AMIDE FORMATION VIA NI-CATALYZED REDUCTIVE COUPLING REACTIONS WITH ISOCYANATES

Eloísa Sofía Serrano Robledo

UNIVERSITAT
ROVIRA i VIRGILI

Amide Formation via Ni-Catalyzed Reductive Coupling Reactions with Isocyanates

---

Eloísa S. Serrano Robledo

DOCTORAL THESIS
2018

Amide Formation via Ni-Catalyzed Reductive Coupling Reactions with Isocyanates

Eloísa S. Serrano Robledo

DOCTORAL THESIS
Supervised by Prof. Rubén F. Martín Romo
Institut Català d'Investigació Química (ICIQ)
Universitat Rovira i Virgili (URV)
Department of Analytical Chemistry & Organic Chemistry

UNIVERSITAT ROVIRA i VIRGILI

ICIQ Institut Català d'Investigació Química

Tarragona 2018

UNIVERSITAT ROVIRA I VIRGILI
AMIDE FORMATION VIA NI-CATALYZED REDUCTIVE COUPLING REACTIONS WITH ISOCYANATES
Eloísa Sofía Serrano Robledo

UNIVERSITAT ROVIRA i VIRGILI

ICIQ
Institut Català d'Investigació Química

Prof. Rubén Martín Romo, Group Leader at the Institute of Chemical Research of Catalonia (ICIQ) and Research Professor of the Catalan Institution for Research and Advanced Studies (ICREA),

STATES that the present study, entitled "Amide Formation via Ni-Catalyzed Reductive Coupling Reactions with Isocyanates", presented by Eloísa S. Serrano Robledo for awarding the degree of Doctor, has been carried out under his supervision at the Institute of Chemical Research of Catalonia (ICIQ).

Tarragona, May 2018

Doctoral Thesis Supervisor

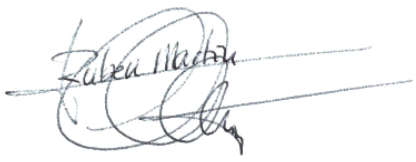

Prof. Rubén Martín Romo

UNIVERSITAT ROVIRA I VIRGILI
AMIDE FORMATION VIA NI-CATALYZED REDUCTIVE COUPLING REACTIONS WITH ISOCYANATES
Eloísa Sofía Serrano Robledo

List of Publications

At the time of printing, the results reported herein have been published in the following journals:

1. Serrano, E. & Martin, R. Nickel-Catalyzed Reductive Amidation of Unactivated Alkyl Bromides. *Angew. Chem. Int. Ed.* **55,** 11207–11211 (2016).

2. Wang, X., Nakajima, M., Serrano, E. & Martin, R. Alkyl Bromides as Mild Hydride Sources in Ni-Catalyzed Hydroamidation of Alkynes with Isocyanates. *J. Am. Chem. Soc.* **138,** 15531–15534 (2016).

The author has also contributed to the following reviews:

3. Juliá-Hernández, F., Gaydou, M., Serrano, E., van Gemmeren, M. & Martin, R. Ni- and Fe-Catalyzed Carboxylation of Unsaturated Hydrocarbons with CO_2. *Topics in Current Chemistry* **374,** 45 (2016).

4. Serrano, E. & Martin, R. Forging Amide Bonds via Metal-Catalyzed Cross-Coupling Reactions with Isocyanates. *Eur. J. Org. Chem*. 10.1002/ejoc.201800175 (2018).

UNIVERSITAT ROVIRA I VIRGILI
AMIDE FORMATION VIA NI-CATALYZED REDUCTIVE COUPLING REACTIONS WITH ISOCYANATES
Eloísa Sofía Serrano Robledo

Table of Contents

Preface

The entirety of the work presented in this dissertation has been performed at the Institute of Chemical Research of Catalonia (ICIQ), during the period of February 2014 to April 2018 under the supervision of Professor Rubén Martín. The present manuscript is divided into five main parts: a general introduction, three research chapters, and a final chapter in which the general conclusions of the work are presented. Each of the research chapters consists of an introduction and a summary of the overall aims of the project, followed by a discussion of the experimental results, conclusions, and finally an experimental section.

In Chapter 1, the principles of reductive cross-electrophile coupling are presented alongside aspects of nickel catalysis that are relevant to this thesis. This is followed by an overview of the existing metal-catalyzed amidation methods using isocyanates as amide sources. The final section of this chapter has been the subject of our recent review, published in *Eur. J. Org. Chem*. 10.1002/ejoc.201800175 (2018).

The second chapter, "*Ni-Catalyzed Reductive Amidation of Unactivated Alkyl Halides with Isocyanates*", describes the synthesis of aliphatic amides from primary alkyl bromides in combination with aryl and alkyl isocyanates, via a Ni-catalyzed reductive cross-coupling. In addition, the synthesis of *N*-tertiary amides has been achieved via the sequential coupling of three different electrophiles. Preliminary mechanistic studies and stoichiometric experiments have indicated the involvement of single-electron transfer processes and the possible intermedacy of Ni(I)-species. In the last section of this chapter, preliminary results for the amidation of unactivated alkyl chlorides are described. Parts of the results presented in Chapter 1 have been published in *Angew. Chem. Int. Ed*. ***55*****,** 11207–11211 (2016).

In the third chapter, "*Towards a Ni-Catalyzed Regiodivergent Amidation of Secondary Alkyl Halides: Unlocking a Reactivity Relay"*, our efforts towards the development of retained and remote Ni-catalyzed amidations of unactivated secondary alkyl halides are divided into two sections. The first describes the retained amidation of unactivated secondary alkyl bromides, in which the unproductive β-hydride elimination from secondary alkyl bromides is minimized by the use of low reaction temperatures and fine-tuned bipyridine-type ligands. In the second section, the efforts towards the optimization of a Ni-catalyzed chain-walking amidation of unactivated acyclic secondary alkyl bromides are presented. Part of the results obtained on the amidation of secondary alkyl bromides has been published in *Angew. Chem. Int. Ed*. ***55*****,** 11207–11211 (2016), but the majority of this chapter discusses unpublished results. The work described has been performed in collaboration with Dr. Alicia Monleón, Alberto Tampieri, Dr. Francisco Juliá-Hernández and Andreu Tortajada.

The last research chapter, "*Ni-Catalyzed Hydroamidation of Alkynes with Isocyanates using Alkyl Bromides as Hydride Sources*", describes the synthesis of acrylamides from aryl-, alkyl-, boryl-, and silyl-substituted alkynes in combination with aryl and alkyl isocyanates. The sensitivity of isocyanates to nucleophiles, including hydride sources, prompted us to take advantage of the facile β-hydride elimination from alkyl halides for the *in situ* formation of catalytic amounts of Ni—H species. Preliminary mechanistic studies provided evidence against an oxidative cyclization pathway between the nickel, the isocyanate and the alkyne coupling partners, and instead pointed towards a hydrometallation pathway. In parallel to Chapter 2, stoichiometric studies with Ni(0) complexes suggested the intermediacy of Ni(I) species. Parts of the contents of this chapter have been published in *J. Am. Chem. Soc*. ***138*****,** 15531–15534 (2016). The work was performed in collaboration with Dr. Xueqiang Wang and Dr. Masaki Nakajima.

UNIVERSITAT ROVIRA I VIRGILI
AMIDE FORMATION VIA NI-CATALYZED REDUCTIVE COUPLING REACTIONS WITH ISOCYANATES
Eloísa Sofía Serrano Robledo

List of Abbreviations & Acronyms

acac =acetylacetonate
APCI = Atmospheric-Pressure Ionization
BHT = 2,6-di-*tert*-butyl-4-methylphenol
bipy = 2,2'-bipyridine
bmim = 1-butyl-3-methylimidazolium
Bpin = 4,4,5,5-tetramethyl-1,3,2-dioxaboronic ester
Bz = benzoyl
cat = catalytic
COD = 1,5-cyclooctadiene
Cp = cyclopentyl
Cy = cyclohexyl
DFT = Density Functional Theory
DMA = *N,N*-dimethylacetamide
DMF = *N,N*-dimethylformamide
DMSO = dimethyl sulfoxide
dppb = 1,4-bis(diphenylphosphino)butane
dppe = 1,2-bis(diphenylphosphino)ethane
dppf = 1,1′-ferrocenediyl-bis(diphenylphosphine)
dppp = 1,4-bis(diphenylphosphino)propane
equiv = equivalents
ESI = Electron Spray Ionisation
EtOAc = Ethyl acetate
GC – FID = Gas Chromatography with Flame Ionization Detector
GC – MS = Gas Chromatography coupled to Mass Spectrometry
h = hour(s)
Het = heterocycle
IPr = 1,3-Bis(2,6-diisopropylphenyl)imidazol-2-ylidene
L = ligand
LED = light-emitting diode
M = metal
Mes = mesityl
MIDA = *N*-methyliminodiacetic acid
n = oxidation state
n. d. = not determined
NBS = *N*-bromosuccinimide
NCS = *N*-chlorosuccinimide
NHC = *N*-heterocyclic carbene
NIS = *N*-iodosuccinimide
NMP = *N*-methyl-2-pyrrolidone
NMR = Nuclear Magnetic Resonnance
phen = 1,10-phenanthroline
Piv = pivalate
PMHS = poly(methylhydrosiloxane)

precat = precatalyst
PyOx = 2-(2'-pyridyl)oxazoline
rt = room temperature
SET = single-electron transfer
SIPr = 1,3-Bis(2,6-di-*i*-propylphenyl)imidazolidin-2-ylidene
S_N = nucleophilic substitution
T = temperature
TBAB = tetrabutylammonium bromide
TBAC = tetrabutylammonium chloride
TBAF = tetrabutylammonium fluoride
TBAI = tetrabutylammonium iodide
TBDPS = tert-butyldiphenylsilyl
TDAE = tetrakis(dimethylamino)ethylene
TEMPO = 2,2,6,6-Tetramethyl-1-piperidinyloxy
Tf = trifluoromethanesulfonyl
THF = tetrahydrofuran
TMEDA = tetramethylethylenediamine
Tol = tolyl

Abstract

Recently, reductive cross-electrophile couplings have become powerful alternatives to classical cross-coupling reactions for the formation of both C—C and C—X bonds.[1–3] The use of two electrophiles instead of an electrophile and a nucleophile offers numerous advantages. For example, the absence of strongly basic reagents allows these reactions to occur under milder conditions, resulting in a broader functional group tolerance. In addition, the use of readily available starting materials circumvents the need to prepare air- and moisture-sensitive organometallic reagents, offering a more practical set-up. Within these methods, nickel catalysis has become a valuable tool for the selective cross-coupling of two electrophiles in the presence of a metallic or organic reductant, via two-electron or single-electron transfer processes.

In line with the Martin group's interest in developing strategies that use heteroallenes such as CO_2 to access value-added compounds,[4,5] this Doctoral Thesis focuses on the development of novel nickel-catalyzed reductive coupling reactions for the synthesis of amides from isocyanates. The ubiquity of amides in biologically relevant molecules such as peptides, proteins, agrochemicals and pharmaceuticals, as well as in synthetic materials, continually prompts the development of novel methods for amide synthesis. The transformations developed herein contribute to the development of new synthetic routes towards amides via metal-catalyzed C—C bond formation, which are an alternative to more traditional C—N bond-forming methods (Scheme 1).

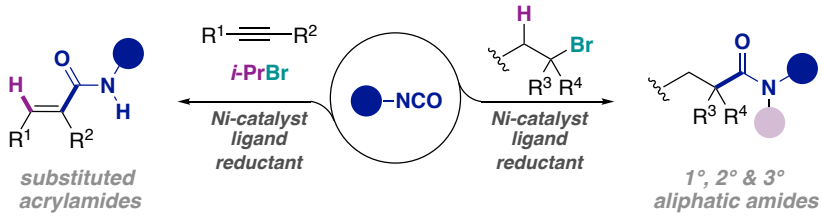

Scheme 1. Amide formation via Ni-catalyzed reductive coupling reactions with isocyanates

Our first strategy aimed to synthesize aliphatic amides from unactivated alkyl bromides using isocyanates as amide synthons (Scheme 2).[6] The successful development of this transformation was based on the identification of a catalytic system that properly balanced the reactivity of both coupling partners. Alkyl halides are challenging substrates due to their slower oxidative addition compared to aryl or alkenyl halides, and have a high propensity to undergo unproductive reactions such as reduction, homodimerization and β-hydride elimination.[7] On the other hand, isocyanates are highly reactive, readily coordinate to low-valent transition metal complexes, and easily undergo dimerization and trimerization reactions.[8] Optimized reaction conditions used a cheap Ni(II) source in combination with bipyridine-type ligands and Mn as the reducing agent. The transformation allowed primary, secondary and tertiary alkyl bromides to be coupled with both aryl and alkyl isocyanates to generate *N*-secondary amides. Furthermore, *N*-primary amides could be accessed by the deprotection of the *tert*-butyl group under Lewis acid conditions, and *N*-tertiary amides could be obtained via the sequential addition of a third electrophile in a one-pot protocol. Stoichiometric studies with Ni(0) and Ni(II)-bipyridine complexes, in the presence or absence of Mn, pointed towards a mechanism that involves alkyl-Ni(I) species. Additionally, a racemic mixture of products was obtained when an enantiopure alkyl bromide substrate was employed, suggesting that single-electron transfer processes are likely to be occurring.

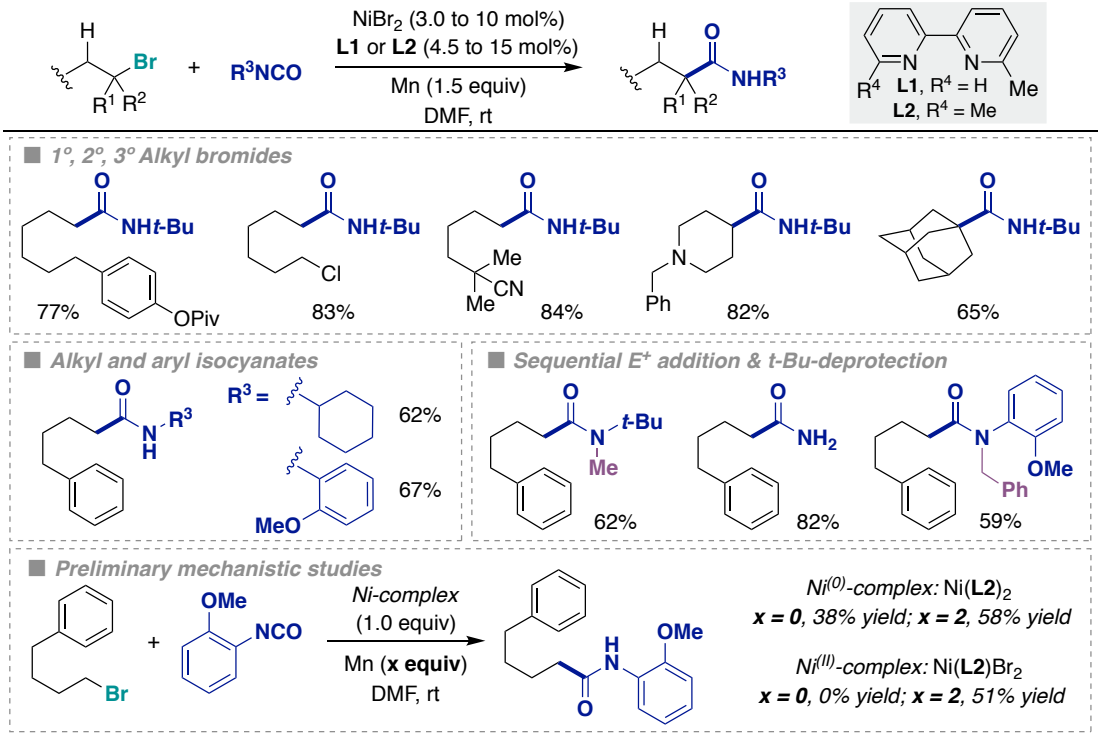

Scheme 2. Ni-catalyzed reductive coupling of unactivated alkyl bromides with isocyanates

One of the limitations of our first strategy was that unactivated acyclic secondary alkyl bromides often provided low yields of the desired secondary amide, mainly due to the formation of β-hydride elimination products. This initial drawback was successfully overcome by the suppression of the undesired β-hydride elimination using low reaction temperatures and finely-tuned bipyridine ligands. Under our newly optimized reaction conditions, high yields of the corresponding amides were obtained with a wide range of secondary alkyl bromides possessing different substitution patterns and functional groups. The Ni-catalyzed chain-walking carboxylation of alkyl bromides recently developed in our group,[9] inspired us to pursue the regiodivergent amidation of acyclic secondary alkyl halides to obtain their remote and retained functionalization under different reaction conditions (Scheme 3). The optimization of the chain-walking amidation is challenging, as – in contrast to the project developed with CO_2[9] – selectivity issues are encountered due to the ready amidation of the secondary alkyl positions of the chain by the more reactive isocyanate coupling partner. The optimization of the reaction temperature and the π–acceptor bipyridine ligand will be pivotal in tuning the reactivity of the Ni-catalyst towards fast β-hydride elimination and migratory insertion, which will lead to high levels of regioselectivity towards the linear amide product. This project is still undergoing in our laboratories.

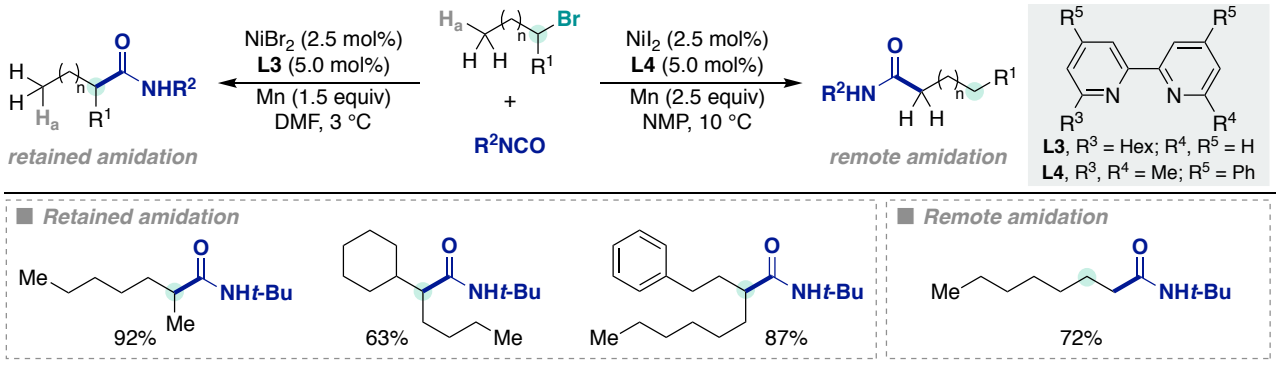

Scheme 3. Towards a regiodivergent amidation of secondary alkyl bromides with isocyanates

Our final venture into amide formation focused on the synthesis of acrylamides via the hydroamidation of alkynes using isocyanates (Scheme 4).[10] At the outset of these studies, one of the primary challenges was the sensitivity of isocyanates to nucleophiles, including hydride sources. In this project, we took advantage of the propensity of alkyl bromides to undergo β-hydride elimination, especially in the presence of Ni-catalysts bearing π-acceptor ligands, to generate catalytic amounts of Ni—H species that could perform the hydrometallation step. The optimization of the reaction conditions led to a system using a Ni(II) salt, phenanthroline-type ligands, Mn as the reducing agent, and isopropyl bromide as the sacrificial hydride source. The transformation provided acrylamides with high levels of diastereoselectivity, showed a broad functional group tolerance, and displayed a wide substrate scope, as aryl-, alkyl-, silyl- and boryl-substituted acetylenes could be coupled with aryl and alkyl isocyanates. Preliminary mechanistic studies showed that oxidative cyclization of the alkyne and the isocyanate is highly unlikely, since no product was detected in stoichiometric reactions in the absence of a hydride source. Moreover, the use of d_7-isopropyl bromide as the starting material led to full deuterium incorporation in the acrylamide product. These studies indicate that the transformation likely begins with the hydrometallation of the alkyne by an *in situ* generated Ni-hydride species, followed by insertion of the isocyanate.

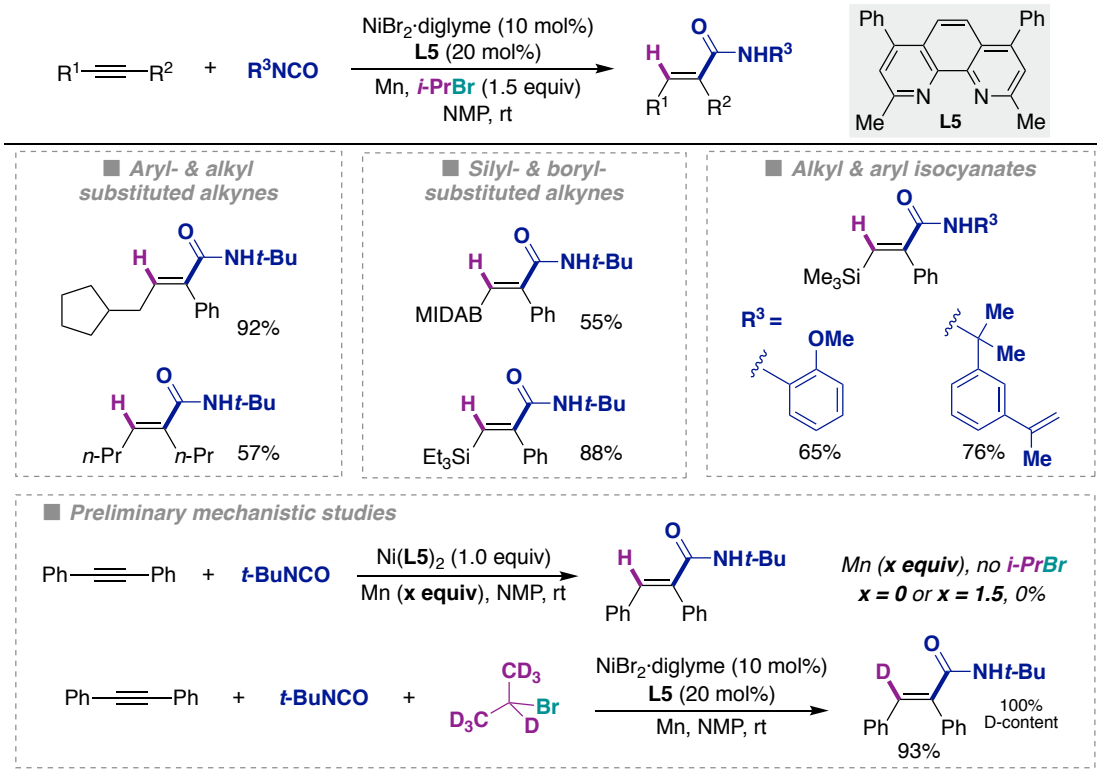

Scheme 4. Ni-catalyzed hydroamidation of alkynes with isocyanates using alkyl bromides as hydride source

In conclusion, we have developed new methods for the synthesis of amides via Ni-catalyzed reductive couplings with isocyanates. A key factor common to the above transformations is the need to carefully control β-hydride elimination reactions, to either achieve the retentive amidation of the starting materials, or to promote the formation of Ni—H species, which can undergo chain-walking processes to functionalize remote positions or can be transferred to other substrates and used in a hydrometallation step.

Bibliography:

1. Weix, D. J. Methods and Mechanisms for Cross-Electrophile Coupling of Csp^2 Halides with Alkyl Electrophiles. *Acc. Chem. Res.* **48,** 1767–1775 (2015).
2. Knappke, C. E. I. *et al.* Reductive Cross-Coupling Reactions between Two Electrophiles. *Chem. Eur. J.* **20,** 6828–6842 (2014).
3. Richmond, E. & Moran, J. Recent Advances in Nickel Catalysis Enabled by Stoichiometric Metallic Reducing Agents. *Synthesis* **50,** 499–513 (2018).
4. Börjesson, M., Moragas, T., Gallego, D. & Martin, R. Metal-Catalyzed Carboxylation of Organic (Pseudo)halides with CO_2. *ACS Catalysis* **6,** 6739–6749 (2016).
5. Correa, A. & Martin, R. Ni-Catalyzed Direct Reductive Amidation via C-O Bond Cleavage. *J. Am. Chem. Soc.* **136,** 7253–7256 (2014).
6. Serrano, E. & Martin, R. Nickel-Catalyzed Reductive Amidation of Unactivated Alkyl Bromides. *Angew. Chem. Int. Ed.* **55,** 11207–11211 (2016).
7. Cárdenas, D. J. Advances in Functional-Group-Tolerant Metal-Catalyzed Alkyl-Alkyl Cross-Coupling Reactions. *Angew. Chem. Int. Ed.* **42,** 384–387 (2003).
8. Braunstein, P. & Nobel, D. Transition-Metal-Mediated Reactions of Organic Isocyanates. *Chem. Rev.* **89,** 1927–1945 (1989).
9. Juliá-Hernández, F., Moragas, T., Cornella, J. & Martin, R. Remote carboxylation of halogenated aliphatic hydrocarbons with carbon dioxide. *Nature* **545,** 84–88 (2017).
10. Wang, X., Nakajima, M., Serrano, E. & Martin, R. Alkyl Bromides as Mild Hydride Sources in Ni-Catalyzed Hydroamidation of Alkynes with Isocyanates. *J. Am. Chem. Soc.* **138,** 15531–15534 (2016).

Chapter 1.

General Introduction

1.1. Reductive Cross-Electrophile Couplings

Metal-catalyzed cross-coupling reactions have revolutionized the way chemists build C—C and C—heteroatom bonds in organic molecules.[1] These transformations are based on the union of an organic electrophile with a nucleophilic (organometallic) reagent through the formation of C—metal bonds (Scheme 1.1, left). The electrophilic coupling partners are often organohalides or pseudohalides, whereas the nucleophiles can be alkenes, alkynes, carbon- or heteroatom-based nucleophiles, or organometallic compounds. The high efficiency, mild conditions and broad functional group tolerance associated with these reactions have contributed to their widespread use in synthetic organic chemistry and target-oriented synthesis, both in academia and industry. The importance of the field was recognized by the 2010 Nobel Prize in Chemistry awarded to Professors Richard F. Heck, Ei-ichi Negishi and Akira Suzuki, for their discoveries in Pd-catalyzed cross-coupling reactions for the formation of C—C single bonds.[2]

One of the drawbacks associated with traditional cross-coupling reactions is that, in many cases, the organometallic reagent needs to be prepared from organic(pseudo)halides by metallation reactions, which adds an extra synthetic step. Additionally, the sensitivity of most organometallic species requires the rigorous exclusion of moisture and dioxygen from the reactions, and the basicity and nucleophilicity of these reagents (or of the additives needed for their activation), often diminishes the functional group tolerance. A more straightforward approach would be the direct use of two electrophiles as coupling partners to form the same kind of C—C bonds. To this end, metal-catalyzed reductive cross-electrophile couplings have recently become useful alternatives to cross-coupling reactions, in which two electrophilic partners can be combined in the presence of a stoichiometric reducing agent (Scheme 1.1, right).[3,4] Among the advantages of these protocols are their experimental simplicity, the wide commercial availability of organic halides compared to organometallic reagents, and the enhanced chemoselectivity that results from the mild conditions given by the formation of transient organometallic intermediates, instead of the use of stoichiometric organometallic reagents.

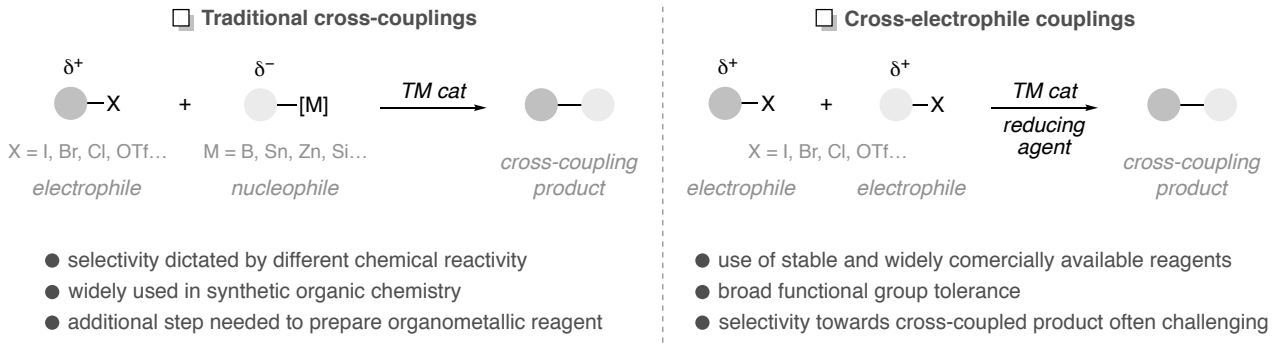

Scheme 1.1. Traditional cross-coupling and reductive cross-electrophile coupling reactions

The first examples of reductive cross-couplings date back to the discovery of sodium-mediated dimerization reactions of alkyl halides by Wurtz,[5] the cross-coupling of aryl halides and alkyl halides (the Wurtz-Fittig reaction),[6] and the Cu-mediated biaryl formation pioneered by Ullmann.[7] Later developments in the field include the Nozaki-Hiyama-Kishi reaction,[8,9] which initially used Ni-catalysts in combination with stoichiometric amounts of Cr, and later Ni/Cr-catalytic systems with Mn as the stoichiometric reducing agent.[10] Subsequent reports relied on the use of electrochemical processes;[11–14] however, the requirement for special laboratory equipment and sacrificial anodes has hampered the routine use and further development of these protocols, until recently.[15]

In the last decades, the successful development of catalytic cross-electrophile couplings has made the formation of C(sp^2)—C(sp^3), C(sp^2)—C(sp^2) bonds, and although less developed, even C(sp^3)—C(sp^3) bonds, from simple electrophiles possible. Recent catalytic systems are based on Co, Pd, and Fe, but primarily rely on Ni catalysts.[16] In these protocols, the reductant provides the necessary electrons to balance the redox equation of the reaction. Specifically, it reduces the transient catalytic metal-species within the catalytic cycle and affords reaction turnover. Moreover, it can also react directly with the substrate to *in situ* and slowly generate the corresponding organometallic nucleophile via metal-insertion reactions; however, labeling the second case as a reductive cross-coupling is debatable.[3] Common reducing agents employed in these transformations are metallic powders of Mn, Zn, Mg, as well as organic reductants such as B_2pin_2[17] and TDAE,[18] albeit to a lesser extent.

In traditional metal-catalyzed cross-coupling reactions, the selective formation of cross-coupled products relies on the different chemical nature of the nucleophile and electrophile used as starting materials. These react with the transition metal-catalyst via distinct pathways (i.e. transmetallation and oxidative addition), providing high selectivity towards the desired product. In contrast, the coupling partners used in cross-electrophile couplings have similar reactivities, which often lead to undesired homocoupling reactions instead of the formation of the targeted cross-coupled product. Reaching high levels of selectivity in cross-electrophile couplings is therefore one of the major challenges to be surmounted. Different strategies to increase the selectivity in these protocols include: the addition of an excess of one reagent, the electronic differentiation of the starting materials, catalyst-substrate steric matching, and the development of reactions that couple substrates for which oxidative addition occurs via two different mechanisms, such as through two-electron polar or radical pathways.[19] The study and understanding of the mechanisms by which cross-electrophile couplings operate has not only contributed to advances within the field, but has also inspired the design of novel transformations, particularly of dual nickel/photoredox systems in which the photoredox cycle replaces the reducing agent.

In recent years, our group has extensively contributed to the field of reductive carboxylation reactions using CO_2 as a C1-synthon as means to access valuable carboxylic acids from simple electrophilic coupling partners.[20] These processes fall into the category of cross-electrophile coupling reactions, in which a reducing agent is required to drive the reaction forward. The efforts carried out by our group have allowed to couple CO_2 with aryl halides, benzylic electrophiles, alkyl halides, allylic acetates, alcohols and unsaturated hydrocarbons, among others by using, in most instances, Ni catalysts in combination with phosphine or nitrogen-containing ligands in the presence of metal reductants (Scheme 1.2).

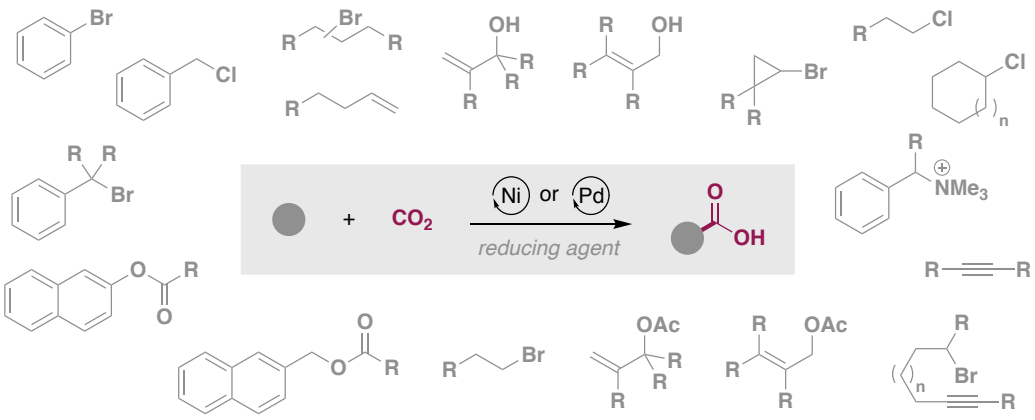

Scheme 1.2. Reductive cross-coupling reactions with CO_2 developed in the Martin group

1.2. General Characteristics of Nickel Catalysts

Nickel belongs to the group 10 metals of the periodic table, and it is the 24th most abundant element in the Earth's crust, being more abundant than Cu, Zn and Pb. The use of nickel as a mediator in organic transformations was pioneered by the Nobel Prize-winning work of Sabatier for the hydrogenation of ethylene. Further progress in the field was overshadowed by rapid developments in Pd chemistry, perhaps due to the difficulties associated with the control of organonickel species that contributed to the false impression that nickel was not suitable for synthetic applications. However, over time, a variety of synthetically useful and robust Ni-catalyzed transformations were developed including cross-coupling reactions (such as Kumada-Corriu, Suzuki-Miyaura, Negishi and Hiyama reactions), as well as cyclizations and polymerization reactions, among others. A renewed interest in nickel catalysts within the last decades has led to the design of novel chemical transformations that exploit the versatility of earth-abundant nickel salts.[21] Important advancements have been accomplished in the Mizoroki-Heck reaction, reductive cross-coupling reactions, C—O[22] and C—N[23] bond activations, C—H bond functionalizations, asymmetric couplings,[24] and metallaphotoredox reactions,[25] among others. The utility of nickel-catalyzed transformations is demonstrated in industrial applications such as the Shell Higher Olefin Process (SHOP) for the production of α-olefins and DuPont's hydrocyanation of butadiene for adiponitrile synthesis. Additionally, nickel catalysts have found a broad application in the synthesis of pharmaceuticals and agrochemicals.

Nickel	*Palladium*
Oxidation states	
0, **+1**, **+2**, **+3**, +4	**0**, +1, **+2**, +3, **+4**
Atomic radius	
smaller than Pd	larger than Ni
Electronegativity (Pauling)	
1.91	2.20
Reactivity	
relatively more reactive than Pd bond strength Ni—C < Pd—C	relatively more reactive than Pt bond strength Pd—C < Pt—C
Polar or radical pathways	
radical pathways favored homolytic cleavage trend Ni—C > Pd—C	two-electron (polar) pathways more common homolytic cleavage trend Pd—C > Pt—C
Favored elementary steps	
facile oxidative addition facile migratory insertion	facile reductive elimination facile β-hydride elimination
Binding to unsaturated compounds	
strong binding binding to alkenes: ΔE = 34.3 kcal/mol binding to alkynes: ΔE = 41.6 kcal/mol	less favored binding binding to alkenes: ΔE = 16.1 kcal/mol binding to alkynes: ΔE = 17.9 kcal/mol
Catalytic cycles	
Ni(0)/Ni(II) Ni(0)/Ni(II)/Ni(I) **Ni(I)/Ni(III)** Ni(I)	**Pd(0)/Pd(II)** Pd(II)/Pd(III)/Pd(IV) Pd(0)/Pd(I)/Pd(II) **Pd(II)/Pd(IV)**

Table 1.1. General characteristics of nickel and palladium catalysts

The differences between the general characteristics of nickel and palladium catalysts are highlighted in Table 1.1.[21,26,27] Although the modulation of the electronic properties of the metal centers by ligand coordination alters

their reactivity, it is possible to outline some general trends. For example: nickel is a smaller and hence more nucleophilic metal that can activate less reactive starting materials such as C—O and C—N electrophiles. Pd is a more electronegative atom than Ni, a property that reflects in its higher second ionization potential (Pd(II) = 19.43 vs. Ni(II) = 18.17 eV).[28] In general, the weaker Ni—C bond gives rise to more reactive intermediates and to radical pathways via homolytic bond cleavage. The loss of electron density on the metal during oxidative addition is facilitated by the more electropositive character of Ni compared to Pd. Conversely, a more facile reductive elimination is observed with the latter. Pd—alkyl complexes are more prone to β-hydride elimination than Ni—alkyl species due to a better agostic interaction resulting from the more effective σ-donation of the C—$H_β$ σ-bond to the lower-lying empty *d* orbital of Pd, which weakens the C—H bond.[29] The microscopic reverse reaction, migratory insertion, is therefore more favored with Ni than with Pd. Moreover, the more favored π-back donation from Ni results in a stronger binding to alkenes and alkynes, and thus in the more facile activation of these motifs.[27] Finally, as odd oxidation states are easily accessible with Ni, different catalytic manifolds can be designed. From these properties, it derives that the complementary reactivity of Ni and Pd can be exploited in the development of alternative chemical transformations.

1.3. The Amide Functional Group

Amides are one of the most prevalent functional groups in nature, as they constitute the core linkages of amino acids in peptides and proteins. The stability of peptide bonds arises from the mesomeric stabilization of amides, in which delocalization of the nitrogen lone pair imparts a double bond character to the C—N bond. This generates a zwitterionic species and forces coplanarity on the O—C(R)—N(R)$_2$ system. Overall, the resulting resonance structures account for the lower nucleophilicity of the carbonyl group, and the higher rotational barrier around the C—N bond (Scheme 1.3, top).[30]

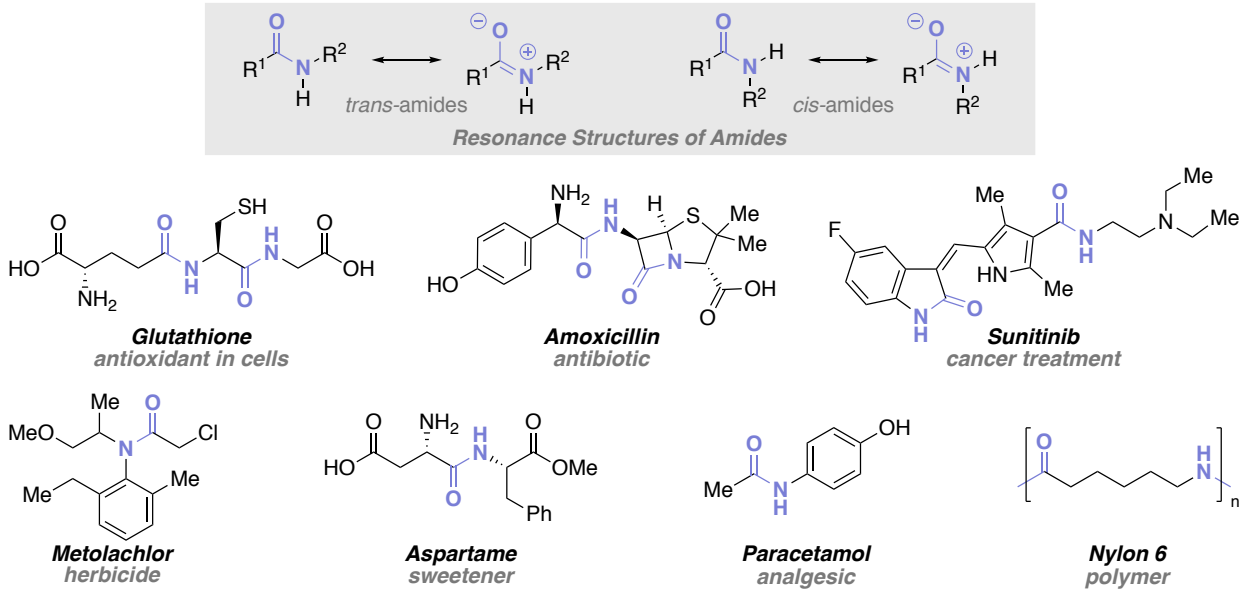

Scheme 1.3. Resonance structures of amides and examples of relevant amide-containing molecules

Besides being a key functional group in nature, amides are widespread in biologically active compounds such as agrochemicals and pharmaceuticals, and in synthetic materials such as polymers and hydrogels (Scheme 1.3, bottom). Indeed, an analysis of known drug databases carried out in 1999 showed that about 25% of all commercialized pharmaceuticals contained amide bonds.[31] In 2003, this functional group was present in 9 out of the 53 top selling small molecule drugs.[32] From this, it is clear that amide bond formation is one of the most

commonly performed reactions in the chemical industry, and that it is particularly important in drug discovery. In fact, according to a 2011's analysis of three large pharmaceutical companies, 16% of all reactions performed corresponded to amide bond formations.[33] A comparative analysis of the medicinal chemistry literature showed that in 2014, 60% of the manuscripts analyzed reported the formation of an amide bond.[34]

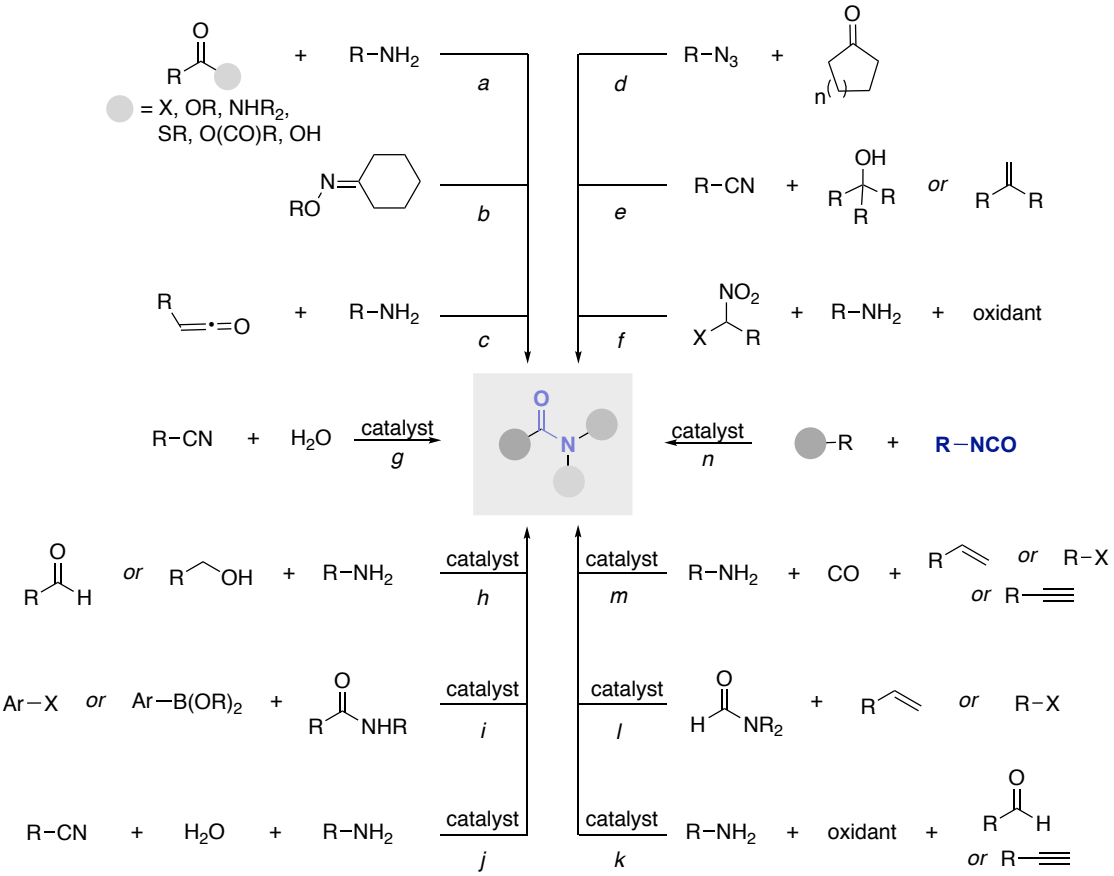

a) condensation of (activated) carboxylic acid derivatives, *b*) Beckmann rearrangement, *c*) addition to ketenes, *d*) Boyer-Schmidt-Aubé rearrangement, *e*) Ritter reaction, *f*) oxidative coupling of α-halo-nitro compounds, *g*) hydration of nitriles, *h*) dehydrogenative amidation, *i*) *N*-arylation cross-couplings, *j*) coupling of nitriles with amines, *k*) oxidative amidation of aldehydes or alkynes, *l*) amidocarbonylation with formamides, *m*) amidocarbonylation using CO and amines, *n*) cross-coupling with isocyanates, among others.

Scheme 1.4. Synthetic approaches towards amide formation

Scheme 1.4 summarizes some of the most important methods for amide bond formation. Amongst these, the formation of C—N bonds by condensation of activated carboxylic acid derivatives with amines is the most prevalent method in both industry and academia (Scheme 1.4, *path a*). The direct dehydrative condensation of a carboxylic acid and an amine would be ideal, but it is an uphill process that requires harsh conditions; therefore, the reaction requires the derivatization of the carboxylic acid into an acyl chloride or anhydride, the addition of an activating agent, or the addition of stoichiometric amounts of a coupling reagent.[35] Numerous such reagents have been developed, and overall, the advances achieved in the field currently give access to a large variety of peptides.[36–38] Nevertheless, this classical route to amide bonds encounters significant drawbacks for the synthesis of highly hindered amides, is limited to the use of nucleophilic amines, has low atom-economy, and generates by-products and side-products that are difficult to separate from the desired amides. These drawbacks have prompted the development of numerous alternative methods that produce less waste, have a broad functional group tolerance and give access to a large variety of amide scaffolds.[39] Current alternative methods to the use of activated carboxylic acids include enzymatic processes, transition metal and organocatalytic transformations,[40]

the use of amino or carboxylic acid surrogates, direct amidation of carboxylic acids and transamidation reactions,[41] and chemical ligation techniques for long peptide synthesis.[42,43] In 2007, the ACS Green Chemistry Institute Pharmaceutical Roundtable listed the development of "amide formation avoiding poor atom economy reagents" as one of the top priorities of organic chemistry, with a special interest in the development of catalytic and environmentally-friendly methods.[44] In this Doctoral Thesis, we have developed synthetic methods that contribute to the use of isocyanates as amide synthons via transition metal-catalyzed C—C bond formations.

Furthermore, amides can serve as useful synthons for a variety of functional group interconversions, via both C—N and C—C bond-cleavage processes (Scheme 1.5). Recently developed methods take advantage of the activation of these bonds by transition metal catalysts (i.e. Pd and Ni), and use amides as surrogates for commonly employed organic halides in transformations that overcome the robustness of the amide bond by distortion of its planarity.[45]

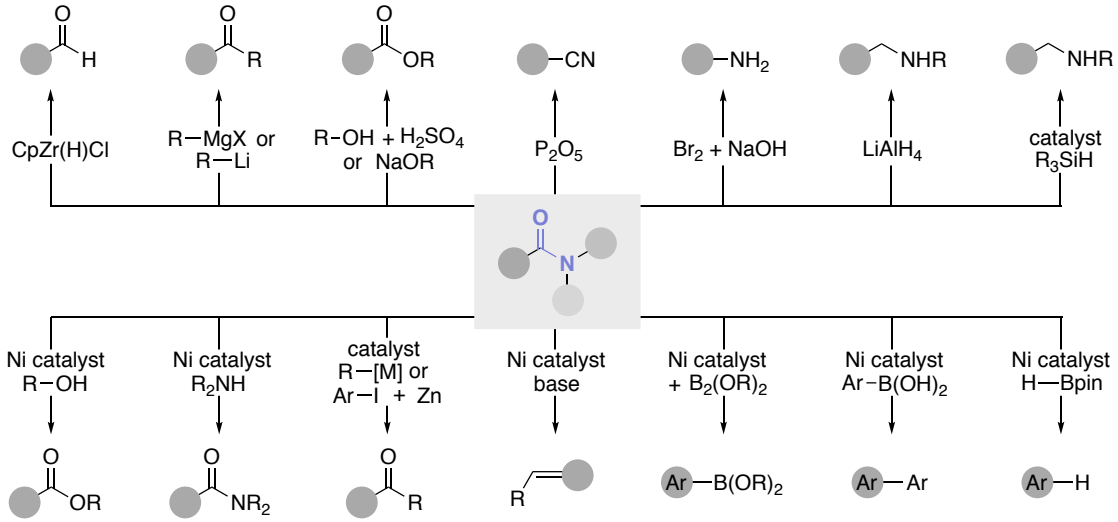

Scheme 1.5. Amides as synthons in organic synthesis

1.4. Isocyanates as Amide Synthons

1.4.1. General Aspects of Isocyanates

The cumulative bond system of isocyanates is isoelectronic with inert carbon dioxide, but the polarization generated by the amido group results in a much higher reactivity (Scheme 1.6, top). Even though the nitrogen and oxygen atoms present in the molecule are nucleophilic, the strong electrophilic character of the central carbon atom dictates the reactivity of isocyanates, and thus they usually behave as electrophiles. The reactivity is also influenced by the nitrogen substituent; with aromatic isocyanates being more reactive than alkyl or cycloalkyl substituted isocyanates for electronic reasons.[46,47]

Isocyanates were first synthesized by Wurtz in 1848 by alkylation of cyanate salts with sulfuric acid esters,[48] and later in 1884 by Hentschel from amines and phosgene.[49] Their synthesis was followed by extensive studies on their reactivity, with a particular interest in their reactions with amines and alcohols, to generate ureas and carbamates, as well as in their dimerization and trimerization reactions. The discoveries made by O. Bayer in 1937 on the synthesis of polyurethanes by polymerization reactions of diisocyanates and diols, ushered the use of isocyanates in modern organic chemistry.[50] For example, isocyanates are useful reagents in cycloaddition reactions, rearrangements, and in a variety of metal-catalyzed transformations.

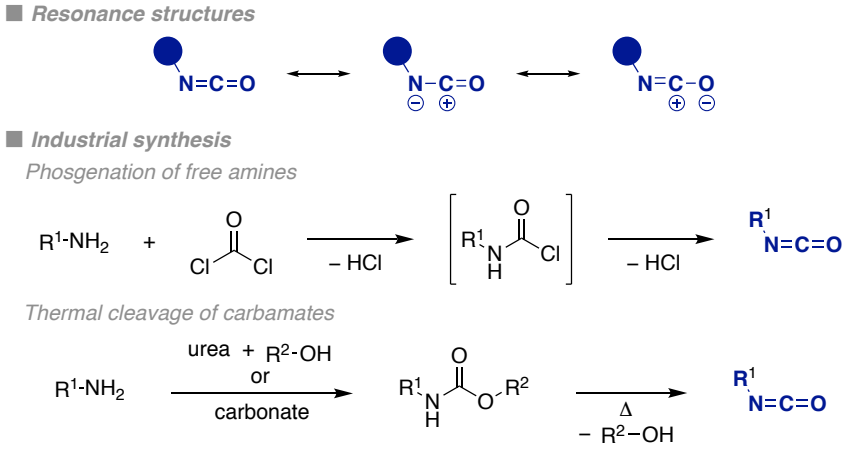

Scheme 1.6. Resonance structures of isocyanates and common industrial synthetic methods

Nowadays, numerous aromatic and aliphatic isocyanates are commercially available. Their large-scale industrial synthesis still mainly relies on phosgenation reactions of amines or amine salts, or on the thermal cleavage of urethanes (Scheme 1.6, bottom). Other phosgene-free methods have extensively been studied, but their use in industry has not been widely adopted.[51] On a laboratory scale, aryl and alkyl isocyanates can be prepared from the corresponding carboxylic acid or carboxylic acid derivative via Curtius, Lossen or Hofmann rearrangements, as well as from amines by reaction with oxalyl chloride, phosgene surrogates such as triphosgene or diphosgene,[52,53] or activated carbonates,[54,55] among other methods.[56–58]

1.4.2. Activation of Isocyanates by Transition Metals

Isocyanates can coordinate to transition metals in side-on η^2-C,N or η^2-C,O fashion, the former being more common due to the lower electronegativity of the nitrogen atom.[59,60] Other coordination modes involve μ^2- or even μ^3- in which the isocyanates act as a bridging ligand between different metal centers. Coordination of an isocyanate to a metal deviates the molecule from linearity and significantly lowers its activation energy, hence favoring reactions with less-reactive nucleophilic partners (Figure 1.1).

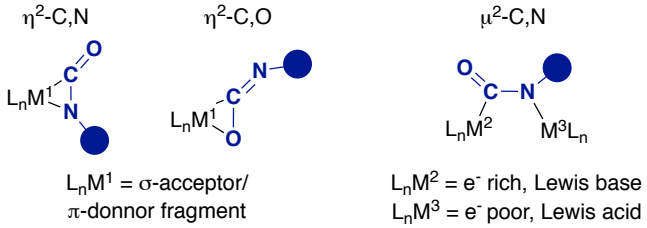

Figure 1.1. Common coordination modes of isocyanates

The activation of isocyanates by metal salts has been exploited for the synthesis of industrially relevant compounds, such as polyurethanes, which are formed by condensation reactions with nucleophiles and diisocyanates; the production of uretdiones, isocyanurates, and related compounds, which are generated by metal-mediated or metal-catalyzed dimerization and (cyclo)trimerization reactions; as well as carbamates and ureas, which are generated by reaction of isocyanates with nucleophiles.[46,51] However, this reactivity hampers the use of isocyanates as amide synthons in metal-catalyzed transformations, as it leads to the generation of undesired products, and often increases the amount of isocyanate required for the reaction. Metal catalysts relevant to this Doctoral Thesis, such as Ni(II) halide salts[61] and zero-valent metal complexes,[62,63] have been reported to trimerize aryl and alkyl isocyanates, for example.

Other metal-catalyzed transformations using isocyanates include the ring expansion of epoxides, aziridines and related ring-strained compounds,[64–66] and the generation of heterocyclic frameworks via metal-catalyzed cycloadditions, where isocyanates serve as 2π-components, including asymmetric methods and their use in the total synthesis of natural products.[67–69] Furthermore, isocyanates also serve as amide synthons in the direct addition of organometallic species, or in metal-catalyzed cross couplings and C—H-functionalization reactions.[70] Earlier reports of the use of isocyanates in transition-metal-mediated reactions were extensively reviewed by Braunstein and Nobel,[59] and newer examples have been summarized and put in context in recent reviews.[71,72]

1.4.3. Direct Addition of Organometallic Reagents to Isocyanates

The direct addition of organometallic reagents to a diverse range of isocyanates was studied prior to their use as amide synthons in metal-catalyzed cross-coupling reactions. These methods have mostly been developed using well-defined organometallic species such as Grignard reagents, organolithium, and organozinc derivatives. Although these species can be accessed via classical metalation techniques, their air sensitivity, high reactivity, and low functional group tolerance are the major drawbacks that have restricted their wide application for the synthesis of amides. The direct addition of Grignard reagents to isocyanates can be traced back to the seminal work of Blaise[73] and Gilman in the early 20th century.[74,75] This was followed by scattered examples[76–80] until 2012, when the group of Bode developed a general method for the addition of organomagnesium bromides to isocyanates to access sterically hindered and electron-deficient secondary amides (Scheme 1.7).[81] The protocol tolerated sensitive functional groups such as esters and ketones by employing low reaction temperatures. Notably, the use of equimolar amounts of the Grignard reagent and the isocyanate generated the desired products in high yields.

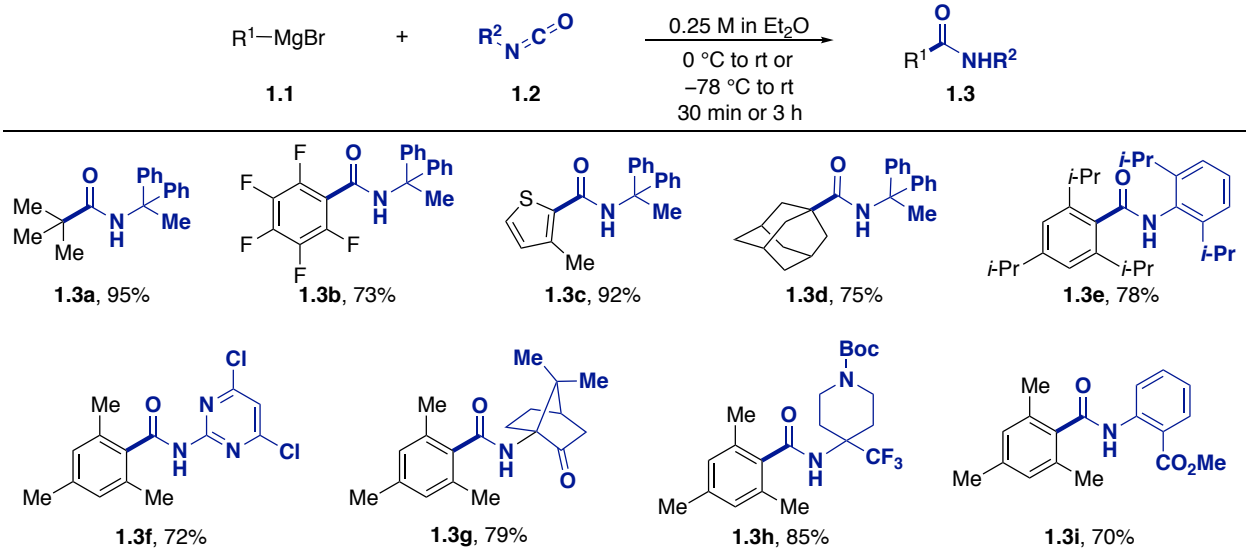

Scheme 1.7. Synthesis of sterically hindered and electron-deficient amides via Grignard addition to isocyanates

The pioneering work of Gilman on the addition of organolithium reagents to isocyanates[82] inspired the development of various methods for the addition of both alkyl and aryl organolithium reagents to iso(thio)cyanates, including the stereospecific addition of chiral alkyllithium reagents.[83–86] However, due to the basicity and high reactivity of organolithium compounds, these protocols often suffer from poor functional group tolerance and lack generality. Furthermore, a variety of organozinc reagents have been added to isocyanates to afford aromatic and aliphatic amides.[87–89] Although these organometallic species have the advantage of displaying a better functional group tolerance, their use for the synthesis of amides still remains limited.

1.4.4. Metal-Catalyzed Amide Synthesis using Isocyanates

1.4.4.1. Metal-Catalyzed Addition of Organometallic Reagents to Isocyanates

One of the first examples of the metal-catalyzed cross-coupling of organometallic reagents and isocyanates was reported in 1987 by Zhang and co-workers (Scheme 1.8).[90] Using catalytic amounts of Cp_2TiCl_2 at low reaction temperatures, linear aliphatic amides could be prepared from a combination of phenyl isocyanate with both linear and branched Grignard reagents. The observed reactivity was proposed to arise from an initial transmetalation of the alkylmagnesium bromide reagent to the titanium catalyst, followed by β-hydride elimination, which generates a Ti—H intermediate and the corresponding alkene. Subsequent migratory insertion places the Ti-catalyst at the less sterically hindered primary carbon. A final isocyanate insertion and transmetalation affords the desired compound and regenerates the Ti-catalyst. In a later report, the authors showed that carrying out the reaction at higher temperatures promoted the selective formation of *N*-methyl-*N,N'*-diphenylurea and *N*-methyl-*N,N'*-diphenylthiourea.[91] These products result from isocyanate reduction and deoxygenation by the Ti—H species. As expected from the use of Grignard reagents, the scope of both reactions was rather limited, and no functional group tolerance was described.

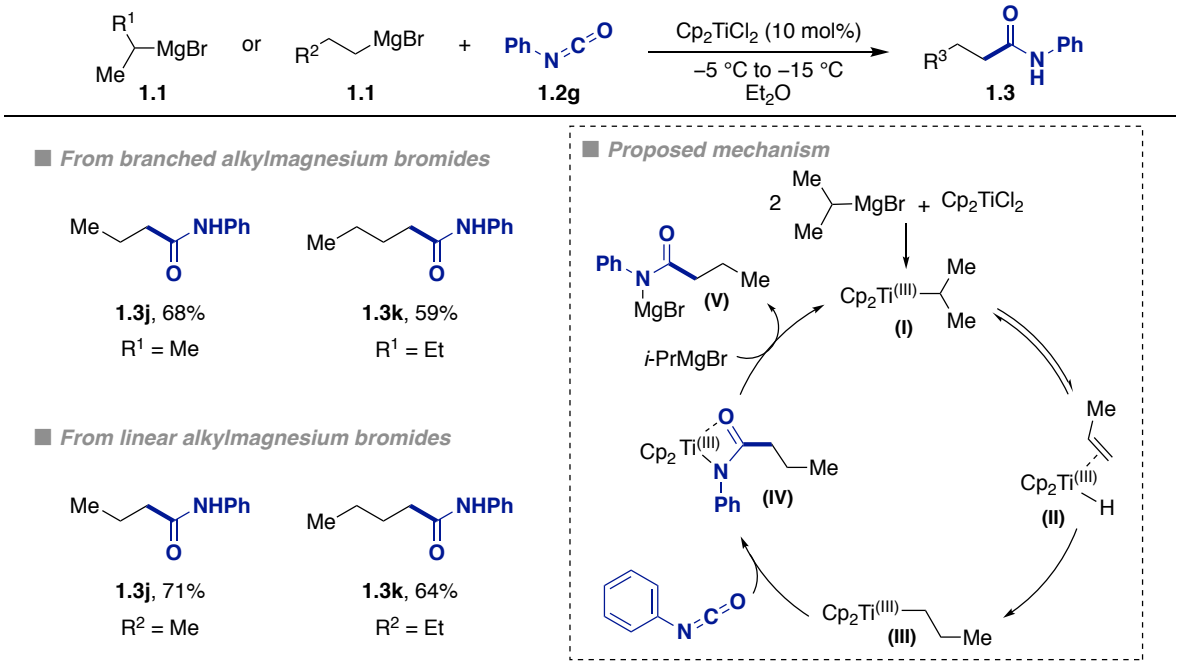

Scheme 1.8. Ti-catalyzed addition of Grignard reagents to isocyanates

Two decades after this work, Mori and co-workers reported the first rhodium-catalyzed arylation and alkenylation of isocyanates using organostannanes (Scheme 1.9).[92] The need for a protic source to promote catalyst turnover in rhodium-catalyzed couplings posed a challenge for the use of isocyanates, as these reagents are prone to decompose to the corresponding primary amine under protic conditions. Although the addition of water indeed resulted in the hydrolysis of the isocyanate, product yields were greatly improved when phenol derivatives were used. Under optimized reaction conditions, aryl and alkyl isocyanates could be coupled to both aryl and alkenyl organostannanes to afford a variety of benzamides and α,β-unsaturated amides. Even though only electron-rich organostannanes could be employed in the transformation, the excellent chemoselectivity associated with the low basicity of organostannane reagents allowed for a broader functional group tolerance than the previous report using Grignard reagents.

The mechanism of the reaction was proposed to proceed via an initial transmetallation of the organostannane to the Rh(I) species, which generates a C(sp^2)—Rh(I) intermediate. Consecutive addition to the isocyanate forms an *N*- or *O*-bound rhodium species, from which protonation of the Rh-amidate by the phenol derivative affords the desired product and regenerates the catalytically active phenoxyrhodium species. It is worth mentioning that a two-fold excess of the isocyanate was needed, due to the competing equilibrium with the corresponding carbamate that is formed by reaction of the isocyanate with the phenol additive.

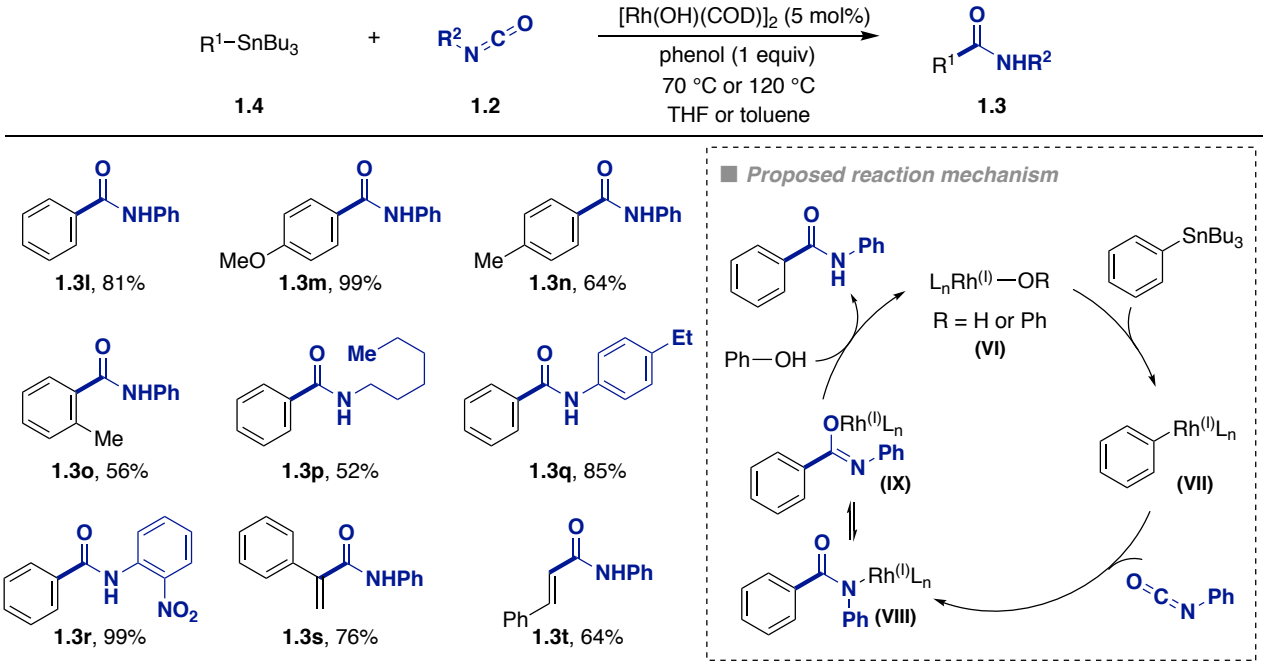

Scheme 1.9. Rh-catalyzed addition of organostannane reagents to aryl and alkyl isocyanates

The use of boronic acid derivatives over other organometallic reagents has numerous advantages; these include their commercial availability, stability, lower toxicity, and the functional group compatibility afforded by milder reaction conditions.[93] Inspired by Mori's work, Murakami and co-workers developed the rhodium-catalyzed addition of aryl and alkenylboronic acids to isocyanates (Scheme 1.10).[94] Compared to the previously developed method using organotin reagents, the functional group tolerance of the transformation was increased as esters, halides, and thienyl groups were well tolerated. In addition, not only could electron-rich aryl boronic acids be employed but electron-poor boroxines could also be used. Although higher reaction temperatures were necessary, the use of these starting materials prevented potential hydrolysis-decarboxylation pathways inherent to electron-poor arylrhodium intermediates. The presence of active protons within the starting materials avoided the need for additives that protonate the product and promote catalyst turnover. However, a three-fold excess of the organometallic partner was needed to obtain high yields of the desired product – possibly due to hydrolysis of the intermediate organorhodium(I) species. Analogous to this transformation, Kianmehr and co-workers reported the Pd-catalyzed cross-coupling of aryl boronic esters and aromatic isocyanates.[95] Although both electron-rich and electron-poor boronic acids could be used, the scope of the reaction was narrow and the desired benzamides were consistently obtained in moderate yields, along with high amounts of biaryl side-products.

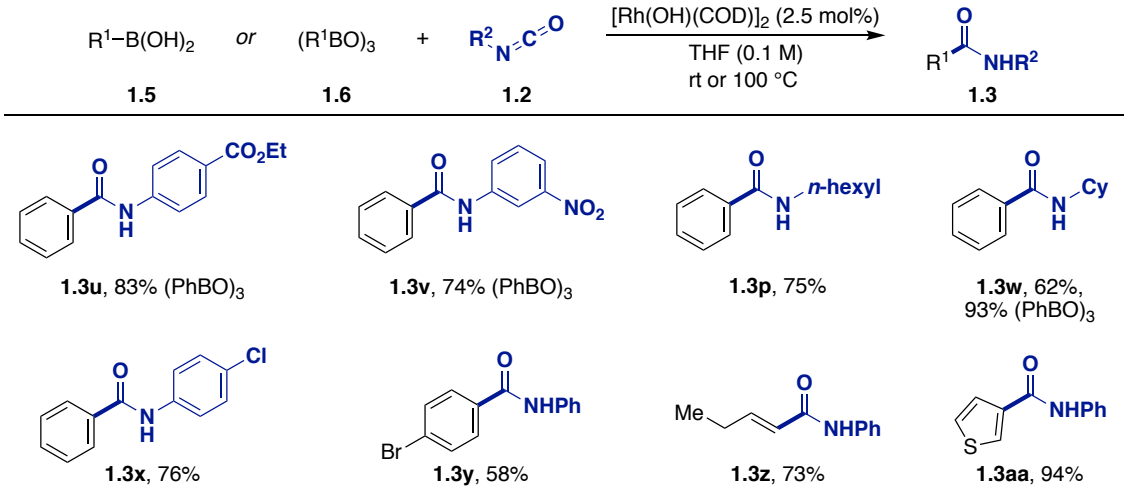

Scheme 1.10. Rh-catalyzed addition of boronic acids to aryl and alkyl isocyanates

In 2015, a more efficient method for the synthesis of benzamides via the Cu-catalyzed amidation of arylboronic esters and isocyanates was reported (Scheme 1.11).[96] The advantages of the transformation included the use of a ligand-free catalytic system based on an earth-abundant and inexpensive catalyst, and the use of a smaller excess of the boronic ester compared to the previously reported methods. Similarly to the use of phenol additives by Mori (vide supra), the authors propose the formation of a carbamate intermediate from the reaction of the isocyanate and the nucleophilic base, which is an additive needed to promote catalyst turnover by formation of a lithium-amidate. Therefore, high reaction temperatures and relatively long reaction times were needed to favor the reverse reaction and recover the isocyanate partner. Nevertheless, the method gave access to a wide scope of benzamides and displayed a good functional group tolerance. These included the formation of sterically hindered products, and amides that would be derived from electron-poor amines, both of which are often difficult to prepare following traditional methods for amide-bond formation.

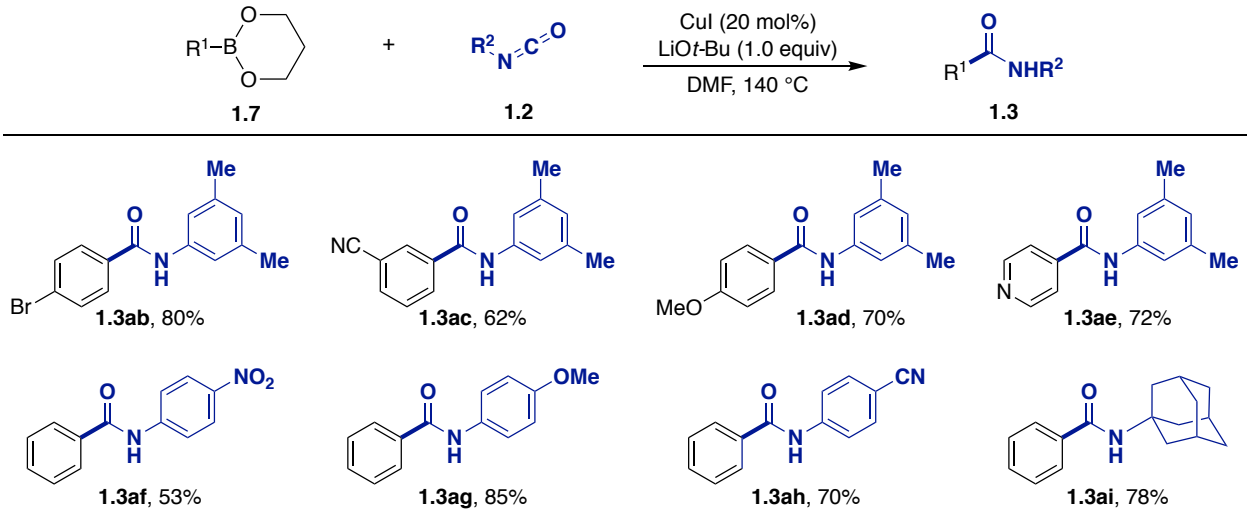

Scheme 1.11. Cu-catalyzed addition of boronic esters to isocyanates

The classical cross-coupling methods described above using organometallic reagents and isocyanates offer an efficient alternative to the traditional amide-bond formation via the condensation of activated carboxylic acids and amines. Specifically, these catalytic methods offer an effective way to access benzamides bearing different substitution patterns and functional groups. The commercial availability of isocyanates and of boronic acids

derivatives renders the more recently developed methods practical and useful. However, the scope of alkyl amides and acrylamides remains limited to a few examples, probably due to the more difficult preparation of alkyl organometallic reagents and the lower reactivity of both alkyl and alkenyl nucleophiles.

In this regard, Nakamura and co-workers reported three discrete examples of the Pd-catalyzed three-component coupling of allylstannanes, allyl chlorides and isocyanates to afford *N*-tertiary aliphatic amides, as part of their extensive studies on the reactivity of bis-π-allylpalladium complexes (Scheme 1.12).[97] In parallel, Solin and co-workers extended the scope of the transformation by using *p*-toluenesulfonyl isocyanate (**1.2t**) to afford bisallylated amides with high regioselectivity (Scheme 1.13).[98] A fine-tuning of the substituents on both coupling partners was found to be essential. Otherwise, mixtures of regioisomers and homo-coupling products were obtained. Moreover, the reaction was limited to the use of **1.2t**, as other isocyanates such as phenyl or 4-nitrophenyl isocyanate only resulted in monoallylated products. These Pd-catalyzed transformations involve the formation of a C—C and a C—N bond through the intermediacy of amphiphilic bis-π-allylpalladium complexes. Formation of the C—C bond occurs via a nucleophilic attack of the Pd-intermediate to the electrophilic isocyanate. This is followed by subsequent intramolecular reaction with the electrophilic π-allylpalladium species to generate the C—N bond.

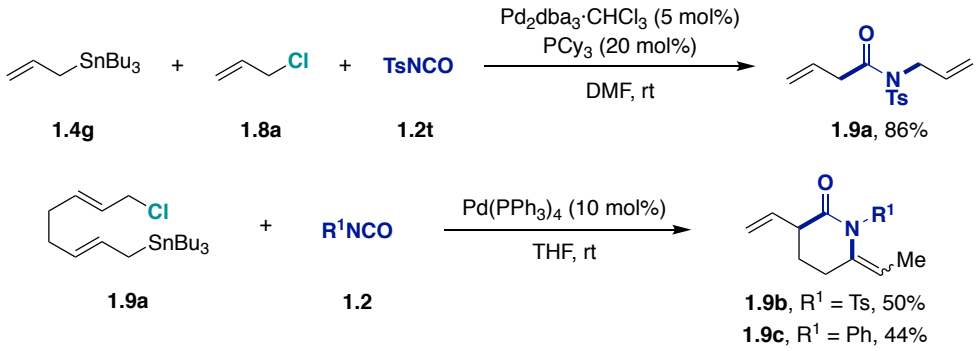

Scheme 1.12. First examples of Pd-catalyzed bis-allylation of isocyanates using allylstannanes and allyl chlorides

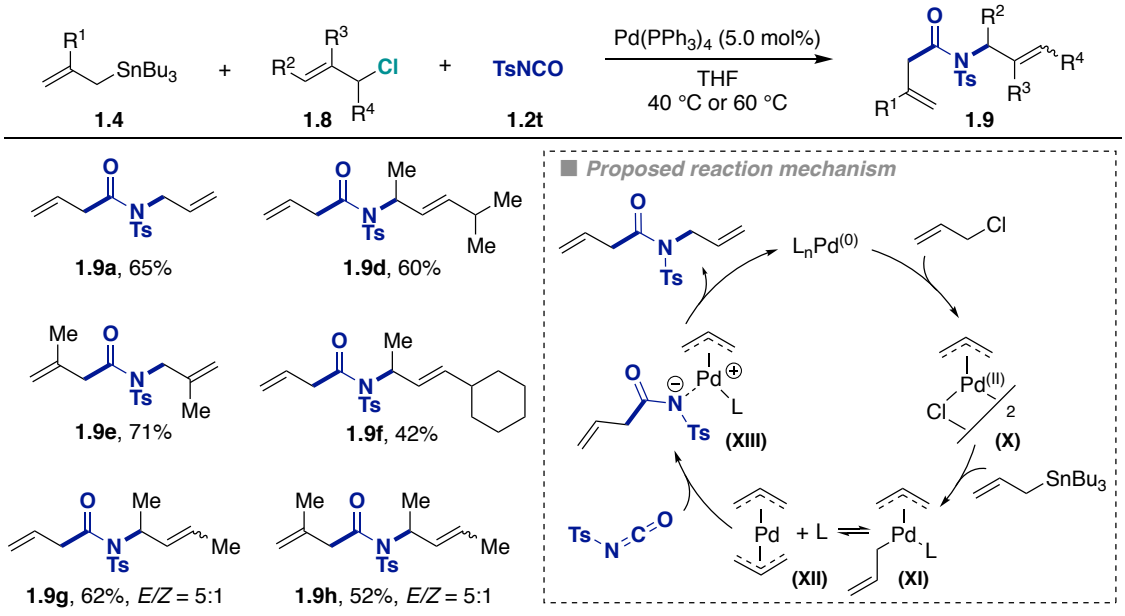

Scheme 1.13. Pd-catalyzed bis-allylation of tosyl isocyanate using allylstannanes and allyl chlorides

1.4.4.2. Metal-Catalyzed Cross-Coupling Reactions of Isocyanates with Unsaturated C—C Bonds

Notwithstanding the utility of organometallic reagents for the synthesis of amides via metal-catalyzed C—C bond formations, illustrated by the previous examples, the development of catalytic methods that use abundant unsaturated hydrocarbons as pro-nucleophiles has several advantages, such as atom-economy, no need for substrate pre-functionalization, and milder reaction conditions. Seminal studies, performed in the 1980's, by Hoberg and co-workers paved the way for the development of the more modern examples of metal-catalyzed amide formation using isocyanates and unsaturated compounds. Specifically, these studies showed that the Ni-stoichiometric and -catalytic coupling of isocyanates with multiple bond systems such as alkynes,[99] alkenes,[100] 1,3-dienes,[101] allenes,[102] aldehydes[103] and imines,[104] occurs via five-membered nickelacycle intermediates, which are generated by oxidative coupling. Although the scope of the reactions was not fully explored, these intermediate species could be characterized and employed in subsequent reactions to generate amides.[59,105] The pioneering work of Hoberg expanded the synthesis of amides from isocyanates and highly reactive organometallic species to the use of less activated coupling partners.

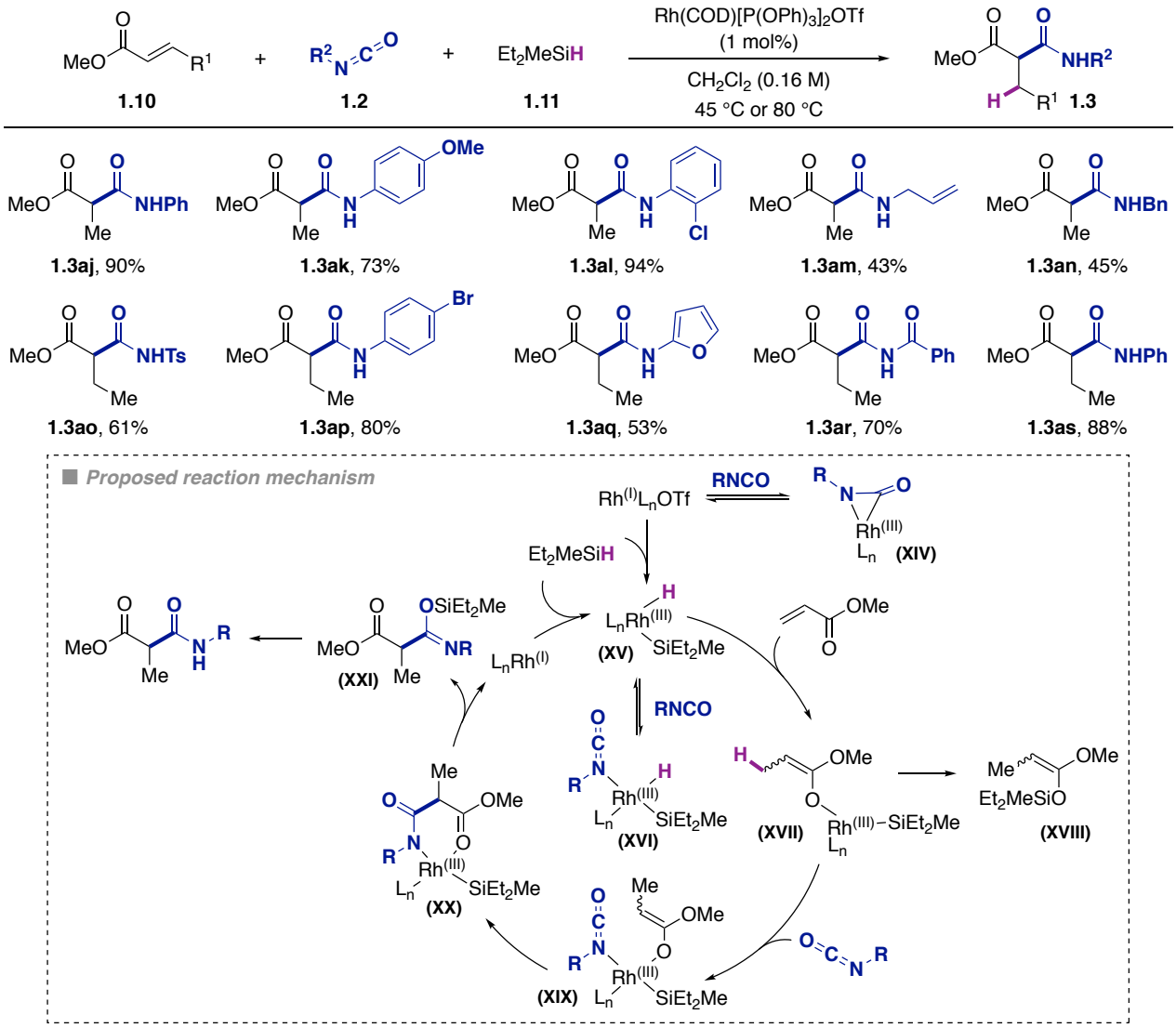

Scheme 1.14. Rh-catalyzed hydrocarbamoylation of α,β-unsaturated carbonyls

In 2001, Muraoka and co-workers reported a Rh-catalyzed formal hydrocarbamoylation of α,β–unsaturated carbonyl compounds with isocyanates using hydrosilanes as the hydride source (Scheme 1.14).[106] Optimal

catalytic conditions used a cationic Rh(I)-complex bearing monodentate phosphine ligands, as bidentate phosphines needed longer reaction times and afforded lower yields of the desired product. Although the reaction was limited to unsubstituted or β-methyl-substituted α,β–unsaturated esters, the reaction was highly regioselective and the scope of the isocyanate partner was broad. Both electron-rich and electron-poor aryl isocyanates were tolerated, including isocyanates substituted by electron-withdrawing groups such as benzoyl or *p*-tosyl groups. In contrast, alkyl isocyanates were less reactive under the reaction conditions, underscoring the importance of having a highly electrophilic isocyanate as the coupling partner. Supported by the isolation of silyl imidate (**XXI**) and of ketene silyl acetal (**XVIII**), the authors propose a mechanism based on the initial oxidative addition of the hydrosilane to the low-valent Rh(I) cationic complex to form a Rh(III)-hydride species. Migratory insertion of the α,β–unsaturated carbonyl compound generates a Rh-enolate intermediate, which defines the regioselectivity of the reaction. Next, coordination of the isocyanate, intramolecular nucleophilic attack to the electrophilic carbon center, and a final reductive elimination afford the silyl imidate intermediate while regenerating the Rh(I)-complex. High reaction temperatures were required to achieve high yields of the desired products, due to the competitive coordination of the isocyanate to the Rh(I)-complex and reversible oxidative addition to form a Rh(III)-species, which compete with the generation of the Rh(I)—H species.

The functionalization of feedstock materials such as alkenes is one of the major goals in organic chemistry; their simplicity and low cost makes them ideal starting materials in catalytic processes that build-up molecular complexity. Previous reports by Hoberg on the stoichiometric and catalytic reactions of phenyl isocyanate and alkenes with Ni(0)-complexes bearing phosphine ligands[107–114] inspired the Jamison group to develop the Ni-catalyzed synthesis of *N*-alkylated acrylamides from α-olefins and isocyanates (Scheme 1.15).[115]

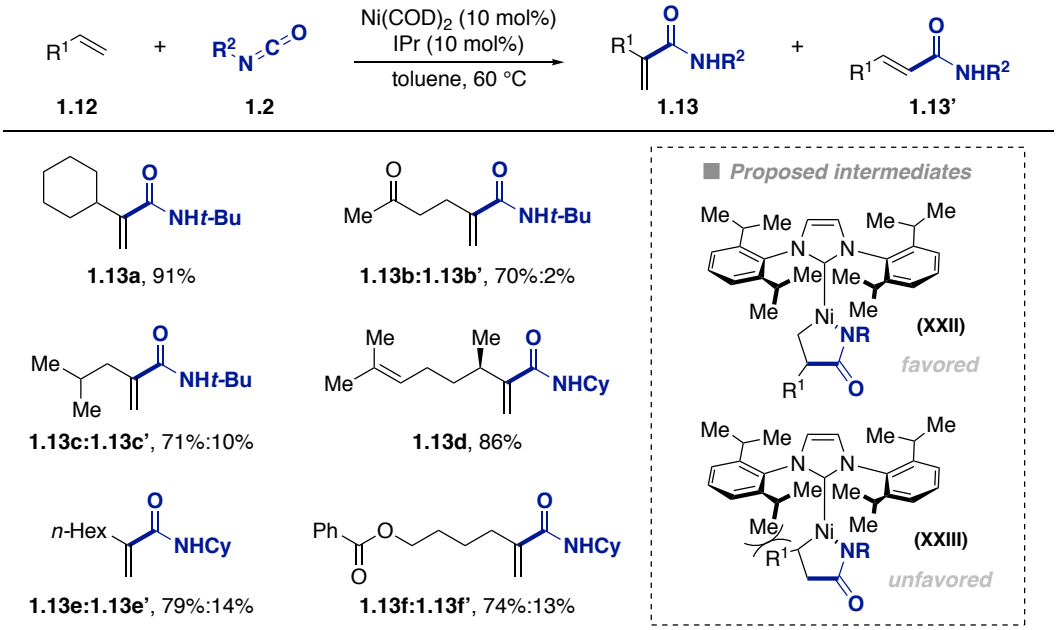

Scheme 1.15. Ni-catalyzed coupling of α-olefins and alkyl isocyanates

Using an *N*-heterocyclic carbene (NHC) as ligand, the authors observed a regioselectivity switch compared to the results obtained by Hoberg; NHCs afforded 1,1-disubstituted acrylamides, whereas the phosphine ligands employed by Hoberg afforded *trans*-disubstituted α,β-unsaturated amides. With this new system, a range of differently substituted α-olefins afforded the desired acrylamides with high yields and good levels of regioselectivity, while unsatisfactory yields were obtained with 1,1-disubstituted, *cis*-, and *trans*-olefins. Although the scope of the isocyanate counterpart was limited to bulky, electron-rich alky isocyanates, the use of *tert*-butyl

isocyanate allowed for the synthesis of *N*-primary amides after deprotection of the *tert*-butyl group under acidic conditions. Unfortunately, the use of other isocyanates gave oligomerization side-products, and attempts to suppress the background NHC-catalyzed trimerization of the isocyanates by pre-forming the Ni-complex led to no improvement.[116] The observed regioselectivity for the formation of 1,1-disubstituted acrylamides was proposed to arise from the preferred azanickelacyclopentanone intermediate, where the alkyl substituent of the parent olefin points away from the steric bulk of the NHC ligand.

The use of isocyanates in combination with unsaturated hydrocarbons has seen widespread application in the synthesis of indole, pyrrole and hydantoin derivatives through tandem reactions. Given the importance of the oxindole scaffold in pharmaceutical compounds and as a synthetic intermediate, Murakami and co-workers reported a series of studies on the Rh- and Pd-catalyzed cyclization reactions of 2-(alkynyl)aryl isocyanates with different coupling partners to afford a variety of 3-alkynlideneoxindoles (Scheme 1.16).

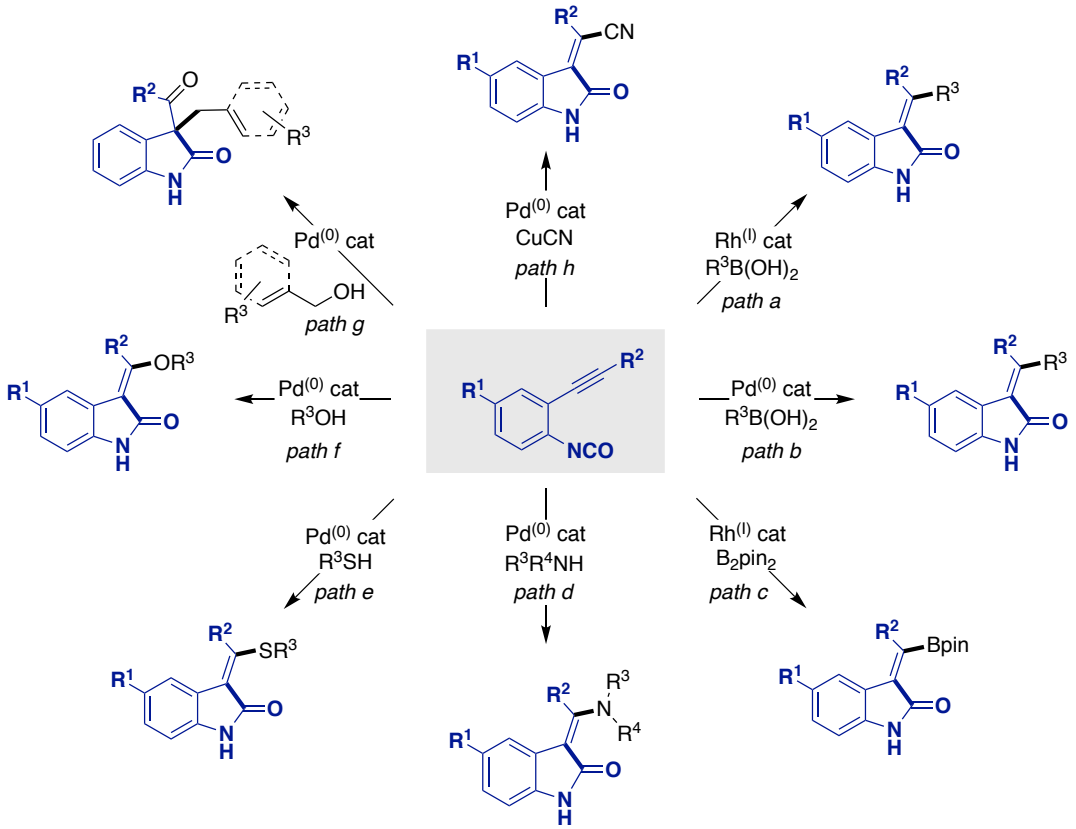

Scheme 1.16. Rh- and Pd-catalyzed synthesis of oxindoles

Their first report used a Rh-catalyst with alkyl or alkenylboronic acids to generate 3-alkylideneoxindoles (*path a*),[117] which was later improved by the use of Pd-catalysis (*path b*).[118] Under these newly optimized conditions, a broader scope for the alkyne terminus and the boronic acids was achieved. The introduction of a handle for further functionalization was possible using B_2pin_2 as coupling partner under Rh-catalysis to afford *E*-borylated 3-alkylideneoxindoles (*path c*).[119] The use of primary and secondary amides gave access to 3-(amidoalkylidene)oxindoles having the amino substituent *cis*- to the carbonyl group (*path d*).[120] As expected, the use of primary amines such as aniline, afforded low yields of the product along with the direct addition of the amine to the isocyanate group. The incorporation of sulfanyl and alkoxyl groups on the alkylidene unit was possible when thiols and alcohols were used in the cyclization reaction (*paths e and f*).[121] Interestingly, when benzyl alcohols were employed as coupling partners, 3,3-disubstituted oxindoles were obtained in one pot

through two Pd-catalyzed processes: an initial oxidative cyclization of 2-(alkynyl)aryl isocyanate and benzylic or allylic alcohols, followed by a [1,3]-rearrangement of the intermediate 3-alkylideneoxindole (*path g*).[122] Finally, 3-(1-cyanoalkylidene)oxindoles could be prepared when copper cyanide was used as the nucleophile (*path h*).[123]

In 2011, the same group described the Ni-catalyzed synthesis of 1,3,5-trisubstituted hydantoins from acrylates and isocyanates (Scheme 1.17).[124] Seminal reports by Hoberg indicated that 1,3-diphenyl-6-methoxycarbonyldihydropyrimidine-2,4-dione could be obtained through the Ni-catalyzed [2+2+2] cycloaddition of one molecule of methyl acrylate and two molecules of phenyl isocyanate when a Ni(0)/PCy_3 catalytic system was used.[125] The key for the selective synthesis of 1,3,5-trisubstittuted hydantoins instead of the reported dihydropyrimidine-2,4-diones was the use of an NHC ligand. The reaction tolerated various aryl isocyanates but gave only isocyanate oligomerization products when using alkyl isocyanates. The authors propose a mechanism based on the initial Ni-catalyzed oxidative cyclization of the acrylate and the isocyanate to afford a 5-membered azanickelacyclopentanone. Subsequent β-hydride elimination and reductive elimination afford an *N*-substituted fumarate intermediate. Next, deprotonation of the amide group by the NHC ligand leads to an amide anion that adds to the second isocyanate molecule. A final cyclization of the anion into the double bond followed by protonation generate the desired product. This mechanistic proposal is supported by time-dependent ^{1}H-NMR studies and by the isolation of a fumarate intermediate after short reaction times, which when re-subjected to the reaction conditions afforded the product. The regioselectivity of the transformation could be explained by the selective formation of an azanickelacyclopentanone in which the electron-withdrawing ester group stabilizes the Ni—C bond.

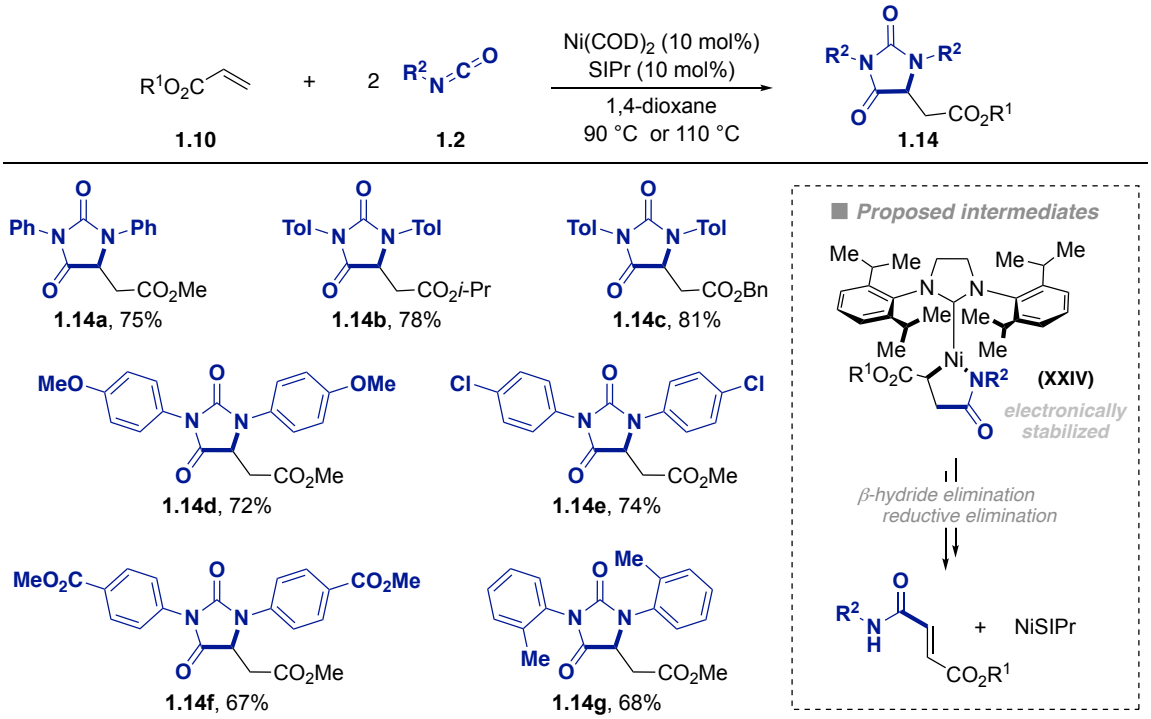

Scheme 1.17. Ni-catalyzed synthesis of 1,3,5-hydantoins from acrylates

The tandem cyclization-addition sequence described above inspired Mizukami and co-workers to develop the Rh-catalyzed synthesis of indole-3-carboxamides from 2-ethynylanilines and isocyanates (Scheme 1.18).[126] The mild reaction conditions allowed for a broad functional group tolerance, especially in the aryl moiety, as well as for the coupling of alkyl and aryl isocyanates. Following the same strategy, Rajesh and co-workers recently

reported the Pd-catalyzed synthesis of furan- and pyrrole-3-carboxamides from isocyanates and 3-alkyne-1,2-diols or 1-amino-3-alkynyl-2-ols, respectively (Scheme 1.19).[127]

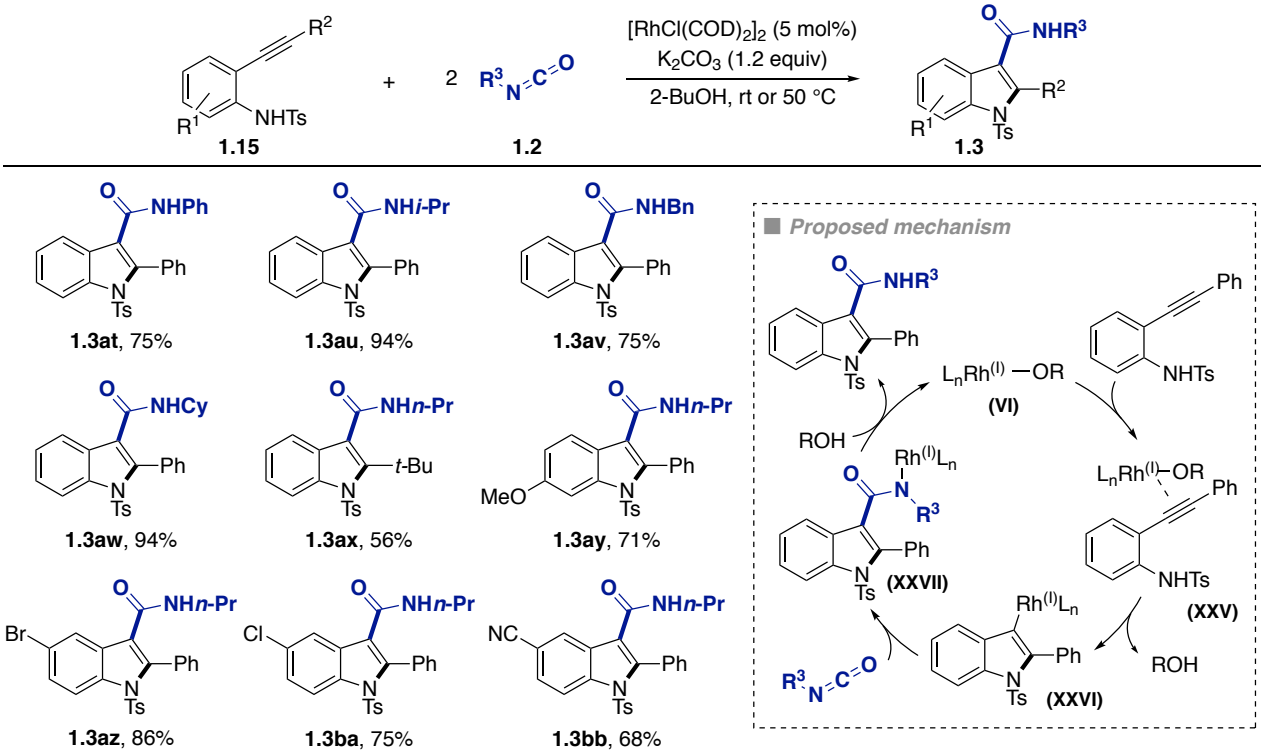

Scheme 1.18. Rh-catalyzed synthesis of indole-3-carboxamides from 2-ethynylanilines and isocyanates

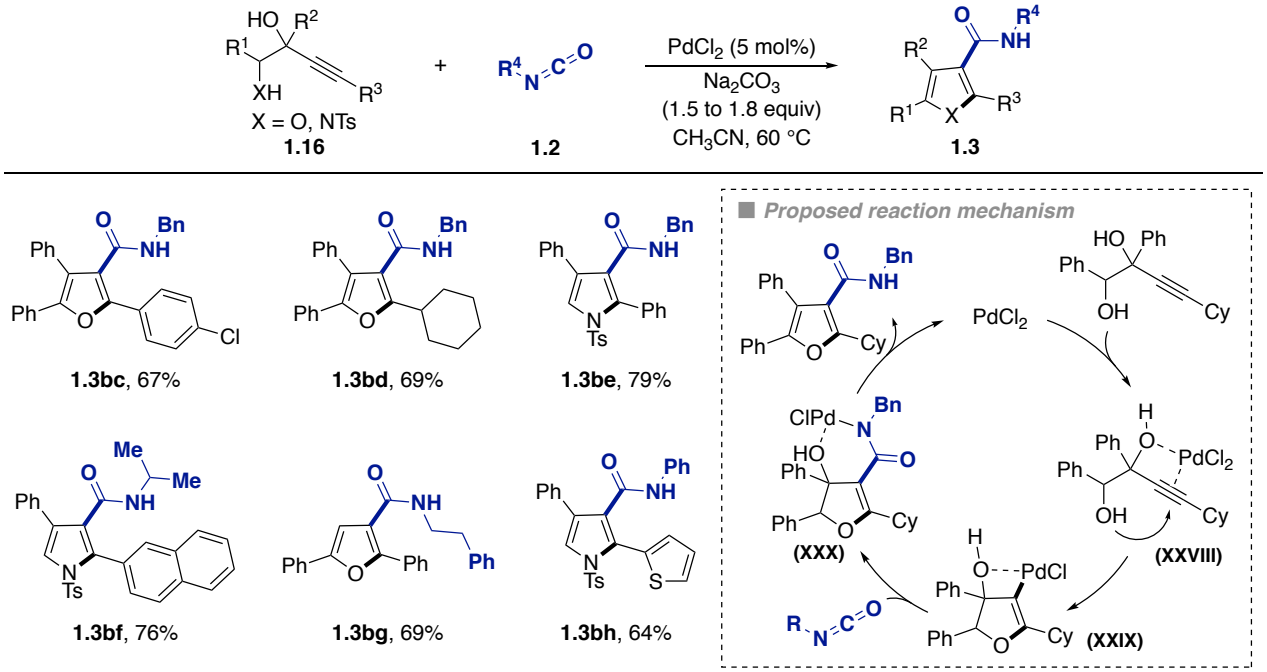

Scheme 1.19. Pd-catalyzed synthesis of furan- and pyrrole-3-carboxamides

1.4.4.3. Metal-Catalyzed Reductive Cross-Electrophile Couplings with Isocyanates

The first Ni-catalyzed reductive cross-coupling of aryl halides with isocyanates was reported in 2005, by Hsieh and Cheng (Scheme 1.20).[128] Under optimized reaction conditions, an array of *o*-iodobenzoates could be coupled with various isocyanates to afford phthalimide derivatives in moderate to good yields. The undesired formation of isocyanurate side-products required the use of superstoichiometric amounts of the isocyanate partner, whereas the homocoupling of the aryl halide was diminished by the addition of extra dppe. Moreover, the reaction could be extended to the use of aryl bromides lacking *o*-esters groups, which afforded the corresponding benzamides; however, when aryl iodides were employed, lower yields and increased amounts of reductive homodimerization products were observed. Although the functional group tolerance was not widely studied in this transformation, it is worth mentioning that a large variety of silyloxy, alkyl and aryl isocyanates with different electronic properties were well tolerated.

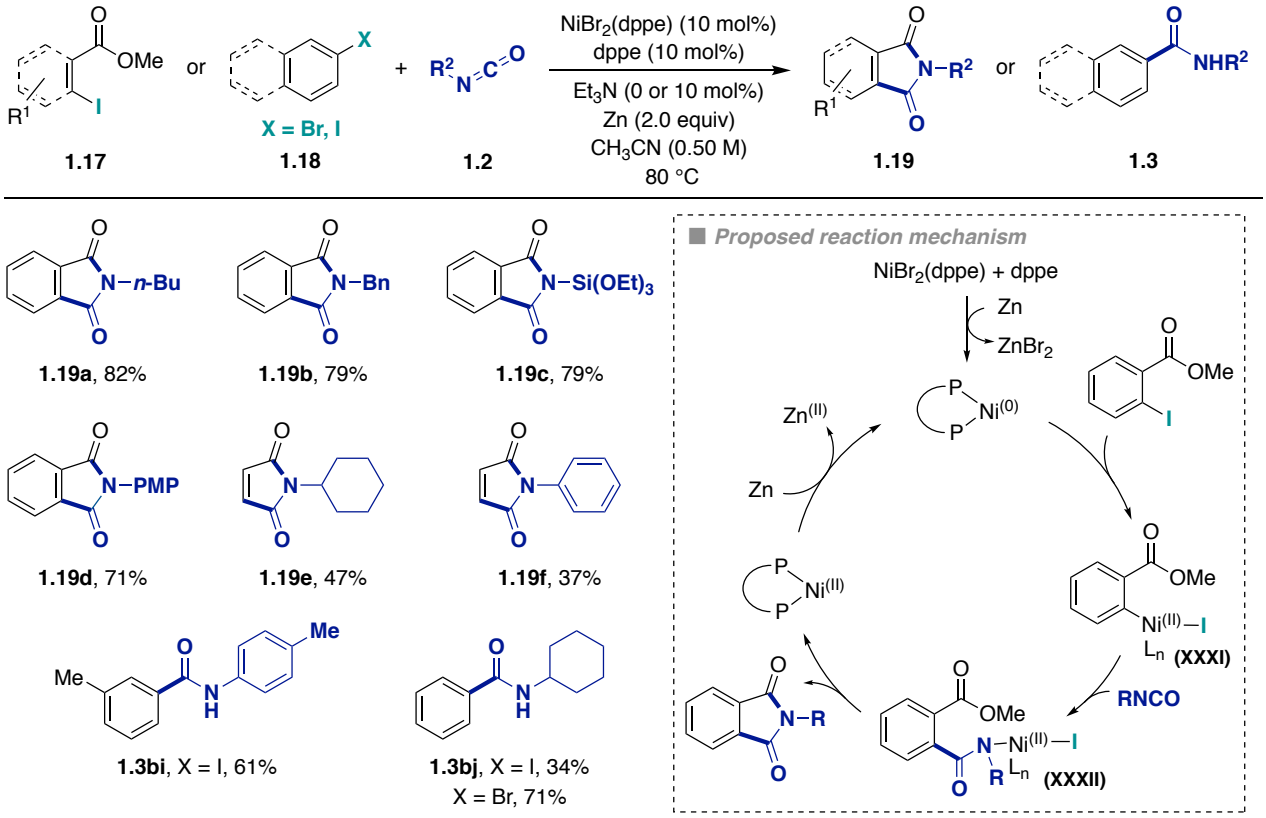

Scheme 1.20. Ni-catalyzed reductive cross-coupling of aryl halides with isocyanates

Although no mechanistic studies were performed, the authors propose an initial Zn-mediated reduction of the Ni(II) precatalyst to generate a Ni(0) species from which an Ar—Ni(II)—I intermediate is formed upon oxidative addition of the *o*-iodobenzoate. Subsequent insertion of the isocyanate into the metal-carbon bond, followed by nucleophilic attack of the Ni-amidate to the *o*-ester group, affords the imide product and a Ni(II) intermediate; which is regenerated to Ni(0) via SET from Zn. The proposed mechanism is supported by the higher yields observed when both electron-rich aryl halides and electron-rich isocyanates were used, which likely enhance the nucleophilic character of the intermediates by raising the HOMO of the Ni—C bond and the Ni—amide bond in (**XXXI**) and (**XXXII**), respectively. Interestingly, the reaction rate of phthalimide formation from *o*-iodobenzoates was increased in the presence of Et_3N, but no additive was necessary to obtain a good reactivity for the synthesis of benzamides from aryl bromides.

Following our group's interest in the development of cross-coupling methodologies for the use of C—O electrophiles as aryl halide surrogates, we reported the Ni-catalyzed reductive coupling of isocyanates with aryl esters and tosylates in 2014 (Scheme 1.21).[129] Using a catalytic system relatively similar to the one employed by Hsieh and Cheng (vide supra), naphthyl pivalates could be coupled with a variety of alkyl isocyanates. In our case, the inclusion of K_2HPO_4 as an additive strongly influenced the efficiency of the reaction by diminishing the formation of undesired carbamate and isocyanurate side-products. However, only low yields of the desired amides were obtained when aryl isocyanates were employed. Moreover, the use of a stronger reductant such as Mn instead of Zn allowed for the coupling of benzylic C(*sp*³)—O electrophiles, even in the presence of C(*sp*²)-pivalates such as in (**1.3bn**). As frequently observed in related cross-couplings of C—O electrophiles, the methodology was restricted to the use of π-extended aryl pivalates. Fortunately, this limitation could be surpassed by the use of aryl tosylates and chlorides, although the addition of NaI was necessary to suppress the reductive homodimerization of the aryl (pseudo)halide partner. In general, the reaction displayed a good functional group tolerance with, amongst others, nitriles, heterocycles, esters, and thioethers being well accommodated. The mechanism of the reaction was proposed to follow a Ni(0)/Ni(II) pathway similar to the one proposed by Hsieh and Cheng for the coupling of *o*-iodobenzoates or aryl halides.

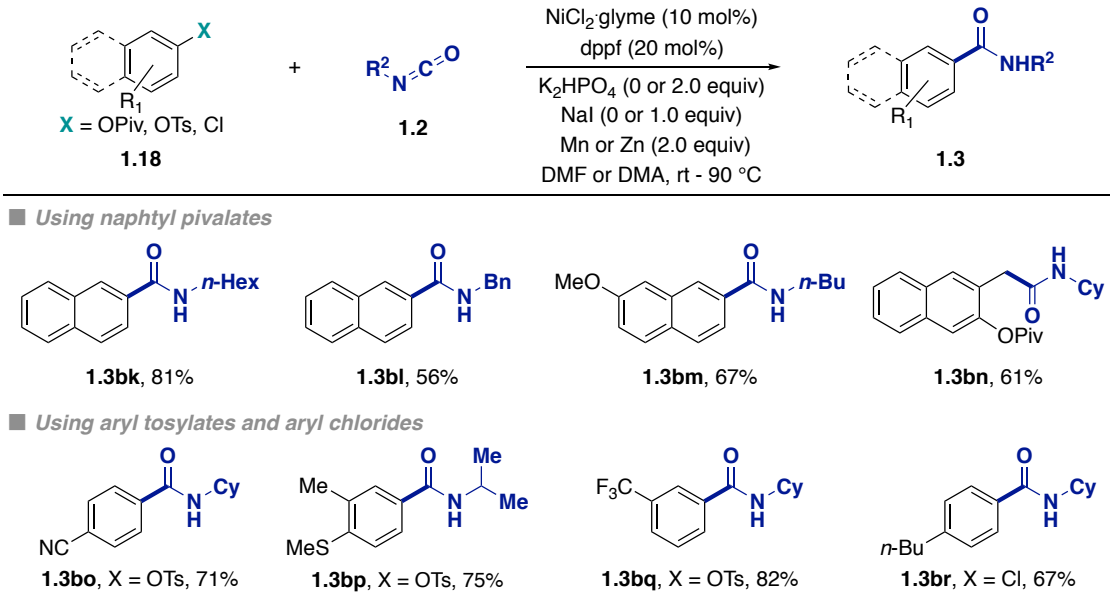

Scheme 1.21. Ni-catalyzed reductive coupling of C—O electrophiles with isocyanates

The two reductive coupling methods described above offer a straightforward alternative to the synthesis of benzamides via traditional cross-coupling methods, as they use bench-stable reagents, a simple reaction set-up, and circumvent the use of organometallic species that are sensitive and need to be synthesized in a separate step. The mild reaction conditions associated with these cross-electrophile couplings allow for a broad functional group tolerance, as illustrated in the scope of aryl (pseudo)halides and isocyanates.

1.4.4.4. Photoredox/Ni-Catalyzed Synthesis of Amides with Isocyanates

One of the most common disadvantages of cross-electrophile coupling protocols is the use of stoichiometric – or often superstoichiometric – amounts of metal powders as reducing agents. These sacrificial reductants react exothermically during the aqueous acid quench to generate significant amounts of waste and hydrogen gas. In late 2017, the group of Molander reported a redox-neutral method in which alkylsilicate reagents were coupled with isocyanates to generate aliphatic amides under a cooperative nickel/photoredox catalytic system (Scheme

1.22).[130] Under optimized reaction conditions, both primary and cyclic secondary alkyl silicates could be coupled with a large variety of aryl and primary, secondary and tertiary alkyl iso(thio)cyanates. Although only moderate yields of the desired products were usually obtained, the mild reaction conditions associated with metallophotoredox transformations allowed for an outstanding functional group tolerance in both coupling partners, including esters, ketones, nitriles, heterocycles and aryl chlorides, among others.

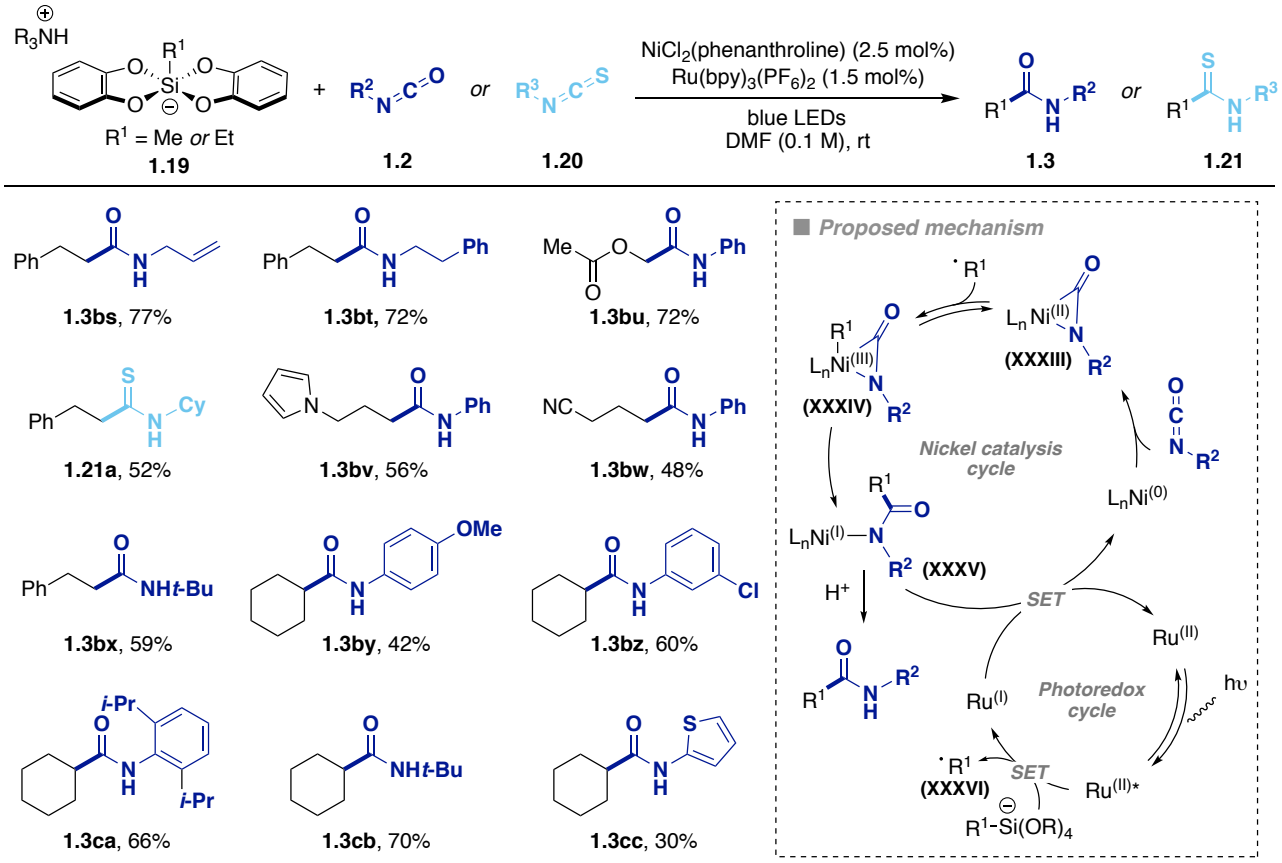

Scheme 1.22. Ni/photoredox-catalyzed amidation of alkylsilcates and isocyanates

Preliminary mechanistic studies were carried out in order to gain some insights into the reaction pathway: the addition of radical scavengers such as TEMPO inhibited the transformation, and no reaction was observed in the absence of photocatalyst, light, or nickel. The use of aprotic alkylsilicate counterions gave only trace amounts of the product, indicating that a proton source was required for catalyst turnover. Addition of 2,6-diisopropylhexyl isocyanate to Ni(0)(phenanthroline)$_2$ resulted in the formation of a new complex, which was identified by the authors as the corresponding oxidative addition adduct; however, this assumption was based only on the changes of the carbonyl stretching frequency in the IR spectrum and the absence of free isocyanate in the NMR spectrum, and could also be tentatively interpreted as a Ni(0) complex with a coordinated isocyanate. Subsequent addition of alkylsilicate and ruthenium photocatalyst to the formed complex yielded the product upon exposure to light.

Based on these findings, the authors proposed a reaction mechanism that starts with the oxidative addition of the isocyanate to the Ni(0) catalyst to form a Ni(II)—amido complex. Addition of the photoredox-generated alkyl radical to this intermediate affords a Ni(III) center. Subsequent reductive elimination and protonation by the ammonium salt generates the desired product and a Ni(I) species, which is reduced by the photocatalyst to close both catalytic cycles. The proposed mechanism was further supported by preliminary computational studies that showed a barrierless oxidative addition of the Ni(0) complex to the isocyanate, compared to a slightly uphill

addition of the alkyl radical to the Ni(0) center. Although the oxidative addition pathway is plausible, the authors cannot completely rule out the possibility of a mechanism that occurs via migratory insertion of the isocyanate to a Ni(I) complex. Moreover, the direct addition of the photoredox-formed radical to the isocyanate was ruled out as no reaction was observed in the absence of nickel; nevertheless, it is possible that the nickel salt is necessary to activate the isocyanate for radical attack.

It is worth mentioning that this dual Ni/photoredox method was developed taking inspiration from the results described in Chapter 2, and serves as an alternative to the use of a stoichiometric electron source. Despite the poor atom economy and the use of not so readily available radical precursors, the broad scope for isocyanates achieved by this method showcases the utility of isocyanates in amide synthesis via metal-catalyzed C—C bond formation.

1.5. General Objectives of this Doctoral Thesis

The ubiquity and importance of amides in peptides, proteins, pharmaceuticals, agrochemicals, and synthetic materials continually encourages the development of novel amidation methods. A particular interest is given to the design of new and alternative chemical transformations that complement and expand the scope of traditional amide-bond formation, which occurs via the condensation of carboxylic acid derivatives and amines. In this regard, the discovery of catalytic amidation methods that are atom-economical, general, and display high chemoselectivity is highly desirable.

One of the main interests of our research group is the development of novel metal-catalyzed transformations using CO_2 for the synthesis of carboxylic acids. Given that this functional group is very often converted to the corresponding amide via the above-mentioned condensation reactions, we postulated that related motifs could be directly accessed using isocyanates. Inspired by previous literature, our group recognized the potential of isocyanates to rapidly generate amides under the mild conditions offered by nickel-catalysis in early 2014, in the Ni-catalyzed reductive amidation of C—O electrophiles *en route* to benzamides.[129]

The general objective of the work presented in this dissertation was to develop new nickel-catalyzed amidation methods using isocyanates as amide synthons. With these transformations, we aimed to give access to a variety of amides under mild conditions, with a particular interest in the preparation of hindered amides that are difficult to access via traditional C—N bond-forming methods. We also anticipated that the markedly higher reactivity of isocyanates compared to CO_2 would offer the possibility of functionalizing less reactive positions. Furthermore, we sought to contribute to the understanding of the mechanisms governing the developed Ni-catalyzed transformations developed herein, with the aim of building on our knowledge of Ni-catalyzed reductive cross-couplings with heteroallenes.

1.6. Bibliography

1. *Metal-Catalyzed Cross-Coupling Reactions*. (eds. de Meijere, A. & Diederich, F.) **1,** (Wiley-VCH Verlag GmbH & Co. KGaA, 2004).
2. The Nobel Prize in Chemistry 2010 - Richard F. Heck, Ei-ichi Negishi and Akira Suzuki. Available at: https://www.nobelprize.org/nobel_prizes/chemistry/laureates/2010/press.pdf. (Accessed: 10th April 2018)
3. Knappke, C. E. I. *et al.* Reductive Cross-Coupling Reactions between Two Electrophiles. *Chem. Eur. J.* **20,** 6828–6842 (2014).
4. Weix, D. J. Methods and Mechanisms for Cross-Electrophile Coupling of Csp^2 Halides with Alkyl Electrophiles. *Acc. Chem. Res.* **48,** 1767–1775 (2015).
5. Wurtz, A. Ueber eine neue Klasse organischer Radicale. *Ann. Chem.* **96,** 364–375 (1855).
6. Tollens, B. & Fittig, R. Ueber die Synthese der Kohlenwasserstoffe der Benzolreihe. *Justus Liebigs Ann. Chem.* **131,** 303–323 (1864).
7. Ullmann, F. & Bielecki, J. Ueber Synthesen in der Biphenylreihe. *Berichte der Dtsch. Chem. Gesellschaft* **34,** 2174–2185 (1901).
8. Okude, Y., Hirano, S., Hiyama, T. & Nozaki, H. Grignard-Type Carbonyl Addition of Allyl Halides by Means of Chromous Salt. A Chemospecific Synthesis of Homoallyl Alcohols. *J. Am. Chem. Soc.* **99,** 3179–3181 (1977).
9. Jin, H., Uenishi, J. I., Christ, W. J. & Kishi, Y. Catalytic Effect of Nickel(II) Chloride and Palladium(II) Acetate on Chromium(II)-Mediated Coupling Reaction of Iodo Olefins with Aldehydes. *J. Am. Chem. Soc.* **108,** 5644–5646 (1986).
10. Fürstner, A. & Shi, N. A Multicomponent Redox System Accounts for the First Nozaki - Hiyama - Kishi Reactions Catalytic in Chromium. *J. Am. Chem. Soc.* **118,** 2533–2534 (1996).
11. Schiavon, G., Bontempelli, G. & Corain, B. Coupling of Organic Halides Electrocatalyzed by the Ni(II)/Ni(I)/Ni(0)-PPh_3 System. A Mechanistic Study based on an Electroanalytical Approach. *J. Chem. Soc. Dalt. Trans.* **5,** 1074–1081 (1981).
12. Amatore, C. & Jutand, A. Rates and Mechanism of Biphenyl Synthesis Catalyzed by Electrogenerated Coordinatively Unsaturated Nickel Complexes. *Organometallics* **7,** 2203–2214 (1988).
13. Amatore, C. & Jutand, A. Activation of Carbon Dioxide by Electron Transfer and Transition Metals. Mechanism of Nickel-Catalyzed Electrocarboxylation of Aromatic Halides. *J. Am. Chem. Soc.* **113,** 2819–2825 (1991).
14. Durandetti, M., Nédélec, J.-Y. & Périchon, J. Nickel-Catalyzed Direct Electrochemical Cross-Coupling between Aryl Halides and Activated Alkyl Halides. *J. Org. Chem.* **61,** 1748–1755 (1996).
15. Yan, M., Kawamata, Y. & Baran, P. S. Synthetic Organic Electrochemistry: Calling All Engineers. *Angew. Chem. Int. Ed.* **57,** 4149–4155 (2018).
16. Wang, X., Dai, Y. & Gong, H. Nickel-Catalyzed Reductive Couplings. *Top. Curr. Chem.* **374,** 43 (2016).
17. Xu, H., Zhao, C., Qian, Q., Deng, W. & Gong, H. Nickel-catalyzed cross-coupling of unactivated alkyl halides using bis(pinacolato)diboron as reductant. *Chem. Sci.* **4,** 4022–4029 (2013).
18. Anka-Lufford, L. L., Huihui, K. M. M., Gower, N. J., Ackerman, L. K. G. & Weix, D. J. Nickel-Catalyzed Cross-Electrophile Coupling with Organic Reductants in Non-Amide Solvents. *Chem. Eur. J.* **22,** 11564–11567 (2016).
19. Everson, D. A. & Weix, D. J. Cross-Electrophile Coupling: Principles of Reactivity and Selectivity. *J. Org. Chem.* **79,** 4793–4798 (2014).
20. Tortajada, A., Juliá-Hernández, F., Börjesson, M., Moragas, T. & Martin, R. Transition Metal-Catalyzed Carboxylation Reactions with carbon Dioxide. *Angew. Chem. Int. Ed.* (2018). doi:10.1002/anie.201803186
21. Tasker, S. Z., Standley, E. A. & Jamison, T. F. Recent Advances in Homogeneous Nickel Catalysis. *Nature* **509,** 299–309 (2014).
22. Rosen, B. M. *et al.* Nickel-catalyzed cross-couplings involving carbon-oxygen bonds. *Chemical Reviews* **111,** 1346–1416 (2011).
23. Dander, J. E. & Garg, N. K. Breaking Amides using Nickel Catalysis. *ACS Catal.* **7,** 1413–1423 (2017).
24. Cherney, A. H., Kadunce, N. T. & Reisman, S. E. Enantioselective and Enantiospecific Transition-Metal-Catalyzed Cross-Coupling Reactions of Organometallic Reagents to Construct C-C Bonds. *Chem. Rev.* **115,** 9587–9652 (2015).
25. Twilton, J. *et al.* The merger of transition metal and photocatalysis. *Nat. Rev. Chem.* **1,** 52 (2017).
26. *Modern Organonickel Chemistry*. (ed. Tamaru, Y.) (Wiley-VCH Verlag GmbH & Co. KGaA, 2005).
27. Ananikov, V. P. Nickel: The 'Spirited Horse' of Transition Metal Catalysis. *ACS Catal.* **5,** 1964–1971 (2015).
28. *CRC Handbook of Chemistry and Physics*. (ed. Lide, D. R.) (CRC Press, 2003).
29. Koga, N., Obara, S., Kitaura, K. & Morokuma, K. Role of Agostic Interaction in β-Elimination of Pd and Ni Complexes. An ab Initio MO Study. *J. Am. Chem. Soc.* **107,** 7109–7116 (1985).
30. *The Amide Linkage: Structural Significance in Chemistry, Biochemistry, and Materials Science*. (eds. Greenberg, A., Breneman, C. M. & Liebman, J. F.) (Wiley-Interscience, 2000).
31. Ghose, A. K., Viswanadhan, V. N. & Wendoloski, J. J. A Knowledge-Based Approach in Designing Combinatorial or Medicinal Chemistry Libraries for Drug Discovery. 1. A Qualitative and Quantitative Characterization of Known Drug Databases. *J. Comb. Chem.* **1,** 55–68 (1999).
32. Carey, J. S., Laffan, D., Thomson, C. & Williams, M. T. Analysis of the reactions used for the preparation of drug candidate molecules. *Org. Biomol. Chem.* **4,** 2337–2347 (2006).
33. Roughley, S. D. & Jordan, A. M. The Medicinal Chemist's Toolbox: An Analysis of Reactions Used in the Pursuit of Drug Candidates. *J. Med. Chem.* **54,** 3451–3479 (2011).
34. Brown, D. G. & Boström, J. Analysis of Past and Present Synthetic Methodologies on Medicinal Chemistry: Where Have All the New Reactions Gone? *J. Med. Chem.* **59,** 4443–4458 (2016).
35. Montalbetti, C. A. G. N. & Falque, V. Amide bond formation and peptide coupling. *Tetrahedron* **61,** 10827–10852 (2005).

36. Albericio, F. Developments in peptide and amide synthesis. *Curr. Opin. Chem. Biol.* **8,** 211–221 (2004).
37. Dunetz, J. R., Magano, J. & Weisenburger, G. A. Large-Scale Applications of Amide Coupling Reagents for the Synthesis of Pharmaceuticals. *Org. Process Res. Dev.* **20,** 140–177 (2016).
38. Valeur, E. & Bradley, M. Amide bond formation: beyond the myth of coupling reagents. *Chem. Soc. Rev.* **38,** 606–631 (2009).
39. Pattabiraman, V. R. & Bode, J. W. Rethinking amide bond synthesis. *Nature* **480,** 471–479 (2011).
40. Allen, C. L. & Williams, J. M. J. Metal-catalysed approaches to amide bond formation. *Chem. Soc. Rev.* **40,** 3405–3415 (2011).
41. Lanigan, R. M. & Sheppard, T. D. Recent Developments in Amide Synthesis: Direct Amidation of Carboxylic Acids and Transamidation Reactions. *Eur. J. Org. Chem.* **2013,** 7453–7465 (2013).
42. De Figueiredo, R. M., Suppo, J. S. & Campagne, J. M. Nonclassical Routes for Amide Bond Formation. *Chem. Rev.* **116,** 12029–12122 (2016).
43. Ojeda-Porras, A. & Gamba-Sánchez, D. Recent Developments in Amide Synthesis Using Nonactivated Starting Materials. *J. Org. Chem.* **81,** 11548–11555 (2016).
44. Constable, D. J. C. *et al.* Key green chemistry research areas—a perspective from pharmaceutical manufacturers. *Green Chem.* **9,** 411–420 (2007).
45. Adachi, S., Kumagai, N. & Shibasaki, M. Conquering amide planarity: Structural distortion and its hidden reactivity. *Tetrahedron Lett.* **59,** 1147–1158 (2018).
46. Ulrich, H. *Chemistry and technology of isocyanates*. (J. Wiley & Sons, 1996).
47. Ulrich, H. *Cumulenes in Click Reactions*. (Wiley, 2009).
48. Wurtz, A. Recherches sur les éthers cyaniques et leurs dérivés. *Comp. Rend.* **27,** 241–243 (1848).
49. Hentschel, W. Zur Darstellung von Phenylcyanat. *Berichte der Dtsch. Chem. Gesellschaft* **17,** 1284–1289 (1884).
50. Ulrich, H. *Cycloaddition Reactions of Heterocumulenes.* (Elsevier Science, 1967).
51. Six, C. & Richter, F. Isocyanates, Organic. in *Ullmann's Encyclopedia of Industrial Chemistry* 63–82 (Wiley-VCH Verlag GmbH & Co. KGaA, 2003).
52. Kurita, K., Matsumura, T. & Iwakura, Y. Trichloromethyl Chloroformate. Reaction with Amines, Amino Acids, and Amino Alcohols. *J. Org. Chem.* **41,** 2070–2071 (1976).
53. Sigurdsson, S. T., Seeger, B., Kutzke, U. & Eckstein, F. A Mild and Simple Method for the Preparation of Isocyanates from Aliphatic Amines Using Trichloromethyl Chloroformate. Synthesis of an Isocyanate Containing an Activated Disulfide. *J. Org. Chem.* **61,** 3883–3884 (1996).
54. Knolker, H. J., Braxmeier, T. & Schlechtingen, G. A Novel Method for the Synthesis of Isocyanates Under Mild Conditions. *Angew. Chem. Int. Ed.* **34,** 2497–2500 (1995).
55. Peerlings, H. W. I. & Meijer, E. W. A mild and convenient method for the preparation of multi-isocyanates starting from primary amines. *Tetrahedron Lett.* **40,** 1021–1024 (1999).
56. Ozaki, S. Recent Advances in Isocyanate Chemistry. *Chem. Rev.* **72,** 457–496 (1972).
57. Mironov, V. F. Organosilicon Synthesis of Isocyanates. *J. Organomet. Chem.* **271,** 207–224 (1984).
58. Gilman, J. W. & Otonari, Y. A. Synthesis of Isocyanates from Carboxylic Acids using Diphenylphosphoryl Azide and 1, 8-Bis(Dimethylamino)Naphthalene. *Synth. Commun.* **23,** 335–341 (1993).
59. Braunstein, P. & Nobel, D. Transition-Metal-Mediated Reactions of Organic Isocyanates. *Chem. Rev.* **89,** 1927–1945 (1989).
60. Villa, J. F. & Powell, H. B. Preparation, Characterization and Lewis Basicity of some Copper(II) and -Nickel(II) Adducts with Organic Isocyanates and Isothiocyanates. *Inorg. Chim. Acta* **32,** 199–204 (1979).
61. Villa, J. F. & Powell, H. B. The Reaction of Some Inorgainc Lewis Bases and Acids with Organic Isocyanates. *Synth. React. Inorg. Met. Chem.* **6,** 59–63 (1976).
62. Paul, F., Moulin, S., Piechaczyk, O., Le Floch, P. & Osborn, J. A. Palladium(0)-Catalyzed Trimerization of Arylisocyanates into 1,3,5-Triarylisocyanurates in the Presence of Diimines: A Nonintuitive Mechanism. *J. Am. Chem. Soc.* **129,** 7294–7304 (2007).
63. Foley, S. R., Yap, G. P. A. & Richeson, D. S. Formation of Novel Tetrasulfido tTin Complexes and Their Ability to Catalyze the Cyclotrimerization of Aryl Isocyanates. *Organometallics* **18,** 4700–4705 (1999).
64. Munegumi, T., Azumaya, I., Kato, T., Masu, H. & Saito, S. [3+2] Cross-Coupling Reactions of Aziridines with Isocyanates Catalyzed by Nickel(II) Iodide. *Org. Lett.* **8,** 379–382 (2006).
65. Baronsky, T. *et al.* Bimetallic Aluminum(salen) Catalyzed Synthesis of Oxazolidinones from Epoxides and Isocyanates. *ACS Catal.* **3,** 790–797 (2013).
66. Wang, P., Qin, J., Yuan, D., Wang, Y. & Yao, Y. Synthesis of Oxazolidinones from Epoxides and Isocyanates Catalyzed by Rare-Earth-Metal Complexes. *ChemCatChem* **7,** 1145–1151 (2015).
67. Perreault, S. & Rovis, T. Multi-Component Cycloaddition Approaches in the Catalytic Asymmetric Synthesis of Alkaloid Targets. *Chem. Soc. Rev.* **38,** 3149–3159 (2009).
68. Chopade, P. R. & Louie, J. [2+2+2] Cycloaddition Reactions Catalyzed by Transition Metal Complexes. *Adv. Synth. Catal.* **348,** 2307–2327 (2006).
69. Thakur, A. & Louie, J. Advances in Nickel-Catalyzed Cycloaddition Reactions To Construct Carbocycles and Heterocycles. *Acc. Chem. Res.* **48,** 2354–2365 (2015).
70. Hummel, J. R., Boerth, J. A. & Ellman, J. A. Transition-Metal-Catalyzed C-H Bond Addition to Carbonyls, Imines, and Related Polarized π Bonds. *Chem. Rev.* **117,** 9163–9227 (2017).
71. Louie, J. Transition Metal Catalyzed Reactions of Carbon Dioxide and Other Heterocumulenes. *Curr. Org. Chem.* **9,** 605–623 (2005).
72. Allen, A. D. & Tidwell, T. T. Ketenes and Other Cumulenes as Reactive Intermediates. *Chem. Rev.* **113,** 7287–7342

(2013).
73. Blaise, E. E. Nouvelles réactions des dérives organométalliques. *Comp. Rend.* **132,** 38–41 (1901).
74. Gilman, H. & Kinney, C. R. The Mechanism of the Reaction of Isocyanates and Isothiocyanates with the Grignard Reagent. *J. Am. Chem. Soc.* **46,** 493–497 (1924).
75. Gilman, H. & Furry, M. The Identification of Organomagnesium Halides by Crytalline Derivatives Prepared from α-Naphthyl Isocyanate. *J. Am. Chem. Soc.* **50,** 1214–1216 (1928).
76. Worrall, D. E. The Action of Butylmagnesium Bromide on the Aromatic Isothiocyanates. *J. Am. Chem. Soc.* **47,** 2974–2976 (1925).
77. Parker, K. A. & Gibbons, E. G. A direct synthesis of primary amides from grignard reagents. *Tetrahedron Lett.* **16,** 981–984 (1975).
78. Einhorn, J. & Luche, J. L. Sonochemical Barbier Reaction with Isocyanates and the Synthetic use of the Organometallic Intermediate. *Tetrahedron Lett.* **27,** 501–504 (1986).
79. Stefanuti, I., Smith, S. A. & Taylor, R. J. . Unsaturated enamides via organometallic addition to isocyanates: the synthesis of Lansamide-I, Lansiumamides A–C and SB-204900. *Tetrahedron Lett.* **41,** 3735–3738 (2000).
80. Antczak, M. I. & Ready, J. M. Two-, Three- and Four-Component Coupling to form Isoquinolones Based on Directed Metalation. *Chem. Sci.* **3,** 1450–1454 (2012).
81. Schäfer, G., Matthey, C. & Bode, J. W. Facile Synthesis of Sterically Hindered and Electron-Deficient Secondary Amides from Isocyanates. *Angew. Chem. Int. Ed.* **51,** 9173–9175 (2012).
82. Gilman, H. & Breuer, F. The Mechanism of Reaction of Phenyl-Sodium and Phenyl-Lithium with Phenyl Isothiocyanate. *J. Am. Chem. Soc.* **55,** 1262–1264 (1933).
83. Lebel, N. A., Cherluck, R. M. & Curtis, E. A. An Improved Synthesis of Amides from the Curtius Reaction. The Reaction of Isocyanates and Organolithium Compounds. *Synthesis* **11,** 678–679 (1973).
84. Coldham, I., Dufour, S., Haxell, T. F. N. & Vennall, G. P. Dynamic resolution of N-alkyl-2-lithiopyrrolidines with the chiral ligand (-)-sparteine. *Tetrahedron* **61,** 3205–3220 (2005).
85. Seel, S. *et al.* Preparation of Stereodefined Secondary Alkyllithium Compounds. *Chem. Eur. J.* **19,** 4614–4622 (2013).
86. Pace, V., Monticelli, S., de la Vega-Hernández, K. & Castoldi, L. Isocyanates and Isothiocyanates as Versatile Platforms for Accessing (Thio)Amide-Type Compounds. *Org. Biomol. Chem.* **14,** 7848–7854 (2016).
87. Schade, M. A., Manolikakes, G. & Knochel, P. Preparation of Primary Amides from Functionalized Organozinc Halides. *Org. Lett.* **12,** 3648–3650 (2010).
88. Haraguchi, R. & Matsubara, S. Preparation of the Zinc Enolate Equivalent of Amides by Zinciomethylation of Isocyanates: Catalytic Asymmetric Reformatsky-Type Reaction. *Synthesis* **46,** 2272–2282 (2014).
89. Yang, H. *et al.* Reaction of Organozinc Halides with Aryl Isocyanates. *Tetrahedron* **69,** 2588–2593 (2013).
90. Zhang, Y., Jiang, J. & Chen, Y. Cp_2TiCl_2-Catalyzed Reaction of Grignard Reagents with Isocyanates, Formation of Carboxamide with Rearranged Carbonskeleton. *Tetrahedron Lett.* **28,** 3815–3816 (1987).
91. Zhang, Y., Jiang, J. & Zhang, Z. Cp_2TiCl_2-Catalyzed Reaction of Grignard Reagents with Isocyanates, Formation of Reduction-Coupling Product of Isocyanates. *Tetrahedron Lett.* **29,** 651–652 (1988).
92. Koike, T., Takahashi, M., Arai, N. & Mori, A. Addition of Organostannanes to Isocyanate Catalyzed by a Rhodium Complex. *Chem. Lett.* **33,** 1364–1365 (2004).
93. *Boronic Acids: Preparation and Applications in Organic Synthesis and Medicine*. (ed. Hall, D. G.) (Wiley-VCH Verlag GmbH & Co. KGaA, 2006).
94. Miura, T., Takahashi, Y. & Murakami, M. Rhodium-Catalysed Addition Reaction of Aryl- and Alkenylboronic Acids to Isocyanates. *Chem. Commun.* **0,** 3577–3579 (2007).
95. Kianmehr, E., Rajabi, A. & Ghanbari, M. Palladium-Catalyzed Addition of Arylboronic Acids to Isocyanates. *Tetrahedron Lett.* **50,** 1687–1688 (2009).
96. Lew, T. T. S., Lim, D. S. W. & Zhang, Y. Copper(I)-Catalyzed Amidation Reaction of Organoboronic Esters and Isocyanates. *Green Chem.* **17,** 5140–5143 (2015).
97. Nakamura, H., Aoyagi, K., Shim, J.-G. & Yamamoto, Y. Catalytic Amphiphilic Allylation via Bis-π-allylpalladium Complexes and its Application to the Synthesis of Medium-Sized Carbocycles. *J. Am. Chem. Soc.* **123,** 372–377 (2001).
98. Solin, N., Narayan, S. & Szabó, K. J. Palladium-Catalyzed Tandem Bis-allylation of Isocyanates. *Org. Lett.* **3,** 909–912 (2001).
99. Hoberg, H. & Oster, B. W. Modellkomplex des nickels für die C-C verknüpfung von alkinen mit isocyanaten. *J. Organomet. Chem.* **234,** C35–C38 (1982).
100. Hernandez, E. & Hoberg, H. CC-Verknüpfung von Styrol mit Isocyanaten an Nickel(0) eine Katalytische Synthese von Zimtsäurenamiden. *J. Organomet. Chem.* **315,** 245–253 (1986).
101. Hernandez, E. & Hoberg, H. Stöichiometrische und Katalytische CC-Verknüpfungen Zwischen 1,3-Butadien und Phenylisocyanat an Nickel(0)-Komplexen. *J. Organomet. Chem.* **327,** 429–436 (1987).
102. Hoberg, H. & Sümmermann, K. Oxidative kupplung von 1,2-dienen mit isocyanaten am lig-nickel(0)-system. *J. Organomet. Chem.* **275,** 239–247 (1984).
103. Hoberg, H. & Sümmermann, K. Nickel(0)-Induzierte Kupplung von Benzaldehyd mit Isocyanaten zu Nickela-heterocyclen. *J. Organomet. Chem.* **264,** 379–385 (1984).
104. Hoberg, H. & Sümmermann, K. Diazanickelacyclopentanone aus Nickel(0), Iminen und Isocyanaten. *J. Organomet. Chem.* **253,** 383–389 (1983).
105. Ohno, K. & Tsuji, J. New Cyclization Reaction of Conjugated Dienes with Isocyanate Catalysed by Palladium Complexes. *J. Chem. Soc. D Chem. Commun.* **0,** 247b–248 (1971).
106. Muraoka, T., Matsuda, I. & Itoh, K. Rhodium-Catalyzed Formal Hydrocarbamoylation toward an α,β-Unsaturated Carbonyl Compound using Aryl Isocyanate and Hydrosilane. *Organometallics* **20,** 4676–4682 (2001).

107. Hoberg, H., Sümmermann, K. & Milchereit, A. C-C-Verknüpfung von Alkenen mit Isocyanaten am Nickel(0). *J. Organomet. Chem.* **288,** 237–248 (1985).
108. Hoberg, H., Sümmermann, K. & Milchereit, A. CC Bond Formation of Alkenes with Isocyanates on Ni^0 Complexes—a New Synthesis of Acrylamides. *Angew. Chem. Int. Ed.* **24,** 325–326 (1985).
109. Hoberg, H. & Hernandez, E. Intermolekulare CC-Verknüpfung von Azanickelacyclopentanonen, α,ω-Disäureamide aus Alkenen und Phenylisocyanat. *J. Organomet. Chem.* **311,** 307–312 (1986).
110. Hoberg, H. & Hernandez, E. Nickel(0)-catalysed Synthesis of Unsaturated Carboxylic Acid Anilides from Ethene and Phenyl Isocyanate. *J. Chem. Soc. Chem. Commun.* **0,** 544–545 (1986).
111. Hernandez, E. & Hoberg, H. Nickel(0)-Katalysierte Bildung von Carbocyclischen Amiden aus α,ω-Dienen und Phenylisocyanat. *J. Organomet. Chem.* **328,** 403–412 (1987).
112. Hoberg, H., Sümmermann, K., Hernandez, E., Ruppin, C. & Guhl, D. Nickel(0)-katalysierte Synthese von Crotonsäureanilid aus Propen und Phenylisocyanat. *J. Organomet. Chem.* **344,** C35–C38 (1988).
113. Hoberg, H. Nickela-Heterocyclen als Intermediate der präparativen Isocyanatchemie. *J. Organomet. Chem.* **358,** 507–517 (1988).
114. Hoberg, H. & Guhl, D. Nickel(O)-Catalyzed Preparation of Isomeric Carboxamides – Ligand-Controlled β-H or β'-H Elimination. *Angew. Chem. Int. Ed.* **28,** 1035–1036 (1989).
115. Schleicher, K. D. & Jamison, T. F. Nickel-Catalyzed Synthesis of Acrylamides from α-Olefins and Isocyanates. *Org. Lett.* **9,** 875–878 (2007).
116. Duong, H. A., Cross, M. J. & Louie, J. N-Heterocyclic Carbenes as Highly Efficient Catalysts for the Cyclotrimerization of Isocyanates. *Org. Lett.* **6,** 4679–4681 (2004).
117. Miura, T., Takahashi, Y. & Murakami, M. Stereoselective Synthesis of 3-Alkylideneoxindoles by Rhodium-Catalyzed Cyclization Reaction of 2-Alkynylaryl Isocyanates with Aryl and Alkenylboronic Acids. *Org. Lett.* **9,** 5075–5077 (2007).
118. Miura, T., Toyoshima, T., Takahashi, Y. & Murakami, M. Stereoselective Synthesis of 3-Alkylideneoxindoles by Palladium-Catalyzed Cyclization Reaction of 2-(Alkynyl)aryl Isocyanates with Organoboron Reagents. *Org. Lett.* **10,** 4887–4889 (2008).
119. Miura, T., Takahashi, Y. & Murakami, M. Rhodium-Catalyzed Borylative Cyclization of 2-Alkynylaryl Isocyanates with Bis(pinacolato)diboron. *Org. Lett.* **10,** 1743–1745 (2008).
120. Miura, T., Toyoshima, T., Takahashi, Y. & Murakami, M. Stereoselective Oxindole Synthesis by Reaction of 2-(Alkynyl)aryl Isocyanates with Amides. *Org. Lett.* **11,** 2141–2143 (2009).
121. Miura, T., Toyoshima, T., Ito, Y. & Murakami, M. Synthesis of Stereodefined 3-Alkylideneoxindoles by Palladium-catalyzed Reactions of 2-(Alkynyl)aryl Isocyanates with Thiols and Alcohols. *Chem. Lett.* **38,** 1174–1175 (2009).
122. Toyoshima, T., Mikano, Y., Miura, T. & Murakami, M. Synthesis of 3,3-Disubstituted Oxindoles by Palladium-Catalyzed Tandem Reaction of 2-(Alkynyl)aryl Isocyanates with Benzylic Alcohols. *Org. Lett.* **12,** 4584–4587 (2010).
123. Miura, T., Toyoshima, T., Kozawa, O. & Murakami, M. Stereoselective Synthesis of 3-(1-Cyanoalkylidene)oxindoles by Palladium-catalyzed Cyclization Reaction of 2-(Alkynyl)aryl Isocyanates with Copper(I) Cyanide. *Chem. Lett.* **39,** 1132–1133 (2010).
124. Miura, T., Mikano, Y. & Murakami, M. Nickel-Catalyzed Synthesis of 1,3,5-Trisubstituted Hydantoins from Acrylates and Isocyanates. *Org. Lett.* **13,** 3560–3563 (2011).
125. Hoberg, H. & Guhl, D. Nickel(0) induzierte und katalysierte CC-Verknüpfungen von Phenylisocyanat mit funktionalisierten Alkenen. *J. Organomet. Chem.* **375,** 245–257 (1989).
126. Mizukami, A., Ise, Y., Kimachi, T. & Inamoto, K. Rhodium-Catalyzed Cyclization of 2-Ethynylanilines in the Presence of Isocyanates: Approach toward Indole-3-carboxamides. *Org. Lett.* **18,** 748–751 (2016).
127. Rajesh, M., Puri, S., Kant, R. & Reddy, M. S. Synthesis of Substituted Furan/Pyrrole-3-carboxamides through a Tandem Nucleopalladation and Isocyanate Insertion. *Org. Lett.* **18,** 4332–4335 (2016).
128. Hsieh, J.-C. & Cheng, C.-H. Nickel-Catalyzed Coupling of Isocyanates with 1,3-Iodoesters and Halobenzenes: a Novel Method for the Synthesis of Imide and Amide Derivatives. *Chem. Commun.* **0,** 4554–4556 (2005).
129. Correa, A. & Martin, R. Ni-Catalyzed Direct Reductive Amidation via C-O Bond Cleavage. *J. Am. Chem. Soc.* **136,** 7253–7256 (2014).
130. Zheng, S., Primer, D. N. & Molander, G. A. Nickel/Photoredox-Catalyzed Amidation via Alkylsilicates and Isocyanates. *ACS Catal.* **7,** 7957–7961 (2017).

UNIVERSITAT ROVIRA I VIRGILI
AMIDE FORMATION VIA NI-CATALYZED REDUCTIVE COUPLING REACTIONS WITH ISOCYANATES
Eloísa Sofía Serrano Robledo

Chapter 2.

Ni-Catalyzed Reductive Amidation of Primary Alkyl Halides with Isocyanates

2.1. Introduction

2.1.1. Metal-Catalyzed Cross-Couplings with Unactivated Alkyl Halides

Unactivated alkyl halides are haloalkanes that, in the β-position, lack activating groups, such as phenyl, vinyl or carbonyl groups, which contain π-orbitals and give oxidative addition intermediates where the metal center is stabilized through π-back donation. Several difficulties are associated with the use of unactivated alkyl halides as electrophiles in cross-coupling reactions.[1–3] Namely, oxidative addition is slower than for aryl or alkenyl halides due to the more electron-rich character of C(sp^3)—X bonds and the lack of a proximal low-lying empty or high-lying occupied orbital that readily interact with the orbitals of the metal. The absence of stabilizing groups in the β-position results in the formation of less stable σ-alkyl-metal intermediates after oxidative addition, in which the presence of β-hydrogens can easily result in β-hydride elimination from coordinatively unsaturated alkyl—metal complexes to afford alkene side-products.[4] Other problems include protodemetalation and the homolytic cleave of the M—C bond that generates alkyl radical species that can dimerize or abstract hydrogen atoms from, for example, the solvent. Additionally, reductive elimination from C(sp^3)—M—C(sp^2) or —C(sp^3) intermediates is slower than C(sp^2)—M—C(sp^2) species, increasing the probability of competitive side-reactions (Scheme 2.1).

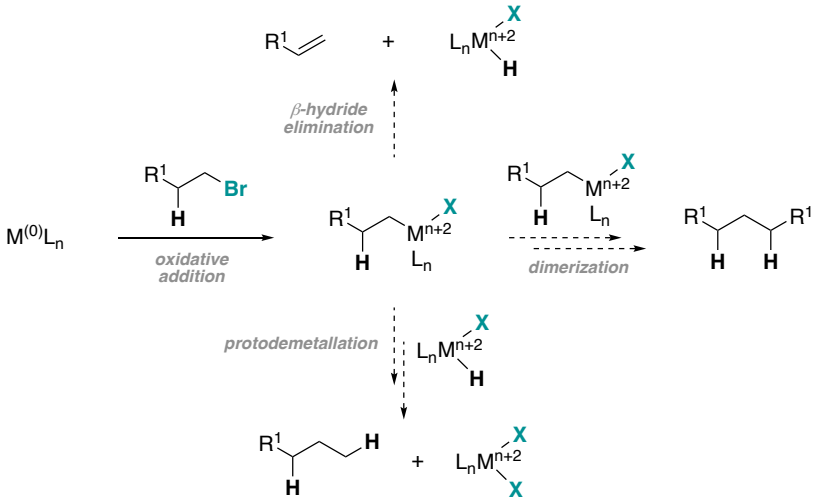

Scheme 2.1. Challenges associated with the use of unactivated alkyl halides in cross-coupling reactions

Since the pioneering work in the 1990's by Suzuki[5] and Knochel[6,7] on the cross-coupling of unactivated alkyl (pseudo)halides with boron and zinc reagents, the last decades have seen remarkable advances in the transition metal-catalyzed cross-coupling of unactivated alkyl electrophiles, and of alkyl-organometallic species. These advances have been achieved using Pd, Fe, Co, Cu, and in particular Ni catalysts.[8–10] The design of new catalytic systems that promote oxidative addition, prevent β-hydride elimination, and accelerate reductive elimination has been fundamental for the development of efficient methods that give high yields of the coupling products and display a broad functional-group tolerance. In many cases, the ligand has played a major role and systems using olefins, bidentate and tridentate amines, alcohols, bulky electron-rich phosphines, and *N*-heterocyclic carbenes (NHC) ligands have proven to be particularly efficient.[3,11] Nowadays the metal-catalyzed cross-coupling of unactivated primary, secondary and tertiary alkyl halides with a large series of nucleophiles is well established. Several examples of Kumada, Suzuki-Miyaura, Negishi, Hiyama, Stille, carbonylation protocols and enantioselective methods, among others have been reported.[12] Moreover, their use in reductive cross-electrophile couplings has seen great advances in the last decade[13–15] and even more recently, metallaphotoredox transformations that use alkyl halides as electrophiles have been reported.[16–18]

The oxidative addition of C(sp^3)-electrophiles is generally proposed to follow a nucleophilic substitution pathway (S_N2) with palladium complexes, in which inversion of the configuration is observed.[19,20] A different activation upon light irradiation has been proposed for alkyl iodides in which radical intermediates are involved.[21] Different mechanistic studies performed on Ni-catalyzed transformations have shown that oxidative addition occurs via single electron transfer (SET) to form alkyl radical species.[22–25]

2.1.1.1. Reductive Cross-Electrophile Couplings with Unactivated Alkyl Halides

Metal-catalyzed reductive cross-electrophile couplings avoid the use of pre-formed organometallic reagents by joining two electrophiles in the presence of a reducing agent. These protocols have several advantages over traditional cross-coupling reactions such as their mild conditions, easy set-up and broad functional group tolerance (vide Chapter 1). The first reductive coupling using alkyl electrophiles was reported as early as 1855 by Wurtz, for the dimerization of alkyl halides using stoichiometric amounts of sodium (Wurtz reaction).[26] This was followed by the cross-coupling of alkyl halides with aryl halides using a similar protocol;[27] however, the harsh conditions and the low efficiency of these methods limited their utilization with functionalized substrates. While the cross-coupling of aryl and activated alkyl electrophiles was further developed using electrochemical processes or metal-catalyzed methods in combination with stoichiometric reducing agents, the use of unactivated alkyl halides as electrophiles was not achieved until several years later. The first reports for the reductive cross-coupling of unactivated alkyl halides and aryl halides were made by Weix and co-workers using Ni-catalysts[28] and by Amatore, Gosmini and co-workers using Co-catalysts[29] employing Mn as source of the electrons, in both cases. Subsequently, the formation of C(sp^3)—C(sp^3) bonds in the homodimerization of unactivated alkyl halides was reported by Weix[30] and by Leigh[31] following two related procedures. The cross-coupling of two different unactivated alkyl halides was achieved by Gong and co-workers; high yields of the cross-couple products were obtained by employing a 3-fold excess of one of the electrophiles,[32] or by using $B_2(pin)_2$ as the reducing agent.[33]

Inspired by these seminal reports, the field of reductive cross-electrophile couplings has significantly expanded throughout the last decade, and nowadays several methods for the coupling unactivated alkyl halides have been reported.[13,14,34] Catalytic systems based on Ni-, Pd-, and to a lesser extent on Co-, and Fe-complexes have been used in combination with Mn, Zn, $B_2(pin)_2$, and the organic reductant TDAE (Scheme 2.2).[35] Although using these systems, the formation of C(sp^3)—C(sp^2) and C(sp^3)—C(sp^3)-bonds can now be achieved with high selectivity using primary, secondary and even tertiary alkyl halides, further improvements are fundamental to secure the future applicability of these strategies.

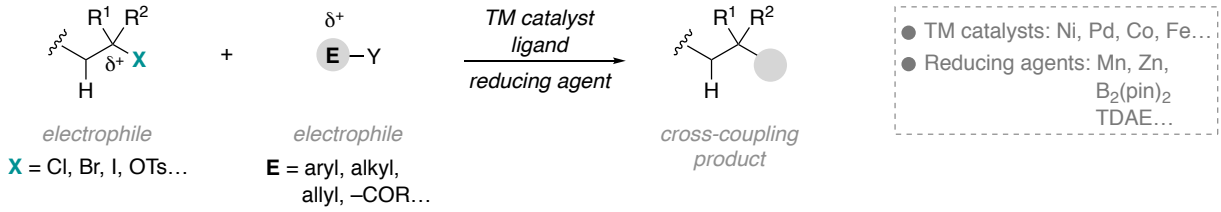

Scheme 2.2. Reductive cross-electrophile couplings with unactivated alkyl halides

2.1.2. Ni-Catalyzed Carboxylation of Unactivated Alkyl Halides

2.1.2.1. Ni-Catalyzed Carboxylation of Unactivated Alkyl Halides and Sulfonates with CO_2

Its abundance, low cost and non-toxicity make carbon dioxide an ideal C1 synthon for the synthesis of value-added organic molecules. The use of transition metals that coordinate and activate CO_2 is a useful means to surmount its thermodynamic and kinetic stability. Our research group has been interested in the development of

efficient methods for the functionalization of CO_2 into organic molecules, in particular using Ni catalysis. Given the isoelectronic nature of isocyanates and CO_2, part of work developed in the Martin group for the Ni-catalyzed synthesis of carboxylic acids via reductive cross-electrophile couplings with CO_2 will be described.

In 2014, the Martin group reported the carboxylation of unactivated alkyl (pseudo)halides using CO_2 at atmospheric pressures for the synthesis of aliphatic acids (Scheme 2.3).[36] Prior to this method, the developed carboxylation protocols were restricted to the use of substrates prone to undergo oxidative addition, including aryl halides and activated alkyl halides such as benzyl halides, or to C—O electrophiles such as aryl pivalates,[37] whereas the functionalization of unactivated alkyl halides possessing β-hydrogen atoms had remained a challenge.

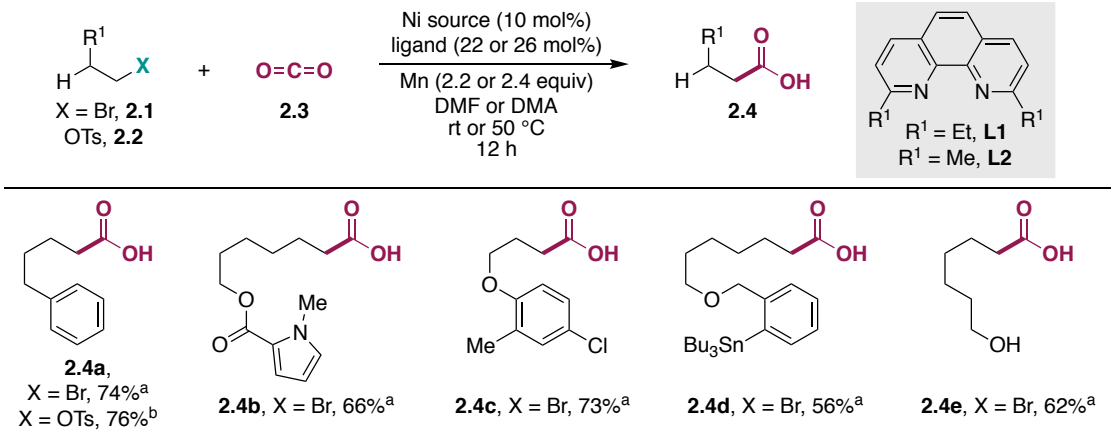

Reaction conditions: [a] **2.1** (0.30 mmol), CO_2 (1 atm), $NiCl_2$·glyme (10 mol%), **L1** (22 mol%), Mn (2.2 equiv), DMA (0.15 M) at rt. [b] **2.1** (0.25 mmol), CO_2 (1 atm), $NiBr_2$·glyme (10 mol%), **L2** (26 mol%), Mn (2.4 equiv), DMF (0.25 M) at 50 °C.

Scheme 2.3. Ni-catalyzed reductive carboxylation of unactivated alkyl bromides and sulfonates with CO_2

Using a Ni(II) precatalyst, phenanthroline-type ligands and Mn as reducing agent, a wide array of primary alkyl bromides and sulfonates were coupled with CO_2 in good yields, and with high chemoselectivity. The identity of the ligand was crucial to prevent common side-reactions associated with the use of unactivated alkyl halides (vide supra). Optimal results were obtained when neocuproine-related ligands were used, while no carboxylation was observed with phenanthroline ligands lacking *ortho*-substituents. Preliminary mechanistic studies showed the formation of a statistical mixture of diastereomers when α,β-bis-deuterated alkyl bromides and tosylates were employed, suggesting that oxidative addition proceeds via a single-electron transfer (SET) process, and that Ni(I) species might be involved in the reaction mechanism.

Next, with the aim of broadening the palette of substrates that can be used to generate carboxylic acids under mild conditions, our group reported the carboxylation of unactivated primary, secondary and tertiary alkyl chlorides, concurrent with the studies that are the subject of this Chapter (Scheme 2.4).[38] In addition to the challenges associated with the cross-coupling of unactivated alkyl halides, it is energetically more costly to form transient nucleophiles from alkyl chlorides than from alkyl bromides. The stronger C(sp^3)—Cl bond (BDE = 81±5 kcal/mol for CH_3Cl vs. 68±2 kcal/mol at 25 °C for CH_3Br),[39] makes oxidative addition of the metal center into the carbon—halogen bond a more endothermic process. The key to a successful carboxylation was the use of additives such as TBAB and LiCl, higher reaction temperatures and a more electron-donating ligand.

The addition of alkali metal iodide salts (LiI, NaI, KI) or TBAI has previously been proposed to assist electron-transfer processes from Mn to the nickel center by bridging of the polarizable iodide ion.[40–44] A similar behavior was proposed to account for the observed enhanced reactivity when TBAB or NaBr was present in the reaction

mixture.[44] The possible formation of μ-halide bridging complexes could indicate the involvement of inner-sphere electron transfer processes, which are often faster than outer-sphere processes.[45,46] In accordance with the carboxylation of alkyl bromides, *ortho*-substituted phenanthroline-type ligands were essential for the carboxylation to occur, and the use of deuterium-labeled alkyl chlorides led evidence that oxidative addition occurs via SET and the intermediacy of Ni(I) species. Stoichiometric reactions with Ni(0)(**L3**)$_2$ showed that carboxylation takes place in the absence of TBAB; suggesting that no Cl/Br exchange is necessary to generate the carboxylic acid. When stoichiometric amounts of Ni(I)(**L3**)OTf, TBAB and suprastoichiometric amounts of Mn were added to the reaction, good yields of the final acid were observed; indicating that Ni(I) species might be competent in product formation. Unlike previous Ni-catalyzed carboxylations of alkyl halides,[36,47] CO_2 insertion was observed in the absence of Mn when stoichiometric amounts of Ni(0)(**L3**)$_2$ were used; indicating that insertion into alkyl—Ni(II) species cannot be entirely ruled out under the reaction conditions.

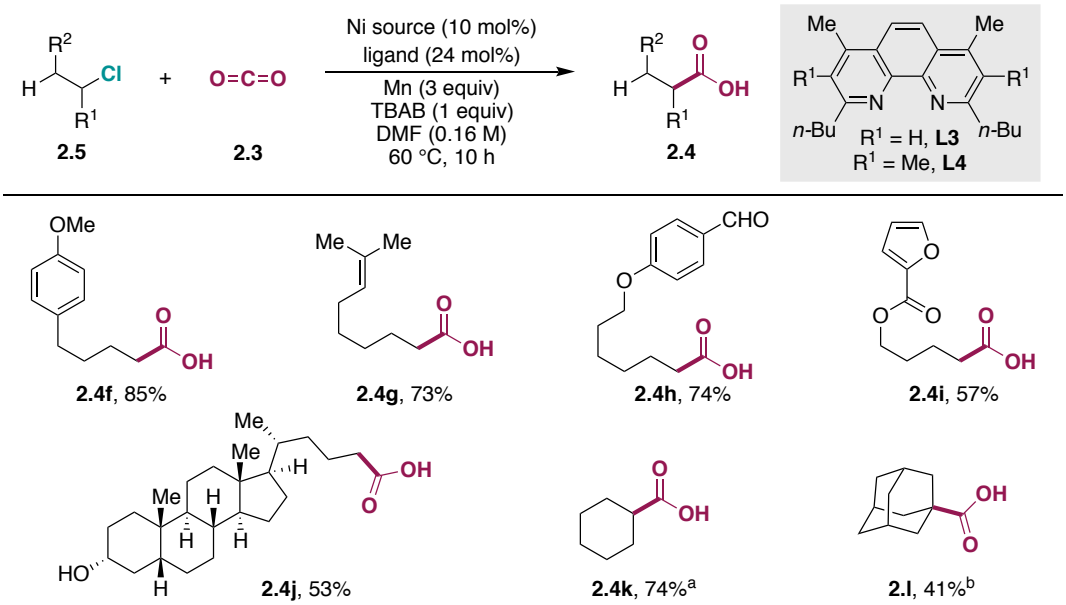

Reaction conditions: 2.4 (0.20 mmol), CO_2 (1 atm), $NiBr_2$·glyme (10 mol%), **L3** (24 mol%), Mn (3 equiv), TBAB (1 equiv), DMF (0.16 M) at 60 °C. [a] using $NiBr_2$·diglyme (10 mol%), **L4** (24 mol%), LiCl (1 equiv) at 90 °C. [a] using $NiBr_2$·diglyme (10 mol%), **L4** (24 mol%), TBAB (2 equiv) and Zn (3 equiv) in DMA at 80 °C.

Scheme 2.4. Ni-catalyzed reductive carboxylation of unactivated alkyl chlorides with CO_2

Scheme 2.5 shows the currently proposed mechanism for the Ni-catalyzed carboxylation of alkyl halides. Although preliminary studies have helped gather some information about the operating pathways, the full mechanistic picture remains unclear. Even though the intermediacy of Ni(I) species preceding CO_2 insertion has been postulated before in the Ni-catalyzed formation of benzoic acids by electrochemical methods,[48] or in reductive cross-coupling methods with activated substrates,[43,49] further in-depth experiments need to be performed in order to clarify whether CO_2 insertion takes place from alkyl—Ni(II) or —Ni(I) species. Other questions that remain unanswered are, for example, the nature of the active catalytic species; the possible involvement of the ligands in the redox process;[50] whether the proposed alkyl—Ni(I) species formed via comproportionation with Ni complexes or by SET from the reducing agent; whether CO_2 insertion occurs via an inner-sphere or an outer-sphere mechanism; and whether the intermediacy of alkylmanganese species can completely be discarded. Additionally, it is possible that the carboxylation of primary, secondary and tertiary halides follow different pathways.[51]

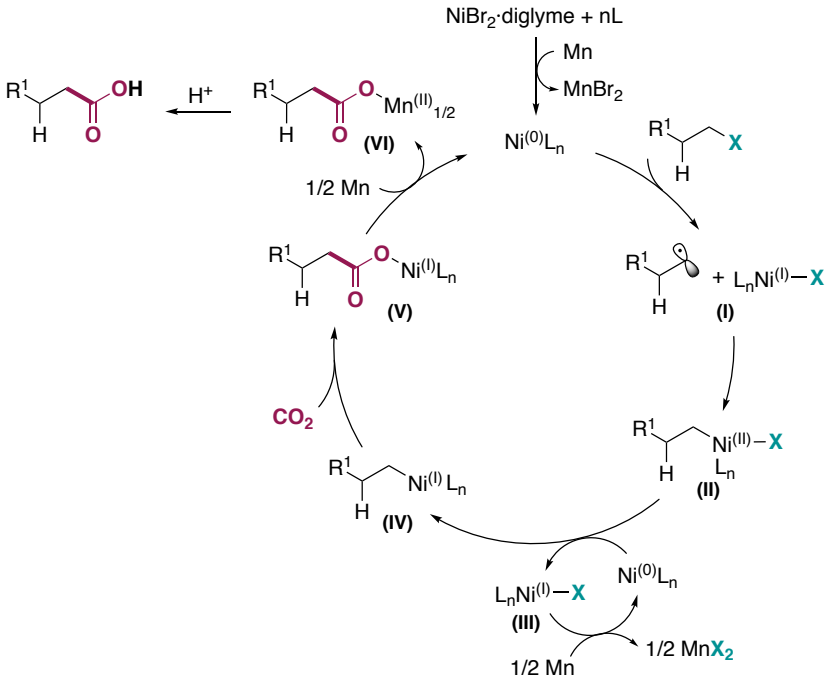

Scheme 2.5. Proposed reaction mechanism for the Ni-catalyzed carboxylation of unactivated (pseudo)halides

2.1.2.2. Ni-Catalyzed Cyclization/Carboxylation of Unactivated Primary and Secondary Alkyl Halides with CO_2

Recently, our group reported the Ni-catalyzed tandem cyclization/carboxylation of unactivated primary and secondary alkyl bromides[51] or chlorides[38] bearing a pending alkyne, to afford tetra-substituted-*exo*-cyclic olefins in which CO_2 insertion occurred at a distal position (Scheme 2.6). The use of differently substituted phenanthroline-type ligands afforded optimal results depending on the alkyl halide that was used as starting material; still, as previously observed, *ortho*-substituted ligands were in most cases essential for reactivity. One of the most important features of this protocol is the divergent synthesis of *syn*- and *anti*-carboxylated olefins from primary and secondary alkyl halides, respectively. The anti-selectivity observed for secondary alkyl halides was proposed to arise from the formation of vinyl radicals – with sp^2 character – that rapidly interconvert (**VIII** and **X**), and recombine with Ni to form a vinyl—Ni(II) species. The major product is proposed to arise from the vinyl—Ni species wherein the steric interaction between the Ni-center and the alkyl substituents in the cycle is minimized (**XI**).

Interestingly, preliminary mechanistic studies showed that different reaction mechanisms might be operating when starting from primary or secondary unactivated alkyl bromides. Experimental evidence points towards an oxidative addition occurring via a polar S_N2 mechanism for primary alkyl bromides, as the carboxylation of a deuterium-labeled primary alkyl bromide was observed to occur with inversion of the configuration, and no inhibition was observed when radical scavengers were added to the reaction. In the case of secondary alkyl bromides, the observation that the reaction was completely inhibited upon the addition of radical scavengers and the *anti*-selectivity obtained for the carboxylation, point towards an oxidative addition occurring via radical intermediates. For both type of substrates, stoichiometric experiments with Ni(0)L_2 complexes, in the absence and presence of Mn, showed that no carboxylation takes place in the absence of reducing agent; suggesting that CO_2 insertion occurs from the more nucleophilic vinyl—Ni(I) species.

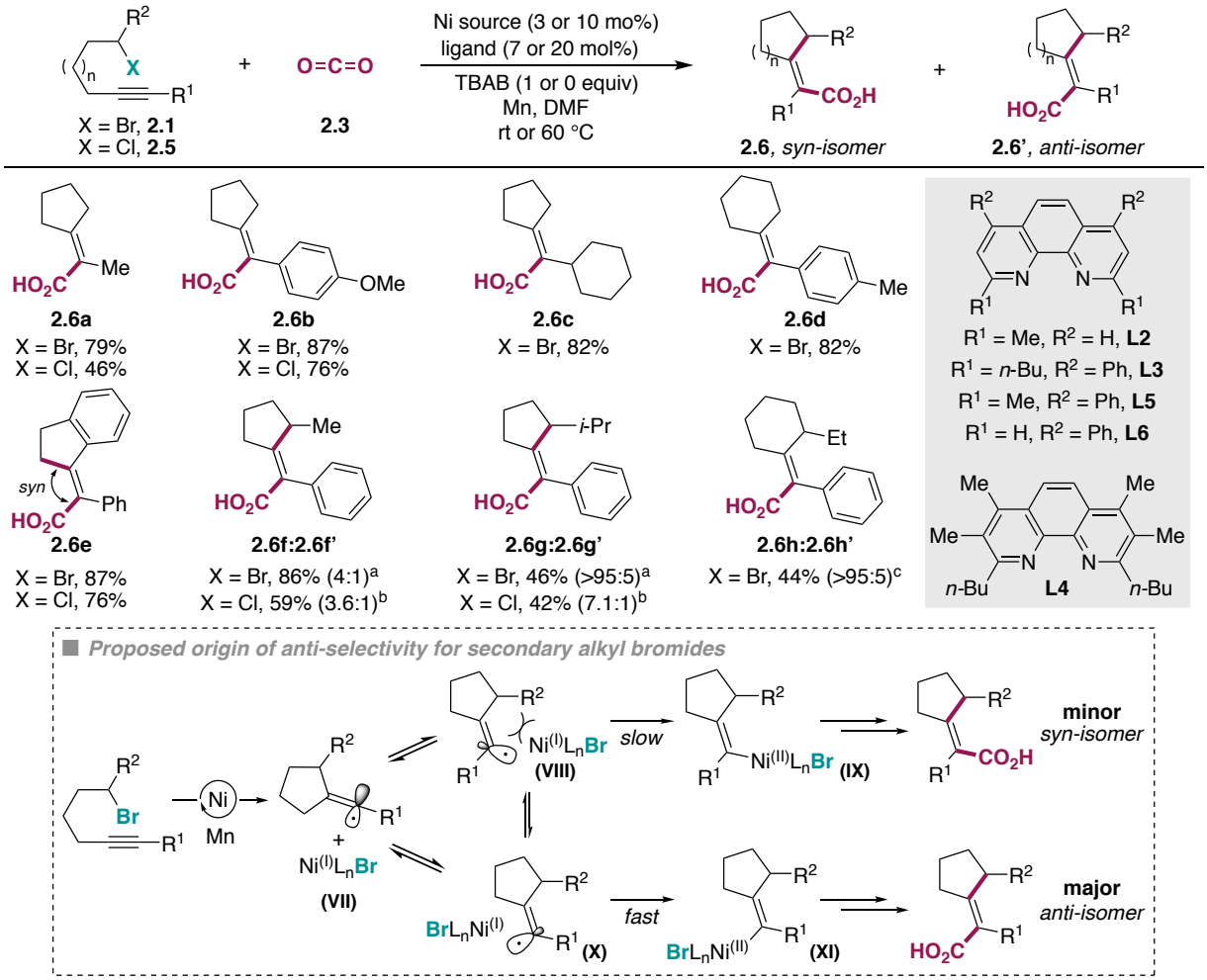

Reaction conditions: for X = Br, **2.1** (0.30 mmol), CO_2 (1 atm), $NiBr_2$·diglyme (10 mol%), **L5** (20 mol%), Mn (2.2 equiv), DMF (0.15 M) at rt. for X = Cl, **2.5** (0.20 mmol), CO_2 (1 atm), $NiBr_2$·glyme (3 mol%), **L3** (7 mol%), Mn (3 equiv), TBAB (1 equiv), DMF (0.16 M) at 60 °C. [a] using **L2**. [b] using **L4** and at 70 °C. [c] using **L6**.

Scheme 2.6. Ni-catalyzed cascade cyclization/carboxylation of unactivated alkyl halides with CO_2

2.2. General Aim of the Project

At the outset of this Doctoral Thesis, the state-of-the-art of the synthesis of amides *via* C—C bond formation showed a scarcity of methods for the preparation of aliphatic amides possessing β-hydrogens. Previously reported approaches rely on the direct addition of alkyl-organometallic species to isocyanates,[52–56] but these present the recurrent limitations associated with the use of organometallic reagents; such as the need for their preparation, their inherent low stability – associated with the presence of β-hydrogens –, the necessity for rigorous anhydrous and oxygen-free conditions, as well as a low functional group tolerance. Other previously reported methods include the use of CO and amines for the aminocarbonylation of alkenes[57–59] or unactivated alkyl iodides.[60,61] And even though the scope of these reactions has been expanded to the use of more basic amines[62,63] and the synthesis of branched amides,[64] during the development of this thesis, these methods require high pressures of CO and high reaction temperatures.

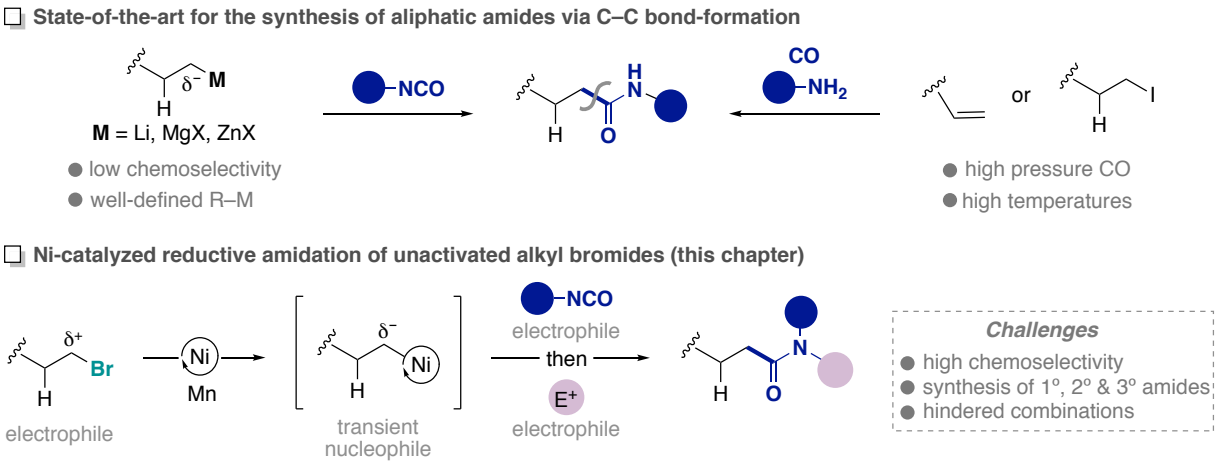

Scheme 2.7. Ni-catalyzed amidation of unactivated alkyl bromides

In view of the state-of-the-art, we recognized that a general approach for the chemoselective and catalytic synthesis of *N*-primary, -secondary and -tertiary alkyl amides with various substitution patterns and wide functional group compatibility remained to be implemented. Given the expertise of our group in reductive cross-electrophile couplings with CO_2 and isocyanates,[65,66] we hypothesized that the development of a protocol starting from unactivated alkyl halides and isocyanates would constitute a simple and efficient method for the preparation of aliphatic amides. The ample commercial availability of both coupling partners, combined with the mild conditions and easy set-up, characteristic of reductive cross-electrophile couplings, offer important advantages over the aforementioned methods (Scheme 2.7).

2.3. Ni-Catalyzed Reductive Amidation of Unactivated Primary Alkyl Bromides

2.3.1. Optimization of the Reaction Conditions

The feasibility of the amidation of unactivated alkyl halides with isocyanates was initially studied using (4-bromobutyl)benzene (**2.1a**) and cyclohexyl isocyanate (**2.7a**), as model substrates (Scheme 2.8). The choice of the model system was based on previous studies carried out in our group on the amidation of aryl pivalates and (pseudo)halides,[66] and the carboxylation of unactivated alkyl bromides.[36] With this initial system, considerable screening of the reaction conditions, including parameters such as ligand, nickel sources, reducing agents, solvents and additives, was performed. However, the decomposition over time of cyclohexyl isocyanate to cyclohexyl urea and cyclohexyl isocyanurate caused reproducibility issues. This prompted us to evaluate the different reaction parameters using *tert*-butyl isocyanate (**2.7b**) instead.

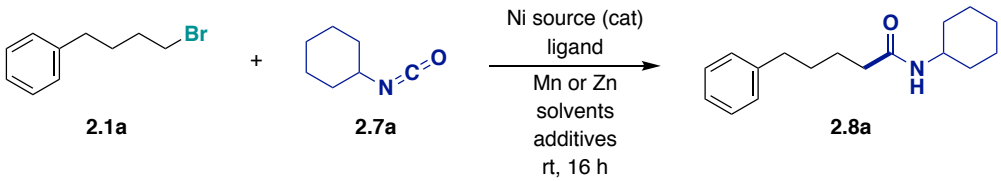

Scheme 2.8. Initial model system for the screening of optimal conditions

The choice of **2.7b** for the screening of reaction conditions, and subsequent preparative scope of alkyl bromides has several advantages. Specifically, the use of **2.7b** in the synthesis of acrylamides from α-olefins and isocyanates by Jamison and co-workers[67] demonstrated the successful application of this isocyanate in Ni-catalyzed protocols. Cleaner reaction crudes were consistently obtained as the formation of isocyanate side-

products was diminished[68] – probably due to the steric hindrance imparted by the *tert*-butyl substituent that prevents isocyanurate formation and related oligomerization reactions. Moreover, *N*-primary amides can be readily obtained by deprotection of the *tert*-butyl group under Brønsted or Lewis acid conditions.[69,70]

The fine-tuning of the reaction conditions with the second model system was based on the results of the preliminary screening with cyclohexyl isocyanate. Our first efforts focused on the identification of an optimal ligand that afforded high selectivity towards the cross-coupling amidation product, along with a decrease in unproductive pathways from both the alkyl bromide and the isocyanate (Scheme 2.9). For the former, undesired side-reactions include β-hydride elimination, reduction and the formation of homodimerization products. For the isocyanate partner, decomposition pathways involve urea formation, trimerization (isocyanurate formation) and even oligomerization, as a result of the strong binding of isocyanates to low-valent transition metal complexes.[71] Therefore, a catalytic system with a good balance of reactivity and selectivity is needed to prevent the side reactions associated to both electrophiles and to promote the formation of the cross-couple product under mild conditions.

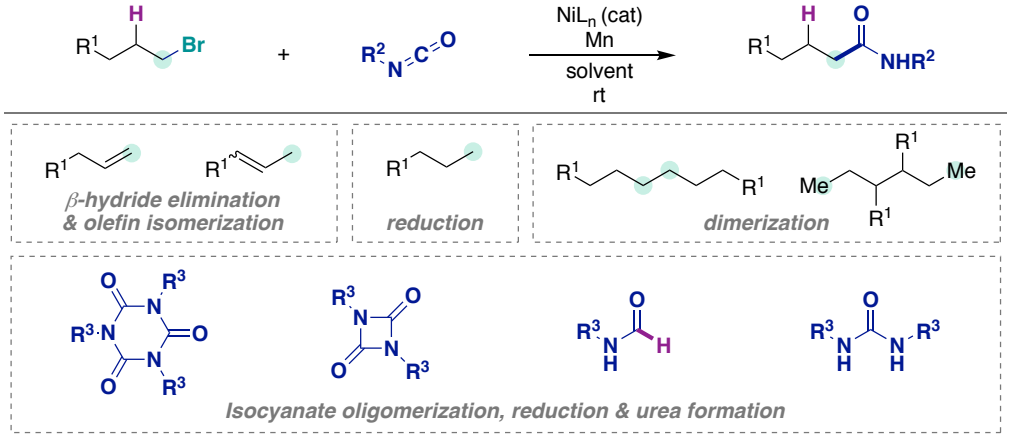

Scheme 2.9. Possible alkyl halide and isocyanate side products

Based on our group's knowledge on the carboxylation of alkyl bromides,[36] as well as on different reported protocols for the cross-coupling of alkyl halides,[11] special attention was paid to the use of phenanthroline- and bipyridine-type ligands (Table 2.1, selected ligands shown). The use of the latter was crucial for success, since lower yields of the desired amide were obtained using phenanthroline-type ligands (entries 1 to 7), whereas terpyridines or phosphines gave no desired product but led to full conversion of the alkyl bromide to undesired products, instead (entries 8 and 9). Finally, 6-methyl-2,2'-bipyridine (**L8**) (entry 2) was identified as the optimal ligand for the studied system. Under these conditions only trace amounts of homodimerization, reduction products, or even alkenes, arising from β-hydride elimination, were detected in the crude reaction mixtures.

As shown in entries 1, 4 and 5, the lack of *ortho*-substituents in the ligand leads to low yields or no formation of the desired product. This is a recurrent observation in several of the carboxylation protocols reported by our group,[37] as well as in other Ni-catalyzed reductive cross-couplings.[72] A plausible explanation for the need for *ortho*-substituted-ligands could be a gain in the stabilization of alkyl—Ni intermediates against β-hydride elimination. This would be achieved by the steric hindrance imparted by the substituent that distorts the geometry and prevents the co-planar rearrangement of the metal and the C—H$_\beta$ σ-bond necessary for β-hydride elimination.

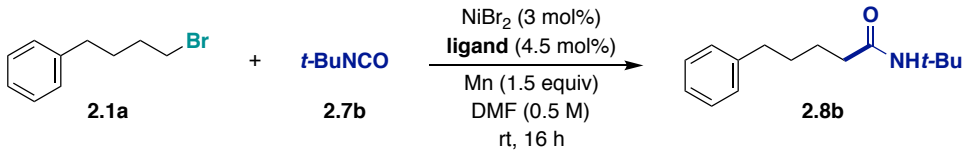

Entry	Ligand	Conversion of 2.1a (%)[a]	Yield of 2.8b (%)[a]
1	2,2'-bipyridine (**L7**)	100	39
2	6-methyl-2,2'-bipyridine (**L8**)	100	95 (86)[b]
3	6,6'-dimethyl-2,2'-bipyridine (**L9**)	100	55
4	4,4'-di-*tert*-butyl-2,2'-bipyridine (**L10**)	3	0
5	1,10-phenanthroline (**L11**)	11	0
6	neocuproine (**L2**)	100	33
7	bathocuproine (**L5**)	100	30
8	6.6''-dimethyl-2,2':6',2''-terpyridine (**L12**)	100	0
9	PPh_3 (**L13**)	6	0

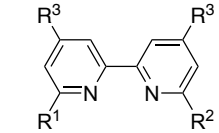

R^1, R^2, R^3 = H, **L7**
R^1 = Me; R^2, R^3 = H, **L8**
R^1, R^2 = Me; R^3 = H, **L9**
R^1, R^2 = H; R^3 = *t*-Bu, **L10**

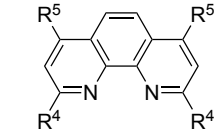

R^4 = Me; R^5 = H, **L2**
R^4 = Me; R^5 = Ph, **L5**
R^4, R^5 = H, **L11**

Reaction conditions: 2.1a (0.50 mmol), **2.7b** (0.75 mmol), $NiBr_2$ (3 mol%), ligand (4.5 mol%), Mn (0.75 mmol), DMF (1 mL) at rt, 16 h. [a] GC conversion and yield using *n*-decane as the internal standard. Mass balance accounts for β-hydride elimination, reduction and homodimerization side-products. [b] Yield of isolated product.

Table 2.1. Screening of ligands

Next, the effect of different solvents on the reaction outcome was studied (Table 2.2). The best results were obtained with amide-containing polar aprotic solvents, such as DMF and DMA (entries 1 and 2). Whereas more coordinating solvents such as acetonitrile (entry 5) or non-polar solvents such as toluene (entry 6) gave no desired product and low conversion. It is important to note that under optimal reaction conditions, older batches of DMF gave lower yields of the desired product, which is probably due to solvent decomposition over time to give dimethylamine and formic acid.

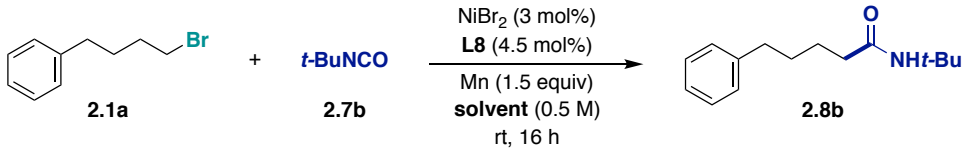

Entry	Solvent	Conversion of 2.1a (%)[a]	Yield of 2.8b (%)[a]
1	DMF	100	97
2	DMA	100	90
3	NMP	17	0
4	DMSO	34	0
5	CH_3CN	0	0
6	toluene	10	0

Reaction conditions: 2.1a (0.50 mmol), **2.7b** (0.75 mmol), $NiBr_2$ (3 mol%), **L8** (4.5 mol%), Mn (0.75 mmol), solvent (1 mL) at rt, 16 h. [a] GC conversion and yield using *n*-decane as the internal standard. Mass balance accounts for β-hydride elimination, reduction and homodimerization side-products.

Table 2.2. Screening of solvents

The higher yields observed in DMF and DMA could be explained by their high dielectric constant (ε = 38.25 at 20 °C and 38.85 at 21 °C, respectively),[73] which aids in the stabilization of charges of, for example the Mn-amidate product obtained prior to acid-quench. Similarly, putative cationic reaction intermediates could be stabilized, in

which DMF can coordinate to the metal center instead of a halide ligand.[74,75] It has been described that coordinating solvents such as acetonitrile, DMSO and DMF promote the formation of cationic $[(bipy)Ni(Mes)]^+$ from [(bipy)Ni(Mes)Br] complexes, as opposed to the neutral complexes that are preferentially formed in other solvents, such as acetone, ether or chlorinated solvents.[76] Additionally, it is possible that the more electrophilic character of cationic Ni(II) intermediates favors its reduction to low-valent Ni species or comproportionation events. Moreover, the longstanding use of DMF as solvent in electrochemistry, might indicate that single-electron transfer processes are favored in this solvent.

Although metal-catalyzed reductive cross-coupling reactions using stoichiometric metal reductants have been conducted in acetonitrile or other non-amide solvents,[13] a large majority of the reported Ni-catalyzed reductive cross-couplings are performed in amide solvents.[77] Recently, Weix and co-workers reported a Ni-catalyzed aryl-alkyl cross-coupling that uses solvents such as acetonitrile or propylene carbonate, when tetrakis(dimethylamino)ethylene (TDAE) is used as an organic reductant,[35] these findings indicate that moving away from metal powders as reducing agents opens the door to the use of more environmentally benign solvents. However, the tedious synthesis of this organic reagent and low commercial availability at a high price, compared to the wide availability and low cost of metal powders, make the use of TDAE less attractive. (Merck prize on April 2018, calculated with the biggest sold quantity and >99.9% purity for the metals, TDAE = 4.2 €/mmol, Mn = 0.14 €/mmol, Zn = 0.04 €/mmol).

Subsequently, other parameters such as the nickel source and the reducing agent were evaluated (Table 2.3). The reaction worked better with nickel sources having bromide counterions (entries 1 and 2) which could act as bridging ligands to facilitate SET processes or favor the formation of cationic species. The use of $Ni(COD)_2$ resulted in low yields of the desired product, probably due to the coordination of COD to the nickel (entry 3). The use of TDAE did not afford the product (entry 4); in retrospect however, it would have been worth to perform the reaction in acetonitrile or other solvents. In contrast to the Ni-catalyzed amidation of aryl pivalates possessing an extended π-system,[66] no desired product was observed when zinc was used as reducing agent (entry 5). The lower reduction potential of Zn with respect to Mn could explain this experimental result ($E°$ = −0.76 and −1.185 V vs. SHE at 25 °C, respectively[73]). It is possible that a stronger reducing agent is needed for the reduction of primary alkyl—Ni(II) intermediates to primary alkyl—Ni(I) species, from which a subsequent isocyanate insertion would be more likely to occur (vide infra, mechanistic discussion).

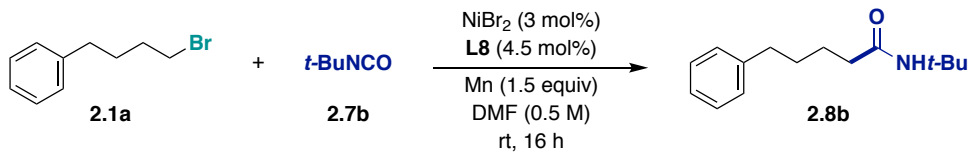

Entry	Deviation from Standard Conditions	Conversion of 2.1a (%)[a]	Yield of 2.8b (%)[a]
1	none	100	97
2	$NiCl_2$·glyme instead of $NiBr_2$	100	80
3	$Ni(COD)_2$ instead of $NiBr_2$	100	45
4	TDAE	n.d.	0
5	Zn instead of Mn	39	0

Reaction conditions: 2.1a (0.50 mmol), **2.7b** (0.75 mmol), $NiBr_2$ (3 mol%), **L8** (4.5 mol%), Mn (0.75 mmol), DMF (1 mL) at rt, 16 h. [a] GC conversion and yield using *n*-decane as the internal standard. Mass balance accounts for β-hydride elimination, reduction and homodimerization side-products.

Table 2.3. Screening of nickel sources and reducing agents

Fine-tuning of the reaction conditions revealed that smaller amounts of isocyanate **2.7b** provided reduced yields of the amide product, showing that a small excess is needed to account for the loss of isocyanate, mainly due to urea formation (Table 2.4, entry 2). Similarly, the use of an equimolar nickel-to-ligand ratio gave lower yields (entry 3). Very likely, a slight excess of the ligand is needed to ensure that all the nickel is coordinated, and possibly to stabilize, for example, nickel(0) species present in the catalytic cycle. Interestingly, higher catalyst loadings gave higher amounts of undesired products (entry 4). This result can be rationalized by a higher concentration of alkyl—Ni species, which for example, instead of inserting isocyanate afford dimerization products or undergo other unproductive pathways.

Furthermore, no reactivity was observed when lowering the catalyst loading to 1 mol%, probably due to the sensitivity of the reaction to traces of oxygen and moisture, which on low scale could readily lead to catalyst decomposition (entry 5). Using lower amounts of Mn had an adverse effect (entry 6), a result that could probably be expected as the Mn was used without prior activation, and the heterogeneity of the reaction might prevent the use of stoichiometric amounts of the reducing agent. Finally, full conversion without product formation was observed when (4-iodobutyl)benzene was used as electrophile. Instead, alkenes were obtained as major products along with some reduced starting material (entry 7). A more positive result was obtained when an alkyl sulfonate (entry 8) was used as substrate, indicating that this methodology can be extended to the use of alkyl pseudohalides.[36] It is worth mentioning that carrying out the reaction at temperatures higher than 25 °C had a deleterious effect on the yield of the desired product, and increased side-product formation. When the reaction was carried out at 40 °C, decomposition of the Ni-catalyst and precipitation of some nickel-black was observed. Later studies on the formation of Ni(0)-complexes with bipyridine ligands showed a similar trend, indicating that the stability of these complexes likely diminishes at higher temperatures (vide infra).

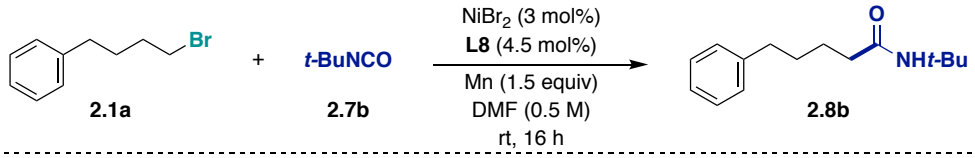

2.1a 2.7b 2.8b

Entry	Deviation from Standard Conditions	Conversion of 2.1a (%)[a]	Yield of 2.8b (%)[a]
1	none	100	95
2	1 equiv instead of 1.5 equiv of **2.7b**	100	86
3	3.0 mol% instead of 4.5 mol% of ligand **L8**	100	85
4	5 mol% of $NiBr_2$ and 10 mol% of **L8**	100	86
5[b]	1 mol% of $NiBr_2$ and 1.5 mol% of **L8**	0	0
6	1.2 equiv instead of 1.5 equiv Mn	100	89
7	(4-iodobutyl)benzene instead of **2.1a**	100	0
8	4-phenylbutyl-4-methylbenzenesulfonate	100	40
9	(4-chlorobutyl)benzene instead of **2.1a**	0	0

Reaction conditions: 2.1a (0.50 mmol), **2.7b** (0.75 mmol), $NiBr_2$ (3 mol%), **L8** (4.5 mol%), Mn (0.75 mmol), DMF (1 mL) at rt, 16 h. [a] GC conversion and yield using *n*-decane as the internal standard. Mass balance accounts for β-hydride elimination, reduction and homodimerization side-products. [b] Reaction carried out at 1 mmol scale.

Table 2.4. Fine-tuning of the reaction conditions

Finally, blank experiments were performed to corroborate that all the reaction parameters were necessary for the amidation to take place. Table 2.5 shows that without nickel, ligand or Mn, no amide product is formed (entries 2 to 4). Omission of **2.7b** led to almost full consumption of the alkyl bromide to generate homodimers, reduced and β-hydride elimination products (entry 5). Importantly, if the reaction was carried out under air, instead of argon, no reactivity was observed (entry 6).

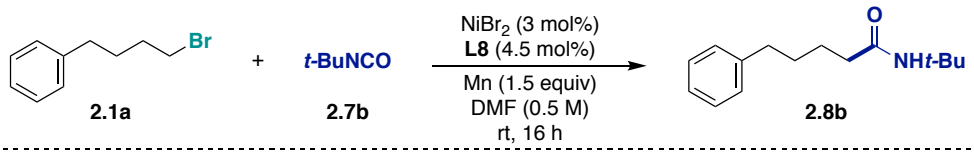

Entry	NiBr2	L8	Mn	Conversion of 2.1a (%)[a]	Yield of 2.8b (%)[a]
1	✓	✓	✓	100	95
2	✗	✓	✓	0	0
3	✓	✗	✓	29[b]	0
4	✓	✓	✗	0	0
5[c]	✓	✓	✓	80[b]	0
6[d]	✓	✓	✓	0	0

Reaction conditions: 2.1a (0.50 mmol), **2.7b** (0.75 mmol), $NiBr_2$ (3 mol%), **L8** (4.5 mol%), Mn (0.75 mmol), DMF (1 mL) at rt, 16 h. ✗ = indicates that the reagent was omitted from the reaction mixture; ✓ = indicates that the reagent was added to the reaction mixture. [a] GC yield using *n*-decane as the internal standard. [b] Mass balance accounts for β-hydride elimination, reduction and homodimerization side-products. [c] **2.7b** was omitted from reaction mixture. [d] reaction carried out under air.

Table 2.5. Blank experiments

2.3.2. Preparative Substrate Scope

2.3.2.1. Scope of Unactivated Primary Alkyl Bromides

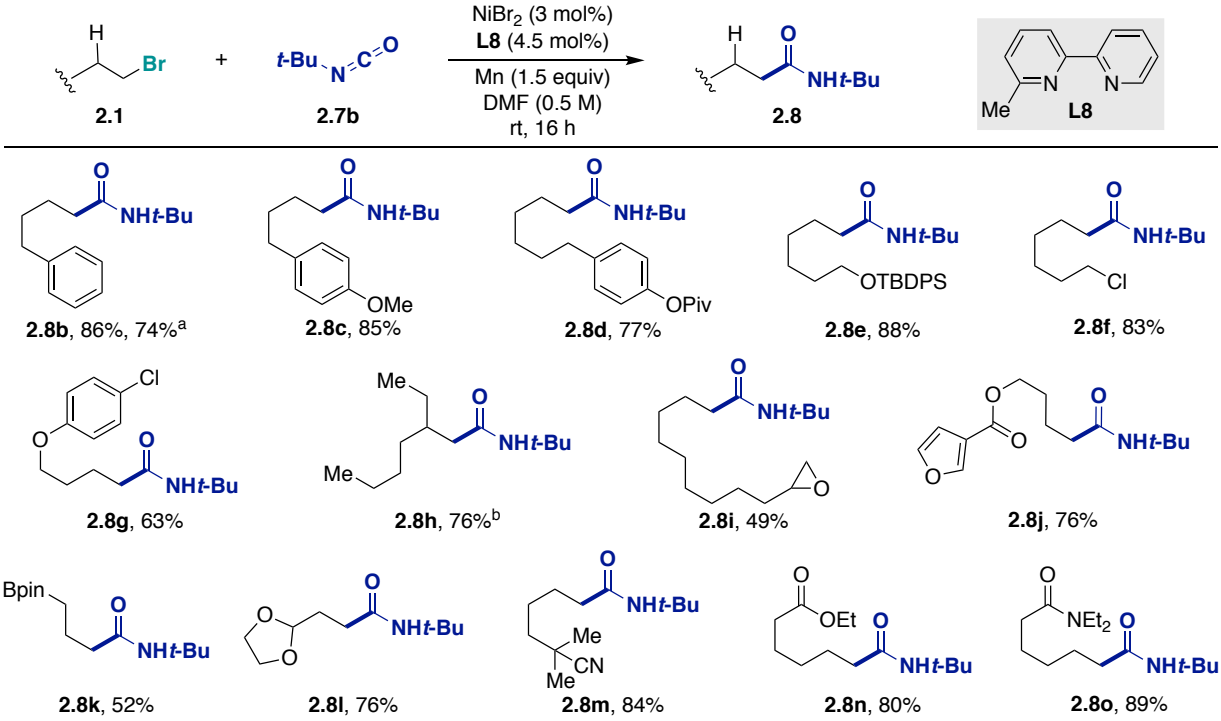

Reaction conditions: 2.1 (0.50 mmol), **2.7b** (0.75 mmol), $NiBr_2$ (3 mol%), **L8** (4.5 mol%), Mn (0.75 mmol), DMF (1 mL) at rt, 16 h. Isolated yields, average of at least two independent runs. [a] **2.1** (4.69 mmol). [b] $NiBr_2$ (5 mol %), **L8** (7.5 mol %).

Scheme 2.10. Scope of primary alkyl bromides with *tert*-butyl isocyanate

Having optimized the reaction conditions, the scope of the transformation was studied by evaluating a range of unactivated primary alkyl bromides in combination with *tert*-butyl isocyanate (**2.7b**). In line with the mild reaction conditions, characteristic of reductive cross-coupling protocols, the transformation allowed for the preparation of a diverse array of amides with high chemoselectivity, and satisfactory yields (Scheme 2.10). Substrates commonly employed in Ni-catalyzed cross-couplings containing aryl ethers (**2.8c**), pivalates (**2.8d**) and chlorides (**2.8g**) were well accommodated. Various functional groups such as silyl ethers (**2.8e**), acetals (**2.8l**),

nitriles (**2.8m**), esters (**2.8d, 2.8j, 2.8n**), amides (**2.8o**) and furans (**2.8j**) were well tolerated. Albeit in lower yields, terminal epoxides (**2.8i**) could be coupled. Under slightly modified reaction conditions, primary alkyl bromides with increased steric hindrance (**2.8h**) afforded the desired amide. Importantly, alkyl chlorides (**2.8f**) and alkyl boronic esters (**2.8k**) remained untouched, leaving an additional handle for further functionalization.[38,78] Finally, satisfactory yields were obtained when the reaction was performed in large scale, starting from 4.69 mmol (1.00 g) of **2.1a**.

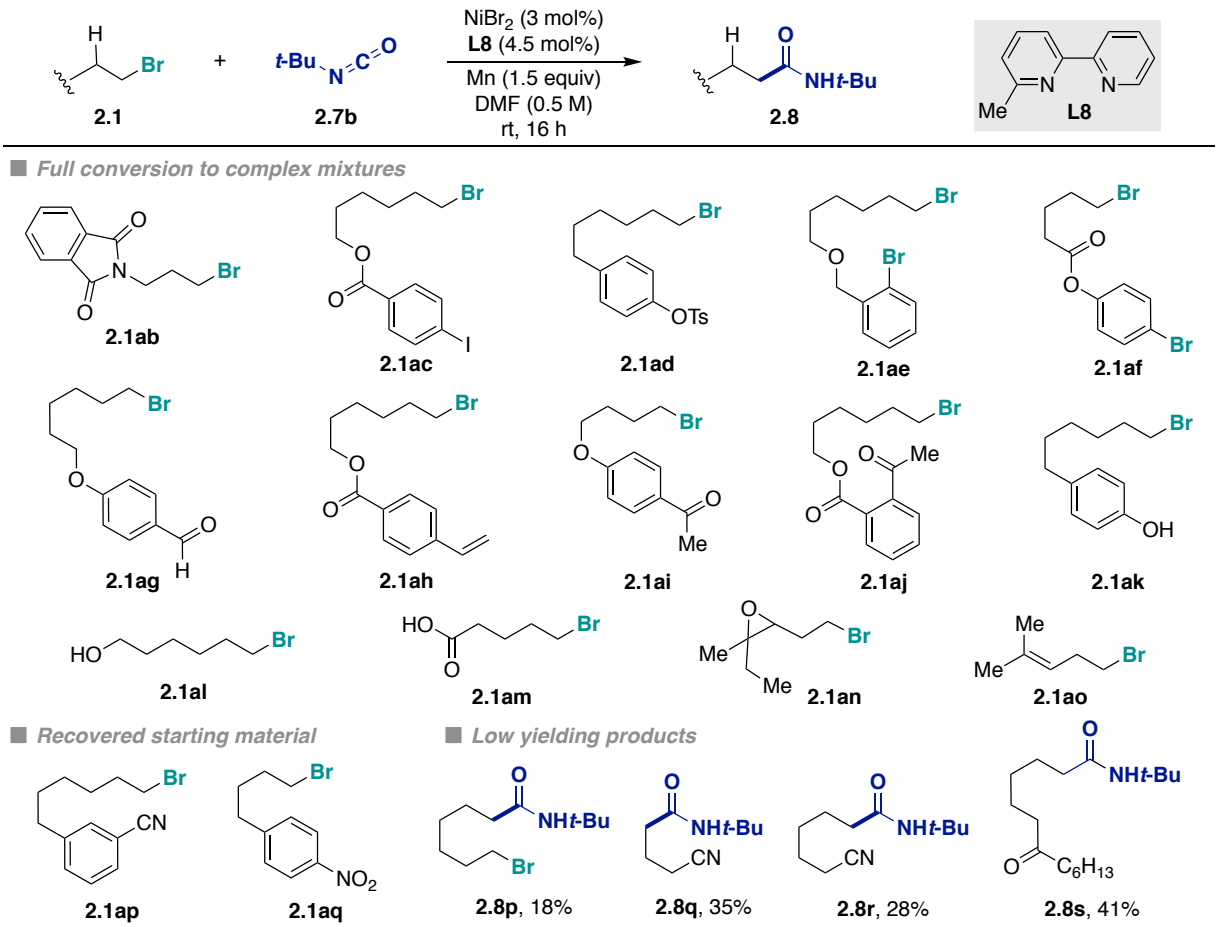

Reaction conditions: **2.1** (0.50 mmol), **2.7b** (0.75 mmol), $NiBr_2$ (3 mol%), **L8** (4.5 mol%), Mn (0.75 mmol), DMF (1 mL) at rt, 16 h. Isolated yields.

Scheme 2.11.Unsuccessful and unsatisfactory substrates for the amidation of primary alkyl bromides

The limitations of the developed method were identified as well (Scheme 2.11). For some of the evaluated substrates full conversion into complex mixtures of unidentified products, dimers, alkenes, and in some cases amides were obtained. For example, functional groups used in metal-catalyzed cross-coupling reactions such as aryl iodides (**2.1ac**), tosylates (**2.1ad)** and bromides (**2.1ae**, **2.1af**) failed to afford the desired amides. Complex mixtures were observed with substrates bearing functional groups such as phthalimide (**12.7ab**), aldehydes (**2.1ag**), alkenes (**2.1ah**, **2.1ao**) and ketones (**2.1ai**, **2.1aj**), probably due to the formation of Ni—H species, after β-hydride elimination, which could react with electrophilic functionalities. Not surprisingly, substrates bearing nucleophilic functional groups such as phenols (**2.1ak**), alcohols (**2.1al**) and acids (**2.1am**) interfered with the reaction, likely by reacting with the isocyanate to form carbamates.[79] Substrate **2.1an** gave only trace amounts of the desired amide, probably due to the distance between the resulting amidate and the epoxide, which can lead to lactam formation via epoxide opening, and subsequent undesired reactions with the isocyanate partner. No reaction was observed with alkyl bromides substituted with aryl moieties bearing nitro (**2.1aq**) or strong σ-donor

groups such as nitriles (**2.1ap**), which could have poisoned the nickel catalyst. Likewise, unhindered alkyl nitriles gave low yields of amides **2.8q** and **2.8r**. Moreover, the selective mono-amidation of 1,5-dibromopentane was met with little success, as a mixture of mono-amidated, di-amidated and side-products was observed (**2.8p**).

2.3.2.2. Scope of Aryl and Alkyl Isocyanates

Scheme 2.12 shows the preparative scope of isocyanates. Higher catalyst loadings and a re-optimization of the reaction conditions were needed when moving away from *tert*-butyl isocyanate. Gratifyingly, other alkyl isocyanates were tolerated, although moderate to low yields of the desired amides were obtained (**2.8a**, **2.8t**, **2.8u**). One of the difficulties of working with alkyl isocyanates is their high sensitivity to moisture, which even leads to decomposition to urea and isocyanurates when stored in a glovebox. Efforts to increase the yield by purification of the isocyanates were made. Although filtration through a short plug of dried neutral alumina, inside a nitrogen-filled glovebox led to a small improvement, distillation of the isocyanates did not have a strong positive effect. Only aromatic isocyanates having *ortho*-substituents were well tolerated (**2.8v**, **2.8w**, **2.8x**) In some cases, the synthesis of *N*-aryl-substituted amides required the use 6,6'-dimethyl-2,2'-bipyridine (**L9**) as ligand, and equimolar amounts of the aromatic isocyanate. The addition of an excess of the latter led to the formation of considerable amounts of *N*-acylureas, arising from the nucleophilic attack of the metal-amidate product to the isocyanate partner and to urea formation (Scheme 2.13).

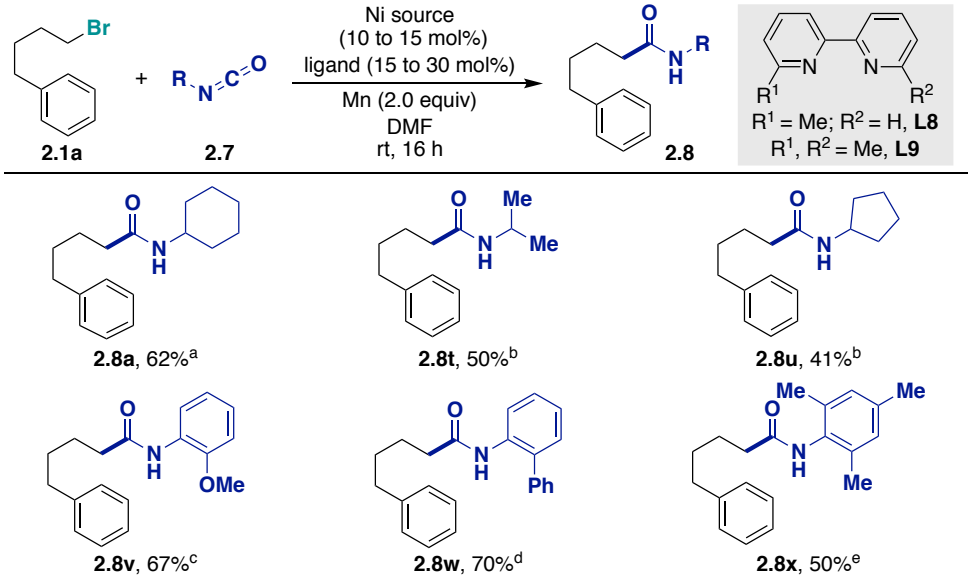

Reaction conditions: **2.1a** (0.50 mmol), Mn (1.0 mmol), DMF (1 mL) at rt, 16 h. [a] **2.7**(1 mmol), $NiBr_2$ (10 mol %), **L8** (15 mol %). [b] **2.7c-d** (1.5 mmol), [(TMEDA)Ni(*o*-tolyl)Cl] (15 mol %), **L8** (30 mol %), DMF (2 mL). [c] **2.7e** (0.5 mmol), $NiBr_2$ (10 mol %), **L9** (20 mol %). [d] **2.7f** (1 mmol), $NiBr_2$ (10 mol %), **L9** (20 mol %). [e] **2.7g** (0.5 mmol), $NiBr_2$ (10 mol %), **L8** (20 mol %). Yields of isolated products, average of at least two independent runs.

Scheme 2.12. Scope of alkyl and aryl isocyanates

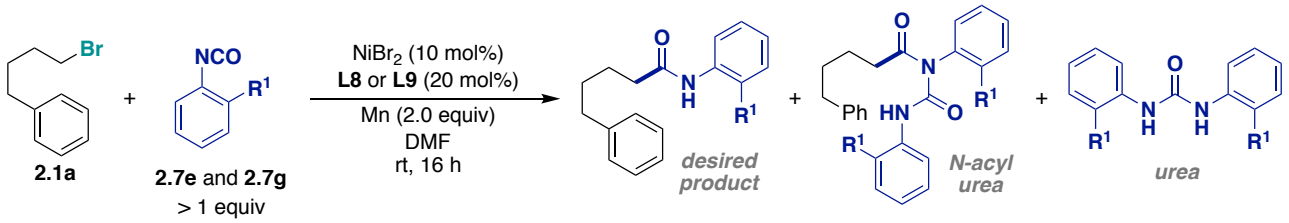

Scheme 2.13. Mass balance obtained with aromatic isocyanates 2.8e and 2.8g

A list of isocyanates that under optimized reaction conditions either failed to afford, or gave low yields (<20%), or merely traces of the desired alkyl amides is shown in Scheme 2.14. In most of the cases, and independently of the electronic properties of the substrate, the listed aryl and alkyl isocyanates gave trimerization and oligomerization products. The formation of these side-products is known to be catalyzed by metals (including Ni[68]), pyridines, tertiary amines, ammonium salts, among others,[80] and represents one of the major challenges to be overcome when using isocyanates as amide synthons in metal-catalyzed transformations.

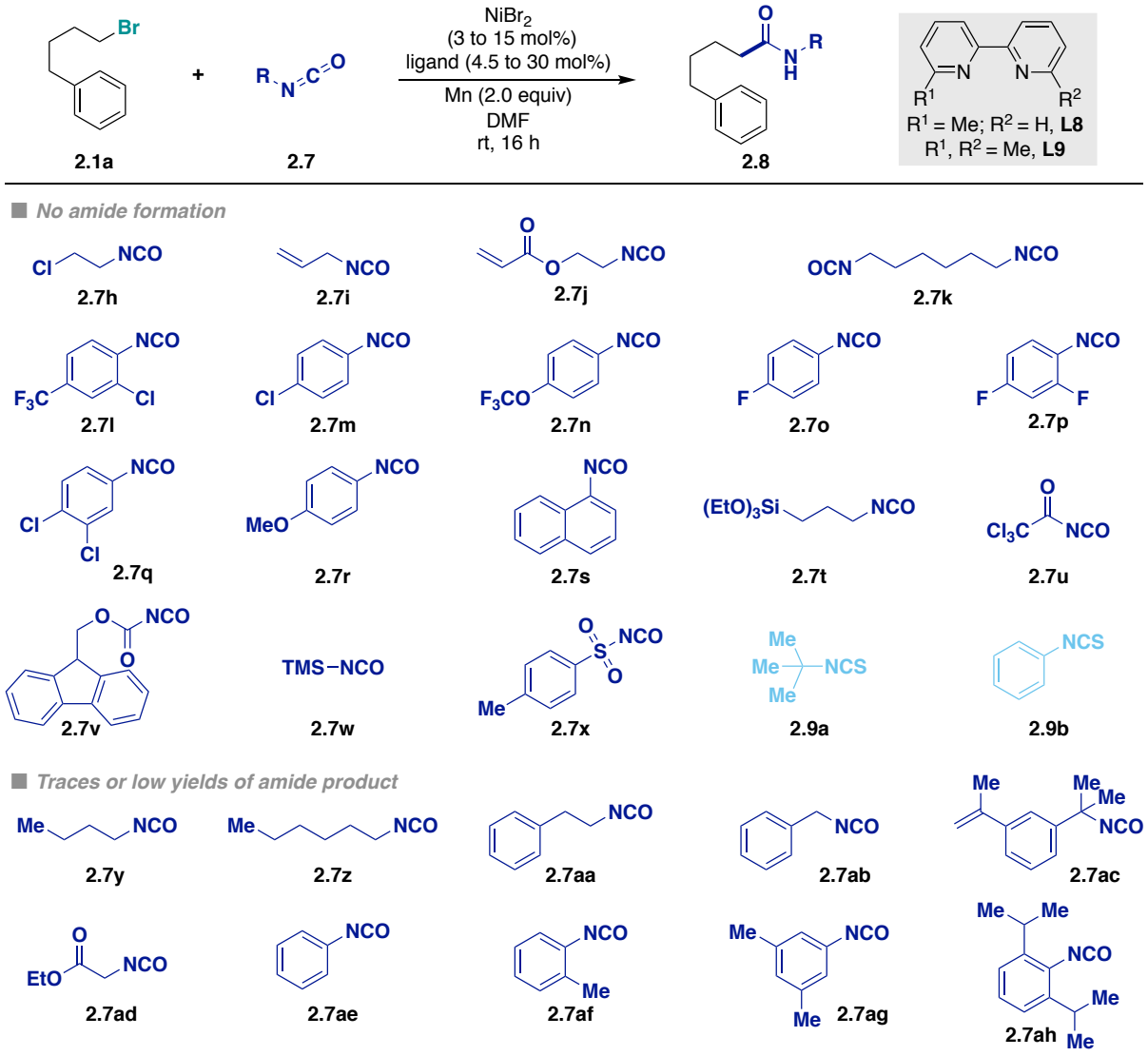

Reaction conditions: 2.1a (0.50 mmol), **2.8** (0.5 to 1.5 mmol), Mn (1.0 mmol), $NiBr_2$ (3 to 15 mol%), ligand (4.5 to 30 mol%), DMF (1 mL) at rt, 16 h.

Scheme 2.14. Unsuccessful isocyanate coupling partners

It is important to mention that extensive screening of conditions, including ligands, additives, solvents, reducing agents, nickel sources, and other variables such as the slow addition of the isocyanate, was performed with phenyl (**2.7ae**), hexyl (**2.7z**), butyl (**2.7y**), and phenethyl isocyanate (**2.7aa**). In all cases the trimerization of the isocyanate could not be prevented, and only small amounts of the desired amides could be obtained. Furthermore, no conversion of **2.1a** was observed when isothiocyanates (**2.9a** and **2.9b**) were used as starting materials. The presence of the less electronegative sulfur atom renders the molecule a better σ-donor, thus coordination to the nickel center is stronger, possibly leading to catalyst poisoning. Up to now, the scope of

isocyanates remains one of the major limitations of the developed amidation protocol, as the reaction is rather limited to the use of bulky, electron-rich isocyanates. Similar limitations were already encountered for the amidation of α-olefins by Jamison and co-workers.[67]

2.3.3. Synthesis of *N*-Tertiary and *N*-Primary Amides

The current developed metal-catalyzed amidations with isocyanates often result in the formation of *N*-secondary amides, except in those cases were a suitable electrophile is present in the starting material; such as for the synthesis of *N*-substituted phthalimides reported by Cheng,[81] or of hydantoins by Murakami.[82] The development of a unified catalytic method that allows for the synthesis of *N*-primary, -secondary and -tertiary amides would be of high interest as means to rapidly build a library of differently substituted amides from the same precursor. The next sections will focus on the approaches taken towards this goal.

2.3.3.1. Synthesis of N-Tertiary Amides via Sequential Addition of a Third Electrophile

The design principle for the synthesis of *N*-tertiary amides consisted of evaluating the synthetic potential of the *in situ* formed metal-amidate **XII** shown in Scheme 2.15, which is the product of the reaction prior to acid quench. In these species, the nitrogen-metal bond has a nucleophilic character that could potentially be intercepted by an appropriate electrophile. This hypothesis was tested by the direct addition of a third electrophile to the reaction mixture after completion of the Ni-catalyzed amidation. Strong electrophiles such as methyl iodide, allyl bromide and benzyl bromide could be used for the synthesis of *N*-tertiary amides from 2-methoxyphenyl-substituted amides (**2.11a**, **2.11b** and **2.11c**). On the other hand, this idea was met with less success for *tert*-butyl-substituted amides, as only methyl iodide afforded *N*-tertiary amide **2.11b**. The obtained results could be explained by the steric hindrance of the bulky *tert*-butyl group, which prevents the addition of bigger electrophiles than methyl iodide. Taking into account that two amide molecules are needed to complete the electron valence when Mn-amidates are formed, the steric properties of the metal-amidate could play an important role in its reactivity. Contrarily, when 2-methoxyphenyl-amidates are used, the formation of a five-membered metala-cycle by coordination of the methoxy group of the aromatic moiety and the amide's nitrogen to the Mn would impart less steric hindrance and could potentially stabilize the metal-amidate, making it more prone to undergo a reaction with the third electrophile.

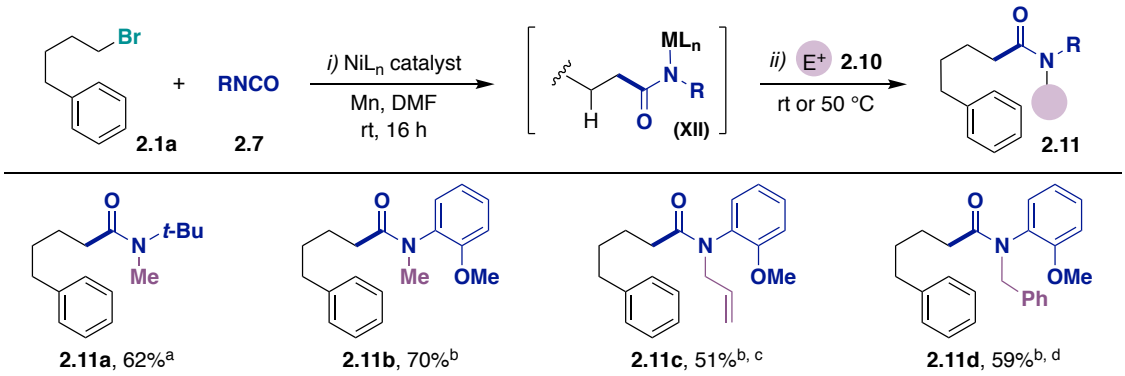

Reaction conditions: [a] **2.1a** (0.50 mmol), **2.7b** (0.75 mmol), Mn (0.75 mmol), $NiBr_2$ (3 mol%), **L8** (4.5 mol%), DMF (1 mL) at rt, 16 h, then MeI (2 equiv), 50 °C. [b] **2.1a** (0.50 mmol), **2.7e** (0.5 mmol), Mn (1.0 mmol), $NiBr_2$ (10 mol%), **L9** (20 mol%), DMF (1 mL) at rt, 16 h, then MeI (5 equiv), rt. [c] Using allyl bromide (10 equiv), 50 °C. [d] Using benzyl bromide (5 equiv), 50 °C. Yields of isolated products, average of at least two independent runs.

Scheme 2.15. Synthesis of *N*-tertiary amides via sequential addition of a third electrophile

With the aim of exploring the possible groups that could be introduced following this design principle, an array of electrophiles was tested under different reaction conditions (Scheme 2.16). For the reactions using *tert*-butyl

isocyanate a range of alkyl halides, strong methylating and ethylating agents, and protecting groups, among others were tested. In some cases, no reaction took place and full or partial recovery of the *N*-secondary amide (**2.8b**) and the electrophile was observed after acid quench. When chloroformates were used (**2.10p** and **2.10q**) complex reaction mixtures and partial decomposition of **2.8b** were observed. The addition of benzoyl chloride and *p*-toluene sulfonyl chloride led to the formation of 5-phenylpentanenitrile, in which a Von Braun amide degradation could have taken place.[83] Unfortunately, for those reactions using 2-methoxyphenyl isocyanate, the use of other alkyl halides (**2.10e** and **2.10t**), Meerwein's salt (**2.10u**), acyl chlorides (**2.10x**, **2.10r**) or chloro-substituted aromatic scaffolds (**2.10v**, **2.10w** and **2.10y**), prone to undergo nucleophilic aromatic substitution, led to partial recovery of the *N*-secondary amide and no *N*-tertiary amide formation.

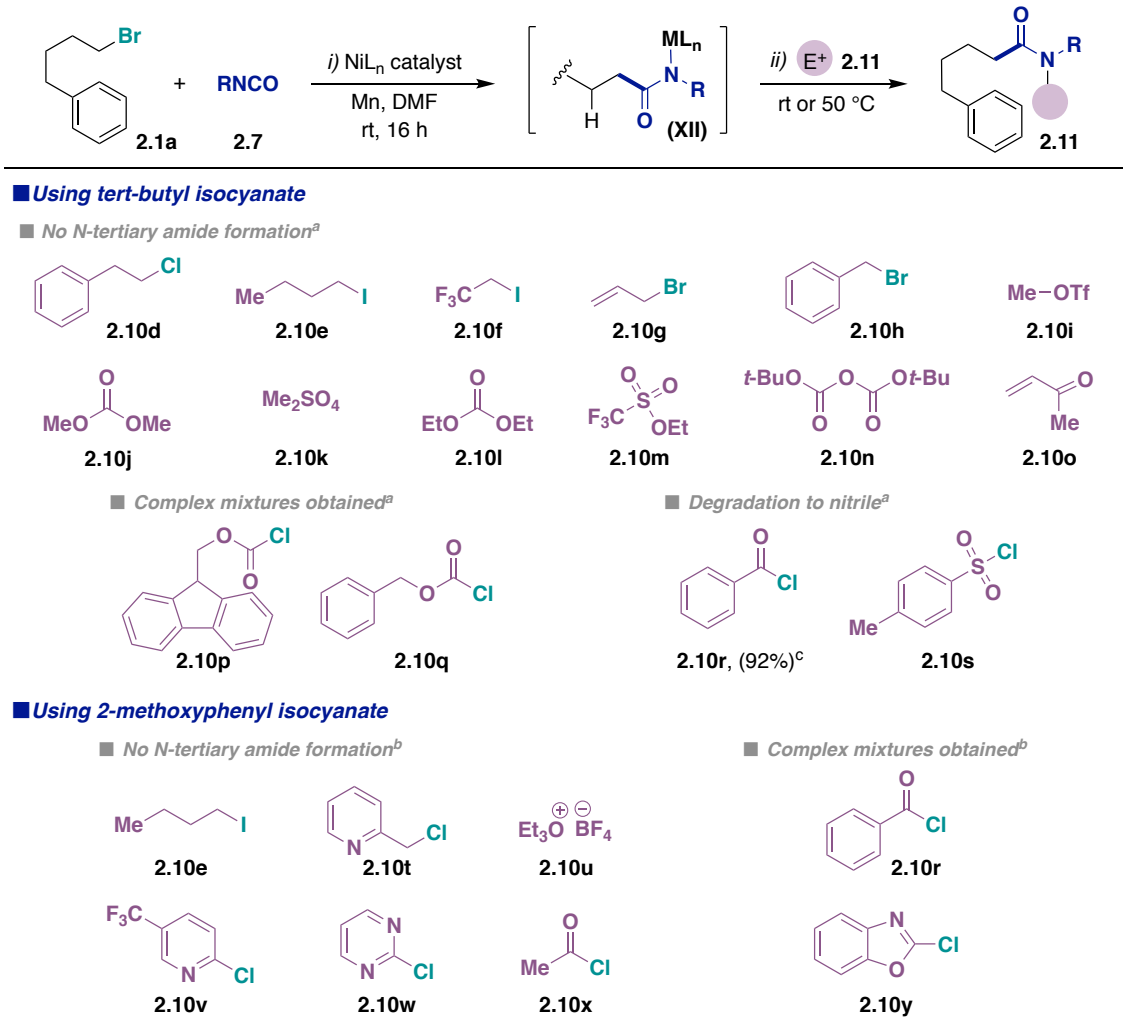

Reaction conditions: [a] **2.1a** (0.50 mmol), **2.7b** (0.75 mmol), Mn (0.75 mmol), $NiBr_2$ (3 mol%), **L8** (4.5 mol%), DMF (1 mL) at rt, 16 h. Then **2.10** (1 to 10 equiv), rt to 50 °C, 16 h. [b] **2.1a** (0.50 mmol), **2.7e** (0.5 mmol), Mn (1.0 mmol), $NiBr_2$ (10 mol%), **L9** (20 mol%), DMF (1 mL) at rt, 16 h. Then **2.10** (1 to 10 equiv), rt to 50 °C. [c] Isolated yield of 5-phenylpentanenitrile.

Scheme 2.16. Unsuccessful electrophiles for the synthesis of *N*-tertiary amides

2.3.3.2. Synthesis of N-Primary and N-Methyl Amides

One of the major synthetic advantages of using **2.7b** as the amide synthon is the possible deprotection of the obtained *N-tert*-butyl amides under Brønsted or Lewis acid conditions. Following a reported method,[70] amide **2.8b** could be deprotected in high yields to afford the primary amide **2.12a**. When trifluoroacetic acid was added either to the reaction crude or to the isolated product,[69,67] the desired amide **2.12a** was isolated in 93 to 97% yield along

with an inseparable impurity, in which the substitution pattern of the aromatic group had changed (Scheme 2.17). Using similar Brønsted acid conditions, compound **2.12b** could be obtained in good yields (Scheme 2.18).

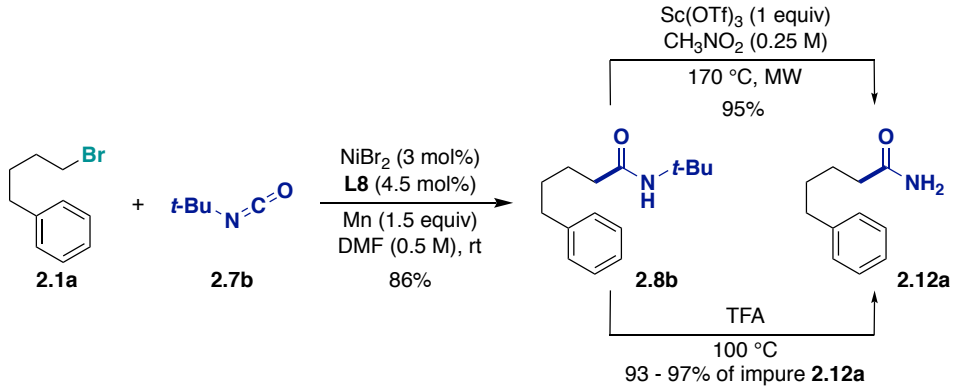

Scheme 2.17.Deprotection of *N*-(*tert*-butyl)-5-phenylpentanamide

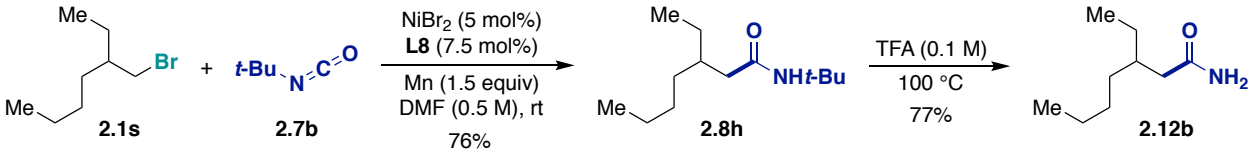

Scheme 2.18. Deprotection of *N*-(*tert*-butyl)-3-ethylheptanamide

The use of methyl isocyanate as amide synthon is precluded by its high toxicity and flammability.[84] The combination of the synthesis of *N*-tertiary amides via the sequential addition of a third electrophile, followed by deprotection of the *tert*-butyl group under catalytic-Lewis acid conditions,[85] allowed for the synthesis of *N*-methyl substituted amide **2.13** (Scheme 2.19), which constitutes a formal use of methyl isocyanate.

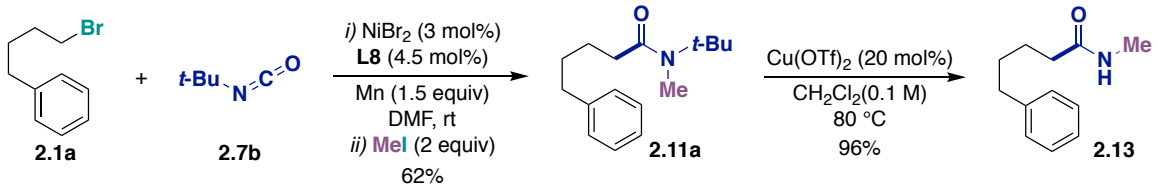

Scheme 2.19. Sequential synthesis of *N*-methyl amide 2.13

2.3.4. Preliminary Mechanistic Studies

2.3.4.1. Intermediacy of Radical Species

The stereochemical course of the reaction was studied with the aim of gaining some insight into the reaction mechanism. Subjecting deuterium-labelled compound **2.1aw** to the optimized reaction conditions afforded amide **2.8y** as a statistical mixture of diastereomers (Scheme 2.20). The obtained result tentatively indicates that oxidative addition of the nickel catalyst to compound **2.1aw** does not invert the stereochemistry present in the starting material, which points against an S_N2-type mechanism for this elementary step.[19,20,51] Instead, oxidative addition is likely to occur with scrambling of the stereochemical information, indicating that a radical intermediate is formed after SET from the nickel catalyst to the alkyl bromide. The rapid pyramidal inversion of the radical results in the loss of the stereochemical information.The intermediacy of **XIII** would ultimately translate into the formation of a diastereomeric mixture of products. However, the obtained result could also be explained by an oxidative addition via an S_N2-type mechanism followed by β-hydride elimination, which would generate an alkene

and a Ni—H species. The formed alkene could afford intermediate **XIII** via olefin coordination and migratory insertion of the Ni—H species and ultimately generate a diastereomeric mixture of products.

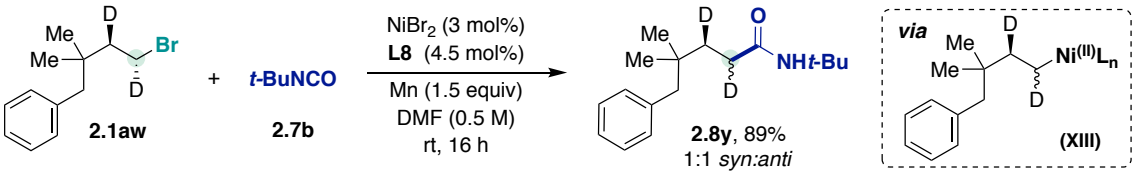

Scheme 2.20. Use of 2.1aw as a probe for the stereochemistry of the reaction

Further evidence for an oxidative addition via radical intermediates was obtained when a racemic mixture of products was obtained starting from enantioenriched secondary alkyl bromide **2.1av** (Scheme 2.21). Although low yields of the secondary amide were obtained – due to competitive β-hydride elimination that afforded large amounts of alkene side-products – this result further indicates the intermediacy of radical species. This hypothesis is in agreement with other Ni-catalyzed cross-couplings of unactivated alkyl halides.[22] Indeed, ample evidence for the involvement of radical intermediates has been found by the group of Weix[86] and Gong[14] in reductive cross-electrophile couplings, and by Fu and co-workers in Suzuki,[87] Hiyama[88] and Stille[89] cross-couplings. It is by taking advantage of the radical nature of the intermediates that Fu[90] and others[91] have developed various enantioselective cross-coupling protocols using secondary alkyl halides.

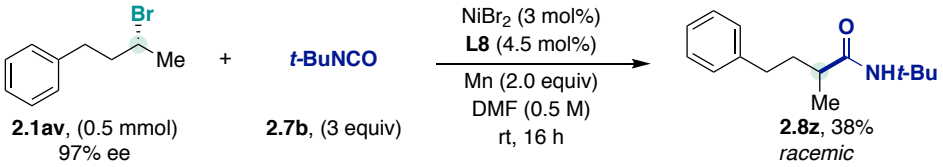

Scheme 2.21. Racemic mixture of amides obtained from an enantioenriched secondary alkyl bromide

Significant inhibition of the reaction was observed when radical scavengers, such as TEMPO and BHT, were added to the reaction mixture (Table 2.6). Although this result alone does not unambiguously indicate the intermediacy of radical species, it does lie in line with the hypothesis of a radical pathway for oxidative addition.

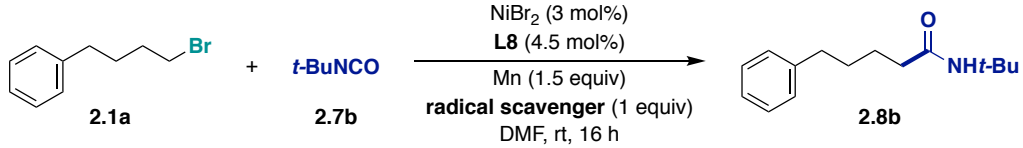

Entry	Conditions	Conversion of 2.1a (%)[a]	Yield of 2.8b (%)[a]
1	Control reaction (no radical scavenger added)[b]	100	95
2	Control reaction (no radical scavenger added)[c]	53	33
3	Tempo (added at t = 0)[b]	0	0
4	Tempo (added after 3h of reaction)[b]	50	27
5	BHT (added at t = 0)[b]	47	34
6	BHT (added after 3 h of reaction)[b]	93	71

Reaction conditions: 2.1a (0.50 mmol), **2.7b** (0.75 mmol), $NiBr_2$ (3 mol%), **L8** (4.5 mol%), Mn (0.75 mmol), DMF (1 mL) at rt, 16 h. [a] GC yield using *n*-decane as the internal standard. [b] Reaction quenched and analyzed after 16 h. [c] Reaction quenched and analyzed after 3 h.

Table 2.6. Effect of the addition of radical scavengers

The ratio of linear and cyclized products from 6-bromo-hex-1-en at different catalyst loadings has been previously used as a probe to study the mechanism of the oxidative addition step of traditional cross-couplings,[92] and of cross-electrophile couplings involving unactivated alkyl halides.[24,25] The oxidative addition of **2.1ax** via SET from Ni(0) results in an alkyl radical, which is prone to fast intramolecular cyclization to afford a second alkyl radical. Recombination of these species with Ni(I)—Br *en route* to alkyl—Ni(II)—Br species can take place via different pathways: in the case of the reductive amidation reaction, the formed alkyl radical could remain in the solvent cage and recombine with the same Ni(I)—Br (Scheme 2.22, right), or could escape from the solvent cage to recombine with a second Ni(I)—Br (Scheme 2.22, left). A constant relationship between the linear and cyclized products (**2.8aa/2.8ab**) at different catalyst loadings is expected for the cage-rebound mechanism, whereas a linear dependence should be observed in if the escape-rebound is operative, as higher Ni concentrations influence the lifetime of the linear radical.[92]

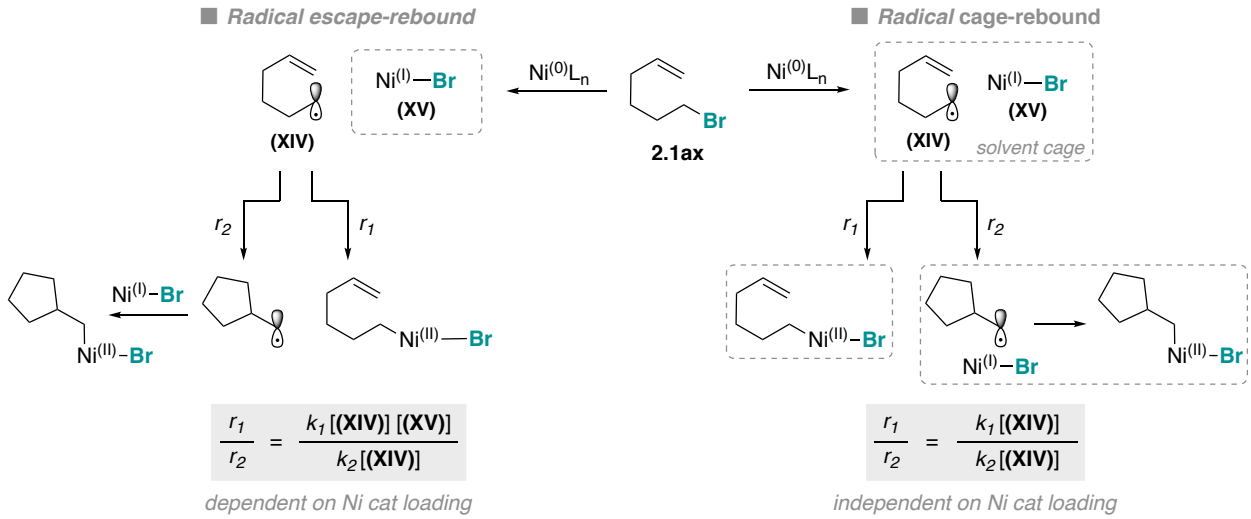

Scheme 2.22. Radical cage-rebound and radical escape-rebound mechanisms

When 6-bromo-hex-1-en was submitted to optimized reaction conditions, higher amounts of linear products were observed at lower catalyst loadings while no cyclized product was observed at 5 or 10 mol% catalyst (Table 2.7). The dependence of the **2.8aa/2.8ab** ratio on the Ni-catalyst loading suggest an escape-rebound mechanism. This result is in agreement with previous studies carried out in reductive cross-electrophile couplings of alkyl halides with aryl halides,[24] alkyl acids[25] and CO_2.[38]

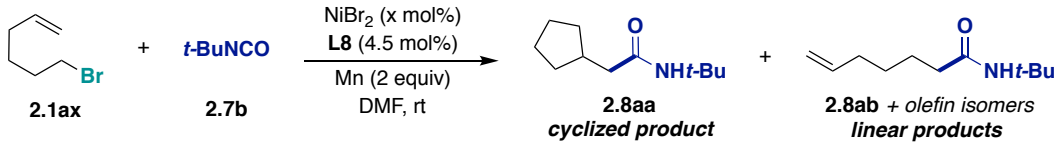

Entry	Ni-catalyst loading (mol%)	Linear/cyclized products ratio (%)[a]
1	1	8,6
2	2	23
3	3	50
4	5	-[b]
5	10	-[b]

Reaction conditions: 2.1ax(0.50 mmol), **2.7b** (0.75 mmol), $NiBr_2$ (x mol%), **L8** (1.5x mol%), Mn (1.0 mmol), DMF (1 mL) at rt, 16 h. [a] GC yield using *n*-decane as the internal standard. [b] No cyclized product was detected.

Table 2.7. Dependence on the Ni-catalyst loading of ratio of linear and cyclized amide products

2.3.4.2. Catalytic and Stoichiometric Experiments with Ni(0) and Ni(II) Complexes

Synthesis of Ni(0) and Ni(II) Complexes with 6,6'-dimethyl-2,2'-bipyridine:

Aiming to perform stoichiometric and catalytic studies with isolated Ni(bipyridine) complexes, large efforts were made to synthesize Ni(**L8**)$_2$ starting from Ni(COD)$_2$ and 6-methyl-2,2'-bipyridine (**L8**). Despite all attempts, the reactions failed to go to completion and mixtures of the desired Ni(**L8**)$_2$ complex, Ni(COD)$_2$, free ligand, and nickel black were consistently obtained. Unfortunately, changing the solvent, concentration, ligand equivalents, temperature, order of addition, amongst other variables had no positive effect, and the isolation of Ni(**L8**)$_2$ proved to be rather challenging. This is in sharp contrast to the formation and isolation of Ni(0) species with phenanthroline-type ligands, which are readily formed from mixtures of the free ligand and Ni(COD)$_2$ in solvents like THF.[93,94]

We thus turned our attention to the synthesis of Ni(**L9**)$_2$ starting from Ni(COD)$_2$ and 6,6'-dimethyl-2,2'-bipyridine (**L9**) (Scheme 2.23). Albeit in low yields, complex **2.14** could be isolated as a dark blue powder, which was characterized by ^{1}H and ^{13}C-NMR. X-ray quality crystals were grown from a saturated solution of the complex in pentane. The ORTEP representation below shows that the nickel atom adopts a distorted tetrahedral geometry. The angle between the planes of the two Ni(**L9**) chelate rings is 78.4 °, which is closer to the tetrahedral geometry (θ = 90 °) than what has been reported for Ni(bipyridine)$_2$ (θ = 51.2°, 47.8 °).[95] This is in line with the presence of *ortho*-substituents that force the geometry to adopt a conformation that minimizes steric hindrance. Interestingly, the average bond length between the carbon atoms that bind the two pyridine units in the ligands is 1.4438(13) Å, which is closer to the radical anion of non-coordinated bipyridine (bipy$^{-\cdot}$ = 1.432(3) Å)[96] than to the neutral ligand (bipy = 1.490(3) Å)[97], a trend that is also observed for Ni(bipyridine)$_2$.[95] Indeed, it has been proposed that Ni(0)-bis-bipyridine complexes are best described as [Ni(I)(bipyridine)^0(bipyridine)$^{-1}$]^0 in which an electron from the metal is delocalized in the two bipyridine moieties.[95,98]

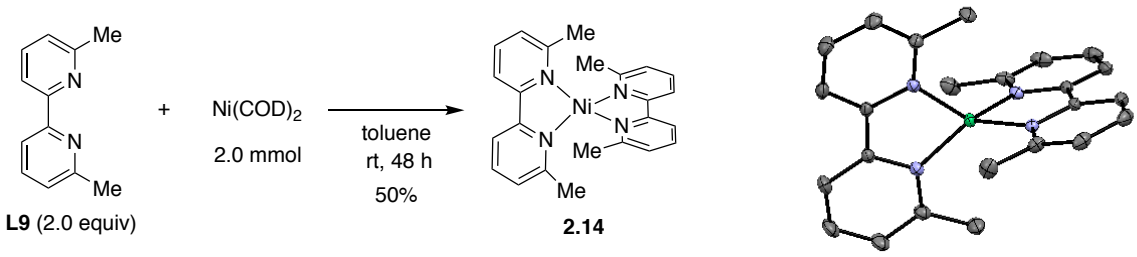

Scheme 2.23. Synthesis and ORTEP representation of Ni(L9)$_2$

Conversely, the synthesis of Ni(II)(bipyridine) complexes is more straightforward. Starting from anhydrous nickel bromide and **L9**, complex **2.15** was obtained as a bright pink-purple powder (Scheme 2.24). Although the paramagnetic character of **2.15** hampered the characterization using NMR techniques, X-ray quality crystals were obtained from a dichloromethane: hexanes (5:1) mixture or by slow evaporation from a saturated DMF solution. Ni(II)-complexes are known to adopt both square planar or tetrahedral geometries. In most of the cases a square planar geometry is favored as the 8 *d*-electrons are disposed in molecular orbitals with lower energy; however, depending on the type of coordinated ligands a change to a (distorted) tetrahedral geometry can be enforced.[99] This is the case of complex **2.15**, in which the nickel atom adopts a tetrahedral geometry (the angle between the planes of the Ni(**L9**) chelate rings and Br—Ni—Br is 90 °). This is likely due to the presence of bromine anions that are weak-field ligands and to the steric hindrance imparted by the methyl substituents of the ligand.

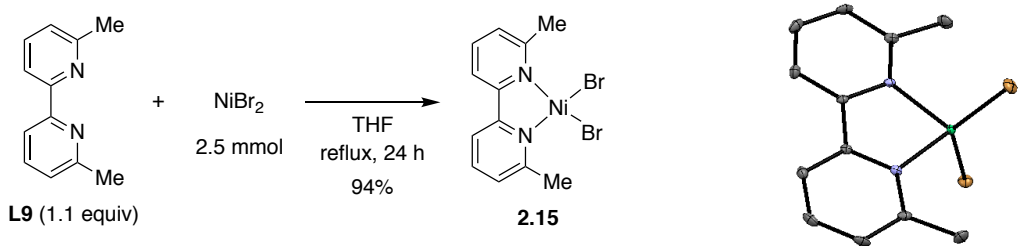

Scheme 2.24. Synthesis and ORTEP representation of Ni(L9)Br_2

Catalytic and Stoichiometric Experiments with Ni(0) and Ni(II) Complexes:

The catalytic competence of complexes **2.14** and **2.15** was evaluated to corroborate if comparable yields of amide **2.8v** were obtained when replacing the optimized catalytic system by the isolated Ni-complexes (Scheme 2.25). Indeed, compound **2.8v** was isolated in a slightly lower, but comparable yield, to those obtained in Scheme 2.12. The formation of β-hydride elimination, reduction and homodimerization products, as well as the formation of *N*-acylureas account for the mass balance.

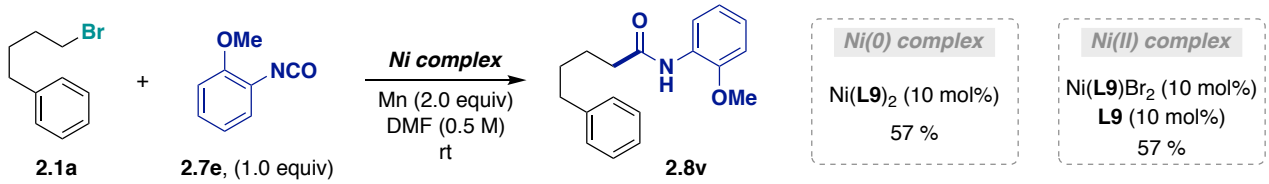

Scheme 2.25. Catalytic experiments with Ni(0) and Ni(II)-6,6'-dimethyl-2,2'-bipyridine complexes

Stoichiometric studies with Ni(II)-complex **2.15** revealed that, as expected, no reaction takes place in the absence of reducing agent, and that comparable yields of **2.8v** are obtained when two equivalents of Mn are used (Scheme 2.26). In parallel to what had been observed for the catalytic version of the transformation, the addition of one extra equivalent of ligand **L9** is necessary to minimize the formation of side-products (Scheme 2.13).

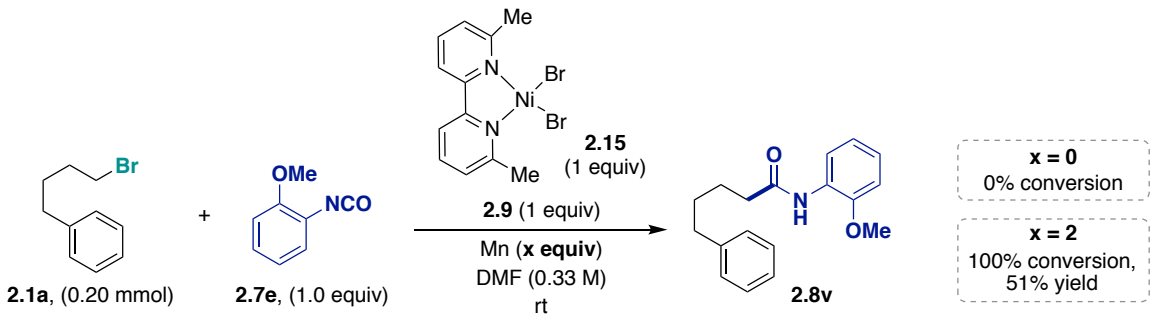

Scheme 2.26. Stoichiometric experiments with Ni(II)-6,6'-dimethyl-2,2'-bipyiridine complex

Subsequently, stoichiometric experiments with Ni(**L9**)$_2$ were performed to test the hypothesis of the intermediacy of alkyl—Ni(I) species formed via comproportionation of Ni(0)(**L9**)$_2$ and *in situ* generated alkyl—Ni(II) species. Interestingly, the use of stoichiometric amounts of Ni(**L9**)$_2$ provided compound **2.8v** regardless whether the reducing agent was added or not to the reaction mixture (Scheme 2.27). The formation of **2.8v** in the absence of Mn needs to be analyzed with precaution, as it does not allow to rule out unambiguously if alkyl—Ni(II) or —Ni(I) species precede isocyanate insertion. The lack of product formation in absence of Mn would have pointed towards the necessity of a comproportionation event to form alkyl—Ni(I) intermediates, which by their

enhanced nucleophilicity could be more prone to isocyanate insertion. Conversely, if a yield higher than 50% would have been obtained, the intermediacy of alkyl—Ni(II) species could have been supposed. However, the low yield and incomplete conversion observed are an ambigous result. Further experiments are required to answer the question whether primary alkyl—Ni(I) species are needed for isocyanate insertion. For example, two equivalents of complex **2.14** could be added to check if higher yields of **2.8v** are obtained. It would be highly interesting to isolate and characterize the reaction intermediates, as well as to evaluate if the ligand is acting as a redox non-innocent ligand by means of EPR spectroscopy and DFT studies.[100]

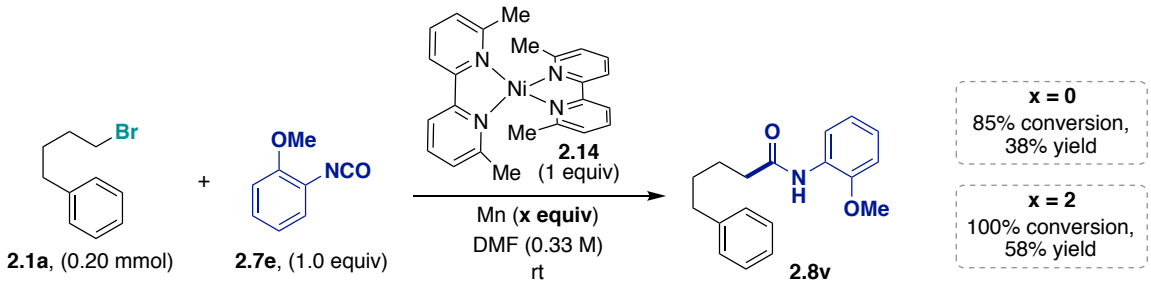

Scheme 2.27. Stoichiometric experiments with Ni(0) -6,6'-dimethyl-2,2'-bipyiridine complex

2.3.5. Plausible Reaction Mechanisms

The next two schemes show possible mechanisms for the developed Ni-catalyzed amidation of alkyl bromides with isocyanates. In both cases, reduction of Ni(II)Br_2 to Ni(0) is proposed to occur via two SET from Mn. This is followed by oxidative addition via SET from the nickel complex to the unactivated alkyl bromide to form an alkyl radical and a Ni(I)—Br species (**XIV**) and subsequent recombination leads to an alkyl—Ni(II)—Br intermediate (**XV**). The two proposed mechanisms then differ in the step that follows oxidative addition; in Scheme 2.28, coordination and isocyanate insertion occurs directly from the alkyl—Ni(II)—Br species (**XV**), whereas in Scheme 2.29 this intermediate is first reduced to afford an alkyl—Ni(I) species (**XIX**). Isocyanate insertion results in the formation of Ni-amidates **XVII** or **XXI**, which in a final step are reductively transmetallated with Mn to generate a Mn-amidate (**XVIII**) and the Ni(0) catalyst. Quenching of the Mn-amidate with a proton source or a suitable electrophile affords the desired products. However, it is important to mention that other mechanisms such as the intermediacy of organomanganese species,[13] and the direct addition of free-radicals to the isocyanates cannot be completely ruled out.[101]

Several details of the mechanisms presented above are worth mentioning: the identity of the Ni(0) species formed after Mn reduction is unknown. Given that the Ni to ligand stoichiometry added to the reaction when using 6-methyl-2,2'-bipyridine (**L8**) is Ni:L = 1:1.5, it is possible that a Ni(0)(**L**) species is formed, which could be stabilized by coordination of the isocyanate. As the best results are obtained with a Ni:L ratio of 1:2 when 6,6'-dimethyl-2,2'-bipyridine (**L9**) is used, a Ni(0)(**L9**)$_2$ species is also plausible in this case. As observed during the ligand screening, the *ortho*-substituents on the ligand have an important role on reactivity. It is very likely that the substituents influence the spatial arrangement of the intermediate Ni-species which would adopt a (distorted) tetrahedral geometry in order to minimize steric hindrance. This geometry is associated with lower reduction potentials, thus favoring the formation of Ni(I) species during the catalytic cycle.[102] The presence of *ortho*-substituents could also disfavor the coordination of two isocyanates to the Ni complex, which would result in the formation of undesired products. It would be interesting to study the effect of the structural changes of the ligand by means of DFT calculations.

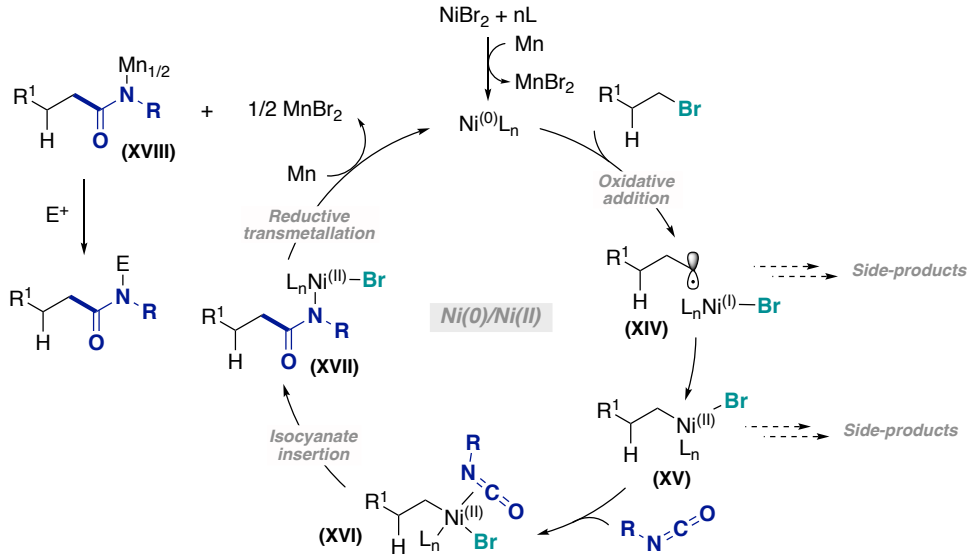

Scheme 2.28.Plausible reaction mechanism via isocyanate insertion to Ni(II) species

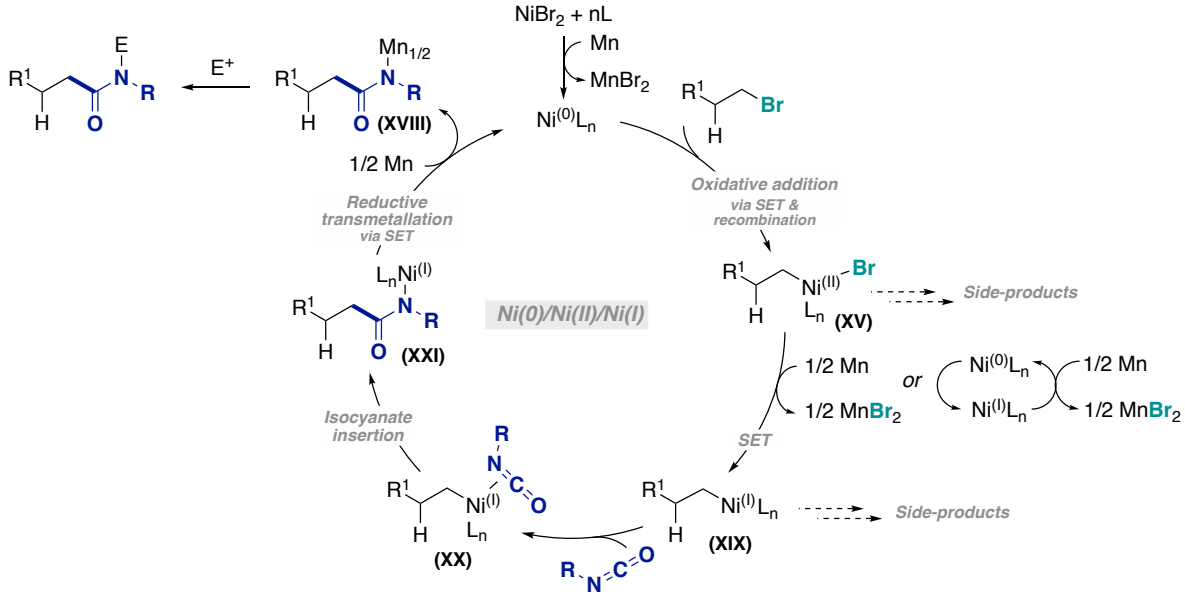

Scheme 2.29. Plausible reaction mechanism via isocyanate insertion to Ni(I) species

The reduction of the alkyl—Ni(II) species (**XV**) can occur via SET from Mn[103] or by comproportionation with Ni(0) species.[104–106] Currently, the experimental results do not allow to identify the more probable scenario. Furthermore, the intermediacy of alkyl—Ni(I) species has been postulated based on the results obtained from the stoichiometric experiments with Ni(0)(**L9**)$_2$ and Ni(II)(**L9**)Br$_2$ complexes in the presence and absence of Mn, but more solid experimental evidence needs to be gathered. It would be highly interesting to determine the reduction potential of these intermediates using cyclic voltammetry and to use them in stoichiometric experiments. However, the isolation of alkyl—Ni(II) oxidative addition complexes has proven rather challenging. For example, Yamamoto and co-workers described the synthesis of a Ni(Et)(X)(bipy) complex, which could be characterized but disproportionated in solution.[107] Vicic and co-workers reported the isolation of an oxidative addition complex of a Ni-terpyridine-type ligand and CH_3I, which lacks β-hydrogens.[23] Disappointing results were found by the authors when 1-iodo-3-phenylpropane was used, as no isolable Ni(II) complex was observed and instead the reaction yielded the homodimer product and NiL_2I_2. Weix and co-workers reported the synthesis and *in situ* use of Ni(C_8H_{17})(I)(**L10**), but no isolation data was given.[24] This is in contrast with the stability observed for

Ni(II)(bipy)(alkyl)$_2$,[108] and for oxidative addition complexes with aryl halides and Ni-complexes bearing bipyridine-type ligands,[24] both of which can be isolated.

As for the mass balance of the reaction, different side-products can be formed from either coupling partner: isocyanate decomposition can result in the formation of trimerization products (isocyanurates) catalyzed by Ni-, Mn-species or by the ligand.[68,71] This is one of the major factors that narrowed the scope of the isocyanates down as only sterically-hindered isocyanates, in which the formation of isocyanurates is prevented, could be successfully coupled under optimized reaction conditions. In some cases, the formation of urea, during the reaction or the work-up, challenged the isolation of the desired products. Possible side-products from the alkyl bromide are olefins, generated by β-hydride elimination, reduced product arising from protodemetallation, and homodimerization products that can be formed either by radical homocoupling or from the alkyl—Ni intermediates. In the latter case, C(sp^3)—C(sp^3) coupling of unactivated alkyl halides under Ni-catalyzed reductive conditions has been proposed to involve Ni(I) and Ni(III) intermediates.[23,30] Nevertheless, transmetallation from two alkyl—Ni(II) species or disproportionation from alkyl—Ni(I) and alkyl—Ni(II) intermediates cannot be ruled out in our case.[109]

2.4. Ni-Catalyzed Reductive Amidation of Unactivated Alkyl Chlorides

With the aim of developing a more general method for synthesis of aliphatic amides that includes the use of less reactive alkyl halides, a screening of the reaction conditions was performed using unactivated alkyl chlorides. The interest in unactivated alkyl chlorides as substrates is also based on the possibility of performing sequential transformations with polyhalogenated alkyl scaffolds as, due to their less reactive nature, alkyl chlorides remain generally untouched under traditional metal-catalyzed conditions. Because of the stronger C—X bond of the alkyl chlorides (BDE = 68±2 kcal/mol at 25 °C for CH_3Br vs. 81±5 kcal/mol for CH_3Cl),[39] which results in a more difficult oxidative addition, they present a markedly lower reactivity than alkyl bromides.

2.4.1. Optimization of the Reaction Conditions using Unactivated Alkyl Chlorides

The first approach towards the optimization of reaction conditions using alkyl chlorides was performed starting from the chlorinated analogue of **2.1a**, (4-chlorobutyl)benzene (Table 2.8). With this substrate, encouraging yields of primary amide **2.8b** were found under reaction conditions inspired on the carboxylation of alkyl chlorides developed by our group.[38] Although no reactivity was observed in the absence of additives, the addition of *tert*-butyl ammonium salts promoted the formation of the desired product.

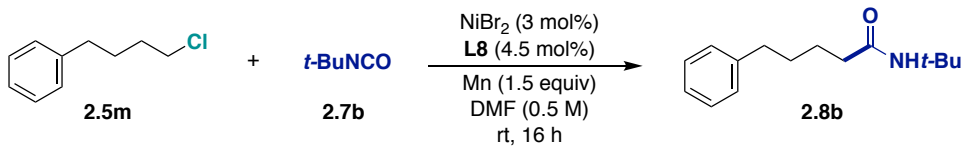

Entry	Deviation from Standard Conditions	Conversion of 2.5m (%)[a]	Yield of 2.8b (%)[a]
1	none	0	0
2	60 °C	0	traces
3	60 °C, TBAI (1 equiv)	86	44
4	40 °C, TBAB (1 equiv)	37	30
5	60 °C, TBAB (1 equiv)	100	55

Reaction conditions: 2.5m (0.25 mmol), **2.7b** (0.50 mmol), $NiBr_2$ (3.0 mol%), **L8** (4.5 mol%), Mn (0.38 mmol), DMF (0.5 mL) at rt, 16 h. [a] GC-FID conversion and yield using *n*-decane as internal standard.

Table 2.8. Preliminary results obtained for the amidation of alkyl chlorides

Encouraged by these results, a more detailed screening was performed using commercially available 1-chloroheptane. The first variable to be evaluated was the reaction temperature in the presence of TBAB or NaI – two of the successful additives for the carboxylation of alkyl chlorides (Table 2.9).[38] Entries 2 and 6 show that a slightly higher selectivity between the amidation product and undesired side-products is achieved at 40 °C. Although some reactivity is also obtained at higher temperatures, this experimental result lies in line with previous observations made during this Thesis regarding the deleterious influence of higher temperatures on the amidation with isocyanates and nickel-bipyridine complexes. This is in contrast to what has been observed in our group for different carboxylations with CO_2 using Ni complexes bearing less-flexible phenanthroline-type ligands and even bipyridine-type ligands.[36,38,110–113] One might suspect the increased propensity of isocyanates to undergo side-reactions at high temperatures to be the main cause of the deleterious defect; however, a combination of the type of substrate, the ligand and the isocyanate's intrinsic reactivity are more likely to be the cause, as successful amidations with isocyanates have been performed at temperatures as high as 140 °C (vide Chapter 1).[66,81] As for the mass balance, the remaining of the conversion of **2.5n** led to the formation of heptene isomers and in some cases of dimers. High amounts of urea and oxalamide from *tert*-butyl isocyanate were detected in the reaction crudes, as well.

Next, the effect of different halide salts was studied at 40 °C but with longer reaction times in order to check if further conversion of **2.5n** was reached (Table 2.10). Similar results were found in the presence of TBAB, TBAI and NaI (entries 1, 2 and 7). Aiming to boost up the yield, three equivalents of *tert*-butyl isocyanate were added to reactions containing these additives but no improvement was observed (yields in parenthesis). As the remaining *tert*-butyl isocyanate cannot be reliably quantified due to the acidic work-up of the reaction and the analytic technique used, it is not possible to hypothesize if the unchanged yield is due to degradation of the isocyanate at early stages of the reaction or to catalyst decomposition. Nevertheless, this observation points towards a mismatch between the low reactivity of the alkyl chloride and the current amidation conditions.

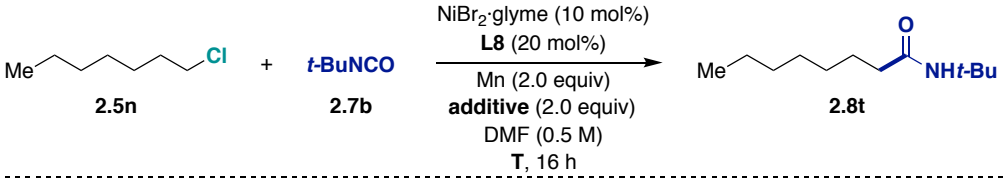

Entry	Additive	Temperature	Conversion of 2.5n (%)[a]	Yield of 2.8t (%)[a]
1	TBAB	30	20	8
2		40	45	20
3		50	58	21
4		60	55	7
5	NaI	30	12	4
6		40	29	10
7		50	65	6
8		60	93	5

Reaction conditions: 2.5n (0.25 mmol), **2.7b** (0.38 mmol), $NiBr_2$·glyme (10 mol%), **L8** (20 mol%), Mn (0.50 mmol), additive (2 equiv), DMF (0.5 mL), 16 h. [a] GC-FID conversion and yield using *n*-decane as internal standard.

Table 2.9. Screening of temperatures in the presence of TBAB and NaI as additives

As previously mentioned in the introduction of this Chapter, halide-containing additives have been used in different reductive cross-electrophile couplings to improve the reactivity of the system when using aryl and alkyl chlorides as starting materials.[40–44] It has been proposed that the extra halides can serve as bridging ligands that

favor inner-sphere electron transfer processes.[45,46] Although traces of 1-bromoheptane were detected by GC-MS using TBAB as additive, which could indicate that a Finkelstein reaction is taking place to form the alkyl bromide that further reacts to afford the desired amide, there is currently not enough information to elucidate the exact role of the additive.

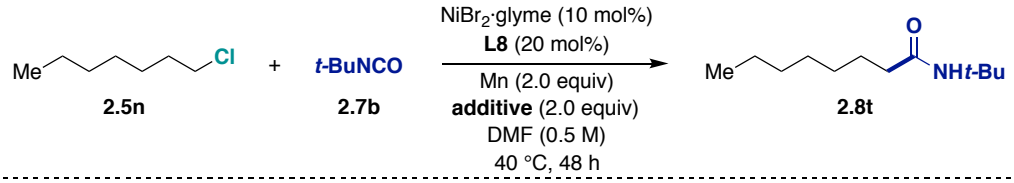

Entry	Additive	Conversion of 2.5n (%)[a]	Yield of 2.8t (%)[a]
1	TBAB	71 (72)	29 (28)
2	TBAI	66 (74)	24 (27)
3	TBAC	38	4
4	LiCl	21	1
5	LiBr	60	11
6	NaBr	64	19
7	NaI	68 (75)	22 (25)
8	$MgBr_2$	50	0
9	$MgCl_2$	23	0
10	none	12	0

Reaction conditions: 2.5n (0.25 mmol), **2.7b** (0.38 mmol), $NiBr_2$·glyme (10 mol%), **L8** (20 mol%), Mn (0.50 mmol), additive (1 equiv), DMF (0.5 mL) at 40 °C, 48h. [a] GC-FID conversion and yield using *n*-decane as internal standard. Yields in parenthesis correspond to the use of 3 equiv of **2.7b**.

Table 2.10. Screening of halide salts as additives

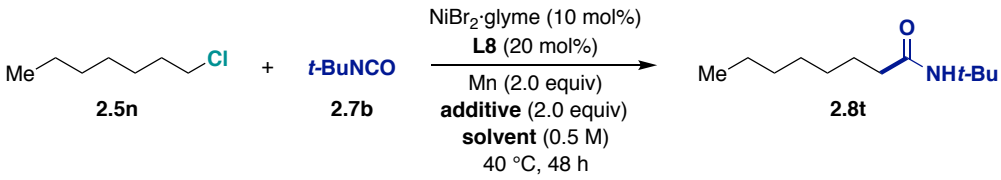

Entry	Additive	Solvent	Conversion of 2.5n (%)[a]	Yield of 2.8t (%)[a]
1		DMF	66	26
2	TBAB	DMA	81	29
3		NMP	90	37
4		DMF	66	23
5	TBAI	DMA	79	26
6		NMP	84	31
7		DMF	69	22
8	NaI	DMA	86	27
9		NMP	89	28

Reaction conditions: 2.5n (0.25 mmol), **2.7b** (0.38 mmol), $NiBr_2$·glyme (10 mol%), **L8** (20 mol%), Mn (0.50 mmol), additive (1 equiv), solvent (0.5 mL) at 25 °C, 48 h. [a] GC-FID conversion and yield using *n*-decane as internal standard.

Table 2.11. Screening of solvents using different halide salts as additives

The optimization of the reaction conditions was continued by performing the reaction in different solvents and in the presence of the best additives found during the previous screenings (Table 2.11). The three amide-containing solvents tested were chosen as they had previously afforded good reactivity in the amidations

reactions, as well as in many of the carboxylation reactions developed by our group. Though no striking differences were found, a slightly better yield was obtained in NMP using TBAB as additive (entry 3). As mentioned throughout this Thesis, these solvents have high dielectric constants[73] that help stabilize ionic reaction intermediates. Moreover, studies performed with Pd[74] and Ni[75,76] complexes have pointed out the preferable formation of cationic reaction intermediates in solvents such as DMSO, acetonitrile and DMF, in which the solvent can coordinate and help stabilize the metal center.

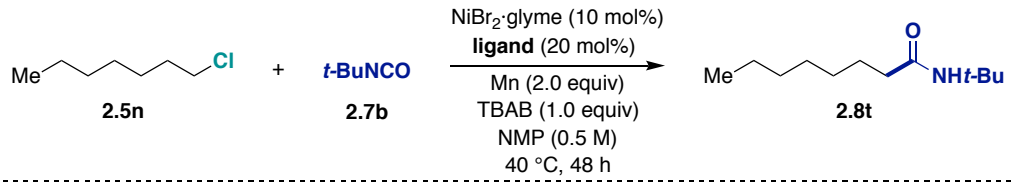

Entry	Ligand	Conversion of 2.5n (%)[a]	Yield of 2.8t (%)[a]
1	2,2'-bipyridine (**L7**)	93	33
2	6-methyl-2,2'-bipyridine (**L8**)	90	37
3	6,6'-dimethyl-2,2'-bipyridine (**L9**)	100	23
4	6-methyl-4,4'-diphenyl-2,2'-bipyridine (**L14**)	89	33
5	6-methyl-4,4'-dimethyl-2,2'-bipyridine (**L15**)	92	28
6	6,6'-dimethyl-4,4'-diphenyl-2,2'-bipyridine (**L16**)	100	16
7	4,4'-bis(4-methoxyphenyl)-6,6'-dimethyl-2,2'-bipyridine (**L17**)	100	24
8	5,5'-dimethyl-2,2'-bipyridine (**L18**)	91	39
9	neocuproine (**L2**)	100	20
10	bathocuproine (**L5**)	94	15
11	1,10-phenanthroline (**L11**)	88	19
12	2-methyl-1,10-phenanthroline (**L19**)	90	16
13	6,6''-dimethyl-2,2':6',2''-terpyridine (**L12**)	100	25
14	PPh_3 (**L13**)	96	27
15	dppf (**L20**)	92	15

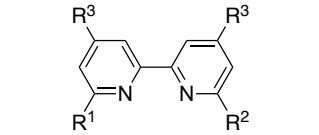

R^1, R^2, R^3 = H, **L7**
R^1 = Me; R^2, R^3 = H, **L8**
R^1, R^2 = Me; R^3 = H, **L9**
R^1 = Me; R^2 = H; R^3 = Ph, **L14**
R^1 = Me; R^2 = H; R^3 = Me, **L15**
R^1, R^2 = Me; R^3 = Ph, **L16**
R^1, R^2 = Me; R^3 = *p*-OMePh, **L17**

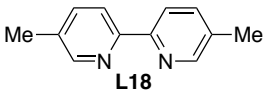

L18

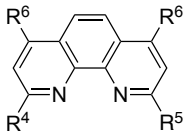

R^4, R^5 = Me; R^6 = H, **L2**
R^4, R^5 = Me; R^6 = Ph, **L5**
R^4, R^5, R^6 = H, **L11**
R^4 = Me; R^5, R^6 = H, **L19**

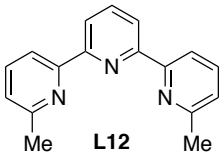

L12

Reaction conditions: 2.5n (0.25 mmol), **2.7b** (0.38 mmol), $NiBr_2$·glyme (10 mol%), ligand (20 mol%), Mn (0.50 mmol), TBAB (1 equiv), NMP (0.5 mL) at 40 °C, 48 h. [a] GC-FID conversion and yield using *n*-decane as internal standard.

Table 2.12. Screening of nitrogen-containing ligands in the presence of TBAB

With these new conditions, a set of bipyridine-, phenanthroline-type and phosphine ligands was screened (Table 2.12, selected ligands shown). In contrast to the amidation of primary alkyl bromides (vide supra), a broader range of ligands afforded the amidation of **2.5n**. Specifically, for the alkyl bromides no reactivity had been observed with most of the ligands that lacked *ortho*-substituents, terpyridines or even phosphine ligands. The similar yields obtained with several of the ligands shown in Table 2.12 are an encouraging result. However, their striking contrast with the previous screening for the alkyl bromide calls for a re-confirmation. If reproducible,

these results might indicate that the amidation of primary alkyl chlorides could be performed with ligands different than bipyridines. This could potentially unlock the use of other isocyanates, as is the case of the amidations using phosphine ligands that tolerate a wider range of isocyanates (vide Chapter 1).

A final screening of different nickel sources was performed using 6-methyl-2,2'-bipyridine (**L8**). Higher yields and a better selectivity were found when using nickel iodide (Table 2.13, entry 1). Other nickel sources, except for $NiBr_2$ and Ni(acac) gave good results, but with lower amounts of the desired amide. As opposed to the results observed with the alkyl bromides, the nature of the nickel counteranion does not seem to have such an important role. This is probably due to the presence of one equivalent of TBAB which ensures that sufficient bromide ions are present in the reaction media. Lastly, having identified NiI_2 as better nickel source, it would be worth to perform a second iteration to evaluate different additives and ligands. Other parameters such as the concentration of the reaction, the reducing agent and the equivalents of the different variables, could as well help achieve a more efficient amidation of unactivated alkyl chlorides.

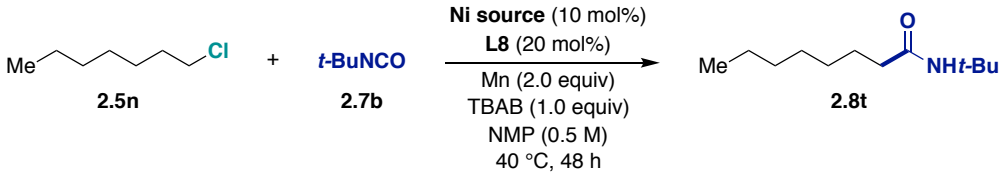

Entry	Ni source	Conversion of 2.5n (%)[a]	Yield of 2.8t (%)[a]
1	NiI_2	64	51
2	$NiBr_2$·diglyme	73	51
3	$NiBr_2$·glyme	74	38
4	$NiBr_2$	55	4
5	$NiCl_2$·glyme	69	47
6	$NiCl_2$	67	47
7	$Ni(acac)_2$	34	6
8	[(TMEDA)Ni(*o*-tolyl)Cl]	76	42

Reaction conditions: 2.5n (0.25 mmol), **2.7b** (0.38 mmol), Ni source (10 mol%), **L8** (20 mol%), Mn (0.50 mmol), TBAB (1 equiv), NMP (0.5 mL) at 40 °C, 48 h. [a] GC-FID conversion and yield using *n*-decane as internal standard.

Table 2.13. Screening of nickel sources in the presence of TBAB

2.5. Conclusions

This chapter summarizes the efforts towards the development of a Ni-catalyzed reductive amidation of unactivated primary alkyl halides with isocyanates. Starting from alkyl bromides and using a catalytic system based on the combination of nickel bromide, bipyridine-type ligands and Mn as the reducing agent, the competitive side-reactions common to unactivated alkyl electrophiles could be surmounted and good yields of the desired aliphatic amides were achieved. The mild reaction conditions characteristic of reductive cross-electrophile coupling protocols allowed for a broad functional group tolerance and for the coupling of alkyl and aryl isocyanates. However, under optimized reaction conditions only bulky, electron rich isocyanates could be used as coupling partners, representing one of the major drawbacks of the developed methodology. A formal cross-coupling reaction of three different electrophiles in a one-pot fashion was developed by the sequential addition of a third electrophile, which quenches the product of the reaction. With this strategy, hindered *N*-tertiary amides and *N*-methyl-amides could easily be prepared. Preliminary mechanistic studies suggested that oxidative addition occurs via radical intermediates, and that alkyl—Ni(I) species might be involved in the reaction and precede isocyanate insertion. Further mechanistic studies are still needed to fully unveil the elementary steps of the mechanism. Finally, preliminary results for the amidation of unactivated alkyl chlorides in the presence of TBAB are described. The encouraging yields obtained with different ligands could potentially unlock the coupling of a broader scope of isocyanates.

The use of Mn as reducing agent could be viewed as a drawback as H_2 is generated upon quenching of the reaction. Inspired by our findings, in 2017 the Molander group designed a dual Ni/photoredox method for the coupling of alkylsilicates and (thio)isocyanates that circumvents the use of metal powders as reducing agents.[114] The main advantage of this method is the wide scope of isocyanates, as the yields of the desired aliphatic amides were often moderate and the synthesis of alkylsilicates is less attractive from a synthetic and economic standpoint than the use of alkyl halides and Mn.

2.6. Bibliography

1. Cárdenas, D. J. Towards Efficient and Wide-Scope Metal-Catalyzed Alkyl-Alkyl Cross-Coupling Reactions. *Angew. Chem. Int. Ed.* **38,** 3018–3020 (1999).
2. Cárdenas, D. J. Advances in Functional-Group-Tolerant Metal-Catalyzed Alkyl-Alkyl Cross-Coupling Reactions. *Angew. Chem. Int. Ed.* **42,** 384–387 (2003).
3. Kambe, N., Iwasaki, T. & Terao, J. Pd-catalyzed cross-coupling reactions of alkyl halides. *Chem. Soc. Rev.* **40,** 4937–4947 (2011).
4. Crabtree, R. H. *The Organometallic Chemistry of the Transition Metals*. (John Wiley & Sons, Inc., 2014).
5. Ishiyama, T., Abe, S., Miyaura, N. & Suzuki, A. Palladium-Catalyzed Alkyl-Alkyl Cross-Coupling Reaction of 9-Alkyl-9-BBN Derivatives with Iodoalkanes Possessing β-Hydrogens. *Chem. Lett.* **21,** 691–694 (1992).
6. Devasagayaraj, A., Stüedemann, T. & Knochel, P. A New Nickel-Catalyzed Cross-Coupling Reaction Between sp^3 Carbon Centers. *Angew. Chem. Int. Ed.* **34,** 2723–2725 (1995).
7. Giovannini, R., Stüdemann, T., Dussin, G. & Knochel, P. An Efficient Nickel-Catalyzed Cross-Coupling Between sp3 Carbon Centers. *Angew. Chem. Int. Ed.* **37,** 2387–2390 (1998).
8. Luh, T.-Y., Leung, M.-K. & Wong, K.-T. Transition metal-catalyzed activation of aliphatic C-X bonds in carbon-carbon bond formation. *Chem. Rev.* **100,** 3187–3204 (2000).
9. Frisch, A. C. & Beller, M. Catalysts for Cross-Coupling Reactions with Non-activated Alkyl Halides. *Angew. Chem. Int. Ed.* **44,** 674–688 (2005).
10. Jana, R., Pathak, T. P. & Sigman, M. S. Advances in transition metal (Pd,Ni,Fe)-catalyzed cross-coupling reactions using alkyl-organometallics as reaction partners. *Chem. Rev.* **111,** 1417–1492 (2011).
11. Hu, X. Nickel-catalyzed cross coupling of non-activated alkyl halides: a mechanistic perspective. *Chem. Sci.* **2,** 1867 (2011).
12. Choi, J. & Fu, G. C. Transition Metal-Catalyzed Alkyl-Alkyl Bond Formation: Another Dimension in Cross-Coupling Chemistry. *Science* **356,** eaaf7230 (2017).
13. Knappke, C. E. I. *et al.* Reductive Cross-Coupling Reactions between Two Electrophiles. *Chem. Eur. J.* **20,** 6828–6842 (2014).
14. Wang, X., Dai, Y. & Gong, H. Nickel-Catalyzed Reductive Couplings. *Top. Curr. Chem.* **374,** 43 (2016).
15. Richmond, E. & Moran, J. Recent Advances in Nickel Catalysis Enabled by Stoichiometric Metallic Reducing Agents. *Synthesis* **50,** 499–513 (2018).
16. Duan, Z., Li, W. & Lei, A. Nickel-Catalyzed Reductive Cross-Coupling of Aryl Bromides with Alkyl Bromides: Et_3N as the Terminal Reductant. *Org. Lett.* **18,** 4012–4015 (2016).
17. McCallum, T. & Barriault, L. Direct alkylation of heteroarenes with unactivated bromoalkanes using photoredox gold catalysis. *Chem. Sci.* **7,** 4754–4758 (2016).
18. Zhang, P., Le, C. C. & MacMillan, D. W. C. Silyl Radical Activation of Alkyl Halides in Metallaphotoredox Catalysis: A Unique Pathway for Cross-Electrophile Coupling. *J. Am. Chem. Soc.* **138,** 8084–8087 (2016).
19. Netherton, M. R. & Fu, G. C. Suzuki Cross-Couplings of Alkyl Tosylates that Possess β Hydrogen Atoms: Synthetic and Mechanistic Studies. *Angew. Chem. Int. Ed.* **41,** 3910–3912 (2002).
20. Stokes, B. J., Opra, S. M. & Sigman, M. S. Palladium-Catalyzed Allylic Cross-Coupling Reactions of Primary and Secondary Homoallylic Electrophiles. *J. Am. Chem. Soc.* **134,** 11408–11411 (2012).
21. Liu, Q. *et al.* Recent Advances on Palladium Radical Involved Reactions. *ACS Catalysis* **5,** 6111–6137 (2015).
22. Anderson, T. J., Jones, G. D. & Vicic, D. A. Evidence for a NiI Active Species in the Catalytic Cross-Coupling of Alkyl Electrophiles. *J. Am. Chem. Soc.* **126,** 8100–8101 (2004).
23. Jones, G. D., McFarland, C., Anderson, T. J. & Vicic, D. A. Analysis of Key Steps in the Catalytic Cross-Coupling of Alkyl Electrophiles under Negishi-like Conditions. *Chem. Commun.* **0,** 4211–4213 (2005).
24. Biswas, S. & Weix, D. J. Mechanism and Selectivity in Nickel-Catalyzed Cross-Electrophile Coupling of Aryl Halides with Alkyl Halides. *J. Am. Chem. Soc.* **135,** 16192–16197 (2013).
25. Zhao, C., Jia, X., Wang, X. & Gong, H. Ni-Catalyzed Reductive Coupling of Alkyl Acids with Unactivated Tertiary Alkyl and Glycosyl Halides. *J. Am. Chem. Soc.* **136,** 17645–17651 (2014).
26. Wurtz, A. Ueber eine neue Klasse organischer Radicale. *Ann. Chem.* **96,** 364–375 (1855).
27. Tollens, B. & Fittig, R. Ueber die Synthese der Kohlenwasserstoffe der Benzolreihe. *Justus Liebigs Ann. Chem.* **131,** 303–323 (1864).
28. Everson, D. A., Shrestha, R. & Weix, D. J. Nickel-Catalyzed Reductive Cross-Coupling of Aryl Halides with Alkyl Halides. *J. Am. Chem. Soc.* **132,** 920–921 (2010).
29. Amatore, M. & Gosmini, C. Direct Method for Carbon-Carbon Bond Formation: The Functional Group Tolerant Cobalt-Catalyzed Alkylation of Aryl Halides. *Chem. Eur. J.* **16,** 5848–5852 (2010).
30. Prinsell, M. R., Everson, D. A. & Weix, D. J. Nickel-catalyzed, sodium iodide-promoted reductive dimerization of alkyl halides, alkyl pseudohalides, and allylic acetates. *Chem. Commun.* **46,** 5743–5745 (2010).
31. Goldup, S. M., Leigh, D. A., McBurney, R. T., McGonigal, P. R. & Plant, A. Ligand-assisted nickel-catalysed sp^3–sp^3 homocoupling of unactivated alkyl bromides and its application to the active template synthesis of rotaxanes. *Chem. Sci.* **1,** 383–386 (2010).
32. Yu, X., Yang, T., Wang, S., Xu, H. & Gong, H. Nickel-Catalyzed Reductive Cross-Coupling of Unactivated Alkyl Halides. *Org. Lett.* **13,** 2138–2141 (2011).
33. Xu, H., Zhao, C., Qian, Q., Deng, W. & Gong, H. Nickel-catalyzed cross-coupling of unactivated alkyl halides using bis(pinacolato)diboron as reductant. *Chem. Sci.* **4,** 4022–4029 (2013).

34. Gu, J., Wang, X., Xue, W. & Gong, H. Nickel-catalyzed reductive coupling of alkyl halides with other electrophiles: concept and mechanistic considerations. *Org. Chem. Front.* **2,** 1411–1421 (2015).
35. Anka-Lufford, L. L., Huihui, K. M. M., Gower, N. J., Ackerman, L. K. G. & Weix, D. J. Nickel-Catalyzed Cross-Electrophile Coupling with Organic Reductants in Non-Amide Solvents. *Chem. Eur. J.* **22,** 11564–11567 (2016).
36. Liu, Y., Cornella, J. & Martin, R. Ni-Catalyzed Carboxylation of Unactivated Primary Alkyl Bromides and Sulfonates with CO_2. *J. Am. Chem. Soc.* **136,** 11212–11215 (2014).
37. Börjesson, M., Moragas, T., Gallego, D. & Martin, R. Metal-Catalyzed Carboxylation of Organic (Pseudo)halides with CO_2. *ACS Catalysis* **6,** 6739–6749 (2016).
38. Börjesson, M., Moragas, T. & Martin, R. Ni-Catalyzed Carboxylation of Unactivated Alkyl Chlorides with CO_2. *J. Am. Chem. Soc.* **138,** 7504–7507 (2016).
39. *Bond Dissociation Energies in Simple Molecules*. (ed. Darwent, B. deB) (National Bureau of Standars, 1970).
40. Iyoda, M., Sakaitan, M., Otsuka, H. & Oda, M. Reductive Coupling of Benzyl Halides Using Nickel(0)-Complex Generated in situ in the Presence of Tetraethylammonium Iodide, a Simple and Convenient Synthesis of Bibenzyls. *Chem. Lett.* **14,** 127–130 (1985).
41. Zembayashi, M., Tamao, K., Yoshida, J. & Kumada, M. Nickel-Phosphine Complex-Catalyzed Homo Coupling of Aryl Halides in the Presence of Zinc Powder. *Tetrahedron Lett.* **18,** 4089–4091 (1977).
42. Iyoda, M., Otsuka, H., Sato, K., Nisato, N. & Oda, M. Homocoupling of Aryl Halides Using Nickel(II) Complex and Zinc in the Presence of Et4NI. An Efficient Method for the Synthesis of Biaryls and Bipyridines. *Bull. Chem. Soc. Jpn.* **63,** 80–87 (1990).
43. Fujihara, T., Nogi, K., Xu, T., Terao, J. & Tsuji, Y. Nickel-catalyzed carboxylation of aryl and vinyl chlorides employing carbon dioxide. *J. Am. Chem. Soc.* **134,** 9106–9109 (2012).
44. Colon, I. & Kelsey, D. R. Coupling of Aryl Chlorides by Nickel and Reducing Metals. *J. Org. Chem.* **51,** 2627–2637 (1986).
45. Taube, H. & Gould, E. S. Organic Molecules as Bridging Groups in Electron-Transfer Reactions. *Acc. Chem. Res.* **2,** 321–329 (1969).
46. Sutin, N. Free Energies, Barriers, and Reactivity Patterns in Oxidation-Reduction Reactions. *Acc. Chem. Res.* **1,** 225–231 (1968).
47. Moragas, T. & Martin, R. Nickel-Catalyzed Reductive Carboxylation of Cyclopropyl Motifs with Carbon Dioxide. *Synthesis* **48,** 2816–2822 (2016).
48. Amatore, C. & Jutand, A. Activation of Carbon Dioxide by Electron Transfer and Transition Metals. Mechanism of Nickel-Catalyzed Electrocarboxylation of Aromatic Halides. *J. Am. Chem. Soc.* **113,** 2819–2825 (1991).
49. León, T., Correa, A. & Martin, R. Ni-Catalyzed Direct Carboxylation of Benzyl Halides with CO_2. *J. Am. Chem. Soc.* **135,** 1221–1224 (2013).
50. Lyaskovskyy, V. & De Bruin, B. Redox Non-Innocent Ligands: Versatile New Tools to Control Catalytic Reactions. *ACS Catal.* **2,** 270–279 (2012).
51. Wang, X., Liu, Y. & Martin, R. Ni-Catalyzed Divergent Cyclization/Carboxylation of Unactivated Primary and Secondary Alkyl Halides with CO_2. *J. Am. Chem. Soc.* **137,** 6476–6479 (2015).
52. Coldham, I., Dufour, S., Haxell, T. F. N., Patel, J. J. & Sanchez-Jimenez, G. Dynamic Thermodynamic and Dynamic Kinetic Resolution of 2-Lithiopyrrolidines. *J. Am. Chem. Soc.* **128,** 10943–10951 (2006).
53. Schäfer, G., Matthey, C. & Bode, J. W. Facile Synthesis of Sterically Hindered and Electron-Deficient Secondary Amides from Isocyanates. *Angew. Chem. Int. Ed.* **51,** 9173–9175 (2012).
54. Yang, H. *et al.* Reaction of Organozinc Halides with Aryl Isocyanates. *Tetrahedron* **69,** 2588–2593 (2013).
55. Haraguchi, R. & Matsubara, S. Catalytic Asymmetric Aldol-Type Reaction of Zinc Enolate Equivalent of Amides. *Org. Lett.* **15,** 3378–3380 (2013).
56. Dagousset, G. *et al.* Diastereoselective Synthesis of Open-Chain Secondary Alkyllithium Compounds and Trapping Reactions with Electrophiles. *Angew. Chem. Int. Ed.* **53,** 1425–1429 (2014).
57. Fang, X., Jackstell, R. & Beller, M. Selective Palladium-Catalyzed Aminocarbonylation of Olefins with Aromatic Amines and Nitroarenes. *Angew. Chem. Int. Ed.* **52,** 14089–14093 (2013).
58. Jiménez-Rodriguez, C. *et al.* Selective Formation of α,ω-Ester Amides from the Aminocarbonylation of Castor Oil Derived Methyl 10-Undecenoate and Other Unsaturated Substrates. *Catal. Sci. Technol.* **4,** 2332–2339 (2014).
59. Liu, H., Yan, N. & Dyson, P. J. Acid-Free Regioselective Aminocarbonylation of Alkenes. *Chem. Commun.* **50,** 7848–7851 (2014).
60. Ryu, I. *et al.* Metal Catalyst-Free by Design. The Synthesis of Amides from Alkyl Iodides, Carbon Monoxide and Amines by a Hybrid Radical/Ionic Reaction. *Chem. Commun.* **0,** 1953–1954 (1998).
61. Fukuyama, T., Inouye, T. & Ryu, I. Atom Transfer Carbonylation Using Ionic Liquids as Reaction Media. *J. Organomet. Chem.* **692,** 685–690 (2007).
62. Zhang, G., Gao, B. & Huang, H. Palladium-Catalyzed Hydroaminocarbonylation of Alkenes with Amines: A Strategy to Overcome the Basicity Barrier Imparted by Aliphatic Amines. *Angew. Chem. Int. Ed.* **54,** 7657–7661 (2015).
63. Dong, K. *et al.* Rh(I)-Catalyzed Hydroamidation of Olefins via Selective Activation of N-H Bonds in Aliphatic Amines. *J. Am. Chem. Soc.* **137,** 6053–6058 (2015).
64. Liu, J. *et al.* Selective Palladium-Catalyzed Aminocarbonylation of Olefins to Branched Amides. *Angew. Chem. Int. Ed.* **55,** 13544–13548 (2016).
65. Tortajada, A., Juliá-Hernández, F., Börjesson, M., Moragas, T. & Martin, R. Transition Metal-Catalyzed Carboxylation Reactions with carbon Dioxide. *Angew. Chem. Int. Ed.* (2018). doi:10.1002/anie.201803186
66. Correa, A. & Martin, R. Ni-Catalyzed Direct Reductive Amidation via C-O Bond Cleavage. *J. Am. Chem. Soc.* **136,** 7253–7256 (2014).
67. Schleicher, K. D. & Jamison, T. F. Nickel-Catalyzed Synthesis of Acrylamides from α-Olefins and Isocyanates. *Org. Lett.*

9, 875–878 (2007).
68. Villa, J. F. & Powell, H. B. The Reaction of Some Inorgainc Lewis Bases and Acids with Organic Isocyanates. *Synth. React. Inorg. Met. Chem.* **6,** 59–63 (1976).
69. Lacey, R. N. The Acid-Catalysed Heterolysis of Amides with Alkyl- Nitrogen Fission (AAL). *J. Chem. Soc.* **0,** 1633–1639 (1960).
70. Mahalingam, A. K., Wu, X. & Alterman, M. Convenient Removal of N-tert-butyl from Amides with Scandium Triflate. *Tetrahedron Lett.* **47,** 3051–3053 (2006).
71. Braunstein, P. & Nobel, D. Transition-Metal-Mediated Reactions of Organic Isocyanates. *Chem. Rev.* **89,** 1927–1945 (1989).
72. Chen, F. *et al.* Remote Migratory Cross-Electrophile Coupling and Olefin Hydroarylation Reactions Enabled by in situ Generation of NiH. *J. Am. Chem. Soc.* **139,** 13929–13935 (2017).
73. *CRC Handbook of Chemistry and Physics*. (ed. Lide, D. R.) (CRC Press, 2003).
74. Jutand, A. The Use of Conductivity Measurements for the Characterization of Cationic Palladium(II) Complexes and for the Determination of Kinetic and Thermodynamic Data in Palladium-Catalyzed Reactions. *Eur. J. Inorg. Chem.* **2003,** 2017–2040 (2003).
75. Klein, A. *et al.* Halide ligands - More than just σ-donors? A structural and spectroscopic study of homologous organonickel complexes. *Inorg. Chem.* **47,** 11324–11333 (2008).
76. Feth, M. P., Klein, A. & Bertagnolli, H. Investigation of the Ligand Exchange Behavior of Square-Planar Nickel(II) Complexes by X-ray Absorption Spectroscopy and X-ray Diffraction. *Eur. J. Inorg. Chem.* **2003,** 839–852 (2003).
77. Everson, D. A. & Weix, D. J. Cross-Electrophile Coupling: Principles of Reactivity and Selectivity. *J. Org. Chem.* **79,** 4793–4798 (2014).
78. Atack, T. C. & Cook, S. P. Manganese-Catalyzed Borylation of Unactivated Alkyl Chlorides. *J. Am. Chem. Soc.* **138,** 6139–6142 (2016).
79. Six, C. & Richter, F. Isocyanates, Organic. in *Ullmann's Encyclopedia of Industrial Chemistry* 63–82 (Wiley-VCH Verlag GmbH & Co. KGaA, 2003).
80. Ulrich, H. *Cumulenes in Click Reactions*. (Wiley, 2009).
81. Hsieh, J.-C. & Cheng, C.-H. Nickel-Catalyzed Coupling of Isocyanates with 1,3-Iodoesters and Halobenzenes: a Novel Method for the Synthesis of Imide and Amide Derivatives. *Chem. Commun.* **0,** 4554–4556 (2005).
82. Miura, T., Mikano, Y. & Murakami, M. Nickel-Catalyzed Synthesis of 1,3,5-Trisubstituted Hydantoins from Acrylates and Isocyanates. *Org. Lett.* **13,** 3560–3563 (2011).
83. Phillips, B. A., Fodor, G., Gal, J., Letourneau, F. & Ryan, J. J. Mechanism of the von Braun Amide Degradations with Carbonyl Bromide or Phosphorus Pentabromide. *Tetrahedron* **29,** 3309–3327 (1973).
84. Broughton, E. The Bhopal Disaster and its Aftermath: A Review. *Environmental Health* **4,** 6 (2005).
85. Evans, V., Mahon, M. F. & Webster, R. L. A Mild, Copper-Catalysed Amide Deprotection Strategy: Use of tert-butyl as a Protecting Group. *Tetrahedron* **70,** 7593–7597 (2014).
86. Weix, D. J. Methods and Mechanisms for Cross-Electrophile Coupling of Csp^2 Halides with Alkyl Electrophiles. *Acc. Chem. Res.* **48,** 1767–1775 (2015).
87. Zhou, J. (Steve) & Fu, G. C. Suzuki Cross-Couplings of Unactivated Secondary Alkyl Bromides and Iodides. *J. Am. Chem. Soc.* **126,** 1340–1341 (2004).
88. Powell, D. A. & Fu, G. C. Nickel-Catalyzed Cross-Couplings of Organosilicon Reagents with Unactivated Secondary Alkyl Bromides. *J. Am. Chem. Soc.* **126,** 7788–7789 (2004).
89. Powell, D. A., Maki, T. & Fu, G. C. Stille Cross-Couplings of Unactivated Secondary Alkyl Halides Using Monoorganotin Reagents. *J. Am. Chem. Soc.* **127,** 510–511 (2005).
90. Fu, G. C. Transition-Metal Catalysis of Nucleophilic Substitution Reactions: A Radical Alternative to SN1 and SN2 Processes. *ACS Cent. Sci.* **3,** 692–700 (2017).
91. Cherney, A. H., Kadunce, N. T. & Reisman, S. E. Enantioselective and Enantiospecific Transition-Metal-Catalyzed Cross-Coupling Reactions of Organometallic Reagents to Construct C-C Bonds. *Chem. Rev.* **115,** 9587–9652 (2015).
92. Breitenfeld, J., Ruiz, J., Wodrich, M. D. & Hu, X. Bimetallic Oxidative Addition Involving Radical Intermediates in Nickel-Catalyzed Alkyl–Alkyl Kumada Coupling Reactions. *J. Am. Chem. Soc.* **135,** 12004–12012 (2013).
93. Pallenberg, A. J., Marschner, T. M. & Barnhart, D. M. Phenanthroline Complexes of the d10 Metals Nickel(0), Zinc(ll) and Silver(I) –comparison to copper(I) species. *Polyhedron* **16,** 2711–2719 (1997).
94. Powers, D. C., Anderson, B. L. & Nocera, D. G. Two-Electron HCl to H_2 Photocycle Promoted by Ni(II) Polypyridyl Halide Complexes. *J. Am. Chem. Soc.* **135,** 18876–18883 (2013).
95. Wang, M., England, J., Weyhermüller, T. & Wieghardt, K. Electronic Structures of 'Low-Valent' Neutral Complexes $[NiL_2]^0$ (S = 0; L = bpy, phen, tpy) - An Experimental and DFT Computational Study. *Eur. J. Inorg. Chem.* **2015,** 1511–1523 (2015).
96. Gore-Randall, E., Irwin, M., Denning, M. S. & Goicoechea, J. M. Synthesis and Characterization of Alkali-Metal Salts of 2,2′-and 2,4′-Bipyridyl Radicals and Dianions. *Inorg. Chem.* **48,** 8304–8316 (2009).
97. Chisholm, M. H., Huffman, J. C. & Rothwell, I. P. Bis(2,2'-bipyridyl)diisopropoxymolybdenum(II). Structural and Spectroscopic Evidence for Molybdenum-to-Bipyridyl -π* Bonding. *J. Am. Chem. Soc.* **103,** 4945–4947 (1981).
98. King, A. E. *et al.* Ni(bpy)(cod): A Convenient Entryway into the Efficient Hydroboration of Ketones, Aldehydes, and Imines. *Eur. J. Inorg. Chem.* **2016,** 1635–1640 (2016).
99. *Modern Organonickel Chemistry*. (ed. Tamaru, Y.) (Wiley-VCH Verlag GmbH & Co. KGaA, 2005).
100. Ciszewski, J. T. *et al.* Redox Trends in Terpyridine Nickel Complexes. *Inorg. Chem.* **50,** 8630–8635 (2011).
101. Yoshimitsu, T., Matsuda, K., Nagaoka, H., Tsukamoto, K. & Tanaka, T. Radical Fixation of Functionalized Carbon Resources: α-sp^3C-H Carbamoylation of Tertiary Amines with Aryl Isocyanates. *Org. Lett.* **9,** 5115–5118 (2007).

102. Dietrich-Buchecker, C. O., Sauvage, J. P. & Kern, J. M. Synthesis and Electrochemical Studies of Catenates: Stabilization of Low Oxidation States by Interlocked Macrocyclic Ligands. *J. Am. Chem. Soc.* **111,** 7791–7800 (1989).
103. Fujihara, T. *et al.* Nickel-Catalyzed Double Carboxylation of Alkynes Employing Carbon Dioxide. *Org. Lett.* **16,** 4960–4963 (2014).
104. Jones, G. D. *et al.* Ligand Redox Effects in the Synthesis, Electronic Structure, and Reactivity of an Alkyl-Alkyl Cross-Coupling Catalyst. *J. Am. Chem. Soc.* **128,** 13175–13183 (2006).
105. Velian, A., Lin, S., Miller, A. J. M., Day, M. W. & Agapie, T. Synthesis and C-C coupling reactivity of a dinuclear Ni^{I}-Ni^{I} Complex Supported by a Terphenyl Diphosphine. *J. Am. Chem. Soc.* **132,** 6296–6297 (2010).
106. Cornella, J., Gómez-Bengoa, E. & Martin, R. Combined Experimental and Theoretical Study on the Reductive Cleavage of Inert C–O Bonds with Silanes: Ruling out a Classical Ni(0)/Ni(II) Catalytic Couple and Evidence for Ni(I) Intermediates. *J. Am. Chem. Soc.* **135,** 1997–2009 (2013).
107. Yamamoto, T., Kohara, T. & Yamamoto, A. Preparation and Properties of Monoalkylnickel(II) Complexes Having a Phenoxo, Benzenethiolato, Oximato, β-Diketonato, or Halo Ligand. *Bull. Chem. Soc. Jpn.* **54,** 2010–2016 (1981).
108. Yamamoto, T., Yamamoto, A. & Ikeda, S. Study of Organo(dipyridyl) nickel Complexes. I. Stability and Activation of the Alkyl-Nickel Bonds of Dialkyl(dipyridyl)nickel by Coordination with Various Substituted Olefins. *J. Am. Chem. Soc.* **93,** 3350–3359 (1971).
109. Everson, D. A., Jones, B. A. & Weix, D. J. Replacing Conventional Carbon Nucleophiles with Electrophiles: Nickel-Catalyzed Reductive Alkylation of Aryl Bromides and Chlorides. *J. Am. Chem. Soc.* **134,** 6146–6159 (2012).
110. Wang, X., Nakajima, M. & Martin, R. Ni-Catalyzed Regioselective Hydrocarboxylation of Alkynes with CO_2 by Using Simple Alcohols as Proton Sources. *J. Am. Chem. Soc.* **137,** 8924–8927 (2015).
111. Moragas, T., Gaydou, M. & Martin, R. Nickel-Catalyzed Carboxylation of Benzylic C-N Bonds with CO_2. *Angew. Chem. Int. Ed.* **55,** 5053–5057 (2016).
112. Tortajada, A., Ninokata, R. & Martin, R. Ni-Catalyzed Site-Selective Dicarboxylation of 1,3-Dienes with CO_2. *J. Am. Chem. Soc.* **140,** 2050–2053 (2018).
113. Gaydou, M., Moragas, T., Juliá-Hernández, F. & Martin, R. Site-Selective Catalytic Carboxylation of Unsaturated Hydrocarbons with CO_2 and Water. *J. Am. Chem. Soc.* **139,** 12161–12164 (2017).
114. Zheng, S., Primer, D. N. & Molander, G. A. Nickel/Photoredox-Catalyzed Amidation via Alkylsilicates and Isocyanates. *ACS Catal.* **7,** 7957–7961 (2017).
115. Pelter, A., Ward, R. S. & Rao, R. R. An Approach to the Biomimetic Synthesis of Aryltetralin Lignans. *Tetrahedron* **41,** 2933–2938 (1985).
116. Kosui, N., Waki, M., Kato, T. & Izumiya, N. Preparation of Homologs of L-2-Amino-5-(p-methoxyphenyl)pentanoic Acid. *Bull. Chem. Soc. Jpn.* **55,** 918–920 (1982).
117. Nguyen, C. *et al.* Acyclic Nucleoside Analogues as Inhibitors of Plasmodium falciparum dUTPase. *J. Med. Chem.* **49,** 4183–4195 (2006).
118. Zhou, J. (Steve) & Fu, G. C. Palladium-Catalyzed Negishi Cross-Coupling Reactions of Unactivated Alkyl Iodides, Bromides, Chlorides, and Tosylates. *J. Am. Chem. Soc.* **125,** 12527–12530 (2003).
119. Nallasivam, J. L. & Fernandes, R. A. A Cascade Aza-Cope/Aza-Prins Cyclization Leading to Piperidine Derivatives. *Eur. J. Org. Chem.* **2015,** 2012–2022 (2015).
120. Denmark, S. E. & Cresswell, A. J. Iron-Catalyzed Cross-Coupling of Unactivated Secondary Alkyl Thioethers and Sulfones with Aryl Grignard Reagents. *J. Org. Chem.* **78,** 12593–12628 (2013).
121. Kauffmann, T., König, J. & Woltermann, A. Nucleophile Alkylierung und Arylierung des 2,2'-Bipyridyls. *Chem. Ber.* **109,** 3864–3868 (1976).
122. Mundinger, S., Jakob, U., Bichovski, P. & Bannwarth, W. Modification and Optimization of the Bis-picolylamide-Based Relay Protection for Carboxylic Acids to be Cleaved by Unusual Complexation with Cu^{2+} Salts. *J. Org. Chem.* **77,** 8968–8979 (2012).
123. Zhang, Y., Pittman, C. U., Arockiasamy, A. & King, R. L. Studies of Organoclays with Functionalized Pillaring Agents. *J. Appl. Polym. Sci.* **121,** 2430–2441 (2011).
124. Kim, I. H. *et al.* Optimization of Amide-Based Inhibitors of Soluble Epoxide Hydrolase with Improved Water Solubility. *J. Med. Chem.* **48,** 3621–3629 (2005).
125. Shields, J. D., Gray, E. E. & Doyle, A. G. A Modular, Air-Stable Nickel Precatalyst. *Org. Lett.* **17,** 2166–2169 (2015).
126. Magano, J. & Monfette, S. Development of an Air-Stable, Broadly Applicable Nickel Source for Nickel-Catalyzed Cross-Coupling. *ACS Catal.* **5,** 3120–3123 (2015).

2.7. Experimental Section

2.7.1. General Considerations

Reagents. $NiBr_2$ (anhydrous, 98% purity, a better reproducibility was found when stored in a glovebox), manganese powder (99.9% trace metal basis), 1-bromo-4-phenylbutane (95.0% purity), *tert*-butyl isocyanate (97% purity), and cyclohexyl isocyanate (98% purity) were purchased from Aldrich. Other isocyanates were purchased from TCI (NOTE: *the purity of the isocyanates was found crucial for the reaction*; higher yields and better reproducibility were achieved by purifying the isocyanates through a short plug of dried neutral alumina inside a nitrogen-filled glovebox. Old batches of isocyanates provide consistently lower yields and variable results). Anhydrous *N,N*-dimethylformamide (DMF, 99.8% purity) and anhydrous *N,N*-dimethylacetamide (DMA, 99.5% purity) were purchased from Acros Organics (NOTE: *it is critical to have appropriately dried DMF and DMA to obtain reproducible results*, since old batches of these solvents provided variable results). 1-bromo-6-chlorohexane was purchased from TCI. 3-Bromopropylboronic acid pinacol ester, ethyl 6-bromohexanoate, bromocyclohexane and endo-norbornane-2-carboxylic acid (98%) were purchased from AlfaAesar. 2-(2-bromoethyl)-1,3-dioxolane, 6-Bromo-2,2-dimethylhexanenitrile, exo-2-bromonorbornane (98%) were purchased from Aldrich. 4-bromotetrahydropyran was purchased from Fluorochem. 1-bromoadamantane was purchased from Fluka. Compounds 1-bromo-4-(4-methoxyphenyl)butane,[115, 116] 4-(6- bromohexyl)phenyl pivalate,[36] 1-bromo-6-(*tert*-butyldiphenylsilyloxy)hexane,[117] 6-bromo-*N,N*-diethylhexanamide,[118] 1-benzyl-4-bromopiperidine,[119] (*rac*)-(3-bromobutyl)benzene,[120] (*R*)-(3-bromobutyl)benzene[120] were prepared following literature procedures. All other reagents were purchased from commercial sources and used as received.

Analytical methods. ^1H NMR and ^{13}C NMR spectra and melting points (where applicable) are included for all compounds. ^1H and ^{13}C-NMR spectra were recorded on a Bruker 300 MHz, 400 MHz and 500 MHz at 20 °C. All ^1H-NMR spectra are reported in parts per million (ppm) downfield of TMS and are reported relative to the signal of residual $CHCl_3$ (7.26 ppm), unless otherwise indicated. All ^{13}C-NMR spectra are reported in ppm relative to residual $CHCl_3$ (77.2 ppm), unless otherwise indicated, and were measured with ^1H decoupling. Coupling constants, *J*, are reported in Hertz. HSQC, HMBC, DEPTQ and COSY experiments were used to assist the assignment of the signals. Melting points were measured using open glass capillaries in a Büchi B540 apparatus. IR spectra were measured on a Bruker Optics FT-IR GmbH Alpha spectrometer with a Platinum-ATR module. Gas chromatographic analyses were performed on a Hewlett-Packard 6890 gas chromatography instrument with an FID detector. UltraPerformance Convergence Chromatography (UPC2) analysis was performed on an Acquity UPC2 Waters instrument equipped with a ChiralPack ID column eluting with CO_2/acetonitrile and monitored using a photodiode array detector (PDA). Column chromatography was performed with EM Science silica gel 60 (230-400 mesh). Thin layer chromatography was carried out using Merck TLC Silica gel 60 F_{254}. $KMnO_4$ or vanillin stains were used as TLC stains for aliphatic amides.

2.7.2. Optimization Details

General Procedure A: Ni-Catalyzed Reductive Amidation of 2.1a with 2.7b. An oven-dried screw-capped test tube containing a stirring bar was charged with the nickel source, ligand and Mn (1.50 equiv). The reaction tube was then evacuated and back-filled with dry argon (this sequence was repeated three times). The appropriate solvent, *tert*-butyl isocyanate (1.50 equiv) and (4-bromobutyl)benzene (42.0 µL, 0.250 mmol; 1 equiv) were added sequentially via syringe or Hamilton syringe under argon atmosphere. The resulting solution was stirred for 16 h at 25 °C. After this time, the crude reaction mixture was carefully quenched with 5% aq. HCl (1 mL). For screening reactions, ethyl acetate was added to the crude and *n*-decane was used as internal standard. A sample of the obtained solution was filtered through a silica-celite plug, eluted with ethyl acetate and analyzed by GC-FID.

NOTE: Reaction mixtures should turn dark green (when 6-methyl-2,2'-bypyridine (**L8**) is used as ligand) or dark brown-green (when 6,6'-dimethyl-2,2'-bypyridine (**L9**) is used as ligand) within 2 h. Colorless reaction mixtures are an indication of no complex formation and should be discarded.

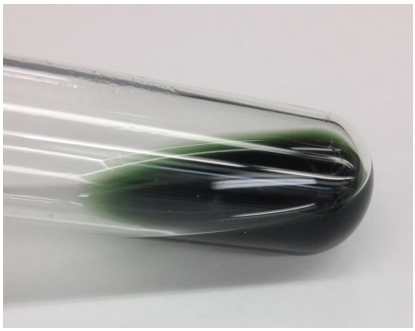

L8 used as ligand with t-BuNCO

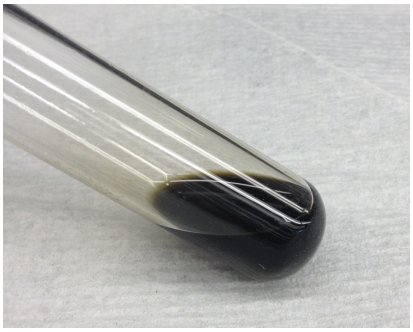

L9 used as ligand with ArNCO

2.7.3. Synthesis of Starting Materials

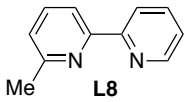

L8

6-methyl-2,2'-bipyridine (L8). The tittle compound was prepared following a slightly modified literature procedure.[121] Methyl lithium (25 mL of a 1.6 M solution in diethyl ether, 40 mmol; 1 equiv), was added slowly to a solution of bipyridine (6.2 g, 40 mmol; 1 equiv) in dry diethyl ether (200 mL, 0.2 M), under argon, at 0 °C and under vigorous agitation. The resulting red solution was heated at reflux for 4 h and after cooling to room temperature, the reaction mixture was quenched with brine (200 mL). The resulting biphasic yellow mixture was separated and the organic phase was extracted with diethyl ether (3 × 50 mL), dried over $MgSO_4$ and evaporated under reduced pressure. The obtained dark orange crude product was dissolved in acetone (50 mL) and a solution of $KMnO_4$ in acetone was added slowly until the color remained purple (the end point is best observed if the resulting MnO_2 is removed by filtration). The obtained crude solution was filtered through a silica-celite plug, concentrated under reduced pressure and purified through column chromatography on silica gel (hexanes/ethyl acetate 90:10) to afford the product as a light-yellow oil (3.6 g, 53% yield). The NMR spectroscopic data correspond to those previously reported in the literature.[122] ^{1}H-NMR (300 MHz, $CDCl_3$) δ 8.67 (ddd, *J* = 4.8, 1.7, 0.9 Hz, 1H, Ar), 8.40 (dt, *J* = 8.0, 1.0 Hz, 1H, Ar), 8.16 (d, *J* = 7.8 Hz, 1H, Ar), 7.80 (td, *J* = 7.8, 1.8 Hz, 1H, Ar), 7.70 (t, *J* = 7.7 Hz, 1H, Ar), 7.28 (ddd, *J* = 7.9, 5.0, 1.4 Hz, 1H, Ar), 7.17 (dd, *J* = 7.7, 1.0 Hz, 1H, Ar), 2.63 (s, 3H, CH_3) ppm. ^{13}C-NMR (75 MHz, $CDCl_3$) δ 158.1, 156.7, 155.7, 149.3, 137.2, 137.0, 123.6, 123.4, 121.3, 118.2, 24.8 ppm. IR (neat, cm^{-1}): 3060, 3012, 2921, 1581, 1459, 1426, 1082, 767, 620.

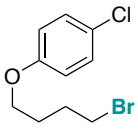

1-(4-bromobutoxy)-chlorobenzene (2.1s). To a solution of 4-chlorophenol (1.0 g, 7.8 mmol; 1 equiv) in acetone (40 mL, 0.2 M) were added K_2CO_3 (2.2 g, 16 mmol; 2 equiv) and 1,4-dibromobutane (1.9 mL, 16 mmol; 2 equiv). The resulting solution was heated at reflux for 12 h, then cooled to room temperature, filtered through celite, eluted with acetone and concentrated under reduced pressure. The resulting crude product was purified by column chromatography (hexanes/ethyl acetate 99:1) to afford the product as a pale yellow solid (1.94 g, 95% yield). m.p.: 34.4 – 36.3 °C. ^{1}H-NMR (500 MHz, $CDCl_3$) δ 7.25 – 7.20 (m, 2H, *Ar*), 6.85 – 6.78 (m, 2H, *Ar*), 3.96 (t, *J* = 6.1 Hz, 2H, *CH₂-O*), 3.48 (t, *J* = 6.6 Hz, 2H, *CH₂-Br*), 2.10 – 2.02 (m, 2H, *CH₂*), 1.98 – 1.90 (m, 2H, *CH₂*) ppm. ^{13}C-NMR (126 MHz, $CDCl_3$) δ 157.6, 129.4, 125.7, 115.8, 67.3, 33.5, 29.5, 28.0 ppm. IR (neat, cm^{-1}): 2956, 2920, 1490, 1467, 1242, 1031, 823, 664. HRMS (ESI^+) [$C_{10}H_{12}ClBrO$] (M+Na) calcd. 261.9760, found 261.9761.

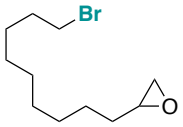

2-(9-bromononyl)oxirane (2.1u). To a solution of 11-bromoundec-1-ene (1.99 g, 8.53 mmol; 1 equiv) in acetone (15 mL, 0.57 M), mCPBA (3.15 g, 12.8 mmol; 1.50 equiv) in acetone (10 mL) was added portion-wise at 0 °C. The resulting solution was slowly warmed to room temperature and stirred for 16 h. The solvent was then removed under reduced pressure and the obtained crude product was dissolved in dichloromethane (10 mL) and filtered through a celite plug. The crude mixture was concentrated under reduced pressure and purified by column chromatography (hexanes/dichloromethane 20:1 to 10:1) to afford the product as a clear oil (1.20 g, 56% yield). The NMR spectroscopic data correspond to those previously reported in the literature.[123] ^{1}H-NMR (400 MHz, $CDCl_3$) δ 3.38 (t, *J* = 6.8 Hz, 2H, *CH*$_2$), 2.88 (tdd, *J* = 5.4, 3.9, 2.7 Hz, 1H, *CH-O*), 2.72 (dd, *J* = 5.0, 4.0 Hz, 1H, *CH-O*), 2.43 (dd, *J* = 5.1, 2.7 Hz, 1H, *CH-O*), 1.83 (dt, *J* = 14.5, 6.9 Hz, 2H, *CH*$_2$), 1.55 – 1.25 (m, 14H, *CH*$_2$) ppm. ^{13}C-NMR (101 MHz, $CDCl_3$) δ 52.4, 47.2, 34.1, 32.9, 32.6, 29.5, 29.5, 29.4, 28.8, 28.2, 26.0 ppm. IR (neat, cm^{-1}): 2925, 2854, 1463, 1259, 834. HRMS (APCI$^+$) [$C_{11}H_{21}BrO$] (M+H) calcd. 249.0849 found 249.0846.

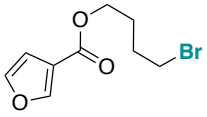

4-bromobutyl furan-3-carboxylate (2.1v). To a solution of furan-2-carboxylic acid (1.0 g, 8.9 mmol; 1 equiv) in acetone (60 mL, 0.15 M) were added K_2CO_3 (3.7 g, 27 mmol; 3 equiv) and 1,4-dibromobutane (3.2 mL, 27 mmol; 3 equiv). The resulting solution was heated at reflux for 48 h, then cooled down to room temperature, filtered through celite, eluted with acetone and concentrated under reduced pressure. The resulting crude mixture was purified by column chromatography (hexanes/ethyl acetate 1:0 to 9:1) to afford the product as a pale-yellow oil (2.10 g, 96% yield). ^{1}H-NMR (400 MHz, $CDCl_3$) δ 8.01 (dd, *J* = 1.6, 0.8 Hz, 1H, *Ar*), 7.43 (t, *J* = 1.7 Hz, 1H, *Ar*), 6.74 (dd, *J* = 1.9, 0.8 Hz, 1H, *Ar*), 4.29 (t, *J* = 6.3 Hz, 2H, *CH*$_2$), 3.47 (t, *J* = 6.5 Hz, 2H, *CH*$_2$), 2.04 – 1.84 (m, 4H, *CH*$_2$) ppm. ^{13}C-NMR (101 MHz, $CDCl_3$) δ 163.2, 147.8, 143.9, 119.5, 109.9, 77.2, 63.6, 33.2, 29.5, 27.5 ppm. IR (neat, cm^{-1}): 2961, 1717, 1578, 1305, 1158, 1075, 969, 761. HRMS (APCI$^+$) [$C_9H_{11}BrO_3$] (M+Na) calcd. 268.9784, found 268.9783.

2.7.4. Preparative Scope

General Procedure B. An oven-dried screw-capped test tube containing a stirring bar was charged, if solid, with the corresponding alkyl bromide (0.50 mmol). Subsequently, $NiBr_2$ (3.3 mg, 0.015 mmol, 3.0 mol%), 6-methyl-2,2'-bipyridine (3.8 mg, 0.023, 4.5 mol%), and Mn (41 mg, 0.75 mmol, 1.5 equiv) were added. The reaction tube was then evacuated and back-filled with dry argon (this sequence was repeated three times) and DMF (1.0 mL) and the corresponding isocyanate (0.75 mmol, 1.5 equiv) were added sequentially under argon flow. In case of liquid alkyl bromides, the corresponding starting material (0.50 mmol) was added under argon flow, via Hamilton syringe. The resulting solution was stirred for 16 h at 25 °C. The crude reaction mixture was carefully quenched with 5% aq. HCl (1 mL) or saturated aq. NH_4Cl (2 mL) (when sensitive functional groups were present). Acid quench was followed by the addition of distilled water (*ca.* 10 mL) and by extraction with dichloromethane (3 × 25 mL). The obtained solution was washed with brine (40 mL), dried over $MgSO_4$, filtered and the solvent was evaporated under reduced pressure. The crude product was purified by column chromatography (hexanes/AcOEt or pentane/Et_2O) to yield the corresponding products.

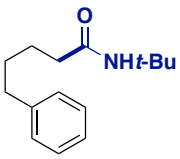

***N*-(*tert*-butyl)-5-phenylpentanamide (2.8b).** Following general procedure B, 1-(4-bromobutyl)-4-methoxybenzene (84.0 µL, 107 mg, 0.500 mmol; 1 equiv) and *tert*-butyl isocyanate (86.0 µL, 74.3 mg, 0.750 mmol; 1.50 equiv) were utilized to deliver **2.8b** as a colorless solid (102 mg 1st run, 100 mg, 2nd run, 86% average yield).

Scale-up reaction: *N*-(*tert*-butyl)-5-phenylpentanamide (2.8b). To an oven-dried 50 mL Schlenk containing a stirring bar were added, under argon atmosphere, $NiBr_2$ (30.8 mg, 0.141 mmol, 3 mol%), 6-methyl-

2,2'-bipyridine (36.0 mg, 0.211 mmol, 4.5 mol%), manganese (387 mg, 7.04 mmol, 1.50 equiv), DMF (9.4 mL), 1-bromo-4-phenylbutane (1.00 g, 4.69 mmol; 1 equiv) and *tert*-butyl isocyanate (0.800 mL, 697 mg, 7.00 mmol; 1.50 equiv). The resulting solution was stirred for 24 h at 25 °C, after which the crude reaction mixture was carefully quenched to protonate the resulting amidate with 5% aq. HCl (10 mL). Acid quench was followed by the addition of distilled water (*ca.* 100 mL) and by extraction with dichloromethane (3 ×100 mL). The obtained solution was washed with brine (100 mL), dried over $MgSO_4$, filtered and the solvent was evaporated under reduced pressure. The crude product was purified by colum- chromatography (pentane/Et_2O 8:2 then 7:3) to afford compound (**2.8b**) as a colorless solid (808 mg, 3.46 mmol; 74% yield). m.p.: 60.8 – 62.4 °C. ^{1}H-NMR (400 MHz, $CDCl_3$) δ 7.30 – 7.24 (m, 2H, *Ar*), 7.20 – 7.15 (m, 3H, *Ar*), 5.19 (s, 1H, *NH*), 2.68 – 2.57 (m, 2H, *CH₂-Ar*), 2.15 – 2.04 (m, 2H, *CH₂-C=O*), 1.64 (dq, J = 8.1, 2.8 Hz, 4H, *CH₂*), 1.33 (s, 9H, *t-Bu*) ppm. ^{13}C-NMR (101 MHz, $CDCl_3$) δ 172.3, 142.5, 128.5, 128.4, 125.9, 51.2, 37.7, 35.9, 31.2, 29.0, 25.6 ppm. IR (neat, cm^{-1}): 3277, 2963, 2861, 1639, 1550, 1453, 1360, 1224, 697. HRMS (ESI^+) [$C_{15}H_{23}NO$] (M+Na) calcd. 256.1672, found 256.1678.

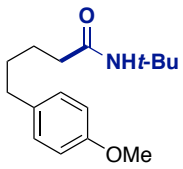

***N*-(*tert*-butyl)-5-(4-methoxyphenyl)pentanamide (2.8c).** Following general procedure B, 1-(4-bromobutyl)-4-methoxybenzene[115, 116] (96.5 µL, 122 mg, 0.500 mmol; 1 equiv), and **2.7b** (86.0 µL, 74.3 mg, 0.750 mmol; 1.50 equiv) were utilized to deliver **2.8c** as a colorless solid (109.5 mg 1st run, 115.8 2nd run, 85% average yield). m.p.: 75.1 – 77.5 °C. ^{1}H-NMR (400 MHz, $CDCl_3$) δ 7.08 (d, *J* = 8.6 Hz, 2H, *Ar*), 6.84 – 6.79 (m, 2H, *Ar*), 5.18 (s, 1H, *NH*), 3.78 (s, 3H, *OCH₃*), 2.57 (t, *J* = 7.1 Hz, 2H, *CH₂*), 2.09 (t, *J* = 7.1 Hz, 2H, *CH₂*), 1.69 – 1.54 (m, 4H, *CH₂-CH₂*), 1.33 (s, 9H, *t-Bu*) ppm. ^{13}C-NMR (101 MHz, $CDCl_3$) δ 172.4, 157.9, 134.6, 129.4, 113.9, 55.4, 51.2, 37.7, 34.9, 31.4, 29.0, 25.5 ppm. IR (neat, cm^{-1}): 3339, 2931, 1642, 1536, 1510, 1455, 1243, 1029, 812. HRMS (ESI^-) [$C_{16}H_{25}NO_2$] (M-H) calcd. 262.1813, found 262.1810.

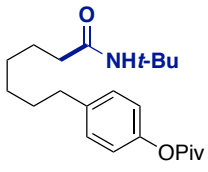

***N*-(*tert*-butyl)-7-(4-pivaloxylphenyl)heptanamide (2.8d).** Following general procedure B, 4-(6-bromohexyl)phenyl pivalate[36] (170.6 mg, 0.5000 mmol; 1 equiv) and **2.7b** (86.0 µL, 74.3 mg, 0.750 mmol; 1.50 equiv) were utilized to deliver **2.8d** as a colorless solid (137.6 mg 1st run, 141.8 2nd run, 77% average yield). m.p.: 88.0 – 89.6 °C. ^{1}H-NMR (500 MHz, $CDCl_3$) δ 7.17 – 7.13 (m, 2H, *Ar*), 6.96 – 9.62 (m, 2H, *Ar*), 5.21 (s, 1H, *NH*), 2.62 – 2.55 (m, 2H, *CH₂*), 2.09 – 2.02 (m, 2H, *CH₂*), 1.65 – 1.54 (m, 4H, *CH₂*), 1.35 (s, 9H, *CH₃*), 1.34 (s, 9H, *CH₃*), 1.35 – 1.31 (m, 4H, *CH₂*) ppm. ^{13}C-NMR (126 MHz, $CDCl_3$) δ 177.4, 172.5, 149.2, 140.1, 129.3, 121.3, 51.2, 39.2, 37.8, 35.4, 31.4, 29.2, 29.2, 29.0, 27.3 25.8 ppm. IR (neat, cm^{-1}): 3301, 2965, 2928, 2854, 1742, 1645, 1548, 1196, 1132. HRMS (ESI^+) [$C_{22}H_{35}NO_3$] (M+H) calcd. 362.2690, found 362.2699.

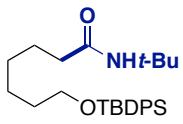

***N*-(*tert*-butyl)-7-((*tert*-butyldiphenylsilyl)oxy)heptanamide (2.8e).** Following general procedure B, ((6-bromohexyl)oxy)(tert-butyl)diphenylsilane[117] (291 mg, 0.500 mmol; 1 equiv) and **2.7b** (86.0 µL, 74.3 mg, 0.750 mmol; 1.50 equiv) were utilized to deliver **2.8e** as a clear oil (178.6 mg 1st run, 203.4 mg 2nd run, 202.7 mg 3rd run, 88% average yield). ^{1}H-NMR (400 MHz, $CDCl_3$) δ 7.66 (dd, *J* = 7.8, 1.7 Hz, 4H, *Ar*), 7.45 – 7.34 (m, 6H, *Ar*), 5.20 (s, 1H, *NH*), 3.65 (t, *J* = 6.4 Hz, 2H, *CH₂-O*), 2.05 (t, *J* = 7.6 Hz, 2H, *CH₂-C=O*), 1.65 – 1.50 (m, 4H, *CH₂-CH₂*), 1.41 – 1.26 (m, 4H, *CH₂-CH₂*), 1.34 (s, 9H, *N-t-Bu*), 1.05 (s, 9H, *Si-t-Bu*) ppm. ^{13}C-NMR (101 MHz, $CDCl_3$) δ 172.5, 135.7, 134.3, 129.6, 127.7, 64.0, 51.2, 37.8, 32.6, 29.1, 29.0, 27.0, 25.9, 25.7, 19.4 ppm. IR (neat, cm^{-1}): 3308, 2930, 2857, 1644, 1545, 1107, 700, 503. HRMS (ESI^-) [$C_{27}H_{41}NO_2Si$] (M-H) calcd. 438.2834, found 438.2825.

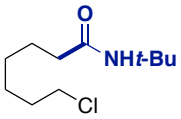

***N*-(*tert*-butyl)-7-chloroheptanamide (2.8f).** Following general procedure B, 1-bromo-6-chlorohexane (99.8 mg, 0.500 mmol; 1 equiv) and **2.7b** (86.0 µL, 74.3 mg, 0.750 mmol; 1.50 equiv) were utilized to deliver **2.8f** as a pale-yellow oil (89.2 mg 1st run, 93.5 mg 2nd run, 83% average yield). ^{1}H-NMR (500 MHz, $CDCl_3$) δ 5.23 (s, 1H, *NH*), 3.52 (t, *J* = 6.7 Hz, 2H, *CH₂*), 2.08 (t, *J* = 7.5 Hz, 2H, *CH₂*), 1.77 (p, *J* = 6.8 Hz, 2H, *CH₂*), 1.61 (p, *J* = 7.5 Hz, 2H, *CH₂)*, 1.48 – 1.42 (m, 2H, *CH₂*), 1.34 (s, 11H, *CH₂ + t-Bu*) ppm. ^{13}C-NMR (126 MHz, $CDCl_3$) δ 172.3, 51.2, 45.2, 37.6, 32.5, 29.0, 28.5, 26.7, 25.6 ppm. IR (neat, cm^{-1}): 3308, 2932, 2861, 1643, 1544, 1453, 1362, 1225. HRMS (ESI$^+$) [$C_{11}H_{22}ClNO$] (M+Na) calcd. 242.1282, found 242.1276.

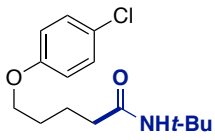

***N*-(*tert*-butyl)-5-(4-chlorophenoxy)pentanamide (2.8g).** Following general procedure B, 1-(4-bromobutoxy)-4-chlorobenzene (131.8 mg, 0.5000 mmol; 1 equiv) and **2.7b** (86.0 µL, 74.3 mg, 0.750 mmol; 1.50 equiv) were utilized to deliver **2.8g** as a colorless solid (92.6 mg 1st run, 86.5 mg 2nd run, 63% average yield). m.p.: 109.6 – 111.6 °C. ^{1}H-NMR (500 MHz, $CDCl_3$) δ 7.24 – 7.19 (m, 2H, *Ar*), 6.82 – 6.78 (m, 2H, *Ar*), 5.26 (s, 1H, *NH*), 3.98 – 3.88 (m, 2H, *CH₂-O*), 2.20 – 2.11 (m, 2H, *CH₂–C=O*), 1.85 – 1.73 (m, 4H, *CH₂-CH₂*), 1.34 (s, 9H, *CH₃*) ppm. ^{13}C-NMR (126 MHz, $CDCl_3$) δ 172.0, 157.7, 129.4, 125.6, 115.9, 68.1, 51.3, 37.3, 29.0, 28.8, 22.5 ppm. IR (neat, cm^{-1}): 3273, 2943, 1642, 1553, 1493, 1224, 820, 666. HRMS (ESI$^+$) [$C_{15}H_{22}ClNO_2$] (M+H) calcd. 284.1412, found 284.1405.

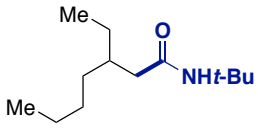

***N*-(*tert*-butyl)-3-ethylheptanamide (2.8h).** Following general procedure B, 3-(bromomethyl)heptane (89.0 µL, 96,6 mg, 0.500 mmol; 1 equiv), **2.7b** (86.0 µL, 74.3 mg, 0.750 mmol; 1.50 equiv), $NiBr_2$ (5.5 mg, 0.025 mmol; 5 mol%) and 6-methyl-2,2'-bipyridine (6.4 mg, 0.038 mmol; 7.5 mol%) were utilized to deliver **2.8h** as a yellow oil (79.7 mg 1st run, 81.6 mg 2nd run, 76% average yield).^{1}H-NMR (400 MHz, $CDCl_3$) δ 5.23 (s, 1H, *NH*), 1.99 (dd, *J* = 7.1, 2.1 Hz, 2H, CH_2-C=O), 1.79 (td, *J* = 12.9, 6.4 Hz, 1H, CH), 1.37 – 1.23 (m, 8H, CH_2 x 4) 1.34 (s, 9H, *t-Bu)*, 0.94 – 0.81 (m, 6H, *CH₃* x 2) ppm. ^{13}C-NMR (101 MHz, $CDCl_3$) δ 172.5, 51.3, 42.7, 36.9, 33.1, 29.0, 28.9, 26.4, 23.1, 14.2, 11.0 ppm. IR (neat, cm^{-1}): 3305, 2960, 2926, 1641, 1545, 1453, 1361, 1226. HRMS (ESI$^-$) [$C_{13}H_{27}NO$] (M-H) calcd. 212.2020, found 212.2019.

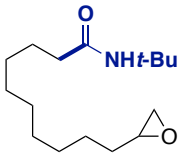

***N*-(*tert*-butyl)-10-(oxiran-2-yl)decanamide (2.8i).** Following general procedure B, 2-(9-bromononyl)oxirane (124.6 mg, 0.5000 mmol; 1 equiv) and **2.7b** (86.0 µL, 74.3 mg, 0.750 mmol; 1.50 equiv) were utilized to deliver **2.8i** as a colorless solid (68.0 mg 1st run, 63.0 mg 2nd run, 49% average yield). m.p.: 38.0 – 40.1 °C. ^{1}H-NMR (400 MHz, $CDCl_3$) δ 5.20 (s, 1H, *NH*), 2.95 – 2.85 (m, 1H, *CH-O*), 2.74 (dd, *J* = 5.0, 4.0 Hz, 1H, *CH-O*), 2.46 (dd, *J* = 5.0, 2.7 Hz, 1H, *CH-O*), 2.11 – 2.03 (m, 2H, *CH₂*), 1.57 (d, *J* = 12.1 Hz, 4H, *CH₂*), 1.54 – 1.39 (m, 4H, *CH₂*), 1.34 (s, 9H, *t-Bu*), 1.29 (s, 8H, *CH₂*) ppm. ^{13}C-NMR (126 MHz, $CDCl_3$) δ 172.6, 52.5, 51.2, 47.3, 37.9, 32.6, 29.6, 29.5, 29.5, 29.5, 29.3, 29.0, 26.1, 25.9 ppm. IR (neat, cm^{-1}): 3312, 2964, 2916, 2851, 1641, 1544, 1359, 1226. HRMS (ESI$^+$) [$C_{16}H_{31}NO_2$] (M+Na) calcd. 292.2247, found 292.2252.

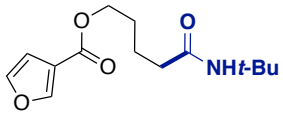

***N*-(*tert*-butylamino)-5-oxopentyl furan-3-carboxylate (2.8j).** Following general procedure B, 4-bromobutyl furan-3-carboxylate (123.5 mg, 0.5000 mmol; 1 equiv) and **2.7b** (86.0 µL, 74.3 mg, 0.750 mmol; 1.50 equiv) were utilized to deliver **2.8j** as a clear oil (104.3 mg 1st run, 98.7 mg 2nd run, 76% average yield). ^{1}H-NMR (400 MHz $CDCl_3$) δ 8.01 (dd, *J* = 1.5, 0.7 Hz, 1H, *Ar*), 7.42 (t, *J* = 1.7 Hz, 1H, *Ar*), 6.73 (dd, *J* = 1.9, 0.7 Hz, 1H, *Ar*), 5.26 (s, 1H, *NH*), 4.32 – 4.19 (m, 2H, *CH₂*), 2.18 – 2.08 (m, 2H, *CH₂*), 1.74 (dt, *J* = 5.0, 2.6 Hz, 4H, *CH₂*), 1.34 (s, 9H, *t-Bu*) ppm. ^{13}C-NMR (126 MHz, $CDCl_3$) δ 171.9, 163.3, 147.8, 143.8, 119.6, 109.9, 64.2, 51.3, 37.0, 29.0, 28.3, 22.3 ppm. IR (neat, cm^{-1}): 3312, 2963, 1720, 1645, 1508, 1305, 1158, 761. HRMS (ESI$^+$) [$C_{14}H_{21}NO_4$] (M+Na) calcd. 290.1363, found 290.1372.

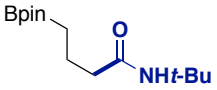

***N*-(*tert*-butyl)-4-(4,4,5,5-tetramethyl-1,3,2-dioxaborolan-2-yl)butanamide (2.8k).** Following general procedure B, 2-(3-bromopropyl)-4,4,5,5-tetramethyl-1,3,2-dioxaborolane (124.5 mg, 0.5000 mmol; 1 equiv) and **2.7b** (86.0 µL, 74.3 mg, 0.750 mmol; 1.50 equiv) were utilized to deliver **2.8k** as a pale yellow oil (69.0 mg 1st run, 72.1 mg 2nd run, 52% average yield). ^{1}H-NMR (400 MHz, $CDCl_3$) δ 5.38 (s, 1H, *NH*), 2.09 (t, *J* = 7.5 Hz, 2H, *CH₂*), 1.77 - 1.66 (m, 2H, *CH₂*), 1.33 (s, 9H, *t-Bu*), 1.24 (s, 12H, *CH₃ in pin*), 0.80 (t, *J* = 7.8 Hz, 2H, *CH₂*) ppm. ^{13}C-NMR (126 MHz, $CDCl_3$) δ 172.6, 83.2, 51.1, 40.1, 29.0, 25.0, 20.7 ppm (the carbon directly attached to the boron atom was not observed due to quadrupolar relaxation). IR (neat, cm^{-1}): 3305, 2974, 2931, 1645, 1543, 1365, 1316, 11. HRMS (ESI$^+$) [C14H28NO3^{10}B] (M+H) calcd. 269.2271, found 269.2270.

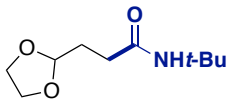

***N*-(*tert*-butyl)-3-(1,3-dioxolan-2-yl)propanamide (2.8l).** Following general procedure B, 2-(2-bromoethyl)-1,3-dioxolane (58.7 µL, 90.5 mg, 0.500 mmol; 1 equiv) and **2.7b** (86.0 µL, 74.3 mg, 0.750 mmol; 1.50 equiv) were utilized to deliver **2.8l** as an off-white solid (74.2 mg 1st run, 77.1 mg 2nd run, 76% average yield). m.p.: 64.0 – 66.8 °C. ^{1}H-NMR (500 MHz, $CDCl_3$) δ 5.44 (s, 1H, *NH*), 4.91 (t, *J* = 4.5 Hz, 1H, *CH-O*), 4.01 – 3.91 (m, 2H, *CH₂-O*), 3.90 – 3.81 (m, 2H, *CH₂-O*), 2.22 (dd, *J* = 8.1, 6.8 Hz, 2H, *CH₂-C=O*), 1.98 (td, *J* = 7.5, 4.5 Hz, 2H, *CH₂*), 1.33 (s, 9H, *t-Bu*) ppm. ^{13}C-NMR (126 MHz, $CDCl_3$) δ 171.7, 103.7, 65.1, 51.2, 31.7, 29.6, 28.9 ppm. IR (neat, cm^{-1}): 3293, 2966, 2928, 1642, 1554, 1449, 1361, 1133. HRMS (ESI$^+$) [$C_{10}H_{19}NO_3$] (M+Na) calcd. 224.1257, found 224.1261.

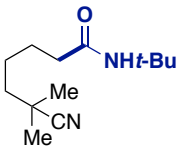

***N*-(*tert*-butyl)-6-cyano-6-methylheptanamide (2.8m).** Following general procedure B, 6-bromo-2,2-dimethylhexanenitrile (102.1 mg, 0.5000 mmol; 1 equiv) and **2.7b** (86.0 µL, 74.3 mg, 0.750 mmol; 1.50 equiv) were utilized to deliver **2.8m** as a yellow solid (97.0 mg 1st run, 92.3 mg 2nd run, 84% average yield). m.p.: 69.5 – 71.2 °C. ^{1}H-NMR (500 MHz, $CDCl_3$) δ 5.29 (s, 1H, *NH*), 2.10 (t, *J* = 7.4 Hz, 2H, *CH₂-C=O*), 1.69 – 1.59 (m, 2H, *CH₂*), 1.56 – 1.42 (m, 4H, *CH₂*), 1.33 (s, 9H, *t-Bu*), 1.32 (s, 6H, *CH₃ + CH₃*) ppm. ^{13}C-NMR (126 MHz, $CDCl_3$) δ 172.0, 125.2, 51.3, 40.9, 37.4, 32.5, 29.0, 26.8, 25.6, 25.0 ppm. IR (neat, cm^{-1}): 3283, 2967, 2929, 2235, 1636, 1557, 1360, 1228. HRMS (ESI$^+$) [$C_{13}H_{24}N_2O$] (M+H) calcd. 225.1961, found 225.1960.

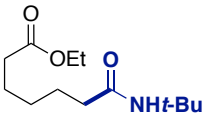

Ethyl 7-(*tert*-butylamino)-7-oxoheptanoate (2.8n). Following general procedure B, ethyl 6-bromohexanoate (89.0 µL, 112 mg, 0.500 mmol; 1 equiv) and **2.7b** (86.0 µL, 74.3 mg, 0.750 mmol; 1.50 equiv) were utilized to deliver **2.8n** as a clear oil (96.8 mg 1st run, 96.0 mg 2nd run, 80% average yield). ^{1}H-NMR (400 MHz, $CDCl_3$) δ 5.24 (s, 1H, *NH*), 4.11 (q, J = 7.1 Hz, 2H, *CH₂-O*), 2.29 (t, *J* = 7.5 Hz, 2H, *CH₂*), 2.12 – 2.03 (m, 2H, *CH₂*), 1.62 (dtd, *J* = 15.3, 7.3, 5.3 Hz, 4H, *CH₂-CH₂*), 1.37 – 1.30 (m, 2H, *CH₂*), 1.33 (s, 9H, *t-Bu*), 1.24 (t, *J* = 7.1 Hz, 3H, *CH₃*) ppm. ^{13}C-NMR (126 MHz, $CDCl_3$) δ 173.8, 172.3, 60.3, 51.2, 37.5, 34.2, 28.9, 28.7, 25.4, 24.7, 14.3 ppm. IR (neat, cm^{-1}): 3314, 2964, 2933, 1734, 1645, 1542, 1224, 1181. HRMS (ESI$^-$) [$C_{13}H_{25}NO_3$] (M-H) calcd. 242.1762, found 242.1757.

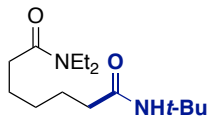

***N*¹-(*tert*-butyl)-*N*⁷,*N*⁷-diethylheptanediamide (2.8o).** Following general procedure B, 6-bromo-N,N-diethylhexanamide[118] (125.1 mg, 0.5000 mmol; 1 equiv) and **2.7b** (86.0 µL, 74.3 mg, 0.750 mmol; 1.50 equiv) were utilized to deliver **2.8o** as a pale yellow solid (116.1 mg 1st run, 125.0 mg 2nd run, 119.1 mg 3rd run, 89% average yield) after purification through column chromatography (CH_2Cl_2:MeOH 99:1, 95: 5 then 90:10). m.p.: 56.8 – 58.5 °C. ^{1}H-NMR (400 MHz, $CDCl_3$) δ 5.30 (s, 1H, *NH*), 3.36 (q, *J* = 7.1 Hz, 2H, *CH₂-N*), 3.29 (q, *J* = 7.1 Hz, 2H, *CH₂-N*), 2.33 – 2.24 (m, 2H, *CH₂-C=O*), 2.09 (t, *J* = 7.5 Hz, 2H, *CH₂-C=O*), 1.72 – 1.58 (m, 4H, *CH₂-CH₂*), 1.39 – 1.32 (m, 2H, *CH₂*), 1.33 (s, 9H, *t-Bu*), 1.16 (t, *J* = 7.1 Hz, 3H, *CH₃*), 1.10 (t, *J* = 7.1 Hz, 3H, *CH₃*) ppm. ^{13}C-NMR (126 MHz, $CDCl_3$) δ 172.5, 172.0, 51.0, 41.9, 40.0, 37.3, 32.8, 28.9,

28.8, 25.5, 25.0, 14.4, 13.1 ppm. IR (neat, cm^{-1}): 3311, 2969, 2943, 1636, 1543, 1451, 1425, 1271, 1220. HRMS (ESI^+) [$C_{15}H_{30}N_2O_2$] (M+Na) calcd. 293.2199, found 293.2205.

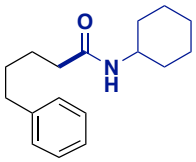

***N*-cyclohexyl-5-phenylpentanamide (2.8a).** Following general procedure B, (4-bromobutyl)benzene (84.0 µL, 107 mg, 0.500 mmol; 1 equiv), cyclohexyl isocyanate (128.0 µL, 128.2 mg, 1.000 mmol; 2 equiv), $NiBr_2$ (11.0 mg, 0.050 mmol, 10 mol%), Mn (55 mg, 1.0 mmol, 2.0 equiv) and 6-methyl-2,2'-bipyridine (12.70 mg, 0.076 mmol, 15 mol%) were utilized to deliver **2.8a** as a colorless solid (75.9 mg 1st run, 84.6 mg 2nd run, 62% average yield). The characterization data correspond to those previously reported in the literature.[124] m.p.: 93.2 – 96.6 °C. ^{1}H-NMR (400 MHz, $CDCl_3$) δ 7.31 - 7.24 (m, 2H, *Ar*), 7.17 (t, *J* = 6.8 Hz, 3H, *Ar*), 5.39 - 5.23 (m, 1H, *NH*), 3.76 (td, *J* = 14.8, 7.3 Hz, 1H, *CH-Cy-N*), 2.62 (t, *J* = 7.1 Hz, 2H, *CH_2*), 2.15 (t, *J* = 7.1 Hz, 2H, *CH_2*), 1.89 (dd, *J* = 12.4, 3.4 Hz, 2H, *CH_2*), 1.74 - 1.57 (m, 7H, *CH_2*), 1.41 - 1.30 (m, 2H, *CH_2*), 1.21 - 1.02 (m, 3H, *CH_2*) ppm. ^{13}C-NMR (101 MHz, $CDCl_3$) δ 171.9, 142.4, 128.5, 128.4, 125.9, 48.2, 37.0, 35.8, 33.4, 31.2, 25.7, 25.6, 25.0 ppm. IR (neat, cm^{-1}): 3303, 2927, 2851, 1635, 1542, 1445, 695. HRMS (ESI^+) [$C_{17}H_{26}NO$] (M+H) calcd. 260.2009, found 260.2009. *Note: old batches of cyclohexyl isocyanate provided inferior results.*

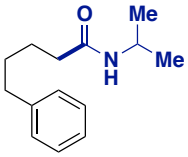

***N*-isopropyl-5-phenylpentanamide (2.8t).** Following general procedure B, (4-bromobutyl)benzene (84.0 µL, 107 mg, 0.500 mmol; 1 equiv), isopropyl isocyanate (150.0 µL, 130.0 mg, 1.530 mmol; 3.1 equiv), [(TMEDA)Ni(o-tolyl)Cl][125, 126] (22.6 mg, 0.0750 mmol, 15 mol%), 6-methyl-2,2'-bipyridine (25.5 mg, 0.150 mmol, 30 mol%), Mn (55 mg, 1.0 mmol, 2.0 equiv) and DMF (2 mL) were utilized to deliver **2.8t** as a colorless solid (54.4 mg 1st run, 54.6 mg 2nd run, 50% average yield). m.p.: 55.4 – 58.1 °C. ^{1}H-NMR (400 MHz, $CDCl_3$) δ 7.31 – 7.23 (m, 2H, *Ar*), 7.17 (t, *J* = 6.7 Hz, 3H, Ar), 5.32 (s, 1H, NH), 4.14 – 4.00 (m, 1H, CH-iPr-N), 2.62 (t, J = 7.1 Hz, 2H, CH_2), 2.14 (t, *J* = 7.1 Hz, 2H, *CH_2*), 1.65 (dq, *J* = 7.5, 3.7, 2.9 Hz, 4H, *CH_2*), 1.12 (d, *J* = 6.6 Hz, 6H, *CH_3*) ppm. ^{13}C-NMR (101 MHz, $CDCl_3$) δ 172.0, 142.4, 128.5, 128.4, 125.9, 77.2, 41.3, 36.9, 35.8, 31.2, 25.5, 22.9 ppm. IR (neat, cm^{-1}): 3311, 2974, 2934, 2858, 1637, 1533, 1453, 698. HRMS (ESI^+) [$C_{14}H_{22}NO$] (M+H) calcd. 220.1696, found 220.1700. *Note: the purity of isopropyl isocyanate was found to have a particularly strong influence in the outcome of the reaction. Better results were obtained when filtering the isocyanates through a short plug of dried neutral alumina inside the glovebox.*

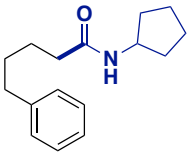

***N*-isopropyl-5-phenylpentanamide (2.8u).** Following general procedure B, (4-bromobutyl)benzene (84.0 µL, 107 mg, 0.500 mmol; 1 equiv), cyclopentyl isocyanate (170.0 µL, 167.6 mg, 1.510 mmol; 3.0 equiv), [(TMEDA)Ni(o-tolyl)Cl][125, 126] (22.6 mg, 0.0750 mmol, 15 mol%), 6-methyl-2,2'-bipyridine (25.5 mg, 0.150 mmol, 30 mol%), Mn (55 mg, 1.0 mmol, 2.0 equiv) and DMF (2 mL) were utilized to deliver **2.8u** as a pale-yellow solid (53.0 mg 1st run, 48.7 mg 2nd run, 41% average yield). m.p.: 53.9 – 56.6 °C. ^{1}H-NMR (400 MHz, $CDCl_3$) δ 7.31 – 7.23 (m, 2H, *Ar*), 7.17 (t, *J* = 6.7 Hz, 3H, Ar), 5.32 (s, 1H, NH), 4.14 – 4.00 (m, 1H, CH-iPr-N), 2.62 (t, J = 7.1 Hz, 2H, CH_2), 2.14 (t, *J* = 7.1 Hz, 2H, *CH_2*), 1.65 (dq, *J* = 7.5, 3.7, 2.9 Hz, 4H, *CH_2*), 1.12 (d, *J* = 6.6 Hz, 6H, *CH_3*) ppm. ^{13}C-NMR (101 MHz, $CDCl_3$) δ 172.0, 142.4, 128.5, 128.4, 125.9, 77.2, 41.3, 36.9, 35.8, 31.2, 25.5, 22.9 ppm. IR (neat, cm^{-1}): 3304, 2930, 2858, 1636, 1543, 1496, 1451, 698. HRMS (ESI^+) [$C_{16}H_{24}NO$] (M+H) calcd. 246.1852, found 246.1858. *Note: the purity of cyclopentyl isocyanate was found to have a particularly strong influence in the outcome of the reaction. Better results were obtained when filtering the isocyanates through a short plug of dried neutral alumina inside the glovebox.*

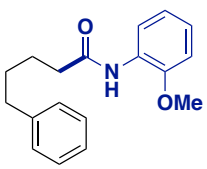

***N*-(2-methoxyphenyl)-5-phenylpentanamide (2.8v).** Following general procedure B, (4-bromobutyl)benzene (84.0 µL, 107 mg, 0.500 mmol; 1 equiv), 2-methoxyphenyl isocyanate (66.5 µL, 74.6 mg, 0.500 mmol; 1 equiv), $NiBr_2$ (11.0 mg, 0.05 mmol, 10 mol%) and **L9** (18.4 mg, 0.100 mmol, 20 mol%) and Mn (55 mg, 1.0 mmol, 2.0 equiv), were utilized

to deliver **2.8v** as a pale-yellow oil (93.0 mg 1st run, 95.9 mg 2nd run, 67% average yield). ^{1}H-NMR (500 MHz, $CDCl_3$) δ 8.39 (d, *J* = 7.5 Hz, 1H, *Ar*), 7.74 (s, 1H, *NH*), 7.31 - 7.25 (m, 2H, *Ar*), 7.19 (d, *J* = 7.2 Hz, 3H, *Ar*), 7.03 (t, *J* = 7.8 Hz, 1H, *Ar*), 7.00 - 6.93 (m, 1H, *Ar*), 6.87 (d, *J* = 8.1 Hz, 1H, *Ar*), 3.87 (s, 3H, *OMe*), 2.67 (t, *J* = 7.5 Hz, 2H, CH_2), 2.41 (t, *J* = 7.3 Hz, 2H, CH_2), 1.84 - 1.69 (m, 4H, CH_2) ppm. ^{13}C-NMR (101 MHz, $CDCl_3$) δ 171.1, 147.8, 142.3, 128.5, 128.4, 127.9, 125.9, 123.6, 121.3, 119.9, 110.0, 55.8, 38.1, 35.9, 31.2, 25.4. ppm. IR (neat, cm^{-1}): 3421, 3325, 2933, 1677, 1599, 1519, 1457, 744, 698. HRMS (ESI$^+$) [$C_{18}H_{22}NO_2$] (M+H) calcd. 284.1645, found 284.1649. *Note: higher amounts of 2-methoxyphenyl isocyanate resulted in lower yields due to the formation of an acyl urea side product coming from the addition of a second isocyanate molecule.*

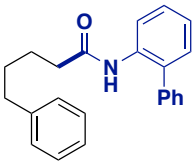

***N*-([1,1'-biphenyl]-2-yl)-5-phenylpentanamide (2.8w).** Following general procedure B, (4-bromobutyl)benzene (84.0 µL, 107 mg, 0.500 mmol; 1 equiv), 2-biphenyl isocyanate (171 µL, 195 mg, 1.00 mmol; 2 equiv), $NiBr_2$ (11.0 mg, 0.05 mmol, 10 mol%) and **L9** (18.4 mg, 0.100 mmol, 20 mol%) and Mn (55 mg, 1.0 mmol, 2.0 equiv), were utilized to deliver **2.8w** as a colorless solid (114.9 mg 1st run, 128.8 mg 2nd run, 74% average yield). m.p.: 74.1 – 76.4 °C. ^{1}H-NMR (500 MHz, $CDCl_3$) δ 8.31 (d, J = 8.1 Hz, 1H, *Ar*), 7.50 – 7.34 (m, 6H, *Ar*), 7.32 – 7.23 (m, 3H, *Ar + NH*), 7.18 (dd, *J* = 21.8, 7.1 Hz, 5H, *Ar*), 2.61 (t, *J* = 7.0 Hz, 2H, CH_2), 2.21 (t, *J* = 7.0 Hz, 2H, CH_2), 1.71 – 1.59 (m, 4H, CH_2) ppm. ^{13}C-NMR (126 MHz, $CDCl_3$) δ 171.0, 142.1, 138.2, 134.8, 132.2, 130.1, 129.3, 129.1, 128.5, 128.5, 128.4, 128.1, 125.9, 124.3, 121.7, 37.8, 35.7, 31.0, 25.2 ppm. IR (neat, cm^{-1}): 3213, 3020, 2931, 2858, 1643, 1530, 749, 698. HRMS (ESI$^+$) [$C_{23}H_{23}NO$] (M+H) calcd. 330.1852, found 330.1859.

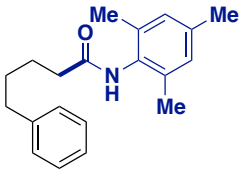

***N*-mesityl-5-phenylpentanamide (2.8x).** Following general procedure B, (4-bromobutyl)benzene (84.0 µL, 107 mg, 0.500 mmol; 1 equiv), 2,4,6-trimethylphenyl isocyanate (80.6 mg, 0.500 mmol; 1 equiv), $NiBr_2$ (11.0 mg, 0.05 mmol, 10.0 mol%) and 6-methyl-2,2'-bipyridine (17 mg, 0.10 mmol, 20 mol%) and Mn (55 mg, 1.0 mmol, 2.0 equiv), were utilized to deliver **2.8x** as a colorless solid (70.7 mg 1st run, 75.6 mg 2nd run, 50% average yield). The compound was isolated as a mixture of regioisomers (4.5:1 ratio). m.p.: 127.1 – 129.6 °C. Spectroscopic data of major isomer: ^{1}H-NMR (400 MHz, $CDCl_3$) δ 7.33 – 7.17 (m, 5H, *Ar)*, 6.88 – 6.82 (bs, 1H, *NH*), 6.86 (s, 2H, *Ar*), 2.66 (t, *J* = 7.3 Hz, 2H, CH_2), 2.37 (t, *J* = 7.2 Hz, 2H, CH_2), 2.26 (s, 3H, CH_3), 2.14 (s, 6H, CH_3), 1.84 – 1.68 (m, 4H, CH_2) ppm. ^{13}C-NMR (101 MHz, $CDCl_3$) δ 171.6, 142.3, 136.9, 135.2, 131.4, 128.9, 128.5, 128.4, 125.9, 36.6, 35.8, 31.3, 25.8, 18.4 ppm. IR (neat, cm^{-1}): 3265, 2929, 2852, 1652, 1520, 1454, 1249, 693. HRMS (ESI$^+$) [$C_{20}H_{25}NO$] (M+H) calcd. 296.2009, found 296.2016. *Note: higher quantities of 2,4,6-trimethylphenyl isocyanate resulted in lower yields due to the formation of an acyl urea side product coming from the addition of a second isocyanate molecule.*

2.7.5. Synthesis of *N*-Tertiary and *N*-Primary Amides via Sequential C-C Bond Formation

General procedure C: sequential C-C bond-formation of 2.7a, 2-methoxyphenyl isocyanate and different electrophiles. An oven-dried screw-capped test tube containing a stirring bar was loaded with $NiBr_2$ (10.9 mg, 0.0500 mmol, 10 mol%), **L9** (18.4 mg, 0.100 mmol, 20 mol%) and manganese (55.0 mg, 1.00 mmol, 2 equiv). The reaction tube was then evacuated and back-filled with dry argon (this sequence was repeated three times) and DMF (2.0 mL), 1-bromo-4-phenylbutane (84.0 µL, 107 mg, 0.50 mmol; 1 equiv) and 2-methoxyphenyl isocyanate (66.5 µL, 74.6 mg, 0.500 mmol; 1 equiv) were added sequentially under argon flow. The resulting solution was stirred for 16 h at 25 °C. After this period, the corresponding alkyl electrophile was added under argon pressure and the resulting mixture was stirred at the indicated time and temperature, and then carefully quenched with saturated aq. NH_4Cl (2 mL). Acid quench was followed by the addition of distilled water (*ca.* 10 mL) and by extraction with dichloromethane (3 × 25 mL). The obtained solution was washed with brine (40 mL), dried

over $MgSO_4$, filtered and the solvent was evaporated under reduced pressure. The crude product was purified by column chromatography (pentane/Et_2O) to yield the corresponding products.

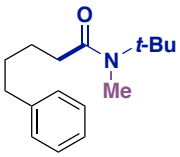

***N*-(*tert*-butyl)-*N*-methyl-5-phenylpentanamide (2.11a).** Following general procedure B, using methyl iodide (62.0 µL, 1.00 mmol; 2 equiv) as alkyl electrophile for 24 h at 50 °C. The title compound (**2.11a**) was obtained as a pale-yellow oil (77.1 mg 1st round, 77.5 2nd round; 62% average yield). ^{1}H-NMR (400 MHz, $CDCl_3$) δ 7.30 – 7.22 (m, 2H, *Ar*), 7.21 – 7.13 (m, 3H, *Ar*), 2.85 (s, 3H, CH_3), 2.64 (t, *J* = 7.1 Hz, 2H, CH_2), 2.35 – 2.24 (m, 2H, CH_2), 1.74 – 1.59 (m, 4H, CH_2), 1.40 (s, 9H, *t-Bu*) ppm. ^{13}C-NMR (101 MHz, $CDCl_3$) δ 173.6, 142.6, 128.5, 128.3, 125.7, 56.7, 36.7, 36.0, 32.0, 31.3, 28.4, 25.1 ppm. IR (neat, cm^{-1}): 2925, 1645, 1453, 1385, 1361, 1110, 698. HRMS (ESI^+) [$C_{16}H_{25}NO$] (M+H) calcd. 248.2009, found 248.2018.

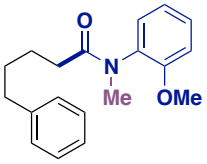

***N*-(2-methoxyphenyl)-*N*-methyl-5-phenylpentanamide (2.11b).** Following general procedure C, using methyl iodide (156 µL, 355 mg, 2.50 mmol; 5 equiv) as alkyl electrophile for 12 h at 25 °C. The title compound (**2.11b**) was obtained as a pale-yellow oil (105.2 mg 1st run, 100.8 mg 2nd run, 70% average yield). ^{1}H-NMR (400 MHz, $CDCl_3$) δ 7.31 (td, *J* = 8.1, 1.7 Hz, 1H, *Ar*), 7.27 – 7.20 (m, 2H, *Ar*), 7.17 – 7.07 (m, 4H, *Ar*), 7.00 – 6.91 (m, 2H, *Ar*), 3.77 (s, 3H, *OMe*), 3.16 (s, 3H, CH_3), 2.52 (t, *J* = 7.5 Hz, 2H, CH_2), 2.09 – 1.94 (m, *J* = 7.2 Hz, 2H, CH_2), 1.66 – 1.56 (m, 2H, CH_2), 1.51 (p, J = 7.4 Hz, 2H, CH_2) ppm. ^{13}C-NMR (101 MHz, $CDCl_3$) δ 173.8, 155.3, 142.6, 132.8, 129.4, 129.3, 128.5, 128.3, 125.7, 121.1, 112.0, 55.5, 36.1, 35.8, 33.4, 31.2, 25.1 ppm. IR (neat, cm^{-1}): 2934, 1653, 1596, 1498, 1382, 1238, 1025, 748, 699. HRMS (ESI^+) [$C_{19}H_{23}NO_2$] (M+H) calcd. 298.1802, found 298.1797.

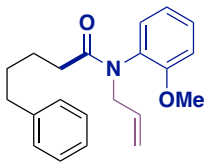

***N*-allyl-*N*-(2-methoxyphenyl)-5-phenylpentanamide (2.11c).** Following general procedure C, using allyl bromide (450 µL, 629 mg, 5.20 mmol; 10.4 equiv) as alkyl electrophile for 12 h at 50 °C. The title compound (**2.11c**) was obtained as a clear oil (80.3 mg 1st run, 84.6 mg 2nd run, 51% average yield). ^{1}H-NMR (500 MHz, $CDCl_3$) δ 7.34 – 7.29 (m, 1H, *Ar*), 7.25 – 7.22 (m, 2H, *Ar*), 7.20 – 7.05 (m, 4H, *Ar*), 6.97 – 6.91 (m, 2H, *Ar*), 5.89 – 5.79 (m, 1H, *CH*), 5.06 – 4.97 (m, 2H, CH_2), 4.55 (dd, *J* = 14.8, 5.9 Hz, 1H, *CH*), 3.90 (dd, *J* = 14.8, 7.0 Hz, 1H, *CH*), 3.77 (s, 3H, OCH_3), 2.52 (t, *J* = 7.6 Hz, 2H, CH_2), 2.02 (h, *J* = 8.0 Hz, 2H, CH_2), 1.61 (dt, *J* = 14.6, 6.8 Hz, 2H, CH_2), 1.52 (p, *J* = 7.4 Hz, 2H, CH_2) ppm. ^{13}C-NMR (126 MHz, $CDCl_3$) δ 173.4, 155.4, 142.6, 133.9, 131.0, 130.3, 129.4, 128.5, 128.3, 125.7, 120.9, 117.3, 111.9, 55.5, 51.2, 35.8, 33.7, 31.2, 25.0 ppm. IR (neat, cm^{-1}): 2931, 1645, 1498, 1393, 1249, 1025, 749, 699. HRMS (ESI^+) [$C_{21}H_{25}NO_2$] (M+H) calcd. 324.1958, found 324.1967.

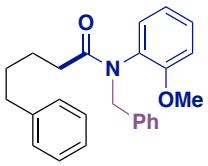

***N*-benzyl-*N*-(2-methoxyphenyl)-5-phenylpentanamide (2.11d).** Following general procedure C, using benzyl bromide (300 µL, 431 mg, 2.52 mmol; 5 equiv) as alkyl electrophile for 12 h at 50 °C. The title compound (**2.11d**) was obtained as a pale-yellow oil (118.8 mg 1st run, 107.7 mg 2nd run, 59% average yield). ^{1}H-NMR (400 MHz, $CDCl_3$) δ 7.32 – 7.09 (m, 11H, *Ar*), 6.93 – 6.76 (m, 3H, *Ar*), 5.30 (d, *J* = 14.3 Hz, 1H, *CH-Ar*), 4.32 (d, J = 14.3 Hz, 1H, *CH-Ar*), 3.68 (s, 3H, OCH_3), 2.58 – 2.51 (m, 2H, CH_2), 2.13 – 1.99 (m, 2H, CH_2), 1.70 – 1.62 (m, 2H, CH_2), 1.60 – 1.50 (m, 2H, CH_2) ppm. ^{13}C-NMR (101 MHz, $CDCl_3$) δ 173.6, 155.3, 142.6, 138.0, 130.9, 130.3, 129.4, 129.1, 128.5, 128.9, 128.1, 127.1, 125.7, 120.7, 111.9, 55.4, 51.8, 35.8, 33.7, 31.2, 25.0 ppm. IR (neat, cm^{-1}): 2931, 1653 ,1497, 1396, 1247, 1025, 747, 697. HRMS (ESI^+) [$C_{25}H_{27}NO_2$] (M+H) calcd. 374.2115, found 374.2122.

2.7.6. *tert*-Butyl Group Deprotection

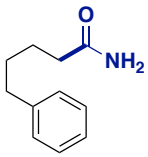

5-phenylpentanamide (2.12a). A microwave vial containing a stirring bar, was charged with *N*-(*tert*-butyl)-5-phenylpentanamide (**2.8b**) (117 mg, 0.500 mmol; 1 equiv), scandium(III) triflate (246 mg, 0.500 mmol; 1 equiv) and nitromethane (2.00 mL). The resulting solution was heated at 170 °C for 1h using a Biotage Microwave Reactor.[70] The reaction mixture was cooled to room temperature and the solvent removed under reduced pressure. The resulting residue was dissolved in dichloromethane, washed with water, dried over $MgSO_4$ and the solvent was evaporated under reduced pressure. The crude product was purified by column chromatography (pentane/AcOEt 1:1 then AcOEt) to afford compound **2.12a** as an off-white solid (81.7 mg; 95% yield; 82% yield after two steps). m.p.: 102.0 – 104.4 °C. ^{1}H-NMR (400 MHz, $CDCl_3$) δ 7.32 – 7.23 (m, 2H, *Ar*), 7.21 – 7.14 (m, 3H, *Ar*), 5.43 (d, *J* = 34.6 Hz, 2H, *NH*$_2$), 2.70 – 2.58 (m, 2H, *CH*$_2$), 2.28 – 2.19 (m, 2H, *CH*$_2$), 1.68 (p, *J* = 3.7 Hz, 4H, *CH*$_2$) ppm. ^{13}C-NMR (101 MHz, $CDCl_3$) δ 175.4, 142.3, 128.5, 128.5, 125.9, 77.2, 35.9, 35.8, 31.1, 25.3 ppm. IR (neat, cm^{-1}): 3401, 3177, 2923, 2853, 1645, 1418, 630. HRMS (ESI$^+$) [$C_{11}H_{15}NO$] (M+Na) calcd. 200.1046, found 200.1048.

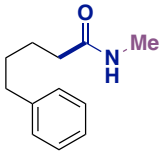

***N*-methyl-5-phenylpentanamide (2.13).** A side-necked sealable tube containing a stirring bar was charged with **2.11a** (124 mg, 0.500 mmol; 1 equiv), copper(II) triflate (36.0 mg, 0.100 mmol; 20 mol%) and dichloromethane (5.00 mL).[85] The resulting solution was heated to 80 °C and followed by TLC until full conversion (*ca.* 48 h). After the reaction mixture was cooled to room temperature, distilled water (15 mL) was added and the resulting mixture extracted with dichloromethane (3 × 10 mL). The organic layer was dried over $MgSO_4$, filtered and the solvent was evaporated under reduced pressure. The crude product was purified by column chromatography (pentane/AcOEt 1:1 then AcOEt) to afford compound **2.13** as a pale-yellow oil (92.0 mg; 96% yield; 60% yield after two steps). ^{1}H-NMR (400 MHz, $CDCl_3$) δ 7.29 – 7.22 (m, 2H, *Ar*), 7.20 – 7.12 (m, 3H, *Ar*), 5.83 (s, 1H, *NH*), 2.75 (d, J = 4.8 Hz, 3H, *CH*$_3$), 2.61 (t, *J* = 7.1 Hz, 2H, *CH*$_2$), 2.17 (t, *J* = 7.1 Hz, 2H, *CH*$_2$), 1.72 – 1.58 (m, 4H, *CH*$_2$) ppm. ^{13}C-NMR (101 MHz, $CDCl_3$) δ 173.7, 142.3, 128.4, 128.4, 125.8, 36.5, 35.7, 31.2, 26.3, 25.5 ppm. IR (neat, cm^{-1}): 3293, 2929, 2857, 1642, 1554, 1453, 1409, 697. HRMS (ESI$^+$) [$C_{12}H_{17}NO$] (M+H) calcd. 192.1383, found 192.1386.

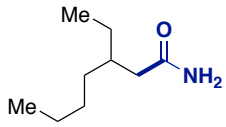

3-ethylheptanamide (2.12b) A Schlenk tube was charged with **2.8h** (53.3 mg, 0.25 mmol) and TFA (2.5 mL) was stirred at 70 °C for 16 hours. The reaction mixture was cooled to room temperature and the excess of TFA was removed under reduced pressure. The crude solid was filtered over a short pad of silica gel (EtOAc) affording the product **2.12b** as an off-white solid (30.4 mg, 77%). m.p.: 63.5 – 65.7 °C. ^{1}H-NMR (400 MHz, $CDCl_3$) δ 5.44 (bs, 1H), 5.60 (bs, 1H), 2.18 – 2.10 (m, 1H), 1.44 – 1.15 (m, 10H).0.93 – 0.83 (m, 6H) ppm. ^{13}C-NMR (101 MHz, $CDCl_3$) δ 40.8, 36.8, 33.1, 28.9, 26.3, 23.1, 14.2, 10.9 ppm.. IR (neat, cm^{-1}): 3347, 3180, 2960, 2924, 1664, 1624, 1410, 1147. HRMS (ESI$^+$) [$C_9H_{20}NO$] (M+H) calcd. 158.1539, found 158.1537.

2.7.7. Mechanistic Experiments

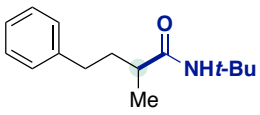

***N*-(*tert*-butyl)-2-methyl-4-phenylbutanamide (2.8z).** Following general procedure B, (*R*)-(3-bromobutyl)benzene[120] (106.6 mg, 0.500 mmol; 1 equiv) and **2.7b** (171 µL, 148 mg, 0.750 mmol; 3.0 equiv) and Mn (55 mg, 1.0 mmol; 2 equiv) were utilized to deliver (rac)-*N*-(*tert*-butyl)-2-methyl-4-phenylbutanamide as a colorless solid (44.8 mg, 38% yield). m.p.: 86.4 – 88.3 °C. ^{1}H-NMR (400 MHz, $CDCl_3$) δ 7.32 - 7.25 (m, 2H, *Ar*), 7.22 - 7.16 (m, 3H, *Ar*), 5.18 (s, 1H, *NH*), 2.65 (dd, *J* = 9.2, 5.1 Hz, 1H, *CH*), 2.62 - 2.50 (m, 1H, *CH*), 2.09 - 1.92 (m, 2H, *CH*$_2$), 1.73 - 1.61 (m, 1H, *CH*), 1.36 (s, 9H, *t-Bu*), 1.12 (d, *J* = 6.6 Hz, 3H, *CH*$_3$) ppm. ^{13}C-NMR (101 MHz, $CDCl_3$) δ 175.6, 142.0, 128.6, 128.5, 126.0, 51.2,

41.6, 36.0, 33.7, 29.0, 18.2 ppm. IR (neat, cm^{-1}): 3315, 2966, 2926, 1643, 1542, 1452, 1360, 1224, 695. HRMS (ESI^+) [$C_{15}H_{23}NO$] (M+H) calcd. 234.1852, found 234.1863.

UPC2 chromatogram of the starting material (*R*)-(3-bromobutyl)benzene (2.1av). Method used: ChiralPak ID column (4.6 mm ϕ x 100 mmL x 3 μm), CO_2/ACN from 0 to 40% ACN during 8 min, 3 ml/min, 1500 psi.

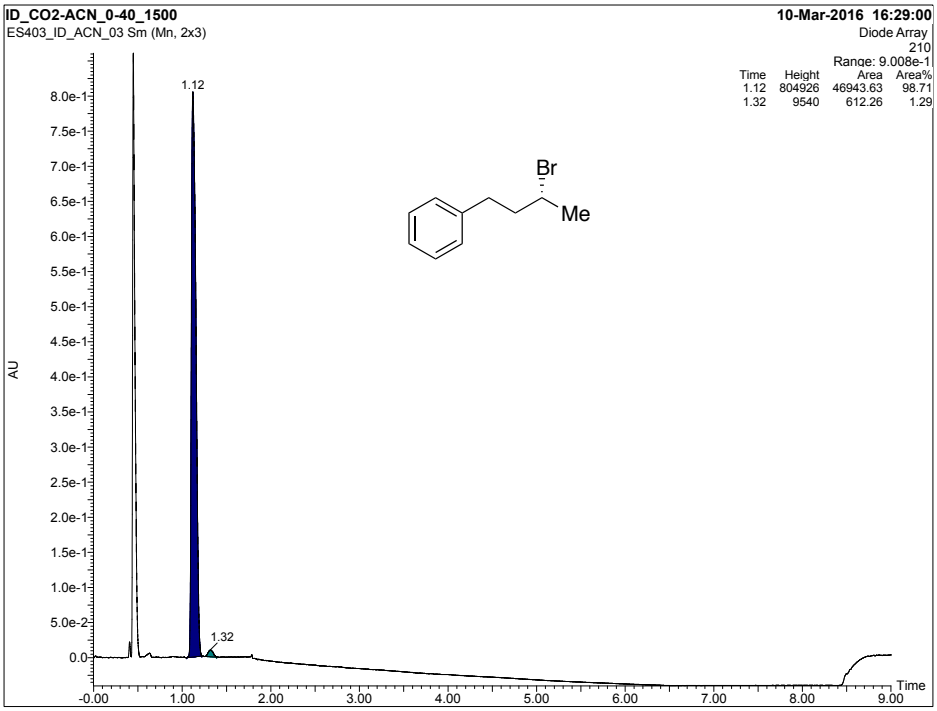

UPC2 chromatogram of the product (rac)-*N*-(*tert*-butyl)-2-methyl-4-phenylbutanamide. Method used: ChiralPak ID column (4.6 mm ϕ x 100 mmL x 3 μm), CO_2/ACN 90:10 for 5 min, 3 ml/min, 1500 psi.

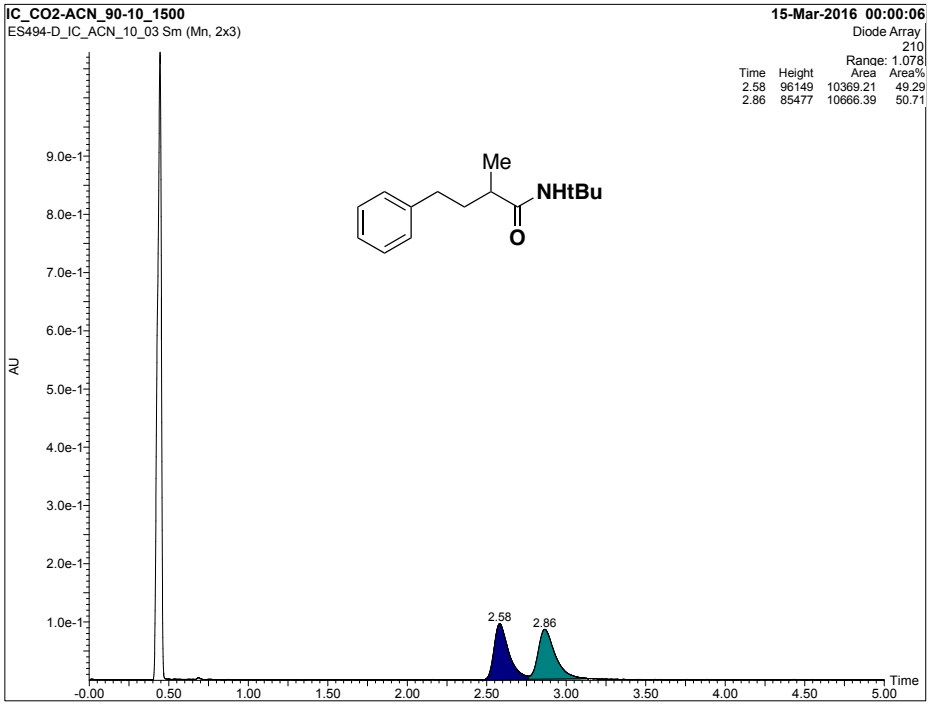

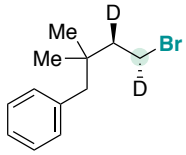

((3R,4R)-4-bromo-2,2-dimethylbutyl-3,4-d$_2$)benzene (2.1aw). A solution of CBr_4 (487 mg, 1.47 mmol; 1.30 equiv) in dichloromethane (1.0 mL) was added dropwise to a solution of (*1R,2R*)-3,3-dimethyl-4-phenylbutan-1,2-d$_2$-1-ol (204 mg, 1.13 mmol; 1 equiv) and triphenylphosphine (385 mg, 1.47 mmol; 1.3 equiv) in dichloromethane (6 mL) at 0°C. The resulting mixture was warmed slowly to room temperature and stirred for 4h. Then the solvent was evaporated under reduced pressure and the crude product purified by column chromatography (pentane) to afford **2.1aw** as a clear oil (261 mg, 95% yield). ^{1}H-NMR (400 MHz, $CDCl_3$) δ 7.33 – 7.20 (m, 3H, *Ar*), 7.16 – 7.09 (m, 2H, *Ar*), 3.42 (d, *J* = 12.4 Hz, 1H, *CH*), 2.53 (s, 2H, *CH$_2$*), 1.85 (d, *J* = 12.3 Hz, 1H, *CH*), 0.91 (s, 6H, *CH$_3$*) ppm. ^{13}C-NMR (101 MHz, $CDCl_3$) δ 138.4, 130.6, 128.0, 126.3, 48.6, 46.8 (*J* = 19,8 Hz), 35.7, 29.2 (*J* = 22.8 Hz), 26.6 ppm. IR (neat, cm^{-1}): 3027, 2957, 2926, 2870, 1467, 1453, 716, 700. HRMS (ESI$^+$) [$C_{12}{}^1H_{15}{}^2H_2Br$] (M+H) calcd. 242.0639, found 242.0634.

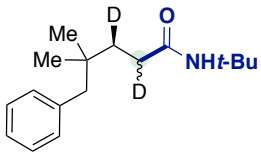

(3S)-*N*-(*tert*-butyl)-4,4-dimethyl-5-phenylpentanamide (2.8y). Following general procedure B, **2.1aw** (122 mg, 0.500 mmol; 1 equiv) and **2.7b** (86.0 µL, 74.3 mg, 0.750 mmol; 1.50 equiv) were utilized to deliver **2.8y** as a pale-yellow oil (116.9 mg, 89% yield). ^{1}H-NMR (500 MHz, $CDCl_3$, 23 °C) δ 7.28 – 7.24 (m, 2H, *Ar*), 7.19 (t, *J* = 7.3 Hz, 1H, *Ar*), 7.14 – 7.10 (m, 2H, *Ar*), 5.31 (s, 1H, *NH*), 2.50 (s, 2H, *CH$_2$*), 2.09 (d, *J* = 9.6 Hz, 1H, *CH*), 1.58 – 1.52 (m, 1H, *CH*), 1.34 (s, 9H, *t-Bu*), 0.85 (s, 6H, *CH$_3$*) ppm. ^{1}H-NMR (500 MHz, $CDCl_3$, -60 °C) δ 7.27 (dt, *J* = 24.3, 7.2 Hz, 3H, *Ar*), 7.14 (d, J = 7.1 Hz, 2H, Ar), 5.70 (s, 1H NH), 2.49 (s, 2H, *CH$_2$*), 2.12 (dd, *J* = 8.7, 4.0 Hz, 1H, *CH*), 1.57 - 1.49 (m, 1H, *CH*), 1.32 (s, 9H, *t-Bu*) ppm. ^{13}C-NMR (126 MHz, $CDCl_3$) δ 172.9, 139.1, 130.7, 127.9, 126.0, 77.2, 51.2, 48.6, 37.3, 34.0, 32.7, 29.0, 26.5 ppm. IR (neat, cm^{-1}): 3306, 2962, 2926, 1639, 1545, 1452, 1225, 701. HRMS (ESI$^+$) [$C_{17}H_{26}D_2NO$] (M+H) calcd. 264.2291, found 264.2296.

2.7.8. Synthesis of Ni(II) and Ni(0) Complexes

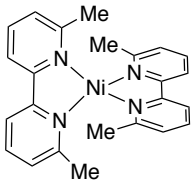

Bis(6,6'-dimethyl-2,2'-bipyridine)nickel(0) (2.14). An oven-dried Schlenk flask containing a stirring bar was introduced into a nitrogen-filled glovebox and charged with $Ni(COD)_2$ (550 mg, 2.00 mmol; 1 equiv) and anhydrous toluene (20.0 mL). To the obtained yellow solution, 6,6'-dimethyl-2,2'-bipyridine (737 mg, 4.00 mmol; 2 equiv) was added slowly, observing a color change from dark green to dark blue. Additional anhydrous toluene (20 mL) was added and the solution was stirred inside the glovebox at room temperature for 48 h. Once outside the glovebox, the solvent was removed under reduced pressure and after full evaporation the dark blue solid was heated to 40 °C under vacuum. Inside the glovebox, the crude solid was re-dissolved in dried pentane (100 mL) (the solid is partially-soluble in pentane), filtered and washed with dried pentane (20 mL). The obtained dark blue solid was dried under reduced pressure, characterized by NMR and used for the stoichiometric reactions (430 mg, 1.00 mmol; 50% yield). X-ray quality crystals were grown from a saturated solution in pentane. ^{1}H-NMR (500 MHz, C_6D_6) δ 8.18 (t, *J* = 7.3 Hz, 4H, *Ar*), 7.48 (d, *J* = 6.3 Hz, 4H, *Ar*), 7.28 (d, *J* = 8.1 Hz, 4H, *Ar*), 2.52 (s, 12H, *CH$_3$*) ppm. ^{13}C-NMR (126 MHz, C_6D_6) δ 159.0, 138.0, 123.8, 119.2, 119.2, 27.7 ppm.

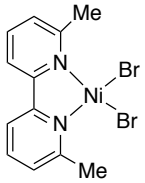

(6,6'-dimethyl-2,2'-bipyridine)nickel(II) dibromide (2.15). An oven-dried two-neck round-bottom flask containing a stirring bar, was charged with anhydrous nickel bromide (542 mg, 2.48 mmol; 1 equiv), 6,6'-dimethyl-2,2'-bipyridine (503 mg, 2.73 mmol; 1.1 equiv) and dried tetrahydrofuran (20.0 mL). The obtained solution was refluxed for 24 h. After cooling to room temperature, the solid was filtered, washed with tetrahydrofuran (20 mL) and hexanes (20 mL) and dried under reduced pressure to afford compound **2.15** as a purple solid (941 mg, 2.34 mmol; 94% yield). The complex was recrystallized form a dichloromethane: hexanes (5:1) mixture or by slow evaporation from a saturated DMF solution to afford purple crystals of paramagnetic **2.15** that were analyzed by X-ray diffraction.

2.7.9. Stoichiometric and Catalytic Experiments with Ni Complexes

2.7.9.1. Catalytic Experiments

With Ni(L9)Br_2 complex (**2.15**):

Following general procedure C, but starting from bis(6,6'-dimethyl-2,2'-bipyridine)nickel(0) (**2.15**) (20.1 mg, 0.0500 mmol; 10 mol%), 6,6'-dimethyl-2,2'-bipyridine (9.2 mg, 0.0500 mmol; 10 mol%), manganese (55.0 mg, 1.00 mmol; 2 equiv), DMF (1.0 mL). After acid quench, dilution with ethyl acetate and using *n*-decane as internal standard, GC-FID analysis showed 100% conversion and 57% yield of product (**2.8v**). Mass balance accounts for *N*-acylurea product (from the attack of the product to a second isocyanate molecule), dimers of **2.1a**, reduced **2.1a** and alkenes coming from β-hydride elimination.

With Ni(L9)$_2$ complex (**2.14**):

Following general procedure C, but starting from bis(6,6'-dimethyl-2,2'-bipyridine)nickel(0) (**2.14**) (10.7 mg, 0.0250 mmol; 10 mol%), manganese (27.5 mg, 0.500 mmol; 2 equiv), DMF (0.5 mL), 1-bromo-4-phenylbutane (53.3 mg, 0.250 mmol; 1 equiv) and 2-methoxyphenyl isocyanate (32.3 µL, 37.3 mg, 0.250 mmol; 1 equiv). After acid quench, dilution with ethyl acetate and using *n*-decane as internal standard, GC-FID analysis showed 100% conversion and 57% yield of product (**2.8v**). Mass balance accounts for *N*-acylurea product (from the attack of the product to a second isocyanate molecule), dimers of **2.1a**, reduced **2.1a** and alkenes coming from β-hydride elimination.

2.7.9.2. Stoichiometric Experiments

Stoichiometric Experiments with Complex **2.14**:

With no manganese: the general procedure C was followed but starting from bis(6,6'-dimethyl-2,2'-bipyridine)nickel(0) (**2.14**) (85.4 mg, 0.200 mmol; 1 equiv), DMF (0.6 mL), 1-bromo-4-phenylbutane (42.6 mg, 0.200 mmol; 1 equiv) and 2-methoxyphenyl isocyanate (26.6 µL, 29.8 mg, 0.200 mmol; 1 equiv). After acid quench, dilution with ethyl acetate and using n-decane as internal standard, GC-FID analysis showed 85% conversion and 38% yield of **2.8v**

With manganese: the general procedure C was followed but starting from bis(6,6'-dimethyl-2,2'-bipyridine)nickel(0) (**2.14**) (85.4 mg, 0.200 mmol; 1 equiv), manganese (22.0 mg, 0.400 mmol; 2 equiv), DMF (0.6 mL), 1-bromo-4-phenylbutane (42.6 mg, 0.200 mmol; 1 equiv) and 2-methoxyphenyl isocyanate (26.6 µL, 29.8 mg, 0.200 mmol; 1 equiv). After acid quench, dilution with ethyl acetate and using n-decane as internal standard, GC-FID analysis showed 100% conversion and 58% yield of product **2.8v**.

Stoichiometric experiments with Complex **2.15**:

General procedure C was followed but starting (6,6'-dimethyl-2,2'- bipyridine)nickel(II) dibromide (**2.15**) (80.5 mg, 0.200 mmol; 1 equiv), manganese (22.0 mg, 0.400 mmol; 2 equiv), DMF (0.6 mL), 6,6'-dimethyl-2,2'-bipyridine (36.8 mg, 0.200 mmol; 1 equiv), 1-bromo-4-phenylbutane (42.6 mg, 0.200 mmol; 1 equiv) and 2-methoxyphenyl isocyanate (26.6 µL, 29.8 mg, 0.200 mmol; 1 equiv). After acid quench, dilution with ethyl acetate and using *n*-decane as internal standard, GC-FID analysis showed 100% conversion and 51% yield of product **2.8v**.

2.7.10. X-ray Crystallographic Analysis

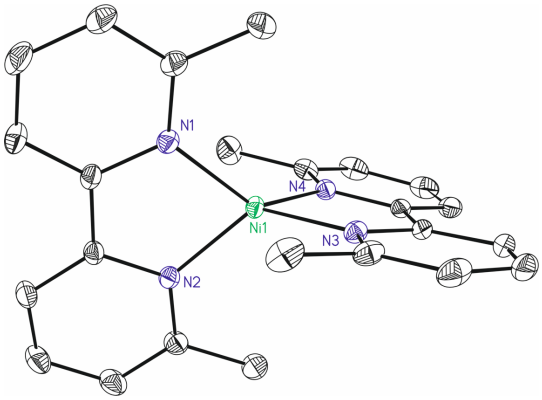

Table 1. Crystal data and structure refinement for **2.14**.

Identification code	**2.14**	
Empirical formula	$C_{36}H_{36}N_6Ni$	
Formula weight	611.42	
Temperature	100(2) K	
Wavelength	0.71073 Å	
Crystal system	Triclinic	
Space group	P-1	
Unit cell dimensions	a = 8.7671(4)Å	⟨= 79.5270(12)°.
	b = 11.7661(5)Å	® = 74.8400(12)°.
	c = 15.4557(6)Å	© = 89.1942(12)°.
Volume	1512.27(11) $Å^3$	
Z	2	
Density (calculated)	1.343 Mg/m^3	
Absorption coefficient	0.678 mm^{-1}	
F(000)	644	
Crystal size	0.30 x 0.30 x 0.04 mm^3	
Theta range for data collection	1.761 to 35.086°.	
Index ranges	-14<=h<=14,-18<=k<=19,-12<=l<=24	
Reflections collected	63396	
Independent reflections	12375[R(int) = 0.0242]	
Completeness to theta =35.086°	92.4%	
Absorption correction	Empirical	
Max. and min. transmission	0.973 and 0.884	
Refinement method	Full-matrix least-squares on F^2	
Data / restraints / parameters	12375/ 0/ 394	
Goodness-of-fit on F^2	1.036	
Final R indices [I>2sigma(I)]	R1 = 0.0304, wR2 = 0.0790	
R indices (all data)	R1 = 0.0369, wR2 = 0.0823	
Largest diff. peak and hole	0.483 and -0.253 $e.Å^{-3}$	

Table 2. Bond lengths [Å] and angles [°] for **2.14**.

Bond lengths----	
Ni1-N2	1.9245(8)

Ni1-N1	1.9296(8)	C16-H16	0.9500
Ni1-N3	1.9306(8)	C17-C18	1.4064(13)
Ni1-N4	1.9337(7)	C17-H17	0.9500
N1-C2	1.3698(12)	C18-C19	1.4411(13)
N1-C6	1.3755(12)	C19-C20	1.4050(12)
N2-C11	1.3704(12)	C20-C21	1.3726(16)
N2-C7	1.3735(11)	C20-H20	0.9500
N3-C14	1.3700(12)	C21-C22	1.4055(17)
N3-C18	1.3758(11)	C21-H21	0.9500
N4-C23	1.3680(12)	C22-C23	1.3800(13)
N4-C19	1.3747(11)	C22-H22	0.9500
C1-C2	1.4965(15)	C23-C24	1.4966(15)
C1-H1A	0.9800	C24-H24A	0.9800
C1-H1B	0.9800	C24-H24B	0.9800
C1-H1C	0.9800	C24-H24C	0.9800
C2-C3	1.3804(13)	N1A-C2A	1.3420(12)
C3-C4	1.4028(16)	N1A-C6A	1.3459(11)
C3-H3	0.9500	N2A-C7A	1.3461(12)
C4-C5	1.3772(15)	N2A-C11A	1.3461(12)
C4-H4	0.9500	C1A-C2A	1.5035(14)
C5-C6	1.4022(12)	C1A-H1A1	0.9800
C5-H5	0.9500	C1A-H1A2	0.9800
C6-C7	1.4465(13)	C1A-H1A3	0.9800
C7-C8	1.4044(13)	C2A-C3A	1.3978(14)
C8-C9	1.3777(15)	C3A-C4A	1.3845(14)
C8-H8	0.9500	C3A-H3A	0.9500
C9-C10	1.4014(15)	C4A-C5A	1.3897(13)
C9-H9	0.9500	C4A-H4A	0.9500
C10-C11	1.3813(14)	C5A-C6A	1.3929(13)
C10-H10	0.9500	C5A-H5A	0.9500
C11-C12	1.4995(14)	C6A-C7A	1.4933(12)
C12-H12A	0.9800	C7A-C8A	1.3953(13)
C12-H12B	0.9800	C8A-C9A	1.3907(13)
C12-H12C	0.9800	C8A-H8A	0.9500
C13-C14	1.5003(15)	C9A-C10A	1.3860(15)
C13-H13A	0.9800	C9A-H9A	0.9500
C13-H13B	0.9800	C10A-C11A	1.3961(15)
C13-H13C	0.9800	C10A-H10A	0.9500
C14-C15	1.3778(14)	C11A-C12A	1.5041(14)
C15-C16	1.4081(17)	C12A-H12D	0.9800
C15-H15	0.9500	C12A-H12E	0.9800
		C12A-H12F	0.9800

Angles----------

C16-C17	1.3762(16)	N2-Ni1-N1	82.86(3)

N2-Ni1-N3	127.74(3)	C8-C9-H9	120.6
N1-Ni1-N3	121.09(3)	C10-C9-H9	120.6
N2-Ni1-N4	115.62(3)	C11-C10-C9	120.30(10)
N1-Ni1-N4	133.39(3)	C11-C10-H10	119.8
N3-Ni1-N4	82.48(3)	C9-C10-H10	119.8
C2-N1-C6	118.10(8)	N2-C11-C10	121.51(9)
C2-N1-Ni1	127.05(6)	N2-C11-C12	116.41(8)
C6-N1-Ni1	114.75(6)	C10-C11-C12	122.08(9)
C11-N2-C7	118.26(8)	C11-C12-H12A	109.5
C11-N2-Ni1	126.69(6)	C11-C12-H12B	109.5
C7-N2-Ni1	114.97(6)	H12A-C12-H12B	109.5
C14-N3-C18	118.09(8)	C11-C12-H12C	109.5
C14-N3-Ni1	126.95(6)	H12A-C12-H12C	109.5
C18-N3-Ni1	114.96(6)	H12B-C12-H12C	109.5
C23-N4-C19	118.31(8)	C14-C13-H13A	109.5
C23-N4-Ni1	126.72(6)	C14-C13-H13B	109.5
C19-N4-Ni1	114.68(6)	H13A-C13-H13B	109.5
C2-C1-H1A	109.5	C14-C13-H13C	109.5
C2-C1-H1B	109.5	H13A-C13-H13C	109.5
H1A-C1-H1B	109.5	H13B-C13-H13C	109.5
C2-C1-H1C	109.5	N3-C14-C15	121.97(9)
H1A-C1-H1C	109.5	N3-C14-C13	116.25(9)
H1B-C1-H1C	109.5	C15-C14-C13	121.78(9)
N1-C2-C3	121.60(9)	C14-C15-C16	119.85(10)
N1-C2-C1	116.18(8)	C14-C15-H15	120.1
C3-C2-C1	122.22(9)	C16-C15-H15	120.1
C2-C3-C4	120.16(10)	C17-C16-C15	119.00(9)
C2-C3-H3	119.9	C17-C16-H16	120.5
C4-C3-H3	119.9	C15-C16-H16	120.5
C5-C4-C3	118.91(9)	C16-C17-C18	119.32(9)
C5-C4-H4	120.5	C16-C17-H17	120.3
C3-C4-H4	120.5	C18-C17-H17	120.3
C4-C5-C6	119.29(9)	N3-C18-C17	121.76(9)
C4-C5-H5	120.4	N3-C18-C19	113.64(8)
C6-C5-H5	120.4	C17-C18-C19	124.58(8)
N1-C6-C5	121.92(9)	N4-C19-C20	121.58(9)
N1-C6-C7	113.59(7)	N4-C19-C18	113.71(7)
C5-C6-C7	124.48(9)	C20-C19-C18	124.71(9)
N2-C7-C8	121.69(8)	C21-C20-C19	119.54(9)
N2-C7-C6	113.67(8)	C21-C20-H20	120.2
C8-C7-C6	124.62(8)	C19-C20-H20	120.2
C9-C8-C7	119.52(9)	C20-C21-C22	118.86(9)
C9-C8-H8	120.2	C20-C21-H21	120.6
		C22-C21-H21	120.6
C7-C8-H8	120.2	C23-C22-C21	120.05(9)
C8-C9-C10	118.71(9)	C23-C22-H22	120.0

C21-C22-H22	120.0	C4A-C5A-H5A	120.7
N4-C23-C22	121.63(9)	C6A-C5A-H5A	120.7
N4-C23-C24	115.89(8)	N1A-C6A-C5A	122.61(8)
C22-C23-C24	122.49(9)	N1A-C6A-C7A	115.91(8)
C23-C24-H24A	109.5	C5A-C6A-C7A	121.48(8)
C23-C24-H24B	109.5	N2A-C7A-C8A	122.78(8)
H24A-C24-H24B	109.5	N2A-C7A-C6A	116.48(8)
C23-C24-H24C	109.5	C8A-C7A-C6A	120.73(8)
H24A-C24-H24C	109.5	C9A-C8A-C7A	118.40(9)
H24B-C24-H24C	109.5	C9A-C8A-H8A	120.8
C2A-N1A-C6A	118.56(8)	C7A-C8A-H8A	120.8
C7A-N2A-C11A	118.54(8)	C10A-C9A-C8A	119.04(9)
C2A-C1A-H1A1	109.5	C10A-C9A-H9A	120.5
C2A-C1A-H1A2	109.5	C8A-C9A-H9A	120.5
H1A1-C1A-H1A2	109.5	C9A-C10A-C11A	119.32(9)
C2A-C1A-H1A3	109.5	C9A-C10A-H10A	120.3
H1A1-C1A-H1A3	109.5	C11A-C10A-H10A	120.3
H1A2-C1A-H1A3	109.5	N2A-C11A-C10A	121.91(9)
N1A-C2A-C3A	122.19(9)	N2A-C11A-C12A	116.69(9)
N1A-C2A-C1A	116.52(9)	C10A-C11A-C12A	121.38(9)
C3A-C2A-C1A	121.28(8)	C11A-C12A-H12D	109.5
C4A-C3A-C2A	118.92(9)	C11A-C12A-H12E	109.5
C4A-C3A-H3A	120.5	H12D-C12A-H12E	109.5
C2A-C3A-H3A	120.5	C11A-C12A-H12F	109.5
C3A-C4A-C5A	119.18(9)	H12D-C12A-H12F	109.5
C3A-C4A-H4A	120.4	H12E-C12A-H12F	109.5
C5A-C4A-H4A	120.4		
C4A-C5A-C6A	118.53(9)		

Table 3. Torsion angles [°] for **2.14**.

C6-N1-C2-C3	1.21(14)	C4-C5-C6-C7	179.43(10)
Ni1-N1-C2-C3	-174.97(8)	C11-N2-C7-C8	-1.22(13)
C6-N1-C2-C1	-178.39(9)	Ni1-N2-C7-C8	175.76(7)
Ni1-N1-C2-C1	5.43(13)	C11-N2-C7-C6	-179.89(8)
N1-C2-C3-C4	-0.12(17)	Ni1-N2-C7-C6	-2.92(10)
C1-C2-C3-C4	179.45(11)	N1-C6-C7-N2	4.32(11)
C2-C3-C4-C5	-0.78(18)	C5-C6-C7-N2	-174.63(9)
C3-C4-C5-C6	0.56(17)	N1-C6-C7-C8	-174.31(9)
C2-N1-C6-C5	-1.43(13)	C5-C6-C7-C8	6.74(15)
Ni1-N1-C6-C5	175.21(7)	N2-C7-C8-C9	0.36(15)
C2-N1-C6-C7	179.58(8)	C6-C7-C8-C9	178.89(10)
Ni1-N1-C6-C7	-3.77(10)	C7-C8-C9-C10	0.14(16)
C4-C5-C6-N1	0.56(15)	C8-C9-C10-C11	0.23(17)
		C7-N2-C11-C10	1.60(14)
		Ni1-N2-C11-C10	-174.99(8)

C7-N2-C11-C12	-178.07(9)
Ni1-N2-C11-C12	5.35(13)
C9-C10-C11-N2	-1.13(16)
C9-C10-C11-C12	178.51(10)
C18-N3-C14-C15	-0.05(13)
Ni1-N3-C14-C15	-179.93(7)
C18-N3-C14-C13	179.05(8)
Ni1-N3-C14-C13	-0.83(12)
N3-C14-C15-C16	0.89(15)
C13-C14-C15-C16	-178.16(9)
C14-C15-C16-C17	-1.01(15)
C15-C16-C17-C18	0.31(15)
C14-N3-C18-C17	-0.67(13)
Ni1-N3-C18-C17	179.22(7)
C14-N3-C18-C19	-178.81(8)
Ni1-N3-C18-C19	1.09(9)
C16-C17-C18-N3	0.54(14)
C16-C17-C18-C19	178.46(9)
C23-N4-C19-C20	-1.95(13)
Ni1-N4-C19-C20	172.21(7)
C23-N4-C19-C18	177.97(8)
Ni1-N4-C19-C18	-7.87(9)
N3-C18-C19-N4	4.39(11)
C17-C18-C19-N4	-173.68(8)
N3-C18-C19-C20	-175.69(8)
C17-C18-C19-C20	6.24(14)
N4-C19-C20-C21	1.25(14)
C18-C19-C20-C21	-178.67(9)
C19-C20-C21-C22	0.40(14)
C20-C21-C22-C23	-1.31(15)
C19-N4-C23-C22	1.02(13)
Ni1-N4-C23-C22	-172.35(7)
C19-N4-C23-C24	-179.21(8)
Ni1-N4-C23-C24	7.42(12)
C21-C22-C23-N4	0.60(15)
C21-C22-C23-C24	-179.16(10)
C6A-N1A-C2A-C3A	-0.61(13)
C6A-N1A-C2A-C1A	178.99(8)
N1A-C2A-C3A-C4A	0.17(15)
C1A-C2A-C3A-C4A	-179.40(10)
C2A-C3A-C4A-C5A	0.31(15)
C3A-C4A-C5A-C6A	-0.35(15)
C2A-N1A-C6A-C5A	0.57(13)
C2A-N1A-C6A-C7A	-179.16(8)
C4A-C5A-C6A-N1A	-0.09(14)
C4A-C5A-C6A-C7A	179.62(8)
C11A-N2A-C7A-C8A	0.49(13)
C11A-N2A-C7A-C6A	-178.56(8)
N1A-C6A-C7A-N2A	165.83(8)
C5A-C6A-C7A-N2A	-13.90(12)
N1A-C6A-C7A-C8A	-13.23(12)
C5A-C6A-C7A-C8A	167.04(9)
N2A-C7A-C8A-C9A	-0.04(14)
C6A-C7A-C8A-C9A	178.96(8)
C7A-C8A-C9A-C10A	-0.28(14)
C8A-C9A-C10A-C11A	0.16(15)
C7A-N2A-C11A-C10A	-0.61(13)
C7A-N2A-C11A-C12A	177.54(8)
C9A-C10A-C11A-N2A	0.30(15)
C9A-C10A-C11A-C12A	-177.78(10)

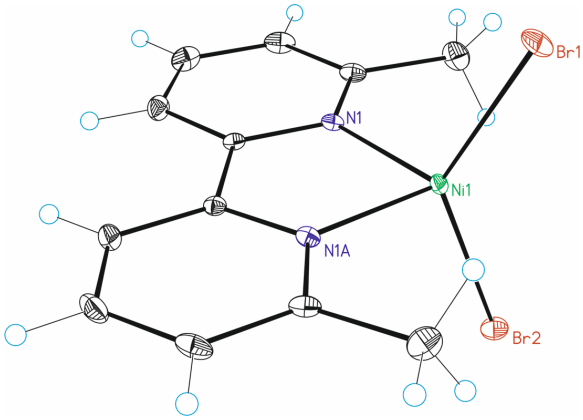

Table 1. Crystal data and structure refinement for **2.15**.

Identification code	**2.15**	
Empirical formula	$C_{12}H_{12}Br_2N_2Ni$	
Formula weight	402.77	
Temperature	100(2) K	
Wavelength	null Å	
Crystal system	Orthorhombic	
Space group	Pnma	
Unit cell dimensions	a = 14.6852(14)Å	a= 90°.
	b = 11.2355(8)Å	b = 90°.
	c = 8.1230(6)Å	g = 90°.
Volume	1340.26(19) $Å^3$	
Z	4	
Density (calculated)	1.996 Mg/m^3	
Absorption coefficient	7.388 mm^{-1}	
F(000)	784	
Crystal size	0.30 x 0.25 x 0.25 mm^3	
Theta range for data collection	2.774 to 32.429°.	
Index ranges	-21<=h<=20,-15<=k<=10,-5<=l<=12	
Reflections collected	9284	
Independent reflections	2250[R(int) = 0.0393]	
Completeness to theta =32.429°	89.4%	
Absorption correction	Multi-scan	
Max. and min. transmission	_exptl_absorpt_correction_T_max 0.7464	
	and _exptl_absorpt_correction_T_min 0.2815	
Refinement method	Full-matrix least-squares on F^2	
Data / restraints / parameters	2250/ 0/ 83	
Goodness-of-fit on F^2	1.078	
Final R indices [I>2sigma(I)]	R1 = 0.0304, wR2 = 0.0673	
R indices (all data)	R1 = 0.0385, wR2 = 0.0697	
Largest diff. peak and hole	0.681 and -1.478 e.$Å^{-3}$	

Table 2. Bond lengths [Å] and angles [°] for **2.15**.

Bond lengths----	
Ni1-N1#1	1.9821(18)
Ni1-N1	1.9821(18)
Ni1-Br1	2.3401(5)
Ni1-Br2	2.3510(5)
N1-C2	1.347(3)
N1-C6	1.353(3)
C1-C2	1.498(3)
C2-C3	1.392(3)
C3-C4	1.384(3)
C4-C5	1.384(4)
C5-C6	1.388(3)
C6-C6#1	1.493(5)
Angles----------	
N1-Ni1-N1#1	83.09(11)
N1-Ni1-Br1#1	110.21(5)
N1-Ni1-Br1	110.21(5)
N1-Ni1-Br2#1	104.79(5)
N1-Ni1-Br2	104.79(5)
Br1-Ni1-Br2	132.564(19)
C2-N1-C6	120.41(19)
C2-N1-Ni1	125.95(14)
C6-N1-Ni1	113.61(15)
N1-C2-C3	119.8(2)
N1-C2-C1	117.4(2)
C3-C2-C1	122.8(2)
C4-C3-C2	120.3(2)
C3-C4-C5	119.3(2)
C4-C5-C6	118.59(19)
N1-C6-C5	121.6(2)
N1-C6-C6#1	114.83(13)
C5-C6-C6#1	123.57(13)

Symmetry transformations used to generate equivalent atoms:
#1 x, -y+1/2, z

Table 3. Torsion angles [°] for **2.15**.

C6-N1-C2-C3	0.0(3)
Ni1-N1-C2-C3	177.98(15)
C6-N1-C2-C1	179.91(18)
Ni1-N1-C2-C1	-2.1(3)
N1-C2-C3-C4	0.5(3)
C1-C2-C3-C4	-179.4(2)
C2-C3-C4-C5	-0.4(3)
C3-C4-C5-C6	-0.2(3)
C2-N1-C6-C5	-0.7(3)
Ni1-N1-C6-C5	-178.84(15)
C2-N1-C6-C6#1	179.42(14)
Ni1-N1-C6-C6#1	1.24(14)
C4-C5-C6-N1	0.7(3)
C4-C5-C6-C6#1	-179.34(13)

Symmetry transformations used to generate equivalent atoms:
#1 x, -y+1/2, z

2.8. ^{1}H-NMR and ^{13}C-NMR Spectra

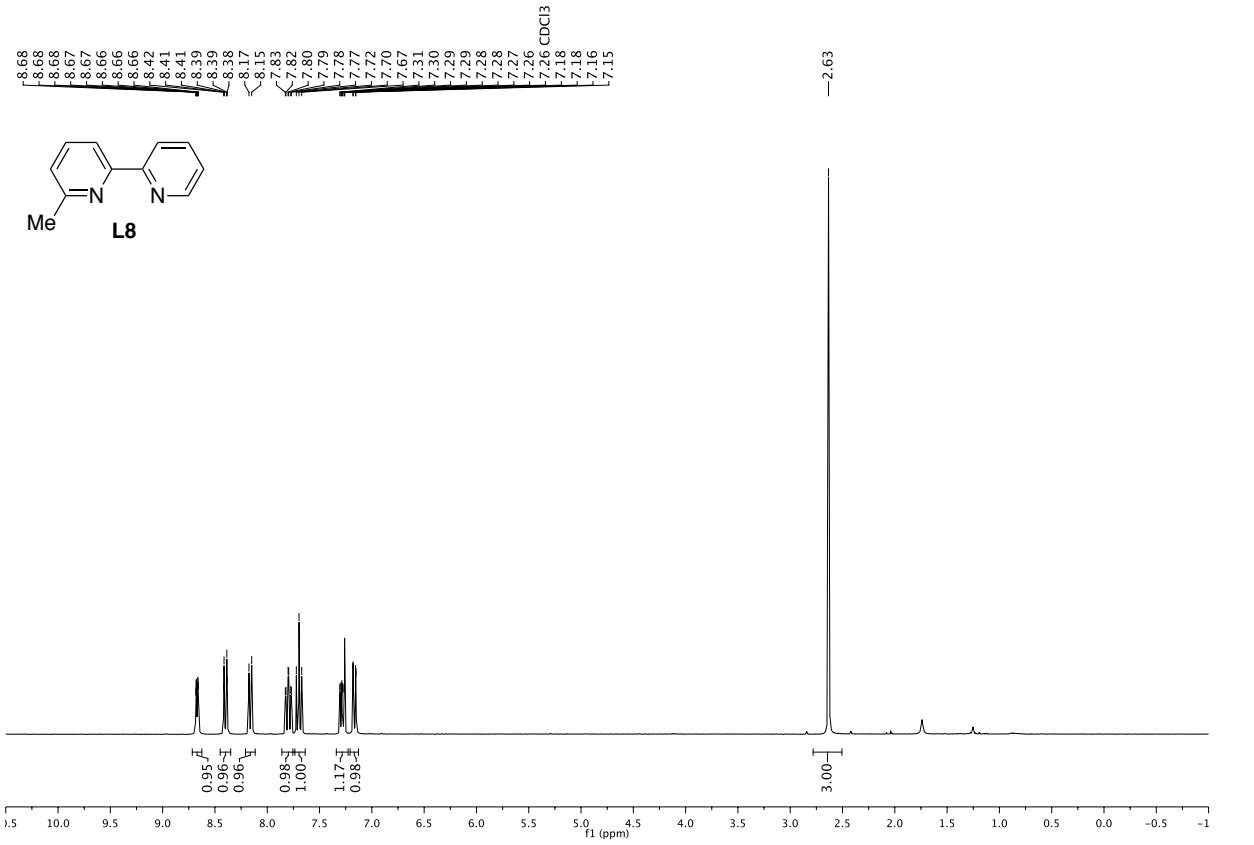

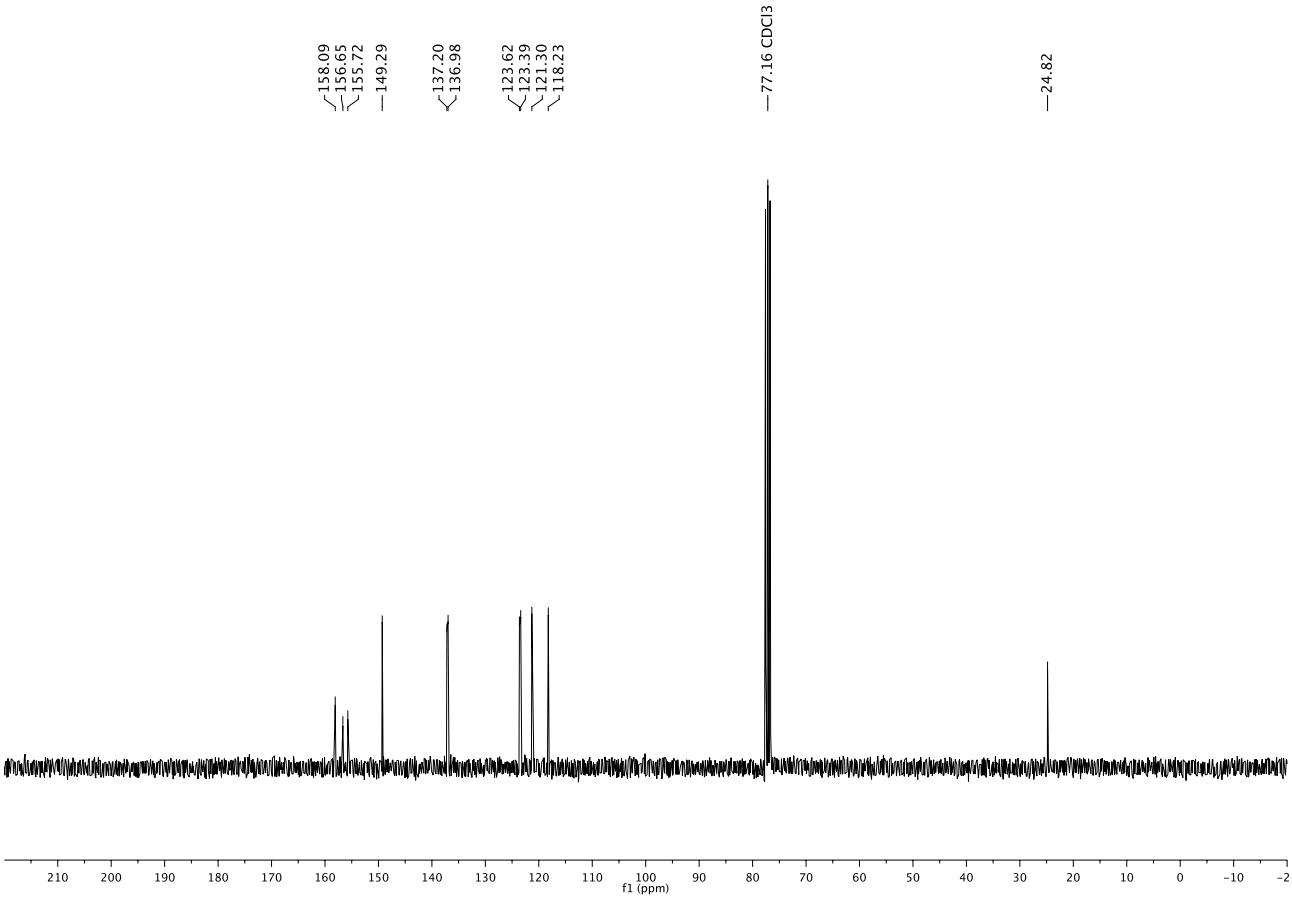

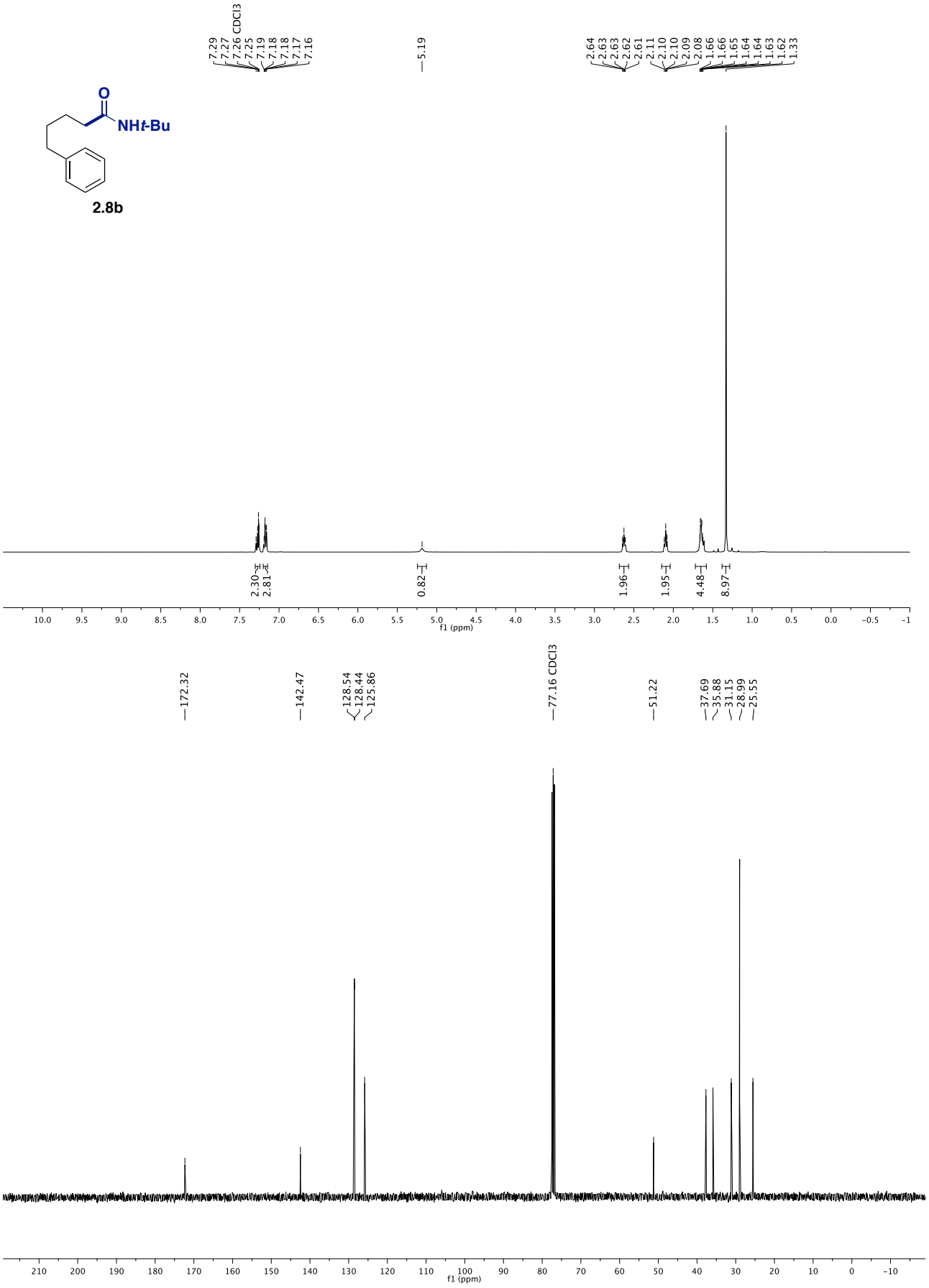
7.29
7.27
7.26 CDCl3
7.25
7.19
7.18
7.18
7.17
7.16
5.19
2.64
2.63
2.63
2.62
2.61
2.11
2.10
2.10
2.09
2.08
1.66
1.66
1.65
1.64
1.64
1.63
1.62
1.33
O
NHt-Bu
2.8b
2.30
2.81
0.82
1.96
1.95
4.48
8.97
f1 (ppm)
172.32
142.47
128.54
128.44
125.86
77.16 CDCl3
51.22
37.69
35.88
31.15
28.99
25.55
f1 (ppm)

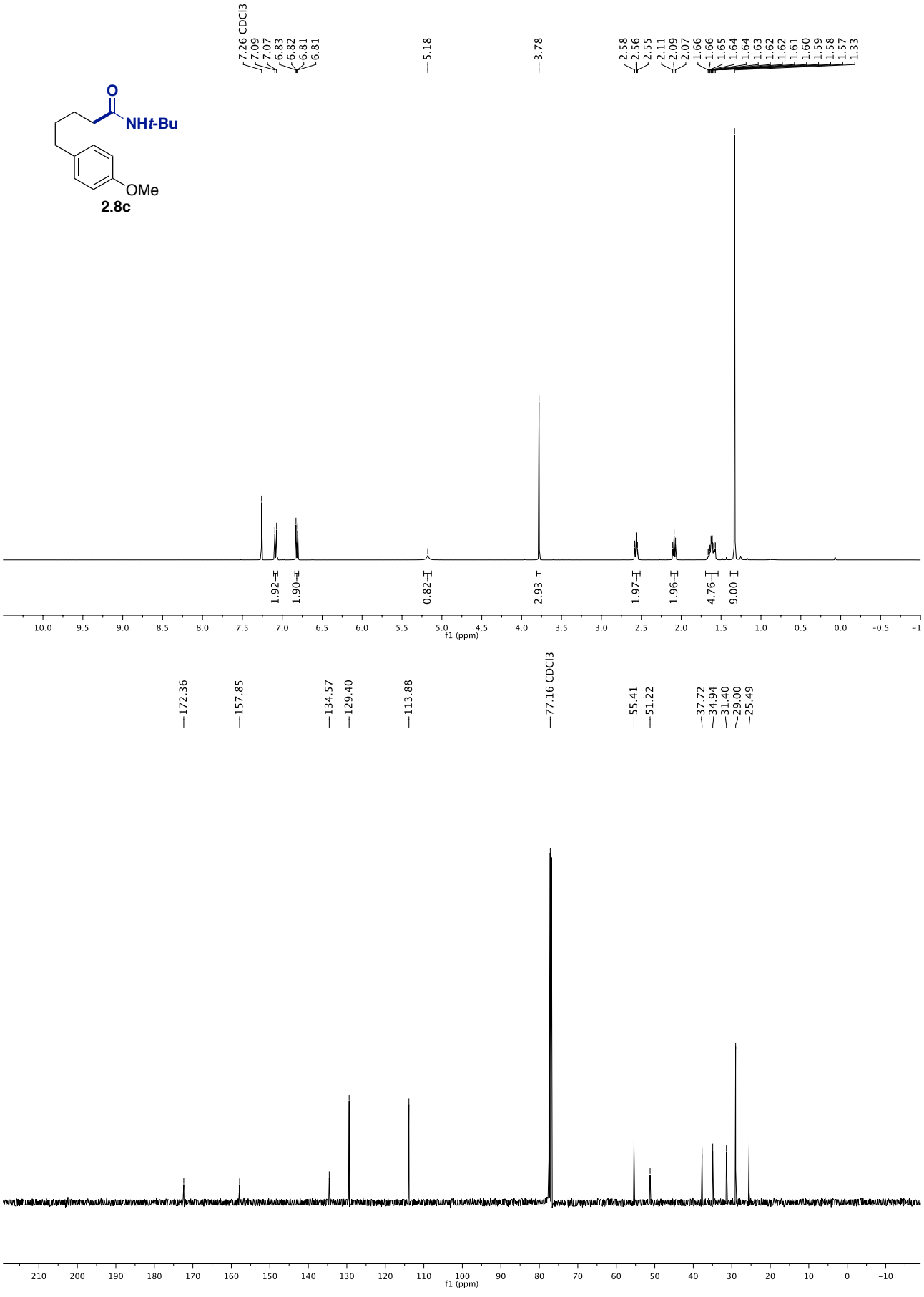
7.26 CDCl3
7.09
7.07
6.83
6.82
6.81
6.81
5.18
3.78
2.58
2.56
2.55
2.11
2.09
2.07
1.66
1.65
1.64
1.64
1.63
1.62
1.62
1.61
1.60
1.59
1.58
1.57
1.33
O
NHt-Bu
OMe
2.8c
1.92
1.90
0.82
2.93
1.97
1.96
4.76
9.00
f1 (ppm)
172.36
157.85
134.57
129.40
113.88
77.16 CDCl3
55.41
51.22
37.72
34.94
31.40
29.00
25.49
f1 (ppm)

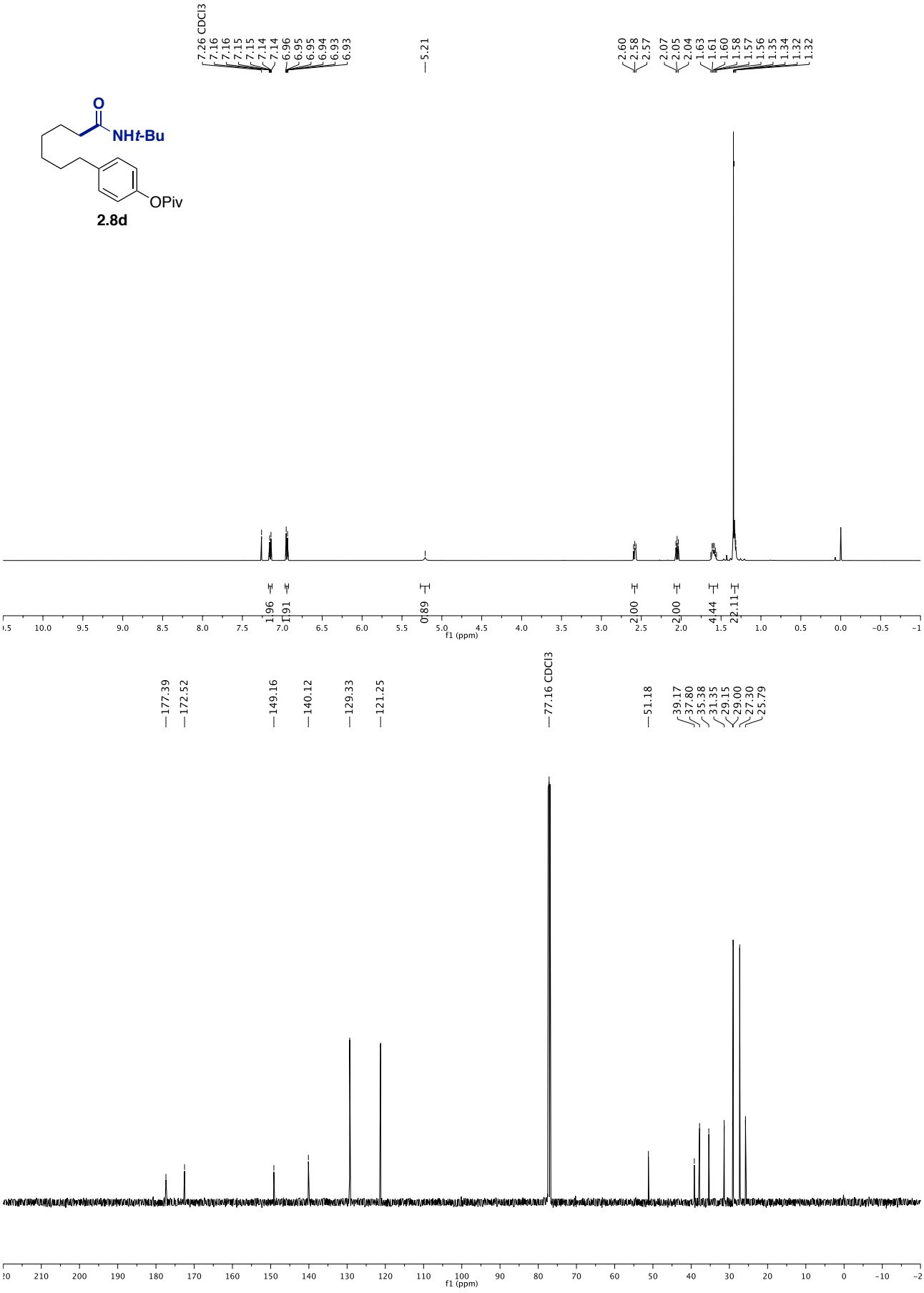
7.26 CDCl3
7.16
7.16
7.15
7.15
7.14
7.14
6.96
6.95
6.95
6.94
6.93
6.93
5.21
2.60
2.58
2.57
2.07
2.05
2.04
1.63
1.61
1.60
1.58
1.57
1.56
1.35
1.34
1.32
1.32
O
NHt-Bu
OPiv
2.8d
1.96
1.91
0.89
2.00
2.00
4.44
22.11
f1 (ppm)
177.39
172.52
149.16
140.12
129.33
121.25
77.16 CDCl3
51.18
39.17
37.80
35.38
31.35
29.15
29.00
27.30
25.79
f1 (ppm)

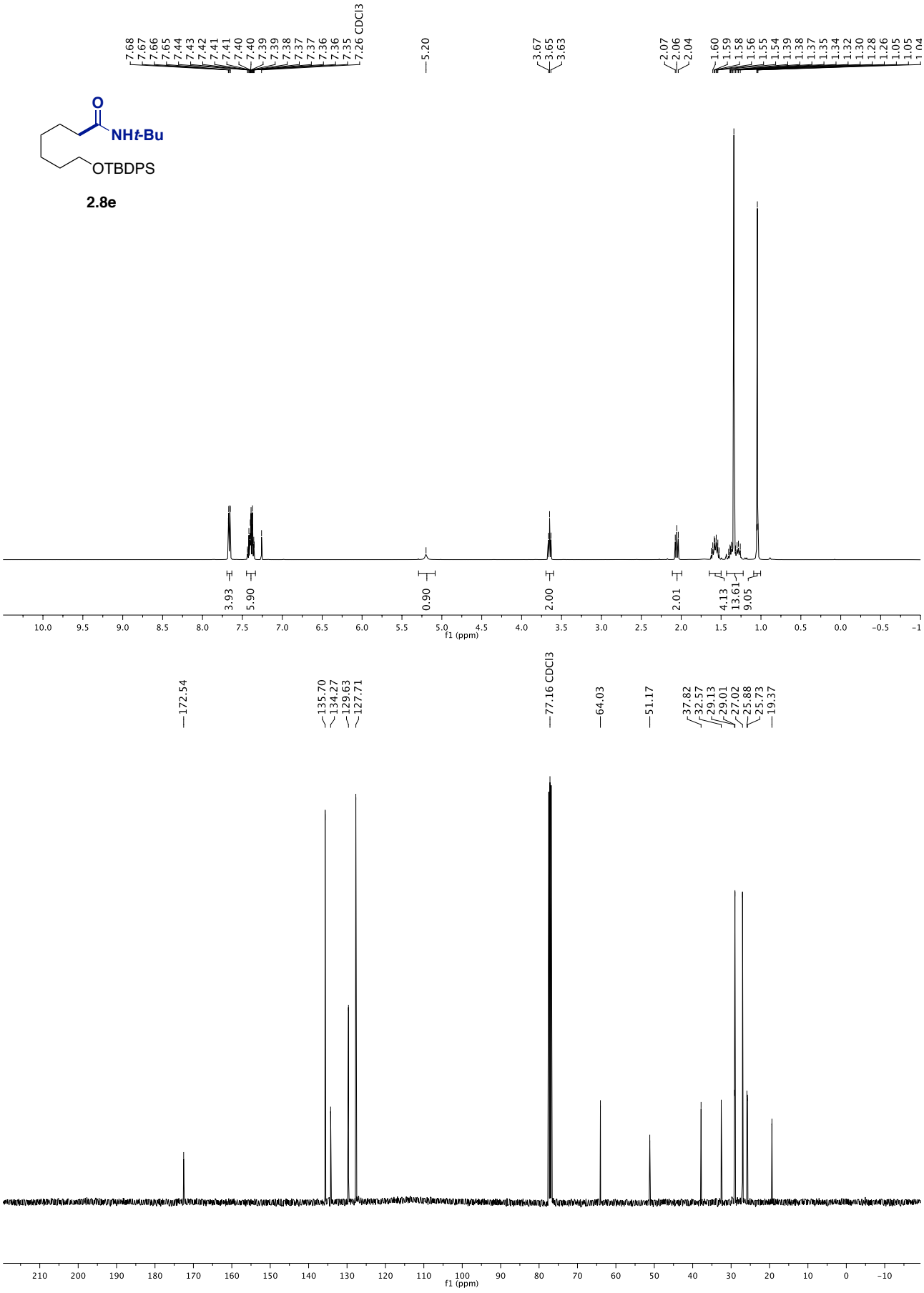
NHt-Bu
OTBDPS
2.8e
f1 (ppm)

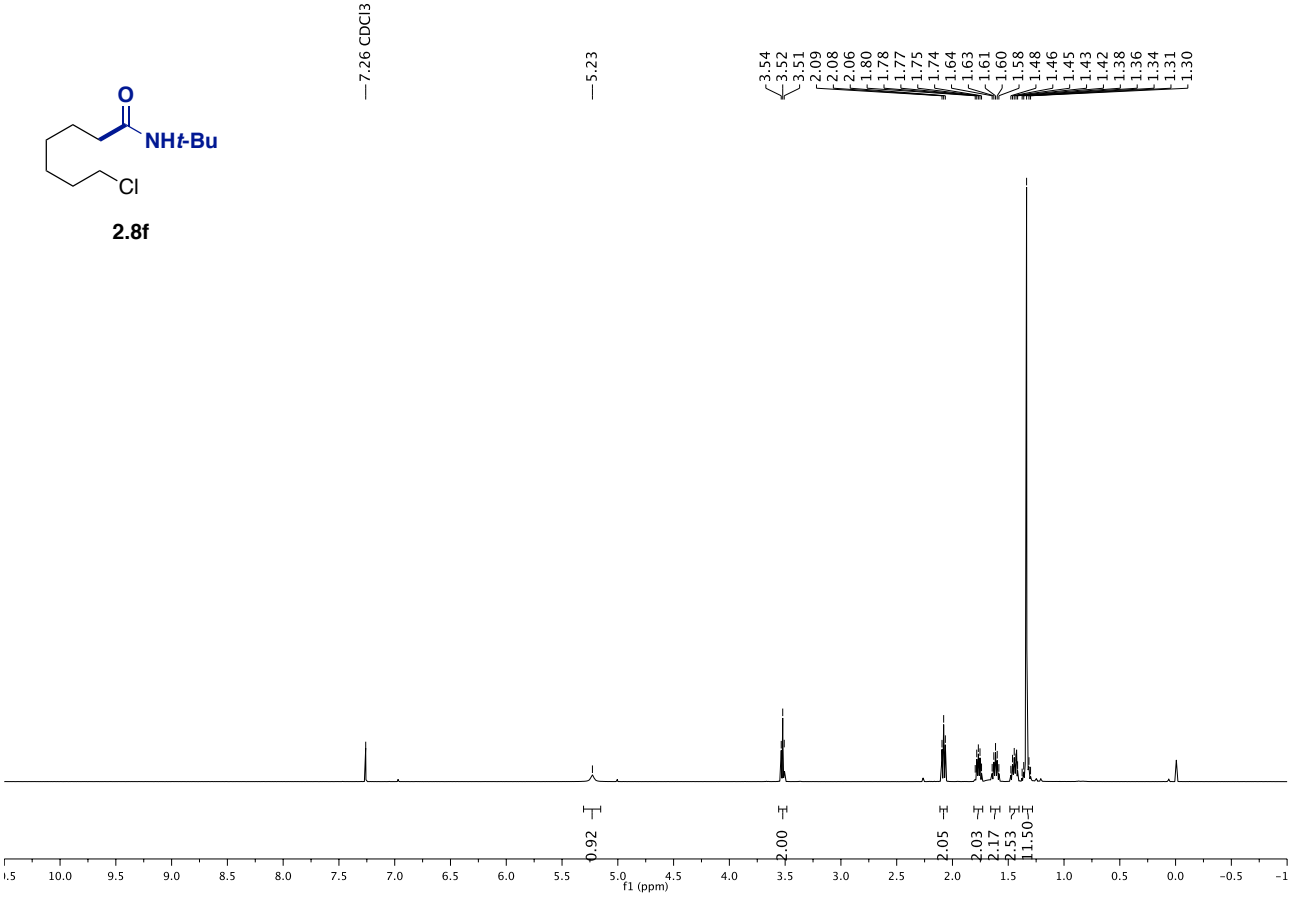
7.26 CDCl3
5.23
3.54
3.52
3.51
2.09
2.08
2.06
1.80
1.78
1.77
1.75
1.74
1.64
1.63
1.61
1.60
1.58
1.48
1.46
1.45
1.43
1.42
1.38
1.36
1.34
1.31
1.30
O
NHt-Bu
Cl
0.92
2.00
2.05
2.03
2.17
2.53
11.50
f1 (ppm)

2.8f

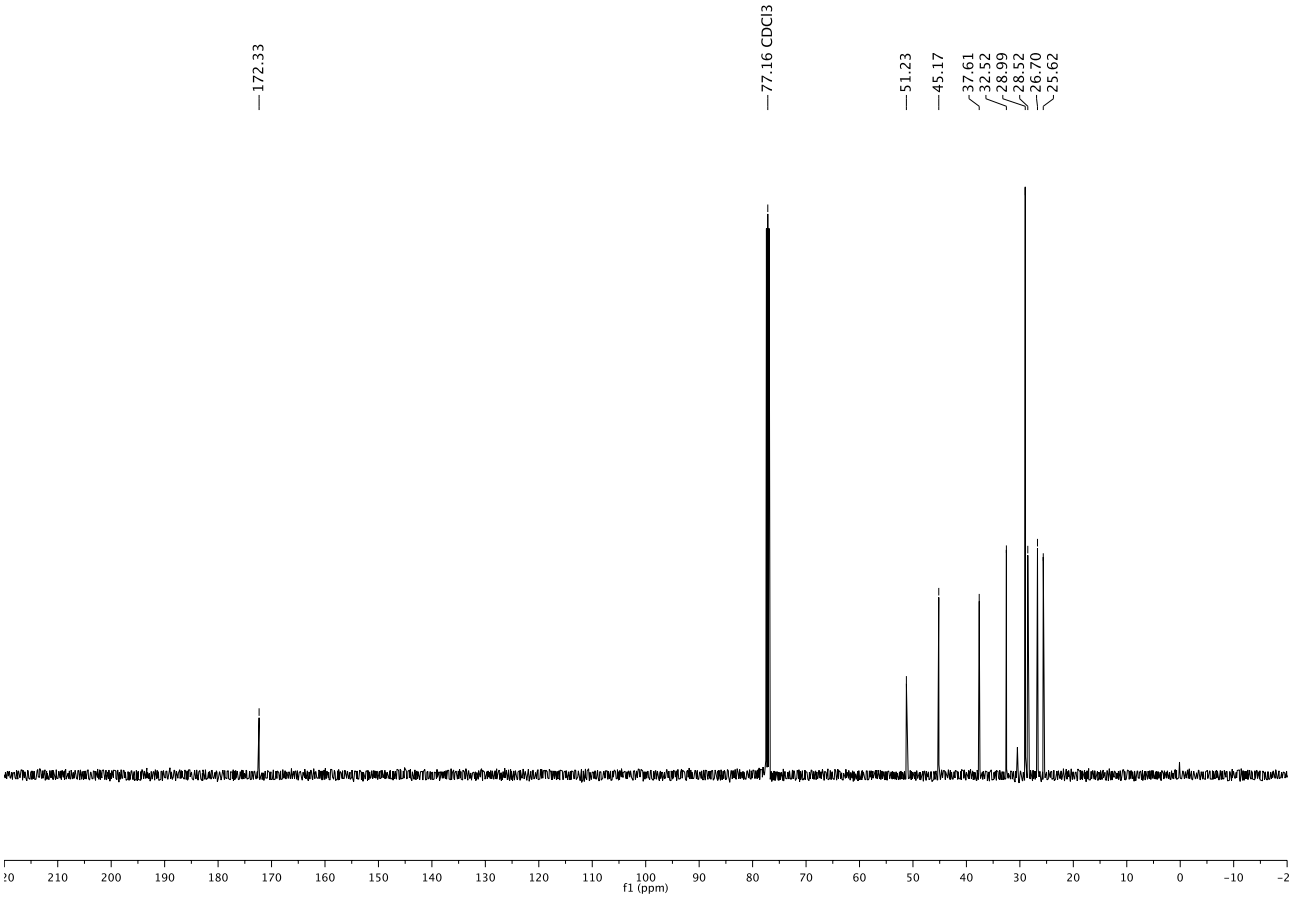
172.33
77.16 CDCl3
51.23
45.17
37.61
32.52
28.99
28.52
26.70
25.62
f1 (ppm)

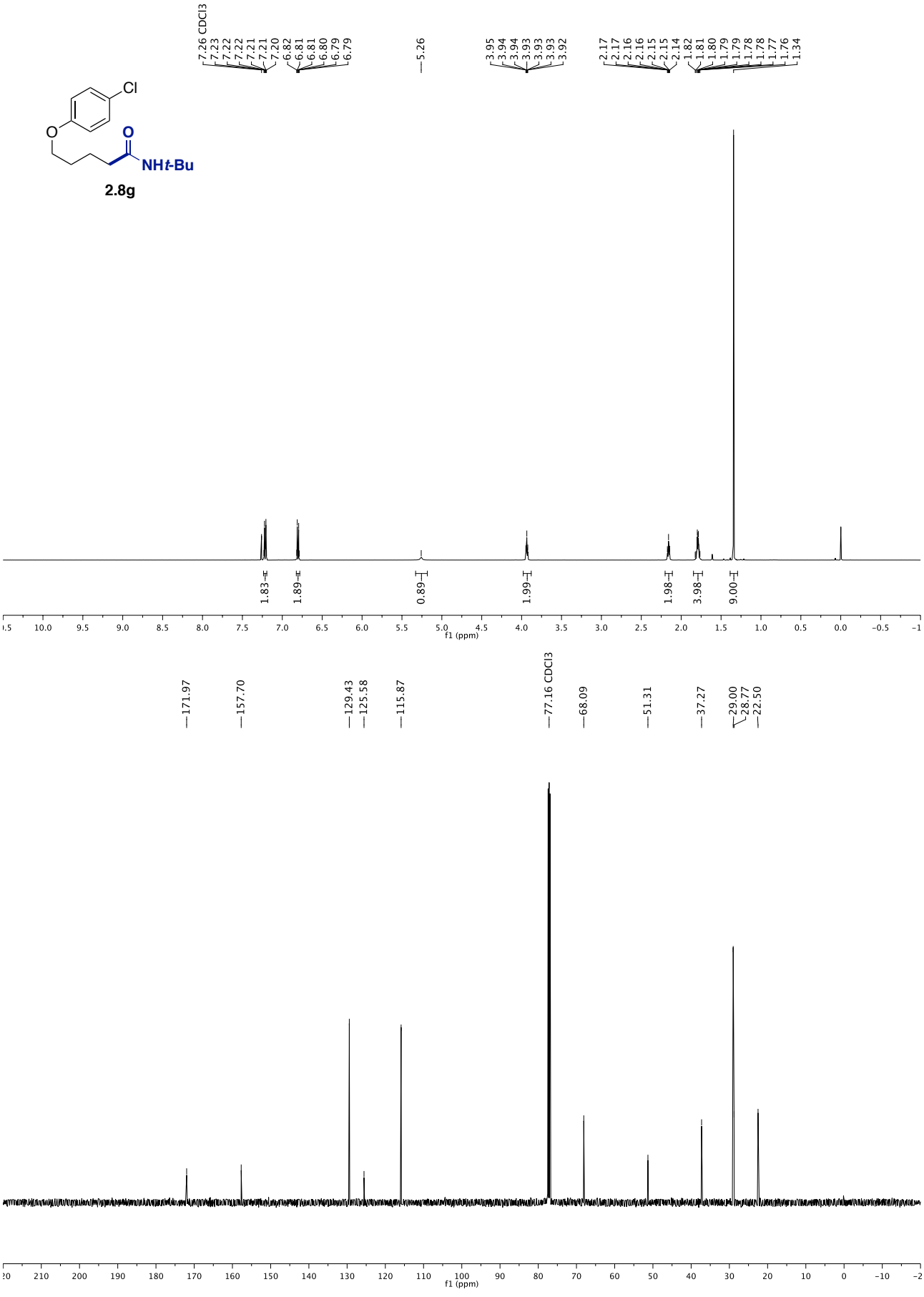
7.26 CDCl3
7.23
7.22
7.22
7.21
7.21
7.20
6.82
6.81
6.81
6.80
6.79
6.79
5.26
3.95
3.94
3.94
3.93
3.93
3.93
3.92
2.17
2.17
2.16
2.16
2.15
2.15
2.14
1.82
1.81
1.80
1.79
1.79
1.78
1.78
1.77
1.76
1.34
Cl
O
O
NHt-Bu
2.8g
1.83
1.89
0.89
1.99
1.98
3.98
9.00
f1 (ppm)
171.97
157.70
129.43
125.58
115.87
77.16 CDCl3
68.09
51.31
37.27
29.00
28.77
22.50
f1 (ppm)

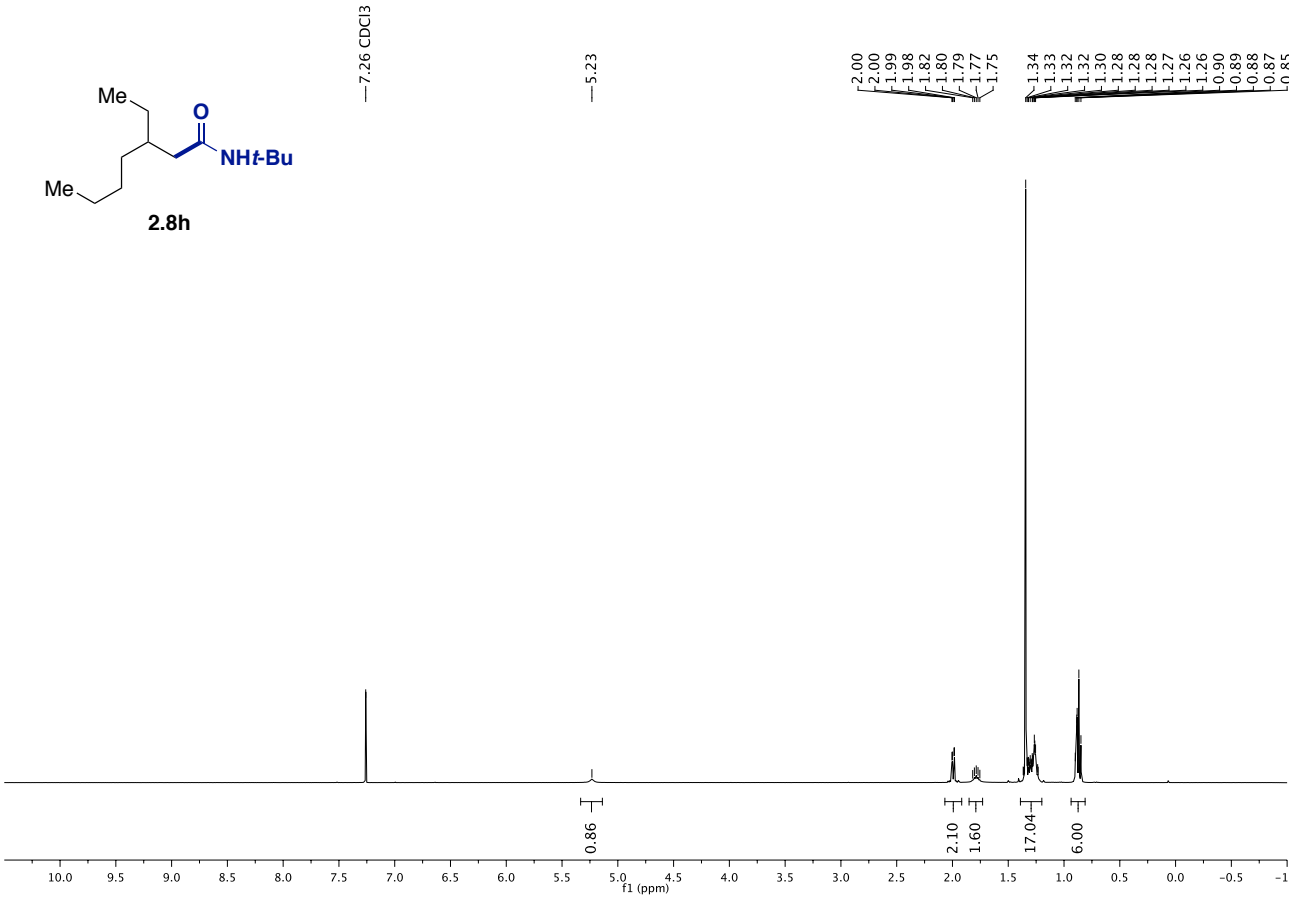
Me
O
NHt-Bu
Me
2.8h
7.26 CDCl3
5.23
2.00
2.00
1.99
1.98
1.82
1.80
1.79
1.77
1.75
1.34
1.33
1.32
1.32
1.30
1.28
1.28
1.28
1.27
1.26
1.26
0.90
0.89
0.88
0.87
0.86
2.10
1.60
17.04
6.00
f1 (ppm)

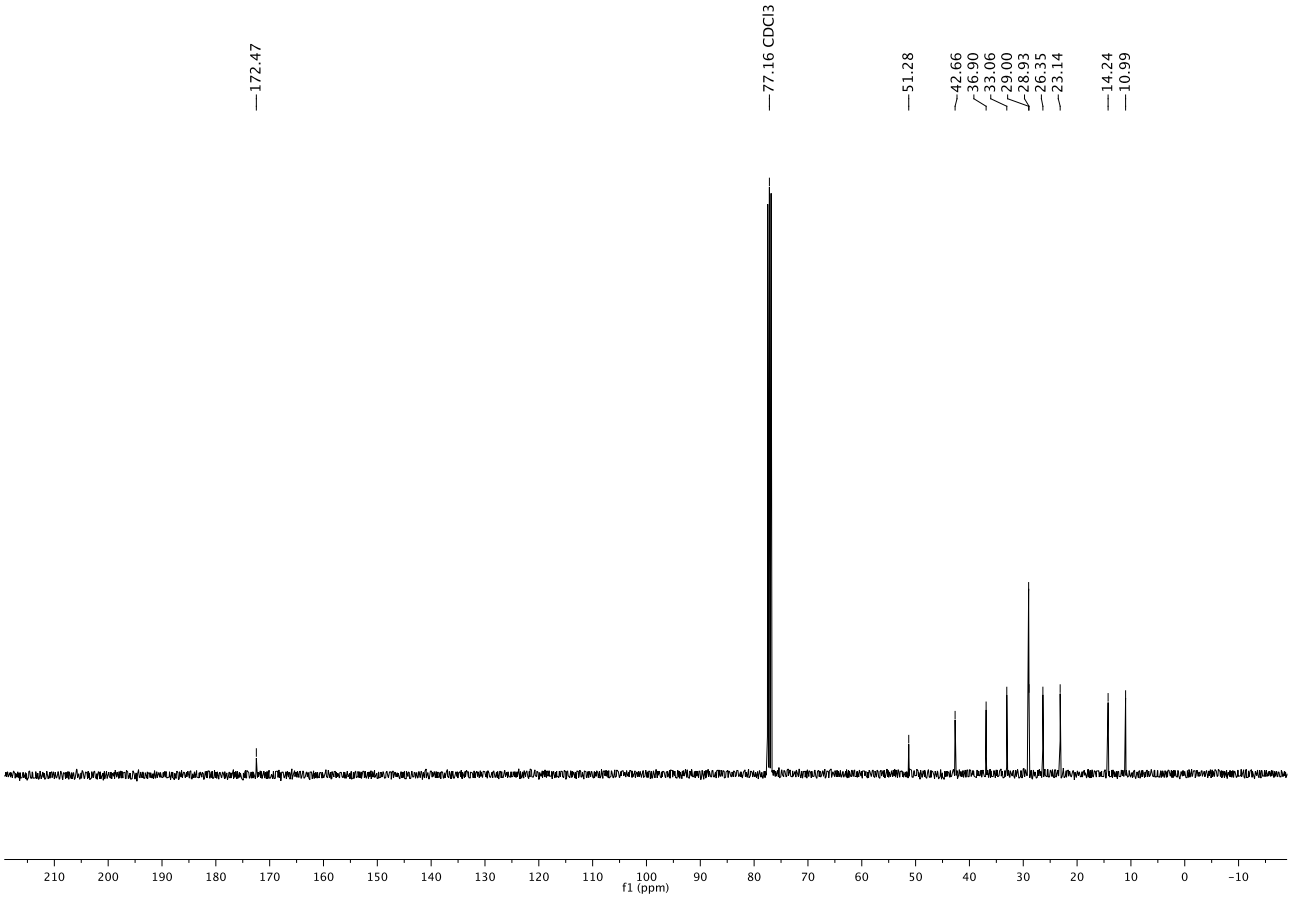
172.47
77.16 CDCl3
51.28
42.66
36.90
33.06
29.00
28.93
26.35
23.14
14.24
10.99
f1 (ppm)

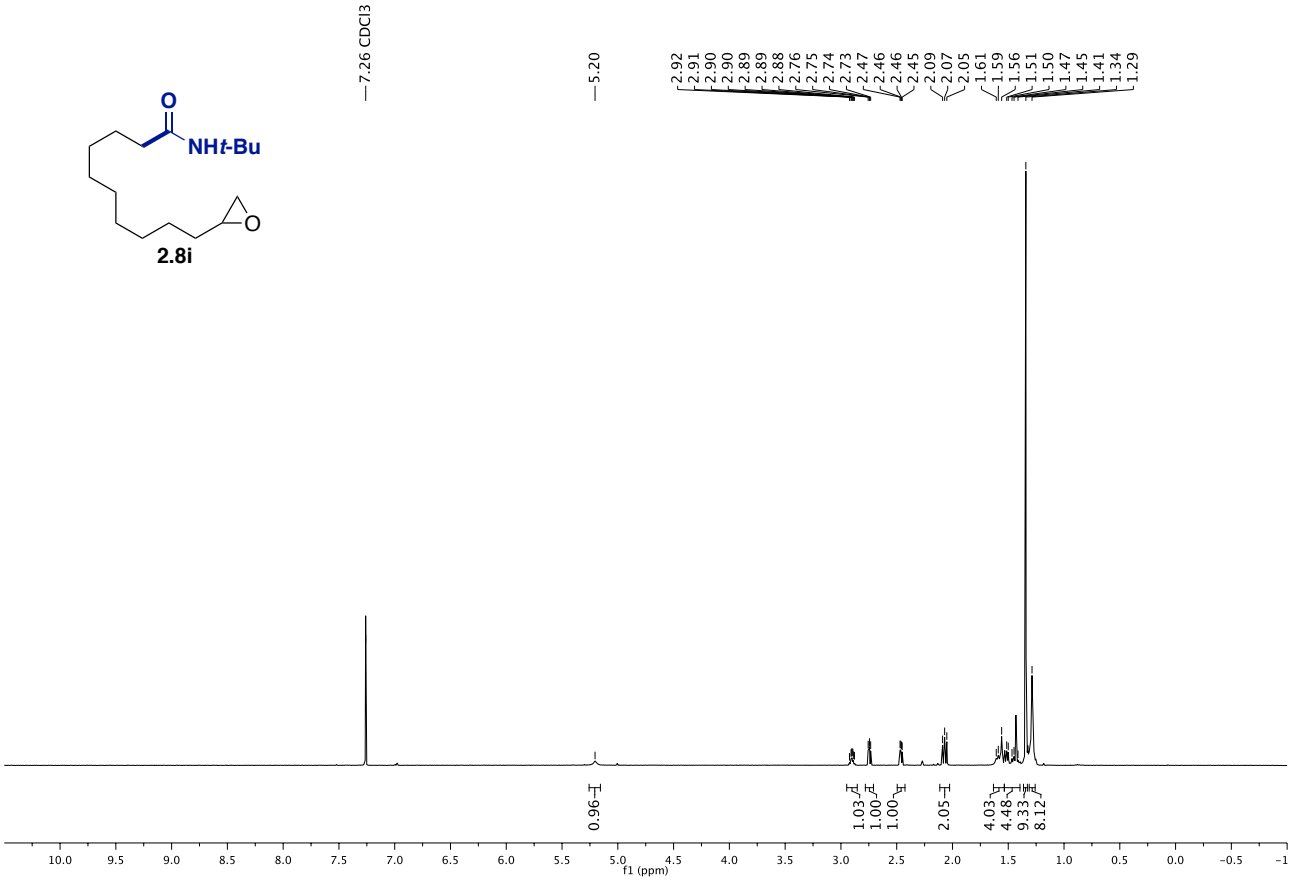
7.26 CDCl3
5.20
2.92
2.91
2.90
2.90
2.89
2.89
2.88
2.76
2.75
2.74
2.73
2.47
2.46
2.45
2.09
2.07
2.05
1.61
1.59
1.56
1.51
1.50
1.47
1.45
1.41
1.34
1.29
O
NHt-Bu
O
2.8i
0.96
1.03
1.00
1.00
2.05
4.03
4.48
9.33
8.12
f1 (ppm)

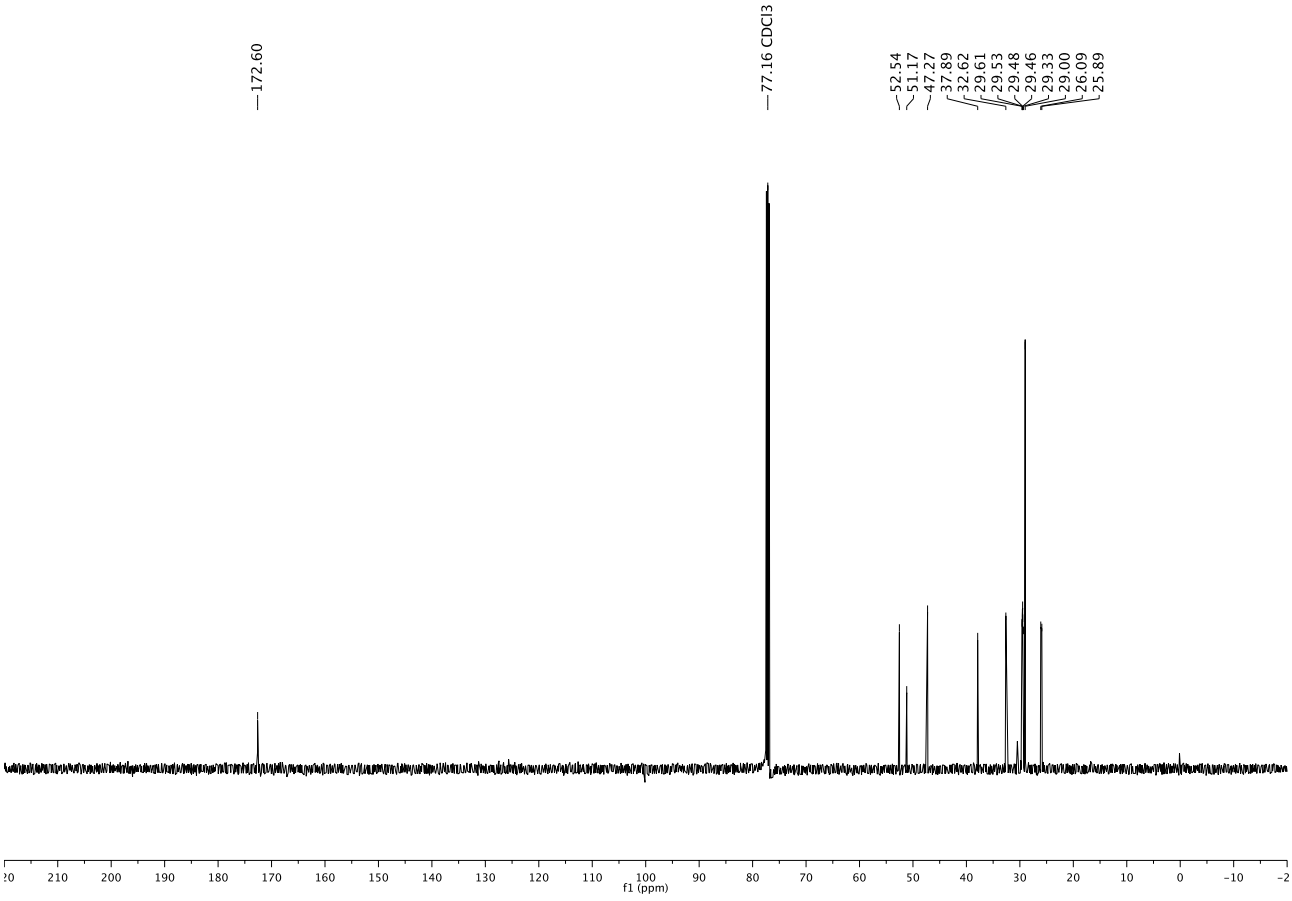
172.60
77.16 CDCl3
52.54
51.17
47.27
37.89
32.62
29.61
29.53
29.48
29.46
29.33
29.00
26.09
25.89
f1 (ppm)

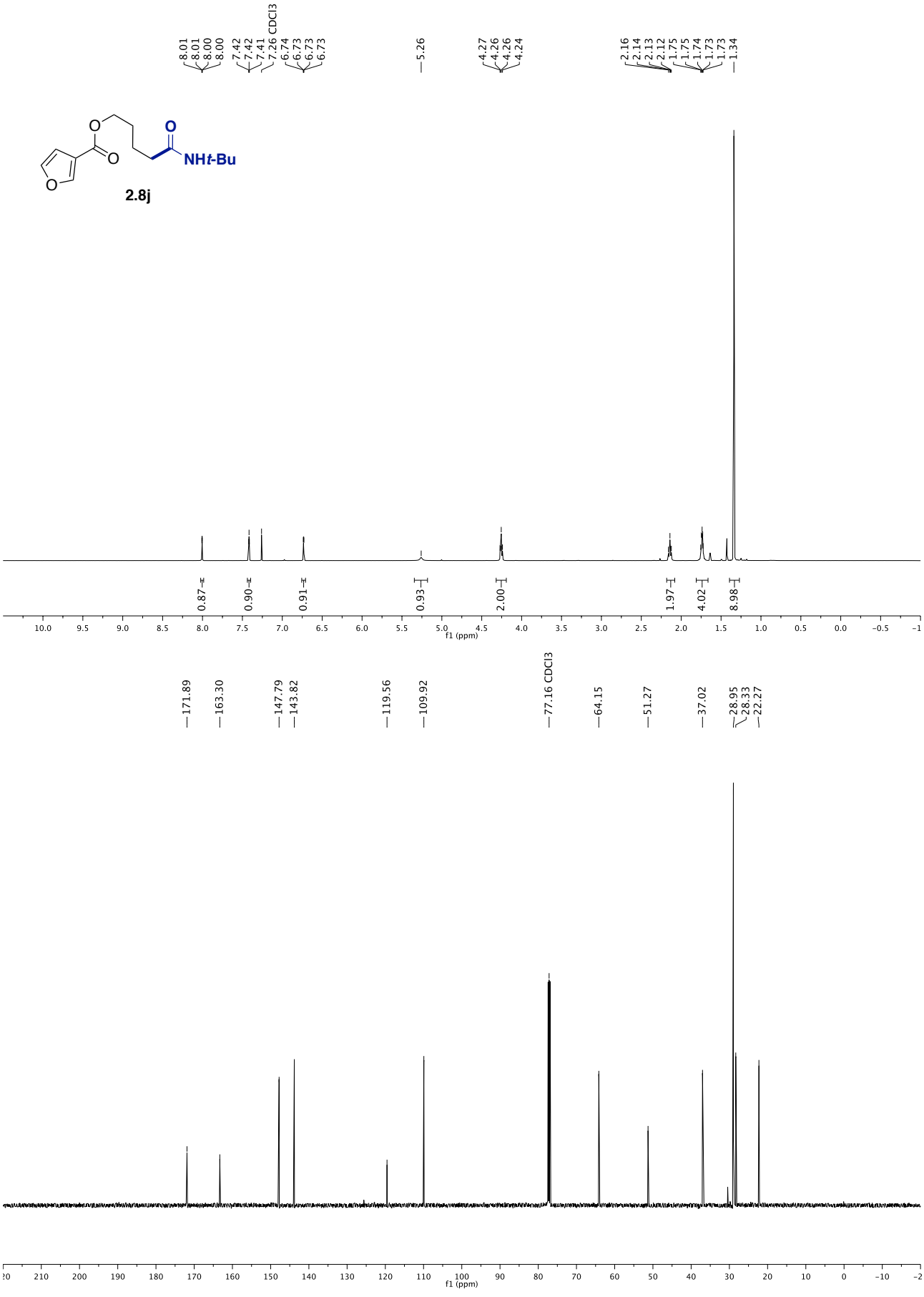
8.01
8.01
8.00
8.00
7.42
7.42
7.41
7.26 CDCl3
6.74
6.73
6.73
6.73
5.26
4.27
4.26
4.26
4.24
2.16
2.14
2.13
2.12
1.75
1.75
1.74
1.73
1.73
1.34
O
O
O
O
NHt-Bu
2.8j
0.87
0.90
0.91
0.93
2.00
1.97
4.02
8.98
f1 (ppm)
171.89
163.30
147.79
143.82
119.56
109.92
77.16 CDCl3
64.15
51.27
37.02
28.95
28.33
22.27
f1 (ppm)

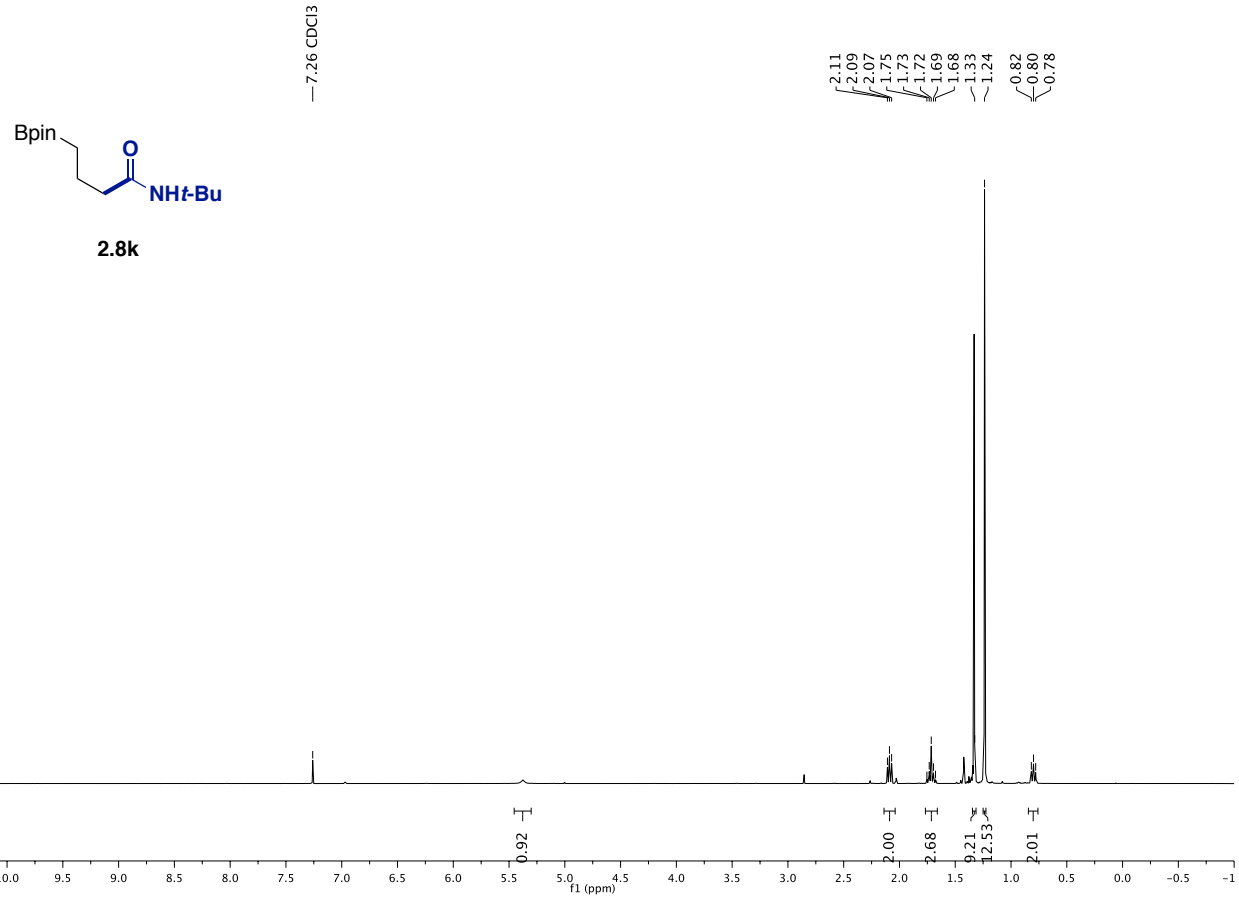
7.26 CDCl3
2.11
2.09
2.07
1.75
1.73
1.72
1.69
1.68
1.33
1.24
0.82
0.80
0.78
Bpin
O
NHt-Bu
2.8k
0.92
2.00
2.68
9.21
12.53
2.01
f1 (ppm)

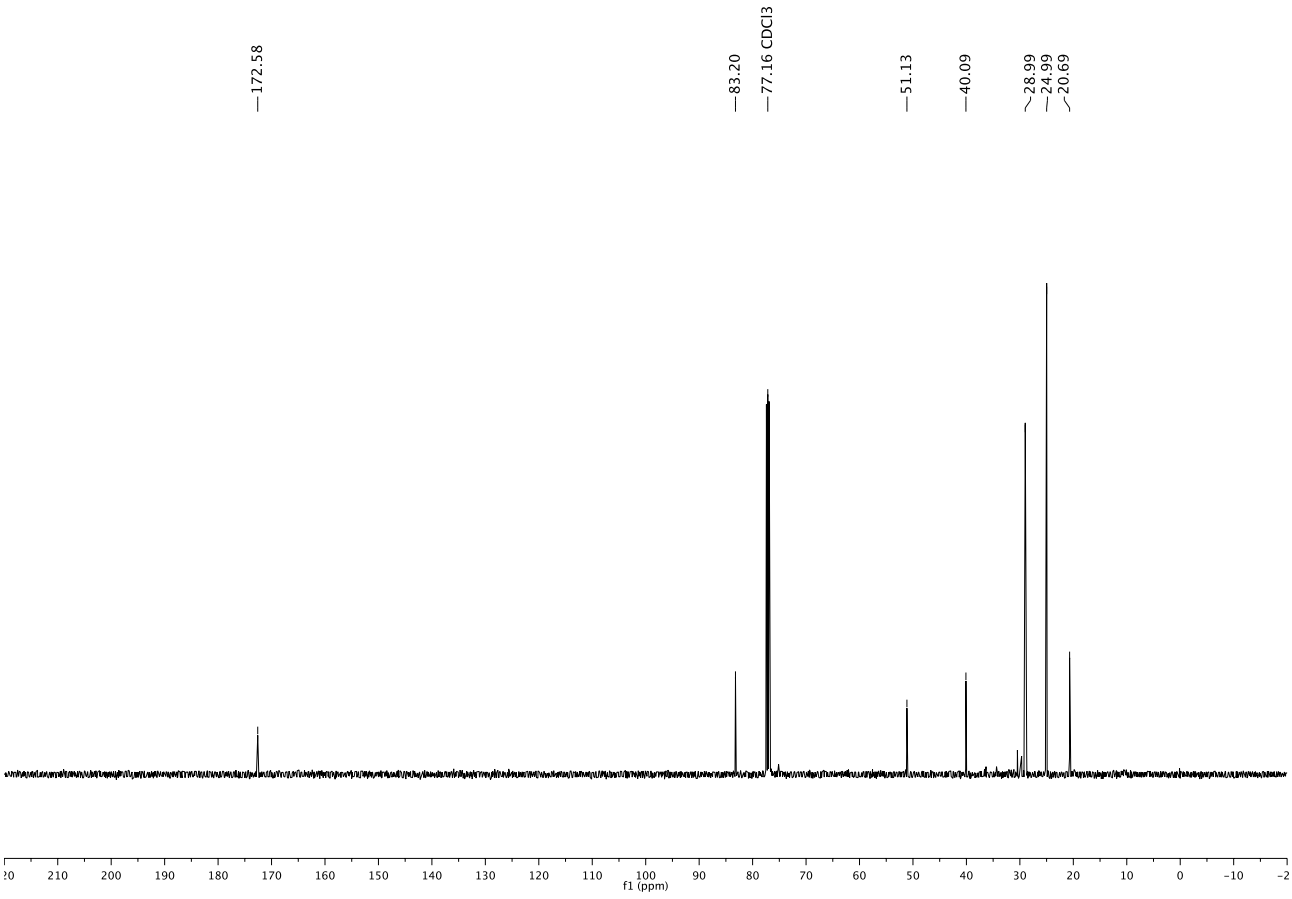
172.58
83.20
77.16 CDCl3
51.13
40.09
28.99
24.99
20.69
f1 (ppm)

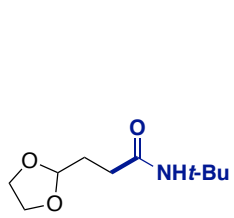
O
O
O
NHt-Bu

2.8l

7.26 CDCl3
5.44
4.92
4.91
4.90
3.99
3.97
3.96
3.96
3.95
3.95
3.94
3.92
3.89
3.87
3.86
3.85
3.85
3.85
3.84
3.82
2.23
2.22
2.20
2.00
1.99
1.98
1.98
1.97
1.96
1.33
0.92
0.95
2.00
1.97
2.00
2.00
9.11
f1 (ppm)

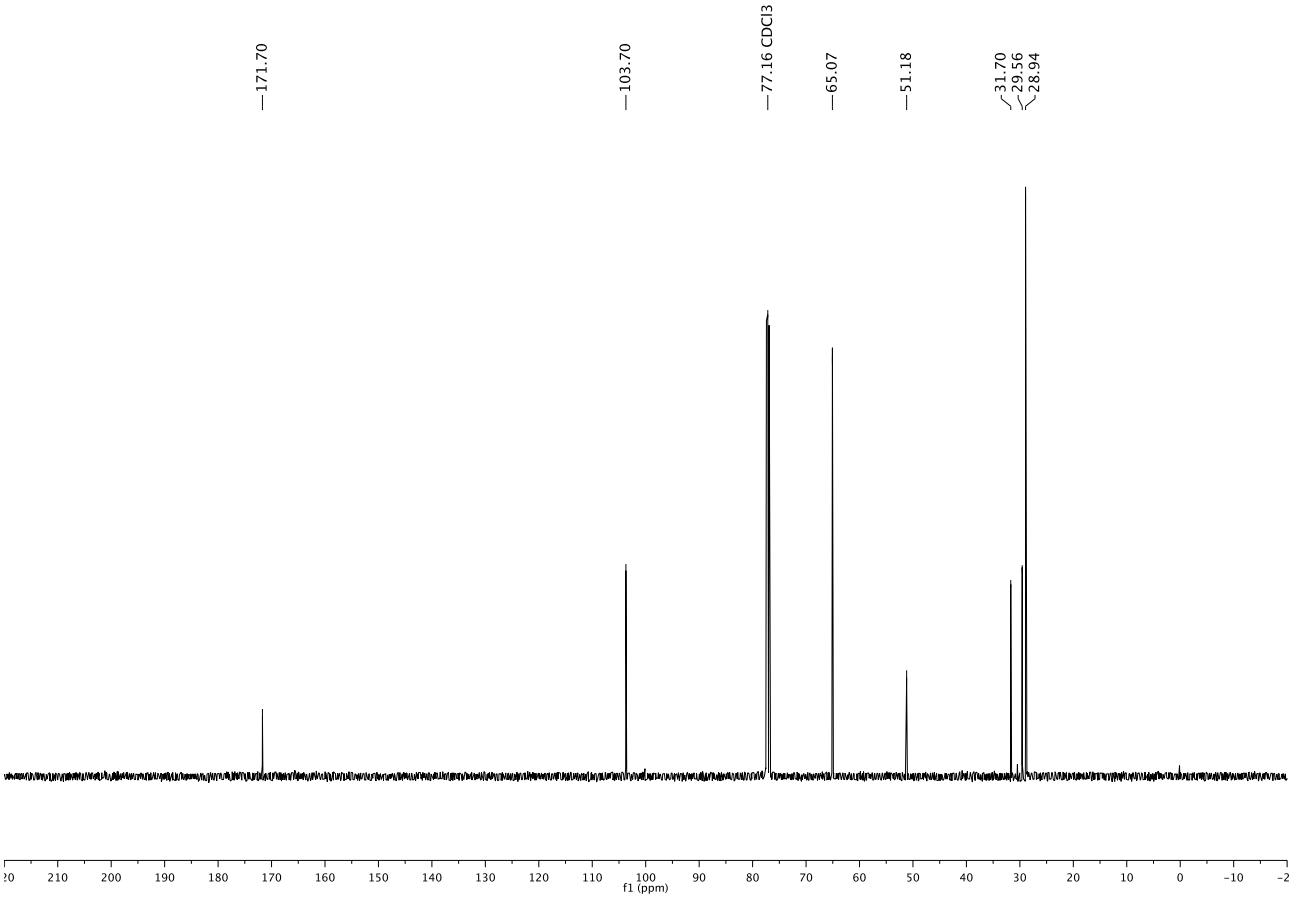
171.70
103.70
77.16 CDCl3
65.07
51.18
31.70
29.56
28.94
f1 (ppm)

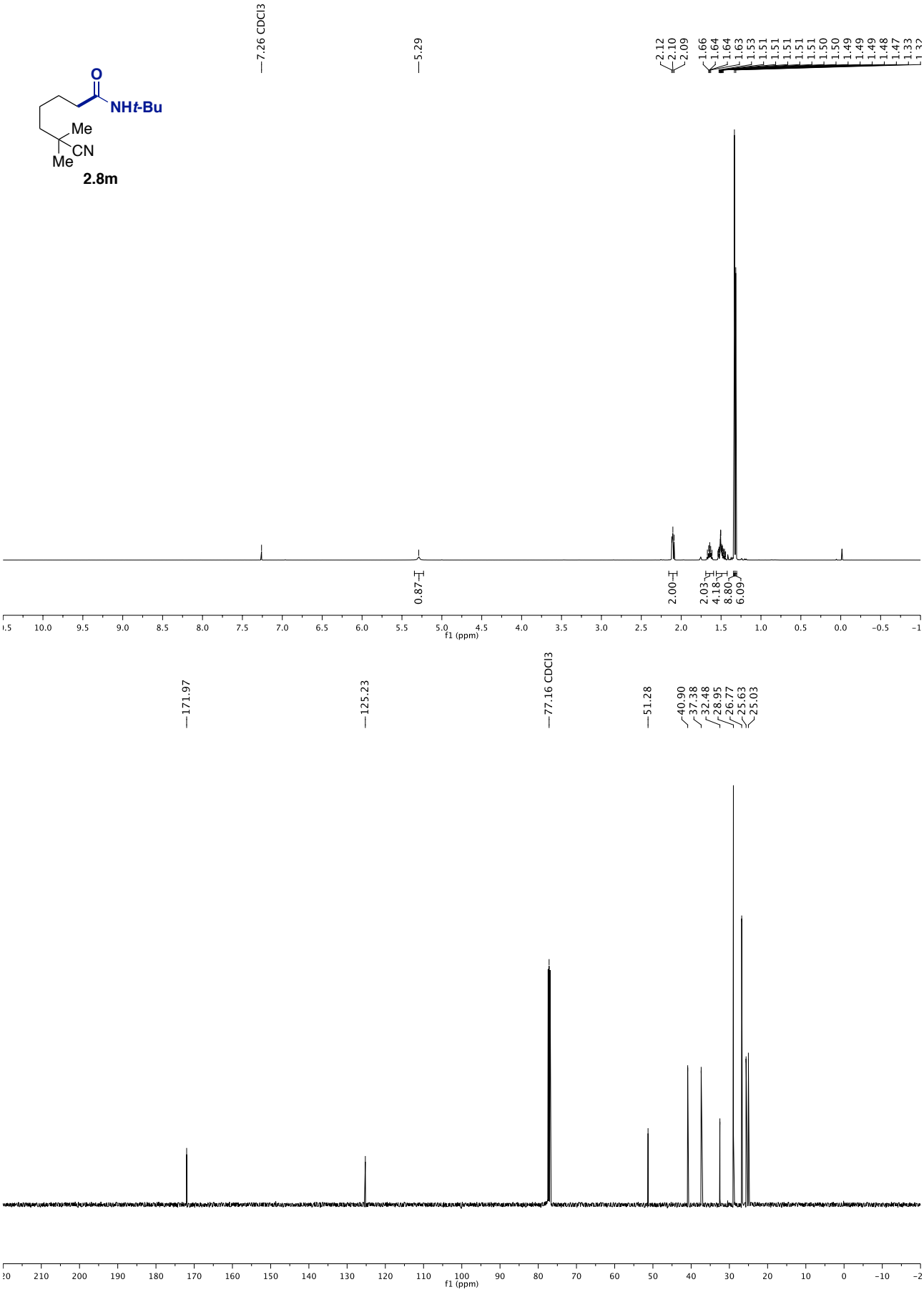
7.26 CDCl3
5.29
2.12
2.10
2.09
1.66
1.64
1.64
1.63
1.53
1.51
1.51
1.51
1.51
1.50
1.50
1.49
1.49
1.49
1.48
1.47
1.33
O
NHt-Bu
Me
CN
Me
2.8m
0.87
2.00
2.03
4.18
8.80
6.09
f1 (ppm)
171.97
125.23
77.16 CDCl3
51.28
40.90
37.38
32.48
28.95
26.77
25.63
25.03
f1 (ppm)

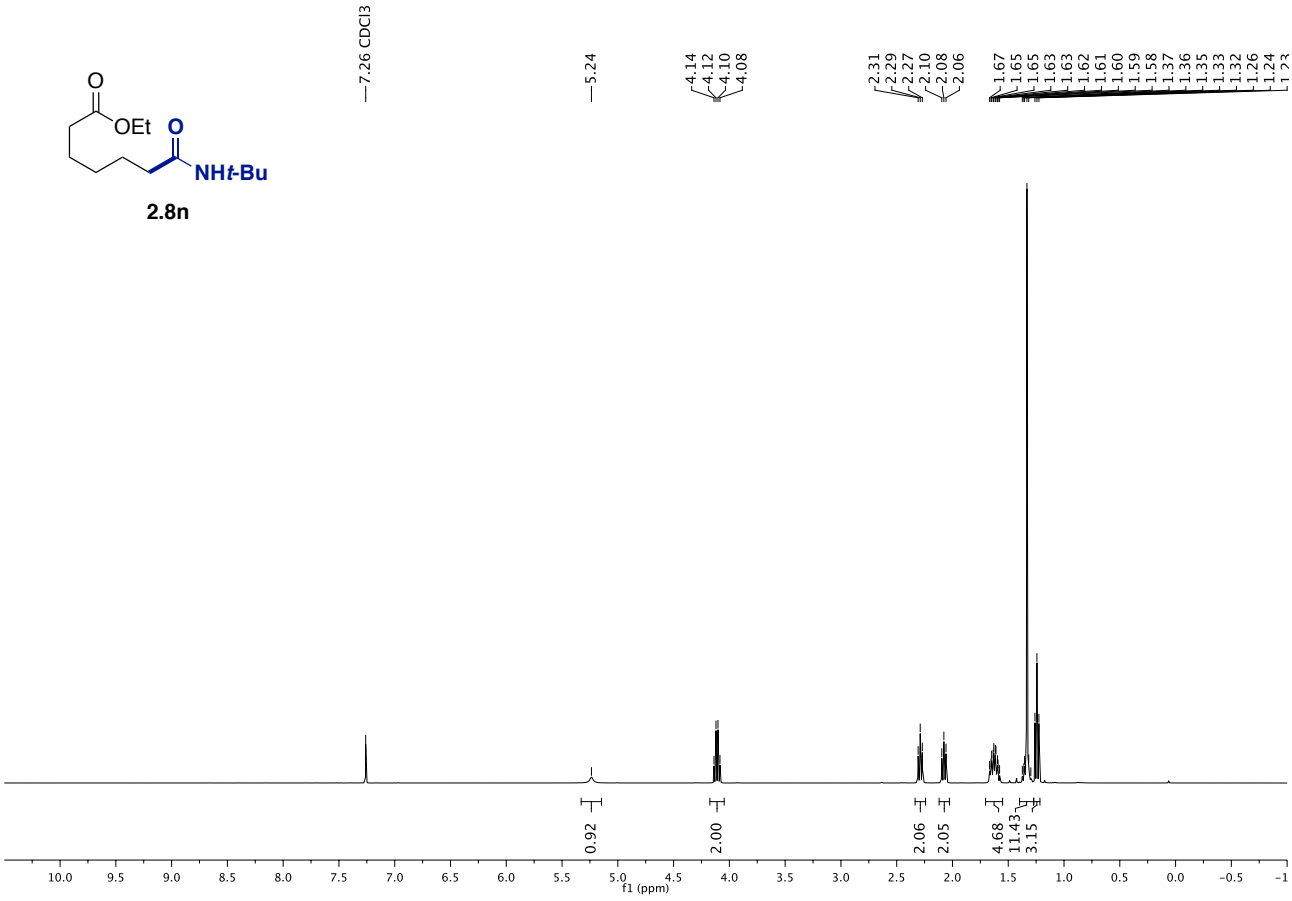
O
OEt
O
NHt-Bu
2.8n
7.26 CDCl3
5.24
4.14
4.12
4.10
4.08
2.31
2.29
2.27
2.10
2.08
2.06
1.67
1.65
1.65
1.63
1.63
1.62
1.61
1.60
1.59
1.58
1.37
1.36
1.35
1.33
1.32
1.26
1.24
0.92
2.00
2.06
2.05
4.68
11.43
3.15
f1 (ppm)

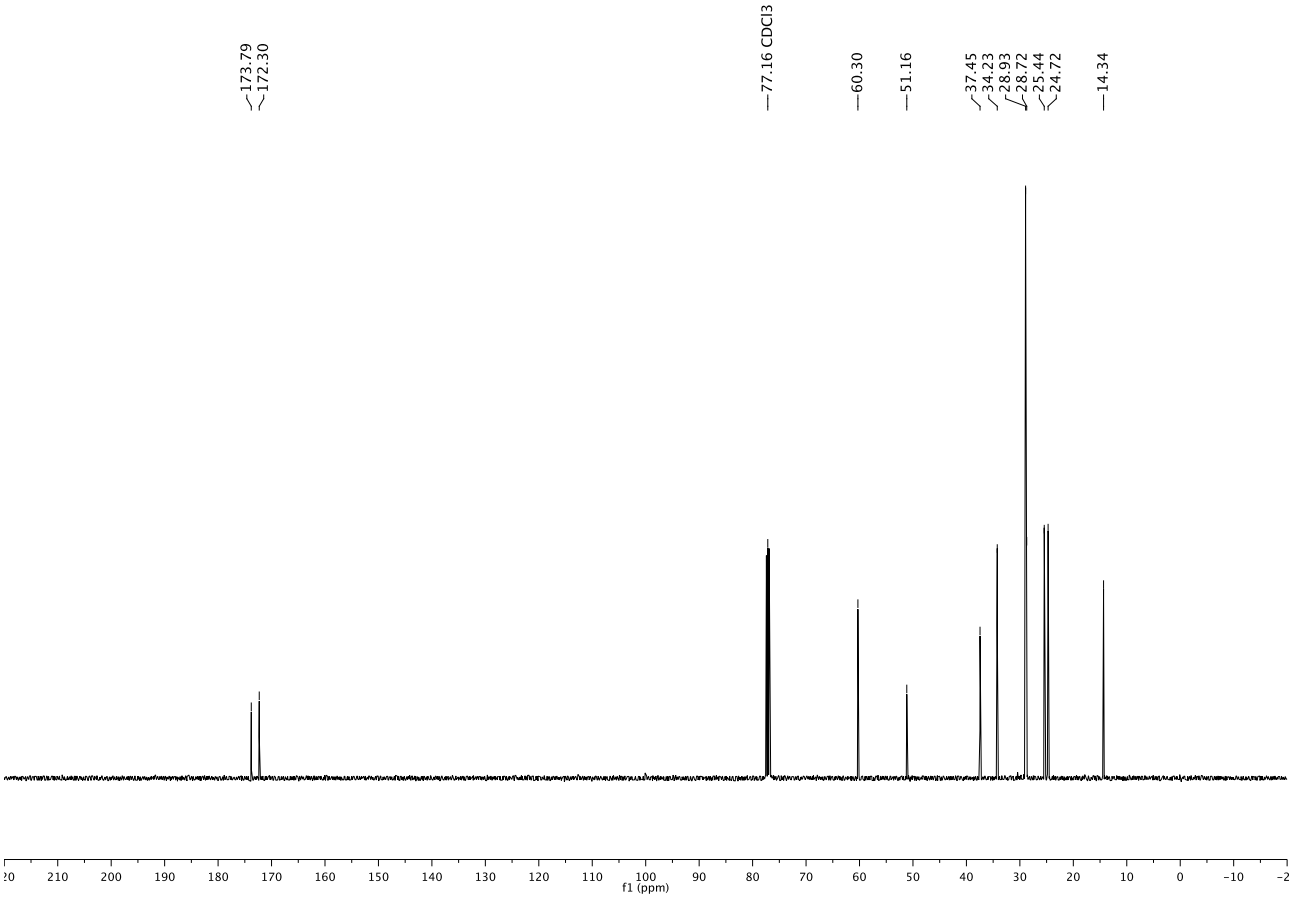
173.79
172.30
77.16 CDCl3
60.30
51.16
37.45
34.23
28.93
28.72
25.44
24.72
14.34
f1 (ppm)

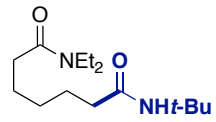
O
NEt2
O
NHt-Bu

2.8o

7.26 CDCl3
5.30
3.39
3.37
3.35
3.33
3.33
3.32
3.30
3.28
3.26
2.31
2.29
2.28
2.27
2.11
2.09
2.08
1.67
1.67
1.66
1.65
1.64
1.63
1.62
1.61
1.38
1.38
1.36
1.34
1.33
1.18
1.16
1.14
1.12
1.10
0.84
2.02
1.95
1.93
1.93
4.76
11.00
3.04
2.93
f1 (ppm)

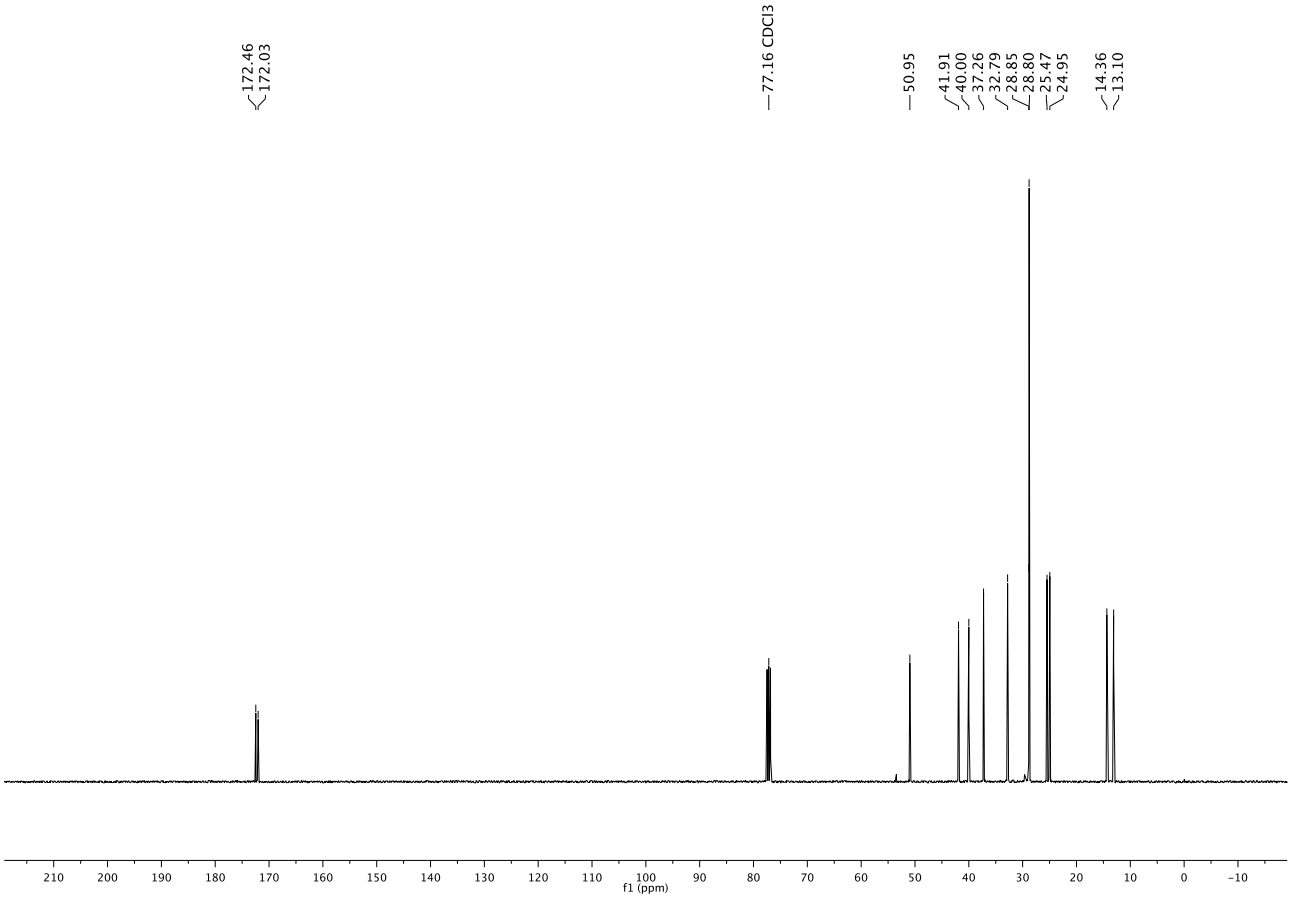
172.46
172.03
77.16 CDCl3
50.95
41.91
40.00
37.26
32.79
28.85
28.80
25.47
24.95
14.36
13.10
f1 (ppm)

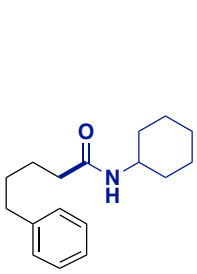

2.8a

7.29
7.27
7.26 CDCl3
7.25
7.19
7.17
7.15
5.32
5.30
3.80
3.79
3.77
3.76
3.75
3.72
3.71
2.64
2.62
2.61
2.16
2.15
2.13
1.91
1.90
1.88
1.87
1.71
1.68
1.67
1.66
1.65
1.59
1.40
1.37
1.34
1.31
1.19
1.16
1.13
1.10
2.20
3.05
0.96
1.00
2.08
2.07
2.17
7.62
2.57
3.36
f1 (ppm)

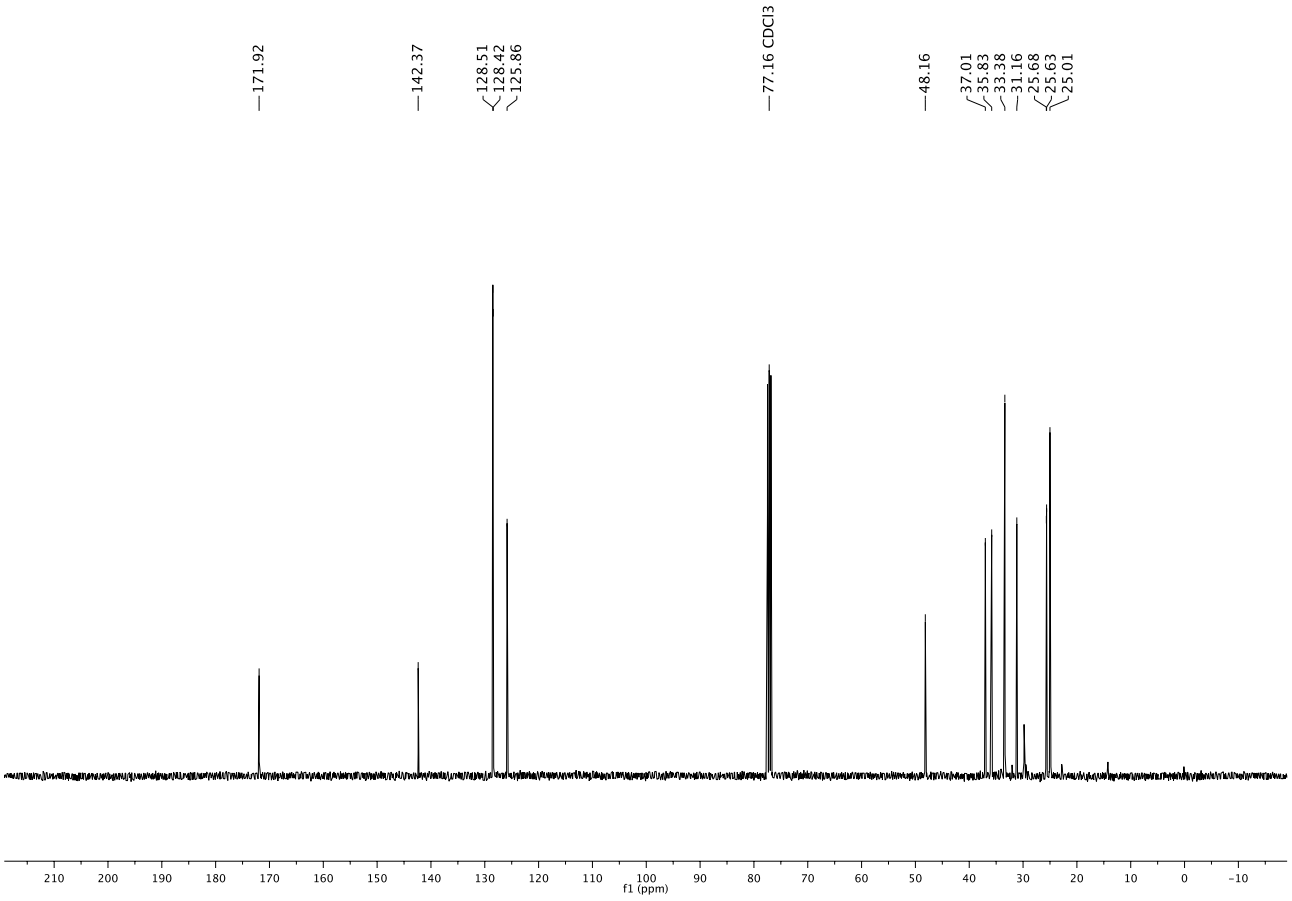
171.92
142.37
128.51
128.42
125.86
77.16 CDCl3
48.16
37.01
35.83
33.38
31.16
25.68
25.63
25.01
f1 (ppm)

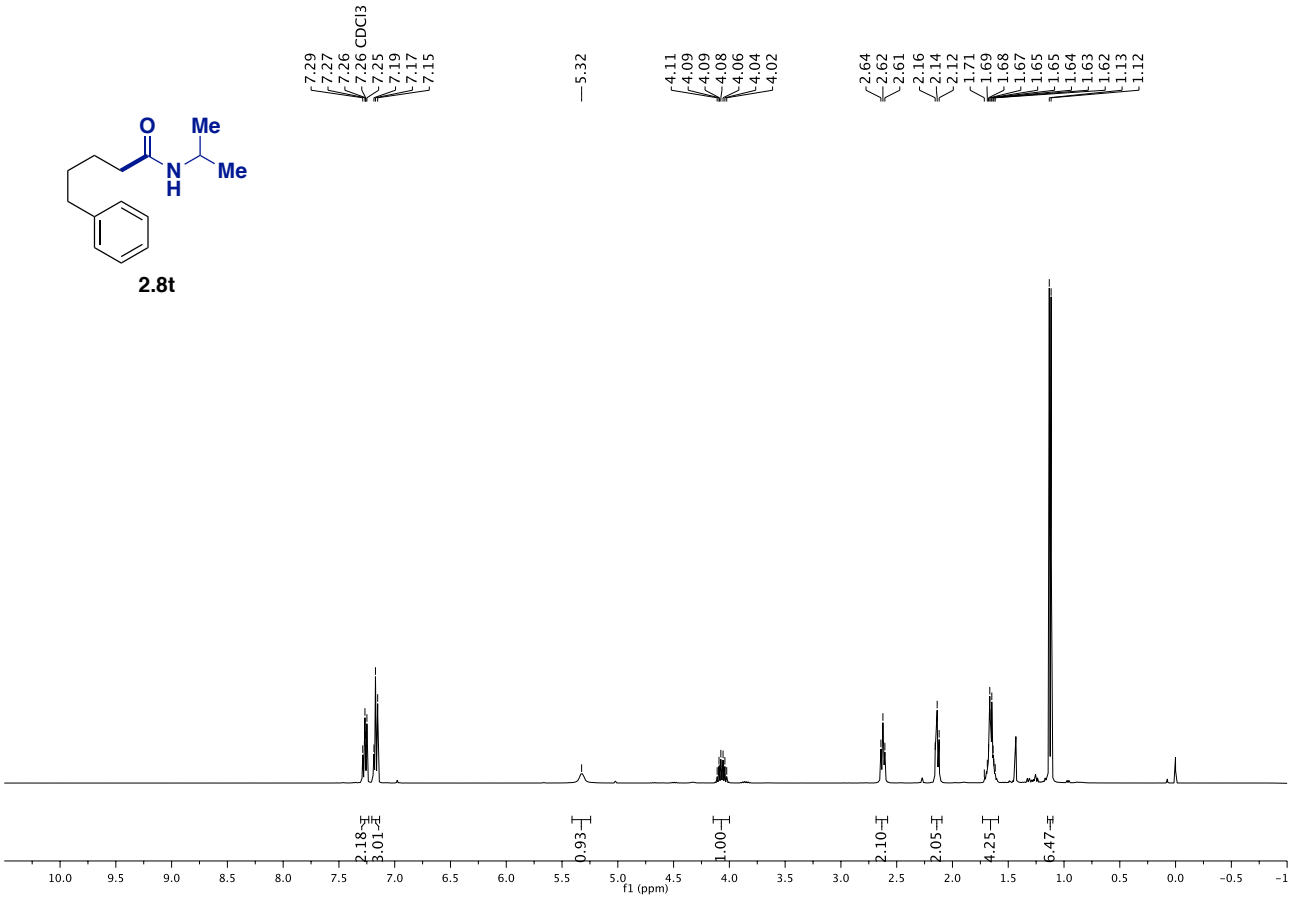
7.29
7.27
7.26
CDCl3
7.25
7.19
7.17
7.15
5.32
4.11
4.09
4.09
4.08
4.06
4.04
4.02
2.64
2.62
2.61
2.16
2.14
2.12
1.71
1.69
1.68
1.67
1.65
1.65
1.64
1.63
1.62
1.13
1.12
O
Me
N
H
Me
2.8t
2.18
3.01
0.93
1.00
2.10
2.05
4.25
6.47
f1 (ppm)

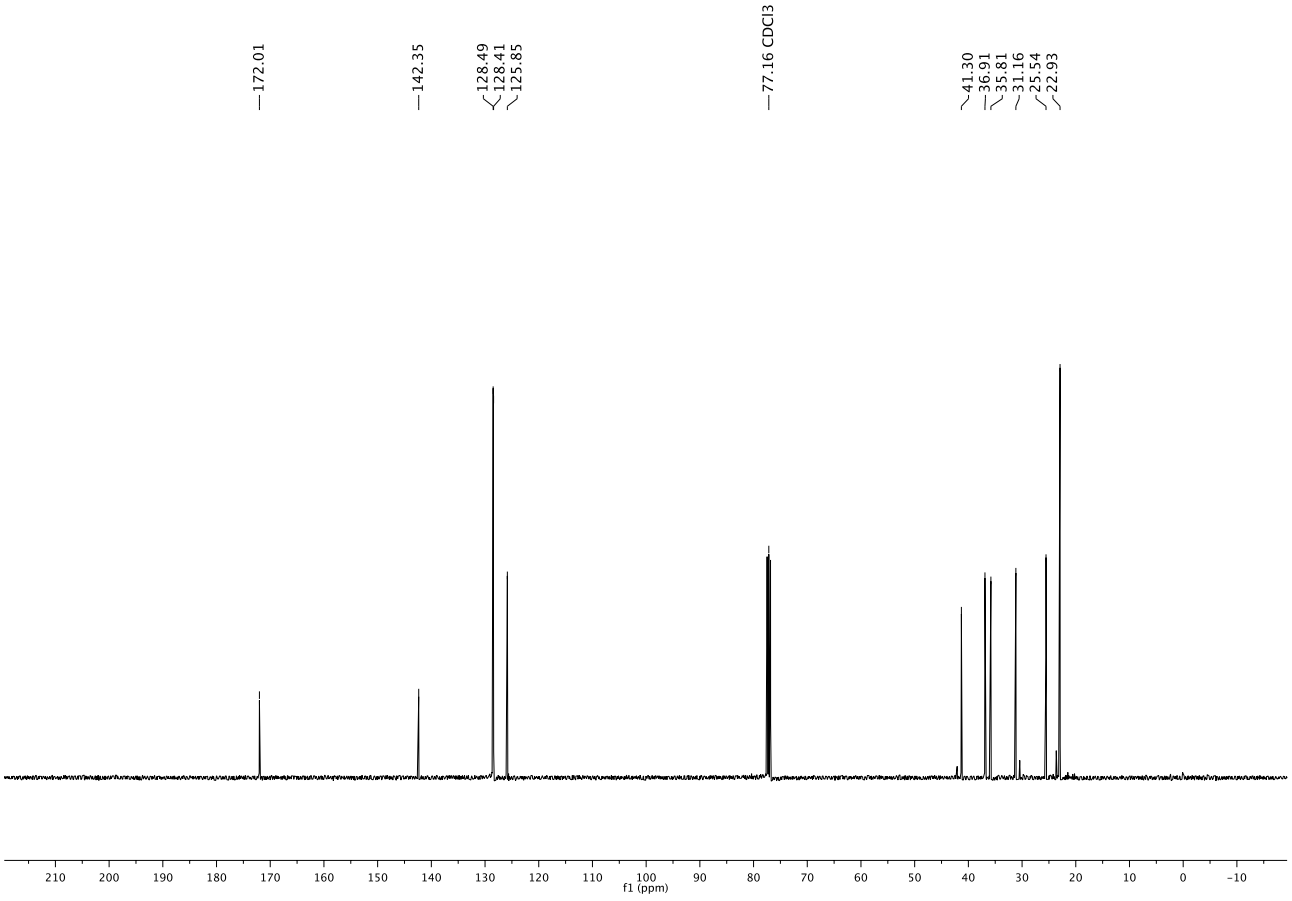
172.01
142.35
128.49
128.41
125.85
77.16 CDCl3
41.30
36.91
35.81
31.16
25.54
22.93
f1 (ppm)

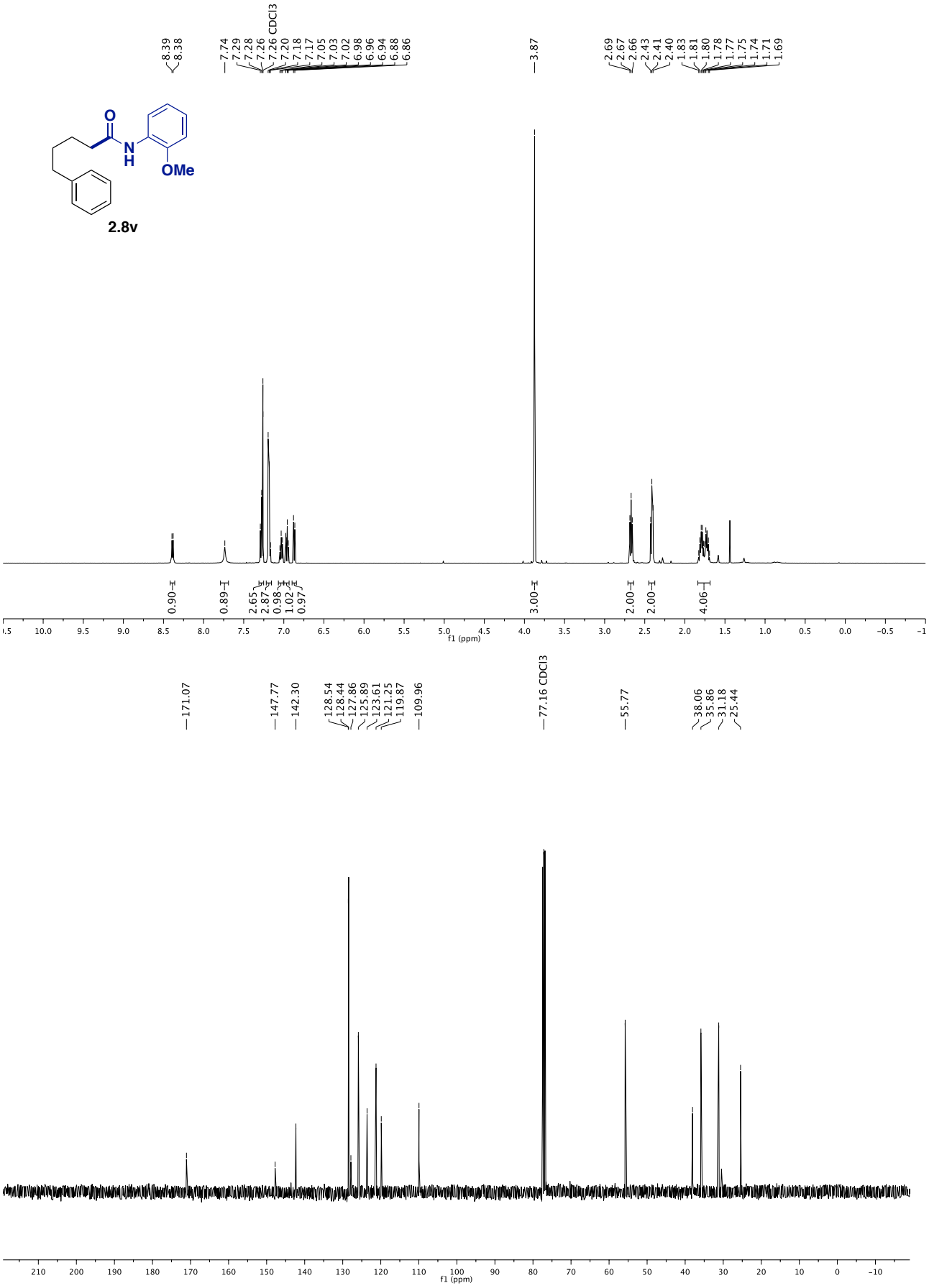
8.39
8.38
7.74
7.29
7.28
7.26
7.26 CDCl3
7.20
7.18
7.17
7.05
7.03
7.02
6.98
6.96
6.94
6.88
6.86
3.87
2.69
2.67
2.66
2.43
2.41
2.40
1.83
1.81
1.80
1.78
1.77
1.75
1.74
1.71
1.69
O
N
H
OMe
2.8v
0.90
0.89
2.65
2.87
0.98
1.02
0.97
3.00
2.00
2.00
4.06
f1 (ppm)
171.07
147.77
142.30
128.54
128.44
127.86
125.89
123.61
121.25
119.87
109.96
77.16 CDCl3
55.77
38.06
35.86
31.18
25.44
f1 (ppm)

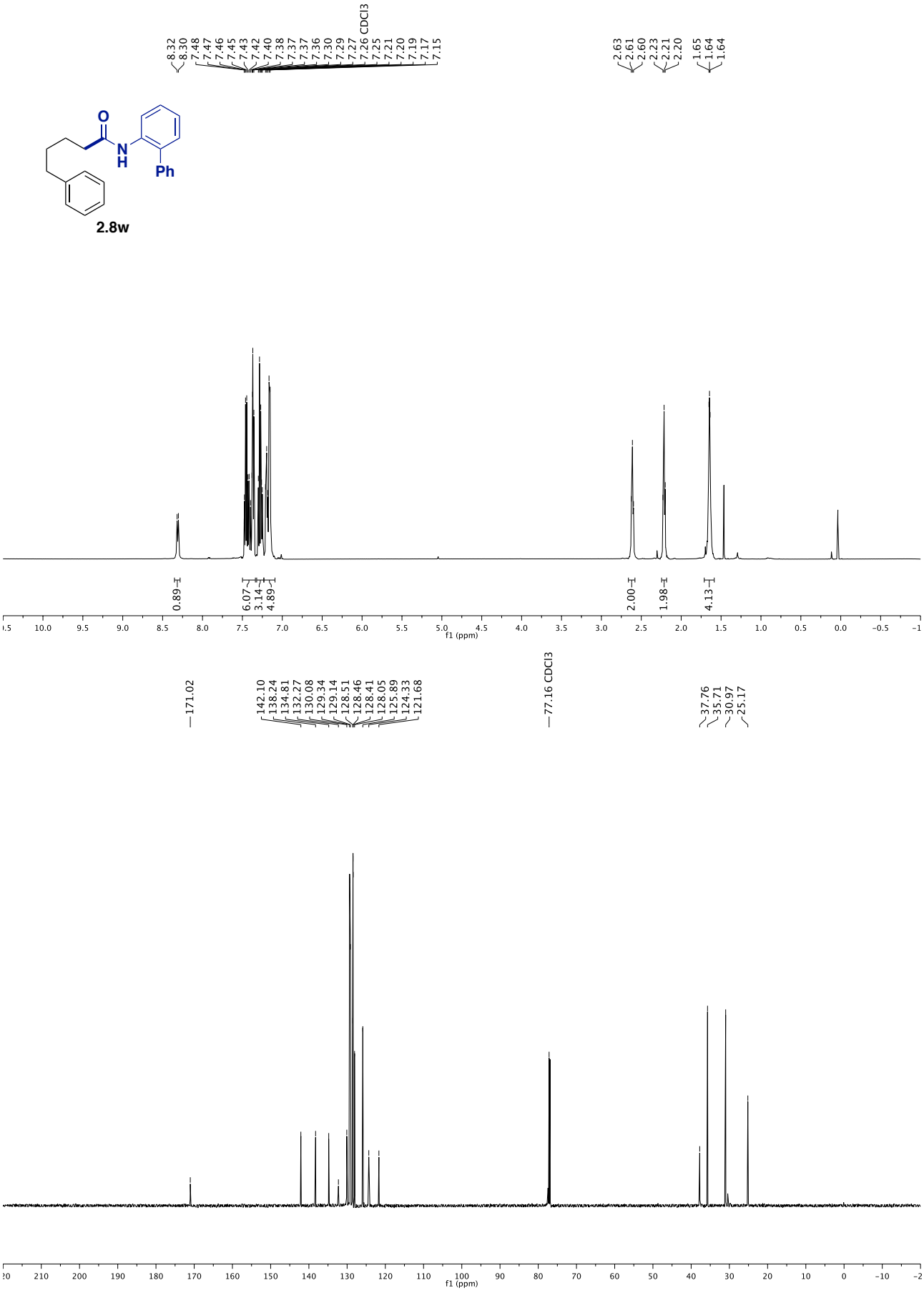
8.32
8.30
7.48
7.47
7.46
7.45
7.43
7.42
7.40
7.38
7.37
7.37
7.36
7.30
7.29
7.27
7.26 CDCl3
7.25
7.21
7.20
7.19
7.17
7.15
2.63
2.61
2.60
2.23
2.21
2.20
1.65
1.64
1.64
O
N
H
Ph
2.8w
0.89
6.07
3.14
4.89
2.00
1.98
4.13
f1 (ppm)
171.02
142.10
138.24
134.81
132.27
130.08
129.34
129.14
128.51
128.46
128.41
128.05
125.89
124.33
121.68
77.16 CDCl3
37.76
35.71
30.97
25.17
f1 (ppm)

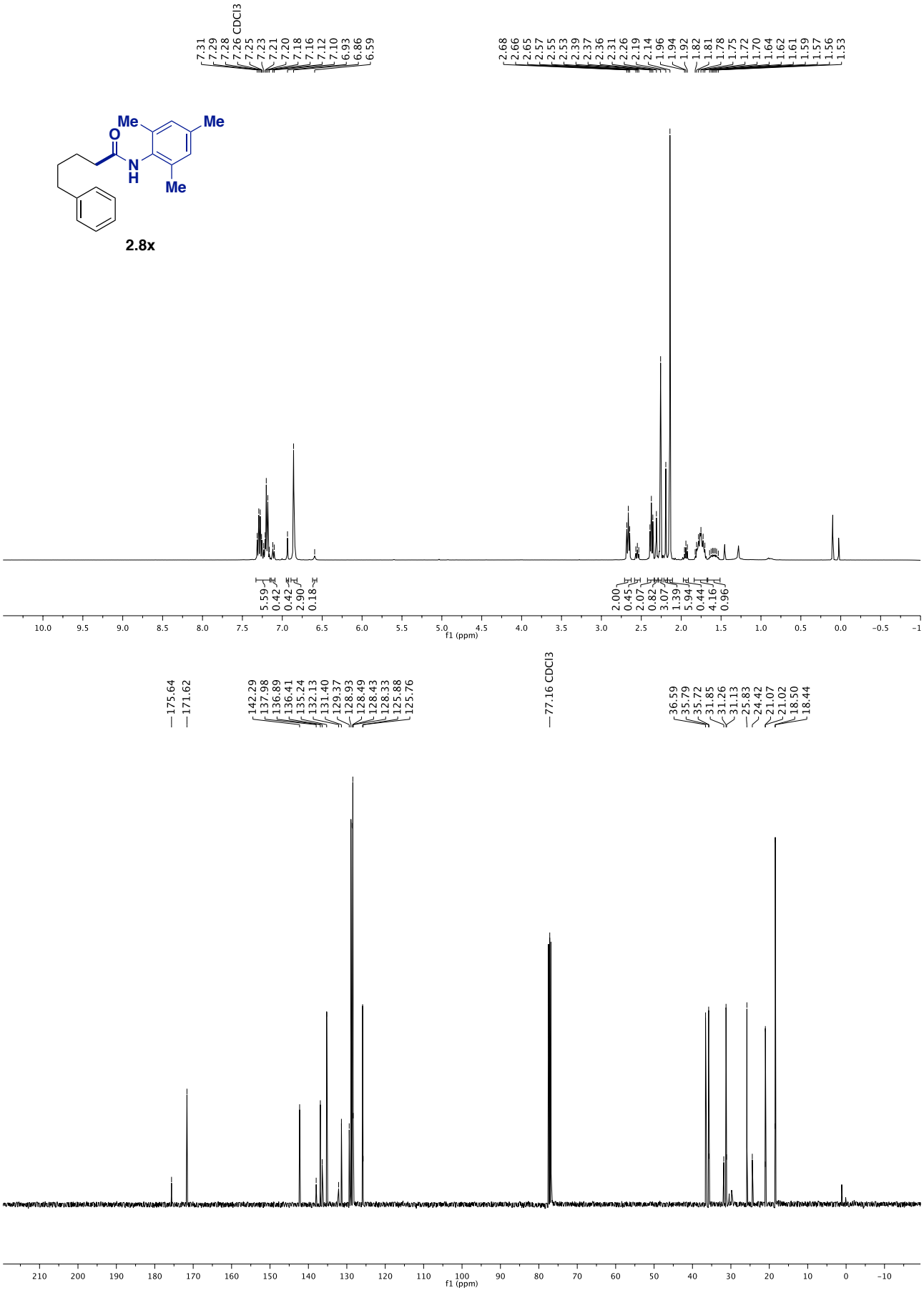
7.31
7.29
7.28
7.26 CDCl3
7.25
7.23
7.21
7.20
7.18
7.16
7.12
7.10
6.93
6.86
6.59
2.68
2.66
2.65
2.57
2.55
2.53
2.39
2.37
2.36
2.31
2.26
2.19
2.14
1.96
1.94
1.92
1.82
1.81
1.78
1.75
1.72
1.70
1.64
1.62
1.61
1.59
1.57
1.56
1.53
Me
Me
O
N
H
Me
2.8x
5.59
0.42
0.42
2.90
0.18
2.00
0.45
2.07
0.82
3.07
1.39
5.94
0.44
4.16
0.96
f1 (ppm)
175.64
171.62
142.29
137.98
136.89
136.41
135.24
132.13
131.40
129.37
128.93
128.49
128.43
128.33
125.88
125.76
77.16 CDCl3
36.59
35.79
35.72
31.85
31.26
31.13
25.83
24.42
21.07
21.02
18.50
18.44
f1 (ppm)

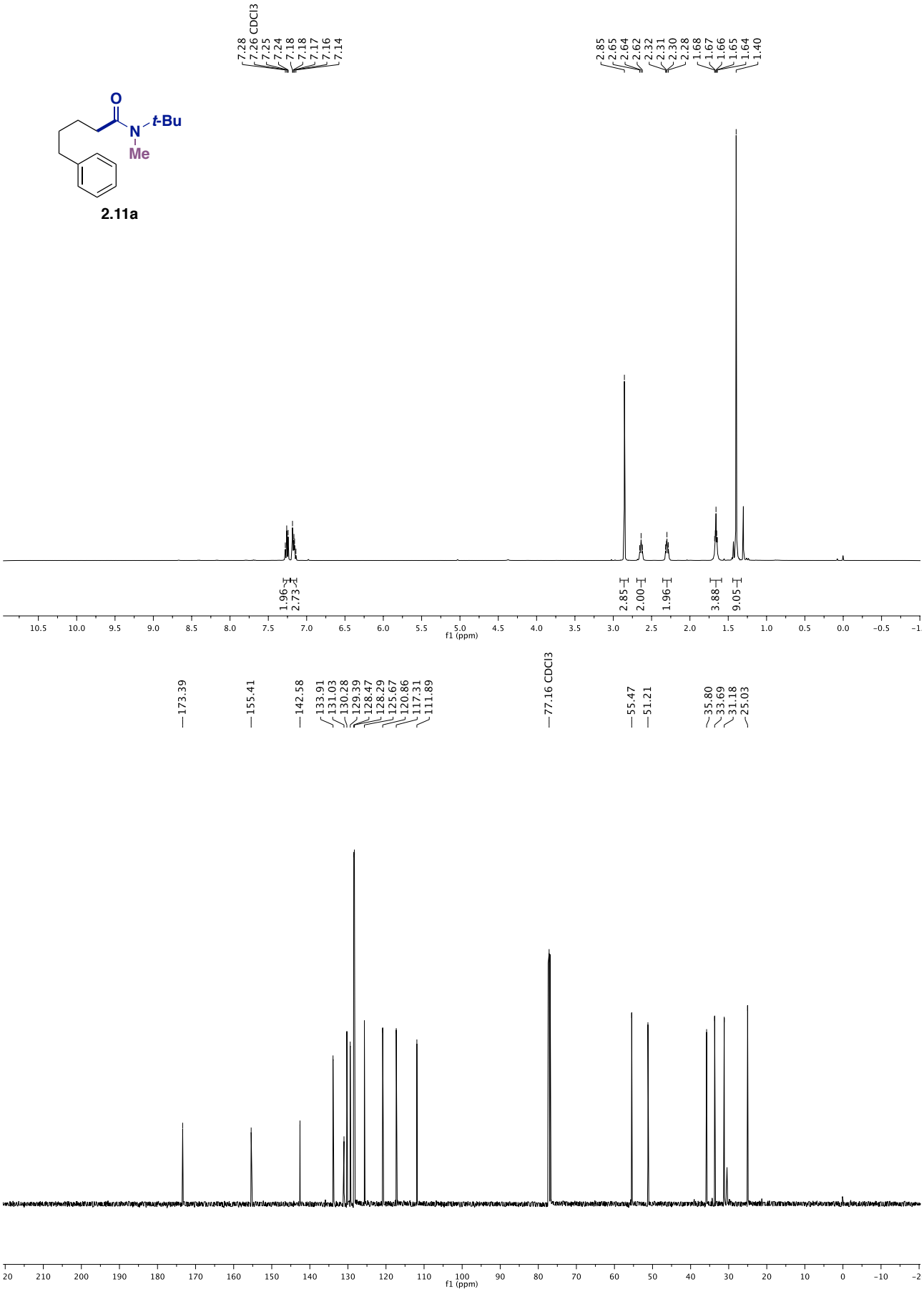
7.28
7.26 CDCl3
7.25
7.24
7.18
7.18
7.17
7.16
7.14
2.85
2.65
2.64
2.62
2.32
2.31
2.30
2.28
1.68
1.67
1.66
1.65
1.64
1.40
O
N
t-Bu
Me
2.11a
1.96
2.73
2.85
2.00
1.96
3.88
9.05
f1 (ppm)
173.39
155.41
142.58
133.91
131.03
130.28
129.39
128.47
128.29
125.67
120.86
117.31
111.89
77.16 CDCl3
55.47
51.21
35.80
33.69
31.18
25.03
f1 (ppm)

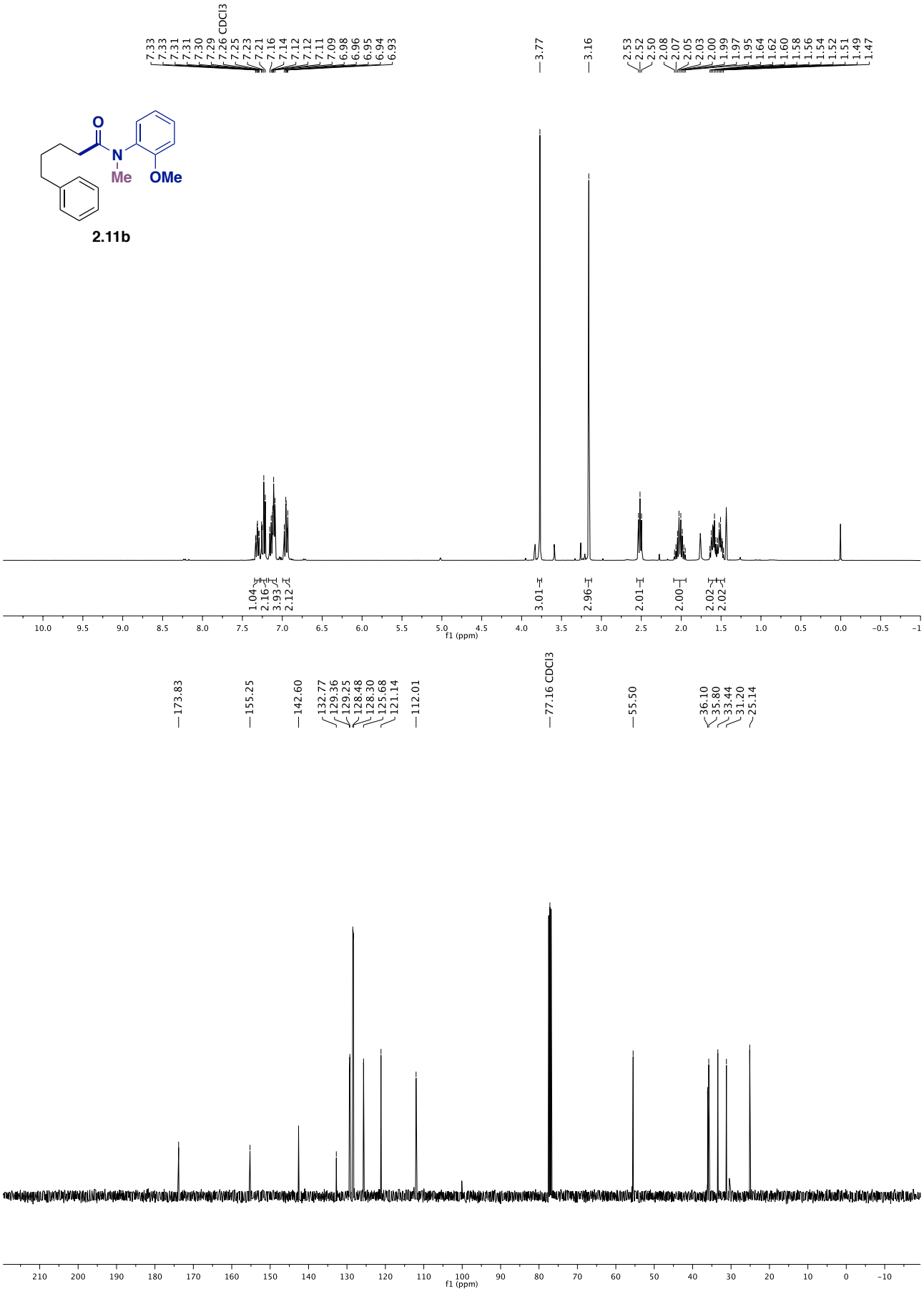
7.33
7.33
7.31
7.31
7.30
7.29
7.26 CDCl3
7.25
7.23
7.21
7.16
7.14
7.12
7.12
7.11
7.09
6.98
6.96
6.95
6.94
6.93
3.77
3.16
2.53
2.52
2.50
2.08
2.07
2.05
2.03
2.00
1.99
1.97
1.95
1.64
1.62
1.60
1.58
1.56
1.54
1.52
1.51
1.49
1.47
O
N
Me
OMe
2.11b
1.04
2.16
3.93
2.12
3.01
2.96
2.01
2.00
2.02
2.02
f1 (ppm)
173.83
155.25
142.60
132.77
129.36
129.25
128.48
128.30
125.68
121.14
112.01
77.16 CDCl3
55.50
36.10
35.80
33.44
31.20
25.14
f1 (ppm)

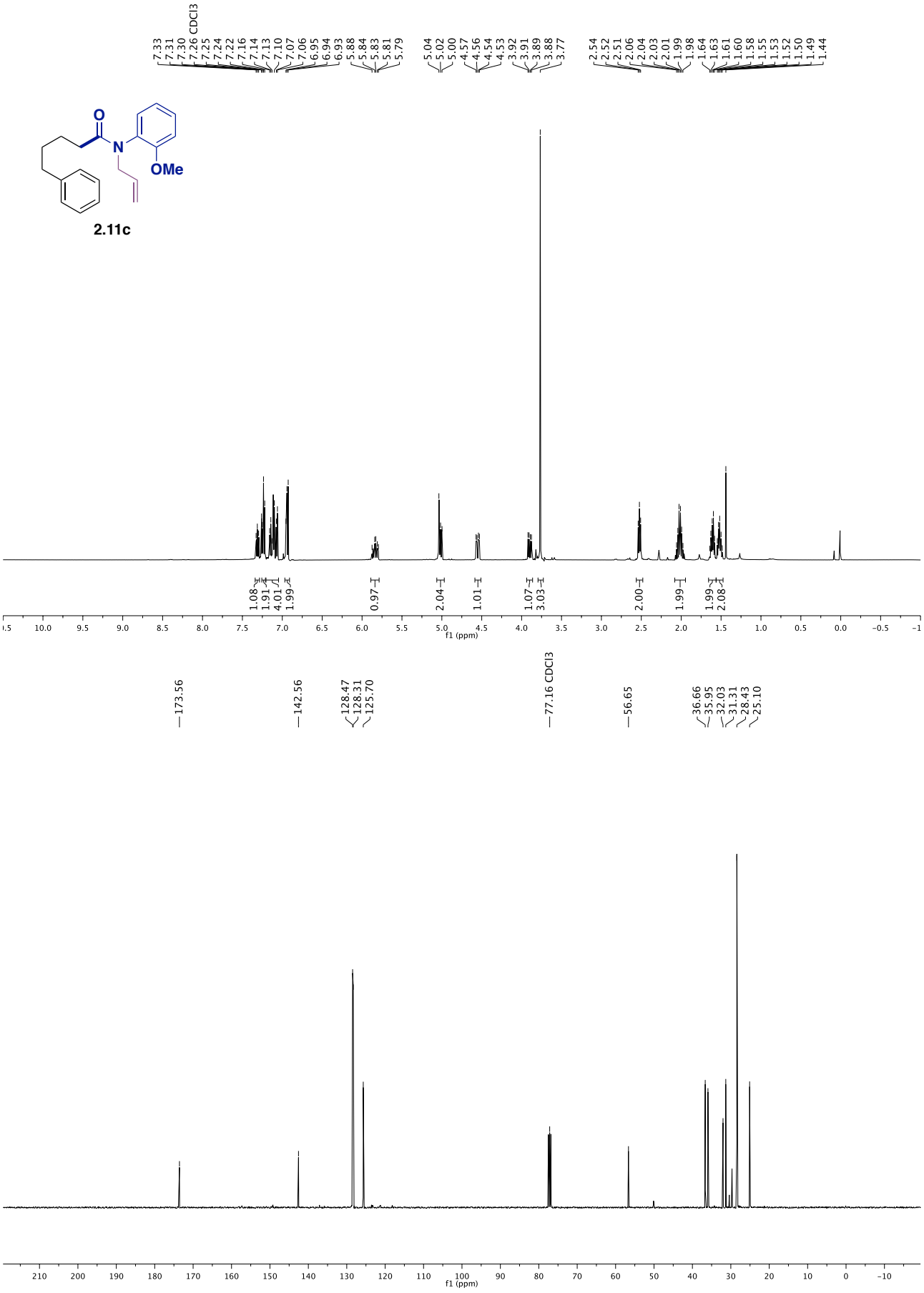
7.33
7.31
7.30
7.26 CDCl3
7.25
7.24
7.22
7.16
7.14
7.13
7.10
7.07
7.06
6.95
6.94
6.93
5.88
5.84
5.83
5.81
5.79
5.04
5.02
5.00
4.57
4.56
4.54
4.53
3.92
3.91
3.89
3.88
3.77
2.54
2.52
2.51
2.06
2.04
2.03
2.01
1.99
1.98
1.64
1.63
1.61
1.60
1.58
1.55
1.53
1.52
1.50
1.49
1.44
O
N
OMe
2.11c
1.08
1.91
4.01
1.99
0.97
2.04
1.01
1.07
3.03
2.00
1.99
1.99
2.08
f1 (ppm)
173.56
142.56
128.47
128.31
125.70
77.16 CDCl3
56.65
36.66
35.95
32.03
31.31
28.43
25.10
f1 (ppm)

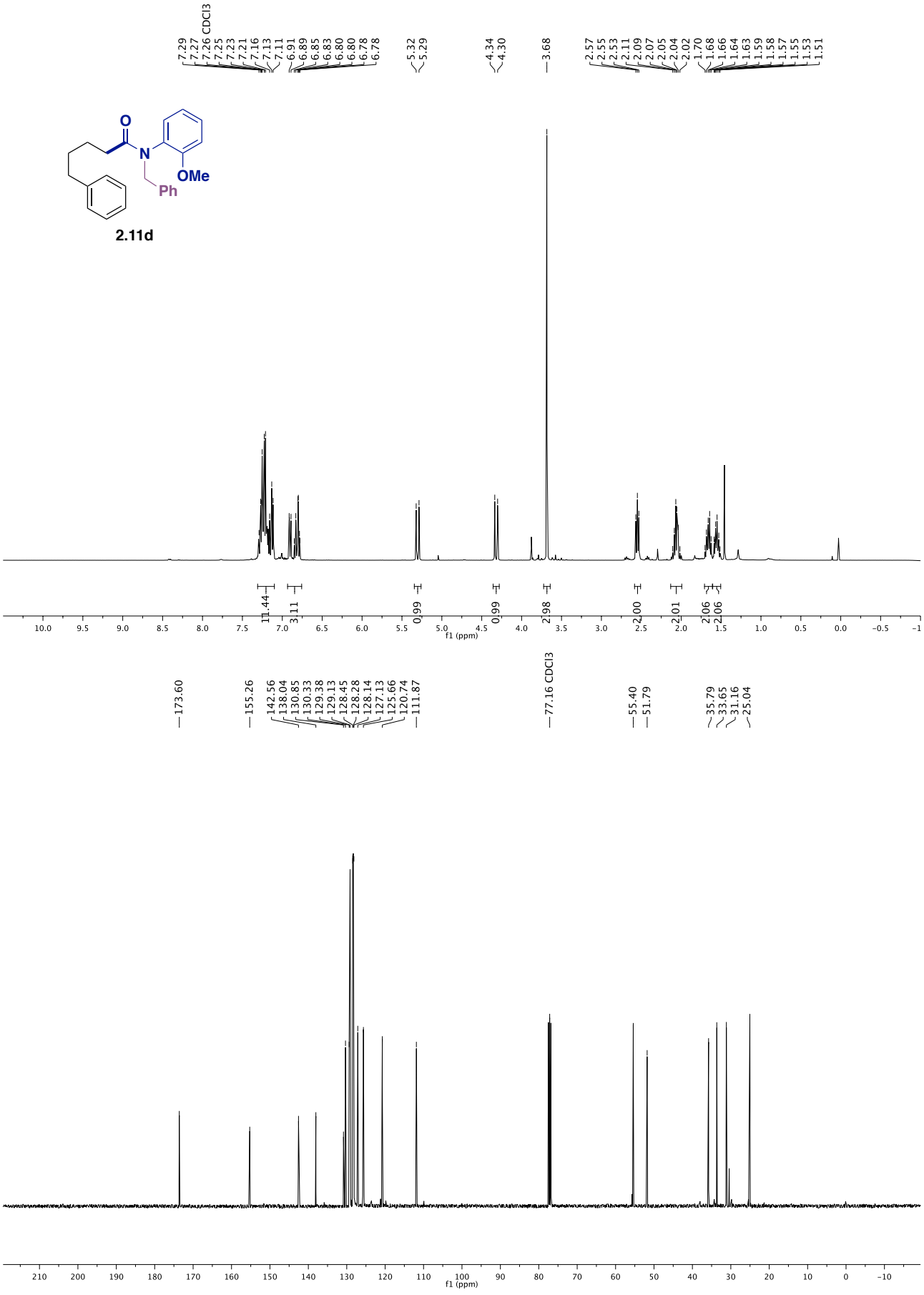
7.29
7.27
7.26 CDCl3
7.25
7.23
7.21
7.16
7.13
7.11
6.91
6.89
6.85
6.83
6.80
6.80
6.78
6.78
5.32
5.29
4.34
4.30
3.68
2.57
2.55
2.53
2.11
2.09
2.07
2.05
2.04
2.02
1.70
1.68
1.66
1.64
1.63
1.59
1.58
1.57
1.55
1.53
1.51
O
N
OMe
Ph
2.11d
11.44
3.11
0.99
0.99
2.98
2.00
2.01
2.06
2.06
f1 (ppm)
173.60
155.26
142.56
138.04
130.85
130.33
129.38
129.13
128.45
128.28
128.14
127.13
125.66
120.74
111.87
77.16 CDCl3
55.40
51.79
35.79
33.65
31.16
25.04
f1 (ppm)

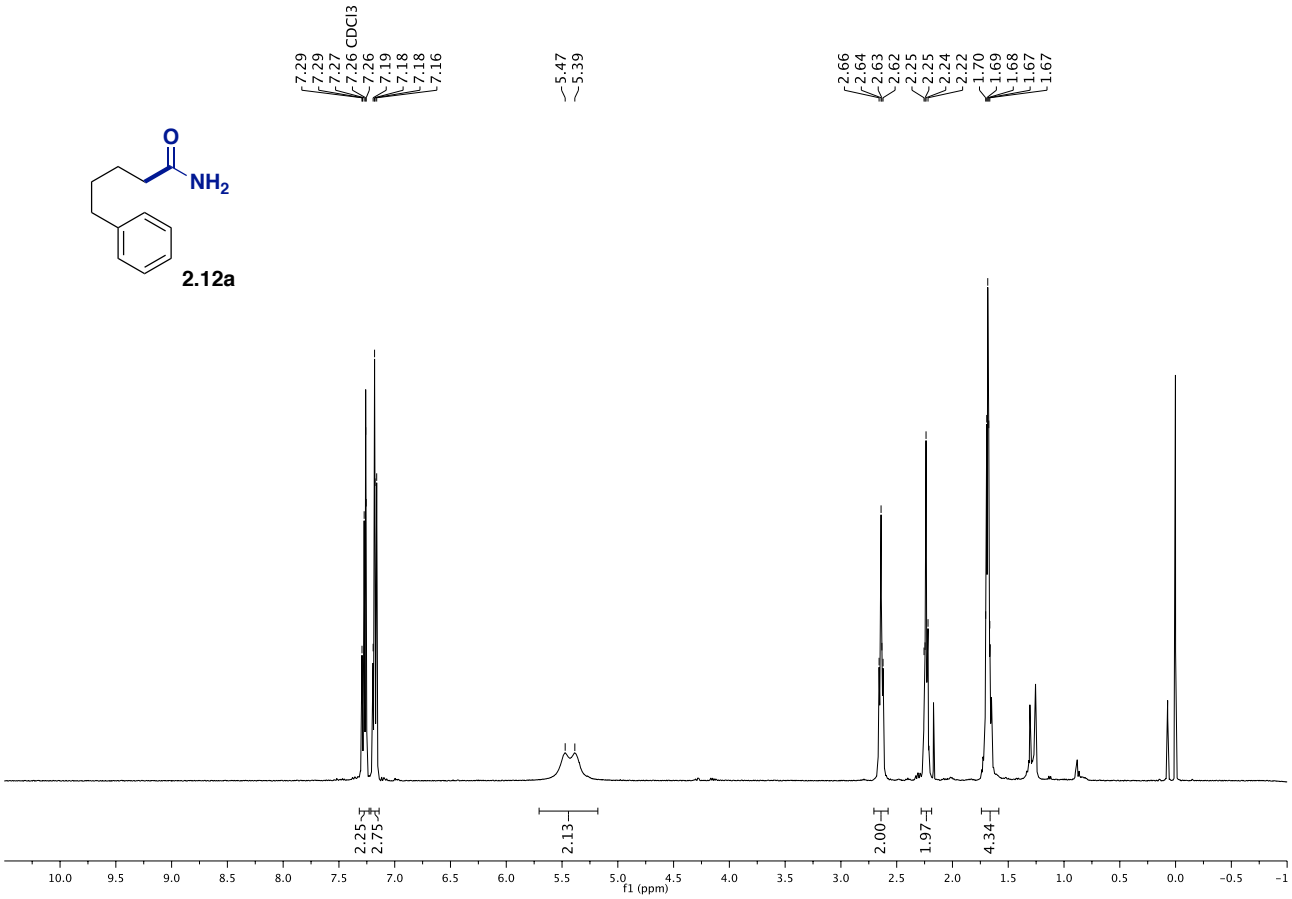
7.29
7.29
7.27
CDCl3
7.26
7.26
7.19
7.18
7.18
7.16
5.47
5.39
2.66
2.64
2.63
2.62
2.25
2.25
2.24
2.22
1.70
1.69
1.68
1.67
1.67
O
NH2
2.12a
2.25
2.75
2.13
2.00
1.97
4.34
f1 (ppm)

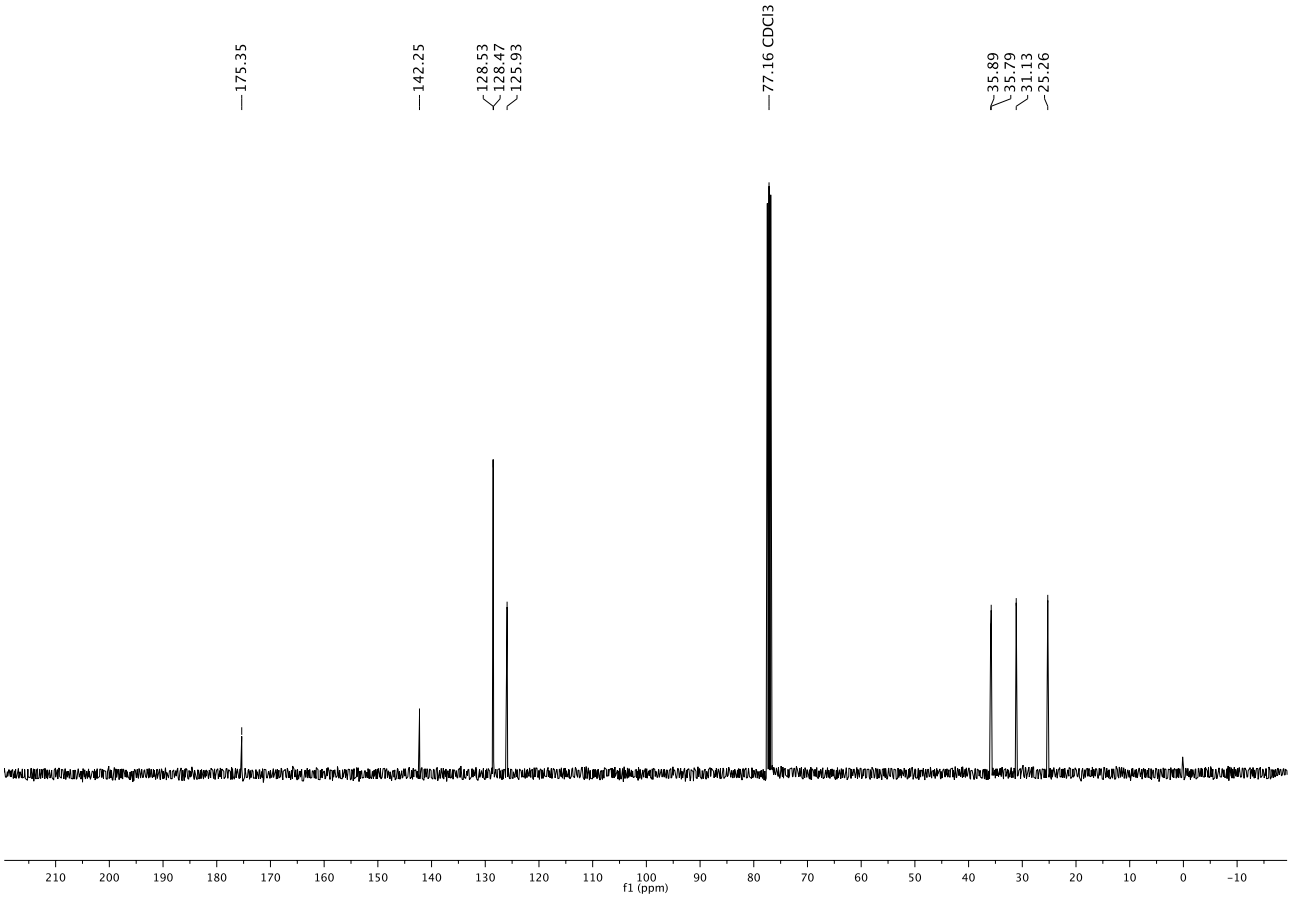
175.35
142.25
128.53
128.47
125.93
77.16 CDCl3
35.89
35.79
31.13
25.26
f1 (ppm)

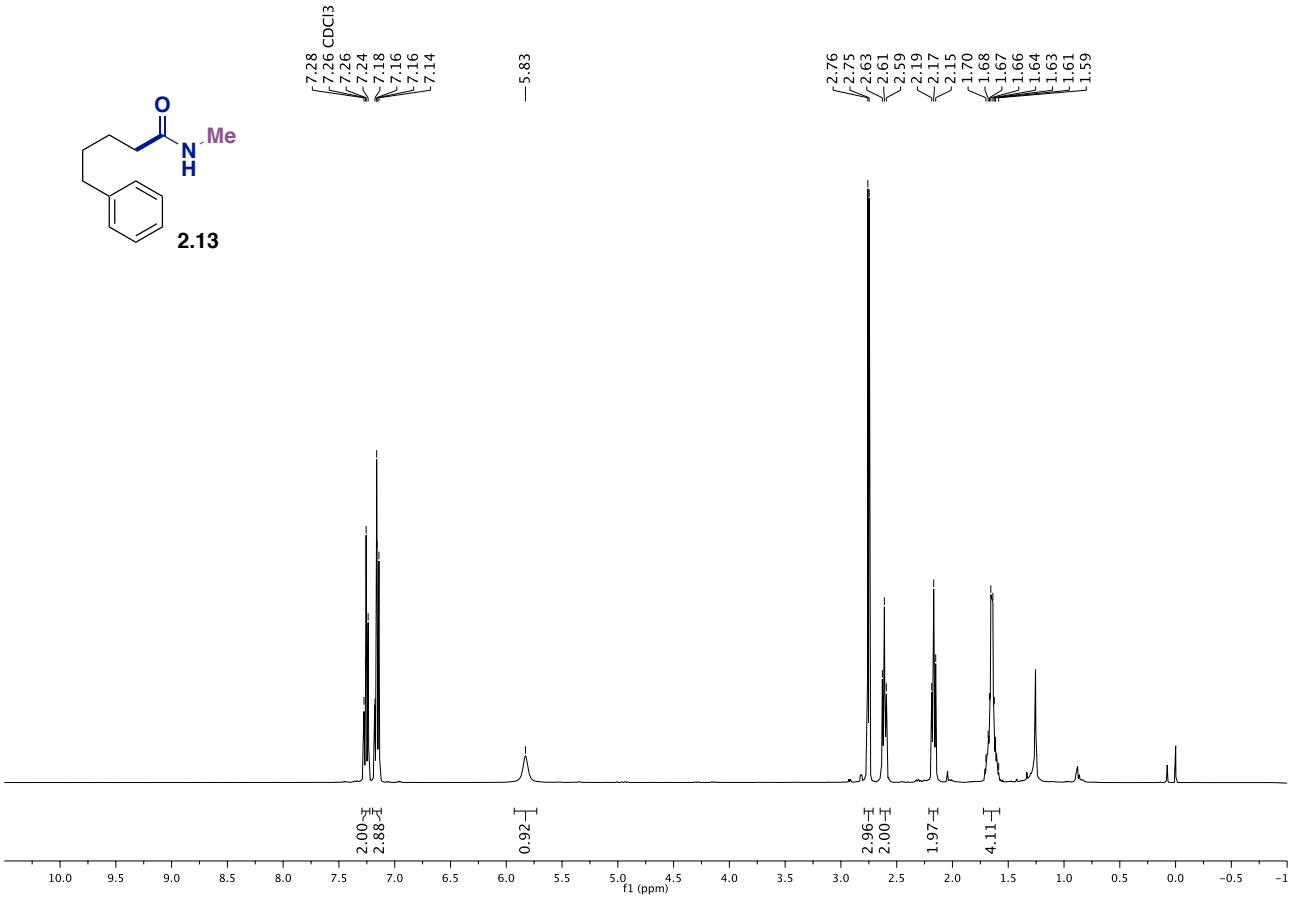
7.28
7.26 CDCl3
7.26
7.24
7.18
7.16
7.16
7.14
5.83
2.76
2.75
2.63
2.61
2.59
2.19
2.17
2.15
1.70
1.68
1.67
1.66
1.64
1.63
1.61
1.59
O
N
H
Me
2.13
2.00
2.88
0.92
2.96
2.00
1.97
4.11
f1 (ppm)

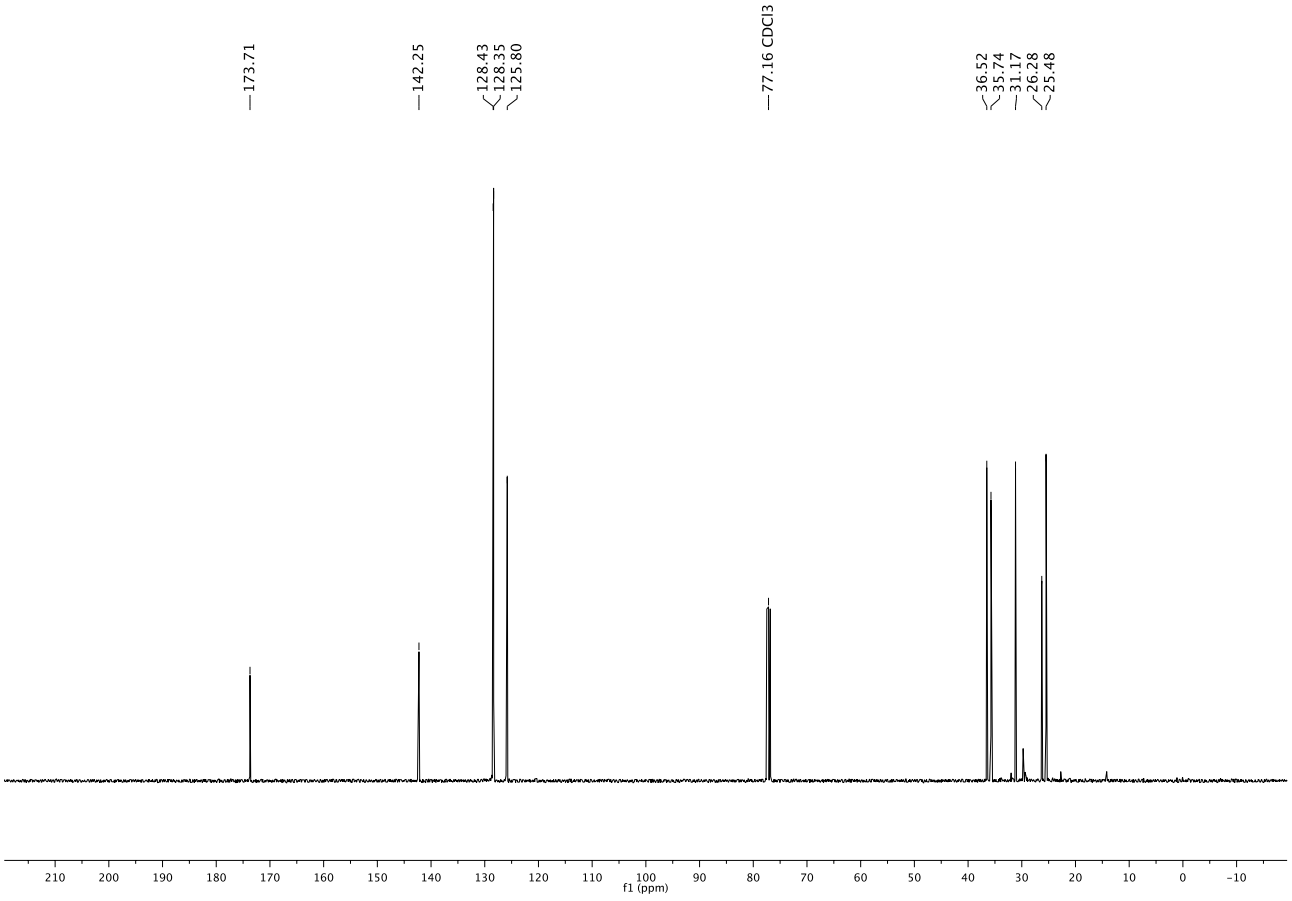
173.71
142.25
128.43
128.35
125.80
77.16 CDCl3
36.52
35.74
31.17
26.28
25.48
f1 (ppm)

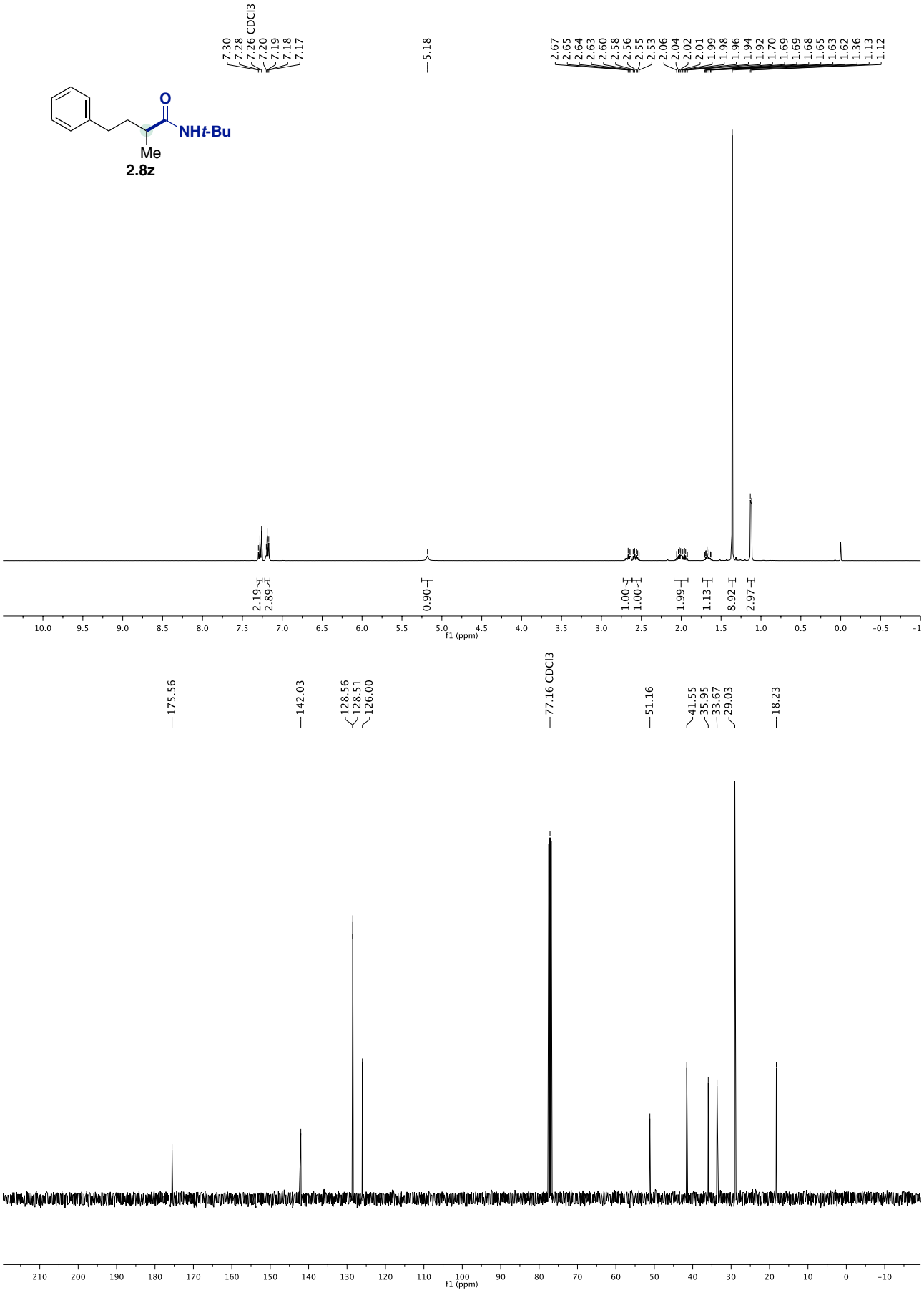
7.30
7.28
7.26 CDCl3
7.20
7.19
7.18
7.17
5.18
2.67
2.65
2.64
2.63
2.60
2.58
2.56
2.55
2.53
2.06
2.04
2.02
2.01
1.99
1.98
1.96
1.94
1.92
1.70
1.69
1.69
1.68
1.65
1.63
1.62
1.36
1.13
1.12
O
NHt-Bu
Me
2.8z
2.19
2.89
0.90
1.00
1.00
1.99
1.13
8.92
2.97
f1 (ppm)
175.56
142.03
128.56
128.51
126.00
77.16 CDCl3
51.16
41.55
35.95
33.67
29.03
18.23
f1 (ppm)

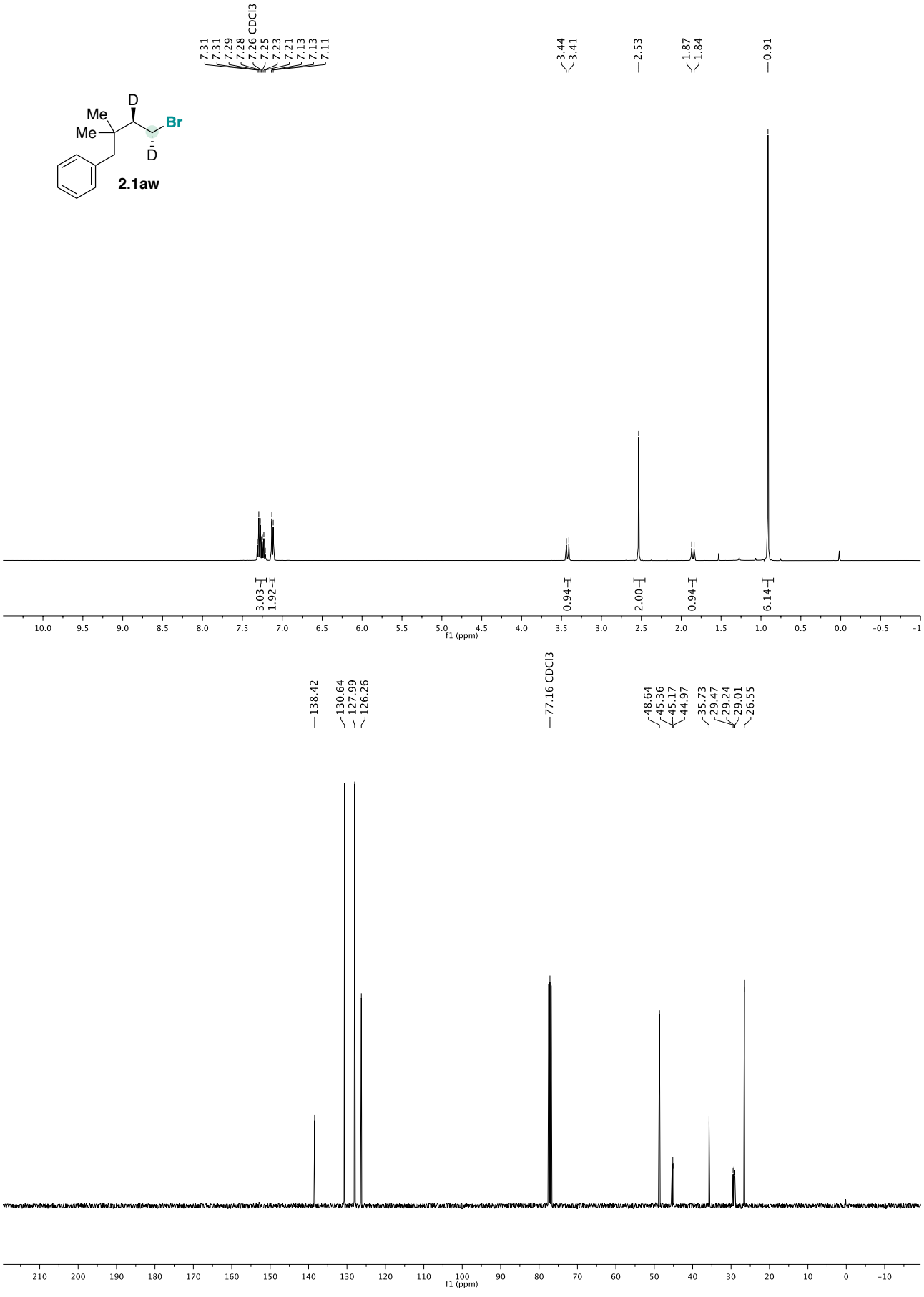
7.31
7.31
7.29
7.28
7.26 CDCl3
7.25
7.23
7.21
7.13
7.13
7.11
3.44
3.41
2.53
1.87
1.84
0.91
Me
Me
D
Br
D
2.1aw
3.03
1.92
0.94
2.00
0.94
6.14
f1 (ppm)
138.42
130.64
127.99
126.26
77.16 CDCl3
48.64
45.36
45.17
44.97
35.73
29.47
29.24
29.01
26.55
f1 (ppm)

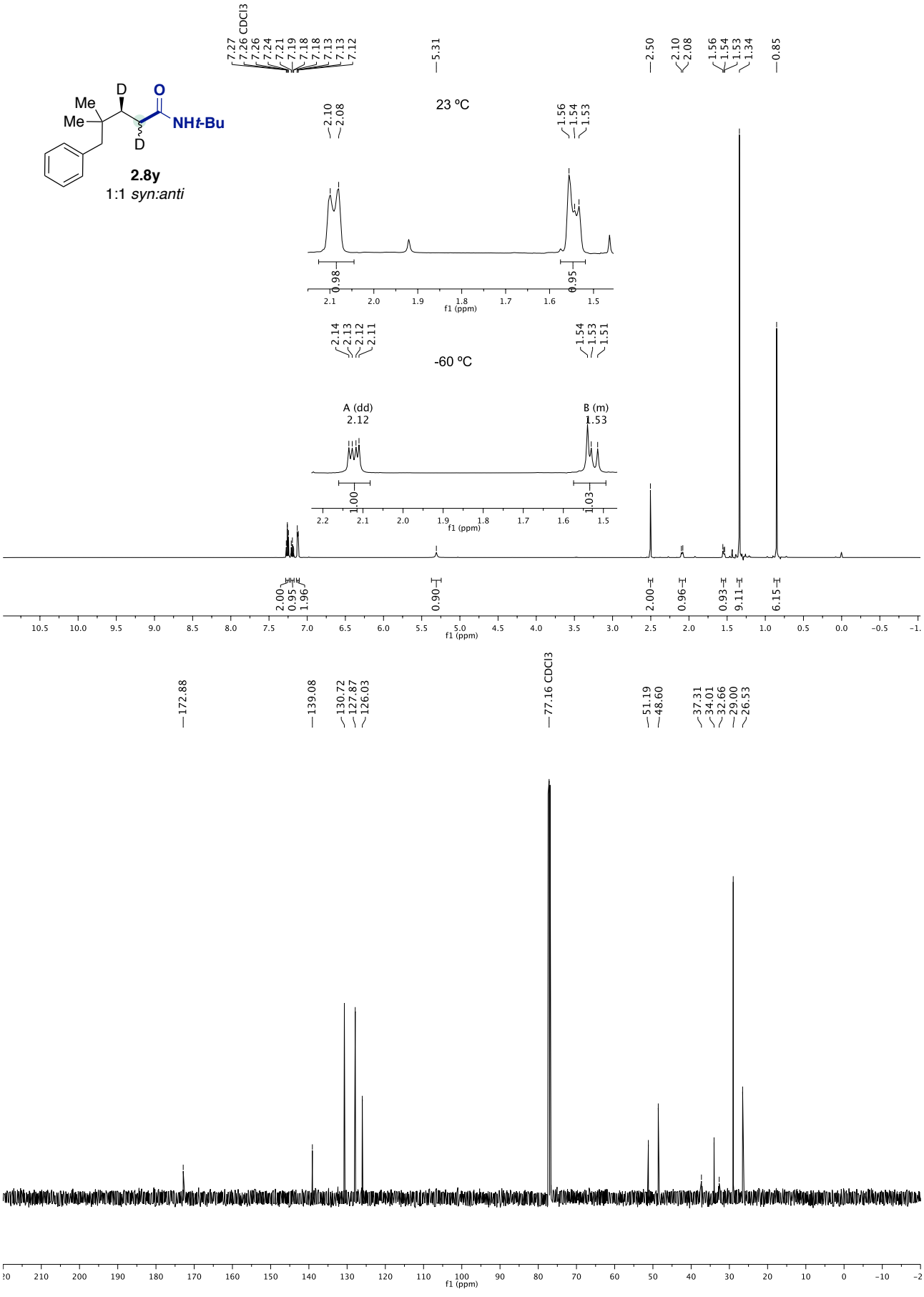
Me
Me
D
O
NHt-Bu
D
2.8y
1:1 syn:anti
23 °C
-60 °C
A (dd)
2.12
B (m)
1.53
CDCl3

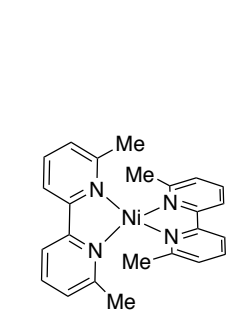

2.14

* Residual ligand

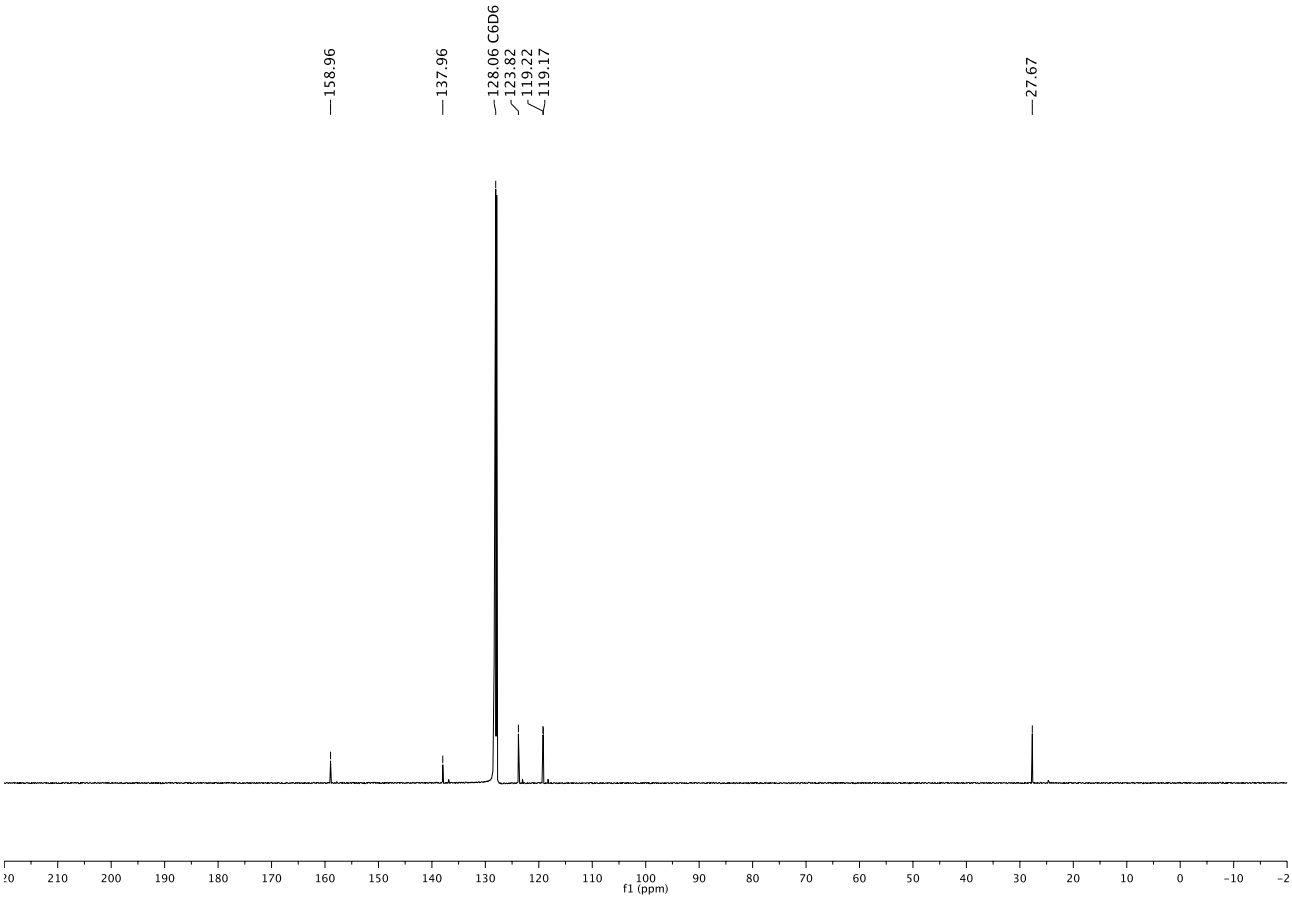

Chapter 3.

Towards a Ni-Catalyzed Regiodivergent Amidation of Secondary Alkyl Halides: Unlocking a Reactivity Relay

In collaboration with Dr. Alicia Monleón, Alberto Tampieri, Dr. Francisco Juliá-Hernández and Andreu Tortajada

3.1. Introduction

3.1.1. Metal-Catalyzed Functionalization of Unactivated Secondary Alkyl Halides

The cross-coupling of unactivated (secondary) alkyl halides is associated with several difficulties: a generally more difficult oxidative addition compared to C(sp^2)-electrophiles, a slower reductive elimination for C(sp^3)—M—C(sp^2)/C(sp^3) than for C(sp^2)—M—C(sp^2) species, and a disposition to undergo undesired pathways such as β-hydride elimination, protodemetallation and dimerization reactions, which arise from the lower stability of alkyl-metal species. Specifically for secondary and tertiary alkyl halides, the added steric hindrance compared to primary alkyl halides hampers oxidative addition, and the presence of additional neighboring β-hydrogens in the alkyl-metal intermediates increases the probability of β-hydride elimination.[1–3]

Since the pioneering report by Fu and Zhou on the Ni-catalyzed Negishi cross-coupling of secondary alkyl bromides and iodides,[4] the use of secondary alkyl halides in catalytic methodologies has unlocked the possibility of disconnecting molecules via non-traditional approaches. These methods have been developed using Ni, Co, Fe and Pd catalysis.[5,6] Due to the lower propensity of Ni to undergo β-hydride elimination compared to more electronegative metals such as Pd, Ni-catalysts have proven particularly suitable for the formation of C(sp^3)—C(sp^2) and C(sp^3)—C(sp^3) bonds from unactivated alkyl halides via traditional cross-coupling reactions with organometallic reagents,[7] reductive cross-electrophile couplings[8–10] or metallaphotoredox reactions.[11–13] The study of the mechanisms of these Ni-catalyzed reactions, which suggested the intermediacy of radical species, inspired the development of enantioselective transformations that start from racemic secondary alkyl halides. These were first described for cross-coupling reactions with organometallic reagents,[14] and more recently in reductive cross-electrophile protocols that start from activated secondary alkyl chlorides.[8,15]

3.1.2. Metal Chain-Walking: A Strategy for Remote sp^3 C—H Functionalization

A wide variety of organic transformations have been developed for the selective functionalization at the most reactive site of a pre-functionalized molecule. An alternative, more challenging, strategy is the selective activation of unreactive C—H bonds far from the initial reactive functional group, termed "remote functionalization". Several strategies have been designed for the remote functionalization of sp^2 C—H bonds; however the activation of sp^3 C—H bonds is considerably more difficult.[16] Among the problems associated with the activation of the latter are their less reactive nature due to a stronger bond energy,[17] the lack of π-bonds that readily interact with transition metals, and the difficult-to-control site-selectivity, which arises from the presence of multiple similar sp^3 C—H bonds within a hydrocarbon scaffold.[18] Different approaches have been followed towards overcoming these challenges that are encountered during the selective functionalization of sp^3 C—H bonds, such as through the use of pre-installed directing groups, or even through more challenging undirected approaches based on the intermediacy of radical species or non-covalent interactions between an enzyme and a substrate.[16,19] Despite these efforts, the site site-selective C—C bond formation at stronger, primary sp^3 C—H bonds remains a challenging task.

An alternative approach towards remote sp^3 C—H functionalization is the use of transition metals capable of migrating the reactive site of a molecule along a hydrocarbon skeleton to reach a terminal primary position where a terminating reaction takes place.[20,21] In this strategy, a suitable transition metal reacts with the substrate's most reactive site to form an alkyl metal intermediate. From this species, the metal is able to migrate via iterative β-hydride elimination/migratory insertion reactions along the hydrocarbon chain, in a process called "chain walking" or "chain running".[22,23] The formation of the active migrating species can be triggered by either reaction between the transition metal and a C=C bond present in the substrate, or by oxidative addition to alkyl electrophiles. Different transition metals such as Zr, Rh, Ru, Ir and Pd have been used to achieve chain-walking

hydroformylation, hydroboration, hydrosilylation and hydroarylation reactions, among others.[20] More recently, methods that use more sustainable systems based on base-metal catalysts such as Co, Fe and Ni have received increased attention.[21]

The chain-walking strategies that will be discussed in this Chapter are proposed to follow a 1,2-hydride shift mechanism for olefin isomerization which takes place via alkyl intermediates and for which all the steps are reversible (Scheme 3.1).[24] In this pathway, a M—H species (**I**) having a free coordination site binds to the olefin, and subsequently triggers a reversible *syn*-migratory insertion across the C=C bond to generate an alkyl—M intermediate (**IV**). Subsequent β-hydride elimination gives rise to a new M—H species along with an olefin intermediate in which the double bond has migrated within the hydrocarbon chain (**V**). This step requires a vacant coordination site at the metal and a *syn*-coplanar rearrangement with the proximal β-hydrogen. The transfer of a hydride to the metal is a concerted process that occurs through a four-centered transition state, in which the agostic interaction between the *d*-orbitals of the metal and the C—H_β σ-bond facilitates C—H bond cleavage. *Syn*-insertion of the newly formed M—H species and an iterative sequence of the β-hydride elimination/migratory insertion steps moves the metal along the chain in the process called metal "chain walking" or "chain running".

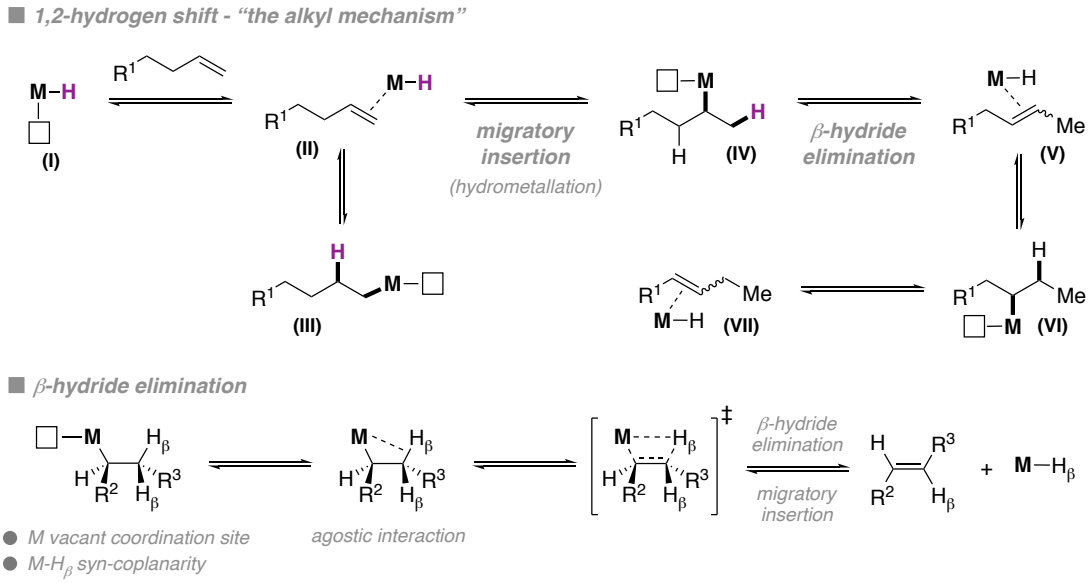

Scheme 3.1. 1,2-hydride shift and β-hydride elimination mechanism

3.1.3. Ni-Catalyzed Chain-Walking Functionalizations

The use of Ni-catalysts capable of olefin isomerization is of high importance in multi-ton industrial processes such as the Shell higher olefin process (SHOP) for ethylene oligomerization to α-olefins and DuPont's hydrocyanation of 1,3-butadiene for adiponitrile production.[25,26] Moreover, in the 1990's, Brookhart and co-workers reported cationic Ni(II)-α-diimine complexes that were highly active in the polymerization of α-olefins. These catalysts were able to generate polymers with linear, unbranched segments via chain-walking olefin isomerization (Scheme 3.2).[23,27] These discoveries form the basis of the more recent development of Ni-catalyzed chain-walking transformations that enable the formal sp^3 C—H functionalization at remote positions within a saturated hydrocarbon chain.

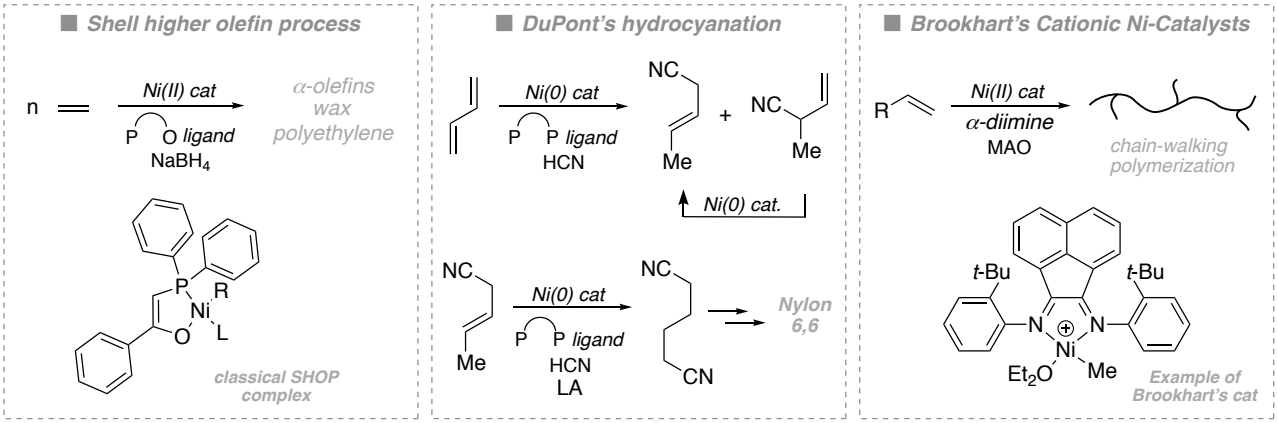

Scheme 3.2. Relevant Ni-catalyzed olefin isomerization processes

3.1.3.1. Ni-Catalyzed Chain-Walking Transformations with Olefins

During the last decade, different Ni-catalyzed protocols for the remote functionalization of olefins have been reported. In 2013, Ong and co-workers developed a tandem olefin isomerization/C—H bond functionalization using Ni catalysts in combination with NHC ligands (Scheme 3.3, top). Under these conditions, a range of heteroarenes bearing acidic C—H bonds could be coupled with activated α-olefins to form 1,1-diarylalkanes. The regioselectivity of the reaction could be switched by the addition of an Al co-catalyst that inhibited olefin isomerization and resulted in the formation of the linear products.[28] An extension to the selective *para*-C—H-alkylation of pyridines was also reported by the same group.[29] In parallel, Hartwig and co-workers reported the linear-selective hydroarylation of unactivated terminal and internal alkenes with trifluoromethyl-substituted arenes, which used a similar catalytic system.[30] In this case, mechanistic experiments together with computational studies suggested that the transformation can be best described as formal chain-walking, and is proposed to follow a pathway where no Ni—H intermediates intervened (Scheme 3.3).

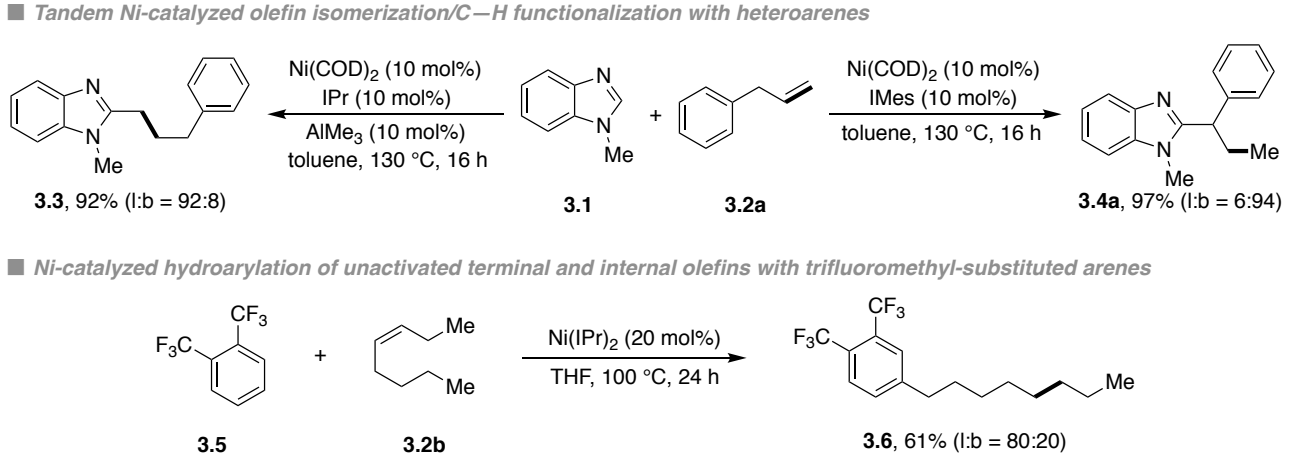

Scheme 3.3. Chain-walking hydroarylation of olefins catalyzed by Ni(0)-NHC complexes

More recently, Zhu and co-workers reported a series of strategies for reductive Ni-catalyzed olefin isomerization/C—C bond formation initiated by hydrometallation of terminal or internal olefins with *in situ* generated Ni—H species (Scheme 3.4). With their first protocol, aryl iodides were coupled with olefins bearing a pendant phenyl moiety to form 1,1-diarylalkanes by using a Ni(II)-bipyridine complex as catalyst. In this system, the Ni—H species, required to trigger the chain walking, were formed using PMHS, which also acted as the

reducing agent. The addition of a fluoride base was necessary to drive Ni—H generation by formation of the strong Si—F bond.[31] In their second protocol, propyl bromide and Mn replaced the silane/CsF system.[32] The use of alkyl bromides for the *in situ* generation of Ni—H species had already been disclosed by our group for the transformation discussed in Chapter 4. Using this new system, the aryl halides scope could be extended to aryl bromides. Finally, the Ni-catalyzed remote C(sp^3)—H alkylation of olefins with alkyl iodides was recently achieved using a PyOx ligand and a silane as hydride source[33] (a system reminiscent to the hydroalkylation of olefins previously developed by Liu and co-workers[34]). In this case, the olefin scope was not limited to substrates bearing a phenyl group in the hydrocarbon chain, which had been used as the driving force for their previous strategies by the formation of a thermodynamically favored benzyl-nickel intermediate. Moreover, good selectivities towards the unrearranged product were obtained when secondary alkyl iodides were employed as substrates. Although in-depth mechanistic studies are needed, Zhu and co-workers proposed that their remote hydrofunctionalization of olefins proceeds via Ni(I)—H and Ni(I)—alkyl intermediates, and that olefin isomerization precedes the oxidative addition of the organic halide.

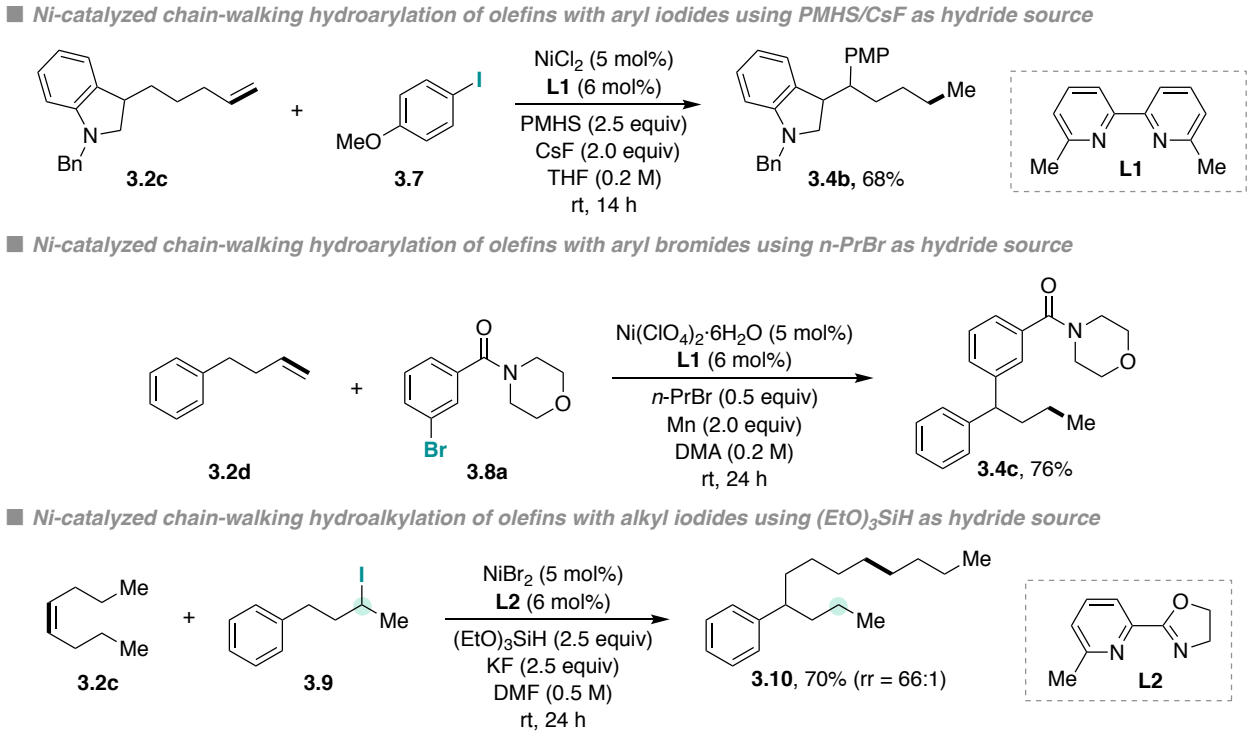

Scheme 3.4. Ni-catalyzed chain-walking hydroarylation and hydroalkylation with *in situ* generated Ni—H species

Building upon their knowledge of Ir- and Pd-catalyzed olefin isomerizations,[35,36] Mazet and co-workers recently reported a one-pot multicatalytic sequence for the stereoselective synthesis of highly substituted alkenes via sequential isomerization/cross-coupling reactions of alkenyl methyl ethers (Scheme 3.5).[37] In this case, the chain-walking migration of C=C bonds was triggered by well-defined Ir- or Pd—H species depending on whether allyl methyl ethers or remote alkenyl methyl ethers were used, respectively. In both cases, the vinyl methyl ethers generated *in situ* could be coupled with Grignard reagents via Ni-catalyzed C—O bond activation using an NHC ligand. This one-pot multicatalytic strategy enables the synthesis of tetra-substituted alkene motifs with good diastereoselectivity, which are difficult to access otherwise.

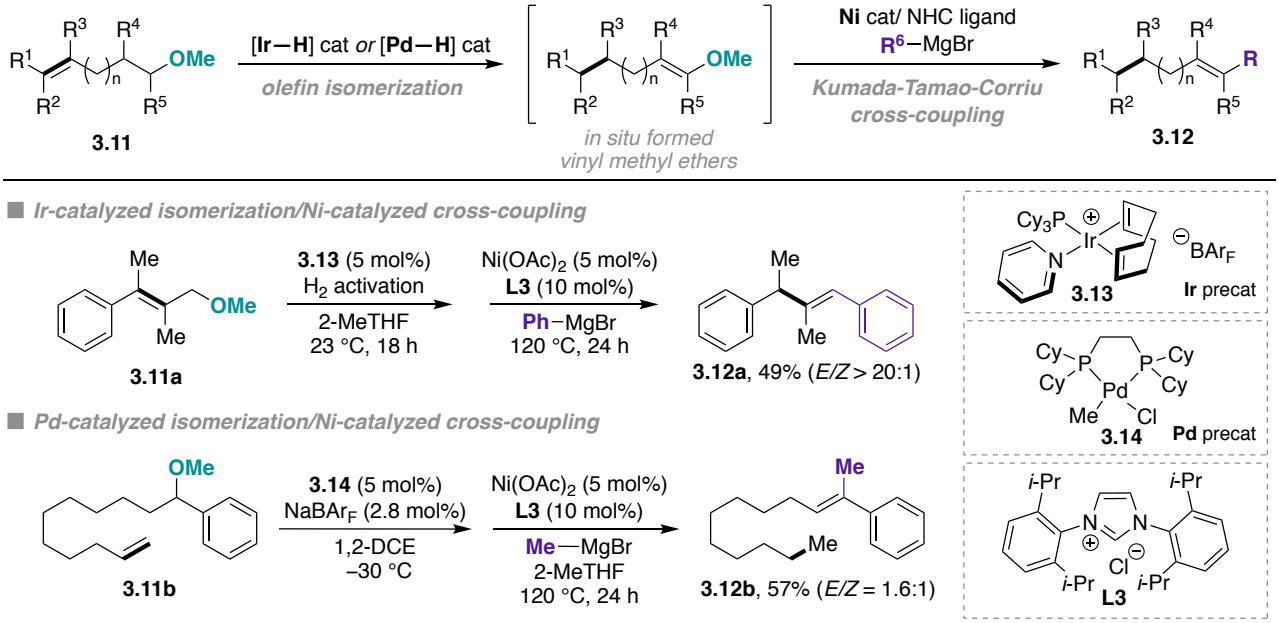

Scheme 3.5. Multicatalytic sequential olefin isomerization/cross-coupling of allylic or alkenyl methyl ethers and Grignard reagents

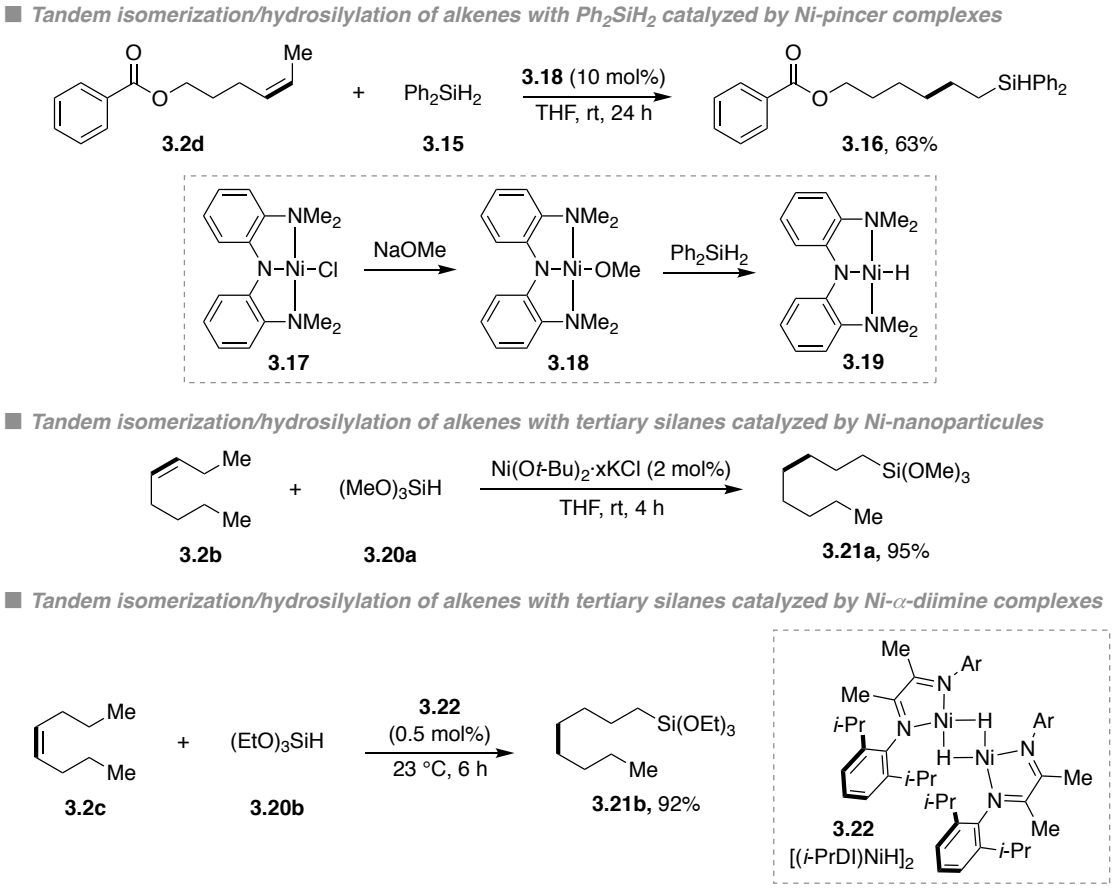

Scheme 3.6. Ni-catalyzed chain-walking hydrosilylations

The Ni-catalyzed remote functionalization of olefins is not just limited to the formation of C—C bonds, as the construction of C—Si bonds has also been reported (Scheme 3.6). In 2015, Hu and co-workers described a highly

chemoselective *anti*-Markovnikov hydrosilylation of unactivated terminal and internal alkenes using diphenylsilane and a Ni(II) bis(amino)amide (N_2N) pincer complex **3.18**, previously developed in their group.[38,39] The transformation was later improved by the use of Ni nanoparticles that catalyze the tandem isomerization/hydrosilylation of unactivated alkenes with tertiary silanes to afford *n*-alkyl silanes, which are more stable and useful products. Although a lower functional group tolerance was observed compared to their first system, the scope and efficiency of the tandem isomerization was improved. Notably, isomeric mixtures of alkanes and even fatty acid-derived internal alkenes provided the desired terminal hydrosilylation products in high yields.[40] Finally, Chirik and co-workers described the use of Ni-catalysts bearing redox-active α-diimine ligands for alkene hydrosilylation. Although the chain-walking hydrosilylation was only studied using 4-octene, high yields of the desired product were isolated using a tertiary silane.[41]

3.1.3.2. Ni-Catalyzed Chain-Walking Cross-Electrophile Couplings with Alkyl Bromides

Preceded by a recent report from Baudoin and co-workers on the Pd-catalyzed chain-walking arylation of linear secondary alkyl bromides with aryl triflates via Negishi-type cross-coupling reactions,[42,43] several Ni-catalyzed transformations for the remote arylation of alkyl bromides have been developed (Scheme 3.7).

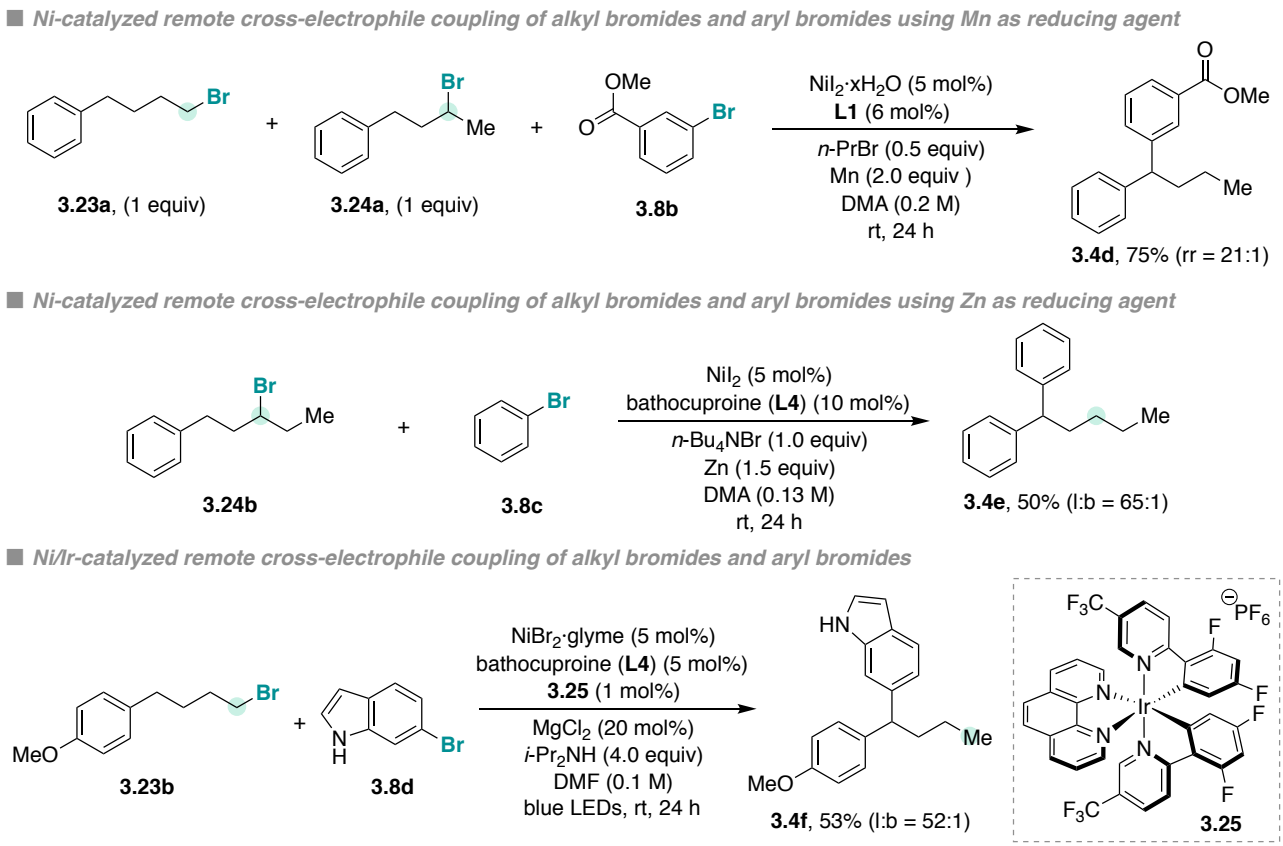

Scheme 3.7. Ni-catalyzed remote cross-electrophile couplings with alkyl bromides

In 2017, Zhu and co-workers reported the Ni-catalyzed reductive hydroarylation of primary and secondary alkyl bromides with aryl bromides using Mn as the reducing agent.[32] As for their related chain-walking hydroarylation of olefins (vide supra), the authors used *n*-propyl bromide as a hydride source, which was necessary in this case to obtain good yields of the desired 1,1-diarylalkanes. Information about the reaction mechanism was obtained by competition experiments between an alkyl bromide, an olefin and an aryl bromide in the absence of an additional hydride source. These generated comparable amounts of both cross-coupled 1,1-

diarylalkane products arising from the olefin and the alkyl bromide. This result suggests that chain-walking occurs with rapid olefin de-coordination and subsequent migratory insertion of the Ni—H into another olefin. Moreover, based on the observation of olefin isomerization in the absence of aryl halide, and a different product distribution depending on the aryl halide used, the authors proposed that the metal-walk occurs prior to oxidative addition.

Independently, Yin and co-workers described a similar Ni-catalyzed reductive hydroarylation protocol, but with Zn as the reducing agent and bathocuproine as the ligand.[44] Interestingly, the addition of an external hydride source was not necessary; however, in this case an ammonium halide was required to increase product yields. In accordance with the cross-electrophile couplings developed by Weix and co-workers, the use of bipyridine and phenanthroline-type ligands lacking *ortho*-substituents afforded the retained cross-coupled products[9] (it is worth mentioning that in their first publication the Weix group had already observed small amounts of chain-walking products for some examples of the Ni-catalyzed coupling of aryl iodides and alkyl iodides[45]). More recently, Yin and co-workers also described an alternative Ni/Ir-photoredox protocol for the remote cross-electrophile coupling of alkyl bromides and aryl halides.[46] The system was similar to the one reported by Lei for the retained cross-coupling of the same starting materials under metallaphotoredox conditions;[47] however, the chain-walking process was promoted with the use of bathocuproine instead of 4,4'-di-*tert*-butyl-2,2'-bipyridine, a privileged ligand for reductive cross-electrophile and metallaphotoredox couplings. The main advantage of this dual catalysis method is the use of the diisopropylamide/photoredox system as the reductant instead of a metal powder.

In contrast to Zhu's reports, but in agreement with Weix's mechanistic studies for their retained cross-electrophile couplings,[48] the remote cross-coupling processes described by Yin are proposed to occur via Ni(III) intermediates (Scheme 3.8, top). In the first step, oxidative addition of the aryl bromide into a Ni(0) species generates an aryl—Ni(II) intermediate (**VIII**). This is followed by alkyl radical addition to afford a Ni(III) species (**IX**). Subsequent iterative β-hydride elimination/migratory insertion of the Ni(III) species ultimately generates a benzyl-nickel(III) intermediate (**XII**), which after reductive elimination affords the desired product. The elementary steps towards the formation of Ni(III) species in this mechanistic proposal are based on previous studies by Weix; however, no further experiments were performed. The possibility of chain-walk by Ni(III) species is questionable, as these are prone to rapid reductive elimination to afford either the reduced or cross-coupled product. The alternative mechanism proposed by Zhu and co-workers is more likely, as Ni(I)—H species are more prone to undergo the sequential migratory insertions/β-hydride eliminations that are required for the chain-walk (Scheme 3.8, bottom). However, the intermediacy of Ni(II) species in Ni-catalyzed chain-walking polymerization reactions could indicate that Ni(II)—H could be the propagating species within the catalytic cycle.[49] Additionally, an alternative mechanism can be proposed in which both starting materials undergo oxidative addition to form Ni(II)—alkyl and Ni(II)—aryl species at a similar rate. Subsequent transmetallation from these intermediates could generate an alkyl—Ni(II)—aryl species, which after reductive elimination would afford the 1,1-diarylalkane product. In order to elucidate the full mechanistic picture, further mechanistic experiments and computational studies are needed.

As shown below, the metal chain-walking with alkyl halides is proposed to start with oxidative addition to the Ni(0)-complex followed by a series of iterative β-hydride elimination and migratory insertion steps, whereas when using olefins as starting materials the metal-walk is triggered by insertion of putative Ni—H species formed *in situ*. It is important to mention that the ability of the Ni-catalyzed system to promote the chain-walking in both strategies is dependent on the substituents adjacent to the nitrogen atom in the ligands used; the use of bipyridine or phenanthroline-type ligands lacking such *ortho*-substituents results in the retained cross-coupling products, as observed by Weix and co-workers,[9] and further shown by Yin and co-workers with the use of 5,5'-dimethyl-2,2'-bipyridine (and other ligands lacking *ortho*-substituents). A thorough investigation on the effect of the *ortho*-

substitution is lacking in the field and will be of crucial interest to the further development of chain walking strategies.

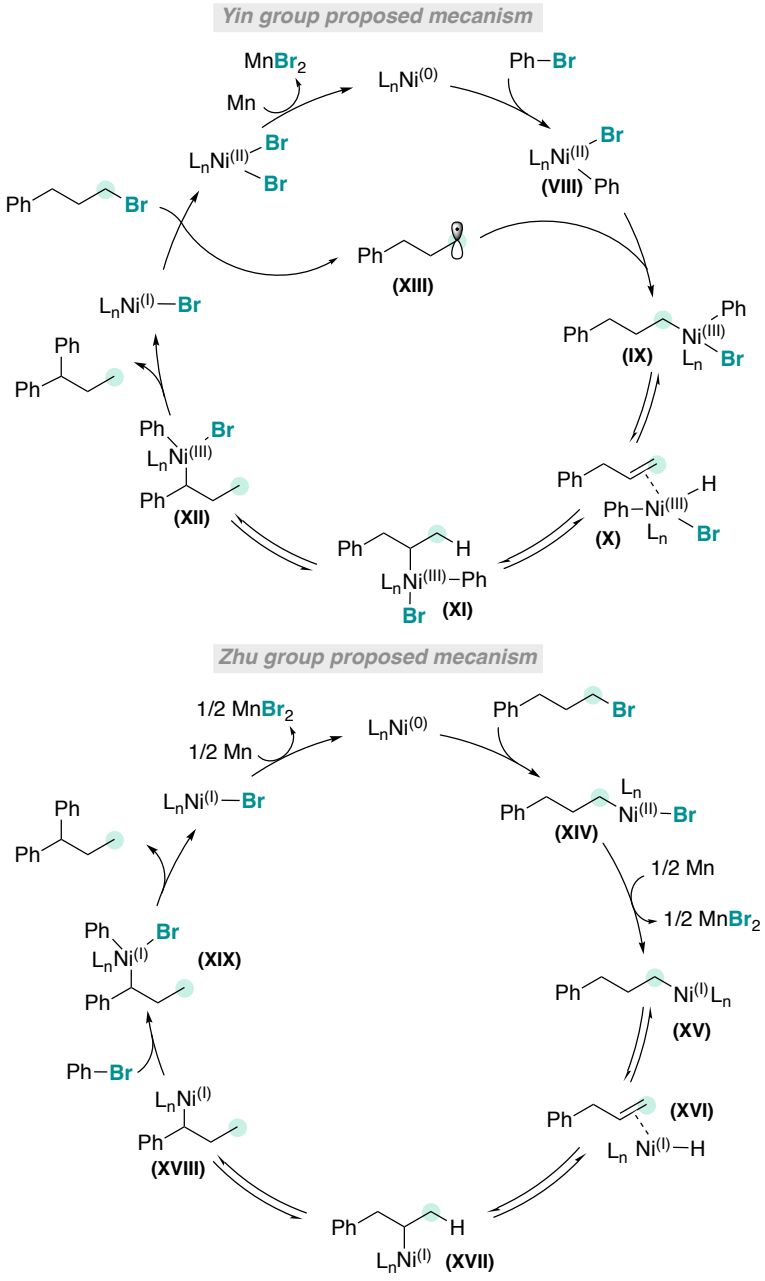

Scheme 3.8. Proposed mechanisms for the remote cross-electrophile coupling of alkyl bromides and aryl halides

3.1.3.3. Ni-Catalyzed Remote Carboxylation of alkyl bromides and olefins with CO_2

In 2017, our group reported the Ni-catalyzed remote reductive carboxylation of unactivated alkyl bromides under atmospheric pressure of CO_2 (Scheme 3.9).[50] A π-acceptor phenanthroline-type ligand bearing long alkyl chains adjacent to the nitrogen atom and *para*-phenyl substituents was key to obtaining high yields of the remote carboxylation products. Conversely, the use of related ligands bearing shorter alkyl chains as *ortho*-substituents or ligands lacking *para*-phenyl rings, such as neocuproine, led to low or only trace amounts of the desired acid. Under the optimized conditions, a broad functional group tolerance was observed and esters, ketones, aryl and alkyl chlorides, heterocycles and alcohols, among others, were well tolerated. Important aspects of this remote

carboxylation method are: a) the thermally-modulated regiodivergent synthesis of carboxylic acids from substrates containing esters or amides, and b) the regioconvergent synthesis of primary acids from crude isomeric mixtures of alkyl bromides, obtained via radical bromination of the corresponding alkane. A similar strategy could also be applied by the bromination of regioisomeric mixtures of alkenes. In contrast to the Ni-catalyzed chain-walking hydroarylations (vide supra), primary carboxylic acids were obtained even when phenyl rings were present in the hydrocarbon chain, showing that stronger primary sp^3 C—H bonds can be remotely functionalized in the presence of weaker sp^3 C—H bonds. This result might be explained by the preferred formation of primary Ni—alkyl intermediates in which the steric interaction between the hydrocarbon chain and the bulky substituents of the ligand is diminished. Importantly, the remote carboxylation can be conducted with little erosion of the enantiomeric ratio of a pre-existing stereocenter located within the hydrocarbon chain. This result suggests that the remote carboxylation proceeds via a non-dissociative mechanism in which the Ni-catalyst remains bound to the substrate to achieve the isomerization and functionalization at the same molecule.

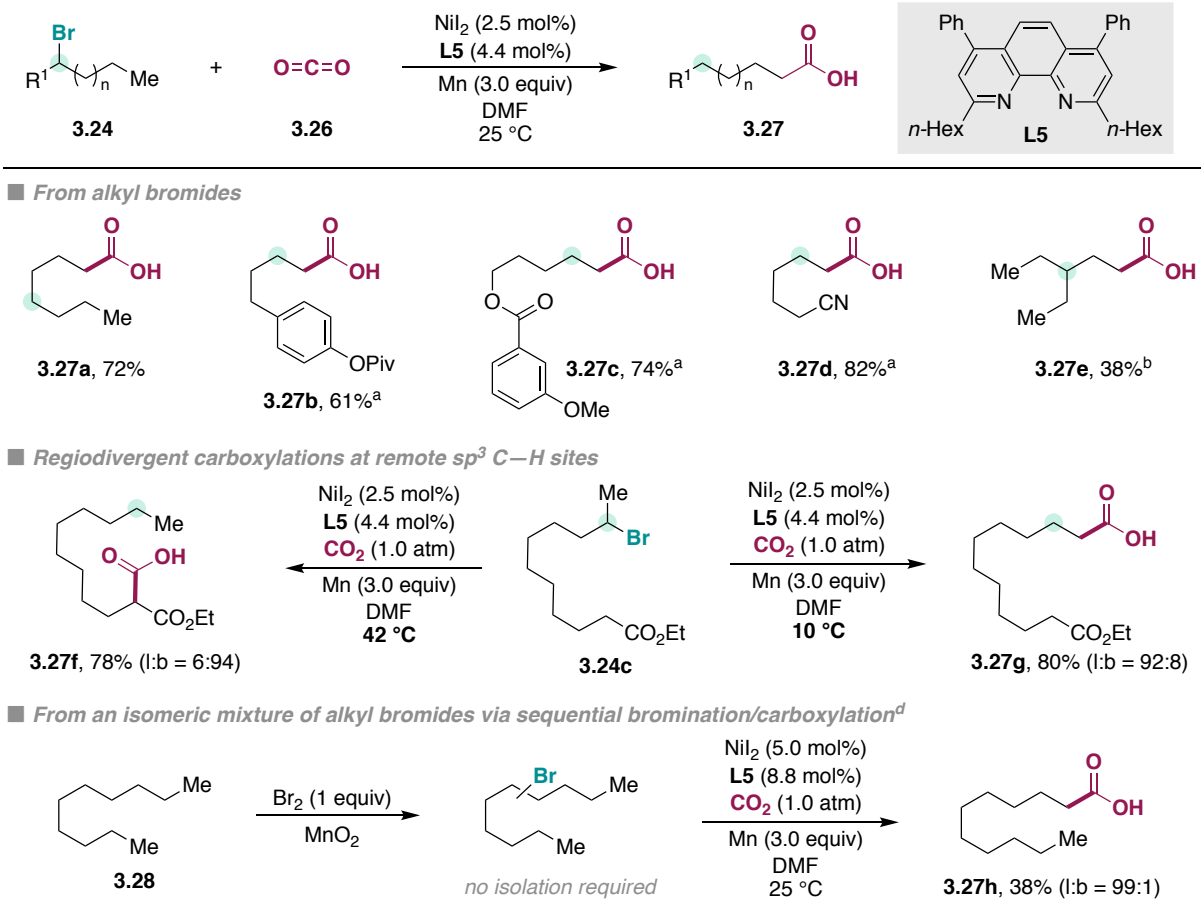

Reaction conditions: 3.24 (0.50 mmol), CO_2 (1 atm), NiI_2 (2.5 mol%), **L5** (4.4 mol%), Mn (3.0 equiv), DMF (1 M) at 25 °C, 20 h. [a] At 10 °C. [b] NiI_2 (10 mol%). [d] Br_2 (1 equiv), MnO_2 (2 equiv), alkane (0.02 M).

Scheme 3.9. Ni-catalyzed remote reductive carboxylation of alkyl bromides with CO_2

Recently, our group reported the remote reductive hydrocarboxylation of terminal and internal unactivated olefins with CO_2 via a Ni-catalyzed chain-walking processes using water as formal hydride source (Scheme 3.10).[51] This transformation avoids the use of halogenated substrates and uses feedstock materials such as water, CO_2 and olefins, instead. Another important advantage of this protocol is the use of water as an abundant and innocuous formal hydride source, rather than silanes or organometallic reagents that are often used to generate the propagating M—H species. Deuteration experiments using D_2O were consistent with the participation of water as

a formal hydride source; however, whether Ni—H species form under the optimized reaction conditions still remains unclear.

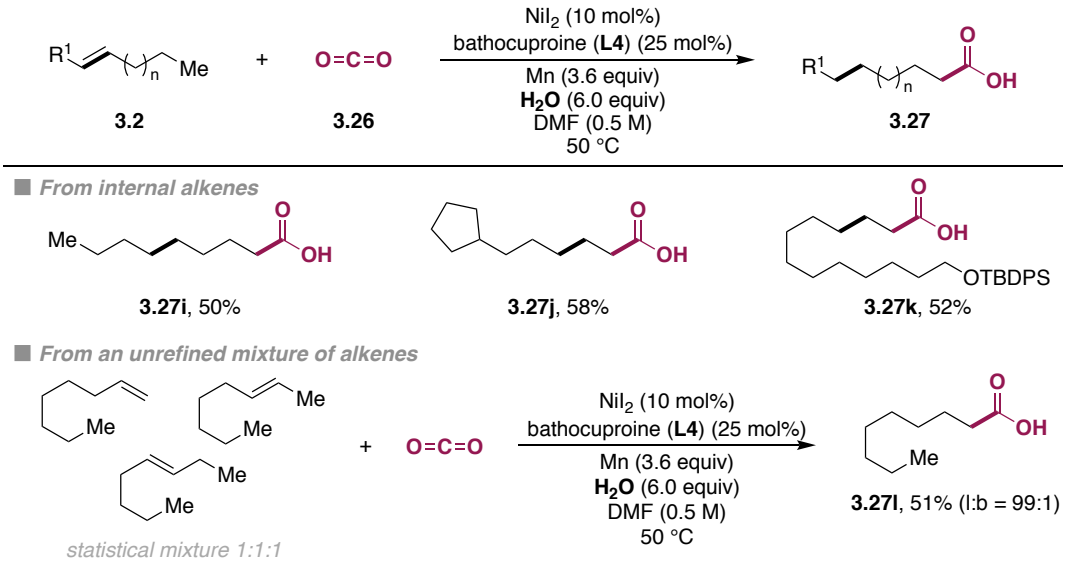

Reaction conditions: 3.2 (0.20 mmol), CO_2 (1 atm), NiI_2 (10 mol%), bathocuproine (**L4**) (25 mol%), H_2O (6.0 equiv) Mn (3.6 equiv), DMF (0.50 M) at 50 °C, 20 h.

Scheme 3.10. Ni-catalyzed remote reductive carboxylation of olefins with CO_2 using water as hydride source

3.2. General Aim of the Project

Regiodivergent transformations are a useful tool for the synthesis of different motifs from the same building block. Encouraged by our group's recent findings in remote carboxylation reactions with CO_2, we hypothesized that the use of isocyanates as coupling partners could allow enable the development of a regiodivergent transformation of secondary alkyl halides for the synthesis of aliphatic primary and secondary amides, depending on the reaction conditions (Scheme 3.11). Achieving this goal requires the design of two different catalytic systems that either suppress or facilitate β-hydride elimination from the alkyl-metal intermediates generated upon oxidative addition into the C—X bond.

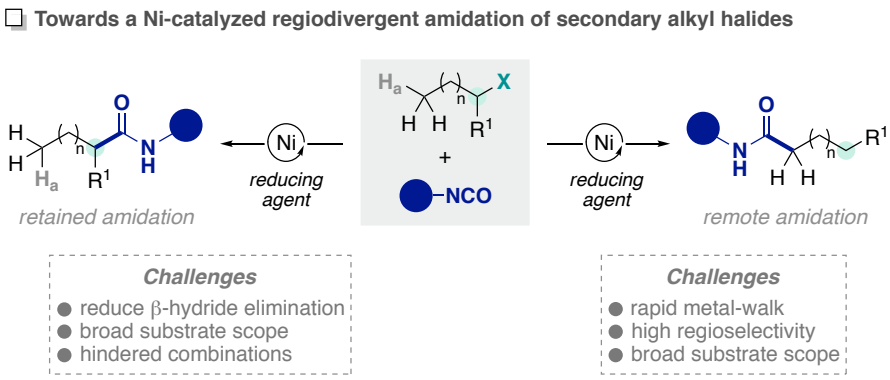

Scheme 3.11. Towards a Ni-catalyzed regiodivergent synthesis of amides from secondary alkyl halides

The major challenges associated with the development of an amidation of secondary alkyl halides are the higher propensity of branched alkyl—Ni species to undergo undesired pathways, such as β-hydride elimination, and the increased steric hindrance of the substrate that could result in a more difficult isocyanate insertion into the alkyl—Ni intermediate. On the other hand, the development of a remote amidation of primary sp^3 C—H bonds

is made challenging by the strong binding properties of isocyanates to transition metals, their higher reactivity and higher solubility compared to CO_2, which facilitate the amidation at the initial reactive site. Therefore, a catalytic system needs to be designed that is capable of efficient metal migration through sequential β-hydride elimination/migratory insertion along the hydrocarbon chain until reaching the primary sp^3 position, without the formation of internal amides.

3.3. Ni-Catalyzed Reductive Amidation of Unactivated Secondary Alkyl Bromides with Isocyanates

3.3.1. First Approach Towards the Retained Amidation of Unactivated Secondary and Tertiary Alkyl Bromides

The first efforts towards the Ni-catalyzed amidation of secondary and tertiary alkyl bromides with isocyanates were made using similar reaction conditions to those optimized in Chapter 2 for the amidation of primary alkyl bromides (Scheme 3.12). Under these conditions, good yields of the corresponding secondary amides were obtained with a small set of cyclic alkyl bromides (**3.29a** to **3.29d**). Conversely, linear secondary alkyl bromides afforded lower yields and higher amounts of olefin side products. This could be explained by the higher degree of rotational freedom in the acyclic system which increases the chance for a suitable agostic interaction leading to β-hydride elimination. In line with the results found in Chapter 2, further evidence for a radical mechanism for the oxidative addition was provided by the amidation of *exo*-2-bromonorbornane, which resulted in a diastereomeric mixture of *exo* and *endo* amides (**3.29d**). The amidation of sterically more demanding tertiary alkyl bromides was limited to substrates not prone to β-hydride elimination, and afforded moderate yields of the desired amide (**3.29f**). At the time that these results were published, very few reductive couplings with tertiary alkyl halides had been reported.[52,53] Since then, the formation of all-carbon quaternary centers using reductive cross-coupling techniques has seen some advances, but still remains challenging.[54–56]

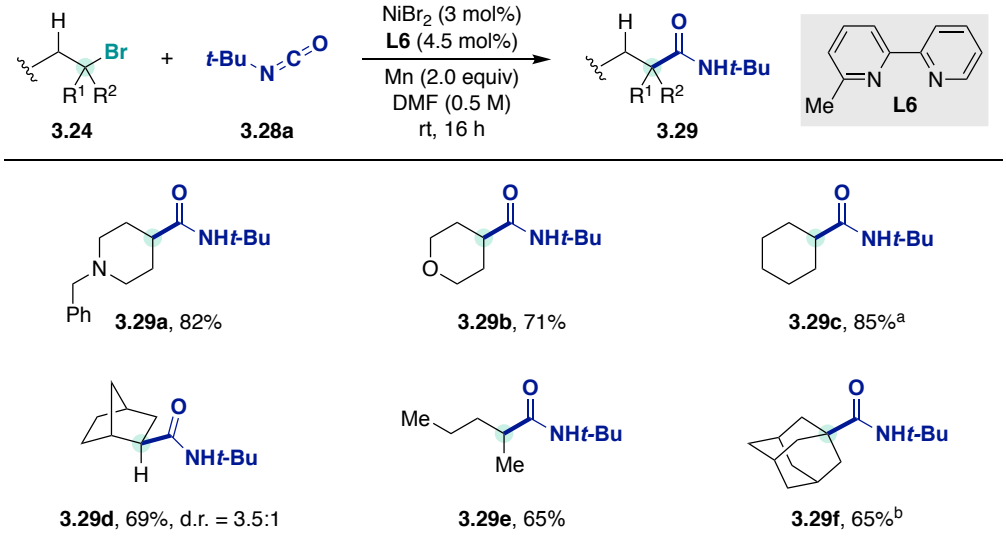

Reaction conditions: **3.24** (0.50 mmol), **3.28a** (1.5 mmol), Mn (1.0 mmol), $NiBr_2$ (3.0 mol%), **L6** (4.5 mol%), DMF (1.0 mL) at rt, 16 h. [a] Using **3.28a** (0.75 mmol), $NiBr_2$ (5.0 mol%), **L6** (7.5 mol%). [b] Using $NiBr_2$ (10 mol%), **L6** (15 mol%).

Scheme 3.12. First scope of secondary and tertiary alkyl bromides

Unfortunately, under these reaction conditions a wide range of substrates failed to afford the targeted amides in good yield, mostly due to the competitive formation of β-hydride elimination products. In some cases, it was not possible to overcome the facile β-hydride elimination or the dimerization of the alkyl bromide starting material,

and only traces or low yields of the corresponding amides were observed. During these studies, the temperature was identified as a crucial variable, as irreproducible product yields were obtained when the reaction temperature was not carefully controlled (Scheme 3.13).

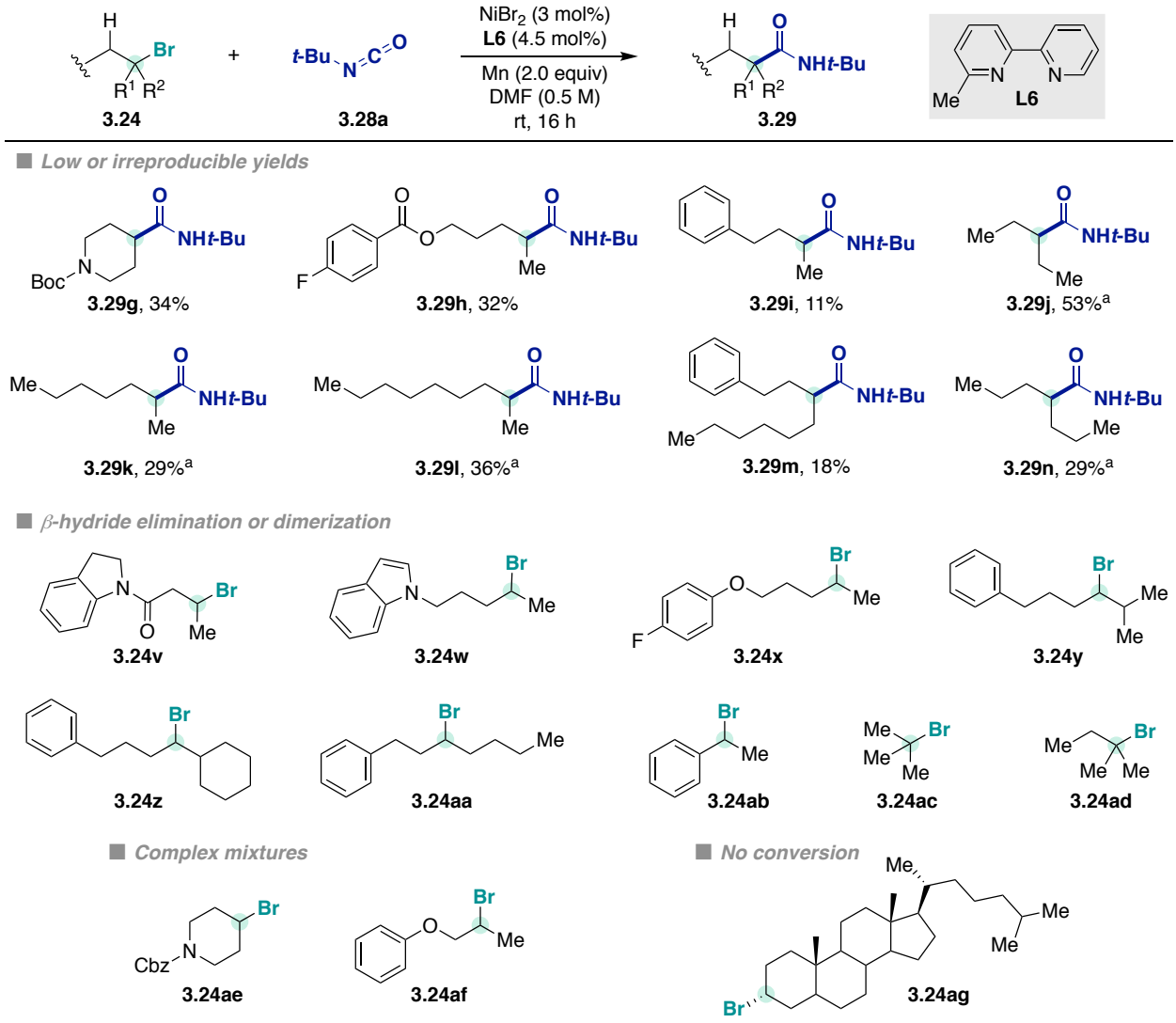

Reaction conditions: 3.24 (0.50 mmol), **3.28a** (1.5 mmol), Mn (1.0 mmol), $NiBr_2$ (3.0 mol%), **L6** (4.5 mol%), DMF (1.0 mL) at 25 °C, 16 h. [a] Best isolated yields, variable yields as low as 10% were obtained when rt was not controlled.

Scheme 3.13. Unsatisfactory amidation of secondary and tertiary alkyl bromides

3.3.2. Re-evaluation of the Reaction Conditions for Linear Alkyl Bromides

The low and variable yields obtained with the majority of the linear secondary alkyl bromides that were tested prompted us to perform a re-optimization of the reaction conditions. This started by the evaluation of different ligands at low reaction temperatures, using 3-bromoheptane as the model substrate (Table 3.1). During this and the following screening, the reaction temperature was reliably controlled by the use of a new set-up, in which the reaction vessel was placed in an aluminum block having an internal circulation system connected to a chiller (see Experimental Section). When a set of different substituted bipyridine- and phenanthroline-type ligands was used, a high regioselectivity towards the retained amidation product was achieved in all cases. In line with the results obtained in Chapter 2, bipyridine-type ligands afforded superior results compared to phenanthroline-type ligands (entry 7 vs. 12, for example). Whereas good yields of the desired product were obtained using **L6** and **L7**, even more encouraging results were observed with **L8**. As shown in entry 3, this ligand provided higher yields of amide

3.29o without reaching complete conversion of **3.24ah**, leaving room for further optimization of other parameters. Importantly, only trace amounts of the chain-walking amidation product **3.29p** were observed with all ligands tested. The formation of product **3.29k** is likely due to the presence of 2-bromoheptane in the 3-bromoheptane used for the screening, and not the product of a chain-walking process.

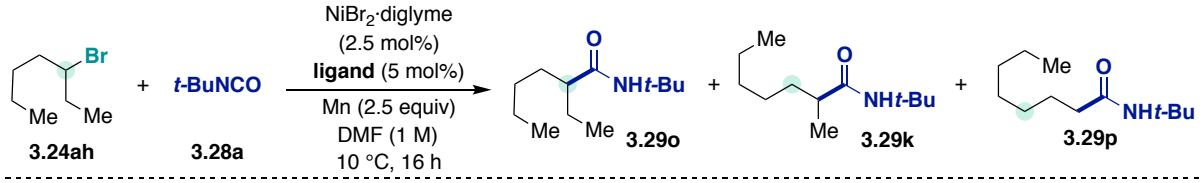

Entry	Ligand	Conversion of 3.24ah (%)[a]	Yield of 3.29o: 3.29k: 3.29p (%)[a]
1	6-methyl-2,2'-bipyridine (**L6**)	100	71: 6: 0
2	6-*n*-butyl-2,2'-bipyridine (**L7**)	97	76: 7: 0
3	6-*n*-hexyl-2,2'-bipyridine (**L8**)	94	81: 7: 0
4	6-isoproyl-2,2'-bipyridine (**L9**)	100	41: 4: 0
5	6-(trifluoromethyl)-2,2'-bipyridine (**L10**)	48	0: 1: 3
6	6-methyl-4-(trifluoromethyl)-2,2'-bipyridine (**L11**)	41	4: 0: 0
7	6-methyl-4,4'-diphenyl-2,2'-bipyridine (**L12**)	100	61: 6: 0
8	6-methyl-4,4'-dimethyl-2,2'-bipyridine (**L13**)	100	30: 2: 0
9	6-methyl-4,4'-bis(trifluoromethyl)-2,2'-bipyridine (**L14**)	100	21: 3: 1
10	4,4'-dimethoxy-6-methyl-2,2'-bipyridine (**L15**)	100	4: 0: 0
11	5,5'-dimethyl-2,2'-bipyridine (**L16**)	95	32: 4: 0
12	2-methyl-4,7-diphenyl-1,10-phenanthroline (**L17**)	100	23: 3: 4
13	2,4,7-trimethyl-1,10-phenanthroline (**L18**)	100	26: 3: 0

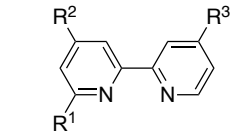

R^1 = Me; R^2, R^3 = H, **L6**
R^1 = *n*-Bu; R^2, R^3 = H, **L7**
R^1 = *n*-Hex; R^2, R^3 = H, **L8**
R^1 = *i*-Pr; R^2, R^3 = H,**L9**
R^1 = CF_3; R^2, R^3 = H, **L10**
R^1 = Me; R^2 = CF_3; R^3 = H, **L11**
R^1 = Me; R^2, R^3 = Ph, **L12**
R^1 = Me; R^2, R^3 = Me, **L13**
R^1 = Me; R^2, R^3 = CF_3,**L14**
R^1 = Me; R^2, R^3 = OMe, **L15**

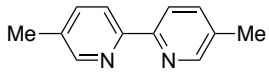

L16

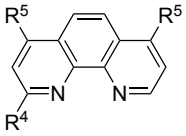

R^4 = Me; R^5 = Ph, **L17**
R^4, R^5 = Me, **L18**

Reaction conditions: 3.24ah (0.50 mmol), **3.28a** (0.75 mmol), $NiBr_2$·diglyme (2.5 mol%), ligand (5.0 mol%), Mn (1.25 mmol), DMF (0.5 mL) at 10 °C, 16 h. [a] GC-FID conversion and yield using *n*-decane as internal standard. Commercially available and used **3.24ah** contained ca. 5% of 2-bromoheptane. Mass balance accounts for heptenes, formamide, urea and oxalamide.

Table 3.1. Screening of nitrogen-containing ligands

The GC-FID and GC-MS analysis of the crude reaction mixtures provided useful insights into the mass balance of the reaction (Scheme 3.14). In all cases, non-negligible amounts of heptene isomers were observed along with smaller amounts of homodimers. As shown in Chapter 2, 1,3-di-*tert*-butylurea arising from the decomposition of *tert*-butyl isocyanate during the reaction or the reaction work-up was observed. Additionally, other side-products derived from the isocyanate such as, N^1,N^2-di-*tert*-butyloxalamide and *N*-*tert*-butylformamide, could be detected. The formation of oxalamides has been reported to be catalyzed by Ni(0) complexes via the oxidative coupling of the corresponding isocyanate,[57] whereas the formamide very likely arises from the reduction of the isocyanate by Ni—H species, which are formed via β-hydride elimination from the starting alkyl halide.

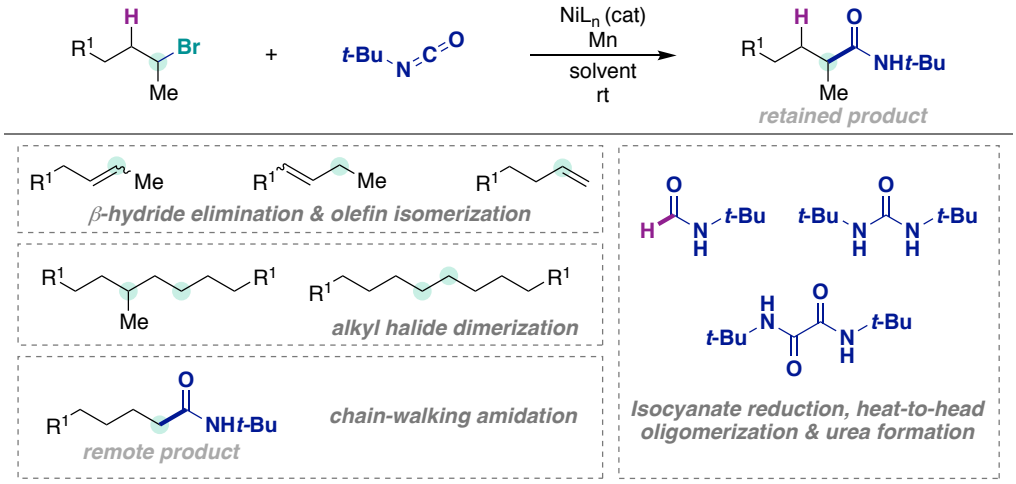

Scheme 3.14. Possible side-products formed during the reaction

Second, different nickel sources were evaluated using 6-*n*-hexyl-2,2'-bipyridine (**L8**) as the ligand (Table 3.2). Once again, readily available $NiBr_2$ provided the best results in terms of yield, whereas most of the other tested nickel sources failed to reach full conversion even after 24 h, and afforded lower amounts of the **3.29o**. Paralleling the results from Chapter 2 and 4, nickel bromide salts afforded superior results compared to those with a chloride counterion. This might indicate the need for a more polarizable and labile ligand that could favor the formation of transient cationic nickel species during the reaction. Additionally, the lower reduction potential of $NiBr_2$ compared to $NiCl_2$ could facilitate the formation of the initial catalytically active species.[58,59] In contrast to the results obtained in Chapter 2, the use of $Ni(COD)_2$ resulted in comparable yields to those obtained with $NiBr_2$ (entries 4 and 7). This observation might suggest differences between the amidation mechanism of primary alkyl bromides and secondary alkyl bromides.

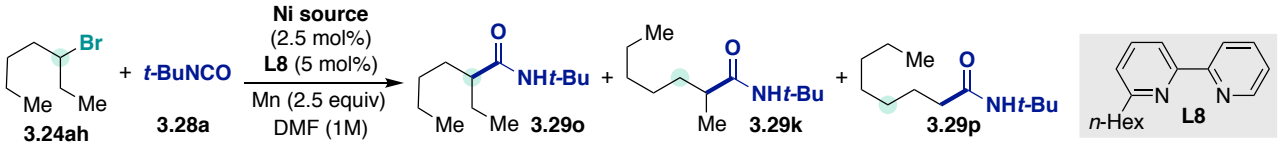

Entry	Ni source	Conversion of 3.24ah (%)[a]	Yield of 3.29o: 3.29k: 3.29p (%)[a]
1	NiI_2	100	69: 6: 0
2	$NiBr_2$·diglyme	71 (92)	51: 5: 0 (68: 6: 0)
3	$NiBr_2$·diglyme[b]	77	58: 5: 0
4	$NiBr_2$·glyme	55 (70)	42: 4: 0 (52: 5: 0)
5	$NiBr_2$	100	73: 6: 0
6	$NiCl_2$·diglyme	43 (60)	50: 5: 0 (47: 7: 0)
7	$Ni(COD)_2$	(100)	(75: 6: 0)
8	[(TMEDA)Ni(*o*-tolyl)Cl]	74	57: 5: 0

Reaction conditions: 3.24ah (0.50 mmol), **3.28a** (0.75 mmol), Ni source (2.5 mol%), **L8** (5.0 mol%), Mn (1.25 mmol), DMF (0.5 mL) at 10 °C, 16 h. [a] GC-FID conversion and yield using *n*-decane as internal standard. [b] DMF (1 mL). Yields in parenthesis correspond to 24 h reaction. Commercially available and used **3.24ah** contained ca. 5% of 2-bromoheptane. Mass balance accounts for heptenes, formamide, urea and oxalamide.

Table 3.2. Screening of nickel sources

Next, the reaction was carried out at different temperatures to verify its influence on the reaction yields (Table 3.3, entries 1 to 3). Indeed, higher yields were obtained at 10 and 3 °C, with a significant decrease in the formation

of urea, oxalamide and formamide side-products observed at 3 °C. This has an additional advantage, as difficulties were encountered in the separation of the desired product by column chromatography from oxalamide and urea during the study of the scope for the transformation. Additionally, no variation in the reaction outcome was observed when the reaction was performed in different amide-type solvents (Table 3.3, entries 4 to 6).

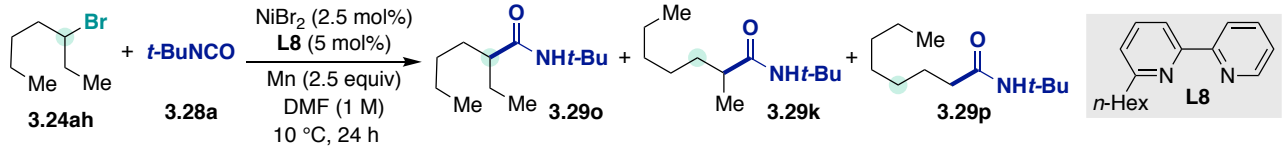

Entry	Deviation from Standard Conditions	Conversion of 3.24ah (%)[a]	Yield of 3.29o: 3.29k: 3.29p (%)[a]
1	none	100	72: 6: 0
2	25 °C	100	56: 5: 0
3	3 °C	100[b]	80: 6: 0
4	DMA; 3 equiv *t*-BuNCO	100	75: 6: 0
5	NMP; 3 equiv *t*-BuNCO	100	74: 6: 0
6	DMF; 3 equiv *t*-BuNCO	100	75: 6: 0

Reaction conditions: 3.24ah (0.50 mmol), **3.28a** (0.75 mmol), $NiBr_2$ (2.5 mol%), **L38** (5.0 mol%), Mn (1.25 mmol), DMF (0.5 mL) at 10 °C, 24 h. [a] GC-FID conversion and yield using *n*-decane as internal standard. [b] Lower amounts of oxalamide and formamide obtained. Commercially available and used **3.24ah** contained ca. 5% of 2-bromoheptane. Mass balance accounts for heptenes, formamide, urea and oxalamide.

Table 3.3. Screening of temperatures and solvents

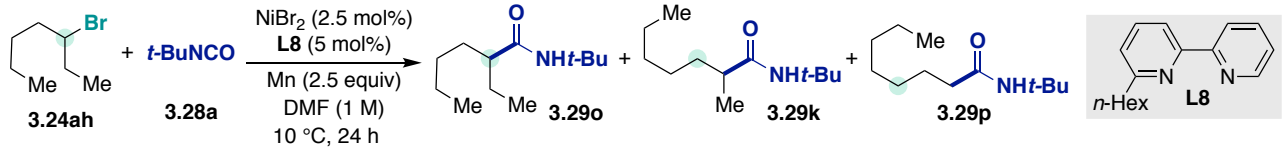

Entry	Deviation from Standard Conditions	Conversion of 3.24ah (%)[a]	Yield of 3.29o: 3.29k: 3.29p (%)[a]
1	none	100	76: 7: 0
2	3.0 equiv *t*-BuNCO	100	78: 7: 0
3	3.0 equiv *t*-BuNCO; 2.0 equiv Mn	100	80: 7: 0
4	3.0 equiv *t*-BuNCO; 2.0 equiv Mn; 1.0 mL DMF	100	78: 7: 0
5	Ni:**L8** 1:1.5	100	73: 6: 0
6	Ni:**L8** 1:2.5	100	77: 7: 0
7	1.0 equiv of Mn	89	60: 6: 0
8	3.0 equiv of Mn	100	76: 7: 0
9	Zn instead of Mn[b]	100	47: 9: 0
10	2-chloroheptane; 1.0 equiv TBAC[c]	38	0: 10: 0
11	2-chloroheptane; 1.0 equiv TBAB[c]	21	0: 1: 0
12	3 °C[d]	100	80: 6: 0

Reaction conditions: 3.24ah (0.50 mmol), **3.28a** (0.75 mmol), $NiBr_2$ (2.5 mol%), **L8** (5.0 mol%), Mn (0.75 mmol), DMF (0.5 mL) at 10 °C, 24 h. [a] GC-FID conversion and yield using *n*-decane as internal standard. [b] Zn (2 equiv). [c] $NiBr_2$·glyme (10 mol%), **L6** (20 mol%), Mn (1.0 mmol), at 40 °C, 48 h. [d] Lower amounts of oxalamide and formamide obtained. Commercially available and used **3.24ah** contained ca. 5% of 2-bromoheptane. Mass balance accounts for heptenes, formamide, urea and oxalamide.

Table 3.4. Fine-tuning of the reaction conditions

Varying the amount of isocyanate, the Ni:**L8** ratio or amount of Mn added to the reaction did not lead to a significant improvement in the yield of the **3.29o** (Table 3.4, entries 1 to 9). Contrary to the results obtained for primary alkyl bromides (vide Chapter 2), the reaction could be conducted using Zn as the reducing agent (entry

9). Unfortunately, the use of other alkyl halides such as 2-chloroheptane led to no product formation, even in the presence of additives known to enhance reactivity in cross-electrophile coupling reactions (entries 10 and 11).[54] Finally, as smaller amounts of oxalamide were formed, a lower reaction temperature was preferred for studying the scope of the transformation (entry 12).

3.3.3. Preparative Substrate Scope

3.3.3.1. Scope of Unactivated Secondary Alkyl Bromides

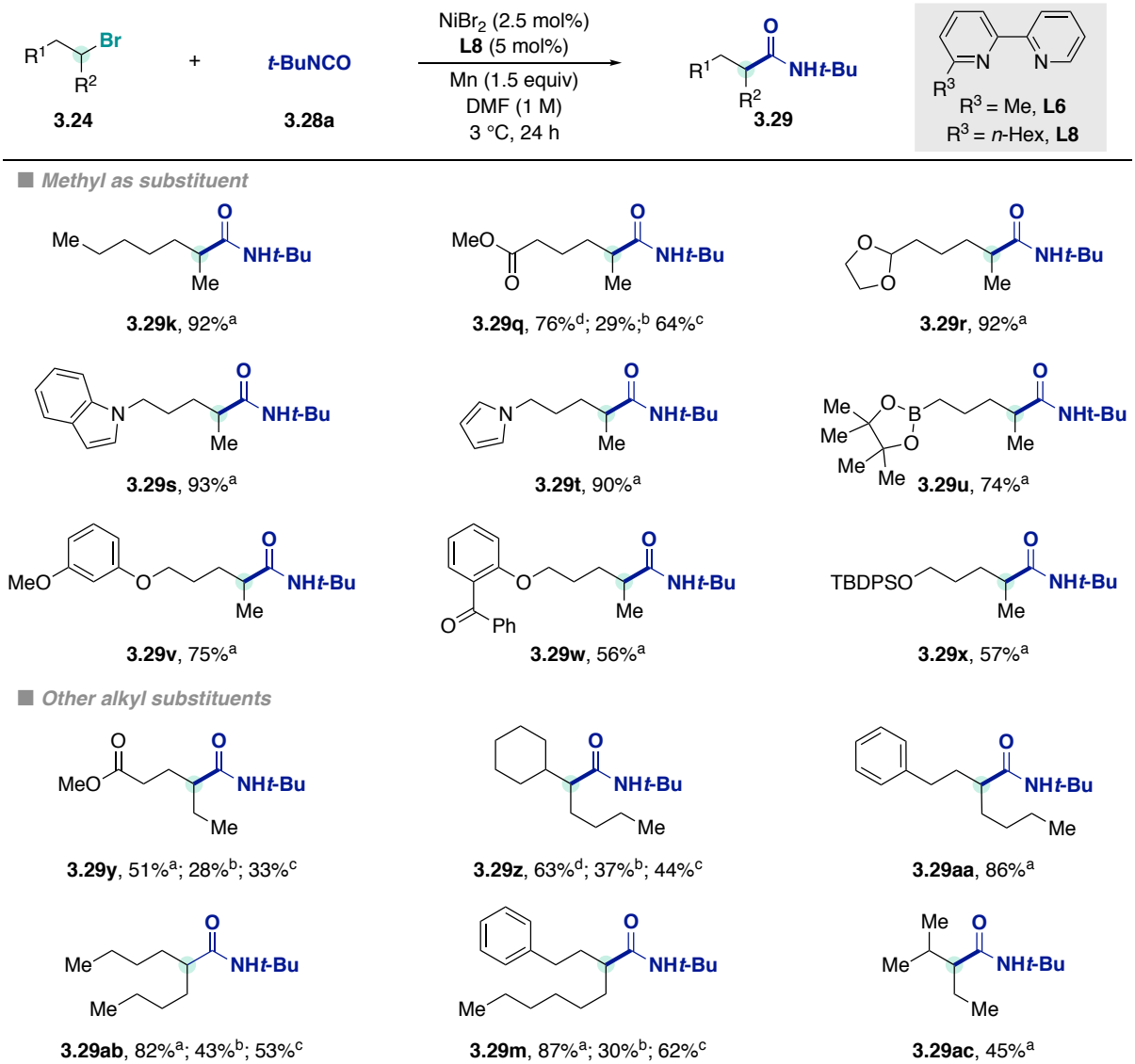

Reaction conditions: [a] **3.24** (0.50 mmol), **3.28a** (0.75 mmol), $NiBr_2$ (2.5 mol%), **L8** (5.0 mol%), Mn (0.75 mmol), DMF (0.5 mL) at 3 °C, 24 h. [b] **3.24** (0.50 mmol), **3.28a** (1.5 mmol), $NiBr_2$ (3 mol%), **L5** (4.5 mol%), Mn (1.0 mmol), DMF (1 mL) at 25 °C, 16 h, as in Chapter 2. [c] As a but using **L5** (5 mol%) instead. [d] As a but using **3.28a** (1.5 mmol) and Mn (1.0 mmol) instead. Isolated yields.

Scheme 3.15. Scope of secondary alkyl bromides with *tert*-butyl isocyanate

The scope of the retentive amidation of unactivated secondary alkyl bromides was performed using *tert*-butyl isocyanate as the coupling partner (Scheme 3.15). The main advantages associated with the use of this isocyanate are the possible deprotection of the *tert*-butyl group using Brønsted[60] or Lewis acids,[61,62] and the decreased

formation of side-products, such as urea and isocyanurates.[63] In order to validate the improvement in the reaction scope achieved by the use of the newly optimized conditions (*conditions a*), a comparison was made between these and the previously developed protocol for primary alkyl bromides (*conditions b*), as well as with the use of 6-methyl-2,2'-bipyridine (**L6**) instead of 6-*n*-hexyl-2,2'-bipyridine (**L8**) at 3 °C (*conditions c*). Importantly, higher and more reliable yields were obtained, even under *conditions b*, by carefully controlling the reaction temperature.

From the results shown in Scheme 3.15, it can be concluded that the new reaction conditions enable the coupling of different secondary alkyl bromides with **3.28a** in high yields and with excellent regioselectivity, without the formation of chain-walking amidation products. Moreover, the system is not limited to the use of methyl-substituted secondary alkyl bromides, and can tolerate internal secondary bromides bearing different substitution patterns and chain-lengths. A general trend is illustrated by products **3.29q**, **3.29y**, **3.29z**, **3.29ab** and **3.29m**, which shows that the improved conditions (*conditions a*) give reliable access to secondary amides in synthetically useful yields, compared to the poor results obtained when the previous protocol is used (*conditions b*). The higher yields obtained with ligand **L8** instead of ligand **L6** (*conditions a* vs. *conditions c*), further indicate that the outcome of the reaction is dependent on both the ligand and the reaction temperature. Indirectly, this observation indicates that these variables have an influence on the β-hydride elimination from the transient alkyl—Ni species generated throughout the course of the reaction.

Unfortunately, not all of the tested substrates successfully afforded the targeted amides (Scheme 3.16). For example, alkyl bromides bearing coordinating groups such as nitriles (**3.24f**) or olefins (**3.24aj**), afforded mixtures of several amide products. Other substrates prone to β-hydride elimination such as **3.24ai** and **3.24k** were also not tolerated. Finally, the use of highly sterically hindered substrates only afforded low yields of the corresponding amide (**3.29ad**).

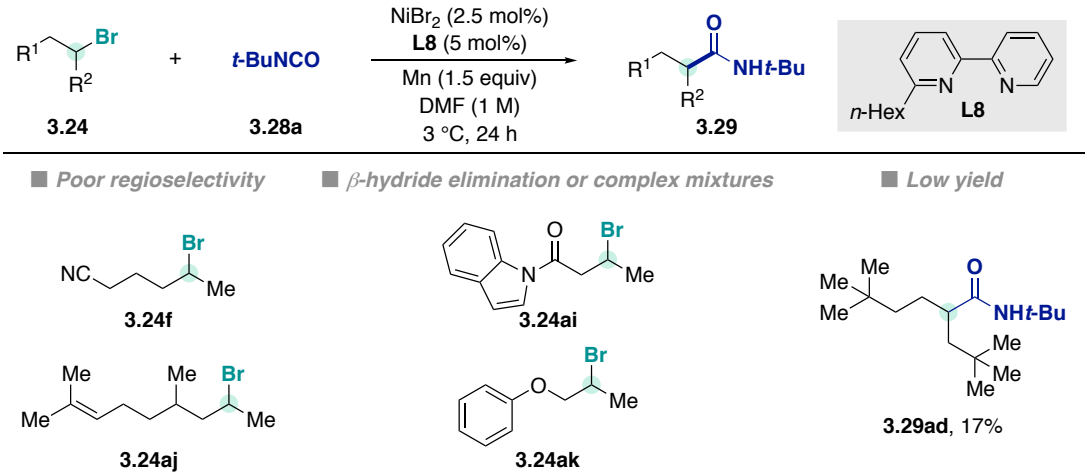

Reaction conditions: **3.24** (0.50 mmol), **3.28a** (0.75 mmol), $NiBr_2$ (2.5 mol%), **L8** (5.0 mol%), Mn (0.75 mmol), DMF (0.5 mL) at 3 °C, 24 h. Isolated yield.

Scheme 3.16. Unsuccessful substrates for the amidation of secondary alkyl bromides with *tert*-butyl isocyanate

3.3.3.1. Scope of Aryl and Alkyl Isocyanates

A preliminary investigation of the scope for the isocyanate coupling partner was performed using 2-bromoheptane and 3-bromoheptane (Scheme 3.17). Unfortunately, difficulties during the isolation of amides **3.29ae** and **3.29af** were encountered as the reaction crudes contained significant amounts of isocyanate side-products. In line with the scope of isocyanates for the amidation of primary alkyl bromides (Chapter 2), a detailed

re-optimization of the reaction conditions is expected to improve the yields of the desired amides with isocyanates other than *tert*-butyl isocyanate. In particular, the study of the ligand, nickel source, isocyanate equivalents, and even the slow addition of the isocyanates at low temperatures will likely be crucial to achieving high yields.

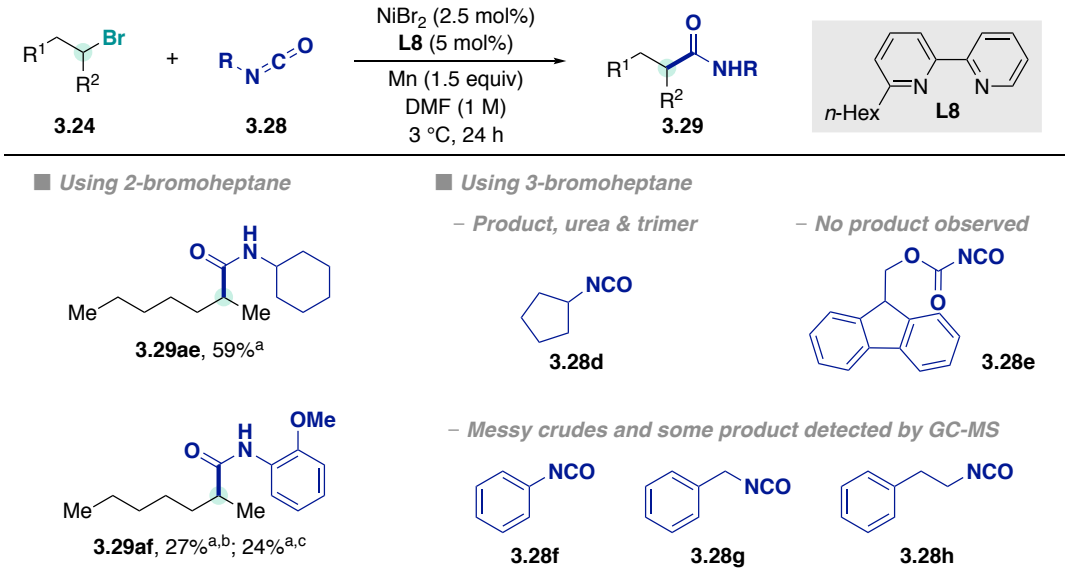

Reaction conditions: **3.24** (0.5 mmol), **3.28** (0.75 mmol), $NiBr_2$ (2.5 mol%), **L8** (5.0 mol%), Mn (0.75 mmol), DMF (0.5 mL) at 3 °C, 24 h. Isolated yields. [a] Isolated along with unknown impurities. [b] Using **3.28c** (0.5 mmol). [c] Using **3.28c** (1 mmol).

Scheme 3.17. Preliminary evaluation of the isocyanate scope

3.4. Remote Amidation of Acyclic Secondary Alkyl Bromides via Ni-Chain-Walking

The Ni-catalyzed chain-walking carboxylation of unactivated secondary alkyl bromides,[50] recently developed by our group, encouraged us to pursue an analogous remote amidation reaction using isocyanates. At first sight, one might expect that given the related transformations that have been successfully developed using either CO_2 or isocyanates, extending the chain-walking protocol to the latter should be straightforward. However, several properties of isocyanates differ significantly from those of CO_2 and challenge the development of a remote amidation. For example, the markedly increased reactivity of isocyanates, their stronger binding to transition metals, and their higher solubility in organic solvents facilitate the functionalization at the initial reaction site and could eventually hamper the steps required for the remote amidation. In contrast, the inertness and low solubility of CO_2 indirectly facilitate the displacement of the Ni catalyst along the alkyl chain towards the terminal position. Carboxylation at the distal, primary sp^3 C—H position is therefore favored over functionalization of the internal positions. Up to now the carboxylation of secondary alkyl halides with CO_2 has only been achieved for cyclic scaffolds at high reaction temperatures.[54] For these reasons, we anticipated that the development of a related chain-walking amidation would be a particularly challenging task. The following tables show a representative set of the conditions that have been tested in order to identify optimal reaction conditions for triggering the remote amidation of unactivated secondary alkyl halides with isocyanates.

The optimization of the remote amidation started with the screening of different nitrogen-containing ligands (Table 3.5 and Table 3.6). With the aim of facilitating comparison of the results, a similar model system to the one used for the retentive amidation was employed (vide supra). As expected from the knowledge acquired during the optimization of the retentive amidation, *ortho*-monosubstituted ligands afforded the secondary amide **3.29k** exclusively (Table 3.5, entries 1 to 3). In contrast, the chain-walking process was facilitated by the use of *ortho*-

disubstituted ligands (entries 4 to 12). This is in agreement with the reported chain-walking transformations using *ortho*-disustituted bipyridine and phenanthroline-type ligands (vide supra). Even though **L1** has been successfully used in Ni-catalyzed remote functionalizations, mixtures of both primary and secondary amides were obtained in our case (entry 4).[31,32] Increasing the steric hindrance of the *ortho*-substituent from methyl to *n*-butyl (entry 5) had a positive effect on regioselectivity but little influence on the overall yield, whereas the use of an isopropyl substituent exerted a negative influence on both parameters (entry 6). The use of a more π-acidic ligand having phenyl substituents at the 4,4'-positions (**L23**) afforded high selectivity towards the primary amide and a promising overall yield (entry 7). This improvement might be explained by a more effective β-hydride elimination due to an increase in the electrophilicity of the Ni-center, and by a better binding of the *in situ* generated alkene via σ-donation to the Ni. However, using this ligand backbone, changes in the length or steric bulk of the alkyl *o*-substituent led to no improvement (entries 8 and 9). Interestingly, the presence of electron-donating or electron-withdrawing substituents on the phenyl ring, which influence the σ-donating and π-accepting ability of the ligand, had no beneficial effect on the regioselectivity or yield of the primary amide.

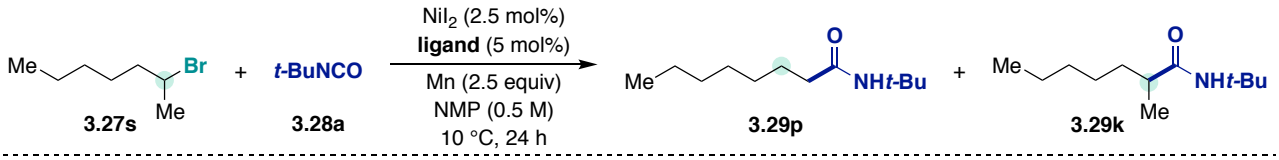

Entry	Ligand	Conversion of 3.27s (%)[a]	Yield of 3.29p: 3.29k (%)[a]
1	4,4',6-trimethyl-2,2'-bipyridine (**L19**)	97	0: 15
2	6-methyl-4,4'-diphenyl-2,2'-bipyridine (**L12**)	91	0: 65
3	4,4'-di-*tert*-butyl-6-methyl-2,2'-bipyridine (**L20**)	99	0: 22
4	6,6'-methyl-2,2'-bipyridine (**L1**)	100	38: 11
5	6,6'-di-*n*-butyl-2,2'-bipyridine (**L21**)	100	53: 6
6	6,6'-diisopropyl-2,2'-bipyridine (**L22**)	100	14: 4
7	6,6'-dimethyl-4,4'-diphenyl-2,2'-bipyridine (**L23**)	100	69: 3 (72)[b]
8	6,6'-diethyl-4,4'-diphenyl-2,2'-bipyridine (**L24**)	50	3: 3
9	6,6'-diisopropyl-4,4'-diphenyl-2,2'-bipyridine (**L25**)	70	53: 3
10	6,6'-dimethyl-4,4'-bis(4-methoxyphenyl)-2,2'-bipyridine (**L26**)	100	61: 12
11	4,4'-bis(4-fluorophenyl)-6,6'-dimethyl-2,2'-bipyridine (**L27**)	100	61: 2
12	6,6'-dimethyl-4,4'-bis(4-(trifluoromethyl)phenyl)-2,2'-bipyridine (**L28**)	74	4: 5

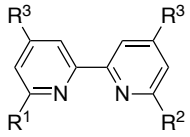

R^1, R^3 = Me; R^2 = H, **L19**
R^1 = Me; R^2 = H; R^3 = Ph, **L12**
R^1 = Me; R^2 = H; R^3 = *t*-Bu, **L20**
R^1, R^2 = Me; R^3 = H, **L1**
R^1, R^2 = *n*-Bu; R^3 = H, **L21**
R^1, R^2 = *i*-Pr; R^3 = H, **L22**
R^1, R^2 = Me; R^3 = Ph, **L23**
R^1, R^2 = Et; R^3 = Ph, **L24**
R^1, R^2 = *i*-Pr; R^3 = Ph, **L25**
R^1, R^2 = Me; R^3 = *p*-OMePh, **L26**
R^1, R^2 = Me; R^3 = *p*-FPh, **L27**
R^1, R^2 = Me; R^3 = *p*-CF_3Ph, **L28**

Reaction conditions: 3.27s (0.50 mmol), **3.28a**(0.75 mmol), NiI_2 (2.5 mol%), ligand (5.0 mol%), Mn (1.25 mmol), NMP (0.5 mL) at 10 °C, 24 h. [a] GC-FID conversion and yield using anisole as internal standard. [b] Isolated yield. Mass balance accounts for heptenes, formamide, urea and oxalamide.

Table 3.5. Screening of bipyridine-type ligands

Prompted by the optimal results observed using phenanthroline-type ligands in the remote carboxylation of unactivated alkyl halides, a set of this class of ligands was evaluated (Table 3.6, entries 1 to 5). Similar to the results obtained with bipyridine-type ligands, the use of *ortho*-monosubstituted phenanthrolines afforded the retained

amide, albeit in low yields (entry 1). In general, higher regioselectivities but lower yields were systematically obtained when using other phenanthroline ligands (entries 2 to 5). Unfortunately, poor results were observed with **L5**, which was the optimal ligand for the remote carboxylation (entry 5).[50] The use of terpyridine was also unsuccessful, with small amounts of the amide products detected in the crude reaction mixtures (entry 6). The poor reactivity observed with this tridentate ligand could be explained by the lack of a vacant coordination site on the alkyl—Ni species, which would be required for the β-hydride elimination step. Other types of ligands, including some that had previously been used in chain-walking transformations, such as PyOx ligands[33,64,65] and α-diimines,[41] led to unsatisfactory outcomes, as well (entries 7 to 11). In view of these results, further screening was continued with 6,6'-dimethyl-4,4'-diphenyl-2,2'-bipyridine (**L23**).

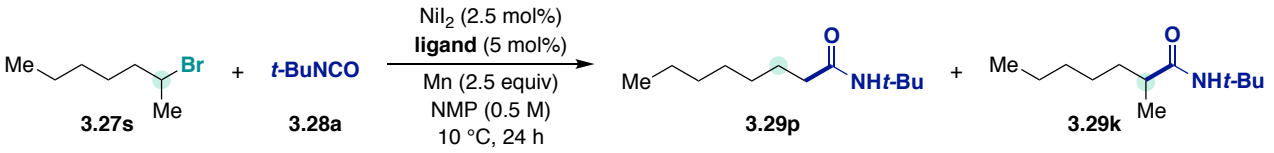

Entry	Ligand	Conversion of 3.27s (%)[a]	Yield of 3.29p: 3.29k (%)[a]
1	2,3,4,7,8-pentamethyl-1,10-phenanthroline (**L29**)	93	0 : 15
2	neocuproine (**L30**)	100	29: 0
3	2,9-diethyl-1,10-phenanthroline (**L31**)	94	33: 3
4	bathocuproine (**L4**)	100	32: 3
5	2,9-dihexyl-4,7-diphenyl-1,10-phenanthroline (**L5**)	56	0: 3
6	4',6,6''-trimethyl-2,2':6',2''-terpyridine (**L32**)	100	1: 3
7	4-isopropyl-2-(6-methylpyridin-2-yl)-4,5-dihydrooxazole (**L33**)	53	1: 3
8	2,6-Bis-[1-(2,6-diisopropylphenylimino)ethyl]pyridine (*i*-PrPDI) (**L34**)	35	0: 3
9	2,3-Bis(2,6-diisopropylphenylimino)butane (*i*-PrDI) (**L35**)	90	2: 3

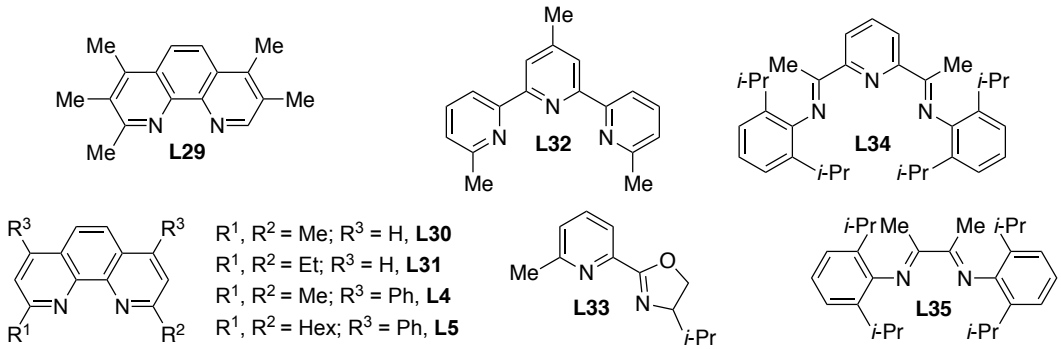

Reaction conditions: 3.27s (0.50 mmol), **3.28s** (0.75 mmol), NiI_2 (2.5 mol%), ligand (5.0 mol%), Mn (1.25 mmol), NMP (0.5 mL) at 10 °C, 24 h. [a] GC-FID conversion and yield using anisole as internal standard. Mass balance accounts for heptenes, formamide, urea and oxalamide.

Table 3.6. Screening of other amine-containing ligands

Table 3.7 shows that the use of different nickel sources had a strong influence in the reaction outcome. Lower yields, and in some cases lower regioselectivities were found when using nickel halide salts other than NiI_2. The superior results obtained with iodide counterions could be tentatively explained by the lower reduction potential of these salts compared to other halides.[58,59] The larger volume and higher lability of iodide could also contribute to the formation of cationic nickel species, especially when using sterically hindered ligands. The poor solubility

of ligand **L23** combined with that of $NiBr_2$ probably explains the limited conversion observed with this nickel source. This contrasts the good results obtained for the retained amidation with 6-*n*-hexyl-2,2'-bipyrdine (**L8**). Switching to other Ni(II) sources such as $(TBA)_2[NiBr_2]$ or $Ni(acac)_2$ had a deleterious impact on the reaction outcome (entries 5 and 7). Unlike the retained amidation, the use of $Ni(COD)_2$ led to low conversion to the desired product (entry 8). This observation could be explained by the presence of the COD ligand occupying the vacant coordination site that is required for the β-hydride elimination step, or potentially displacing the transient alkene formed *in situ*. As expected, the use of precatalyst $NiBr_2$(**L23**), in the presence of additional ligand, affords comparable results to the use of soluble $NiBr_2$ sources (entries 10 vs. 2 and 3). Unfortunately, also no improvement was observed when using the NiI_2(**L23**) precatalyst (entries 11 and 12 vs. 1).

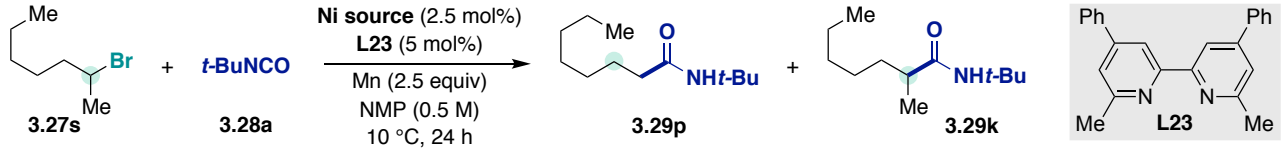

Entry	Ni source	Conversion of 3.27s (%)[a]	Yield of 3.29p: 3.29k (%)[a]
1	NiI_2	100	69: 3
2	$NiBr_2$·diglyme	85	41: 12
3	$NiBr_2$·glyme	100	45: 3
4	$NiBr_2$	6	1: 0
5	$(TBA)_2[NiBr_2]$	15	1: 2
6	$NiCl_2$·glyme	100	16: 3
7	$Ni(acac)_2$	4	0: 1
8	$Ni(COD)_2$	24	2: 3
9	$NiBr_2$(**L23**)	100	8: 3
10	$NiBr_2$(**L23**) and **L23** (2.5 mol%)	97	43: 2
11	NiI_2(**L23**)	100	14: 1
12	NiI_2(**L23**) and **L23** (2.5 mol%)	100	51: 1

Reaction conditions: 3.27s (0.50 mmol), **3.28a** (0.75 mmol), NiI_2(2.5 mol%), **L23** (5.0 mol%), Mn (1.25 mmol), NMP (0.5 mL) at 10 °C, 24 h. [a] GC-FID conversion and yield using anisole as internal standard. [b] DMF (1 mL). Yields in parenthesis correspond to 24 h reaction. Mass balance accounts for heptenes, formamide, urea and oxalamide.

Table 3.7. Screening of nickel sources

Finally, the effect of different additives and variations to the reaction conditions was evaluated (Table 3.8). The reaction was carried out at lower temperatures with the aim of disfavoring the formation of undesired products from the isocyanate that are difficult to separate from the desired amides; however, incomplete conversion and a slightly lower selectivity was observed at 3 °C (entry 2). This result can be explained by a slower β-hydride elimination that results in higher amounts of retained product. Despite the positive effect of ammonium salts in Pd-catalyzed chain-walking transformations,[66,67] their use as additives did not lead to better results (entries 3 to 5). Likewise, the use of iodide-containing additives such as NaI resulted in disappointing yields (entry 6), and the addition of larger amounts of **3.28a** had no strong effect on the overall amidation yield (entry 7).

As will be explained in detail in Chapter 4, Ni—H species can be formed from light alkyl bromides and π-acceptor ligands.[68] As the mass balance of the starting material accounts for the formation of alkenes, and because formamide was detected in the crude reaction mixtures, we hypothesized that the addition of a sacrificial hydride source might ensure that those alkenes re-enter the catalytic cycle via the migratory insertion of Ni—H species across the C=C bond. Although this strategy has improved the efficiency of other Ni-catalyzed chain-walking transformations, it had no positive effect in our case (entries 8 to 10).[32] Lastly, with the hypothesis that more

reactive alkyl iodides could afford cationic nickel species that would result in a more efficient chain-walking amidation, the reaction was performed using 2-iodoheptane. Nevertheless, lower yields of primary amide **3.29p** were obtained, along with large amounts of heptene isomers (entry 11).

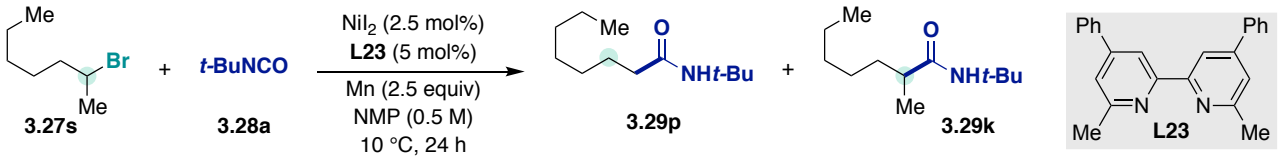

Entry	Deviation from Standard Conditions	Conversion of 3.27s (%)[a]	Yield of 3.29p: 3.29k (%)[a]
1	None	100	69: 3
2	3 °C instead of 10 °C	92	62: 6
3	TBAC (1 equiv)	96	8: 3
4	TBAB (1 equiv)	86	34: 2
5	TBAI (1 equiv)	82	47: 2
6	NaI (1 equiv)	94	12: 3
7	2 equiv *t*-BuNCO instead of 1.5 equiv	100	66: 2
8	*i*-PrBr (0.5 equiv)	100	64: 3
9	*n*-PrBr (0.5 equiv)	100	58: 2
10	*t*-BuBr (0.5 equiv)	91	43: 6
11	2-iodoheptane instead of **3.27s**	100	15: 3

Reaction conditions: 3.27s (0.50 mmol), **3.28a** (0.75 mmol), NiI_2 (2.5 mol%), **L23** (5.0 mol%), Mn (1.25 mmol), NMP (0.5 mL) at 10 °C, 24 h. [a] GC-FID conversion and yield using anisole as internal standard. [b] DMF (1 mL). Yields in parenthesis correspond to 24 h reaction. Mass balance accounts for heptenes, formamide, urea and oxalamide.

Table 3.8. Screening of additives and other parameters

The generality of the current optimized conditions was tested with a small set of unactivated secondary alkyl bromides. Unfortunately, starting from functionalized 2-bromoalkanes, low to moderate yields of the desired primary amides were obtained (Scheme 3.18). From these results it is possible to predict that a lower efficiency will likely be observed when starting from more internal alkyl halides. With the aim of establishing a more robust catalytic protocol that will enable the chain-walking amidation reaction with a variety of substrates, an in-depth optimization of the reaction conditions is currently being performed by other members of the Martin group.

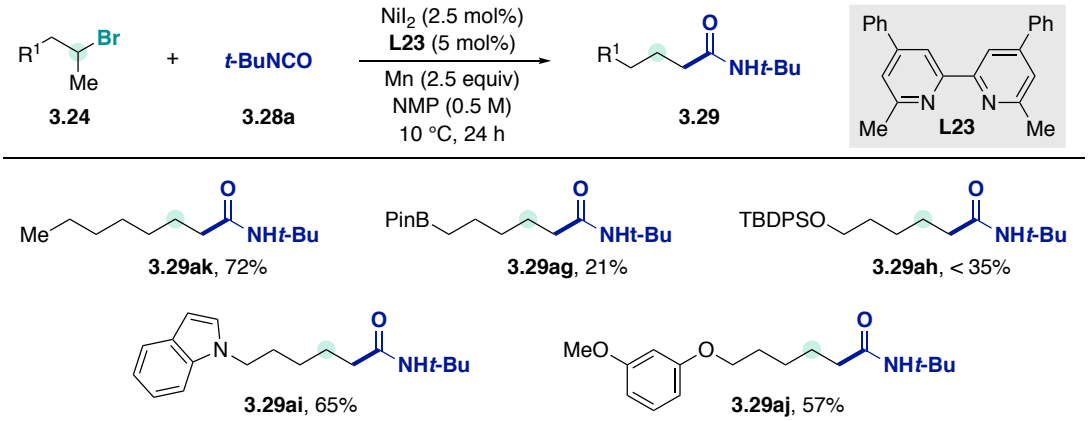

Reaction conditions: 3.24 (0.5 mmol), **3.28a** (0.75 mmol), NiI_2 (2.5 mol%), **L23** (5.0 mol%), Mn (1.25 mmol), NMP (0.25 mL) at 10 °C, 24 h. Isolated yields.

Scheme 3.18. Scope of the chain-walking amidation of secondary alkyl bromides with *tert*-butyl isocyanate

3.5. Proposed Mechanism for the Retained and Remote Amidation of Secondary Alkyl Bromides

Scheme 3.19 shows a mechanistic hypothesis for the retained and remote amidation of secondary alkyl bromides. The retained amidation is proposed to follow a similar pathway as the one described in Chapter 2 for the amidation of primary alkyl bromides. Specifically, it is proposed that the reaction proceeds via alkyl—Ni(I) intermediates (**XXII**), which are obtained by reduction of alkyl—Ni(II) species (**XXI**) via SET from Mn or comproportionation with Ni(0). Subsequent isocyanate insertion into the C—Ni(I) bond, and reductive transmetallation with Mn affords Mn-amidate (**XXV**), which ultimately generates the desired amide upon acidic work-up. However, it is possible that the more nucleophilic character of the secondary alkyl—Ni(II) species (**XXI**) allows isocyanate insertion without the intermediacy of alkyl—Ni(I) species, especially when more electrophilic isocyanates are used. Furthermore, the possibility of a direct reaction of the isocyanate with a transient secondary alkyl radical, generated by SET from Ni(0) and escaping from the solvent cage, cannot be excluded.

The avoidance of β-hydride elimination obtained with *ortho*-monosubstituted ligands is proposed to arise from an increased stabilization of alkyl—Ni intermediates. These species could be stabilized by a non-coplanar arrangement of the Ni—C—C—H_β system caused by the presence of a single *ortho*-substituent in the bipyridine ligand that alters the geometry of the complex. Although a square planar geometry is generally preferred in d^8 complexes for electronic reasons, it is possible that the presence of *ortho*-substituents on the ligands imposes a (distorted) tetrahedral geometry. Such a spatial arrangement would result in a less effective agostic interaction in the alkyl—Ni complexes, which could be further disfavored by the use of more sterically hindered ligands, such as those with longer alkyl chains substituents. This hypothesis is consistent with the higher yields obtained with 6-*n*-hexyl (**L8**) vs. 6-methyl substituted bipyridine (**L6**). Moreover, the change in geometry is associated with a stabilization of low-valent Ni species, and is reflected in the decreased Ni(II)/Ni(I) reduction potential due to the lower-lying orbitals of the (distorted) tetrahedral geometry for a d^8 metal[69] (for example $E_{1/2}$ Ni(II)/Ni(I) = −0.922 V vs. Fc-Fc$^+$ for Ni(**L2.39**)$_2$[54] compared to $E_{1/2}$ Ni(II)/Ni(I) = −1.629 V vs. Fc-Fc$^+$ for Ni(phen)$_3$BF$_4$[70]). Amidation at the initial reaction site is therefore favored as a result of the lower reduction potentials of the alkyl—Ni(II) species that in turn generate alkyl—Ni(I) intermediates that are more prone to isocyanate insertion. Additionally, the presence of a single *ortho*-substituent on the ligand could also facilitate isocyanate insertion into secondary alkyl—Ni intermediate for steric reasons but at the same time block the coordination of two or more isocyanate molecules to the Ni, which would result in the formation of isocyanate side-products. Finally, the temperature has a strong influence on the reaction outcome, as β-hydride elimination is slower at lower reaction temperatures (10 vs. 3 °C).

In contrast to the retained amidation, the chain-walking pathway proceeds via a series of β-hydride elimination/migratory insertion steps that move the metal along the hydrocarbon chain until it reaches the primary sp^3 C—H bond. It is speculated that at the terminal position, both the reduction of the alkyl—Ni(II) species (**XXVIII** to **XXXI**) and the subsequent isocyanate insertion into the C—Ni(I) bond are sterically favored, therefore favoring the formation of the primary amide (**XXX**). As observed during the optimization of the reaction conditions, the elementary steps involved in an effective metal-walk are promoted by the presence of π-acceptor ligands. These enhance the electrophilicity of nickel by removing electron density from the metal center via a stronger π-backbonding interaction with the low-lying π*-orbitals of the ligand. The increased electrophilicity facilitates β-hydride elimination, as it leads to a stronger agostic interaction via an increased σ-donation of the C—H_β bond to the vacant *d*-orbitals of the Ni center. Similarly, coordination between the metal and the transient olefin is stronger due to an improved donation into the empty *d*-orbitals of the Ni.

The regioselectivity switch observed with *ortho*-disubstituted bipyridine ligands is proposed to arise from their increased steric hindrance, leading to the preferential formation of cationic Ni species via bromide extrusion. Such intermediates are more electrophilic and have a vacant coordination site that is needed for effecting β-hydride elimination and subsequent coordination of the resulting alkene. However, it is important to note that the rationale behind the proposed mechanisms and the ligand effects on the regioselectivity is a working hypothesis that needs to be corroborated by computational and structural studies of the relevant nickel intermediates.

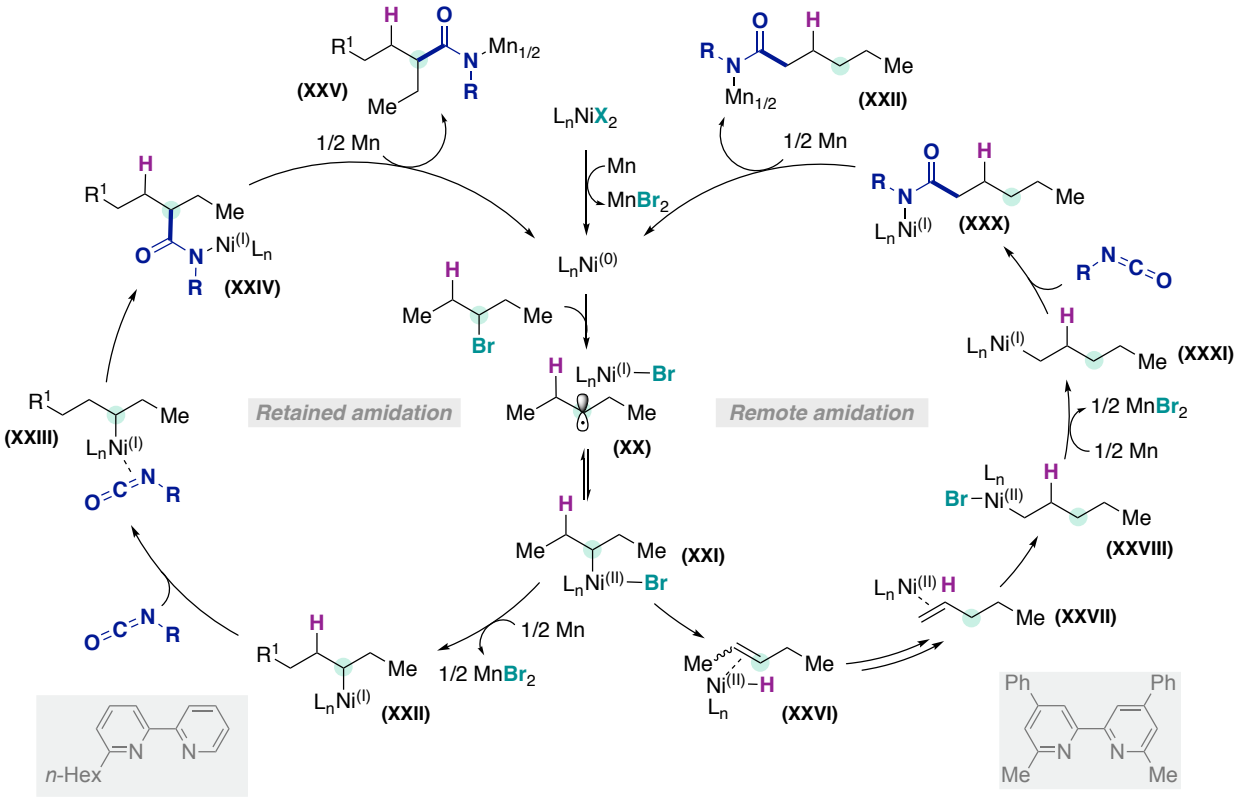

Scheme 3.19. Proposed mechanisms for the Ni-catalyzed retained and remote amidation of secondary alkyl bromides with isocyanates

One of the difficulties with achieving high yields for the remote amidation is the formation of a reactive nickel intermediate at every step of the migration, which could result in the amidation of all the methylenic positions of the chain. Following the mechanism proposed in Scheme 3.19, one could argue that for a successful remote amidation to be developed, it is necessary to find a catalytic system capable of triggering the metal chain-walk at a faster rate than the SET *en route* to the Ni(I) intermediate (**XXII**) that precedes isocyanate insertion. A fast metal-walk would result in an amidation controlled by steric hindrance (kinetic control), in which only the most accessible linear alkyl—Ni intermediate reacts with the isocyanate. Additionally, the detection of olefins in the crude reaction mixtures using the current catalytic system suggests that unproductive dissociative mechanisms are occurring. Preventing olefin de-coordination will thus be a key factor towards developing a more efficient chain-walking amidation. Both the ability to perform the metal-walk and to tightly coordinate the transient alkene can be tuned by changing the electronics of the nickel center. As observed from the ligand screening, the use of π-acceptor ligands effectively increased the regioselectivity of the remote amidation. However, lower yields were obtained when more electron-poor ligands were used, indicating that a fine balance in the electronic properties of the ligand is necessary. The successful use of cationic nickel catalysts in polymerization reactions[23] indicate that the formation of cationic nickel species, which present an enhanced electrophilicity, could result in a more efficient chain-walking process. The formation of these species could be promoted by the addition of halide scavengers

such as $NaBAr_F$ and $NaSbF_6$ to the reaction mixture, or by the use of mixtures of NMP with other coordinating solvents that facilitate halide abstraction.[71–73] Finally, Ni-catalysts with ligands bearing bulky substituents have been shown to prevent olefin exchange processes that often lower the efficiency of the chain-walk in polymerization reactions.[23] A similar beneficial effect was observed in the remote carboxylation of alkyl halides with CO_2 when moving from ethyl to *n*-hexyl substituents.[50] Therefore, the use of bipyridine ligands with long alkyl chains such as *n*-hexyl in the *ortho*-position is worth investigating.

3.6. Conclusions

The efforts towards the development of a regiodivergent amidation of unactivated secondary alkyl bromides with isocyanates as coupling partners are summarized in this Chapter. Initial results on the retained amidation using the catalytic system identified in Chapter 2 only afforded good yields when starting from cyclic secondary alkyl bromides, whereas the use of acyclic substrates mostly led to low and often irreproducible results. A second evaluation of the reaction parameters led to the identification of a new catalytic system that avoided β-hydride elimination from the alkyl—Ni intermediates. Key factors for success were the use of lower reaction temperatures and an *ortho*-monosubstituted bipyridine ligand with a pendant *n*-hexyl chain. With the new conditions, high yields of the desired secondary amides were achieved with a broad scope of acyclic secondary alkyl bromides having different substitution patterns. In line with the results found during this dissertation, the methodology was limited to the use of sterically hindered isocyanates.

In the second section of this Chapter, efforts towards the development of a Ni-catalyzed chain-walking amidation are presented. The screening of different ligands, nickel sources and additives has revealed promising results. Specifically, a change in the regioselectivity of the amidation was achieved with the use of *ortho*-disubstituted ligands. A preliminary survey of the scope of the reaction afforded low to moderate yields, which indicates that a better catalytic system remains to be identified. Further optimization of the reaction conditions is currently ongoing in our laboratories with the aim of identifying a system that promotes a fast and efficient Ni-catalyzed remote amidation of primary sp^3 C—H bonds.

3.7. Bibliography

1. Cárdenas, D. J. Towards Efficient and Wide-Scope Metal-Catalyzed Alkyl-Alkyl Cross-Coupling Reactions. *Angew. Chem. Int. Ed.* **38,** 3018–3020 (1999).
2. Cárdenas, D. J. Advances in Functional-Group-Tolerant Metal-Catalyzed Alkyl-Alkyl Cross-Coupling Reactions. *Angew. Chem. Int. Ed.* **42,** 384–387 (2003).
3. Kambe, N., Iwasaki, T. & Terao, J. Pd-catalyzed cross-coupling reactions of alkyl halides. *Chem. Soc. Rev.* **40,** 4937–4947 (2011).
4. Zhou, J. (Steve) & Fu, G. C. Cross-Couplings of Unactivated Secondary Alkyl Halides: Room-Temperature Nickel-Catalyzed Negishi Reactions of Alkyl Bromides and Iodides. *J. Am. Chem. Soc.* **125,** 14726–14727 (2003).
5. Rudolph, A. & Lautens, M. Secondary alkyl halides in transition-metal-catalyzed cross-coupling reactions. *Angew. Chem. Int. Ed.* **48,** 2656–2670 (2009).
6. Frisch, A. C. & Beller, M. Catalysts for Cross-Coupling Reactions with Non-activated Alkyl Halides. *Angew. Chem. Int. Ed.* **44,** 674–688 (2005).
7. Hu, X. Nickel-catalyzed cross coupling of non-activated alkyl halides: a mechanistic perspective. *Chem. Sci.* **2,** 1867 (2011).
8. Wang, X., Dai, Y. & Gong, H. Nickel-Catalyzed Reductive Couplings. *Top. Curr. Chem.* **374,** 43 (2016).
9. Weix, D. J. Methods and Mechanisms for Cross-Electrophile Coupling of Csp^2 Halides with Alkyl Electrophiles. *Acc. Chem. Res.* **48,** 1767–1775 (2015).
10. Richmond, E. & Moran, J. Recent Advances in Nickel Catalysis Enabled by Stoichiometric Metallic Reducing Agents. *Synthesis* **50,** 499–513 (2018).
11. Duan, Z., Li, W. & Lei, A. Nickel-Catalyzed Reductive Cross-Coupling of Aryl Bromides with Alkyl Bromides: Et_3N as the Terminal Reductant. *Org. Lett.* **18,** 4012–4015 (2016).
12. McCallum, T. & Barriault, L. Direct alkylation of heteroarenes with unactivated bromoalkanes using photoredox gold catalysis. *Chem. Sci.* **7,** 4754–4758 (2016).
13. Zhang, P., Le, C. C. & MacMillan, D. W. C. Silyl Radical Activation of Alkyl Halides in Metallaphotoredox Catalysis: A Unique Pathway for Cross-Electrophile Coupling. *J. Am. Chem. Soc.* **138,** 8084–8087 (2016).
14. Cherney, A. H., Kadunce, N. T. & Reisman, S. E. Enantioselective and Enantiospecific Transition-Metal-Catalyzed Cross-Coupling Reactions of Organometallic Reagents to Construct C-C Bonds. *Chem. Rev.* **115,** 9587–9652 (2015).
15. Cherney, A. H., Kadunce, N. T. & Reisman, S. E. Catalytic Asymmetric Reductive Acyl Cross-Coupling: Synthesis of Enantioenriched Acyclic α,α-Disubstituted Ketones. *J. Am. Chem. Soc.* **135,** 7442–7445 (2013).
16. *Handbook of C–H Transformations*. *Handbook of C–H Transformations* (ed. Dyker, G.) (Wiley-VCH Verlag GmbH & Co. KGaA, 2005). doi:10.1002/9783527619450
17. Xue, X. S., Ji, P., Zhou, B. & Cheng, J. P. The Essential Role of Bond Energetics in C-H Activation/Functionalization. *Chem. Rev.* **117,** 8622–8648 (2017).
18. Li, H., Li, B.-J. & Shi, Z.-J. Challenge and progress: palladium-catalyzed sp^3 C–H activation. *Catal. Sci. Technol.* **1,** 191 (2011).
19. Hartwig, J. F. & Larsen, M. A. Undirected, homogeneous C-H bond functionalization: Challenges and opportunities. *ACS Cent. Sci.* **2,** 281–292 (2016).
20. Vasseur, A., Bruffaerts, J. & Marek, I. Remote Functionalization Through Alkene Isomerization. *Nat. Chem.* **8,** 209–219 (2016).
21. Sommer, H., Juliá-Hernández, F., Martin, R. & Marek, I. Walking Metals for Remote Functionalization. *ACS Cent. Sci.* **4,** 153–165 (2018).
22. Möhring, V. M. & Fink, G. Novel Polymerization of α-Olefins with the Catalyst System Nickel/Aminobis(imino)phosphorane. *Angew. Chem. Int. Ed.* **24,** 1001–1003 (1985).
23. Johnson, L. K., Killian, C. M. & Brookhart, M. New Pd(II)- and Ni(II)-Based Catalysts for Polymerization of Ethylene and α-Olefins. *J. Am. Chem. Soc.* **117,** 6414–6415 (1995).
24. Crabtree, R. H. *The Organometallic Chemistry of the Transition Metals*. (John Wiley & Sons, Inc., 2014).
25. Keim, W. Oligomerization of Ethylene to α-Olefins: Discovery and Development of the Shell Higher Olefin Process (SHOP). *Angew. Chem. Int. Ed.* **52,** 12492–12496 (2013).
26. Bini, L., Müller, C. & Vogt, D. Mechanistic Studies on Hydrocyanation Reactions. *ChemCatChem* **2,** 590–608 (2010).
27. Killian, C. M., Tempel, D. J., Johnson, L. K. & Brookhart, M. Living Polymerization of α-Olefins Using Ni II −α-Diimine Catalysts. Synthesis of New Block Polymers Based on α-Olefins. *J. Am. Chem. Soc.* **118,** 11664–11665 (1996).
28. Lee, W.-C., Wang, C.-H., Lin, Y.-H., Shih, W.-C. & Ong, T.-G. Tandem Isomerization and C-H Activation: Regioselective Hydroheteroarylation of Allylarenes. *Org. Lett.* **15,** 5358–5361 (2013).
29. Lee, W.-C. *et al.* Nickel-catalysed para-CH activation of pyridine with switchable regioselective hydroheteroarylation of allylarenes. *Chem. Commun.* **51,** 17104–17107 (2015).
30. Bair, J. S. *et al.* Linear-Selective Hydroarylation of Unactivated Terminal and Internal Olefins with Trifluoromethyl-Substituted Arenes. *J. Am. Chem. Soc.* **136,** 13098–13101 (2014).
31. He, Y., Cai, Y. & Zhu, S. Mild and Regioselective Benzylic C–H Functionalization: Ni-Catalyzed Reductive Arylation of Remote and Proximal Olefins. *J. Am. Chem. Soc.* **139,** 1061–1064 (2017).
32. Chen, F. *et al.* Remote Migratory Cross-Electrophile Coupling and Olefin Hydroarylation Reactions Enabled by in situ Generation of NiH. *J. Am. Chem. Soc.* **139,** 13929–13935 (2017).
33. Zhou, F., Zhu, J., Zhang, Y. & Zhu, S. NiH-Catalyzed Reductive Relay Hydroalkylation: A Strategy for the Remote C(sp^3)-H Alkylation of Alkenes. *Angew. Chem. Int. Ed.* **130,** 4122–4126 (2018).

34. Lu, X. *et al.* Practical carbon-carbon bond formation from olefins through nickel-catalyzed reductive olefin hydrocarbonation. *Nat. Commun.* **7,** 11129 (2016).
35. Larionov, E., Li, H. & Mazet, C. Well-Defined Transition Metal Hydrides in Catalytic Isomerizations. *Chem. Commun.* **50,** 9816–9826 (2014).
36. Li, H. & Mazet, C. Iridium-Catalyzed Selective Isomerization of Primary Allylic Alcohols. *Acc. Chem. Res.* **49,** 1232–1241 (2016).
37. Romano, C. & Mazet, C. Multicatalytic Stereoselective Synthesis of Highly Substituted Alkenes by Sequential Isomerization/Cross-Coupling Reactions. *J. Am. Chem. Soc.* **140,** 4743–4750 (2018).
38. Buslov, I., Becouse, J., Mazza, S., Montandon-Clerc, M. & Hu, X. Chemoselective Alkene Hydrosilylation Catalyzed by Nickel Pincer Complexes. *Angew. Chem. Int. Ed.* **54,** 14523–14526 (2015).
39. Vechorkin, O., Proust, V. & Hu, X. Functional group tolerant Kumada-Corriu-Tamao coupling of nonactivated alkyl halides with aryl and heteroaryl nucleophiles: Catalysis by a nickel pincer complex permits the coupling of functionalized Grignard reagents. *J. Am. Chem. Soc.* **131,** 9756–9766 (2009).
40. Buslov, I., Song, F. & Hu, X. An Easily Accessed Nickel Nanoparticle Catalyst for Alkene Hydrosilylation with Tertiary Silanes. *Angew. Chem. Int. Ed.* **55,** 12295–12299 (2016).
41. Pappas, I., Treacy, S. & Chirik, P. J. Alkene Hydrosilylation Using Tertiary Silanes with α-Diimine Nickel Catalysts. Redox-Active Ligands Promote a Distinct Mechanistic Pathway from Platinum Catalysts. *ACS Catal.* **6,** 4105–4109 (2016).
42. Dupuy, S., Zhang, K.-F., Goutierre, A.-S. & Baudoin, O. Terminal-Selective Functionalization of Alkyl Chains by Regioconvergent Cross-Coupling. *Angew. Chem. Int. Ed.* **55,** 14793–14797 (2016).
43. Joshi-Pangu, A., Ganesh, M. & Biscoe, M. R. Nickel-Catalyzed Negishi Cross-Coupling Reactions of Secondary Alkylzinc Halides and Aryl Iodides. *Org. Lett.* **13,** 1218–1221 (2011).
44. Peng, L. *et al.* Ligand-Controlled Nickel-Catalyzed Reductive Relay Cross-Coupling of Alkyl Bromides and Aryl Bromides. *ACS Catal.* **8,** 310–313 (2018).
45. Everson, D. A., Shrestha, R. & Weix, D. J. Nickel-Catalyzed Reductive Cross-Coupling of Aryl Halides with Alkyl Halides. *J. Am. Chem. Soc.* **132,** 920–921 (2010).
46. Peng, L., Li, Z. & Yin, G. Photochemical Nickel-Catalyzed Reductive Migratory Cross-Coupling of Alkyl Bromides with Aryl Bromides. *Org. Lett.* **20,** 1880–1883 (2018).
47. Duan, Z., Li, W. & Lei, A. Nickel-Catalyzed Reductive Cross-Coupling of Aryl Bromides with Alkyl Bromides: Et3N as the Terminal Reductant. *Org. Lett.* **18,** 4012–4015 (2016).
48. Biswas, S. & Weix, D. J. Mechanism and Selectivity in Nickel-Catalyzed Cross-Electrophile Coupling of Aryl Halides with Alkyl Halides. *J. Am. Chem. Soc.* **135,** 16192–16197 (2013).
49. Guo, L., Dai, S., Sui, X. & Chen, C. Palladium and Nickel Catalyzed Chain Walking Olefin Polymerization and Copolymerization. *ACS Catal.* **6,** 428–441 (2016).
50. Juliá-Hernández, F., Moragas, T., Cornella, J. & Martin, R. Remote carboxylation of halogenated aliphatic hydrocarbons with carbon dioxide. *Nature* **545,** 84–88 (2017).
51. Gaydou, M., Moragas, T., Juliá-Hernández, F. & Martin, R. Site-Selective Catalytic Carboxylation of Unsaturated Hydrocarbons with CO_2 and Water. *J. Am. Chem. Soc.* **139,** 12161–12164 (2017).
52. Zhao, C., Jia, X., Wang, X. & Gong, H. Ni-Catalyzed Reductive Coupling of Alkyl Acids with Unactivated Tertiary Alkyl and Glycosyl Halides. *J. Am. Chem. Soc.* **136,** 17645–17651 (2014).
53. Wang, X., Wang, S., Xue, W. & Gong, H. Nickel-Catalyzed Reductive Coupling of Aryl Bromides with Tertiary Alkyl Halides. *J. Am. Chem. Soc.* **137,** 11562–11565 (2015).
54. Börjesson, M., Moragas, T. & Martin, R. Ni-Catalyzed Carboxylation of Unactivated Alkyl Chlorides with CO_2. *J. Am. Chem. Soc.* **138,** 7504–7507 (2016).
55. Chen, H., Jia, X., Yu, Y., Qian, Q. & Gong, H. Nickel-Catalyzed Reductive Allylation of Tertiary Alkyl Halides with Allylic Carbonates. *Angew. Chem. Int. Ed.* **56,** 13103–13106 (2017).
56. Lu, X. *et al.* Nickel-Catalyzed Defluorinative Reductive Cross-Coupling of gem-Difluoroalkenes with Unactivated Secondary and Tertiary Alkyl Halides. *J. Am. Chem. Soc.* **139,** 12632–12637 (2017).
57. Hoberg, H., Radine, K. & Milchereit, A. Nickel(0)-induzierte CC-verknüpfung von heterokumulenen: Bildung von oxanilid aus phenylisocyanat. *J. Organomet. Chem.* **280,** C60–C62 (1985).
58. Colon, I. & Kelsey, D. R. Coupling of Aryl Chlorides by Nickel and Reducing Metals. *J. Org. Chem.* **51,** 2627–2637 (1986).
59. Connelly, N. G. & Geiger, W. E. Chemical Redox Agents for Organometallic Chemistry. *Chem. Rev.* **96,** 877–910 (1996).
60. Lacey, R. N. The Acid-Catalysed Heterolysis of Amides with Alkyl- Nitrogen Fission (AAL). *J. Chem. Soc.* **0,** 1633–1639 (1960).
61. Evans, V., Mahon, M. F. & Webster, R. L. A Mild, Copper-Catalysed Amide Deprotection Strategy: Use of tert-butyl as a Protecting Group. *Tetrahedron* **70,** 7593–7597 (2014).
62. Mahalingam, A. K., Wu, X. & Alterman, M. Convenient Removal of N-tert-butyl from Amides with Scandium Triflate. *Tetrahedron Lett.* **47,** 3051–3053 (2006).
63. Schleicher, K. D. & Jamison, T. F. Nickel-Catalyzed Synthesis of Acrylamides from α-Olefins and Isocyanates. *Org. Lett.* **9,** 875–878 (2007).
64. Werner, E. W., Mei, T.-S., Burckle, A. J. & Sigman, M. S. Enantioselective Heck Arylations of Acyclic Alkenyl Alcohols Using a Redox-Relay Strategy. *Science* **333,** 1875–1878 (2011).
65. Chen, Z.-M., Nervig, C. S., DeLuca, R. J. & Sigman, M. S. Palladium-Catalyzed Enantioselective Redox-Relay Heck Alkynylation of Alkenols To Access Propargylic Stereocenters. *Angew. Chem. Int. Ed.* **56,** 6651–6654 (2017).
66. Larock, R. C., Leung, W.-Y. & Stolz-Dunn, S. Synthesis of aryl-substituted aldehydes and ketones via palladium-catalyzed coupling of aryl halides and non-allylic unsaturated alcohols. *Tetrahedron Lett.* **30,** 6629–6632 (1989).
67. Singh, S., Bruffaerts, J., Vasseur, A. & Marek, I. A unique Pd-catalysed Heck arylation as a remote trigger for

cyclopropane selective ring-opening. *Nat. Commun.* **8,** 14200 (2017).
68. Wang, X., Nakajima, M., Serrano, E. & Martin, R. Alkyl Bromides as Mild Hydride Sources in Ni-Catalyzed Hydroamidation of Alkynes with Isocyanates. *J. Am. Chem. Soc.* **138,** 15531–15534 (2016).
69. Dietrich-Buchecker, C. O., Kern, J. M., Sauvage, J. P., Guilhem, J. & Pascard, C. Molecular Structures of a Monovalent and a Divalent Nickel Catenate: Competition between Metal Orbital Requirements and Geometrical Constraints Imposed by the Ligand. *Inorg. Chem.* **33,** 3498–3502 (1994).
70. Ramírez-Delgado, V. *et al.* Electrochemical Behavior of Ni (II) Complexes with N_2S_2 and N_6 Ligands as Potential Catalysts in Hydrogen Evolution Reaction. *J. Mex. Chem. Soc.* **59,** 294–301 (2015).
71. Jutand, A. The Use of Conductivity Measurements for the Characterization of Cationic Palladium(II) Complexes and for the Determination of Kinetic and Thermodynamic Data in Palladium-Catalyzed Reactions. *Eur. J. Inorg. Chem.* **2003,** 2017–2040 (2003).
72. Klein, A. *et al.* Halide ligands - More than just σ-donors? A structural and spectroscopic study of homologous organonickel complexes. *Inorg. Chem.* **47,** 11324–11333 (2008).
73. Feth, M. P., Klein, A. & Bertagnolli, H. Investigation of the Ligand Exchange Behavior of Square-Planar Nickel(II) Complexes by X-ray Absorption Spectroscopy and X-ray Diffraction. *Eur. J. Inorg. Chem.* **2003,** 839–852 (2003).
74. Constable, E. C., Hannon, M. J. & Smith, D. R. Cinnamil - an Oligopyridine Precursor. *Tetrahedron Lett.* **35,** 6657–6660 (1994).
75. Constable, E. C., Housecroft, C. E., Neuburger, M., Poleschak, I. & Zehnder, M. Functionalised 2,2′-bipyridine Ligands for the Preparation of Metallostars; X-ray Structures of Free Ligands and Preparation of Copper(I) and Silver(I) Complexes. *Polyhedron* **22,** 93–108 (2003).
76. Constable, E. C. *et al.* Synthesis and Coordination Chemistry of 4',4''-Disubstituted 2,2':6',2'':6'',2'''-quaterpyridines and Crystal and Molecular structures of Nickel(II) and Cobalt(II) Complexes. *Polyhedron* **19,** 23–34 (2000).
77. Haraguchi, R., Takada, Y. & Matsubara, S. Preparation of Cycloheptane Ring by Nucleophilic Cyclopropanation of 1,2-diketones with Bis(iodozincio)methane. *Org. Biomol. Chem.* **81,** 241–247 (2014).
78. Scheiper, B., Glorius, F., Leitner, A. & Fürstner, A. Catalysis-based enantioselective total synthesis of the macrocyclic spermidine alkaloid isooncinotine. *Proc. Natl. Acad. Sci.* **101,** 11960–11965 (2004).
79. Nallasivam, J. L. & Fernandes, R. A. A Cascade Aza-Cope/Aza-Prins Cyclization Leading to Piperidine Derivatives. *Eur. J. Org. Chem.* **2015,** 2012–2022 (2015).
80. Kalkhambkar, R. G., Waters, S. N. & Laali, K. K. Highly Efficient Synthesis of Amides via Ritter Chemistry with Ionic Liquids. *Tetrahedron Lett.* **52,** 867–871 (2011).

3.8. Experimental Section

3.8.1. General Considerations

Reagents and Reaction Set-up. $NiBr_2$ (anhydrous, 98% purity, a better reproducibility was found when stored in a glovebox), manganese powder (99.9% trace metal basis), *tert*-butyl isocyanate (97% purity), and cyclohexyl isocyanate (98% purity) were purchased from Aldrich. Other isocyanates were purchased from TCI (NOTE: *the purity of the isocyanates was found crucial for the reaction*; higher yields and better reproducibility were achieved by purifying the isocyanates through a short plug of dried neutral alumina inside a nitrogen-filled glovebox. Old batches of isocyanates provide consistently lower yields and variable results). Anhydrous *N,N*-dimethylformamide (DMF, 99.8% purity) and anhydrous *N,N*-dimethylacetamide (DMA, 99.5% purity) were purchased from Acros Organics (NOTE: *it is critical to have appropriately dried DMF and DMA to obtain reproducible results*, since old batches of these solvents provided variable results). Compounds methyl 4-bromohexanoate,[42] methyl 5-bromohexanoate,[42] 1,6-diphenylhexa-1,5-diene-3,4-dione,[74] 4,4'-bis(4-methoxyphenyl)-6,6'-dimethyl-2,2'-bipyridine,[75] 1,6-bis(4-(trifluoromethyl)phenyl)hexa-1,5-diene-3,4-dione[76] and 1,6-bis(4-methoxyphenyl)-hexa-1,5-diene-3,4-dione[77] were prepared following literature procedures. All other reagents were purchased from commercial sources and used as received. The temperature of the reactions was controlled by using a chiller (Huber Minichiller 300) connected to an aluminum block with an internal recirculation circuit (Figure 3.1).

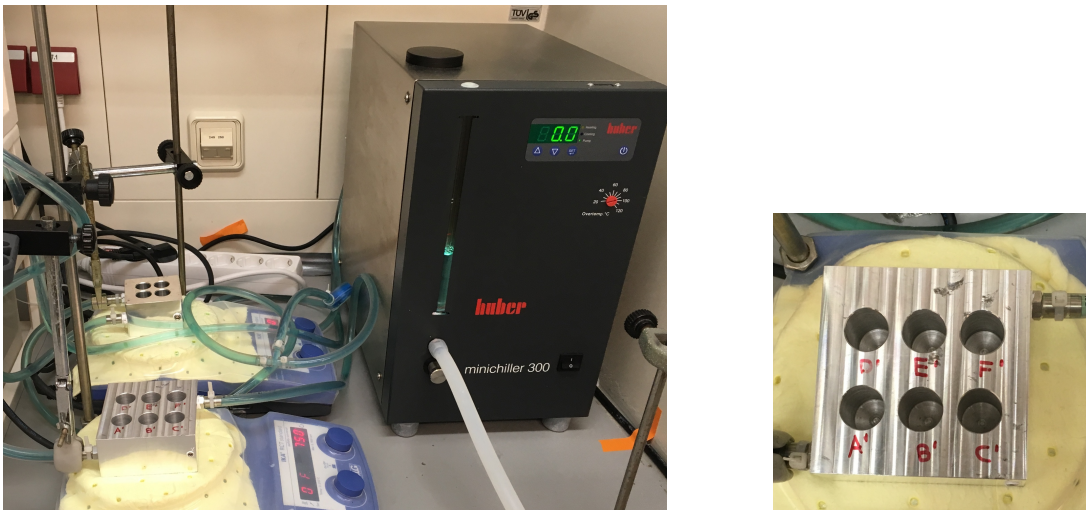

Figure 3.1. Laboratory set-up for low-temperature reactions

Analytical Methods. ^1H and ^{13}C-NMR spectra were recorded on a Bruker 400 MHz and 500 MHz at 20 °C. All ^1H-NMR spectra are reported in parts per million (ppm) downfield of TMS and are reported relative to the signal of residual $CHCl_3$ (7.26 ppm), unless otherwise indicated. All ^{13}C-NMR spectra are reported in ppm relative to residual $CHCl_3$ (77 ppm), unless otherwise indicated, and were measured with ^1H decoupling. Coupling constants, *J*, are reported in Hertz. Melting points were measured using open glass capillaries in a Büchi B540 apparatus. IR spectra were measured on a Bruker Optics FT-IR GmbH Alpha spectrometer with a Platinum-ATR module. Gas chromatographic analyses were performed on a Hewlett-Packard 6890 gas chromatography instrument with an FID detector. Column chromatography was performed with EM Science silica gel 60 (230-400 mesh). Thin layer chromatography was carried out using Merck TLC Silica gel 60 F254. $KMnO_4$ or vanillin stains were used to develop TLCs.

3.8.2. Optimization Details

General Procedure A, Screening Conditions for the Retained Amidation: In a nitrogen-filled glovebox, an oven-dried screw-capped test tube containing a stirring bar was charged with the nickel source, ligand and Mn. The obtained mixture was stirred at rt until a colored complex was obtained (*ca.* 5 to 10 min). Subsequently, 3-bromoheptane (0.5 mmol; 1 equiv) and *tert*-butyl isocyanate (0.75 mmol; 1.5 equiv) were added. The resulting mixture was stirred for 16 to 24 h, at 3 °C using a chiller. The crude reaction mixture was carefully quenched with 5% aq. HCl (1 mL) and extracted with ethyl acetate. A sample of the obtained solution was filtered through a silica-celite plug, eluted with ethyl acetate and analyzed by GC-FID using *n*-decane as internal standard.

General Procedure B, Screening Conditions for the Retained Amidation: In a nitrogen-filled glovebox, an oven-dried screw-capped test tube containing a stirring bar was charged with the nickel source, ligand and Mn. The obtained mixture was stirred at rt, until a colored complex was obtained (*ca.* 5 to 10 min), after which *tert*-butyl isocyanate (0.75 mmol; 1.5 equiv) was added. Subsequently, the reaction mixture was cooled down to 10 °C outside the glovebox, and 2-bromoheptane was added (0.5 mmol; 1 equiv). The resulting mixture was stirred for 24 h, at 10 °C using a chiller. The crude reaction mixture was carefully quenched with 5% aq. HCl (1 mL) and extracted with ethyl acetate. A sample of the obtained solution was filtered through a silica-celite plug, eluted with ethyl acetate and analyzed by GC-FID using anisole as internal standard.

3.8.3. Synthesis of Starting Materials and Ligands

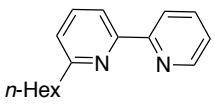

6-hexyl-2,2'-bipyridine (L8). Hexyl lithium (13.9 mL of a 2.3 M in hexane, 32 mmol; 1 equiv), was added slowly to a solution of bipyridine (5.0 g, 32 mmol; 1 equiv) in dry diethyl ether (150 mL, 0.2 M), at −40 °C. The resulting red solution was stirred for 1 h under vigorous agitation. Then, the reaction mixture was quenched with brine (200 mL). The resulting biphasic yellow mixture was separated and the organic phase was extracted with diethyl ether (3 × 50 mL), dried over $MgSO_4$ and evaporated under reduced pressure. The obtained dark orange crude product was dissolved in dichlorometane (50 mL) and MnO_2 (11.1 g, 128 mmol; 4 equiv) were added under vigorous agitation. After 3 h the crude reaction mixture was filtered through a silica-celite plug, concentrated under reduced pressure and purified through column chromatography on silica gel (hexanes/ethyl acetate 99:5) to afford the product as a clear oil (4.38 g, 18.2 mmol, 57% yield). ^{1}H-NMR (400 MHz, $CDCl_3$) δ 8.66 (ddd, *J* = 4.8, 1.8, 0.9 Hz, 1H, *Ar*), 8.44 (dt, *J* = 8.0, 1.1 Hz, 1H, *Ar*), 8.18 (dd, *J* = 7.9, 1.0 Hz, 1H, *Ar*), 7.78 (td, *J* = 7.7, 1.8 Hz, 1H, *Ar*), 7.69 (t, *J* = 7.7 Hz, 1H, *Ar*), 7.26 (ddd, *J* = 7.5, 4.8, 1.2 Hz, 1H, *Ar*), 7.14 (dd, *J* = 7.7, 1.0 Hz, 1H, *Ar*), 2.89 – 2.81 (m, 2H, *CH₂*), 1.86 – 1.72 (m, 2H, *CH₂*), 1.45 – 1.25 (m, 6H, *CH₂* x 3), 0.93 – 0.84 (m, 3H, *CH₃*) ppm. ^{13}C-NMR (101 MHz, $CDCl_3$) δ 162.1, 156.8, 155.6, 149.2, 137.1, 136.9, 123.5, 122.8, 121.3, 118.2, 38.5, 31.9, 29.8, 29.2, 22.7, 14.2 ppm. IR (neat, cm^{-1}): 2925, 2855, 1581, 1563, 1458, 1428, 773. HRMS (ESI^+) [$C_{16}H_{21}N_2$] (M+H) calcd. 241.1699 , found 241.1693

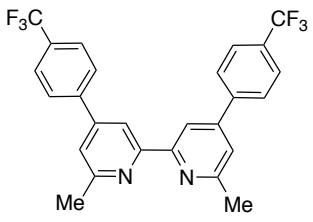

6,6'-dimethyl-4,4'-bis(4-(trifluoromethyl)phenyl)-2,2'-bipyridine (L28). 1,6-bis(4-(trifluoromethyl)phenyl)hexa-1,5-diene-3,4-dione[76] (682 mg, 1.71 mmol; 1 equiv), *N*-acetonylpyridinium chloride (588, 3.42 mmol; 2 equiv), and NH_4OAc (1.05 g, 13.7 mmol; 8 equiv) were added to ethanol (6 mL, 0.3 M). The resulting mixture was heated at reflux for 16 h under Ar. After cooling down, the crude reaction mixture was filtered, and the remaining off-white solid washed with cold ethanol (10 mL x 3), dissolved in $CHCl_3$ and washed with H_2O. The organic phase was separated, dried over $MgSO_4$ and concentrated under reduced pressure. The obtained solid was recrystallized from hot $CHCl_3$ as colorless needles (361 mg, 0.76 mmol, 45% yield). m.p. 258.0 – 260.1 °C. ^{1}H-NMR (400 MHz, $CDCl_3$) δ 8.55 – 8.50 (m, 2H, *Ar*), 7.90 – 7.82 (m, 4H, *Ar*), 7.79 – 7.73 (m, 4H, *Ar*), 7.41 (d, *J* = 1.6 Hz, 2H, *Ar*), 2.73 (s, 6H, *CH₃* x 2) ppm. ^{13}C-NMR

(101 MHz, $CDCl_3$) δ 159.0, 156.6, 148.3, 142.6, 131.0 (q, *J* = 32.5 Hz), 127.8, 126.1 (q, *J* = 3.7 Hz), 124.2 (q, *J* = 272.2 Hz), 121.5, 116.9, 24.9 ppm. ^{19}F-NMR (376 MHz, $CDCl_3$) δ -62.69 ppm. IR (neat, cm^{-1}): 1593, 1548, 1383, 1326, 1284, 1166, 1122, 1107, 1062, 1015, 834, 730. HRMS (ESI^+) [$C_{26}H_{19}F_6N_2$] (M+H) calcd. 473.1447, found 473.1457.

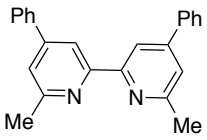

6,6'-dimethyl-4,4'-diphenyl-2,2'-bipyridine (L23). 1,6-diphenylhexa-1,5-diene-3,4-dione[74] (3.30 g, 12.6 mmol; 1 equiv), *N*-acetonylpyridinium chloride (4.30 g, 25.2 mmol; 2 equiv), and NH_4OAc (7.80 g, 101 mmol; 8 equiv) were added to ethanol (42 mL, 0.3 M). The resulting mixture was heated at reflux for 16 h. After cooling down, the crude reaction mixture was filtered, and the remaining off-white solid washed with cold ethanol (10 mL x 3), dissolved in $CHCl_3$ and washed with H_2O. The organic phase was separated, dried over $MgSO_4$ and concentrated under reduced pressure. The obtained solid was recrystallized from hot $CHCl_3$ as colorless needles (1.74 g, 5.16 mmol, 41% yield).m.p. 238.6 – 240.6 °C. ^{1}H-NMR (400 MHz, $CDCl_3$) δ 8.49 (d, *J* = 1.0 Hz, 2H, *Ar*), 7.80 – 7.73 (m, 4H, *Ar*), 7.54 – 7.47 (m, 4H, *Ar*), 7.47 – 7.42 (m, 2H, *Ar*), 7.42 – 7.39 (m, 2H, *Ar*), 2.72 (s, 6H, *CH₃* x 2) ppm. ^{13}C-NMR (101 MHz, $CDCl_3$) δ 158.5, 156.7, 149.7, 139.0, 129.1, 128.9, 127.4, 121.3, 116.9, 24.9 ppm. IR (neat, cm^{-1}): 3061, 3033, 2916, 1741, 1588, 1547, 1494, 1447, 1384, 1073, 871, 763, 692, 620, 502. HRMS (ESI^+) [$C_{24}H_{21}N_2$] (M+H) calcd. 337.1699, found 337.1685.

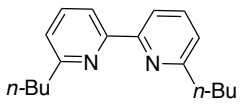

6,6'-dibutyl-2,2'-bipyridine (L21). *Step 1:* A solution of *n*-butylmagnesium chloride (7.4 mL, 2 M in THF, 14.9 mmol; 1.1 equiv) was added over 30 min to a solution of 2,6-dichloropyridine (2.00 g, 13.5 mmol; 1 equiv) and $Fe(acac)_3$ (2.38 mg, 0.672 mmol; 5 mol%), NMP (12 mL) and THF (70 mL) at 0 °C. After completing the addition, the resulting mixture was stirred for 15 min.[78] Then, the reaction was quenched with NH_4Cl (30 mL) and extracted with DCM (30 mL x 3). The organic phase was separated, washed with brine (40 mL), dried over $MgSO_4$ and purified through a short silica gel plug eluted using hexanes/AcOEt 10:1 that afforded an oil. *Step 2:* $NiCl_2{\cdot}6H_2O$ (3.2 g, 13.5 mmol; 1 equiv), PPh_3 (14 g, 54 mmol; 4 equiv) and Zn (883 mg, 13.5 mmol; 1 equiv) were added to a round bottom flask containing DMF (70 mL) and the obtained mixture was purged with Ar for *ca.* 10 min and subsequently heated at 50 °C for 1 h. The oil obtained in *step 1* was dissolved in DMF (20 mL) and added to the reaction flask. The resulting reaction mixture was heated at 50 °C for 3 h. After cooling down to rt, the crude reaction mixture was diluted with 40% aqueous ammonia (100 mL) and extracted with DCM (50 mL x 3), washed with H_2O, brine and dried over $MgSO_4$. A first purification through column chromatography on silica gel is performed to remove PPh_3 by eluting with hexanes, followed by hexanes/AcOEt 99.9:0.1, the resulting oil is purified through a second column chromatography on silica gel using a gradient of hexane:Et_2O 99:1 to 98:2 to afford **L21** as a light-yellow oil (402 mg, 1.50 mmol, 22% yield over 2 steps). ^{1}H-NMR (500 MHz, $CDCl_3$) δ 8.23 (d, *J* = 8.2 Hz, 2H, *Ar*), 7.69 (t, *J* = 7.7 Hz, 2H, *Ar*), 7.13 (d, *J* = 7.2 Hz, 2H, *Ar*), 2.86 (t, *J* = 7.8 Hz, 4H, *CH₂* x 2), 1.79 (p, *J* = 7.6 Hz, 4H, *CH₂* x 2), 1.43 (h, *J* = 7.4 Hz, 4H, *CH₂* x 2), 0.97 (t, *J* = 7.3 Hz, 6H, *CH₃* x 3) ppm. ^{13}C-NMR (126 MHz, $CDCl_3$) δ 161.9, 156.2, 137.0, 122.5, 118.4, 38.3, 32.1, 22.6, 14.2 ppm. IR (neat, cm^{-1}): 3060, 2955, 2928, 2858, 1572, 1437, 1150, 1084, 778, 635. HRMS (ESI^+) [$C_{18}H_{25}N_2$] (M+H) calcd. 269.2012, found 269.2012.

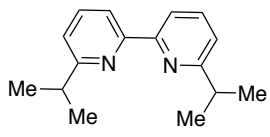

6,6'-diisopropyl-2,2'-bipyridine (L22). *Step 1:* A solution of isopropylmagnesium bromide (15.0 mL, 1 M in THF, 15.0 mmol; 1.1 equiv) was added over 30 min to a solution of 2,6-dichloropyridine (2.00 g, 13.5 mmol; 1 equiv) and $Fe(acac)_3$ (2.38 mg, 0.672 mmol; 5 mol%), NMP (12 mL) and THF (70 mL) at 0 °C. After completing the addition, the resulting mixture was stirred for 15 min.[78] Analysis of an aliquot of the reaction crude revealed the presence of starting material. Addition of extra isopropylmagnesium bromide (8.5 mL, 1 M in THF, 8.5 mmol) was necessary to reach full completion. After completion. the reaction was quenched with NH_4Cl (30 mL) and extracted with DCM (30 mL x 3). The organic phase was separated, washed with brine (40 mL), dried over $MgSO_4$ and

purified through a short silica gel plug eluted using hexanes/AcOEt 10:1 that afforded an oil. *Step 2:* $NiCl_2 \cdot 6H_2O$ (3.2 g, 13.5 mmol; 1 equiv), PPh_3 (14 g, 54 mmol; 4 equiv) and Zn (883 mg, 13.5 mmol; 1 equiv) were added to a round bottom flask containing DMF (70 mL) and the obtained mixture was purged with Ar for *ca.* 10 min and subsequently heated at 50 °C for 1 h. The oil obtained in *step 1* was dissolved in DMF (20 mL) and added to the reaction flask. The resulting reaction mixture was heated at 50 °C for 3 h. After cooling down to rt, the crude reaction mixture was diluted with 40% aqueous ammonia (100 mL) and extracted with DCM (50 mL x 3), washed with H_2O, brine and dried over $MgSO_4$. A first purification through column chromatography on silica gel is performed to remove PPh_3 by eluting with hexanes, followed by hexanes/AcOEt 99.9:0.1, the resulting oil is purified through a second column chromatography on silica gel using a gradient of hexane:AcOEt to afford **L22** as a colorless solid (502 mg, 2.09 mmol, 31% yield over 2 steps). m.p. 34.0 – 36.0 °C. ^{1}H-NMR (500 MHz, $CDCl_3$) δ 8.29 (dd, *J* = 7.8, 1.0 Hz, 2H, *Ar*), 7.71 (t, *J* = 7.7 Hz, 2H, *Ar*), 7.15 (dd, *J* = 7.7, 1.0 Hz, 2H, *Ar*), 3.12 (hept, *J* = 6.9 Hz, 2H, *CH* x 2), 1.36 (d, *J* = 6.9 Hz, 12H, CH_3 x 4) ppm. ^{13}C-NMR (101 MHz, $CDCl_3$) δ 166.6, 155.9, 137.1, 120.5, 118.4, 36.5, 22.8 ppm. IR (neat, cm^{-1}): 3060, 2960, 2927, 2865, 1571, 1432, 1121, 1079, 800, 751, 633. HRMS (ESI^+) [$C_{16}H_{21}N_2$] (M+H) calcd. 241.1699, found 241.1698.

General procedure C, preparation of secondary alkyl bromides: To a solution of the corresponding alcohol in DCM (0.5 M), CBr_4 (1.2 equiv) and PPh_3 (1.2 equiv) were sequentially added at 0 °C. The resulting solution was stirred at rt for 16 h. After completion, the crude reaction mixture was diluted with hexanes and concentrated to half its volume under reduced pressure. The obtained crude mixture was filtered through a short silica plug, eluted with hexanes and concentrated under reduced pressure. Purification through column chromatography on silica gel afforded the desired products.

General procedure D, preparation of secondary alkyl bromides: to a solution of triphenylphosphine (1.2 equiv) in DCM (0.2 M) at 0 °C, bromine (1.2 equiv) was added dropwise and the mixture stirred for 30 min. Then, a solution of the corresponding alcohol (1 equiv) in DCM (0.2 M) and pyridine (1.2 equiv) were subsequently added and the mixture was stirred for 4 h at room temperature. After completion, the mixture was partially concentrated and filtered through a plug of silica eluting with pentane. The filtrate was evaporated and the residue purified by column chromatography on silica gel.

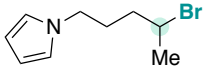

1-(4-bromopentyl)-1*H*-pyrrole. A solution of pyrrole (0.69 mL, 10 mmol; 1 equiv) in DMF (5 mL) was added slowly over a round bottom flask containing NaH (0.48 g of 60% NaH in mineral oil, 12 mmol; 1.2 equiv) in DMF (100 mL), and stirred at rt for 1h. Then, a solution of 1,4-dibromopentane (4 mL, 30 mmol; 3 equiv) in DMF (40 mL) was slowly added and the resulting mixture stirred for 48 h. The crude reaction mixture was evaporated under reduced pressure and the obtained oil purified through column chromatography to afford the title compound as a light-yellow oil (1.06 g, 4.9 mmol; 49% yield). ^{1}H-NMR (500 MHz, $CDCl_3$) δ 6.65 (s, 2H, *Ar*), 6.15 (s, 2H, *Ar*), 4.12 – 4.05 (m, 1H, *CH-Br*), 3.92 (td, *J* = 6.9, 1.3 Hz, 2H, CH_2), 2.08 – 2.00 (m, 1H, CH_2), 1.97 – 1.84 (m, 1H, CH_2), 1.84 – 1.71 (m, 2H, CH_2), 1.69 (d, *J* = 6.7 Hz, 3H, CH_3) ppm. ^{13}C-NMR (75 MHz, $CDCl_3$) δ 120.6, 108.3, 50.9, 49.0, 38.2, 29.9, 26.6 ppm. IR (neat, cm^{-1}): 3099, 2924, 1684, 1499, 1445, 1280, 1088, 1066, 720, 617, 535. HRMS ($APCI^+$) [$C_9H_{15}BrN$] (M+H) calcd. 216.0382, found. 216.0373

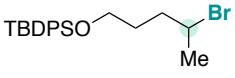

((4-bromopentyl)oxy)(*tert*-butyl)diphenylsilane. Following procedure D, starting from 5-((tert-butyldiphenylsilyl)oxy)pentan-2-ol (5.76 g, 16.8 mmol; 1 equiv), and after purification through column chromatography on silica gel eluting with hexanes/AcOEt 95:5, afforded the title compound as a colorless oil (4.14 g, 10.2 mmol, 61% yield). ^{1}H-NMR (500 MHz, $CDCl_3$) δ 7.68 – 7.66 (m, 4H, *Ar*), 7.46 – 7.36 (m, 6H, *Ar*), 4.14 (dq, *J* = 13.3, 6.6 Hz, 1H, *CH-Br*), 3.69 (t, *J* = 6.2 Hz, 2H, CH_2-*O*), 1.94 – 1.86 (m, 2H, CH_2), 1.83 – 1.73 (m, 1H, CH_2), 1.71 (d, *J* = 6.6 Hz, 3H, CH_3), 1.69 – 1.63 (m, 1H, CH_2), 1.06 (s, 9H, *t-Bu*) ppm. ^{13}C-NMR

(75 MHz, $CDCl_3$) δ 135.7, 134.0, 129.8, 127.8, 63.3, 51.9, 37.8, 30.9, 27.0, 26.7, 19.4 ppm. IR (neat, cm^{-1}): 3071, 3049, 2958, 2931, 2893, 2858, 1472, 1428, 1110, 823, 701, 504. HRMS (APCI$^+$) [$C_{21}H_{29}BrNaOSi$] (M+Na) calcd. 427.1063, found 427.1074.

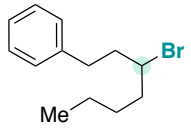

(3-bromoheptyl)benzene. Following general procedure C, starting from 1-phenylheptan-3-ol (2.00 g, 10.4 mmol; 1 equiv) and after purification through column chromatography using hexanes as eluent, the title compound was obtained as a colorless oil (1.44 g, 5.64 mmol, 54% yield). ^{1}H-NMR (400 MHz, $CDCl_3$) δ 7.33 – 7.27 (m, 2H, *Ar*), 7.22 – 7.19 (m, 3H, *Ar*), 3.99 (tt, *J* = 8.2, 4.8 Hz, 1H, *CH-Br*), 2.91 (ddd, *J* = 14.1, 8.7, 5.6 Hz, 1H, CH_2), 2.76 (ddd, *J* = 13.7, 8.8, 7.3 Hz, 1H, CH_2), 2.21 – 2.04 (m, 2H, CH_2), 1.94 – 1.76 (m, 2H, CH_2), 1.58 – 1.46 (m, 1H, CH_2), 1.46 – 1.22 (m, 3H, CH_2, CH_2), 0.91 (t, *J* = 7.2 Hz, 3H, CH_3) ppm. ^{13}C-NMR (101 MHz, $CDCl_3$) δ 141.2, 128.7, 128.6, 126.2, 58.0, 40.9, 39.1, 33.9, 29.8, 22.3, 14.1 ppm. IR (neat, cm^{-1}): 3063, 3027, 2955, 2929, 2860, 1603, 1496, 1454, 1237, 1030, 747, 697. HRMS (EI$^+$) [$C_{13}H_{19}Br$] (M+) calcd. 254.0670, found 254.0675

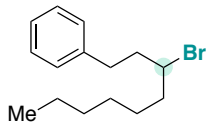

(3-bromononyl)benzene. Following general procedure C, starting from 1-phenylnonan-3-ol (2.29 g, 10.4 mmol; 1 equiv) and after purification through column chromatography using hexanes as eluent, the title compound was obtained as a colorless oil (1.68 g, 5.93 mmol, 57% yield).^{1}H-NMR (400 MHz, $CDCl_3$) δ 7.31-7.28 (m, 2H, *Ar*), 7.22-7.18 (m, 3H, *Ar*), 3.99 (tt, *J* = 8.2, 4.8 Hz, 1H, *CH-Br*), 2.90 (ddd, *J* = 14.1, 8.7, 5.6 Hz, 1H, CH_2), 2.75 (ddd, *J* = 13.7, 8.8, 7.3 Hz, 1H, CH_2), 2.20 – 2.03 (m, 2H, CH_2), 1.93 – 1.76 (m, 2H, CH_2), 1.57 – 1.47 (m, 1H, CH_2), 1.44 – 1.36 (m, 1H, CH_2), 1.32 – 1.27 (m, 6H, CH_2 x 3), 0.88 (t, *J* = 6.8 Hz, 3H, CH_3) ppm. ^{13}C-NMR (101 MHz, $CDCl_3$) δ 141.3, 128.7, 128.6, 126.2, 58.0, 40.9, 39.4, 33.9, 31.8, 28.9, 27.6, 22.7, 14.2 ppm. IR (neat, cm^{-1}): 3063, 3027, 2953, 2926, 2856, 1496, 1454, 1223, 747, 698.

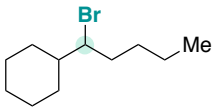

(1-bromopentyl)cyclohexane: Following general procedure C, starting from 1-cyclohexylpentan-1-ol (2.00 g, 11.7 mmol; 1 equiv) and after purification through column chromatography using hexanes as eluent, the title compound was obtained as a colorless. ^{1}H-NMR (400 MHz, $CDCl_3$) δ 3.97 (dt, *J* = 8.8, 4.3 Hz, 1H, *CH-Br*), 1.94 – 1.62 (m, 7H, CH_2 x 3, *CH*), 1.59 – 1.46 (m, 2H, CH_2), 1.45 – 1.08 (m, 8H, CH_2 x 4), 0.96 – 0.85 (m, 3H, CH_3) ppm. ^{13}C-NMR (101 MHz, $CDCl_3$) δ 66.3, 44.6, 36.0, 31.2, 30.3, 29.3, 26.5, 26.4, 26.3, 22.3, 14.1 ppm. IR (neat, cm^{-1}): 2926, 2854, 1449, 1379, 1302, 1243, 1174, 926, 892, 732, 554.

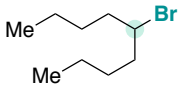

5-bromononane. The title compound was prepared following procedure D. ^{1}H-NMR (500 MHz, $CDCl_3$) δ 4.06 – 4.00 (m, 1H, *CH-Br*), 1.91 – 1.78 (m, 4H, CH_2 x 2), 1.57 – 1.46 (m, 2H, CH_2), 1.45 – 1.23 (m, 6H, CH_2 x 4), 0.92 (t, *J* = 7.3 Hz, 6H, CH_3 x 2) ppm. ^{13}C-NMR (126 MHz, $CDCl_3$) δ 59.1, 39.1, 29.9, 22.3, 14.1 ppm. IR (neat, cm^{-1}): 2957, 2931, 2860, 1465, 1379, 1241, 1182, 936, 732.

3.8.4. Preparative Scope

General Procedure E. *Conditions b*: an oven-dried screw-capped test tube containing a stirring bar was charged, if solid, with the corresponding alkyl bromide (0.50 mmol). Subsequently, $NiBr_2$ (3.3 mg, 0.015 mmol, 3.0 mol%), 6-methyl-2,2'-bipyridine (**L6**) (3.8 mg, 0.023, 4.5 mol%), and Mn (55 mg, 1.0 mmol, 2.0 equiv) were added. The reaction tube was then evacuated and back-filled with dry argon (this sequence was repeated three times) and DMF (1.0 mL) and *tert*-butyl isocyanate (171 μL, 1.5 mmol, 3.0 equiv) were added sequentially under argon flow. In case of liquid alkyl bromides, the corresponding starting material (0.50 mmol) was added under argon flow, via Hamilton syringe. The resulting solution was stirred for 16 h at 25 °C. The crude reaction mixture was

carefully quenched with 5% aq. HCl (1 mL) or saturated aq. NH_4Cl (2 mL) (when sensitive functional groups were present). Acid quench was followed by the addition of distilled water (ca. 10 mL) and by extraction with dichloromethane (3 × 25 mL). The obtained solution was washed with brine (40 mL), dried over $MgSO_4$, filtered and the solvent was evaporated under reduced pressure. The crude product was purified by column chromatography (hexanes/AcOEt or pentane/Et_2O) to yield the corresponding products.

General Procedure F. *Conditions a:* In a nitrogen-filled glovebox, an oven-dried screw-capped test tube containing a stirring bar was charged with $NiBr_2$ (2.7 mg, 0.013 mmol; 2.5 mol%), 6-hexyl-2,2'-bipyridine (**L8**) (6.0 mg, 0.025, 5.0 mol%), Mn (41.2 mg, 0.750 mmol; 1.5 equiv) and DMF (0.5 mL). The obtained mixture was stirred until a deep green color was observed. Subsequently, the corresponding alkyl bromide (0.5 mmol; 1 equiv) and isocyanate (0.75 mmol; 1.5 equiv) were added. The resulting mixture was stirred for 24 h, at 3 °C using a chiller. The crude reaction mixture was carefully quenched with 5% aq. HCl (1 mL) or saturated aq. NH_4Cl (2 mL) (when sensitive functional groups were present). Acid quench was followed by the addition of distilled water (*ca.* 10 mL) and by extraction with ethyl acetate (3 × 15 mL). The organic phase was washed with brine (40 mL), dried over $MgSO_4$, filtered and the solvent was evaporated under reduced pressure. The crude product was purified by column chromatography (hexanes/AcOEt or pentane/Et_2O). *Conditions c:* as *conditions a* but using 6-methyl-2,2'-bipyridine (**L6**) (4.3 mg, 0.025, 5.0 mol%) instead.

General Procedure G. In a nitrogen-filled glovebox, an oven-dried screw-capped test tube containing a stirring bar was charged with NiI_2 (3.9 mg, 0.013 mmol; 2.5 mol%), 6,6'-dimethyl-4,4'-diphenyl-2,2'-bipyridine (**L23**) (8.4 mg, 0.025, 5.0 mol%), Mn (68.7 mg, 1.25 mmol; 2.5 equiv) and NMP (1.0 mL). The obtained mixture was stirred until a deep purple color was observed. Subsequently, the corresponding alkyl bromide (0.5 mmol; 1 equiv) and isocyanate (0.75 mmol; 1.5 equiv) were added. The resulting mixture was stirred for 24 h, at 10 °C using a chiller. The crude reaction mixture was carefully quenched with 5% aq. HCl (1 mL) or saturated aq. NH_4Cl (2 mL) (when sensitive functional groups were present). Acid quench was followed by the addition of distilled water (*ca.* 10 mL) and by extraction with ethyl acetate (3 × 15 mL). The organic phase was washed with brine (40 mL), dried over $MgSO_4$, filtered and the solvent was evaporated under reduced pressure. The crude product was purified by column chromatography (hexanes/AcOEt or pentane/Et_2O).

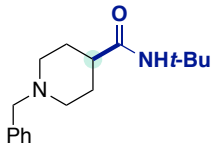

1-benzyl-*N*-(*tert*-butyl)piperidine-4-carboxamide (3.29a). Following general procedure E, 1-benzyl-4-bromopiperidine (127.1 mg, 0.5000 mmol; 1 equiv), *tert*-butyl isocyanate (171 µL, 149 mg, 1.50 mmol; 3 equiv) and Mn (55 mg, 1.0 mmol; 2 equiv) were utilized to deliver **3.29a** as a pale yellow solid (116.9 mg 1st run, 107.4 mg 2nd run, 82% average yield) after purification by column chromatography (CH_2Cl_2 100 with Et_3N 1% then CH_2Cl_2:MeOH 99:1 with Et_3N 1%). m.p.: 108.1 – 111.7 °C. ^{1}H-NMR (500 MHz, $CDCl_3$) δ 7.30 (d, *J* = 4.4 Hz, 4H, *Ar*), 7.27 - 7.22 (m, 1H, *Ar*), 5.24 (s, 1H, *NH*), 3.49 (s, 2H, *CH₂-Ar*), 2.96 - 2.88 (m, 2H, *CH₂*), 1.97 (t, *J* = 11.6 Hz, 3H, *CH₂ + CH*), 1.81 - 1.66 (m, 4H, *CH₂*), 1.33 (s, 9H, *t-Bu*) ppm. ^{13}C-NMR (126 MHz, $CDCl_3$) δ 174.6, 138.6, 129.2, 128.3, 127.1, 63.3, 53.3, 51.1, 44.4, 29.3, 29.0 ppm. IR (neat, cm^{-1}): 3349, 2939, 2763, 1662, 1645, 1534, 1448, 1361, 699. HRMS (ESI^+) [$C_{17}H_{26}N_2O$] (M+H) calcd. 275.2118, found 275.2118.

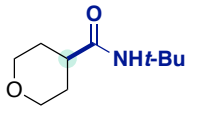

***N*-(*tert*-butyl)tetrahydro-2H-pyran-4-carboxamide (3.29b).** Following general procedure E, 4-bromotetrahydro-2H-pyran (82.5 mg, 0.500 mmol; 1 equiv), *tert*-butyl isocyanate (171 µL, 149 mg, 1.50 mmol; 3 equiv) and Mn (55 mg, 1.0 mmol; 2 equiv) were utilized to deliver **3.29b** as a pale yellow solid (66.0 mg 1st run, 66.1 mg 2nd run, 71% average yield). m.p.: 140.0 – 143.3 °C. ^{1}H-NMR (400 MHz, $CDCl_3$) δ 5.30 (s, 1H, *NH*), 3.98 (ddd, *J* = 11.3, 3.9, 2.2 Hz, 2H, *CH₂*), 3.36 (td, *J* = 11.5,

2.7 Hz, 2H, *CH₂*), 2.24 – 2.15 (m, 1H, *CH*), 1.81 – 1.63 (m, 4H, *CH₂*), 1.32 (s, 9H, *t-Bu*) ppm. ^{13}C-NMR (101 MHz, $CDCl_3$) δ 173.7, 67.4, 51.1, 43.1, 29.5, 28.9 ppm. IR (neat, cm^{-1}): 3339, 2958, 2919, 2849, 1641, 1532, 1360, 1117. HRMS (ESI$^+$) [$C_{10}H_{19}NO_2$] (M+Na) calcd. 208.1308, found 208.1304.

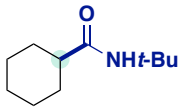

***N*-(*tert*-butyl)cyclohexanecarboxamide (3.29c).** Following general procedure E, bromocyclohexane (91.5 mg, 0.500 mmol; 1 equiv), *tert*-butyl isocyanate (86.0 µL, 74.3 mg, 0.750 mmol; 1.50 equiv), $NiBr_2$ (5.5 mg, 0.025 mmol; 5 mol%), 6-methyl-2,2'-bipyridine (6.4 mg, 0.038 mmol; 7.5 mol%) and Mn (55 mg, 1.0 mmol; 2 equiv) were utilized to deliver **3.29c** as a colorless solid (76.7 mg 1st run, 78.8 mg 2nd run, 85% average yield). The spectroscopic data correspond to those previously reported in the literature.[79] m.p.: 158.7 – 160.2 °C. ^{1}H-NMR (500 MHz, $CDCl_3$) δ 5.22 (s, 1H, *NH*), 1.96 – 1.88 (m, 1H, *CH-C=O*), 1.85 – 1.71 (m, 4H, *CH₂-CH₂*), 1.67 – 1.60 (m, 1H, *CH*), 1.45 – 1.34 (m, 2H, *CH₂*), 1.32 (s, 9H, *t-Bu*), 1.27 – 1.14 (m, 3H, *CH₂ +CH*) ppm. ^{13}C-NMR (101 MHz, $CDCl_3$) δ 175.7, 50.9, 46.5, 29.9, 29.0, 25.9 ppm. IR (neat, cm^{-1}): 3301, 2964, 2929, 2852, 1644, 1545, 1447, 1227. HRMS (ESI$^+$) [$C_{11}H_{21}NO$] (M+H) calcd. 184.1696, found 184.1697.

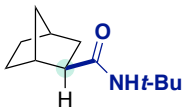

***N*-(*tert*-butyl)bicyclo[2.2.1]heptane-2-carboxamide (3.29d).** Following general procedure E, exo-2-bromonorbornane (98%, only exo isomer) (87.5 mg, 0.500 mmol; 1 equiv), *tert*-butyl isocyanate (171 µL, 149 mg, 1.50 mmol; 3 equiv) and Mn (55 mg, 1.0 mmol; 2 equiv) were utilized to deliver **3.29d** as an off-white solid (69.2 mg 1st run, 64.8 mg 2nd run, 69% average yield). Isolated as a mixture of isomers (*exo:endo* 3.5 : 1.0), the assignment of the isomers was done by comparison with the NMR spectra the *endo* isomer prepared independently from the commercially available *endo*-carboxylic acid (98% purity) – see ^{1}H- and ^{13}C-NMR spectroscopic data. m.p.: 154.4 – 156.5 °C. Spectroscopic data of mayor isomer: ^{1}H-NMR (400 MHz, $CDCl_3$) δ 5.22 (s, 1H, *NH*), 2.34 – 2.30 (m, 1H, *CH*), 2.27 – 2.23 (m, 1H, *CH*), 1.97 (dd, *J* = 8.7, 5.3 Hz, 1H, *CH*), 1.86 – 1.77 (m, 1H, *CH*), 1.58 – 1.52 (m, 1H, *CH*), 1.52 - 1.45 (m, 2H, *CH₂*), 1.41 – 1.35 (m, 2H, *CH₂*), 1.30 (s, 9H, *t-Bu*), 1.20 – 1.07 (m, 2H, *CH₂*) ppm. ^{13}C-NMR (126 MHz, $CDCl_3$): δ 175.3, 51.0, 48.9, 41.8, 36.6, 36.1, 34.5, 30.0, 29.1, 28.8 ppm. IR (neat, cm^{-1}): 3319, 2951, 2869, 1644, 1540, 1451, 1360, 1223. HRMS (ESI$^+$) [$C_{12}H_{21}NO$] (M+Na) calcd. 218.1515, found 218.1515.

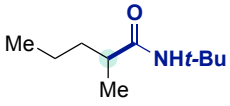

***N*-(*tert*-butyl)-2-methylpentanamide (3.29e).** Following general procedure E, **1w** (90% purity) (83.9 mg, 0.500 mmol; 1 equiv), *tert*-butyl isocyanate (171 µL, 149 mg, 1.50 mmol; 3 equiv) and Mn (55 mg, 1.0 mmol; 2 equiv) were utilized to deliver **3.29e** as an off-white solid (59.6 mg 1st run, 51.8 mg 2nd run, 52.7 mg 3rd run, 64% average yield). m.p.: 81.9 – 84.2 °C. ^{1}H-NMR (400 MHz, $CDCl_3$) δ 5.24 (s, 1H, *NH*), 2.03 (h, *J* = 6.8 Hz, 1H, *CH*), 1.64 – 1.51 (m, 1H, *CH*), 1.32 (s, 9H, *t-Bu*), 1.30 – 1.22 (m, 3H, *CH₂ + CH*), 1.07 (d, *J* = 6.8 Hz, 3H, *CH₃*), 0.88 (t, *J* = 7.1 Hz, 3H, *CH₃*) ppm. ^{13}C-NMR (126 MHz, $CDCl_3$) δ 176.1, 51.1, 42.3, 36.9, 29.0, 20.8, 18.1, 14.3 ppm. IR (neat, cm^{-1}): 3303, 2963, 2929, 1643, 1551, 1360, 1264, 1226. HRMS (ESI$^+$) [$C_{10}H_{21}NO$] (M+Na) calcd. 194.1515, found 194.1521.

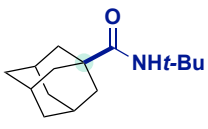

***N*-(*tert*-butyl)adamantane-1-carboxamide (3.29f).** Following general procedure E, **1y** (107.6 mg, 0.5000 mmol; 1 equiv), *tert*-butyl isocyanate (171 µL, 149 mg, 1.50 mmol; 3 equiv) and Mn (55 mg, 1.0 mmol; 2 equiv), $NiBr_2$ (10.9 mg, 0.0500 mmol; 10 mol%) and 6-methyl-2,2'-bipyridine (12.8 mg, 0.0750 mmol; 15 mol%) were utilized to deliver **3.29f** as a colorless solid (75.0 mg 1st run, 77.7 mg 2nd run, 65% average yield). m.p.: 174.5 – 178.5 °C. The spectroscopic data correspond to those previously reported in the literature.[80] ^{1}H-NMR (400 MHz, $CDCl_3$) δ 5.35 (s, 1H, *NH*), 2.05 – 2.00 (m, 3H, *CH*), 1.80 (d, *J* = 2.7 Hz, 6H, *CH₂*), 1.76- 1.64 (m, 6H, *CH₂*), 1.33 (s, 9H, *t-Bu*) ppm. ^{13}C-NMR (101 MHz, $CDCl_3$) δ 177.5, 50.7, 41.0, 39.5, 36.7, 29.0, 28.4 ppm. IR (neat, cm^{-1}): 3350, 2899, 2849, 1635, 1532, 1445, 1286, 1228. HRMS (ESI$^+$) [$C_{15}H_{25}NO$] (M+H) calcd. 236.2009, found 236.2014.

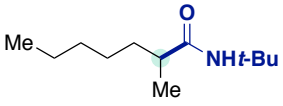

***N*-(*tert*-butyl)-2-methylheptanamide (3.29k).** Following general procedure F and starting from 2-bromoheptane (89.6 mg, 0.500 mmol; 1 equiv) and *tert*-butyl isocyanate (86.0 µL, 74.3 mg, 0.750 mmol; 1.50 equiv), compound **3.29k** was obtained as a colorless solid (91.3 mg 1st run, 91.6 mg 2nd run, 92% average yield). m.p.: 57.9 – 60.2 °C. ^{1}H NMR (500 MHz, $CDCl_3$) δ 5.21 (s, 1H, *NH*), 2.07 – 1.93 (m, 1H, *CH–C=O*), 1.65 – 1.50 (m, 1H, *CH*), 1.34 (s, 9H, *t*-Bu), 1.33 – 1.21 (m, 7H, CH_2), 1.08 (d, *J* = 6.9 Hz, 3H, CH_3–*CH*), 0.87 (t, *J* = 6.9 Hz, 3H, CH_3) ppm. ^{13}C NMR (126 MHz, $CDCl_3$) δ 176.1, 51.1, 42.5, 34.6, 32.0, 29.0, 27.3, 22.7, 18.1, 14.2 ppm. IR (neat, cm^{-1}): 3314, 2961, 2928, 2859, 1646, 1543, 1453, 1362, 1226. HRMS (ESI$^+$) [$C_{12}H_{25}NNaO$] (M+Na) calcd. 222.1828, found 222.1833.

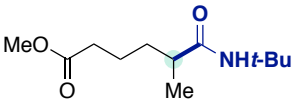

Methyl 6-(*tert*-butylamino)-5-methyl-6-oxohexanoate (3.29q). Following general procedure F slightly modified, and starting from methyl 5-bromohexanoate (104.5 mg, 0.500 mmol; 1 equiv), *tert*-butyl isocyanate (172 µL, 149 mg, 1.5 mmol; 3 equiv) and Mn (55.0 mg, 1.0 mmol; 2 equiv), compound **3.29q** was obtained as a clear oil (90.8 mg, 1st run, 82.7 mg 2nd run, 76% average yield). Alternatively, if instead 6-methyl-2,2'-bipyridine was used as ligand (4.3 mg, 0.025, 5.0 mol%) 73.9 mg (64%) of compound **3.29q** were obtained. When general procedure E was followed, 33.2 mg (29%) of compound **3.29q** were isolated. ^{1}H NMR (500 MHz, $CDCl_3$) δ 5.32 (s, 1H, *NH*), 3.65 (s, 3H, OCH_3), 2.37 – 2.22 (m, 2H, CH_2), 2.10 – 1.98 (m, 1H, *CH–C=O*), 1.68 – 1.52 (m, 3H, CH_2), 1.39 – 1.34 (m, 1H, CH_2), 1.33 (s, 9H, *t-Bu*), 1.09 (d, *J* = 6.8 Hz, 3H, CH_3) ppm. ^{13}C NMR (126 MHz, $CDCl_3$) δ 175.6, 174.1, 51.6, 51.2, 42.2, 34.0, 33.9, 29.0, 22.9, 18.2 ppm. IR (neat, cm^{-1}): 3320, 2965, 2874, 1738, 1647, 1536, 1452, 1224. HRMS (ESI$^+$) [$C_{12}H_{23}NNaO_3$] (M+Na) calcd. 252.1570, found 252.1566.

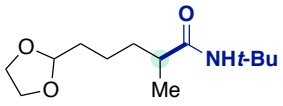

***N*-(*tert*-butyl)-5-(1,3-dioxolan-2-yl)-2-methylpentanamide (3.29r).** Following general procedure F and starting from 2-(4-bromopentyl)-1,3-dioxolane (112.0 mg, 0.500 mmol; 1 equiv) and *tert*-butyl isocyanate (86.0 µL, 74.3 mg, 0.750 mmol; 1.50 equiv), compound **3.29r** was obtained as a yellow oil (112.3 mg 92%). ^{1}H NMR (300 MHz, $CDCl_3$) δ 5.26 (s, 1H, *NH*), 4.83 (t, *J* = 4.8 Hz, 1H, *CH–O*), 3.98 – 3.91 (m, 2H, CH_2–*O*), 3.86 – 3.79 (m, 2H, CH_2–*O*), 2.11 – 1.96 (m, 1H, *CH–C=O*), 1.72 – 1.57 (m, 3H, CH_2), 1.49 – 1.35 (m, 3H, CH_2), 1.33 (s, 9H, *t-Bu*), 1.08 (d, *J* = 6.8 Hz, 3H, CH_3). ^{13}C NMR (75 MHz, $CDCl_3$) δ 175.9, 104.6, 65.0, 51.1, 42.3, 34.4, 33.9, 29.0, 22.1, 18.0 ppm. IR (neat, cm^{-1}): 3316, 2964, 2874, 1647, 1538, 1454, 1363, 1224, 1031. HRMS (ESI$^+$) [$C_{13}H_{25}NNaO_3$] (M+Na) calcd. 266.1727, found 266.1728.

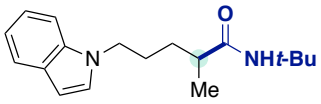

***N*-(*tert*-butyl)-5-(1H-indol-1-yl)-2-methylpentanamide (3.29s).** Following general procedure F and starting from 1-(4-bromopentyl)-1H-indole (133.1 mg, 0.500 mmol; 1 equiv) and *tert*-butyl isocyanate (86.0 µL, 74.3 mg, 0.750 mmol; 1.50 equiv), compound **3.29s** was obtained as a yellow oil (142.9 mg 1st run, 121.7 mg 2nd run, 134.7 3rd run, 93% average yield). ^{1}H NMR (400 MHz, $CDCl_3$) δ 7.63 (dt, *J* = 7.9, 0.9 Hz, 1H, *Ar*), 7.36 – 7.32 (m, 1H, *Ar*), 7.23 – 7.17 (m, 1H, *Ar*), 7.12 – 7.07 (m, 2H, *Ar*), 6.49 (dd, *J* = 3.1, 0.8 Hz, 1H, *Ar*), 5.07 (s, 1H, *NH*), 4.21 – 4.03 (m, 2H, CH_2), 1.93 – 1.87 (m, 1H, *CH–C=O*), 1.87 – 1.78 (m, 2H, CH_2), 1.72 – 1.61 (m, 1H, CH_2), 1.40 – 1.31 (m, 1H, CH_2), 1.29 (s, 9H, *t-Bu*), 1.05 (d, *J* = 6.8 Hz, 3H, CH_3) ppm. ^{13}C NMR (101 MHz, $CDCl_3$) δ 175.4, 136.0, 128.7, 127.9, 121.6, 121.1, 119.4, 109.5, 101.2, 51.2, 46.6, 42.0, 31.9, 28.9, 28.1, 18.4 ppm. IR (neat, cm^{-1}): 3322, 2965, 2931, 2872, 1646, 1510, 1362, 1224, 737. HRMS (ESI$^+$) [$C_{18}H_{26}N_2NaO$] (M+Na) calcd. 309.1937, found 309.1943.

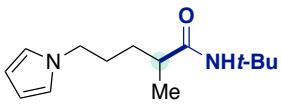

***N*-(*tert*-butyl)-2-methyl-5-(1H-pyrrol-1-yl)pentanamide (3.29t).** Following general procedure F and starting from 1-(4-bromopentyl)-1H-pyrrole (108.1 mg, 0.500 mmol; 1 equiv) and *tert*-butyl isocyanate (86.0 µL, 74.3 mg, 0.750 mmol; 1.50 equiv), compound **3.29t** was obtained as a beige solid (108.0 mg 1st run, 104.9 mg 2nd run, 90% average yield).

m.p.: 59.5 – 61.9 °C. ^{1}H NMR (400 MHz, $CDCl_3$) δ 6.64 (s, 2H, *Ar*), 6.14 (s, 2H, *Ar*), 5.17 (s, 1H, *NH*), 33.96 – 3.87 (m, 1H, *CH*$_2$), 3.87 – 3.78 (m, 1H, *CH*$_2$), 1.96 – 1.85 (m, 1H, *CH–C=O*), 1.80 – 1.69 (m, 2H, *CH*$_2$), 1.68 – 1.56 (m, 1H, *CH*$_2$), 1.33 (s, 9H, *t-Bu*), 1.37 – 1.28 (m, 1H, *CH*$_2$), 1.07 (d, *J* = 6.8 Hz, 3H, *CH*$_3$) ppm. ^{13}C NMR (101 MHz, $CDCl_3$) δ 175.5, 120.6, 108.1, 51.2, 49.8, 41.9, 31.8, 29.5, 29.0, 18.3 ppm. IR (neat, cm^{-1}): 3320, 2965, 2931, 2873, 1645, 1541, 1452, 1088, 719. HRMS (ESI$^+$) [$C_{14}H_{24}N_2NaO$] (M+Na) calcd. 259.1781, found 259.1785.

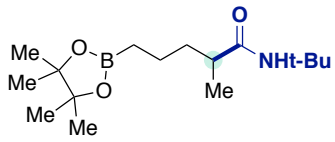

***N*-(*tert*-butyl)-2-methyl-5-(4,4,5,5-tetramethyl-1,3,2-dioxaborolan-2-yl)pentanamide (3.29u).** Following general procedure F and starting from 2-(4-bromopentyl)-4,4,5,5-tetramethyl-1,3,2-dioxaborolane (138.5 mg, 0.500 mmol; 1 equiv) and *tert*-butyl isocyanate (86.0 µL, 74.3 mg, 0.750 mmol; 1.50 equiv), compound **3.29u** was obtained as a clear oil (103.4 mg 1st run, 114.6 mg 2nd run, 74% average yield). ^{1}H NMR (300 MHz, $CDCl_3$) δ 5.24 (s, 1H), 2.11 – 1.95 (m, 1H), 1.67 – 1.51 (m, 1H), 1.47 – 1.35 (m, 3H), 1.33 (s, 9H), 1.23 (s, 12H), 1.07 (d, *J* = 6.8 Hz, 3H), 0.81 – 0.71 (m, 2H).^{13}C NMR (101 MHz, $CDCl_3$) δ 83.1, 51.0, 42.1, 37.3, 29.0, 25.0, 24.7, 21.9, 17.9. ppm. ^{11}B NMR (160 MHz, $CDCl_3$) δ 34.12 ppm. IR (neat, cm^{-1}): 3320, 2973, 2931, 1648, 1542, 1453, 1370, 1318, 1145. HRMS (ESI$^+$) [$C_{16}H_{32}NNaO_3{}^{10}B$] (M+Na) calcd. 319.2404, found 319.2403.

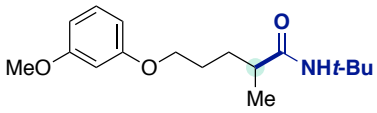

***N*-(*tert*-butyl)-5-(3-methoxyphenoxy)-2-methylpentanamide (3.29v).** Following general procedure F and starting from 1-((4-bromopentyl)oxy)-3-methoxybenzene (136.6 mg, 0.500 mmol; 1 equiv) and *tert*-butyl isocyanate (86.0 µL, 74.3 mg, 0.750 mmol; 1.50 equiv), compound **3.29v** was obtained as a colorless solid (107.1 mg 1st run, 114.2 mg 2nd run, 75% average yield). m.p.: 72.9 – 69.9 °C. ^{1}H NMR (500 MHz, $CDCl_3$) δ 7.17 (t, *J* = 8.2 Hz, 1H, *Ar*), 6.53 – 6.46 (m, 2H, *Ar*), 6.45 (t, *J* = 2.3 Hz, 1H, *Ar*), 5.31 (s, 1H, *NH*), 4.02 – 3.95 (m, 1H, *CH*$_2$–*O*), 3.95 – 3.88 (m, 1H, *CH*$_2$–*O*), 3.79 (s, 3H, *OCH*$_3$), 2.16 – 2.10 (m, 1H, *CH–C=O*), 1.82 – 1.72 (m, 3H, *CH*$_2$), 1.59 – 1.50 (m, 1H, *CH*$_2$), 1.35 (s, 9H, *t-Bu*), 1.13 (d, *J* = 6.8 Hz, 3H, *CH*$_3$) ppm. ^{13}C NMR (126 MHz, $CDCl_3$) δ 175.7, 161.0, 160.3, 130.0, 106.8, 106.4, 101.1, 68.2, 55.4, 51.2, 42.1, 31.3, 29.0, 27.3, 18.3 ppm. IR (neat, cm^{-1}): 3322, 2964, 2873, 1649, 1594, 1493, 1453, 1151, 1046. HRMS (ESI$^+$) [$C_{17}H_{27}NNaO_3$] (M+Na) calcd. 316.1883, found 316.1870.

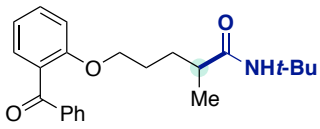

5-(2-benzoylphenoxy)-*N*-(*tert*-butyl)-2-methylpentanamide (3.29w). Following general procedure F and starting from (2-((4-bromopentyl)oxy)phenyl)(phenyl)methanone (173.6 mg, 0.500 mmol; 1 equiv) and *tert*-butyl isocyanate (86.0 µL, 74.3 mg, 0.750 mmol; 1.50 equiv), compound **3.29w** was obtained as a clear oil (103.7 mg, 56%). The branched amide was isolated along with the linear product (22 mg, 6% yield). ^{1}H NMR (500 MHz, $CDCl_3$) δ 7.79 (dd, *J* = 8.4, 1.3 Hz, 2H, *Ar*), 7.58 – 7.50 (m, 1H, *Ar*), 7.47 – 7.40 (m, 3H, *Ar*), 7.37 (dd, *J* = 7.5, 1.7 Hz, 1H, *Ar*), 7.03 (td, *J* = 7.5, 0.9 Hz, 1H, *Ar*), 6.95 (d, *J* = 8.1 Hz, 1H, *Ar*), 5.46 (s, 1H, *NH*), 4.01 – 3.92 (m, 1H, *CH*$_2$–*O*), 3.91 – 3.82 (m, 1H, *CH*$_2$–*O*), 2.01 – 1.93 (m, 1H, *CH–C=O*), 1.53 – 1.43 (m, 3H, *CH*$_2$), 1.28 (s, 9H, *t-Bu*), 1.15 – 1.07 (m, 1H, *CH*$_2$), 0.93 (d, *J* = 6.9 Hz, 3H, *CH*$_3$) ppm. ^{13}C NMR (126 MHz, $CDCl_3$) δ 197.0, 175.8, 157.0, 138.3, 133.0, 132.2, 129.9, 129.9, 129.0, 128.4, 120.6, 112.4, 68.7, 51.1, 41.6, 31.2, 28.9, 26.6, 18.2 ppm. IR (neat, cm^{-1}): 3329, 2965, 2873, 1650, 1598, 1450, 1243, 752, 702. HRMS (ESI$^+$) [$C_{23}H_{29}NNaO_3$] (M+Na) calcd. 390.2040, found 390.2037.

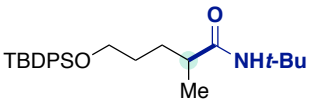

***N*-(*tert*-butyl)-5-((tert-butyldiphenylsilyl)oxy)-2-methylpentanamide (3.29x).** Following general procedure F and starting from ((4-bromopentyl)oxy)(tert-butyl)diphenylsilane (202.7 mg, 0.500 mmol; 1 equiv) and *tert*-butyl isocyanate (86.0 µL, 74.3 mg, 0.750 mmol; 1.50 equiv), compound **3.29x** was obtained as a colorless solid (121.5 mg, 57%). m.p.: 105.1 – 106.4 °C. ^{1}H NMR (300 MHz, $CDCl_3$) δ 7.69 – 7.62 (m, 4H, *Ar*), 7.44 – 7.34 (m, 6H, *Ar*), 5.16 (s, 1H, *NH*), 3.66 (t, *J* = 6.0 Hz, 2H, *CH*$_2$–*O*), 2.09 – 1.96 (m, 1H, *CH*$_2$–*C=O*), 1.71 – 1.49 (m, 4H, *CH*$_2$), 1.32

(s, 9H, *t-Bu*), 1.08 (d, *J* = 6.8 Hz, 3H, *CH₃*), 1.05 (s, 9H, *t-Bu*) ppm. ^{13}C NMR (101 MHz, $CDCl_3$) δ 175.9, 135.7, 134.2, 134.1, 129.7, 127.8, 64.0, 51.1, 42.0, 31.0, 30.4, 29.0, 27.1, 19.4, 18.1 ppm. IR (neat, cm^{-1}): 3270, 2960, 2928, 2854, 1640, 1556, 1263, 1082, 702, 503. HRMS (ESI$^+$) [$C_{26}H_{39}NNaO_2Si$] (M+Na) calcd. 448.2642, found 448.2650.

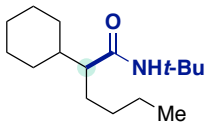

Methyl 4-(*tert*-butylcarbamoyl)hexanoate (3.29y). Following general procedure F, and starting from methyl 4-bromohexanoate (104.5 mg, 0.500 mmol; 1 equiv) and *tert*-butyl isocyanate (86.0 µL, 74.3 mg, 0.750 mmol; 1.50 equiv), compound **3.29y** was obtained as a colorless solid (58.9 mg, 51%). No difference was observed when using the double amount of tert-butyl isocyanate (172 µL, 149 mg, 1.5 mmol; 3.0 equiv) and increasing the Mn loading (55 mg, 1.0 mmol; 2 equiv) as 56.9 mg of compound **3.29y** were isolated. Alternatively, if under these later conditions, 6-methyl-2,2'-bipyridine was used as ligand (4.3 mg, 0.025, 5.0 mol%), 37.9 mg (33%) of compound **3.29y** were obtained. When general procedure E was followed, 32.5 mg (28%) of compound **3.29y** were isolated. m.p.: 45.8 – 48.2 °C. ^{1}H NMR (500 MHz, $CDCl_3$) δ 5.39 (s, 1H, *NH*), 3.67 (s, 3H, *OCH₃*), 2.41 – 2.33 (m, 1H, *CH₂*), 2.31 – 2.23 (m, 1H, *CH₂*), 1.94 – 1.80 (m, 2H, *CH + CH₂*), 1.77 – 1.68 (m, 1H, *CH₂*), 1.67 – 1.56 (m, 1H, *CH₂*), 1.46 – 1.37 (m, 1H, *CH₂*), 1.35 (s, 9H, *t-Bu*), 0.89 (t, *J* = 7.4 Hz, 3H, *CH₃*) ppm. ^{13}C NMR (101 MHz, $CDCl_3$) δ 174.3, 174.1, 51.7, 51.4, 49.0, 31.9, 29.0, 28.1, 26.2, 12.2 ppm. IR (neat, cm^{-1}): 3325, 2964, 2930, 2875, 1736, 1649, 1536, 1454, 1207. HRMS (ESI$^+$) [$C_{12}H_{23}NNaO_3$] (M+Na) calcd. 252.1570, found 252.1567.

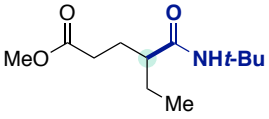

***N*-(*tert*-butyl)-2-cyclohexylhexanamide (3.29az).** Following general procedure F slightly modified, and starting from (1-bromopentyl)cyclohexane (116.6 mg, 0.500 mmol; 1 equiv) and *tert*-butyl isocyanate **3.29ab** (172 µL, 149 mg, 1.5 mmol; 3 equiv) and Mn (82.4 mg, 1.5 mmol; 3 equiv), compound **3.29ab** was obtained as a colorless solid (79.4 mg, 63%). When general procedure E was followed, 47.4 mg (37%) of compound **3.29az** were isolated. m.p.: 173.2 – 175.6 °C. ^{1}H-NMR (400 MHz, $CDCl_3$) δ 5.17 (s, 1H, *NH*), 1.86 – 1.77 (m, 1H, *CH–C=O*), 1.73 – 1.60 (m, 4H, *CH₂*), 1.56 – 1.40 (m, 3H *CH₂*), 1.35 (s, 9H, *t-Bu*), 1.33 – 1.07 (m, 8H, *CH₂*), 0.98 – 0.83 (m, 2H, *CH₂*), 0.87 (t, *J* = 7.2 Hz, 3H, *CH₃*) ppm. ^{13}C NMR (101 MHz, $CDCl_3$) δ 174.8, 55.3, 51.3, 40.5, 31.5, 31.1, 30.2, 29.8, 29.1, 26.7, 26.6, 26.5, 23.0, 14.2 ppm. IR (neat, cm^{-1}): 3299, 2922, 2852, 1638, 1544, 1499, 1360, 1227, 733. HRMS (ESI$^+$) [$C_{16}H_{31}NNaO$] (M+Na) calcd. 276.2298, found 276.2296.

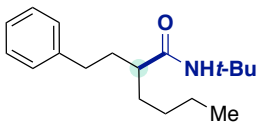

***N*-(*tert*-butyl)-2-phenethylhexanamide (3.29aa).** Following general procedure F and starting from (3-bromoheptyl)benzene (127.6 mg, 0.500 mmol; 1 equiv) and *tert*-butyl isocyanate (86.0 µL, 74.3 mg, 0.750 mmol; 1.50 equiv), compound **3.29ab** was obtained as a colorless solid (117.1 mg 1st run, 120.3 mg 2nd run, 86% average yield). m.p.: 103.6 – 104.8 °C. ^{1}H NMR (400 MHz, $CDCl_3$) δ 7.32 – 7.26 (m, 2H, *Ar*), 7.22 – 7.15 (m, 3H, *Ar*), 5.16 (s, 1H, *NH*), 2.75 – 2.62 (m, 1H, *CH₂*), 2.58 – 2.45 (m, 1H, *CH₂*), 2.01 – 1.88 (m, 1H, *CH₂*), 1.88 – 1.79 (m, 1H, *CH₂*), 1.75 – 1.64 (m, 1H, *CH₂*), 1.64 – 1.55 (m, 1H, *CH₂*), 1.37 (s, 9H, *t-Bu*), 1.43 – 1.14 (m, 5H, *CH₂*), 0.87 (t, *J* = 7.0 Hz, 3H, *CH₃*) ppm. ^{13}C NMR (101 MHz, $CDCl_3$) δ 174.9, 142.1, 128.6, 128.5, 126.0, 51.3, 48.0, 34.6, 33.8, 33.1, 29.9, 29.1, 22.9, 14.2 ppm. IR (neat, cm^{-1}): 3297, 2957, 2929, 2857, 1639, 1551, 1454, 1227, 696. HRMS (ESI$^+$) [$C_{18}H_{29}NNaO$] (M+Na) calcd. 298.2141, found 298.2137.

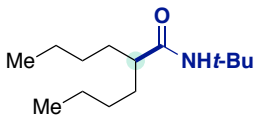

***N*-(*tert*-butyl)-2-butylhexanamide (3.29ab).** Following general procedure F and starting from 5-bromononane (103.6 mg, 0.500 mmol; 1 equiv) and *tert*-butyl isocyanate (86.0 µL, 74.3 mg, 0.750 mmol; 1.50 equiv), compound **3.29ab** was obtained as a colorless solid (91.1 mg 1st run, 95.0 mg 2nd run, 82% average yield). Alternatively, if 6-methyl-2,2'-bipyridine was used as ligand (4.3 mg, 0.025, 5.0 mol%), 60.5 mg (53%) of compound **3.29ab** were obtained. When general procedure E was followed, 48.4 mg (43%) of compound **3.29ab** were isolated. m.p.:

109.3 – 111.9 °C. ^{1}H-NMR (400 MHz, $CDCl_3$) δ 5.20 (s, 1H, *NH*), 1.88 – 1.76 (m, 1H, *CH–C=O*), 1.61 – 1.49 (m, 2H, CH_2), 1.35 (s, 9H, *t-Bu*), 1.40 – 1.14 (m, 10H, CH_2), 0.88 (t, *J* = 7.0 Hz, 6H, CH_3) ppm. ^{13}C NMR (101 MHz, $CDCl_3$) δ 175.5, 51.2, 49.0, 33.1, 30.0, 29.1, 22.9, 14.2 ppm. IR (neat, cm^{-1}): 3297, 2956, 2929, 2857, 1640, 1551, 1360, 1227, 732. HRMS (ESI$^+$) [$C_{14}H_{29}NNaO$] (M+Na) calcd. 250.2141, found 250.2139.

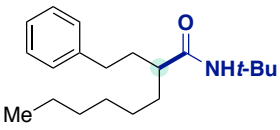

***N*-(tert-butyl)-2-phenethyloctanamide (3.29m).** Following general procedure F and starting from (3-bromononyl)benzene (141.6 mg, 0.500 mmol; 1 equiv) and *tert*-butyl isocyanate (86.0 µL, 74.3 mg, 0.750 mmol; 1.50 equiv), compound **3.29am** was obtained as a colorless solid (131.7 mg, 87%). Alternatively, if 6-methyl-2,2'-bipyridine was used as ligand (4.3 mg, 0.025, 5.0 mol%), 94.6 mg (62%) of compound **3.29am** were obtained. When general procedure E was followed, 45.9 mg (30%) of compound **3.29am** were isolated. m.p.: 72.8 – 74.6 °C. ^{1}H-NMR (500 MHz, $CDCl_3$) δ 7.31 – 7.25 (m, 2H, *Ar*), 7.22 – 7.15 (m, 3H, *Ar*), 5.16 (s, 1H, *NH*), 2.73 – 2.63 (m, 1H, CH_2), 2.56 – 2.47 (m, 1H, CH_2), 1.99 – 1.88 (m, 1H, CH_2), 1.88 – 1.80 (m, 1H, CH_2), 1.74 – 1.64 (m, 1H, CH_2), 1.64 – 1.54 (m, 1H, CH_2), 1.37 (s, 9H, *t-Bu*), 1.42 – 1.32 (m, 1H, CH_2), 1.31 – 1.15 (m, 8H, CH_2), 0.87 (t, J = 7.0 Hz, 3H, CH_3) ppm. ^{13}C NMR (126 MHz, $CDCl_3$) δ 174.9, 142.1, 128.6, 128.5, 126.0, 51.3, 48.0, 34.6, 33.8, 33.4, 31.9, 29.5, 29.1, 27.7, 22.7, 14.2 ppm. IR (neat, cm^{-1}): 3312, 2958, 2926, 2855, 1641, 1542, 1454, 1360, 1226, 697. HRMS (ESI$^+$) [$C_{20}H_{33}NNaO$] (M+Na) calcd. 326.2454, found 326.2442.

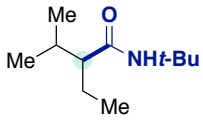

***N*-(*tert*-butyl)-2-ethyl-3-methylbutanamide (3.29ac).** Following general procedure F and starting from 3-bromo-2-methylpentane (82.5 mg, 0.500 mmol; 1 equiv) and *tert*-butyl isocyanate (86.0 µL, 74.3 mg, 0.750 mmol; 1.50 equiv), compound **3.29ac** was obtained as a colorless solid (42.0 mg, 45%). m.p.: 136.8 – 138.5 °C. ^{1}H-NMR (500 MHz, $CDCl_3$) δ 5.21 (s, 1H, *NH*), 1.82 – 1.71 (m, 1H, *CH*), 1.58 – 1.49 (m, 2H, CH_2), 1.47 – 1.40 (m, 1H, CH_2), 1.36 (s, 9H, *t-Bu*), 0.92 (d, *J* = 3.7 Hz, 3H, CH_3), 0.91 (d, *J* = 3.6 Hz, 3H, CH_3), 0.87 (t, *J* = 7.3 Hz, 3H, CH_3) ppm. ^{13}C NMR (126 MHz, $CDCl_3$) δ 174.8, 58.0, 51.3, 31.0, 29.1, 23.6, 21.2, 20.7, 12.5 ppm. IR (neat, cm^{-1}): 3302, 2962, 2929, 2873, 1640, 1544, 1453, 1359, 1226. HRMS (ESI$^+$) [$C_{11}H_{23}NNaO$] (M+Na) calcd. 208.1672, found 208.1668.

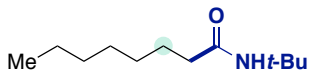

***N*-(*tert*-butyl)octanamide (3.29ak)** Following procedure G and starting from 2-bromoheptane (89.6 mg, 0.500 mmol; 1 equiv) and *tert*-butyl isocyanate (86.0 µL, 74.3 mg, 0.750 mmol; 1.50 equiv), compound **3.29ak** was obtained as a pale-yellow oil (71.8 mg, 72% yield). ^{1}H-NMR (400 MHz, $CDCl_3$) δ 5.26 (s, 1H, *NH*), 2.07 (d, *J* = 7.5 Hz, 2H, CH_2), 1.58 (p, *J* = 7.0 Hz, 2H, CH_2), 1.33 (s, 9H, *t-Bu*), 1.32 – 1.21 (m, 8H, CH_2 x 4), 0.86 (t, *J* = 6.7 Hz, 3H, CH_3) ppm. ^{13}C-NMR (101 MHz, $CDCl_3$) δ 172.7, 51.2, 37.9, 31.8, 29.3, 29.2, 29.0, 25.9, 22.7, 14.2 ppm.

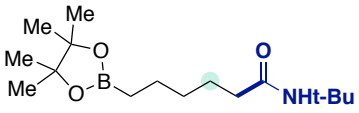

***N*-(*tert*-butyl)-6-(4,4,5,5-tetramethyl-1,3,2-dioxaborolan-2-yl)hexanamide (3.29ag).** Following procedure G and starting from 2-(4-bromopentyl)-4,4,5,5-tetramethyl-1,3,2-dioxaborolane (139 mg, 0.500 mmol; 1 equiv) and *tert*-butyl isocyanate (86.0 µL, 74.3 mg, 0.750 mmol; 1.50 equiv), compound **3.29ag** was obtained as clear oil (31.2 mg, 21% yield). ^{1}H-NMR (400 MHz, $CDCl_3$) δ 5.28 (s, 1H, *NH*), 2.06 (t, *J* = 7.7 Hz, 2H, CH_2), 1.58 (p, *J* = 7.5 Hz, 2H, CH_2), 1.49 – 1.36 (m, 2H, CH_2), 1.36 – 1.27 (m, 11H, *t-Bu*, CH_2), 1.22 (s, 12H, CH_3 x 4), 0.75 (t, *J* = 7.7 Hz, 2H, CH_2) ppm. ^{13}C-NMR (101 MHz, $CDCl_3$) δ 172.8, 83.0, 51.2, 37.8, 32.1, 29.0, 25.8, 24.9, 23.9 ppm. ^{11}B NMR (128 MHz, $CDCl_3$) δ 34.23 ppm.

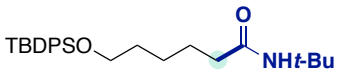

***N*-(*tert*-butyl)-7-((*tert*-butyldiphenylsilyl)oxy)hexanamide (3.29ah).** Following procedure G and starting from ((5-bromopentyl)oxy)(tert-butyl)diphenylsilane (203 mg, 0.500 mmol; 1 equiv) and *tert*-butyl isocyanate (86.0 µL, 74.3 mg, 0.750 mmol; 1.50 equiv), compound **3.29ah** was obtained along with an unknown impurity (43.9 mg, <35% yield of desired product).

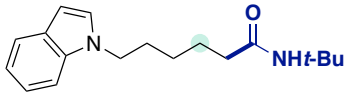

***N*-(*tert*-butyl)-6-(1*H*-indol-1-yl)hexanamide (3.29ai).** Following procedure G and starting from 1-(4-bromopentyl)-1H-indole (133 mg, 0.500 mmol; 1 equiv) and *tert*-butyl isocyanate (86.0 µL, 74.3 mg, 0.750 mmol; 1.50 equiv), compound **3.29ai** was obtained as a red solid (93.0 mg, 65%). m.p. 85 – 87 °C. ^{1}H-NMR (300 MHz, $CDCl_3$) δ 7.62 (dt, *J* = 7.8, 0.9 Hz, 1H, *Ar*), 7.33 (dd, *J* = 8.2, 1.0 Hz, 1H, *Ar*), 7.19 (ddd, *J* = 8.2, 7.0, 1.2 Hz, 1H, *Ar*), 7.12 – 7.06 (m, 2H, *Ar*), 6.48 (dd, *J* = 3.1, 0.9 Hz, 1H, *Ar*), 5.13 (s, 1H, *NH*), 4.13 (t, *J* = 7.0 Hz, 2H, CH_2), 2.03 (t, *J* = 7.4 Hz, 2H, CH_2), 1.92 – 1.79 (m, 2H, CH_2), 1.69 – 1.56 (m, 2H, CH_2), 1.39 – 1.27 (m, 11H, *t-Bu*, CH_2) ppm. ^{13}C-NMR (101 MHz, $CDCl_3$) δ 172.1, 136.0, 128.6, 127.9, 121.4, 121.0, 119.2, 109.4, 101.0, 51.1, 46.2, 37.3, 30.0, 28.9, 26.5, 25.3 ppm. IR (neat, cm^{-1}): 3276, 3080, 2959, 2935, 2857, 1366, 1555, 1455,

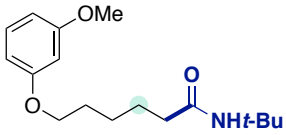

***N*-(*tert*-butyl)-6-(3-methoxyphenoxy)hexanamide (3.29aj).** Following procedure G and starting from 1-((4-bromopentyl)oxy)-3-methoxybenzene (137 mg, 0.500 mmol; 1 equiv) and *tert*-butyl isocyanate (86.0 µL, 74.3 mg, 0.750 mmol; 1.50 equiv), compound **3.29aj** was obtained as a pale-yellow oil (83.6 mg, 57%). ^{1}H-NMR (300 MHz, $CDCl_3$) δ 7.16 (t, *J* = 8.1 Hz, 1H, *Ar*), 6.53 – 6.41 (m, 3H, *Ar*), 5.29 (s, 1H, *NH*), 3.94 (t, *J* = 6.4 Hz, 2H, CH_2), 3.78 (s, 3H, OCH_3), 2.12 (t, *J* = 7.4 Hz, 2H, CH_2), 1.85 – 1.61 (m, 4H, CH_2 x 2), 1.56 – 1.42 (m, 2H, CH_2), 1.34 (s, 9H, *t-Bu*) ppm. ^{13}C-NMR (101 MHz, $CDCl_3$) δ 172.6, 161.0, 160.4, 130.0, 106.8, 106.3, 101.1, 67.8, 55.4, 51.4, 37.6, 29.2, 29.0, 25.8, 25.7 ppm. IR (neat, cm^{-1}): 3313, 29362, 2867, 1645, 1591, 1544, 1492, 1453, 1363, 1285, 1264, 1199, 1149, 1044, 761, 686.

3.9. ^{1}H-NMR and ^{13}C-NMR Spectra

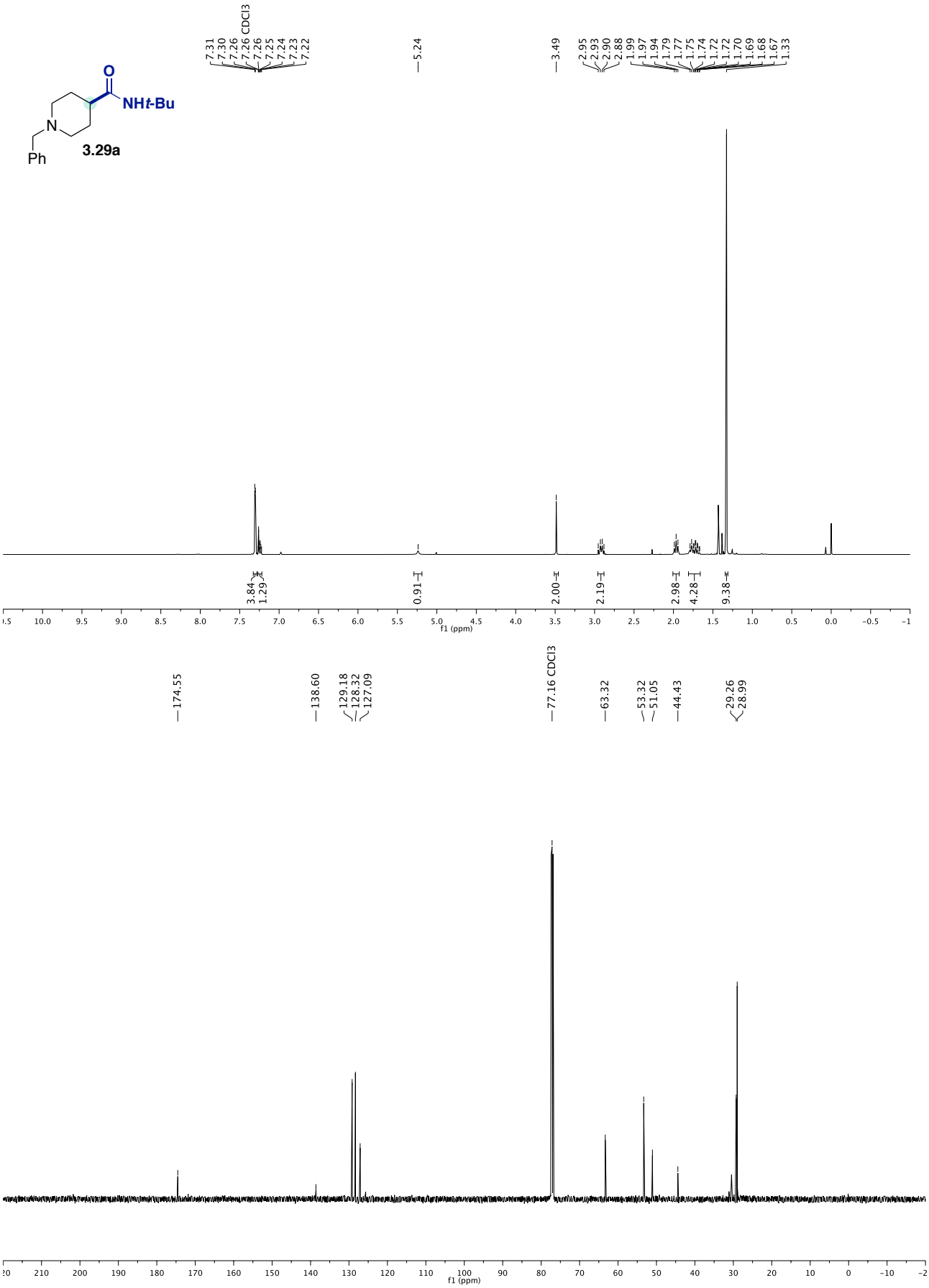

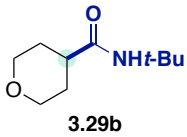
O
NHt-Bu
O

3.29b

7.26 CDCl3
5.30
4.00
3.99
3.99
3.98
3.97
3.97
3.96
3.96
3.40
3.39
3.37
3.36
3.34
3.33
2.24
2.23
2.22
2.20
2.19
2.18
2.16
2.15
1.80
1.79
1.77
1.77
1.76
1.74
1.73
1.71
1.70
1.69
1.69
1.66
1.32
0.91
2.00
1.99
1.03
4.05
9.42
f1 (ppm)

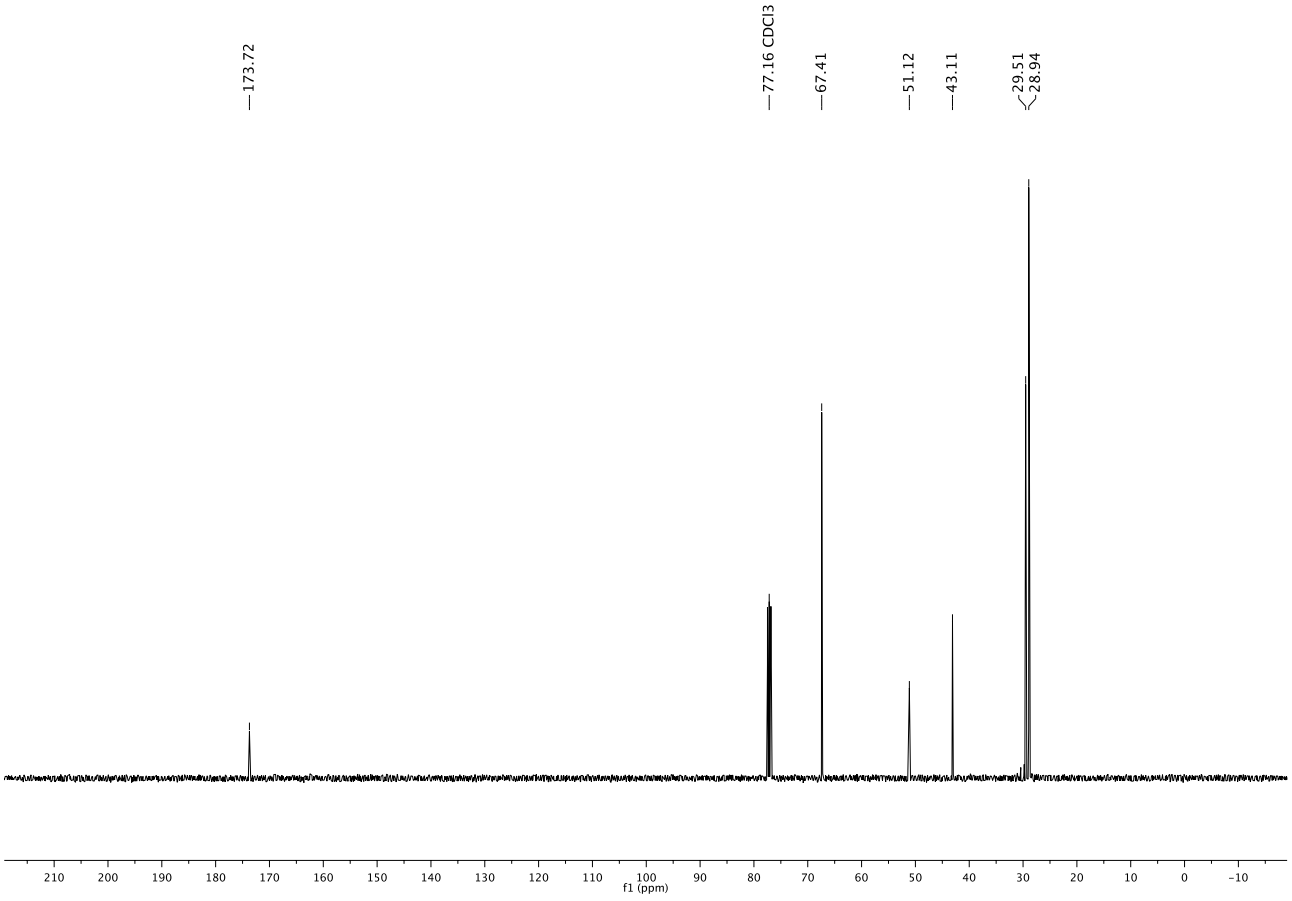
173.72
77.16 CDCl3
67.41
51.12
43.11
29.51
28.94
f1 (ppm)

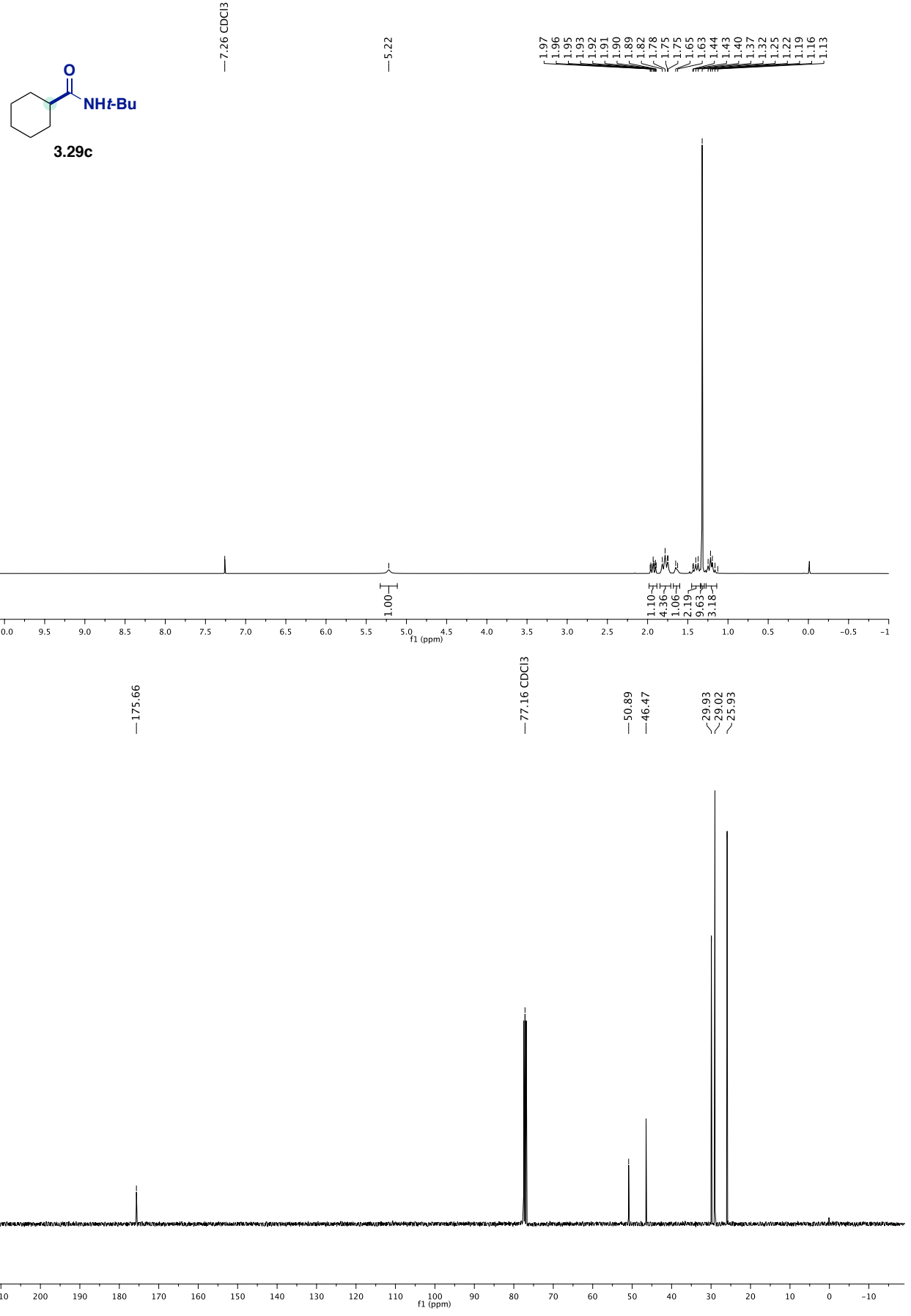
7.26 CDCl3
5.22
1.97
1.96
1.95
1.93
1.92
1.91
1.90
1.89
1.82
1.78
1.75
1.75
1.65
1.63
1.44
1.43
1.40
1.37
1.32
1.25
1.22
1.19
1.16
1.13
O
NHt-Bu
3.29c
1.00
1.10
4.36
1.06
2.19
9.63
3.18
f1 (ppm)
175.66
77.16 CDCl3
50.89
46.47
29.93
29.02
25.93
f1 (ppm)

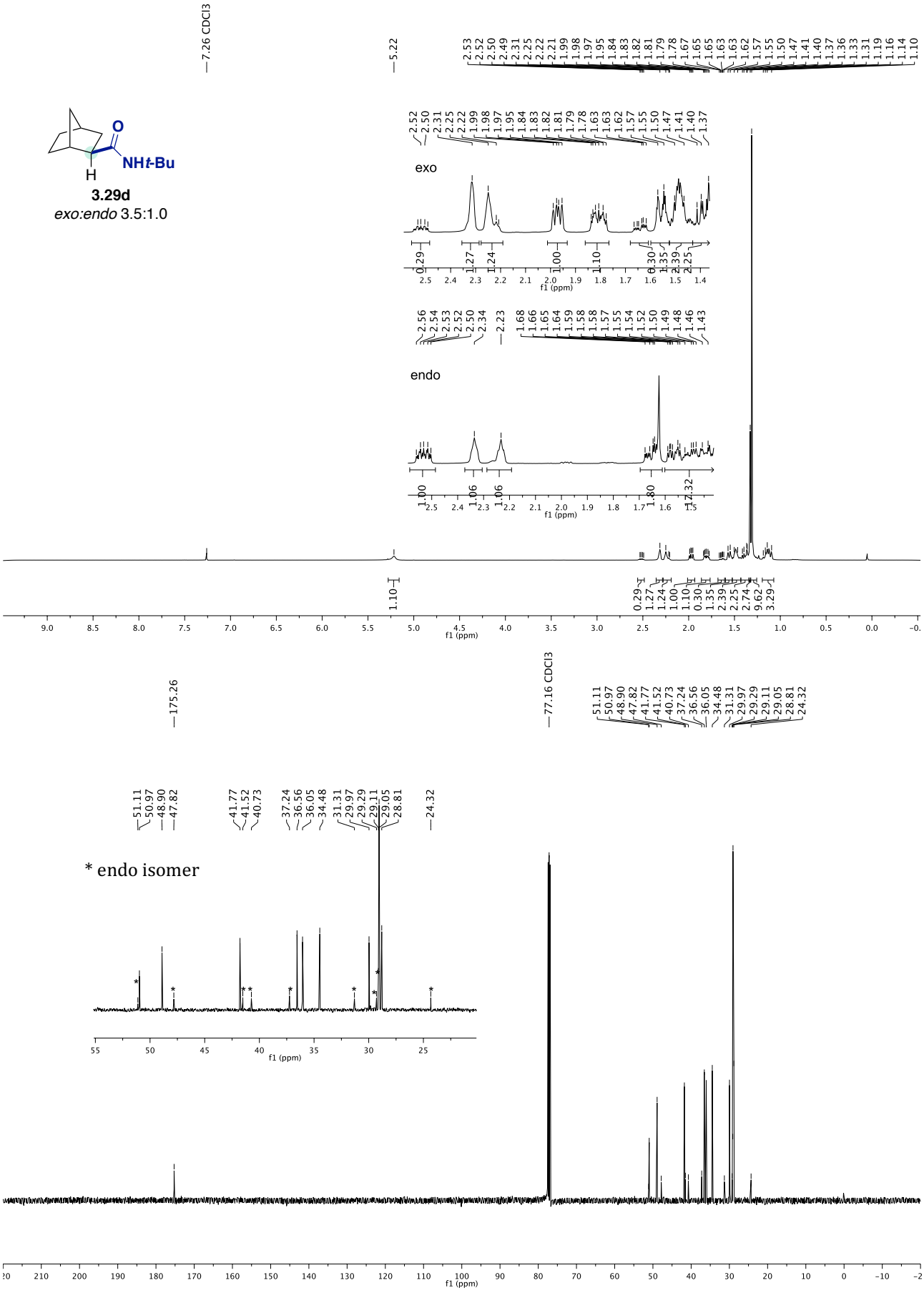
O
NHt-Bu
H
3.29d
exo:endo 3.5:1.0
exo
endo
* endo isomer
f1 (ppm)

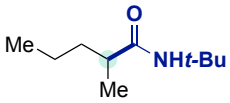
O
Me
NHt-Bu
Me

3.29e

7.26 CDCl3
5.24
2.07
2.05
2.04
2.02
2.00
1.98
1.61
1.58
1.58
1.56
1.54
1.52
1.34
1.32
1.29
1.27
1.26
1.25
1.23
1.08
1.06
0.90
0.88
0.86
1.03
1.00
1.08
9.36
3.17
3.14
3.37
f1 (ppm)

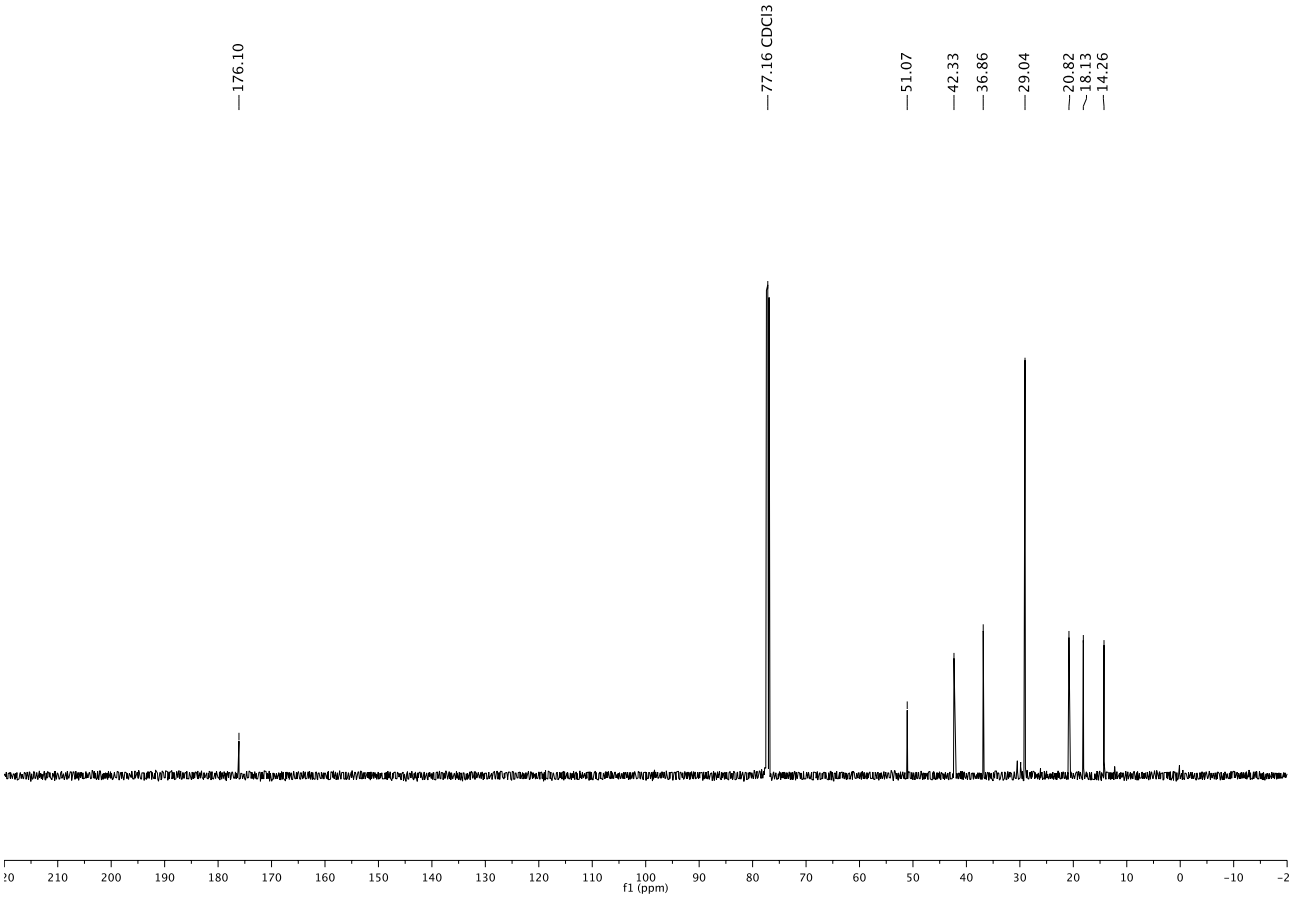
176.10
77.16 CDCl3
51.07
42.33
36.86
29.04
20.82
18.13
14.26
f1 (ppm)

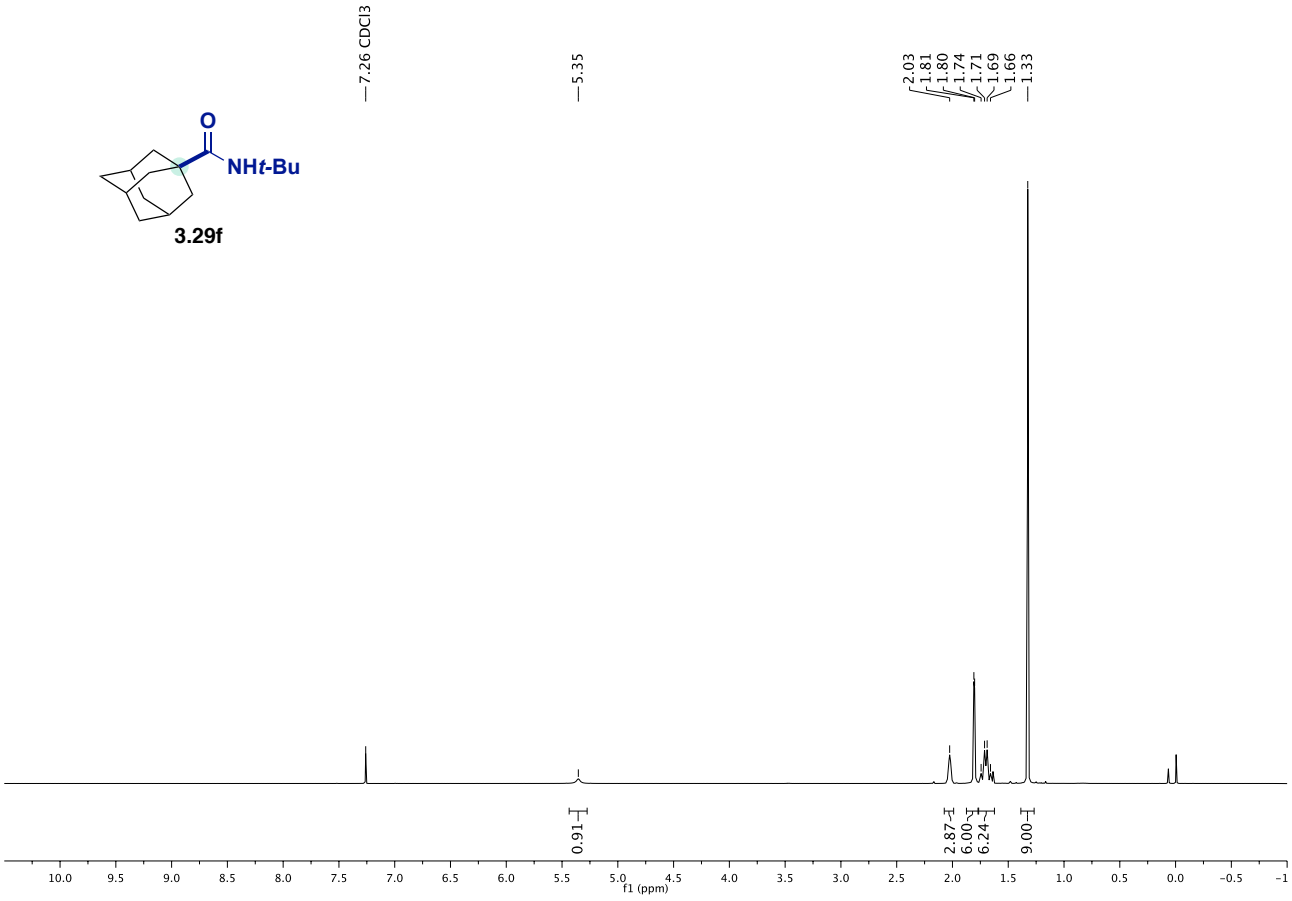
7.26 CDCl3
5.35
2.03
1.81
1.80
1.74
1.71
1.69
1.66
1.33
O
NHt-Bu
3.29f
0.91
2.87
6.00
6.24
9.00
f1 (ppm)

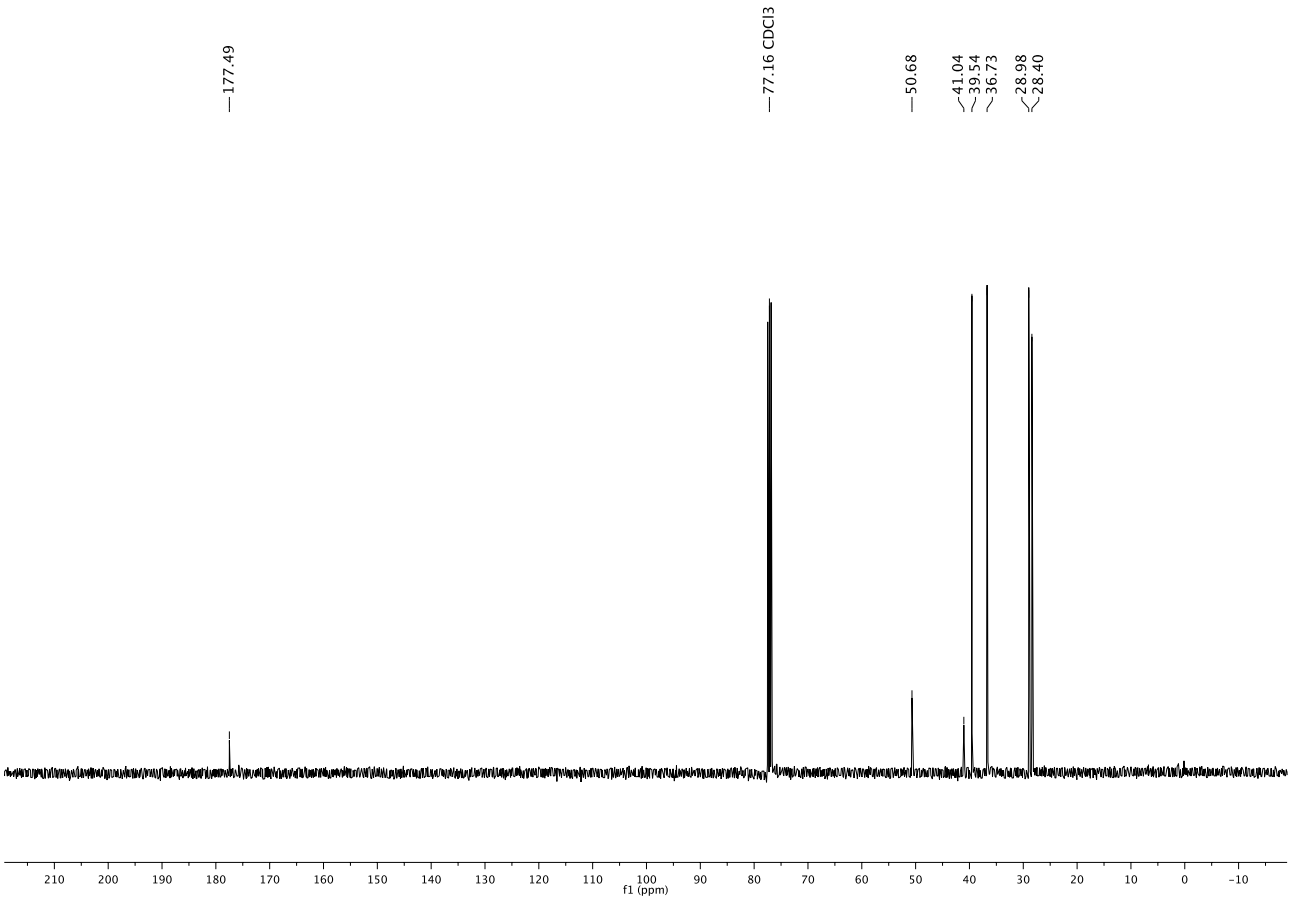
177.49
77.16 CDCl3
50.68
41.04
39.54
36.73
28.98
28.40
f1 (ppm)

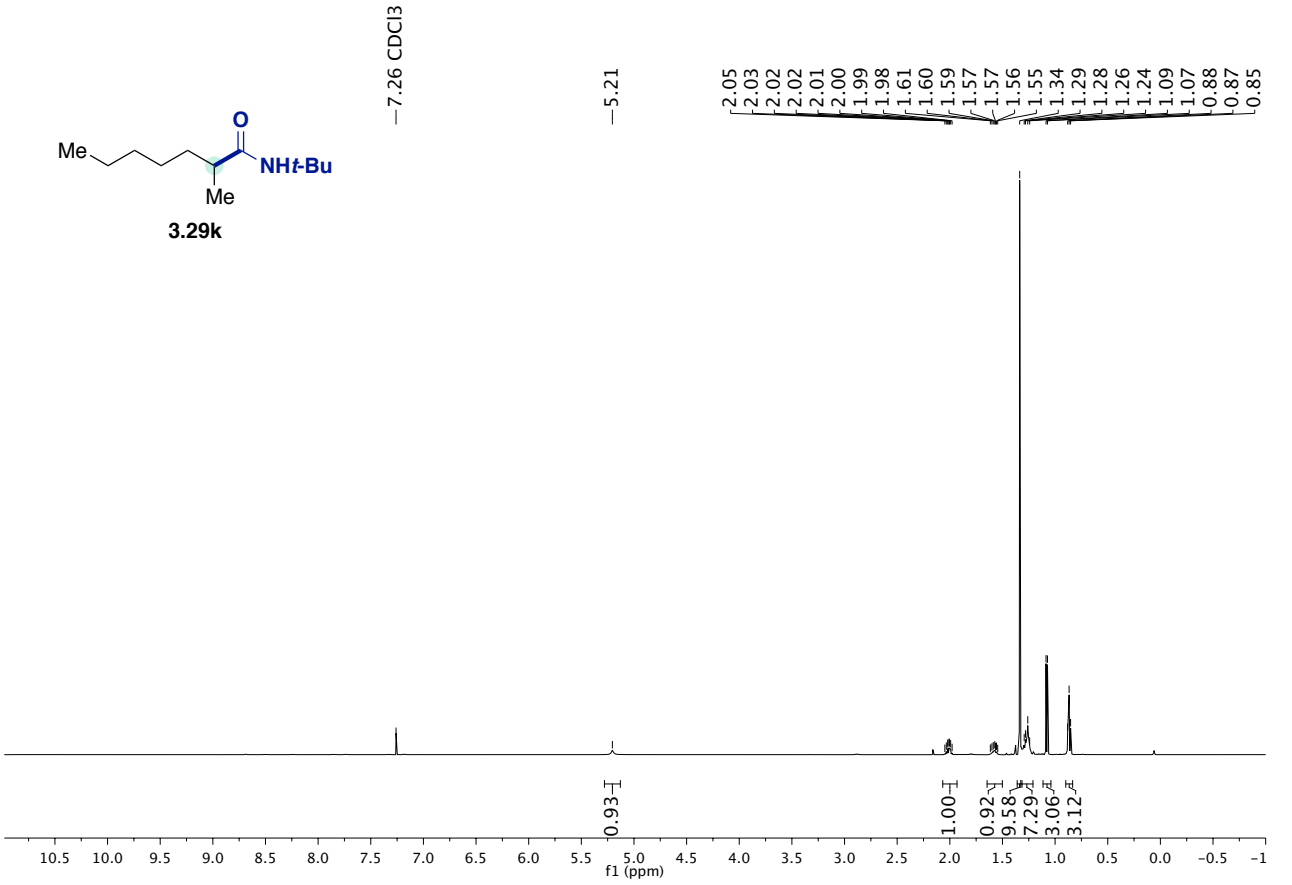
7.26 CDCl3
5.21
2.05
2.03
2.02
2.02
2.01
2.00
1.99
1.98
1.61
1.60
1.59
1.57
1.57
1.56
1.55
1.34
1.29
1.28
1.26
1.24
1.09
1.07
0.88
0.87
0.85
Me
O
NHt-Bu
Me
3.29k
0.93
1.00
0.92
9.58
7.29
3.06
3.12
f1 (ppm)

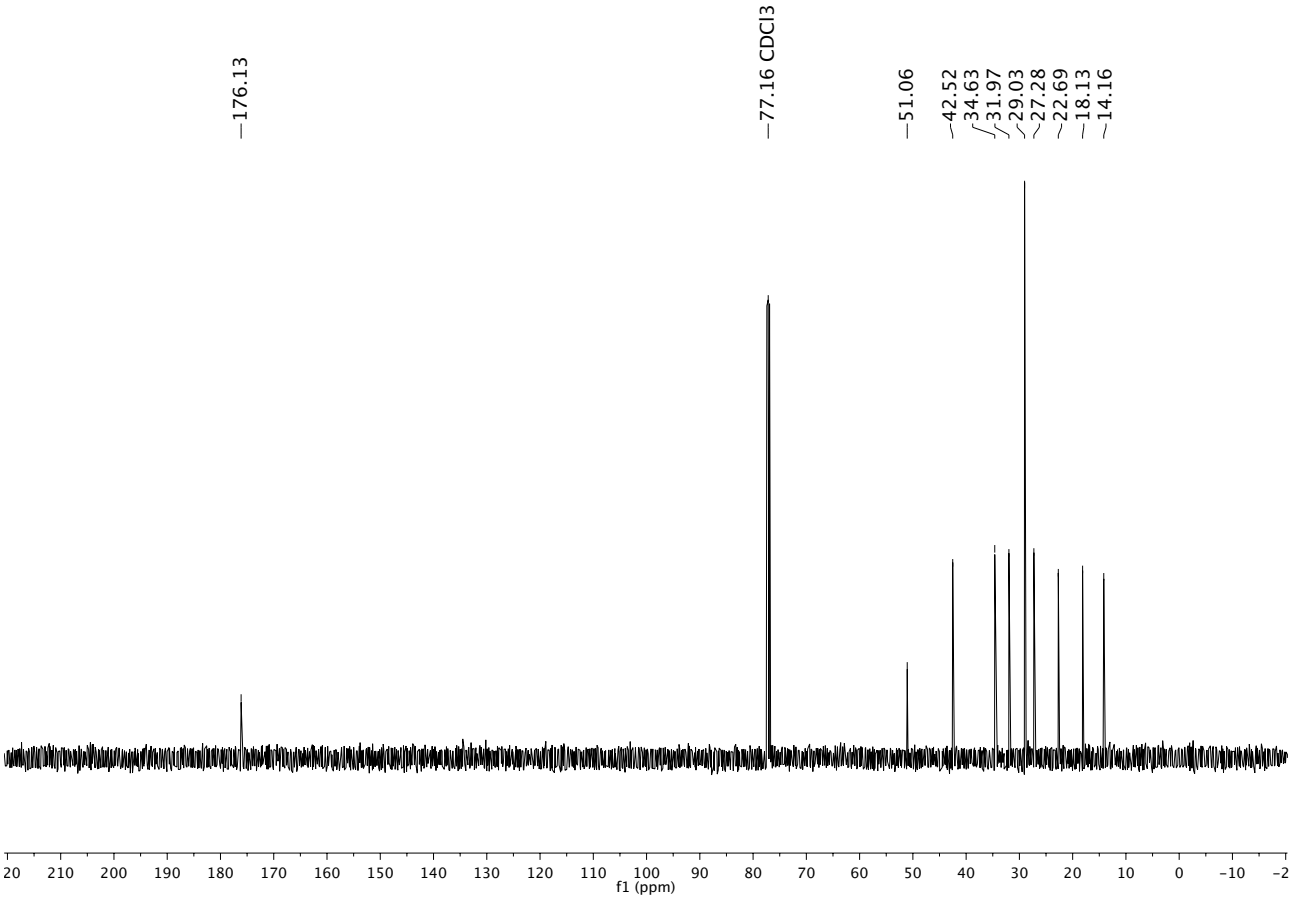
176.13
77.16 CDCl3
51.06
42.52
34.63
31.97
29.03
27.28
22.69
18.13
14.16
f1 (ppm)

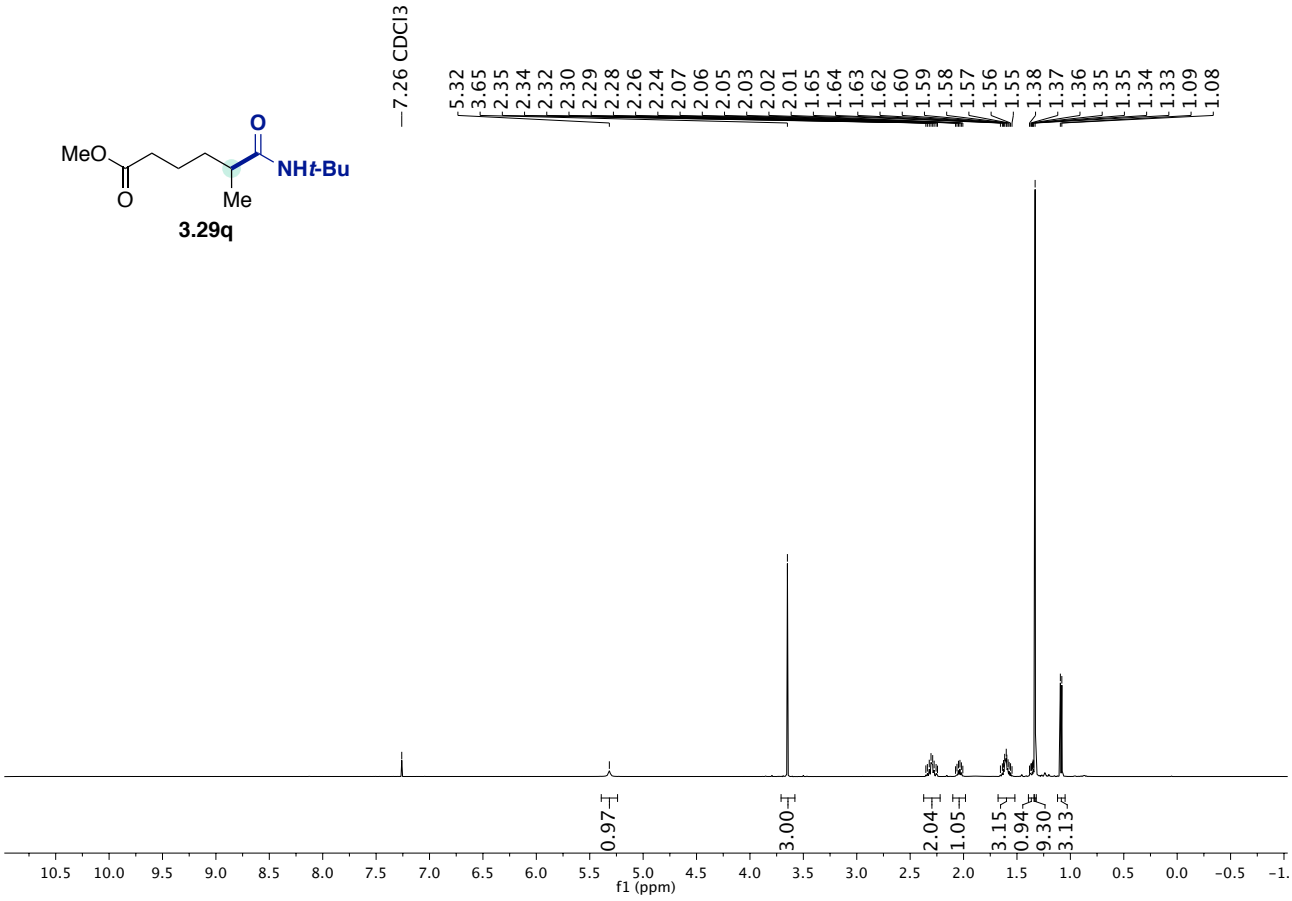
7.26 CDCl3
5.32
3.65
2.35
2.34
2.32
2.30
2.29
2.28
2.26
2.24
2.07
2.06
2.05
2.03
2.02
2.01
1.65
1.64
1.63
1.62
1.60
1.59
1.58
1.57
1.56
1.55
1.38
1.37
1.36
1.35
1.35
1.34
1.33
1.09
1.08
MeO
O
O
NHt-Bu
Me
3.29q
0.97
3.00
2.04
1.05
3.15
0.94
9.30
3.13
f1 (ppm)

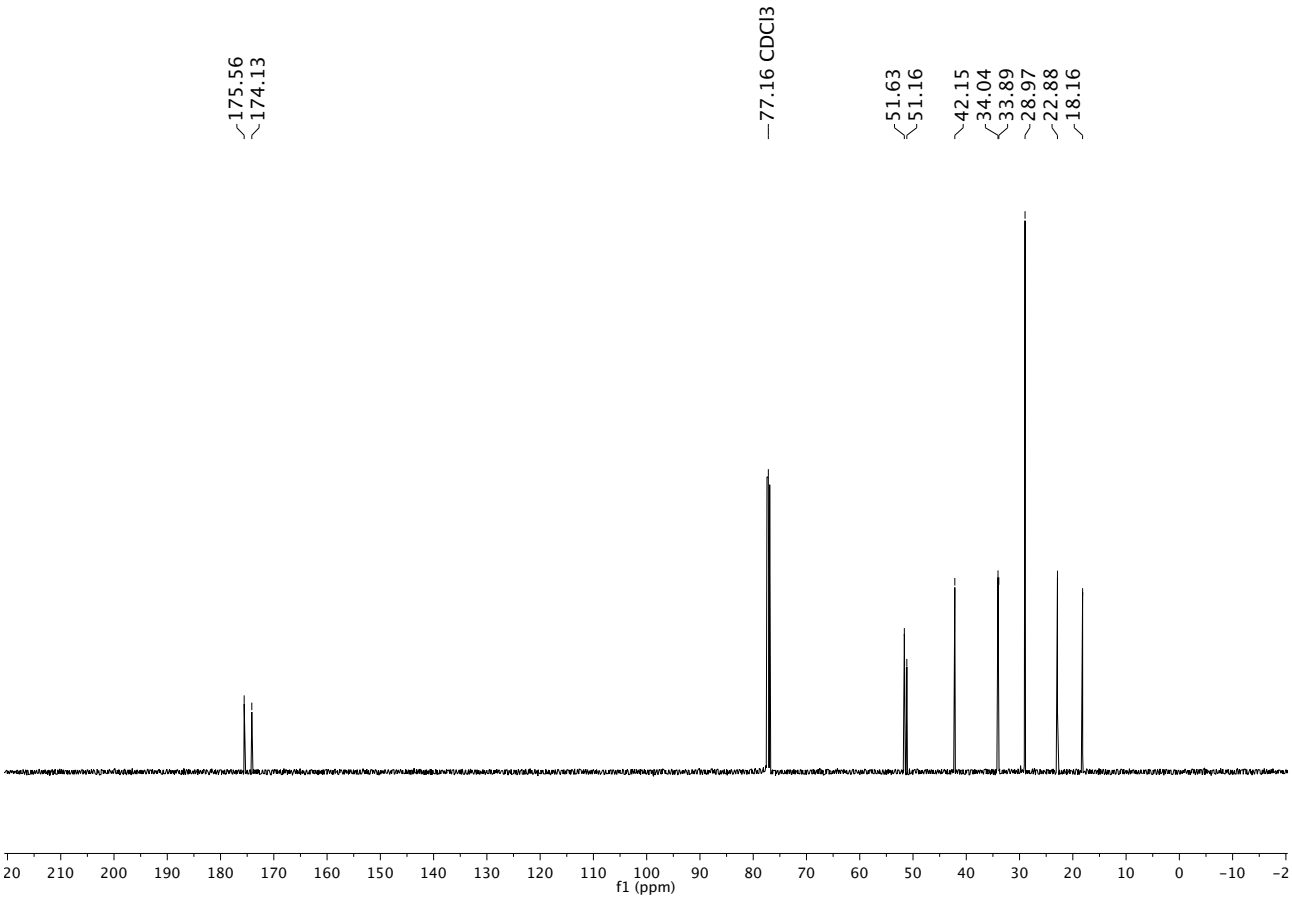
175.56
174.13
77.16 CDCl3
51.63
51.16
42.15
34.04
33.89
28.97
22.88
18.16
f1 (ppm)

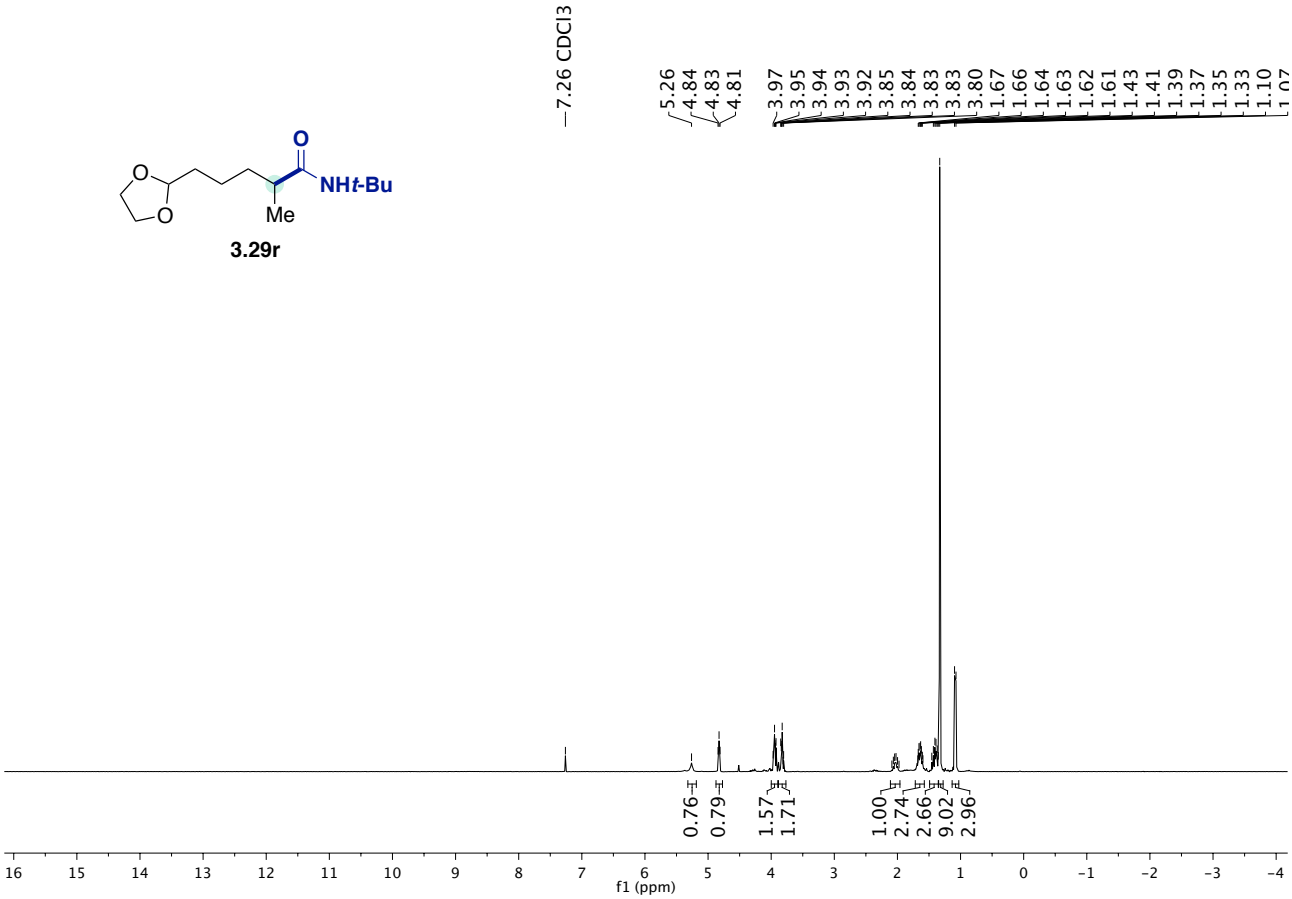
7.26 CDCl3
5.26
4.84
4.83
4.81
3.97
3.95
3.94
3.93
3.92
3.85
3.84
3.83
3.83
3.80
1.67
1.66
1.64
1.63
1.62
1.61
1.43
1.41
1.39
1.37
1.35
1.33
1.10
O
NHt-Bu
Me
O
O
3.29r
0.76
0.79
1.57
1.71
1.00
2.74
2.66
9.02
2.96
f1 (ppm)

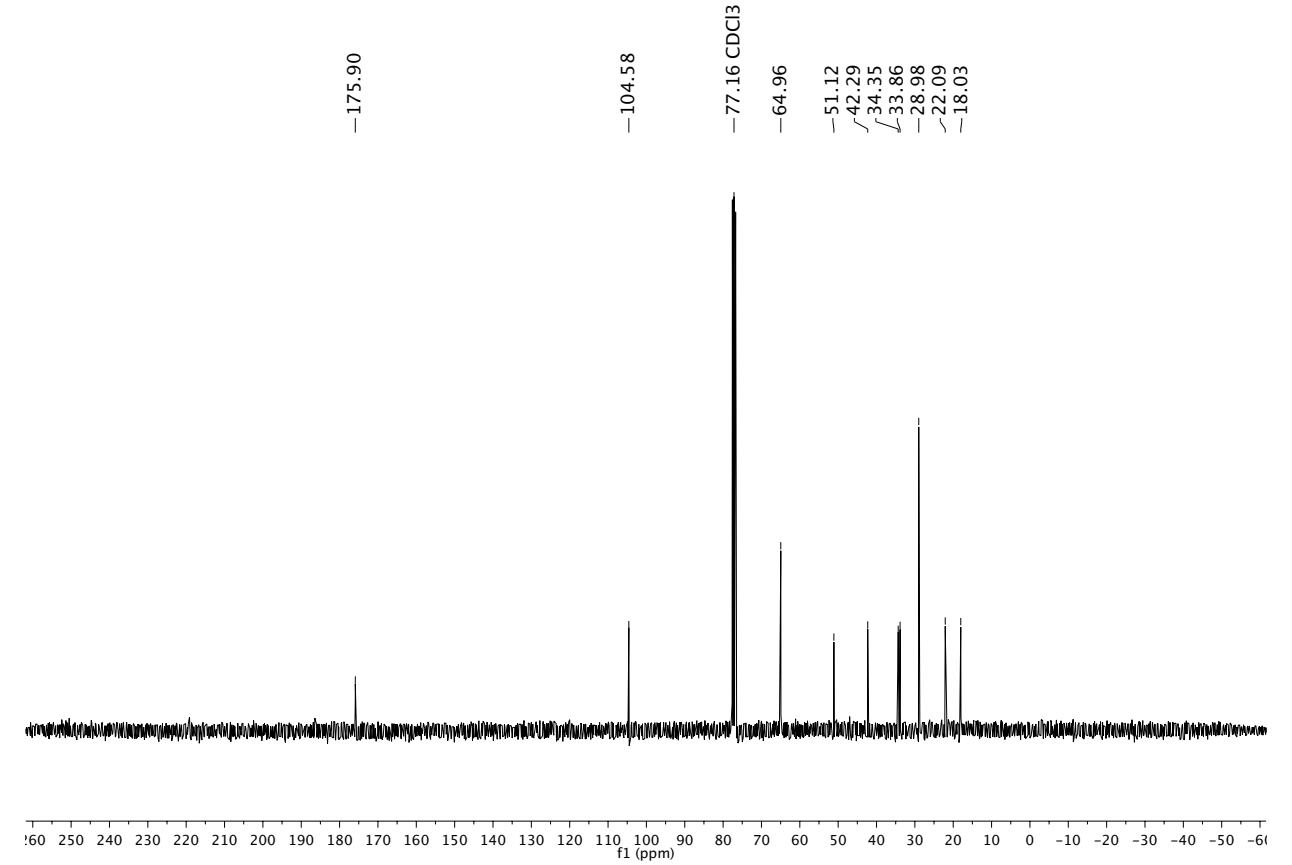
175.90
104.58
77.16 CDCl3
64.96
51.12
42.29
34.35
33.86
28.98
22.09
18.03
f1 (ppm)

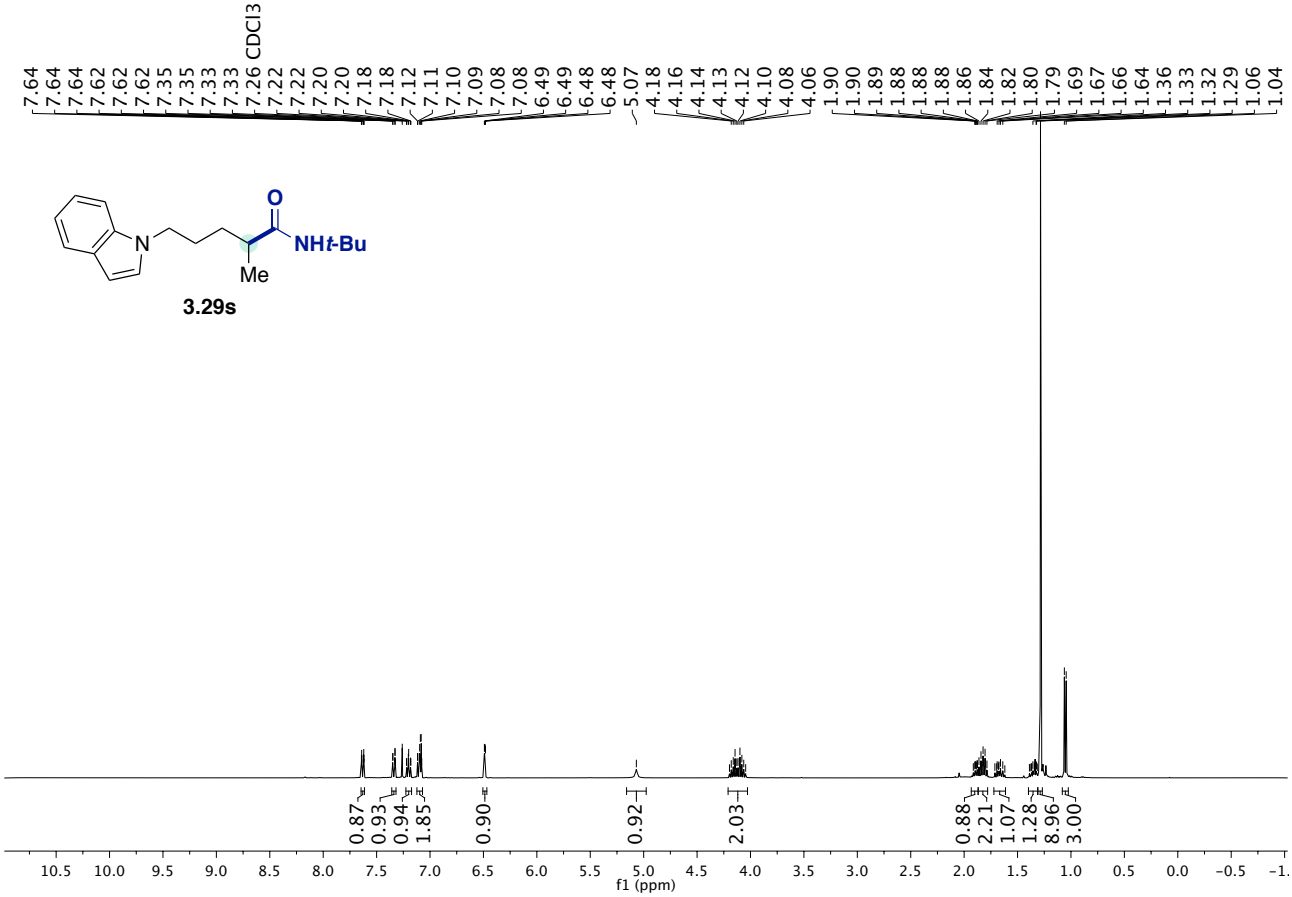
7.64 7.64 7.64 7.62 7.62 7.62 7.35 7.35 7.33 7.33 7.26 CDCl3 7.22 7.22 7.20 7.20 7.18 7.18 7.12 7.11 7.10 7.09 7.08 7.08 6.49 6.49 6.48 6.48 5.07 4.18 4.16 4.14 4.13 4.12 4.10 4.08 4.06 1.90 1.90 1.89 1.88 1.88 1.86 1.84 1.82 1.80 1.79 1.69 1.67 1.66 1.64 1.36 1.33 1.32 1.29 1.06 1.04
O
NHt-Bu
N
Me
3.29s
0.87 0.93 0.94 1.85 0.90 0.92 2.03 0.88 2.21 1.07 1.28 8.96 3.00
f1 (ppm)

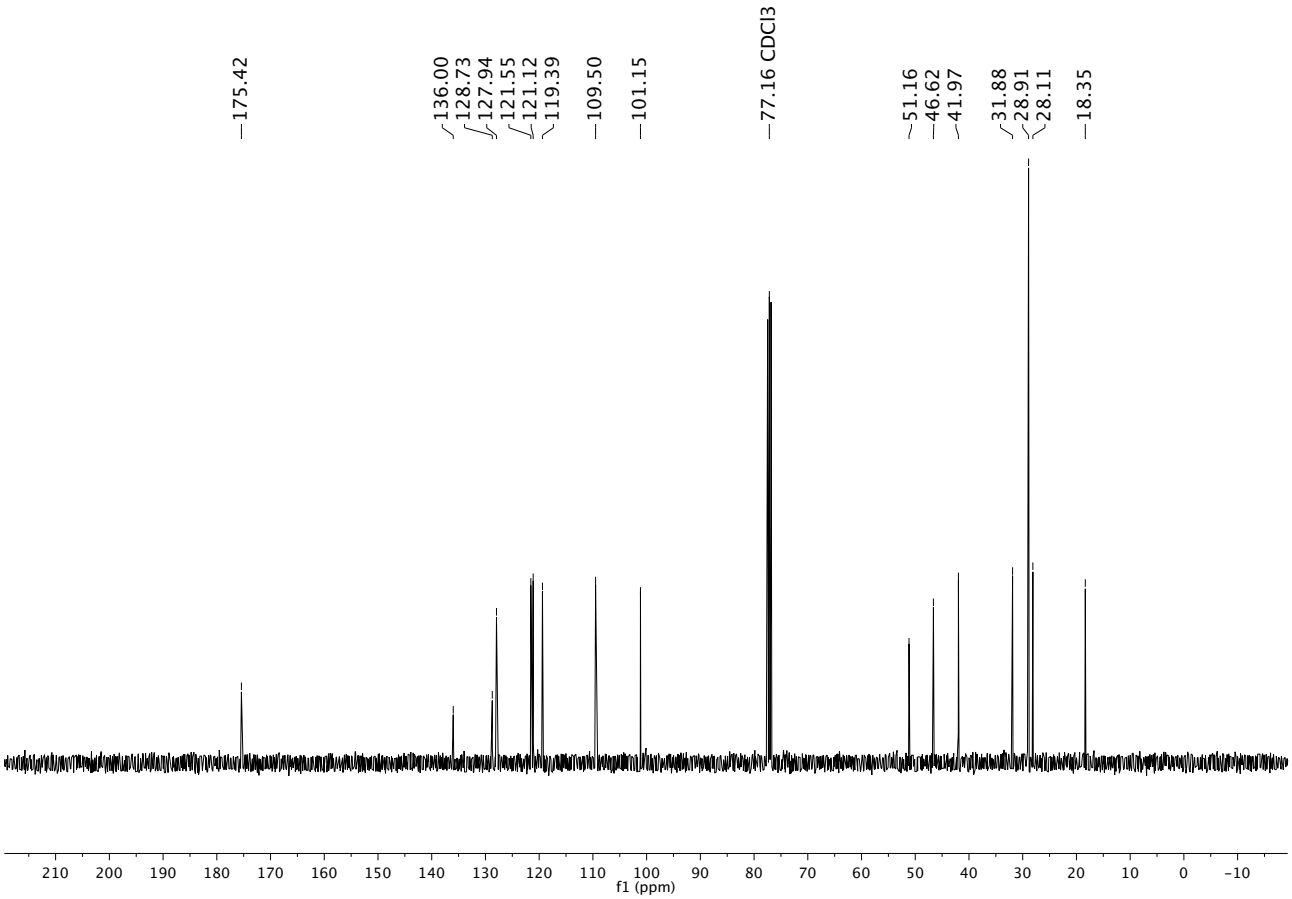
175.42
136.00 128.73 127.94 121.55 121.12 119.39 109.50 101.15 77.16 CDCl3 51.16 46.62 41.97 31.88 28.91 28.11 18.35
f1 (ppm)

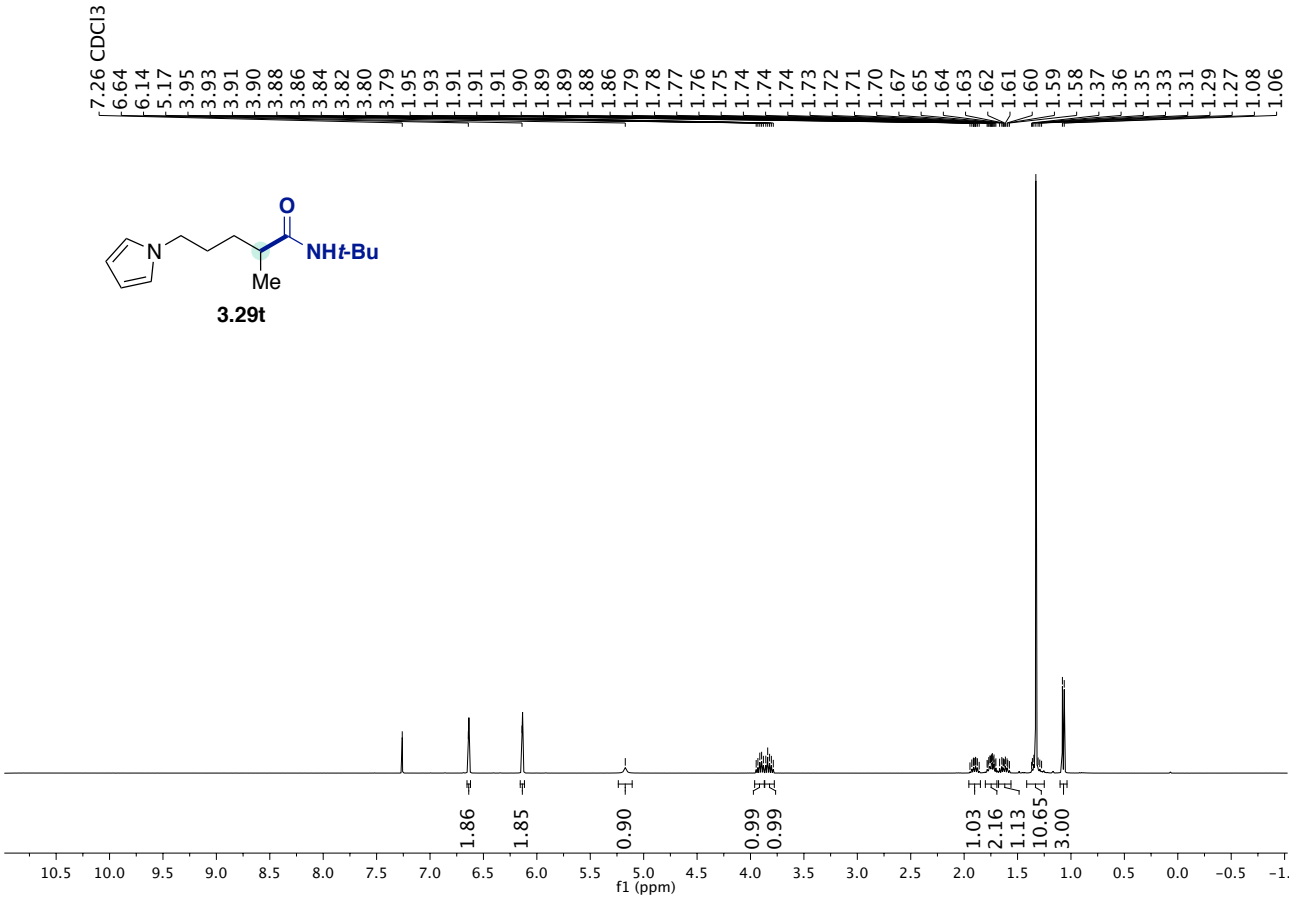
7.26 CDCl3
6.64 6.14 5.17 3.95 3.93 3.91 3.90 3.88 3.86 3.84 3.82 3.80 3.79 1.95 1.93 1.91 1.91 1.91 1.90 1.89 1.89 1.88 1.86 1.79 1.78 1.77 1.76 1.75 1.74 1.74 1.74 1.73 1.72 1.71 1.70 1.67 1.65 1.64 1.63 1.62 1.61 1.60 1.59 1.58 1.37 1.36 1.35 1.33 1.31 1.29 1.27 1.08 1.06
O
NHt-Bu
N
Me
3.29t
1.86 1.85 0.90 0.99 0.99 1.03 2.16 1.13 10.65 3.00
f1 (ppm)

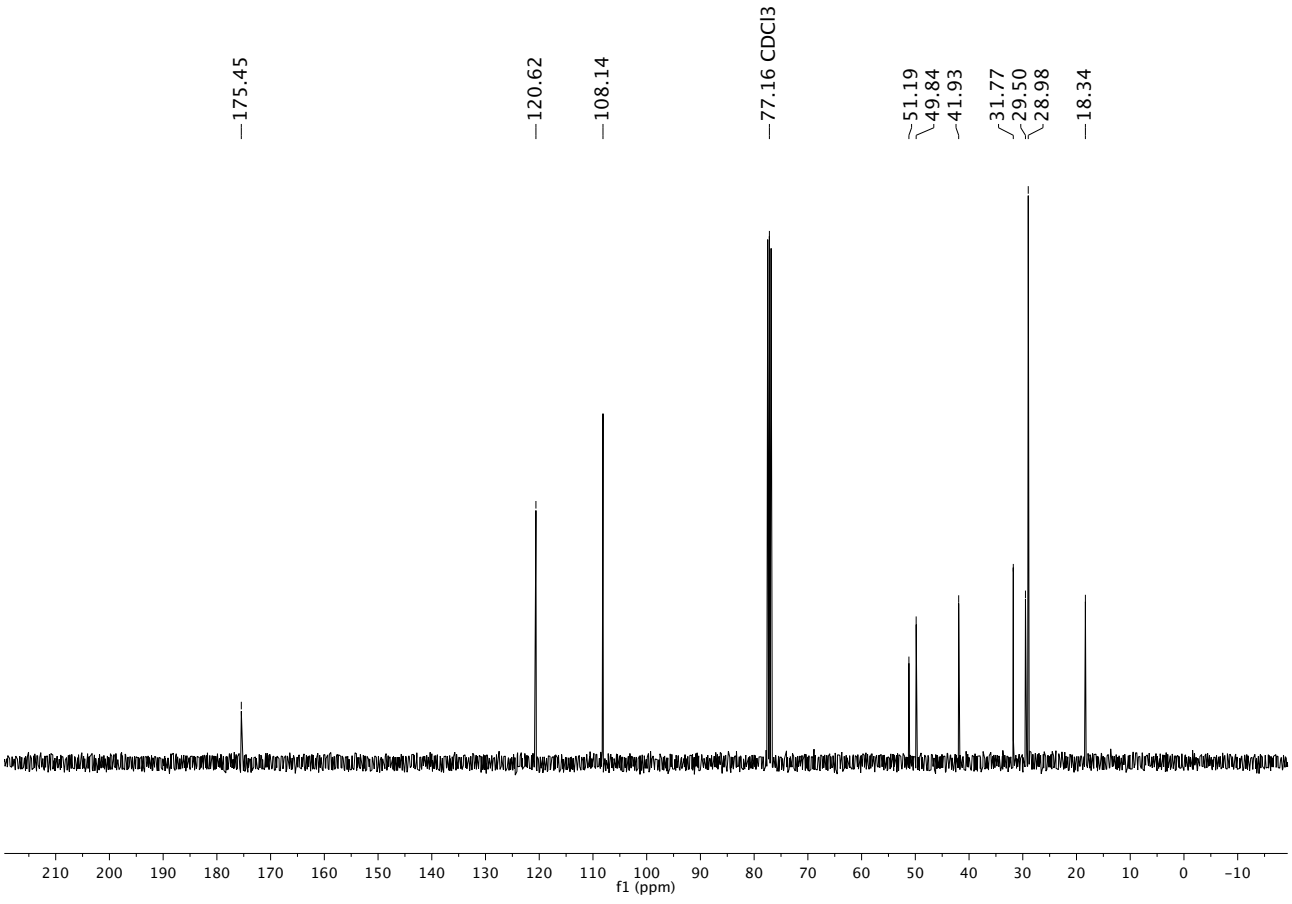
175.45
120.62
108.14
77.16 CDCl3
51.19
49.84
41.93
31.77
29.50
28.98
18.34
f1 (ppm)

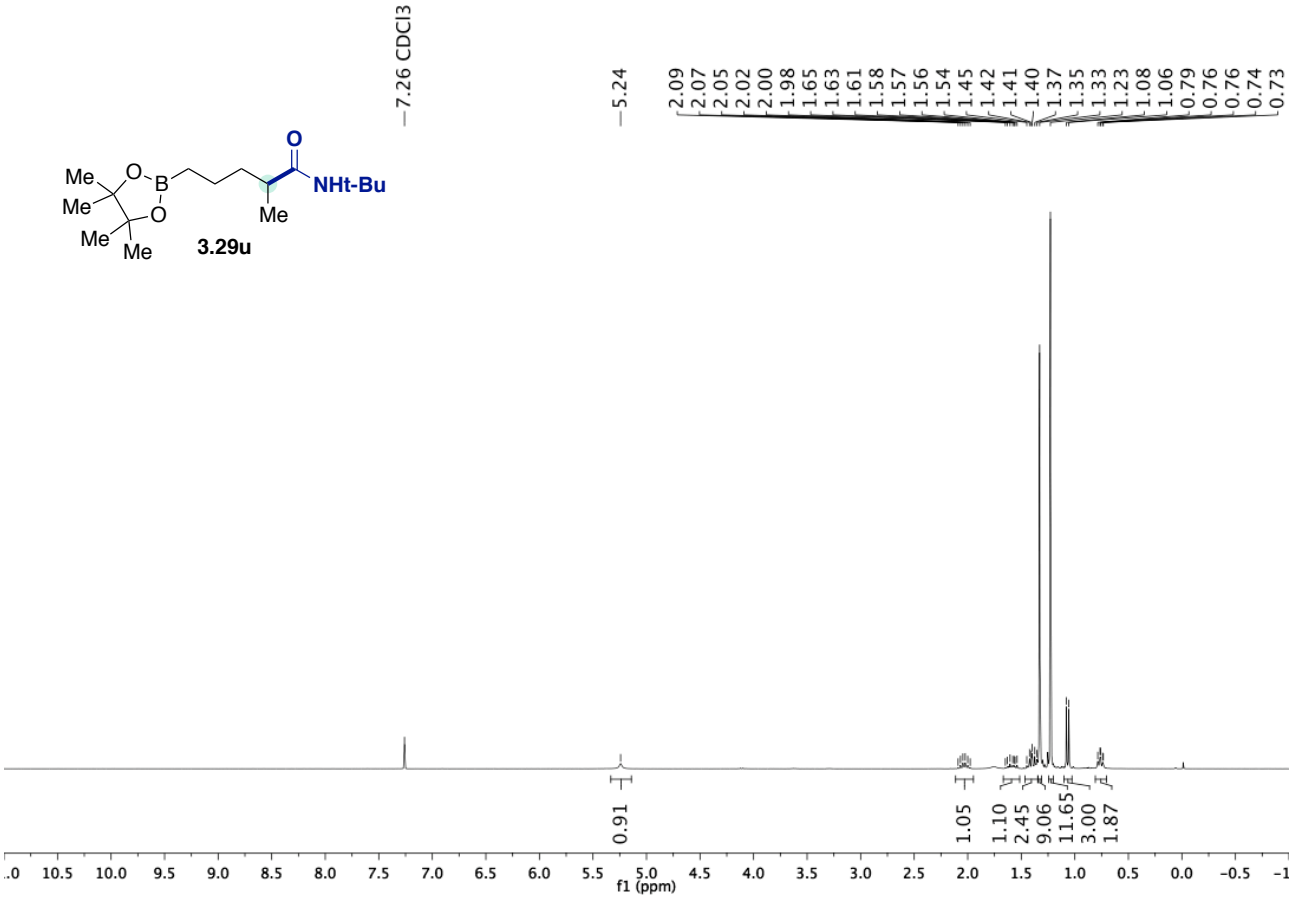
7.26 CDCl3
5.24
2.09
2.07
2.05
2.02
2.00
1.98
1.65
1.63
1.61
1.58
1.57
1.56
1.54
1.45
1.42
1.41
1.40
1.37
1.35
1.33
1.23
1.08
1.06
0.79
0.76
0.76
0.74
0.73
Me
Me
Me
Me
O
B
O
O
NHt-Bu
Me
3.29u
0.91
1.05
1.10
2.45
9.06
11.65
3.00
1.87
f1 (ppm)

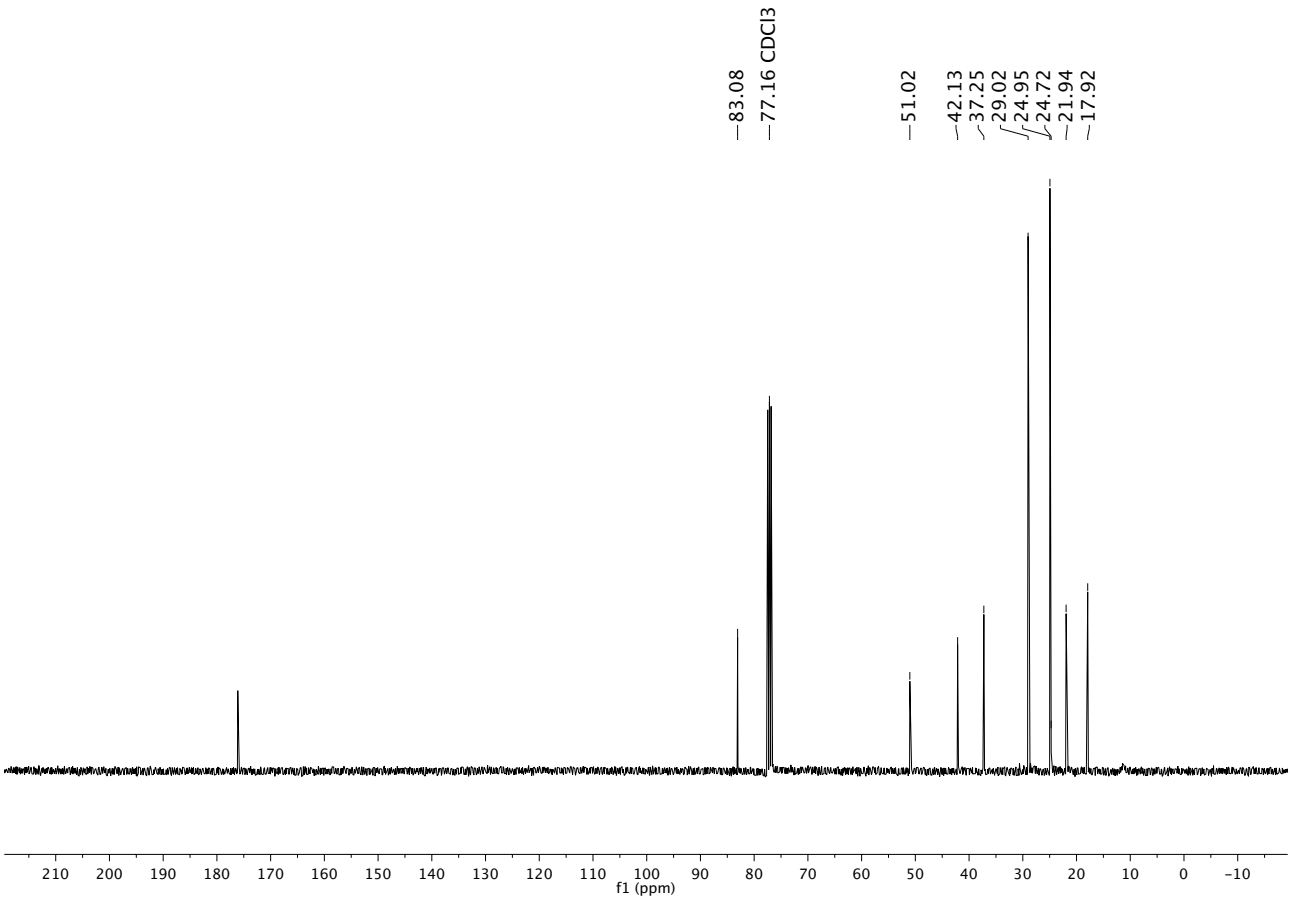
83.08
77.16 CDCl3
51.02
42.13
37.25
29.02
24.95
24.72
21.94
17.92
f1 (ppm)

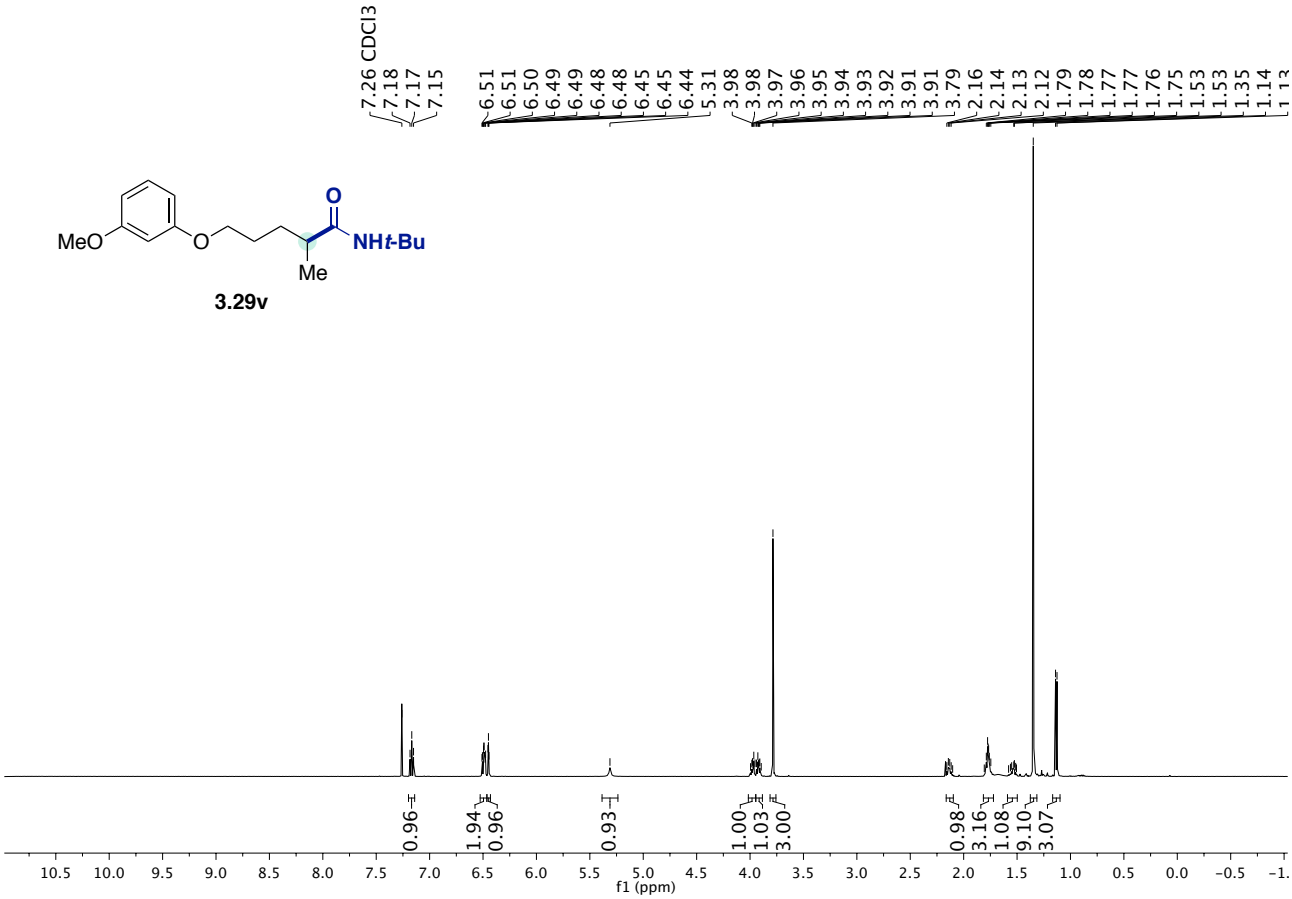
7.26 CDCl3
7.18
7.17
7.15
6.51
6.51
6.50
6.49
6.49
6.48
6.48
6.45
6.45
6.44
5.31
3.98
3.98
3.97
3.96
3.95
3.94
3.93
3.92
3.91
3.91
3.79
2.16
2.14
2.13
2.12
1.79
1.78
1.77
1.77
1.76
1.75
1.53
1.53
1.35
1.14
MeO
O
O
NHt-Bu
Me
0.96
1.94
0.96
0.93
1.00
1.03
3.00
0.98
3.16
1.08
9.10
3.07
f1 (ppm)

3.29v

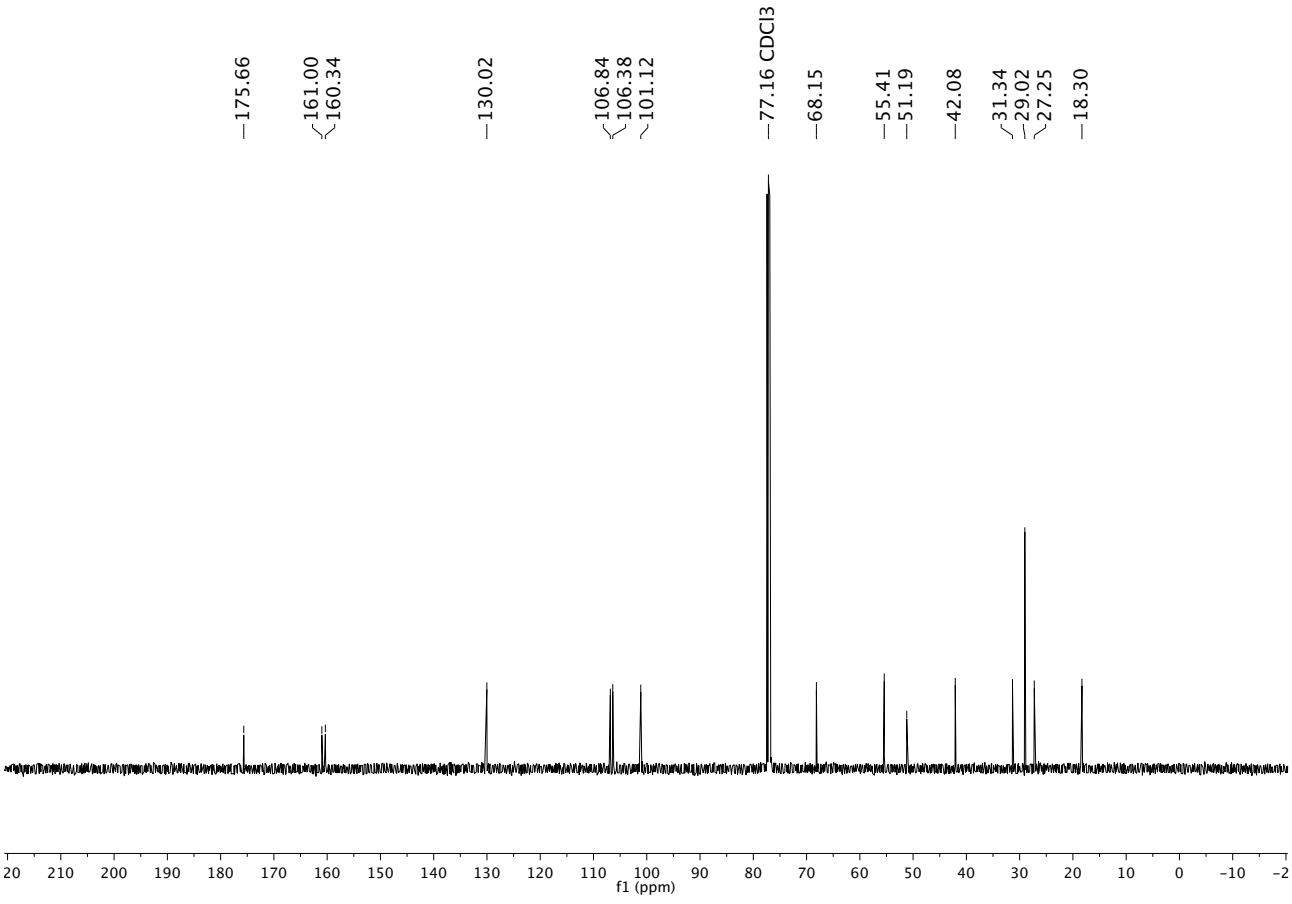
175.66
161.00
160.34
130.02
106.84
106.38
101.12
77.16 CDCl3
68.15
55.41
51.19
42.08
31.34
29.02
27.25
18.30
f1 (ppm)

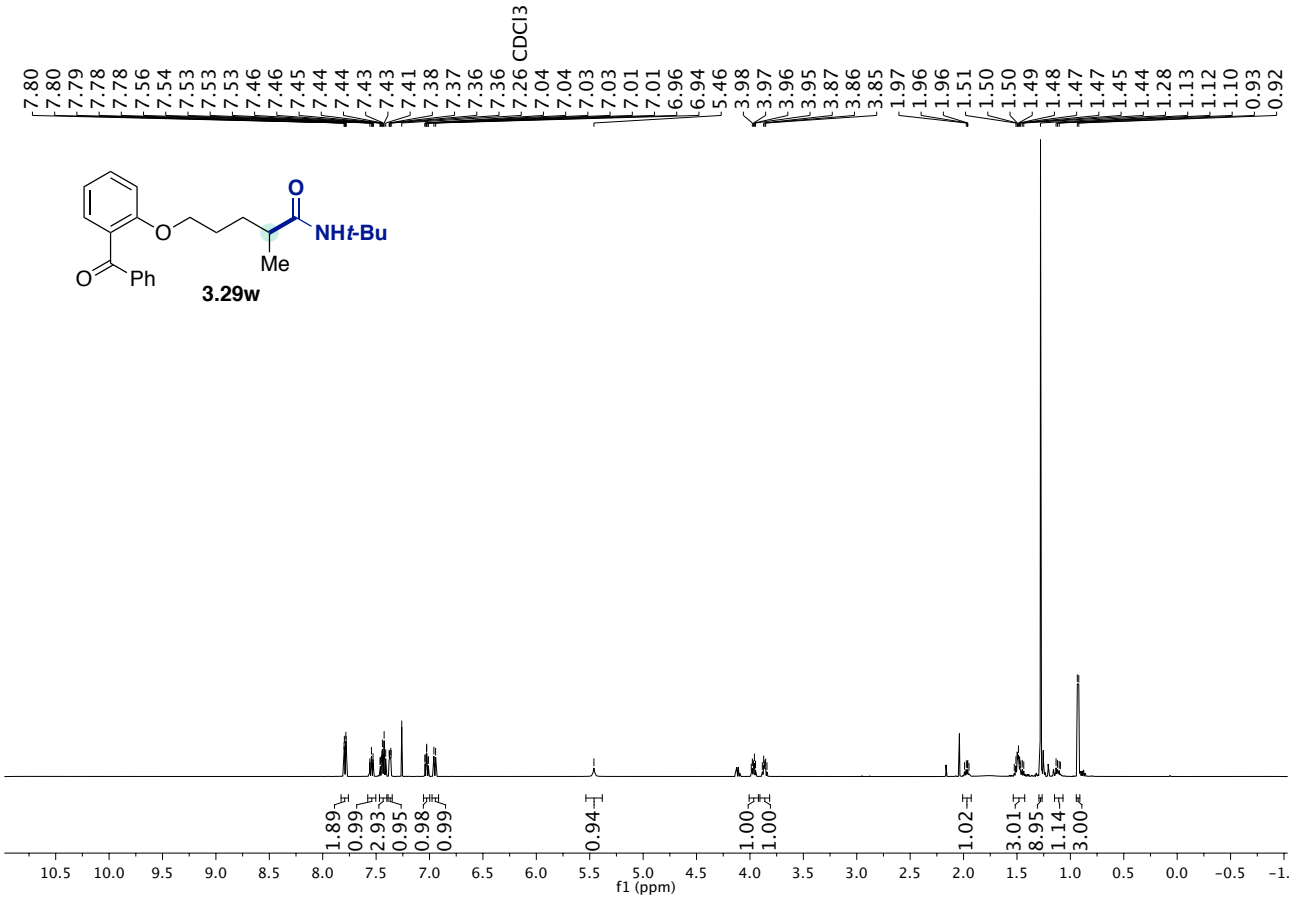
7.80 7.80 7.79 7.78 7.78 7.56 7.54 7.53 7.53 7.53 7.46 7.46 7.45 7.44 7.44 7.43 7.43 7.41 7.38 7.37 7.36 7.36 CDCl3 7.26 7.04 7.04 7.03 7.03 7.01 7.01 6.96 6.94 5.46 3.98 3.97 3.96 3.95 3.87 3.86 3.85 1.97 1.96 1.96 1.51 1.50 1.50 1.49 1.48 1.47 1.47 1.45 1.44 1.28 1.13 1.12 1.10 0.93 0.92
O
NHt-Bu
Me
O
Ph
3.29w
1.89 0.99 2.93 0.95 0.98 0.99 0.94 1.00 1.00 1.02 3.01 8.95 1.14 3.00
f1 (ppm)

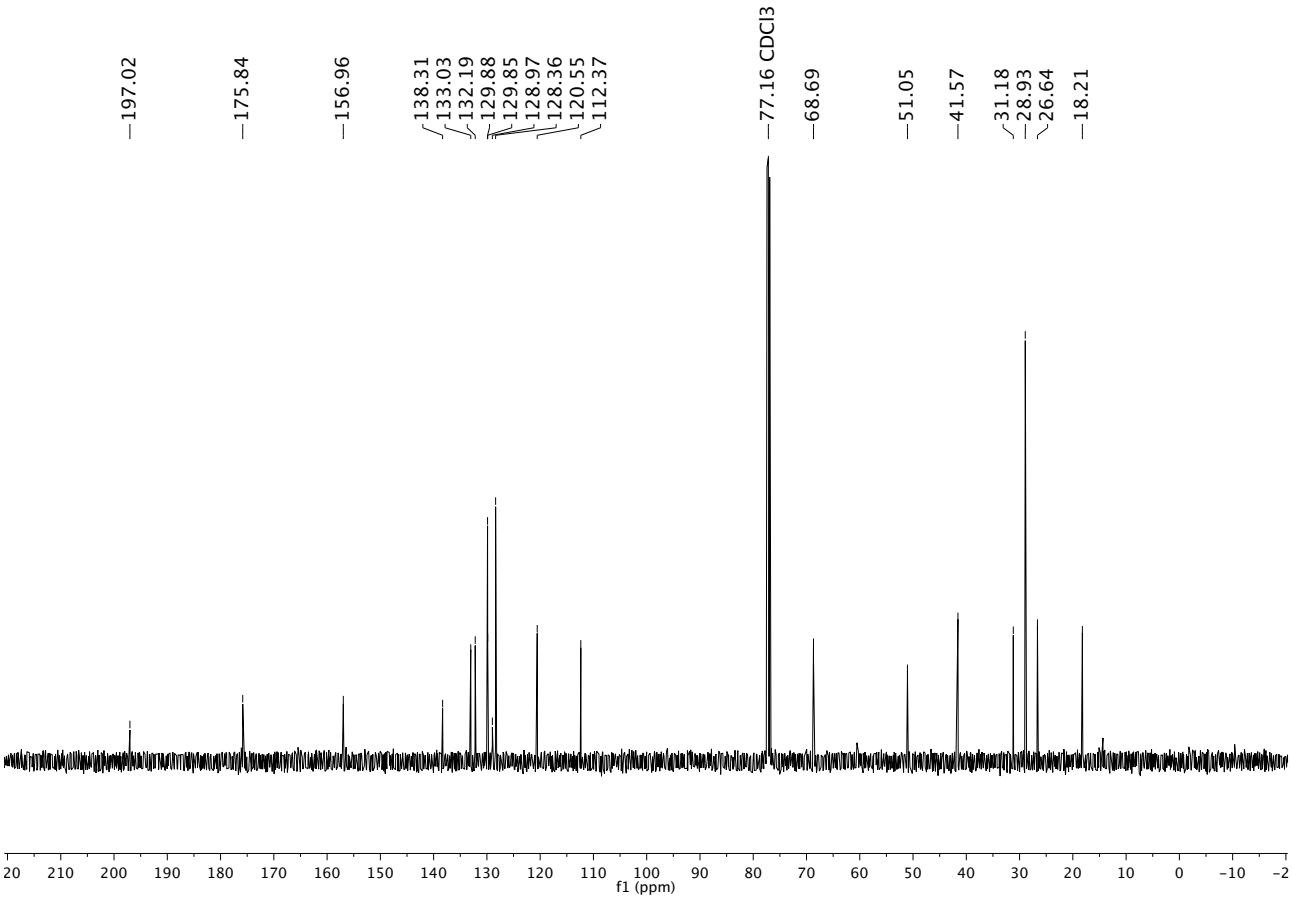
197.02 175.84 156.96 138.31 133.03 132.19 129.88 129.85 128.97 128.36 120.55 112.37 77.16 CDCl3 68.69 51.05 41.57 31.18 28.93 26.64 18.21
f1 (ppm)

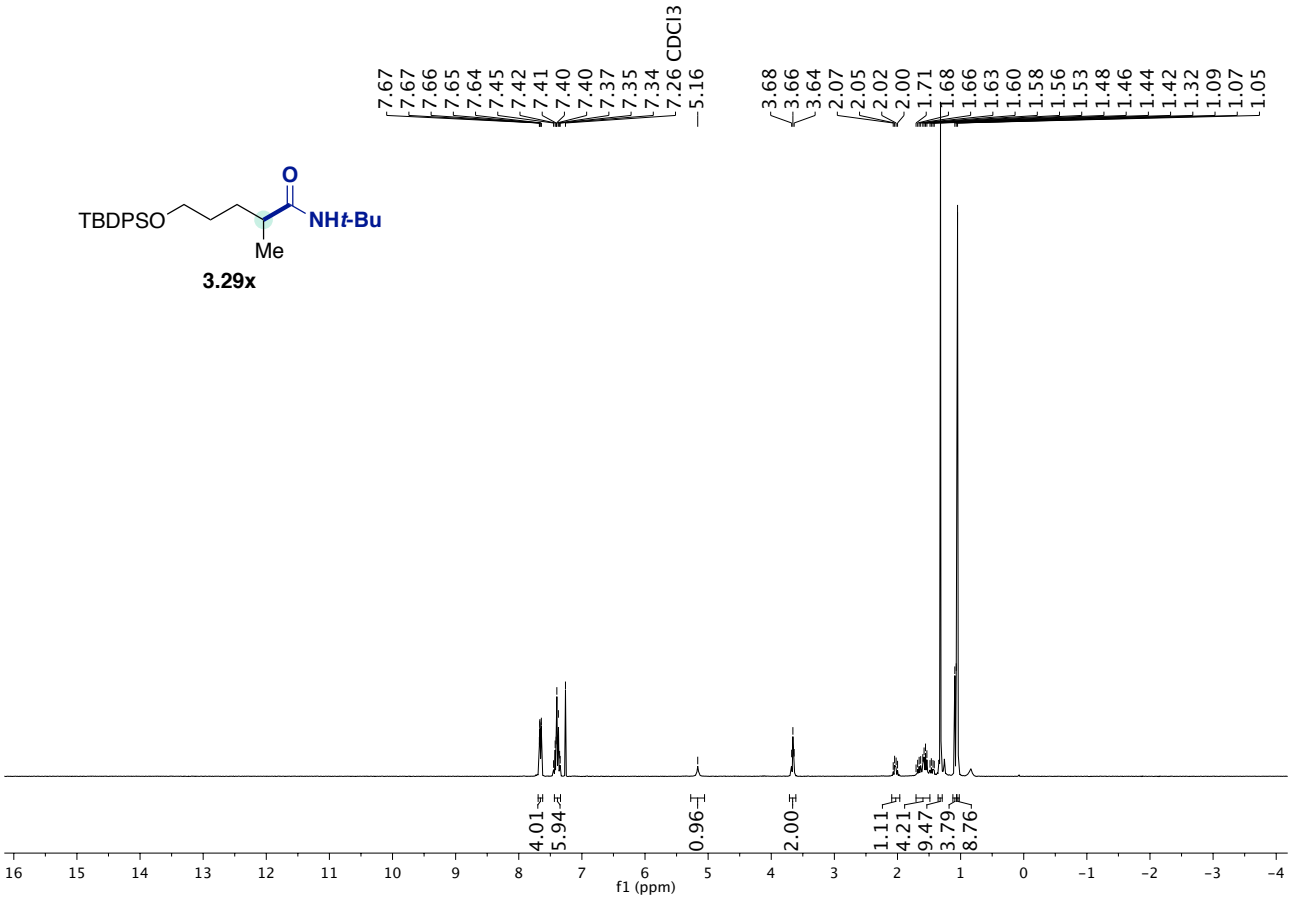
7.67
7.67
7.66
7.65
7.64
7.45
7.42
7.41
7.40
7.40
7.37
7.35
7.34
7.26 CDCl3
5.16
3.68
3.66
3.64
2.07
2.05
2.02
2.00
1.71
1.68
1.66
1.63
1.60
1.58
1.56
1.53
1.48
1.46
1.44
1.42
1.32
1.09
1.07
1.05
TBDPSO
O
NHt-Bu
Me
3.29x
4.01
5.94
0.96
2.00
1.11
4.21
9.47
3.79
8.76
f1 (ppm)

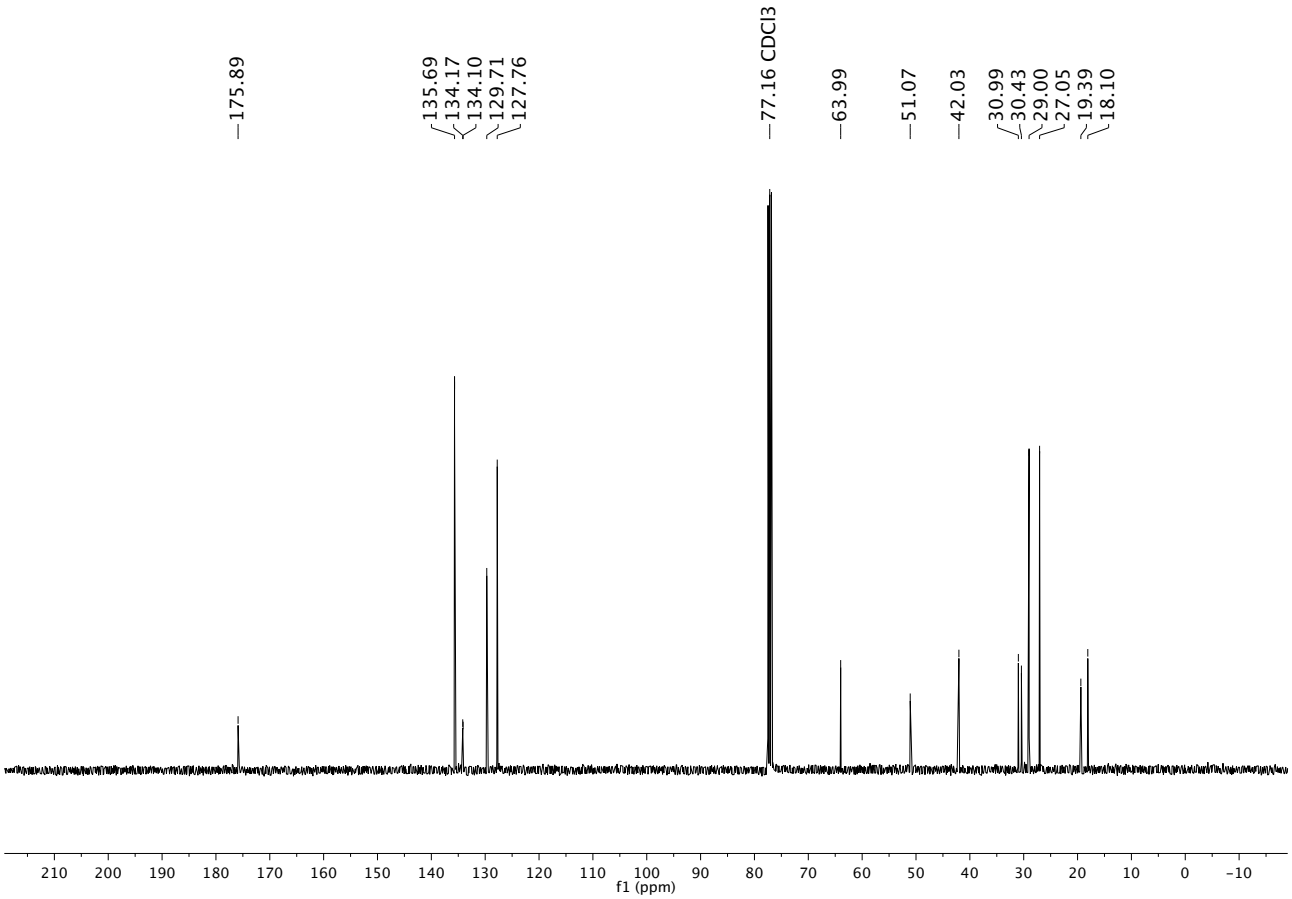
175.89
135.69
134.17
134.10
129.71
127.76
77.16 CDCl3
63.99
51.07
42.03
30.99
30.43
29.00
27.05
19.39
18.10
f1 (ppm)

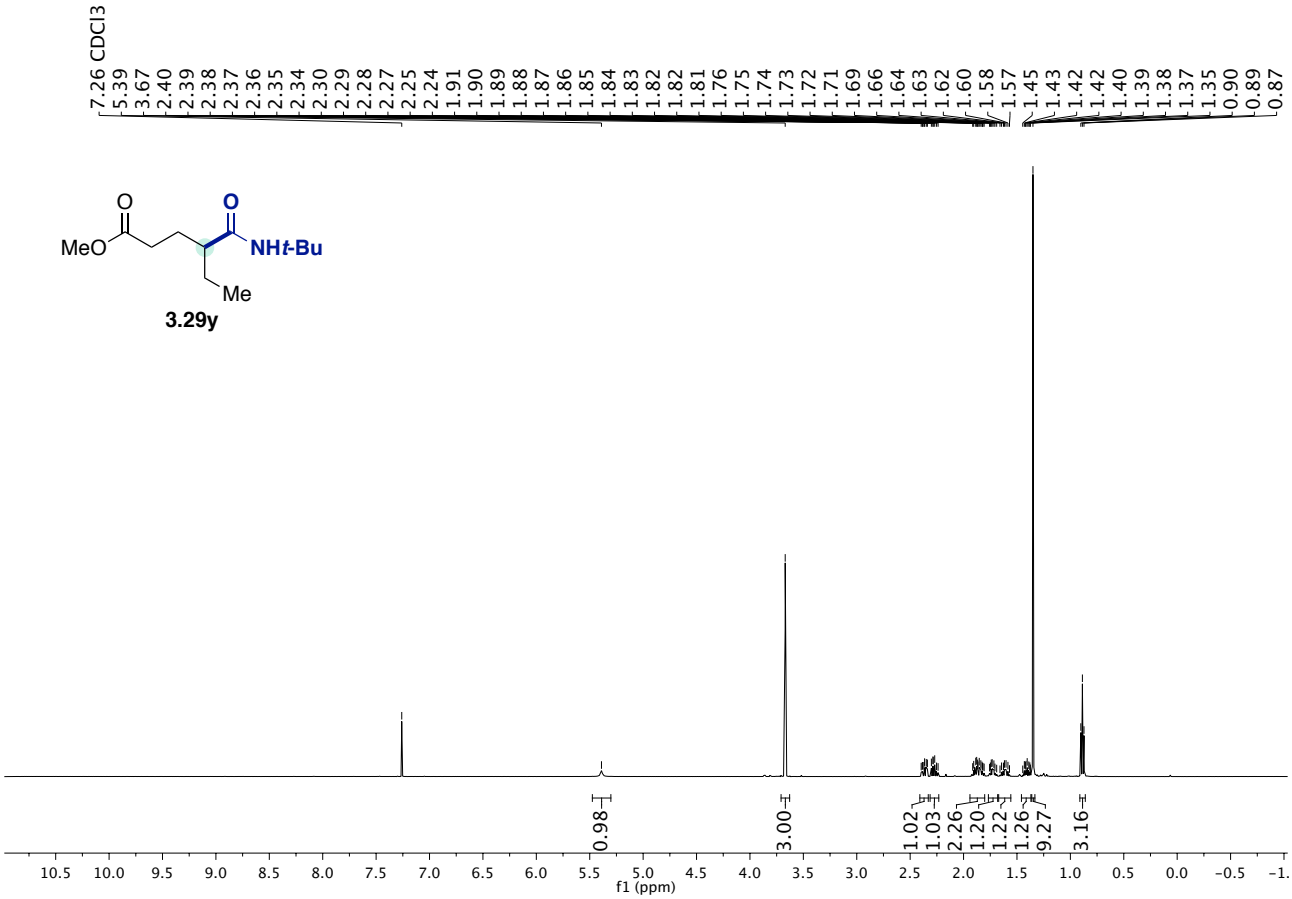
7.26 CDCl3
5.39 3.67 2.40 2.39 2.38 2.37 2.36 2.35 2.34 2.30 2.29 2.28 2.27 2.25 2.24 1.91 1.90 1.89 1.88 1.87 1.86 1.85 1.84 1.83 1.82 1.82 1.81 1.76 1.75 1.74 1.73 1.72 1.71 1.69 1.66 1.64 1.63 1.62 1.60 1.58 1.57 1.45 1.43 1.42 1.42 1.40 1.39 1.38 1.37 1.35 0.90 0.89 0.87
MeO
NHt-Bu
Me
3.29y
0.98 3.00 1.02 1.03 2.26 1.20 1.22 1.26 9.27 3.16
f1 (ppm)

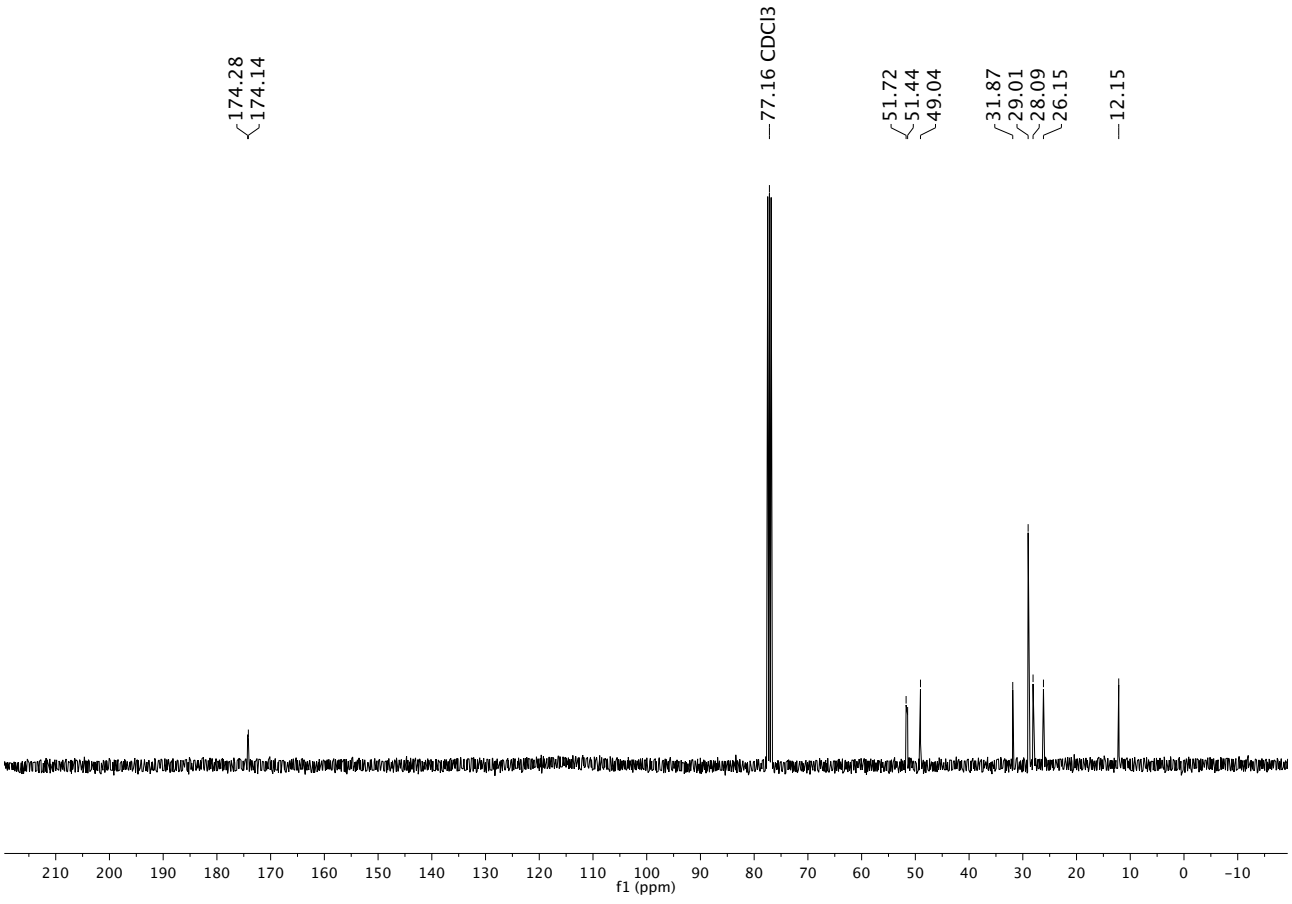
174.28
174.14
77.16 CDCl3
51.72
51.44
49.04
31.87
29.01
28.09
26.15
12.15
f1 (ppm)

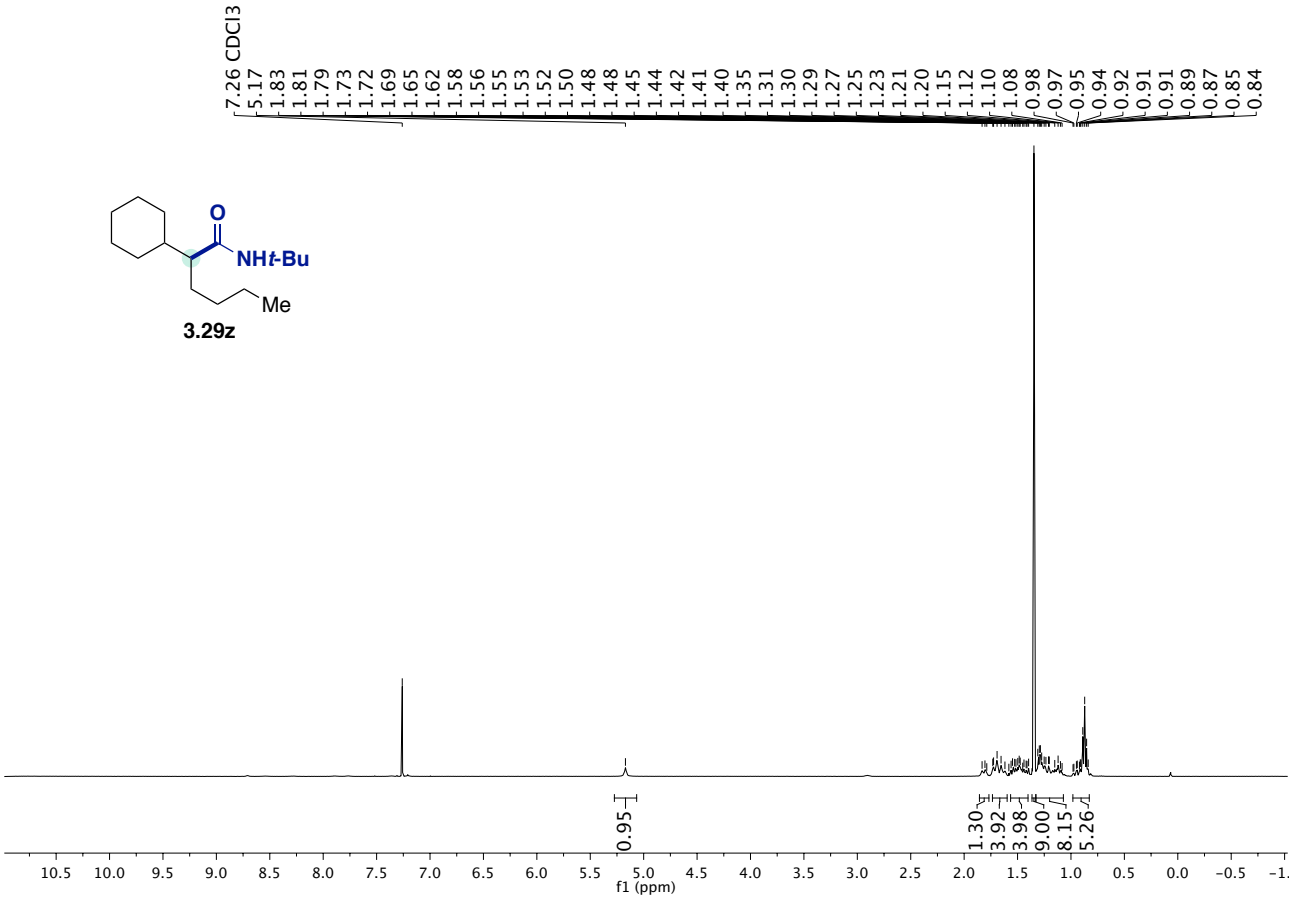
7.26 CDCl3
5.17
1.83
1.81
1.79
1.73
1.72
1.69
1.65
1.62
1.58
1.56
1.55
1.53
1.52
1.50
1.48
1.48
1.45
1.44
1.42
1.41
1.40
1.35
1.31
1.30
1.29
1.27
1.25
1.23
1.21
1.20
1.15
1.12
1.10
1.08
0.98
0.97
0.95
0.94
0.92
0.91
0.91
0.89
0.87
0.85
0.84
O
NHt-Bu
Me
3.29z
0.95
1.30
3.92
3.98
9.00
8.15
5.26
f1 (ppm)

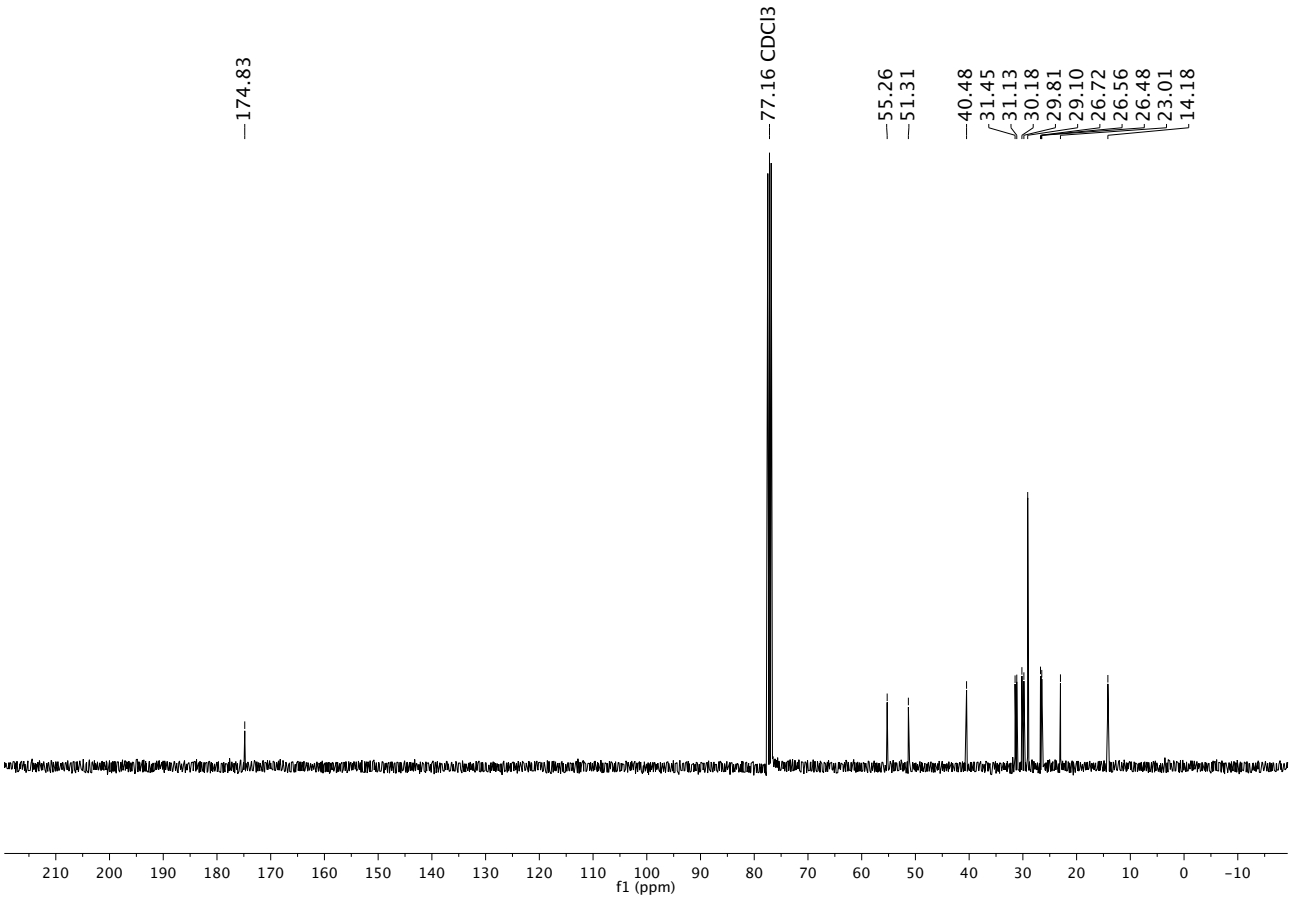
174.83
77.16 CDCl3
55.26
51.31
40.48
31.45
31.13
30.18
29.81
29.10
26.72
26.56
26.48
23.01
14.18
f1 (ppm)

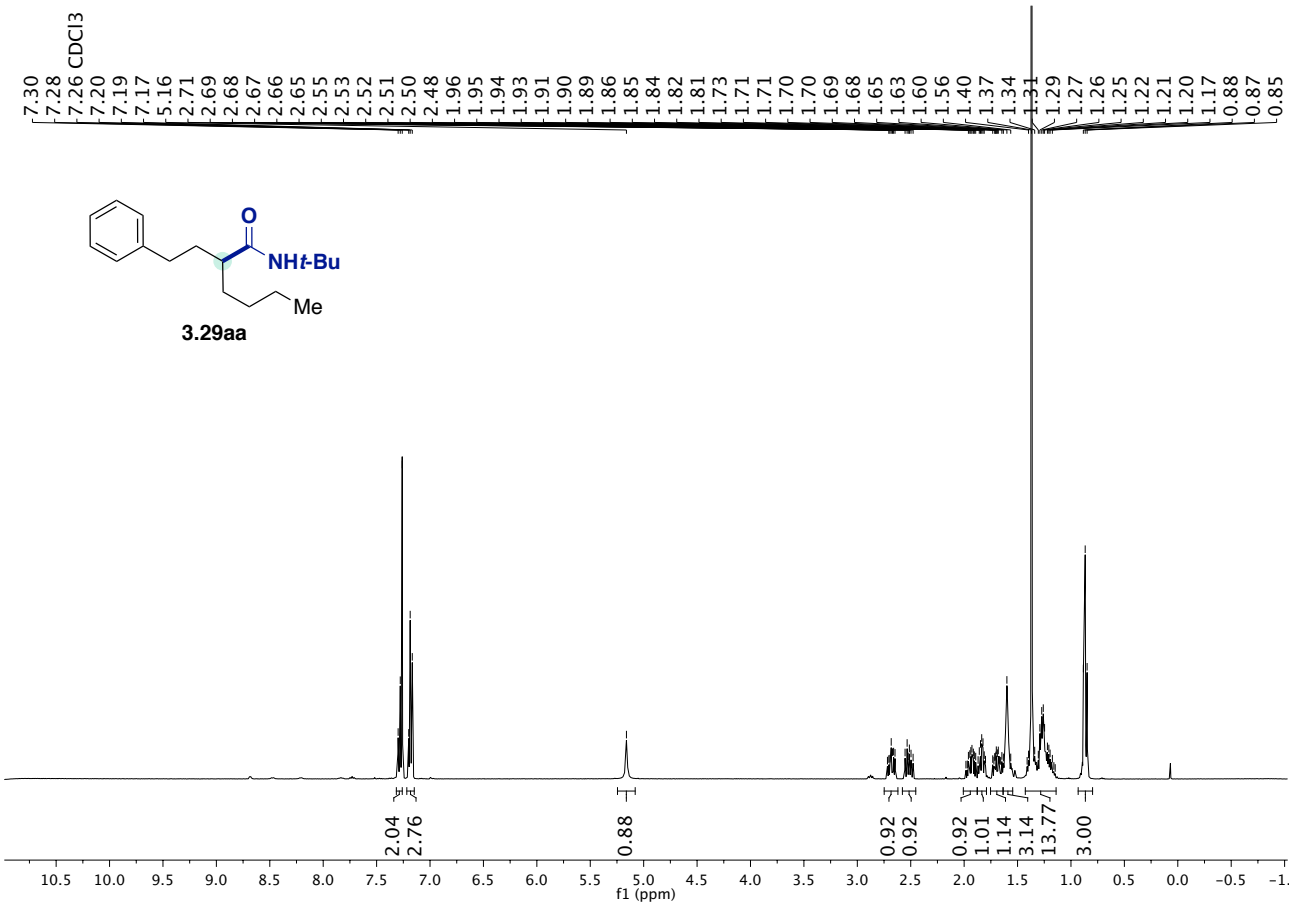
7.30
7.28
CDCl3
7.26
7.20
7.19
7.17
5.16
2.71
2.69
2.68
2.67
2.66
2.65
2.55
2.53
2.52
2.51
2.50
2.48
1.96
1.95
1.94
1.93
1.91
1.90
1.89
1.86
1.85
1.84
1.82
1.81
1.73
1.71
1.71
1.70
1.70
1.69
1.68
1.65
1.63
1.60
1.56
1.40
1.37
1.34
1.31
1.29
1.27
1.26
1.25
1.22
1.21
1.20
1.17
0.88
0.87
0.85
O
NHt-Bu
Me
3.29aa
2.04
2.76
0.88
0.92
0.92
0.92
1.01
1.14
3.14
13.77
3.00
f1 (ppm)

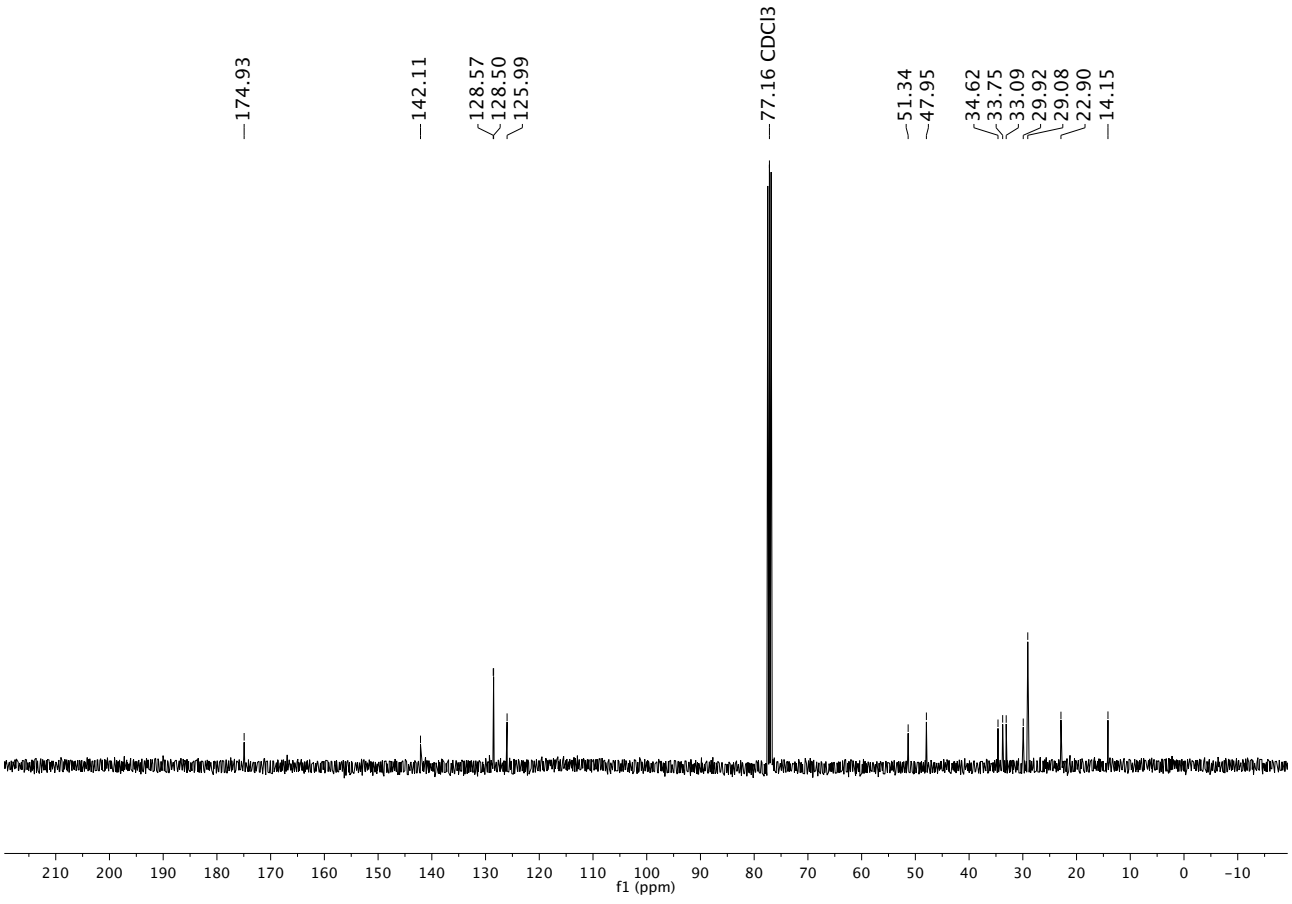
174.93
142.11
128.57
128.50
125.99
77.16 CDCl3
51.34
47.95
34.62
33.75
33.09
29.92
29.08
22.90
14.15
f1 (ppm)

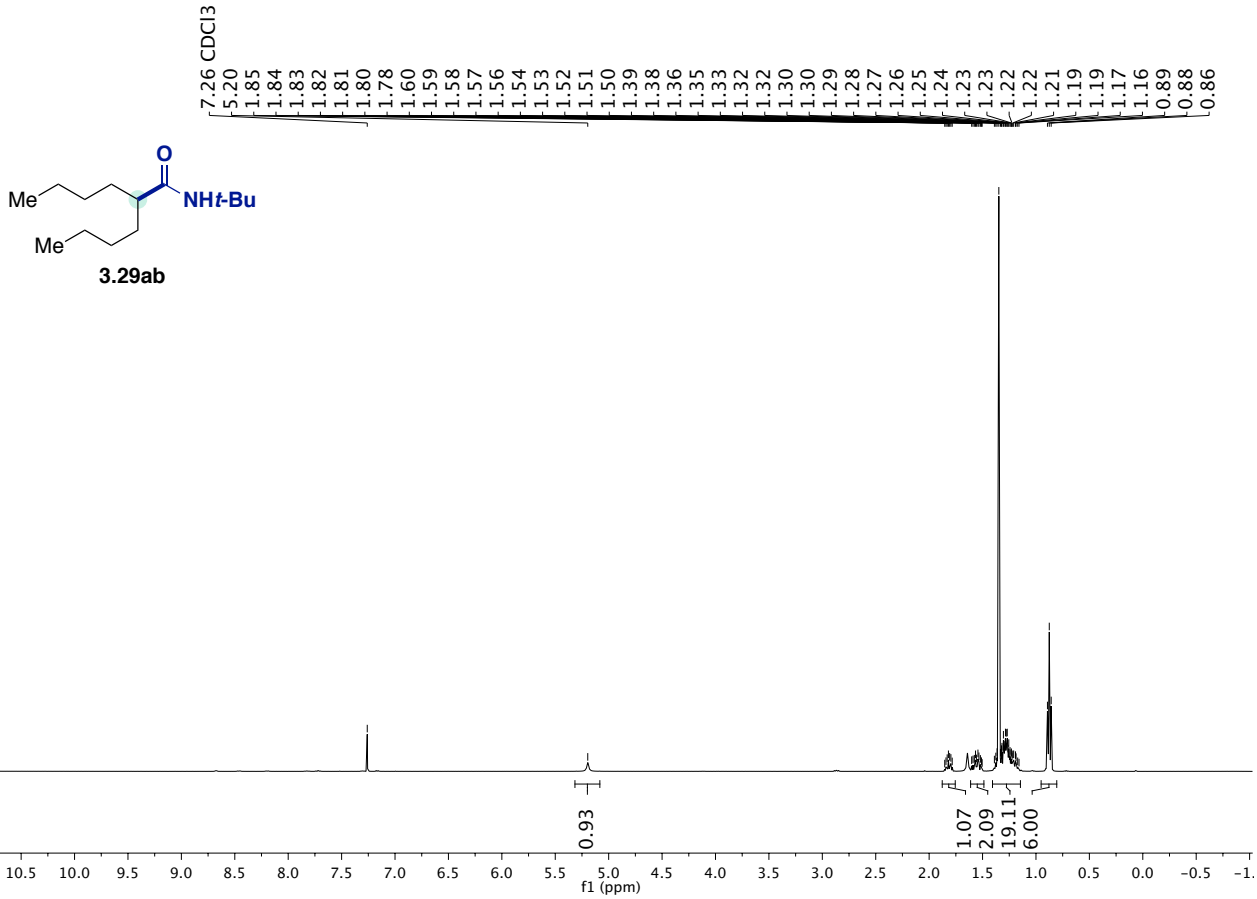
7.26 CDCl3
5.20
1.85
1.84
1.83
1.82
1.81
1.80
1.78
1.60
1.59
1.58
1.57
1.56
1.54
1.53
1.52
1.51
1.50
1.39
1.38
1.36
1.35
1.33
1.32
1.32
1.30
1.30
1.29
1.28
1.27
1.26
1.25
1.24
1.23
1.23
1.22
1.22
1.21
1.19
1.19
1.17
1.16
0.89
0.88
0.86
O
NHt-Bu
Me
Me
3.29ab
0.93
1.07
2.09
19.11
6.00
f1 (ppm)

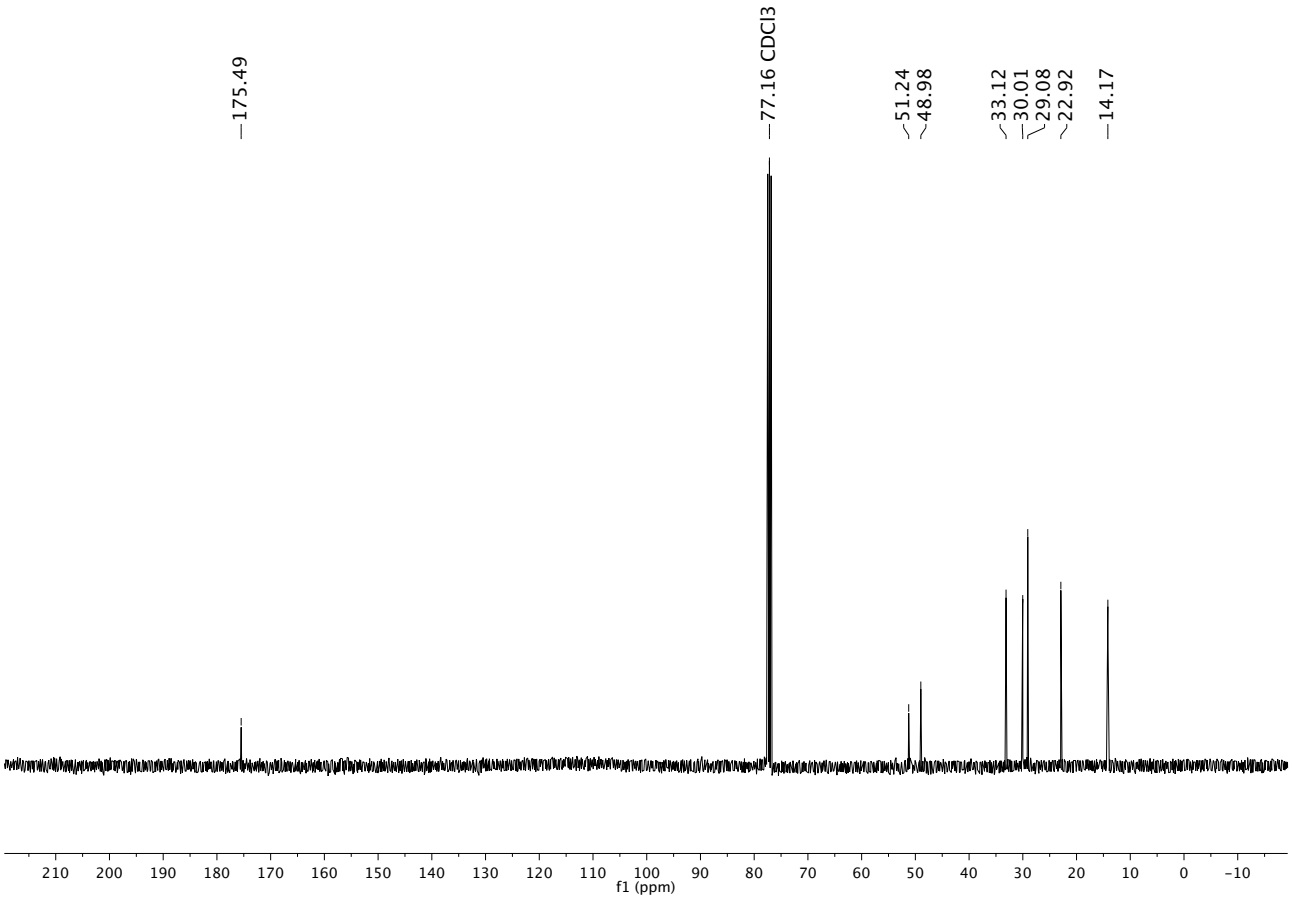
175.49
77.16 CDCl3
51.24
48.98
33.12
30.01
29.08
22.92
14.17
f1 (ppm)

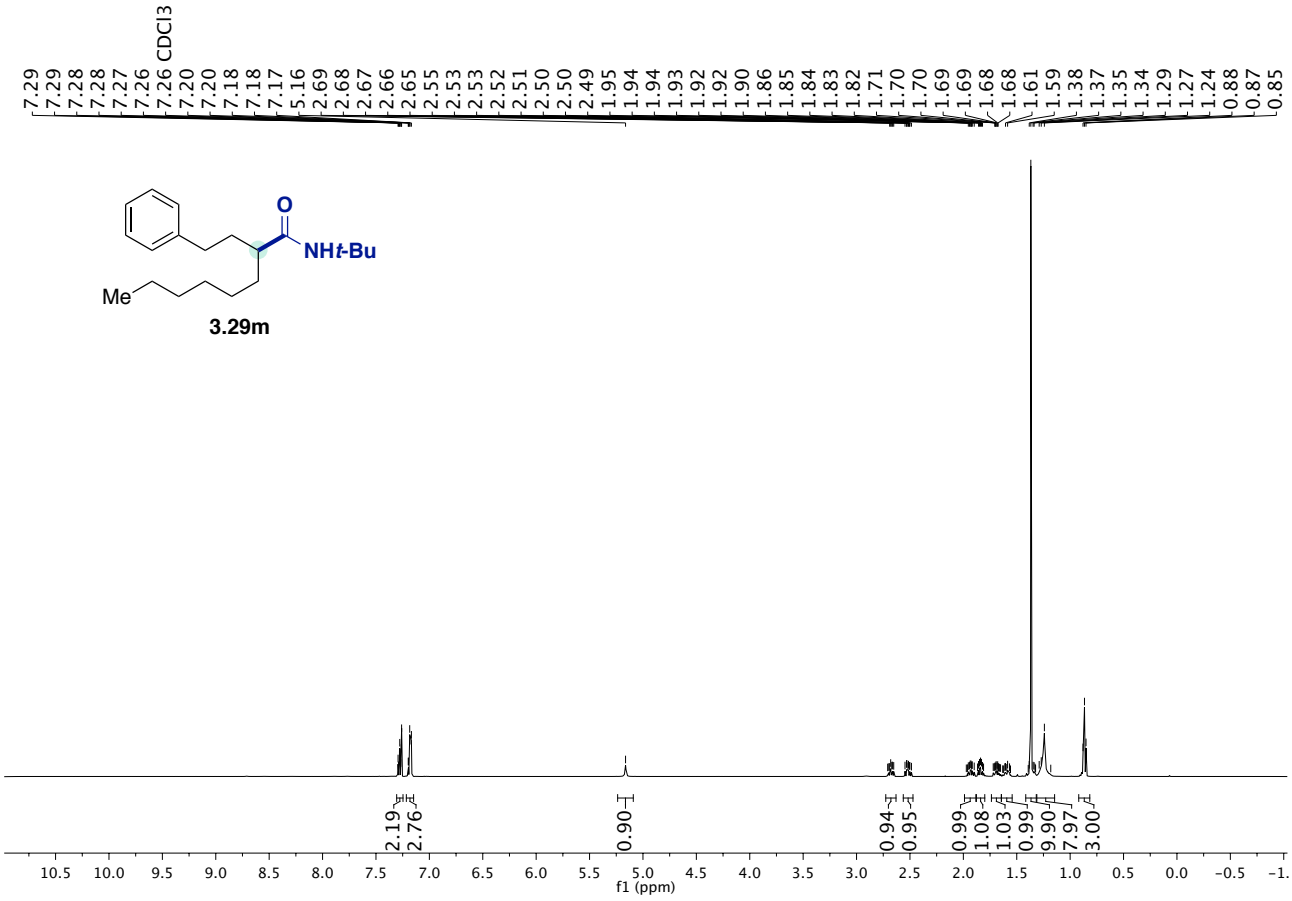
CDCl3
7.29 7.29 7.28 7.28 7.27 7.26 7.26 7.20 7.20 7.18 7.17 5.16 2.69 2.68 2.67 2.66 2.65 2.55 2.53 2.53 2.52 2.51 2.50 2.50 2.49 1.95 1.94 1.94 1.93 1.92 1.92 1.90 1.86 1.85 1.84 1.83 1.82 1.71 1.70 1.70 1.69 1.69 1.68 1.68 1.61 1.59 1.38 1.37 1.35 1.34 1.29 1.27 1.24 0.88 0.87 0.85
O
NHt-Bu
Me
3.29m
2.19 2.76 0.90 0.94 0.95 0.99 1.08 1.03 0.99 9.90 7.97 3.00
f1 (ppm)

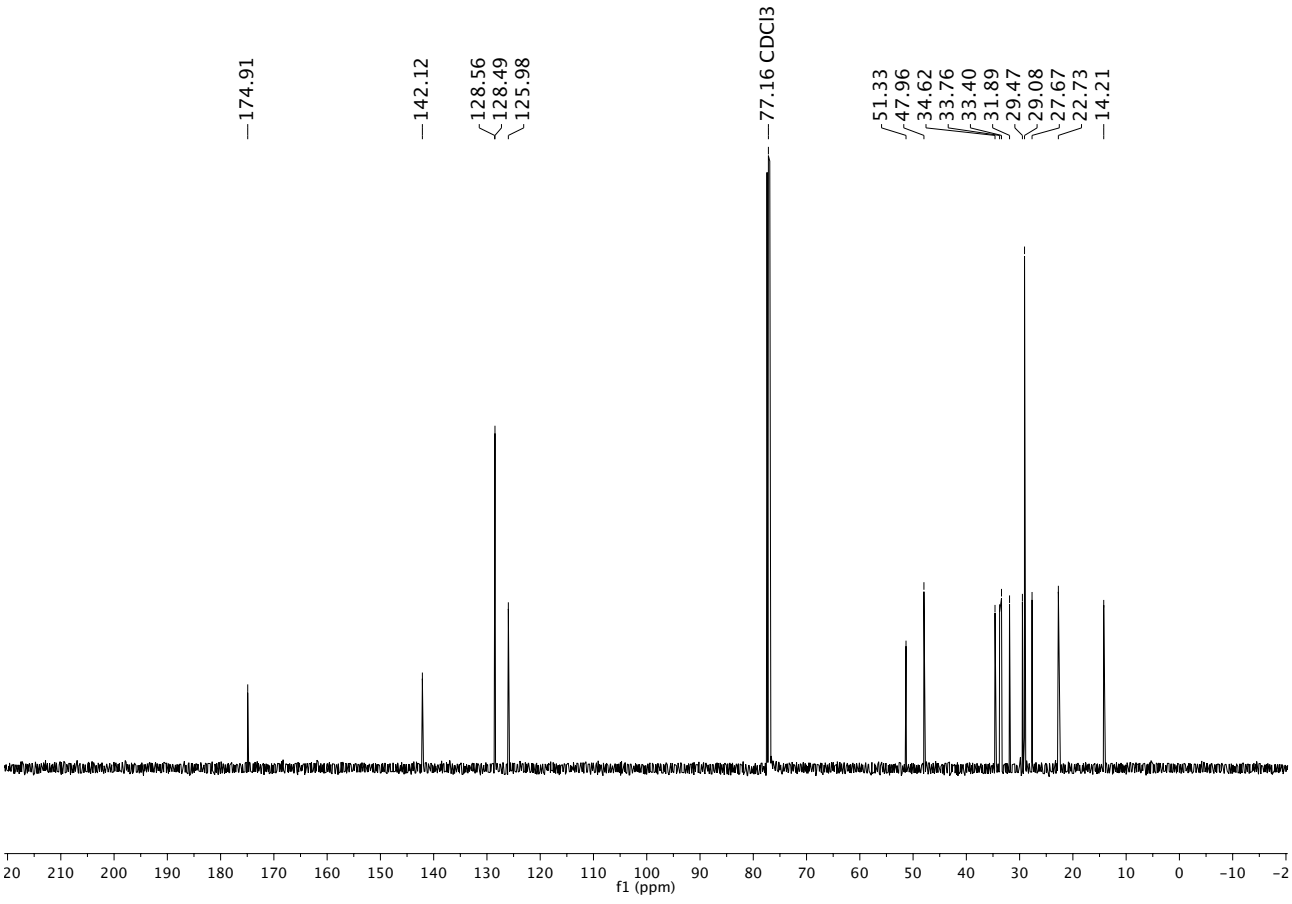
174.91
142.12
128.56
128.49
125.98
77.16 CDCl3
51.33
47.96
34.62
33.76
33.40
31.89
29.47
29.08
27.67
22.73
14.21
f1 (ppm)

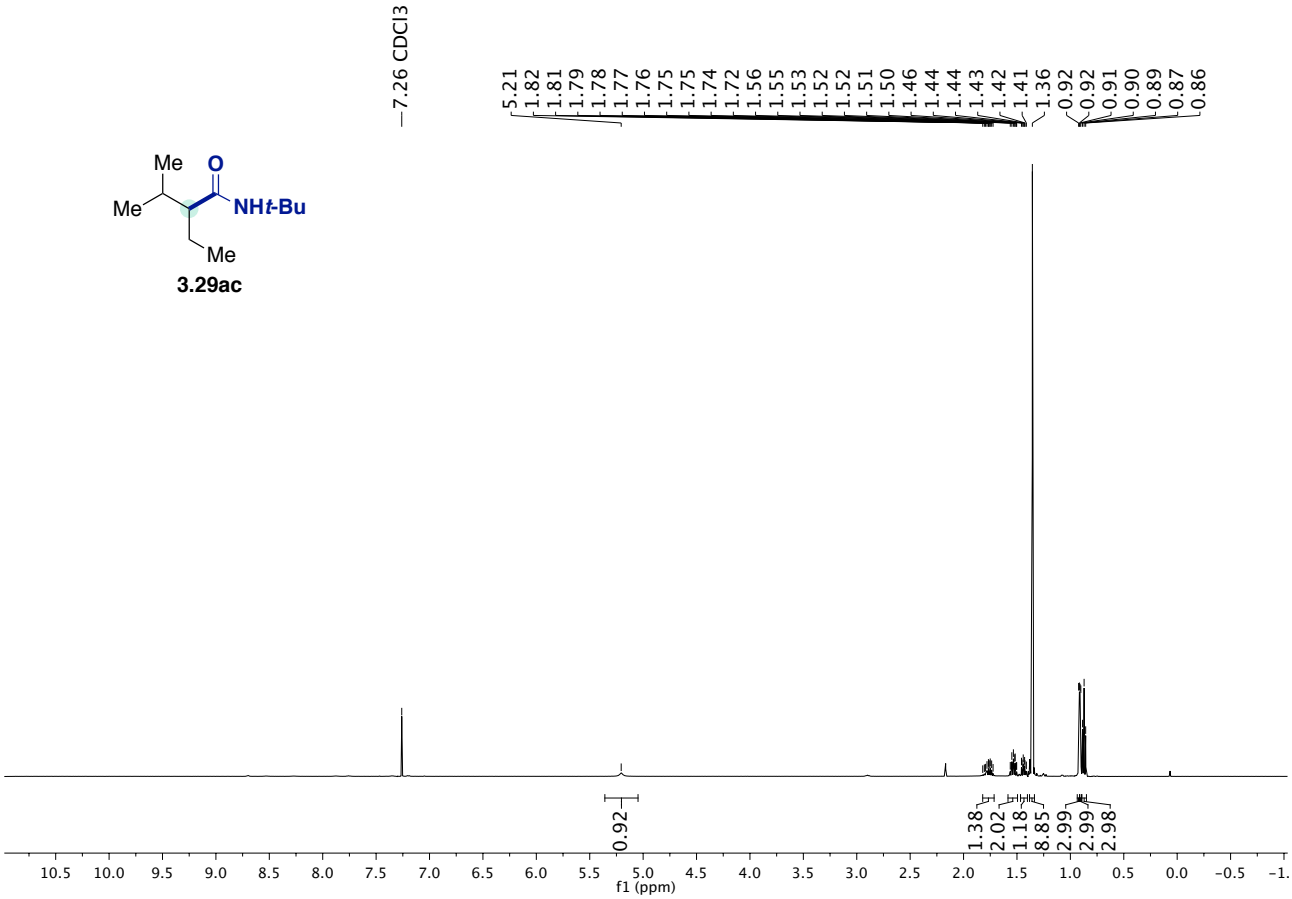
7.26 CDCl3
5.21
1.82
1.81
1.79
1.78
1.77
1.76
1.75
1.75
1.74
1.72
1.56
1.55
1.53
1.52
1.52
1.51
1.50
1.46
1.44
1.44
1.43
1.42
1.41
1.36
0.92
0.92
0.91
0.90
0.89
0.87
0.86
Me
O
Me
NHt-Bu
Me
3.29ac
0.92
1.38
2.02
1.18
8.85
2.99
2.99
2.98
f1 (ppm)

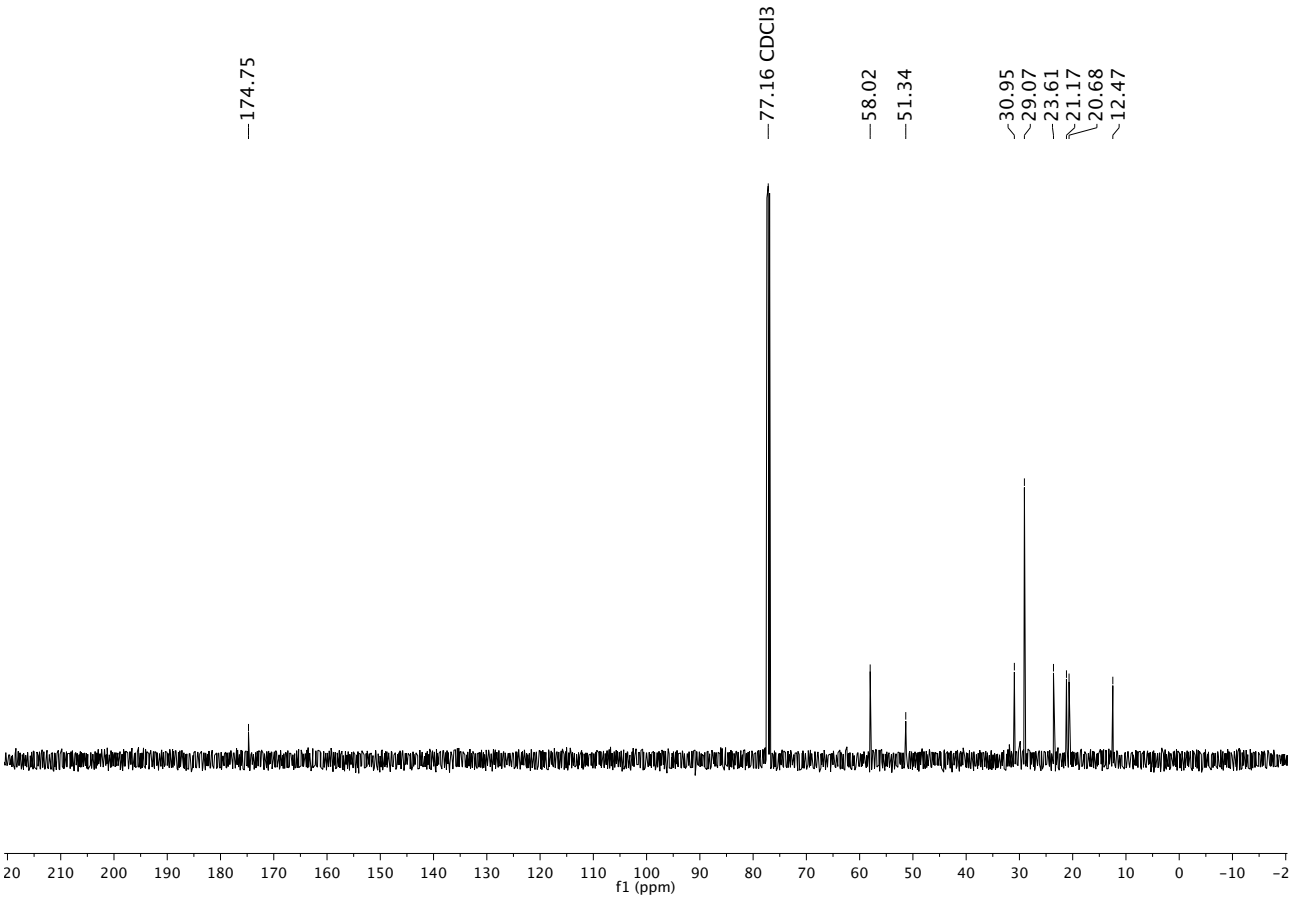
174.75
77.16 CDCl3
58.02
51.34
30.95
29.07
23.61
21.17
20.68
12.47
f1 (ppm)

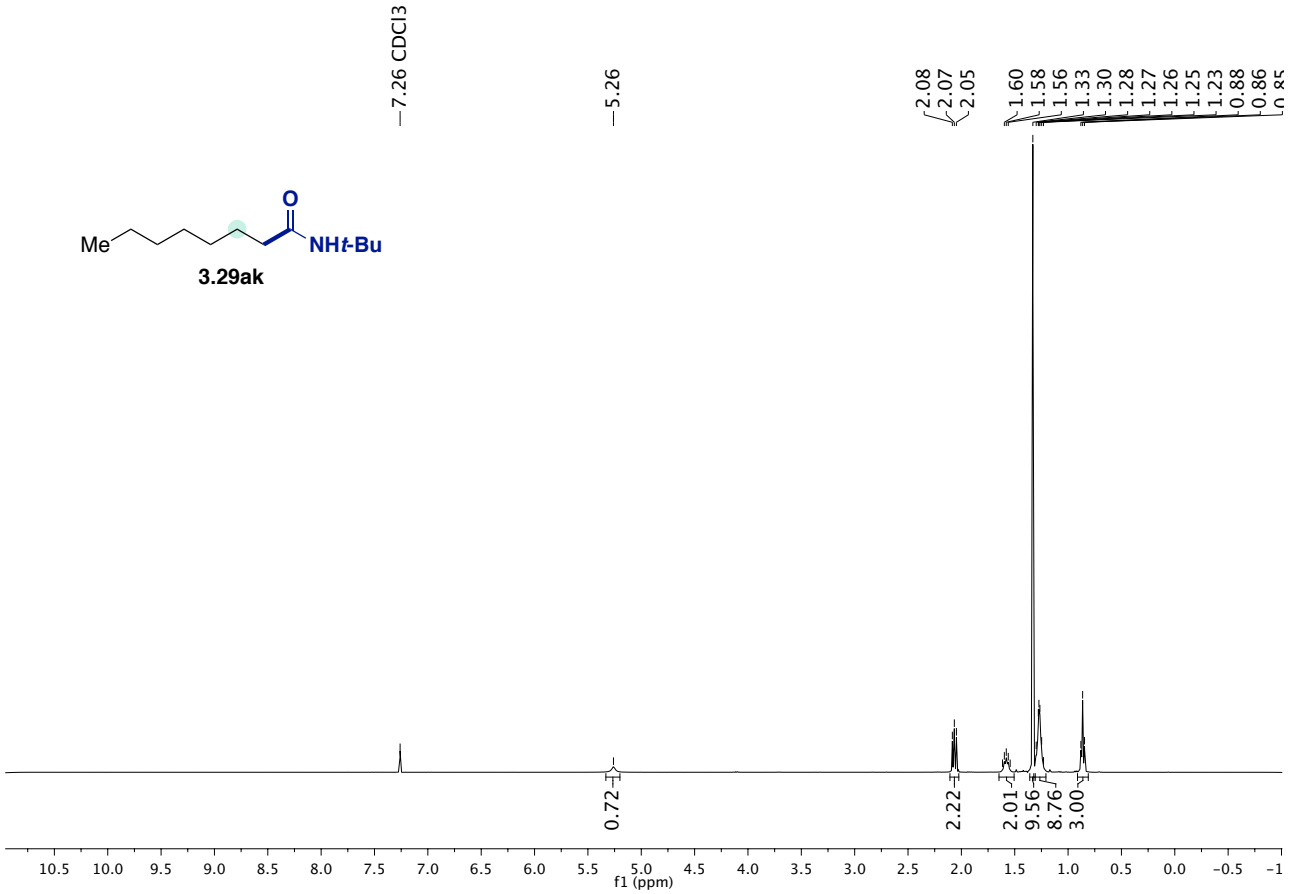
7.26 CDCl3
5.26
2.08
2.07
2.05
1.60
1.58
1.56
1.33
1.30
1.28
1.27
1.26
1.25
1.23
0.88
0.86
Me
O
NHt-Bu
3.29ak
0.72
2.22
2.01
9.56
8.76
3.00
f1 (ppm)

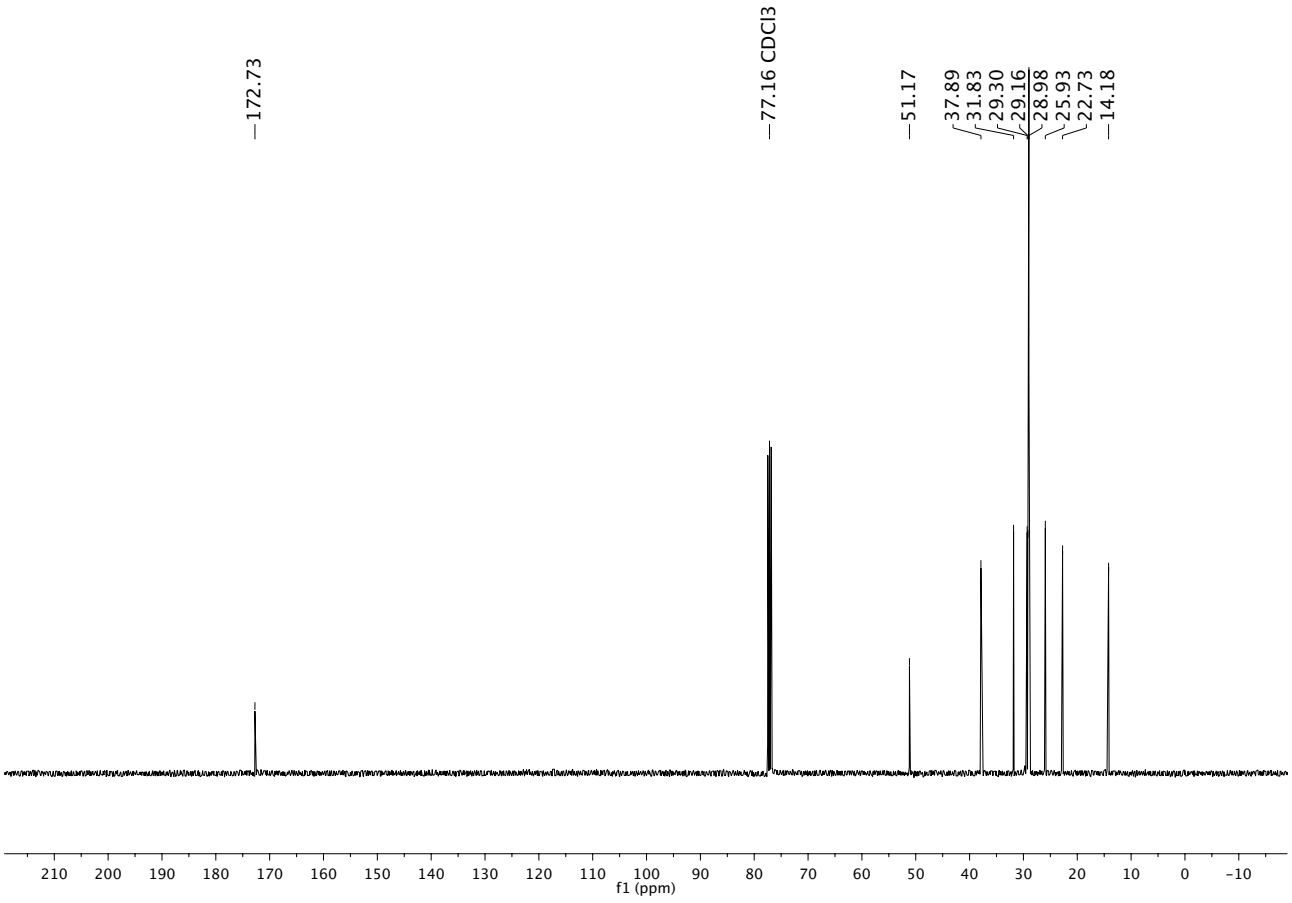
172.73
77.16 CDCl3
51.17
37.89
31.83
29.30
29.16
28.98
25.93
22.73
14.18
f1 (ppm)

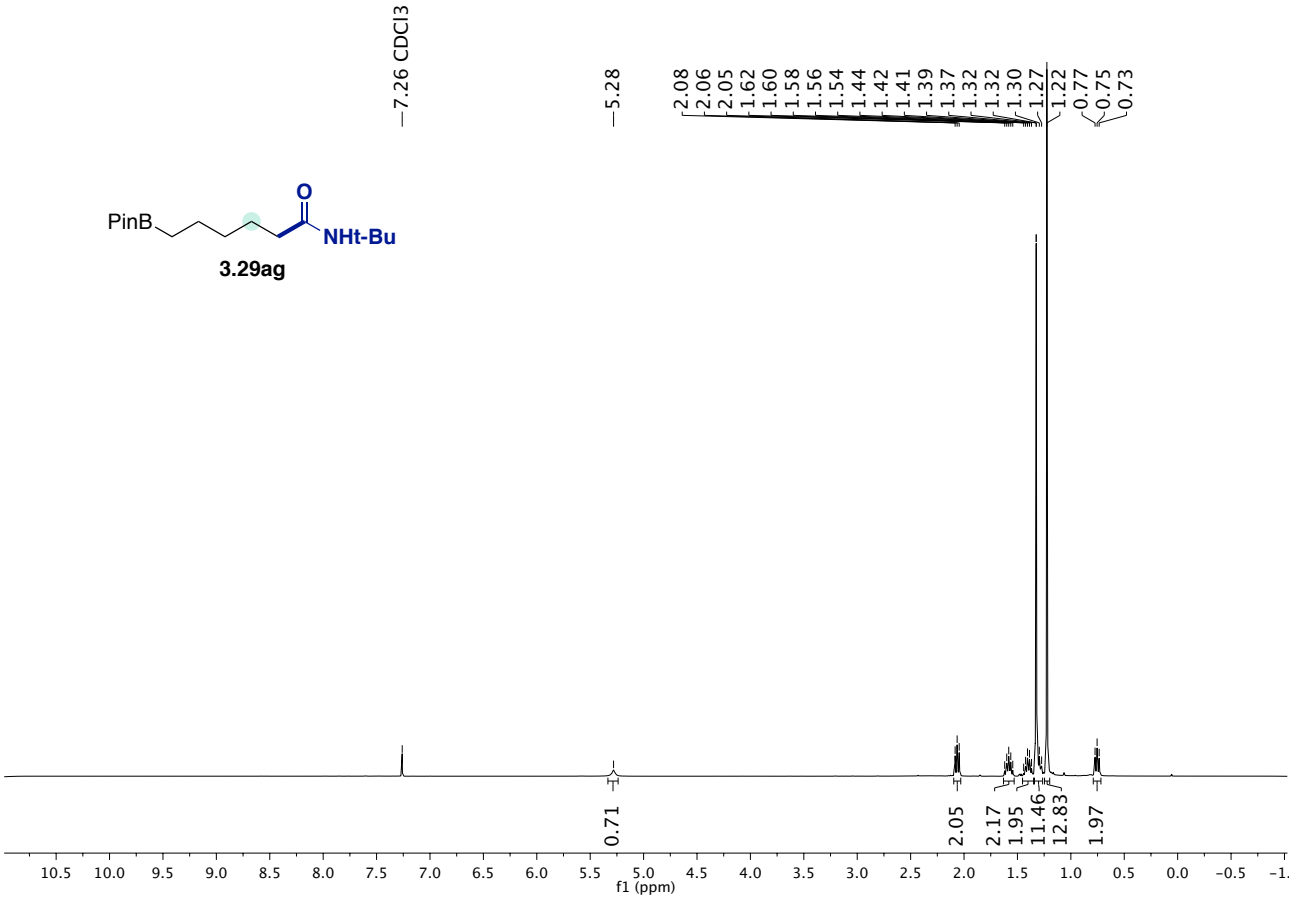
7.26 CDCl3
5.28
2.08
2.06
2.05
1.62
1.60
1.58
1.56
1.54
1.44
1.42
1.41
1.39
1.37
1.32
1.32
1.30
1.27
1.22
0.77
0.75
0.73
PinB
O
NHt-Bu
3.29ag
0.71
2.05
2.17
1.95
11.46
12.83
1.97
f1 (ppm)

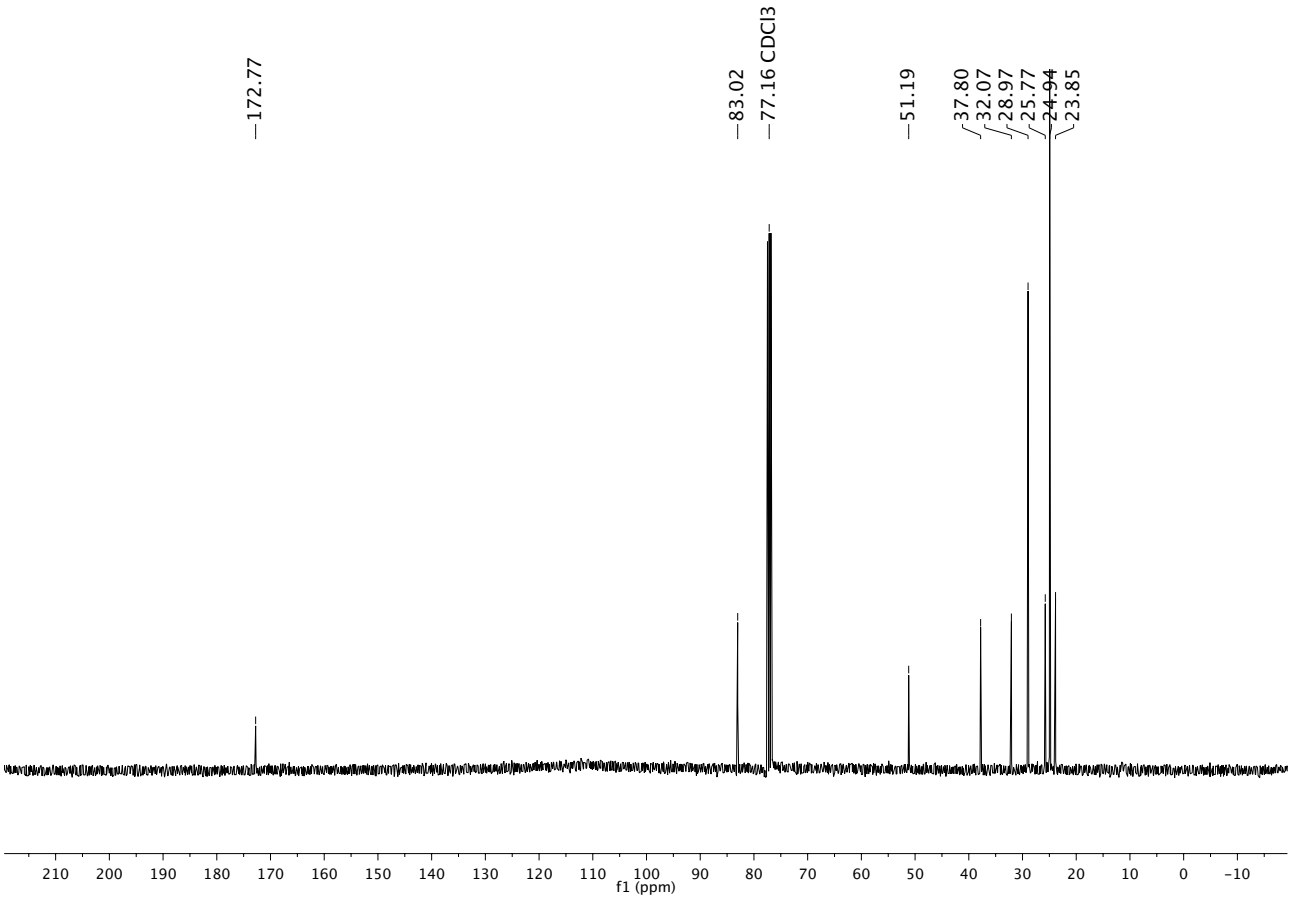
172.77
83.02
77.16 CDCl3
51.19
37.80
32.07
28.97
25.77
24.94
23.85
f1 (ppm)

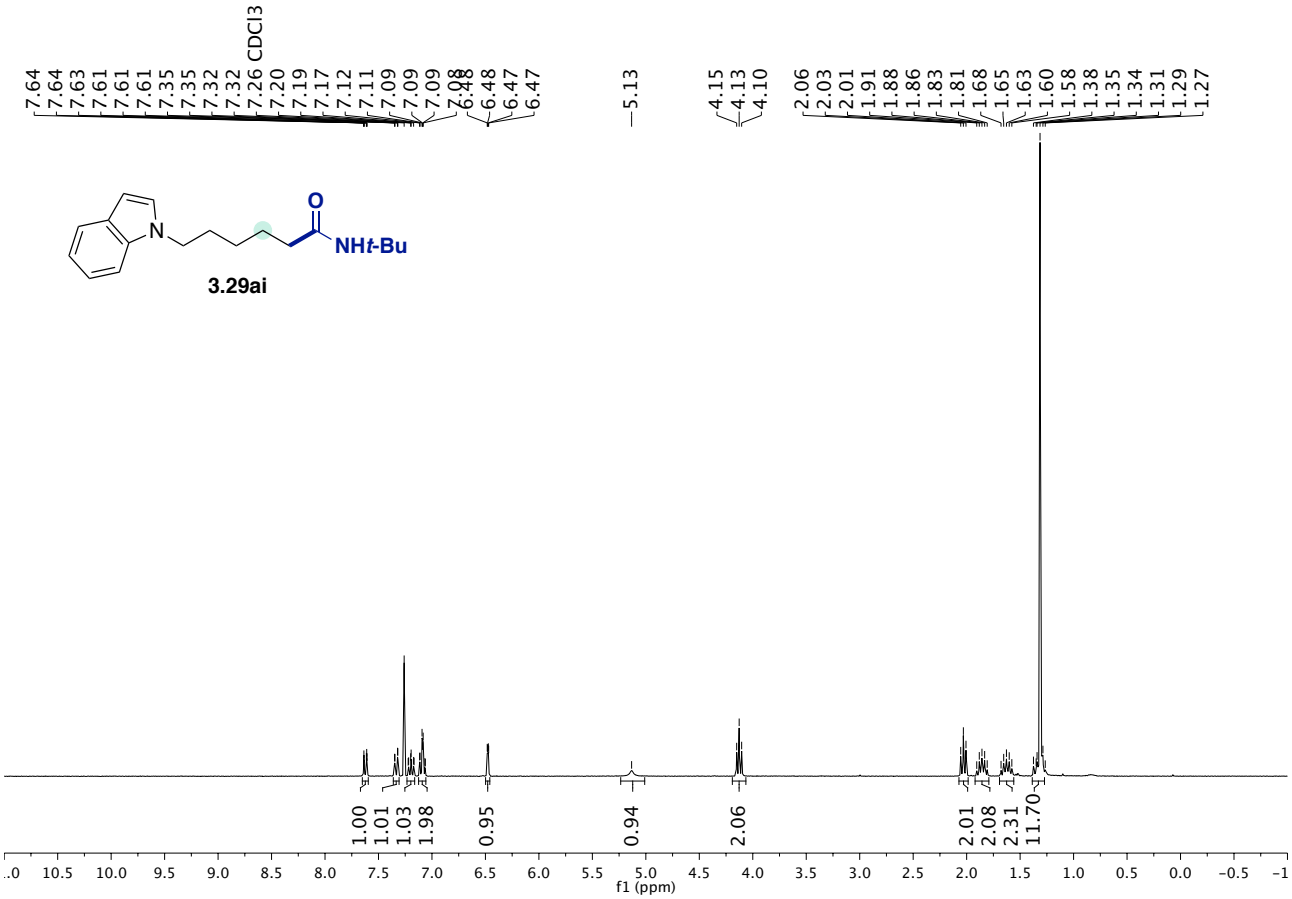
7.64
7.64
7.63
7.61
7.61
7.61
7.35
7.35
7.32
7.32
7.26 CDCl3
7.20
7.19
7.17
7.12
7.11
7.09
7.09
7.09
7.08
6.48
6.47
6.47
5.13
4.15
4.13
4.10
2.06
2.03
2.01
1.91
1.88
1.86
1.83
1.81
1.68
1.65
1.63
1.60
1.58
1.38
1.35
1.34
1.31
1.29
1.27
O
N
NHt-Bu
3.29ai
1.00
1.01
1.03
1.98
0.95
0.94
2.06
2.01
2.08
2.31
11.70
f1 (ppm)

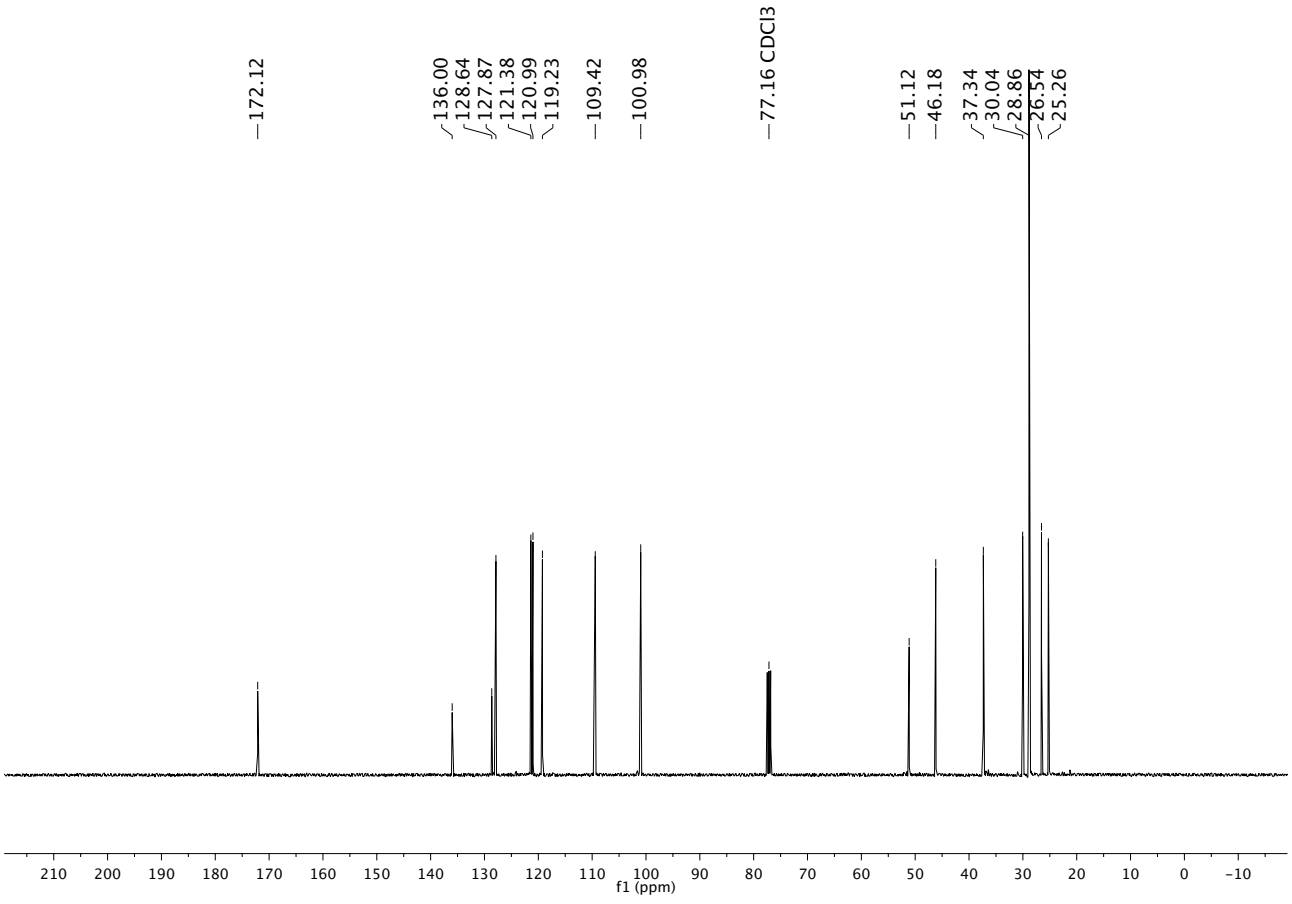
172.12
136.00
128.64
127.87
121.38
120.99
119.23
109.42
100.98
77.16 CDCl3
51.12
46.18
37.34
30.04
28.86
26.54
25.26
f1 (ppm)

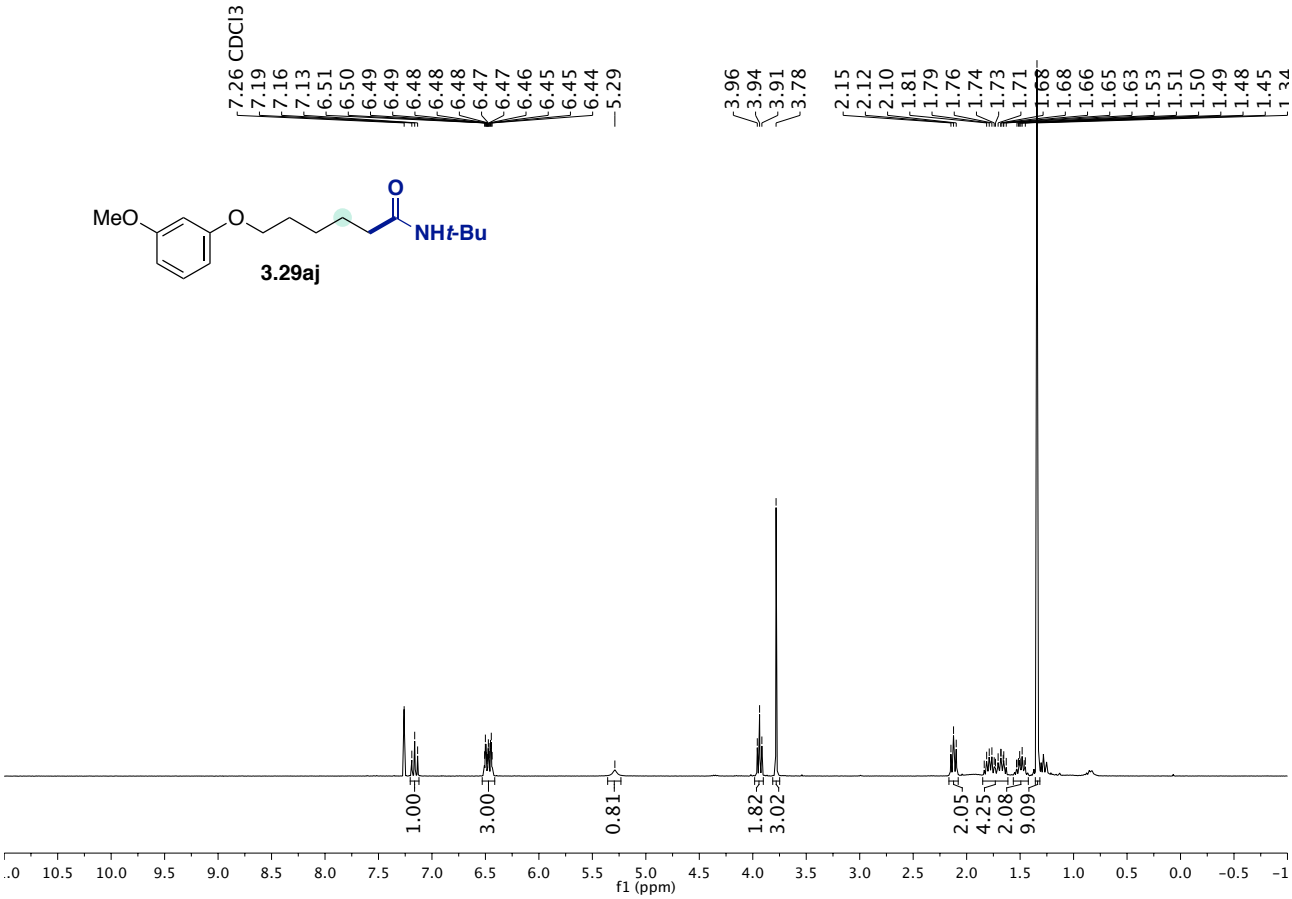
7.26 CDCl3
7.19
7.16
7.13
6.51
6.50
6.49
6.49
6.48
6.48
6.48
6.47
6.47
6.46
6.45
6.45
6.44
5.29
3.96
3.94
3.91
3.78
2.15
2.12
2.10
1.81
1.79
1.76
1.74
1.73
1.71
1.68
1.68
1.66
1.65
1.63
1.53
1.51
1.50
1.49
1.48
1.45
MeO
O
O
NHt-Bu
3.29aj
1.00
3.00
0.81
1.82
3.02
2.05
4.25
2.08
9.09
f1 (ppm)

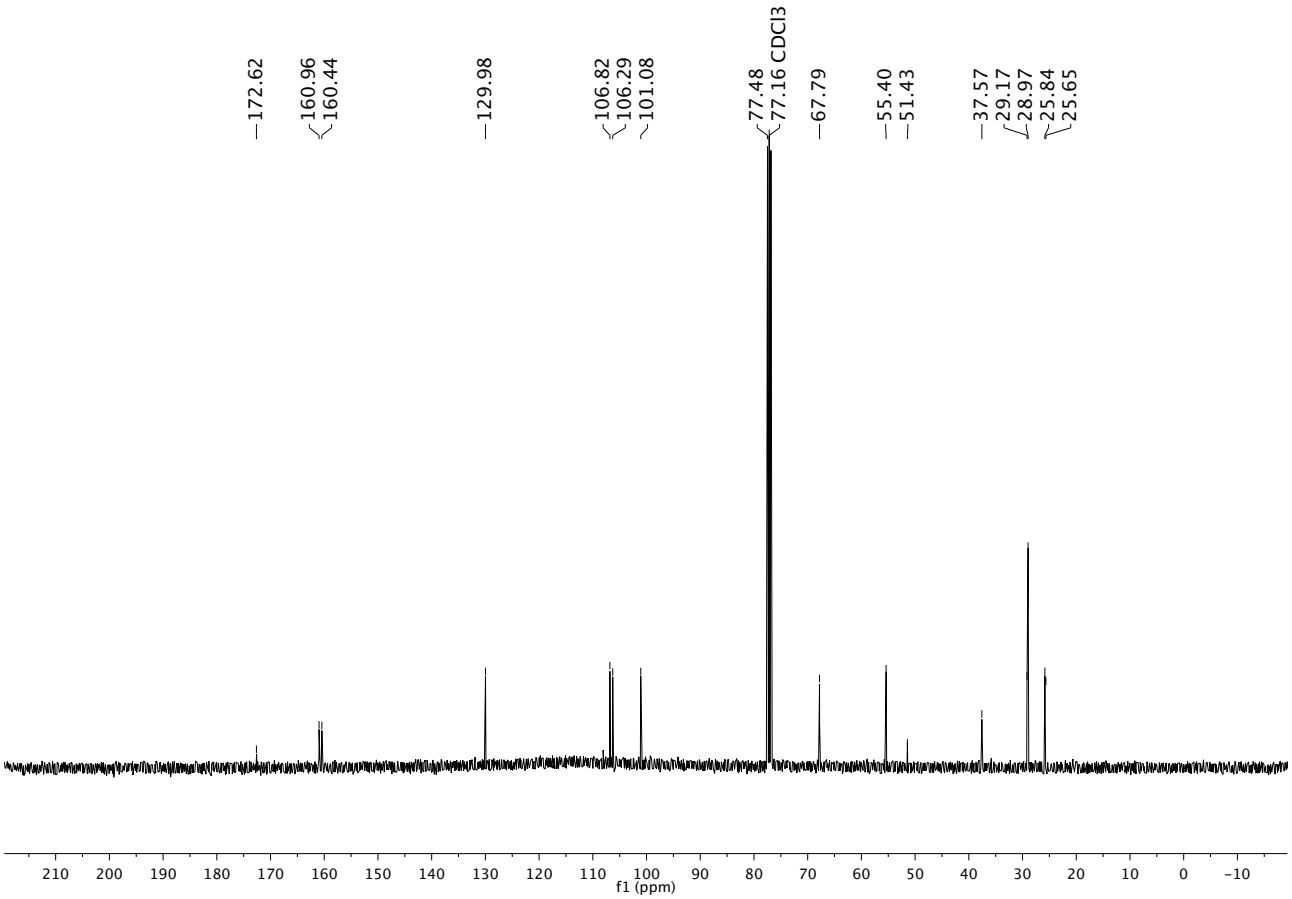
172.62
160.96
160.44
129.98
106.82
106.29
101.08
77.48
77.16 CDCl3
67.79
55.40
51.43
37.57
29.17
28.97
25.84
25.65
f1 (ppm)

UNIVERSITAT ROVIRA I VIRGILI
AMIDE FORMATION VIA NI-CATALYZED REDUCTIVE COUPLING REACTIONS WITH ISOCYANATES
Eloísa Sofía Serrano Robledo

Chapter 4.

Ni-Catalyzed Hydroamidation of Alkynes with Isocyanates using Alkyl Bromides as Hydride Sources

In collaboration with Dr. Xueqiang Wang and Dr. Masaki Nakajima

4.1. Introduction

4.1.1. Hydrometallation of Alkynes

Vinylmetal species have a wide application in organic synthesis, such as in the formation of C—C, C—X, C—M (M = Si, B, Sn) and C—Het (Het = N, O, S, P) bonds for the stereoselective synthesis of substituted olefins. One of the most reliable and direct techniques for their selective synthesis is through the hydrometallation of alkynes (Scheme 4.1). In some cases, the resulting alkenylmetal species are discrete, stable, and isolable. This includes vinylboranes, silanes and stannanes, which are widely used in both Pd-catalyzed cross-coupling reactions and in a variety of transformations such as oxidation, reduction or as nucleophiles. In other cases, vinylmetal species are generated *in situ*, either stoichiometrically or via transition metal-catalysis. The regioselectivity of the obtained products can be *syn*-, *anti*- or a mixture of both; however, even when metal-hydride insertion occurs via *syn*-addition the obtained products can isomerize. The mechanisms by which hydrometallation reactions proceed are diverse and not fully elucidated; nevertheless, it is generally accepted that the first step is the activation of the alkyne via coordination to the metal, and is followed by the addition step. In a *syn*-addition, metal insertion occurs via an inner-sphere mechanism to afford *cis*-products, whereas *trans*-selectivity can be achieved via an *anti*-addition that follows an outer-sphere mechanism.[1] In general, the regioselectivity of the reaction is determined by the steric and electronic properties of both the alkyne and the metal-hydride species.[2,3]

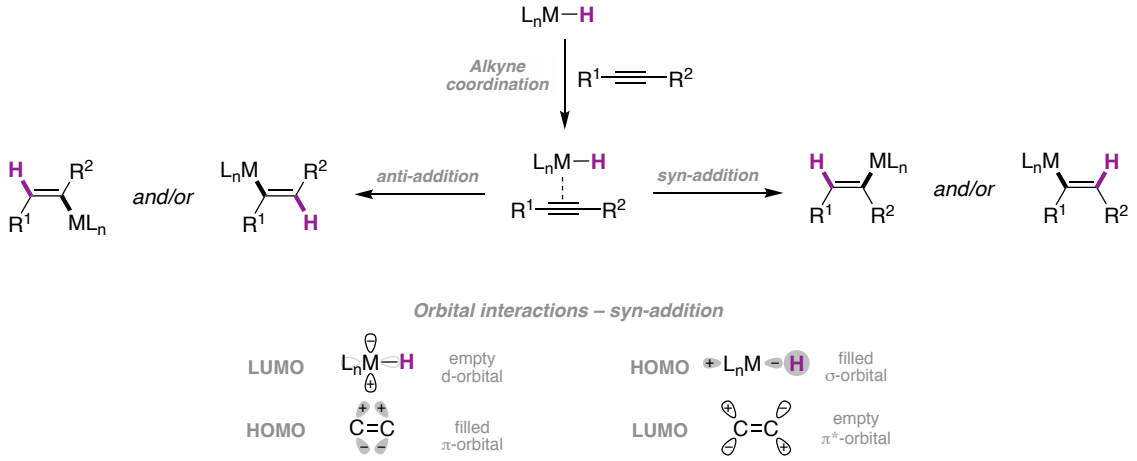

Scheme 4.1. Generation of vinylmetal species via alkyne hydrometallation

Among the most studied methods for the selective synthesis of isolable vinylmetal species are the hydroboration, -silylation and -stannation of alkynes via direct or transition metal-catalyzed methods.[3] The ability of transition metals to form highly reactive, transient vinylmetal species has unlocked the use of metalloid–H reagents that do not add directly to the alkyne in the uncatalyzed process, as well as for the trapping of vinyl-transition metal intermediates with different carbon- or heteroatom-based nucleophiles or electrophiles. Frequently, hydrometallations are performed using discrete hydride donor species, such as silanes, boron hydrides, tin hydrides, aluminum hydrides or zirconocene hydrides, among others. However, their use often reduces the functional group tolerance of the transformation. Other ways to generate transition metal hydrides have been developed, and of these, the protonation of transition metal complexes with an acid, such as acetic acid, to form a cationic metal hydride species has shown to be highly versatile.[4]

4.1.2. Metal-Catalyzed Routes towards Acrylamides

The importance and ubiquity of amides in biologically active molecules and materials continually encourages the design of new chemical transformations for the versatile synthesis of amide-containing molecules. The synthesis of acrylamides is particularly relevant as they serve as monomers for the preparation of polyacrylamides – hydrophilic polymers that find numerous industrial applications such as in solid-liquid separations performed in water treatment, papermaking, oil production and agriculture. Although most of these polymers are made using acrylamide, the simplest and cheapest monomer, other useful monomers include *N*-alkylacrylamide and *N*-alkylmethacrylamides.[5] The acrylamide moiety can also be found in pharmaceuticals and natural products,[6,7] albeit in a lesser extent than their saturated analogues. Moreover, the Michael-acceptor character of acrylamides makes them versatile synthons for the preparation of substituted aliphatic amides. Therefore, the development of chemical routes to prepare diversely functionalized acrylamides will have an impact in the field of polymeric materials, as well as in the synthesis of biologically active compounds.

4.1.2.1. Synthesis of Acrylamides via Ni-Catalyzed Cross-Coupling of α-Olefins with Isocyanates

Taking inspiration from the seminal reports by Hoberg and co-workers on the stoichiometric and catalytic reactions of Ni(0) complexes with alkenes and phenyl isocyanate,[8,9] the Jamison group reported the synthesis of acrylamides from α-olefins and isocyanates to selectively afford 1,1-disubstituted acrylamides (Scheme 4.2).[10,11] Unlike Hoberg's previous studies using Ni(0) complexes and trialkyl phoshines that generated *trans*-disubstituted α,β-unsaturated amides,[12–14] Jamison's protocol afforded an opposite selectivity using $Ni(COD)_2$ in combination with an NHC ligand. The observed regioselectivity was attributed to the selective formation of an azanickelacycle via oxidative coupling of the alkene and the isocyanate, with the olefin substituent pointing away from the bulky NHC ligand.

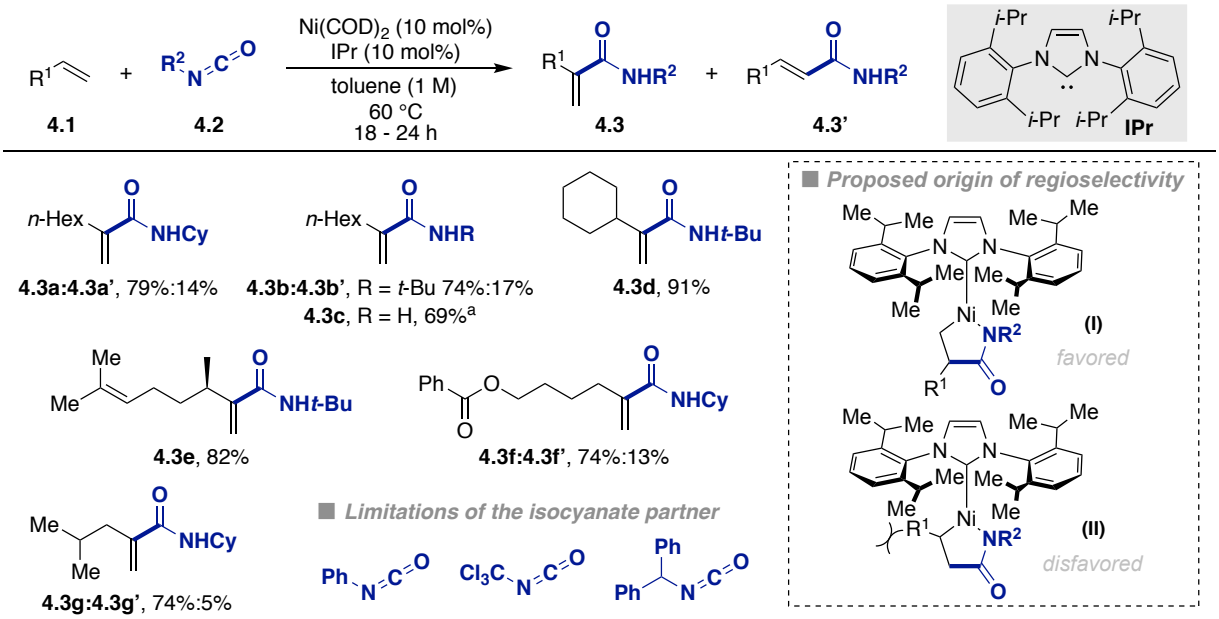

Reaction conditions: **4.1** (0.5 mmol), **4.2** (2 equiv), $Ni(COD)_2$ (10 mol%), IPr (10 mol%), toluene (1 M) at 60 °C, 18 - 24 h. [a] Using **4.3b** (0.2 mmol) in neat TFA (2 mL), 72 °C, 18 h.

Scheme 4.2. Ni-catalyzed synthesis of acrylamides from α-olefins and isocyanates

Under optimized conditions, excellent selectivities towards the 1,1-disubstituted acrylamides were obtained with α-olefins bearing substituents at the allylic and homoallylic position, whereas a slightly lower selectivity was

observed for unbranched α-olefins. Although the abundance and low cost of α-olefins is a considerable advantage in this transformation, a rather limited number of isocyanates could be used as isocyanates other than *tert*-butyl or cyclohexyl led to isocyanate oligomers. Efforts to control the observed side reactions, including the slow or portion-wise addition of the isocyanates, were met with little success. Given that isocyanate trimerization is known to be catalyzed by free NHC ligands,[15] the authors premixed the nickel precatalyst with the ligand prior to the reaction, yet no improvement was observed.[11] The synthetic utility of the reaction could be extended to the synthesis of *N*-primary acrylamides by deprotection of the *tert*-butyl group in neat TFA.

4.1.2.2. Alkynes as Synthons for Acrylamides

Pd-Catalyzed Aminocarbonylations:

Different protocols for the Pd-catalyzed aminocarbonylation of terminal alkynes with primary or secondary amines have been developed. In these methods, the use of Pd catalysts in combination with monodentate or bidentate phosphines affords high yields of the desired branched or linear acrylamides with good regioselectivities (Scheme 4.3).[16–19] Although these reactions are widely used in industry for the synthesis of acrylamides from simple starting materials, they have found limited use in advance target synthesis. The major drawbacks associated with these transformations are the narrow scope of alkynes, as well as the high pressures of CO needed, often in combination with H_2 in syngas mixtures or with strong acids. Although in-depth mechanistic studies are still needed to fully elucidate the mechanism by which aminocarbonylation reactions operate, preliminary studies have suggested the intermediacy of Pd—H species.[20]

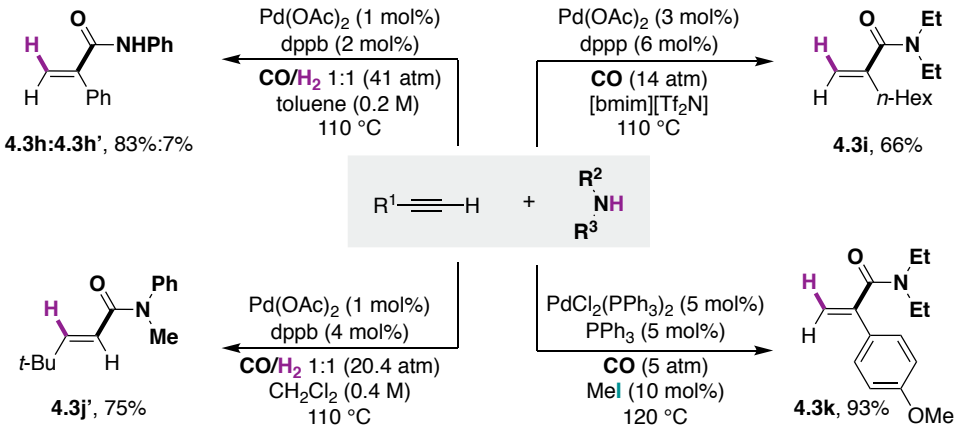

Scheme 4.3. Aminocarbonylation reactions of terminal alkynes using CO and Pd-catalysts

Metal-Catalyzed Intermolecular Hydrocarbamoylations:

The transition metal-catalyzed hydrocarbamoylation of unsaturated C—C triple bonds via insertion into the C—H bond of formamides is an alternative to the use of toxic CO. The application of this strategy to the synthesis of acrylamides was first developed in an intramolecular version starting from alkynylformamides using Rh catalysts.[21] This was followed by the intermolecular synthesis of acrylamides using synergistic Ni and Lewis acid catalysis (Scheme 4.4).[22] In this report, a diverse range of *N*-substituted formamides could be activated and inserted with high regioselectivity across the triple bond of symmetric and asymmetric alkynes. The major limitations of the reaction were the rather limited scope of alkynes and the *in situ* isomerization of the initial (*E*)-acrylamide to give *E/Z* mixtures. The authors proposed a mechanism in which activation of the formamide by coordination to the Lewis acid facilitates the oxidative addition of the C(sp^2)—H bond to the Ni(0) center. Subsequent alkyne coordination sets the basis for a regioselective hydrometallation by avoiding the steric clash between the bulkiest group of the alkyne and the carbamoyl group. A final reductive elimination leads to the desired acrylamide.

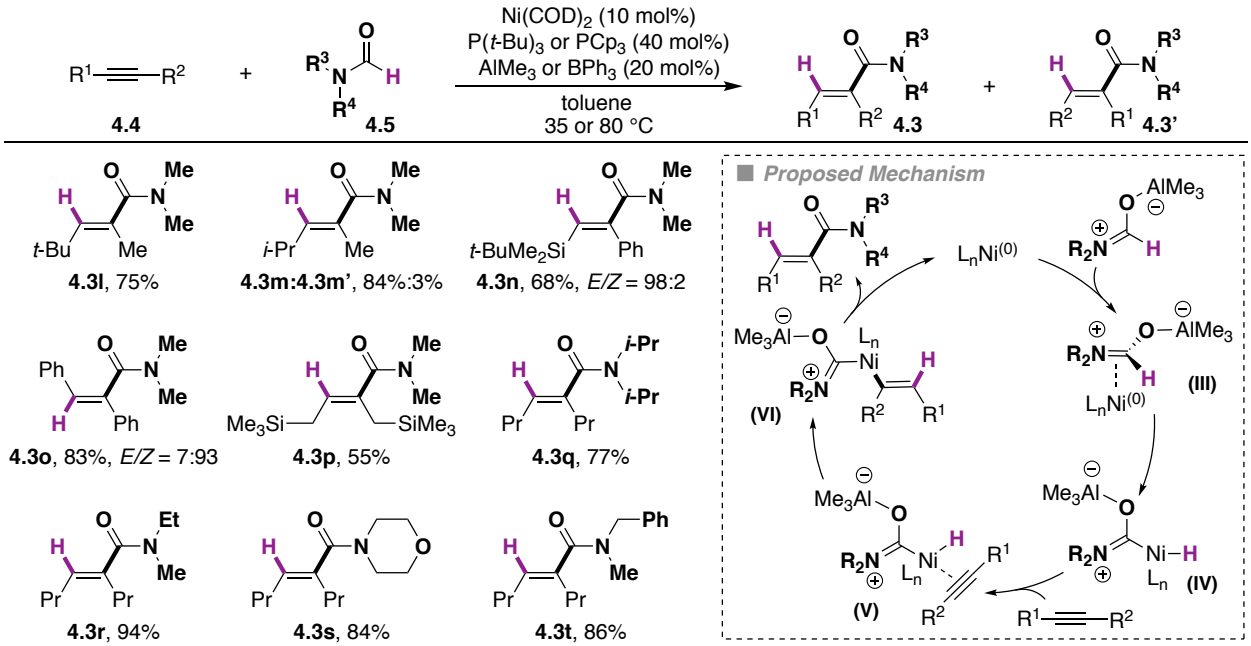

Scheme 4.4. Ni/AlMe$_3$ synergistic catalysis for the hydrocarbamoylation of alkynes using formamides

In a subsequent report, the Tsuji group greatly improved the stereoselectivity and scope of the transformation by using palladium catalysis (Scheme 4.5).[23] The addition of benzoyl chloride was necessary to initiate the reaction by forming catalytic amounts of HCl, which is known to generate Pd—H species *in situ*.[24] Under optimized reaction conditions, a wide variety of internal and terminal alkynes bearing sensitive functional groups were well accommodated, and high *E/Z* ratios were observed.

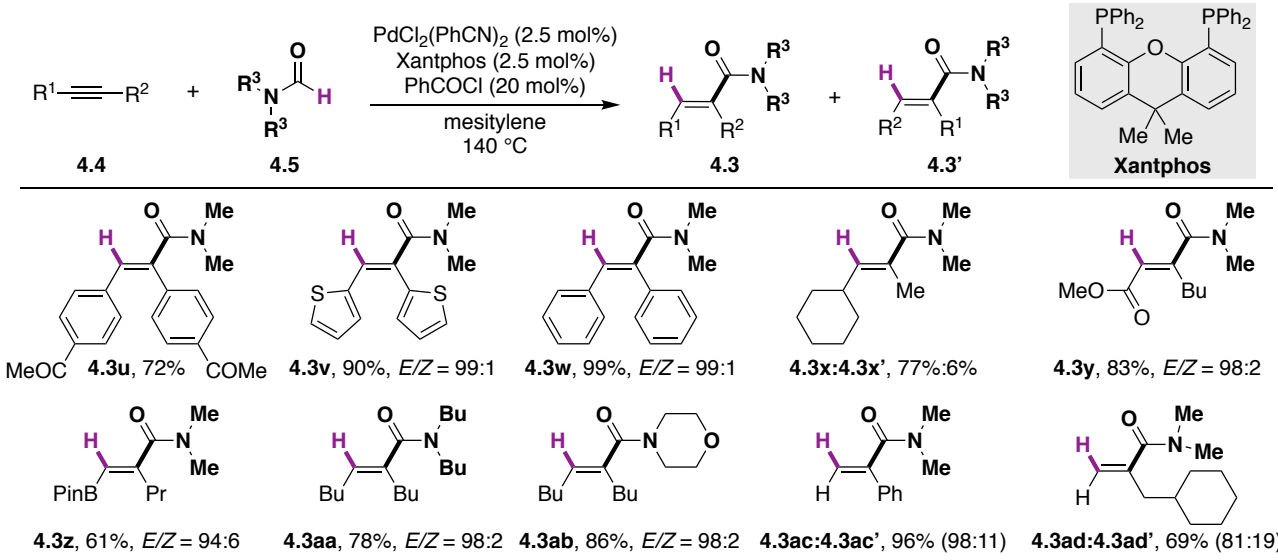

Scheme 4.5. Pd-catalyzed hydrocarbamoylation of alkynes with *N*-substituted formamides

Preliminary mechanistic studies pointed towards a different reaction mechanism using Pd-catalysts from the Ni-catalyzed hydrocarbamoylation depicted above. Specifically, the authors propose a reaction initiated by the insertion of the *in situ*-generated Pd—H species across the alkyne bond, followed by either *a)* insertion into the C=O bond of formamide to generate an alkoxypalladium(II) intermediate that gives rise to the product after β-hydride elimination, or *b)* oxidative addition of the C—H bond in formamide to afford a Pd(IV) intermediate, which

after reductive elimination generates the acrylamide. Both of the proposed pathways regenerate the active Pd—H species. In both the Pd- and the Ni-catalyzed hydrocarbamoylation methods, only a small range of *N,N*-dialkylformamides could be used, and no reaction was observed for either primary or *N*-aryl-substituted formamides.

4.1.3. Ni-Catalyzed Cycloadditions of Alkynes and Isocyanates

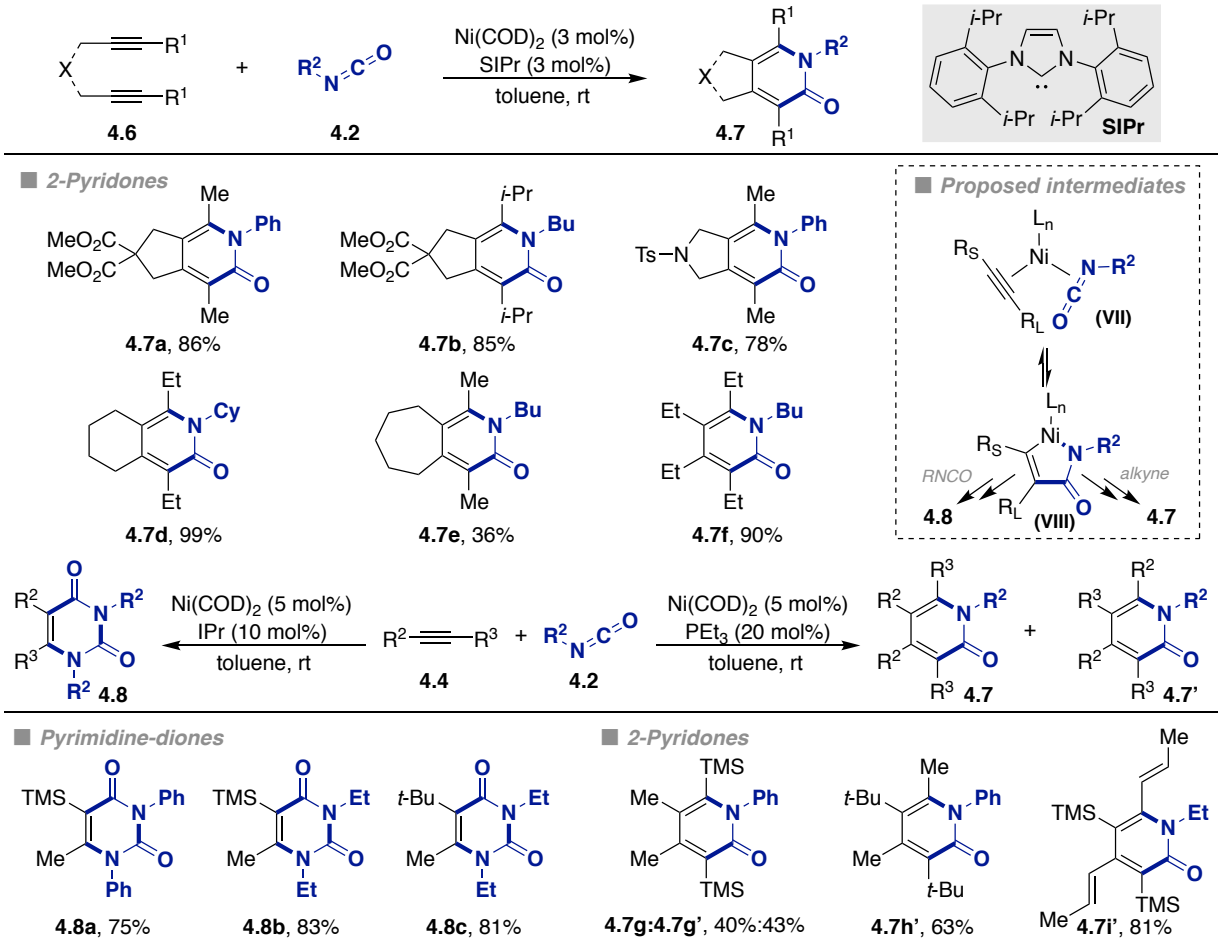

Scheme 4.6. Ni-catalyzed cycloaddition of alkynes and isocyanates to afford 2-pyridiones or pyrimidine-diones

The Ni-catalyzed synthesis of 2-pyridones and pyrimidine-diones from alkynes and isocyanates was reported by Louie (Scheme 4.6). Intramolecular reactions with diynes afforded bicyclic 2-pyridones when a catalytic system based on $Ni(COD)_2$ and an NHC ligand was used.[25] Optimal results for the intermolecular reaction of asymmetric alkynes were obtained with a different catalytic system using triethylphosphine as ligand, although regioisomeric mixtures of products were isolated in these cases.[26] When an excess of the isocyanate was present in the reaction, the coupling of two isocyanate molecules with an unsymmetrical alkyne generated pyrimidine-diones.[27] The optimization of the reaction conditions minimized the formation of side-products arising from the alkyne and the isocyanate coupling partners, both of which readily trimerize to afford polysubstituted benzenes[28] and isocyanurates,[15] respectively. Moreover, the transformations occurred under mild conditions, and aryl as well as alkyl isocyanates were well tolerated. In line with the proposed pathway for the coupling of alkenes and isocyanates by Hoberg and Jamison (vide supra), the mechanism of the reactions was proposed to follow an oxidative coupling between the alkyne, the isocyanate and the nickel center, regardless of the ligand used. The regioselectivity of the products largely depends on the steric factors of the alkyne substituents.

4.1.4. Ni-Catalyzed Hydrocarboxylation of Alkynes with CO_2 using Alcohols as Proton Source

In 2015, our group reported the Ni-catalyzed regioselective formal hydrocarboxylation of alkynes using atmospheric pressures of CO_2 (Scheme 4.7).[29] In contrast to previously reported metal-catalyzed hydrocarboxylations of alkynes,[30,31] no organometallic reagents or silanes were needed, as in this case simple alcohols could be used as proton sources. The mild reaction conditions allowed for a broad functional group tolerance including ketones, heterocycles, esters, and nitriles, among others. Importantly, an opposite regioselectivity was observed compared to classical hydrocarboxylations of alkynes that occur via M—H species, as the carboxylation occurred distal to the aromatic substituent. Preliminary mechanistic studies suggested the ability of the aliphatic alcohol to act as a formal hydride source, as 83% deuterium incorporation into **4.10h** was observed when the reaction was performed with deuterated-isopropyl alcohol. In line with Hoberg's work,[32] an oxidative cyclization between the nickel-center, the alkyne and the activated CO_2 was proposed as a plausible mechanism. The origin of the regioselectivity was attributed to the intermediacy of rapidly interconverting nickelalactones, one of which preferentially reacts with the alcohol in such a way that the steric interactions are minimized. Subsequent protonolysis of the C—Ni(II) bond opens the nickelalactone (**X**), and a final reduction with Mn regenerates the propagating active Ni(0)L_n species.

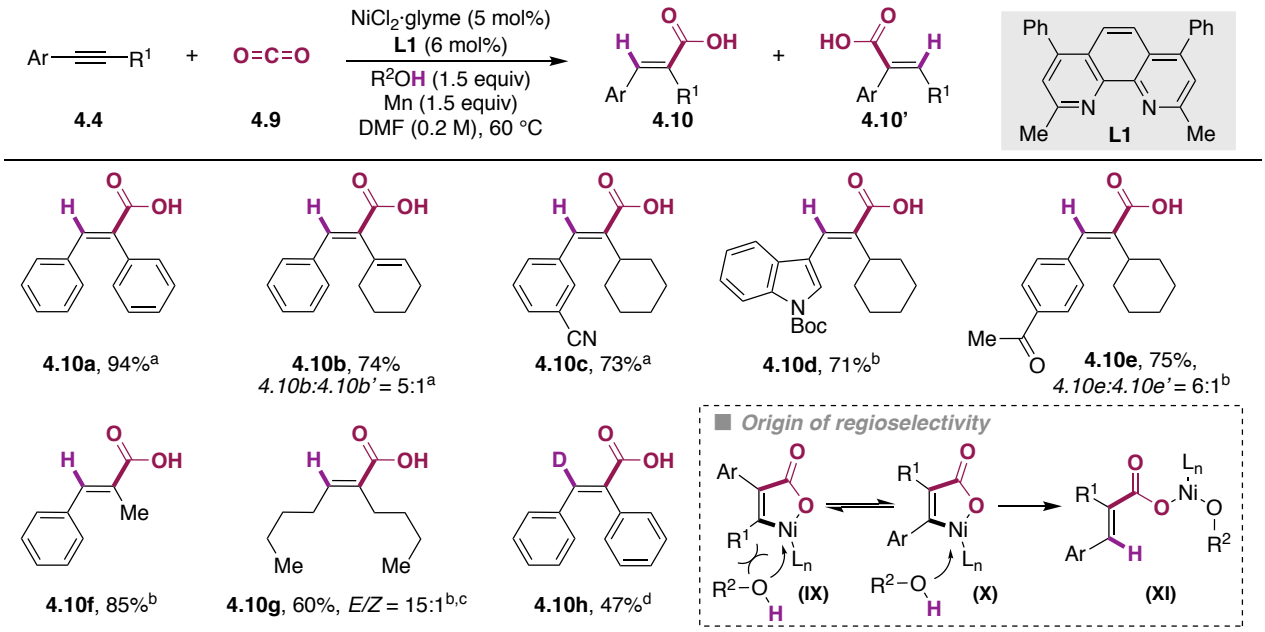

Reaction conditions: **4.4** (0.50 mmol), R^2OH (0.75 mmol), CO_2 (1 atm), $NiCl_2$·glyme (5 mol%), **L1** (6 mol%), Mn (1.5 equiv), DMF (0.20 M) at 60 °C. [a] R^2OH = *i*-PrOH. [b] R^2OH = *t*-BuOH. [c] Using $NiCl_2$·glyme (15 mol%), **L1** (18 mol%) at 80 °C. [d] 83% of D-incorportation using *i*-PrOD.

Scheme 4.7. Ni-catalyzed hydrocarboxylation of alkynes with CO_2 using alcohols as proton sources

4.2. General Aim of the Project

Concerning the current state-of-the-art synthesis of acrylamides, there is a paucity of mild, highly regio- and diastereoselective protocols for the synthesis of acrylamides bearing different alkyl and aryl substituents. For example, the use of isocyanates and alkenes under Ni-catalysis is limited to the generation of 1,1-disubstituted acrylamides. The developed Pd-catalyzed aminocarbonylation methods only tolerate the use of terminal acetylenes and necessitate high pressures of CO. Although metal-catalyzed hydrocarbamoylations show a broader alkyne scope, they are limited to the use of *N,N*-dialkylformamides and need high reaction temperatures.

Inspired by our group's previous work in the hydrocarboxylation of alkynes with CO_2 and in the amidation reactions using isocyanates, we envisaged that a related hydroamidation of alkynes would be a versatile and efficient route to access a wide array of acrylamides under mild reaction conditions. Yet, the need for hydride sources or acids to generate the intermediate M—H species posed a challenge, as these can readily react with the isocyanate coupling partner. To overcome this innate reactivity, we sought to *in situ* generate catalytic amounts of Ni—H species that would readily insert into the alkyne instead of reacting with the isocyanate. Given the known propensity of alkyl halides to undergo unproductive β-hydride elimination[33,34] and the knowledge acquired in Chapter 3, we envisioned to take advantage of this commonly undesired reaction and transform it into a synthetic advantage for the *in situ* and mild generation of Ni—H species. This Chapter describes the development of a Ni-catalyzed hydroamidation of alkynes with isocyanates, using light alkyl bromides as hydride sources (Scheme 4.8).

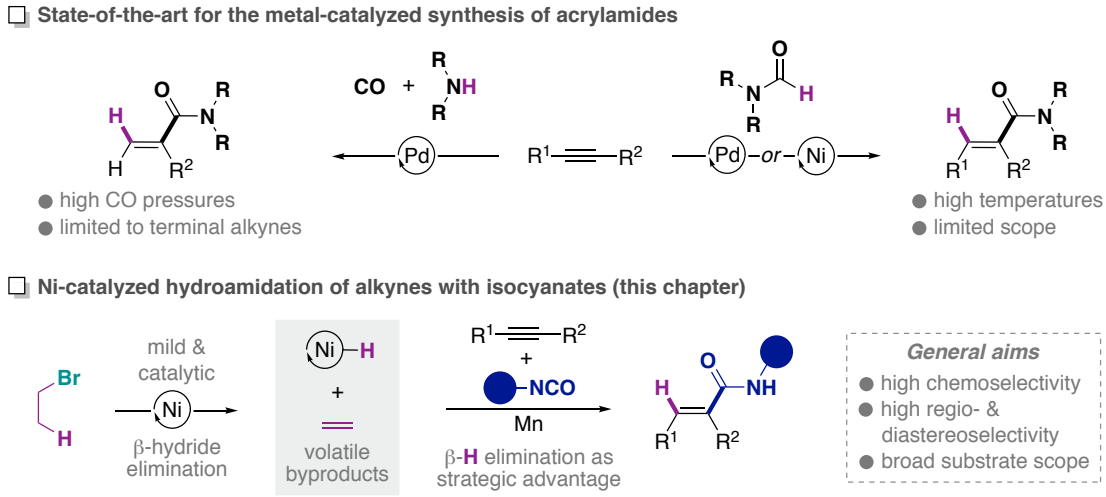

Scheme 4.8. Ni-catalyzed reductive hydroamidation of alkynes with isocyanates using light alkyl bromides as hydride sources

4.3. Ni-Catalyzed Hydroamidation of Alkynes with Isocyanates using Alkyl Bromides as Hydride Sources

4.3.1. Optimization of the Reaction Conditions

The screening for optimal reaction conditions was carried out using diphenylacetylene, *tert*-butyl isocyanate and *n*-butyl bromide as model substrates. The choice of *tert*-butyl isocyanate was based on previous reports that showed its compatibility with Ni-catalysis, as well as the synthetic utility of *N-tert*-butyl-substituted acrylamides for the formation of primary amides by deprotection of the *tert*-butyl group.[10] In line with our previous studies with both CO_2[29] and isocyanates,[35] we focused our attention on nitrogen ligands such as bipyridines, phenanthrolines, and terpyridines that were tested in the presence of catalytic amounts of a nickel(II) salt and Mn as reducing agent, in DMF as solvent (Table 4.1). In line with Chapters 2 and 3, the best yields were obtained with ligands bearing *ortho*-substituents (entry 1 vs. entries 2 and 3, for example). The best balance between selectivity towards the desired acrylamide and reactivity was found when bathocuproine (**L1**) was used as ligand (entry 5).

Scheme 4.9 shows the possible reaction side-products involving the different coupling partners. In all cases shown in Table 4.1, **4.3ae** was formed as a single *E*-diastereomer. The mass balance for the different electrophiles used account for the reduction of **4.4h** to *cis*- and *trans*-stilbene, and GC-MS-detectable amounts of *N*-(*tert*-butyl)pentanamide and hydroalkylation products. Importantly, no oligomerization or significant isocyanate

reduction was observed and only traces of urea were detected in the crude mixtures – which can either be formed during the reaction or upon acidic quenching of the reaction.

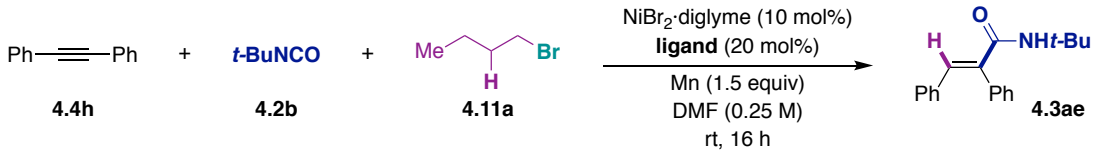

Entry	Ligand	Conversion of 4.4h (%)[a]	Yield of 4.3ae (%)[a]
1	2,2'-bipyridine (**L2**)	66	8
2	6-methyl-2,2'-bipyridine (**L3**)	100	44
3	6,6'-dimethyl-2,2'-bipyridine (**L4**)	94	64
4	1,10-phenanthroline (**L5**)	0	0
5	bathocuproine (**L1**)	79	55
6	neocuproine (**L6**)	94	57
7	2-methyl-1,10-phenanthroline (**L7**)	87	31
8	6.6''-dimethyl-2,2':6',2''-terpyridine (**L8**)	92	18
9	6-methyl-2,2':6',2''-terpyridine (**L9**)	73	5

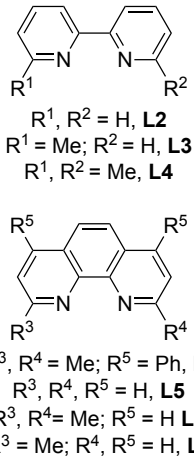

Reaction conditions: **4.4h** (0.25 mmol), **4.2b**(0.38 mmol), **4.11a** (0.38 mmol), $NiBr_2$·diglyme (10 mol%), ligand (20 mol%), Mn (0.38 mmol), DMF (1 mL) at rt, 16 h. [a] HPLC conversion and yield using naphthalene as internal standard. Mass balance accounts for *cis*- and *trans*-stilbene and hydroalkylation of **4.4h**.

Table 4.1. Screening of nitrogen-containing ligands

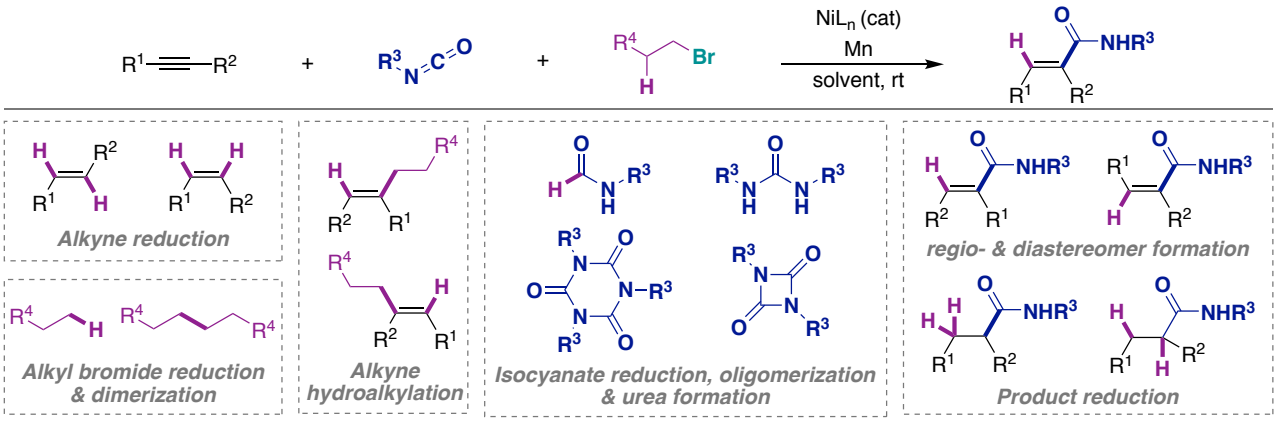

Scheme 4.9. Possible side-products of the studied Ni-catalyzed hydroamidation reaction

Next, a small set of primary and secondary alkyl bromides was evaluated for the ability to act as *in situ* hydride sources (Table 4.2). No improvement was observed when changing the length of the chain of primary alkyl bromides (entries 1 to 3), but higher yields of the desired product were obtained when a secondary alkyl bromide was used (entry 4). This result can be explained by the presence of additional β-hydrogens that increase the probability of β-hydride elimination from the oxidative addition complex. It is important to mention that only small amounts of amidation products coming from isopropyl bromide were detected by GC-MS in the reaction crudes. These products were identified as *N*-(*tert*-butyl)butyramide as the major side-product, and as *N*-(*tert*-butyl)isobutyramide, of which only traces were formed. Indeed, the choice of using light alkyl bromides that generate volatile olefins minimized the formation of aliphatic amides and ensured the availability of Ni—H species that perform the hydrometallation of the alkyne.

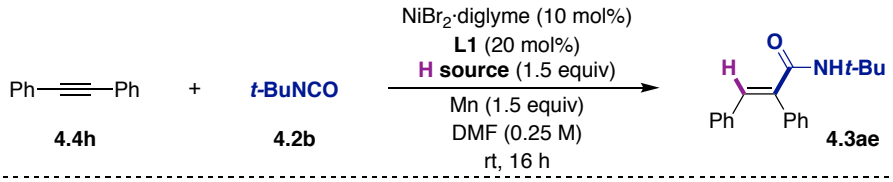

Entry	H source	Conversion of 4.4h (%)[a]	Yield of 4.3ae (%)[a]
1	*n*-BuBr (**4.11a**)	79	55
2	*n*-PrBr (**4.11b**)	100	44
3	EtBr (**4.11c**)	100	54
4	*i*-PrBr (**4.11d**)	100	74

Reaction conditions: **4.4h** (0.25 mmol), **4.2b** (0.38 mmol), **H** source (0.38 mmol), $NiBr_2$·diglyme (10 mol%), **L1** (20 mol%), Mn (0.38 mmol), DMF (1 mL) at rt, 16 h. [a] HPLC conversion and yield using naphthalene as internal standard. Mass balance accounts for *cis*- and *trans*-stilbene and hydroalkylation of **4.4h**.

Table 4.2. Screening of alkyl bromides as hydride sources

As the identity of the solvent has a strong influence in metal-catalyzed reductive couplings, the effect of different polar solvents was studied (Table 4.3). In parallel to previous methods developed in our group using CO_2[36] and isocyanates,[35,37] better results were obtained when using amide-containing solvents (entries 1 to 3), whereas no reactivity was observed when trifluorotoluene or tetrahydrofuran were used (entries 4 and 5). As commented in Chapters 2 and 3, the higher yields observed when amide-containing solvents are employed could be explained by their high dielectric constant,[38] which directly influences the stabilization of charged intermediates. Perhaps more importantly, the formation of cationic intermediates is likely to occur, as it has been shown that donor solvents such as DMF, are able to promote ligand exchange with the halide coordinated to the metal center.[39] Specifically, it has been found that [(bipy)Ni(Mes)Br] complexes form cationic $[(bipy)Ni(Mes)]^+$ species in coordinating solvents such as DMF, acetonitrile and DMSO; whereas in other solvents, such as acetone, ether or chlorinated solvents the neutral complexes are stable.[40,41] These cationic-Ni species are more electrophilic and thus easier to reduce and can comproportionate more readily than the neutral analogs.

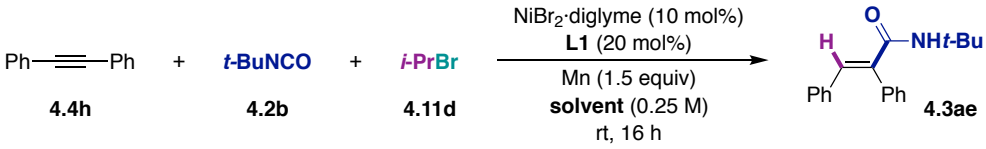

Entry	Solvent	Conversion of 4.4h (%)[a]	Yield of 4.3ae (%)[a]
1	DMF	100	73
2	DMA	58	54
3	NMP	100	91
4	$PhCF_3$	0	0
5	THF	0	0

Reaction conditions: **4.4h** (0.25 mmol), **4.2b** (0.38 mmol), *i*-PrBr (0.38 mmol), $NiBr_2$·diglyme (10 mol%), **L1** (20 mol%), Mn (0.38 mmol), solvent (1 mL) at rt, 16 h. [a] HPLC conversion and yield using naphthalene as internal standard. Mass balance accounts for *cis*- and *trans*-stilbene and hydroalkylation of **4.4h**.

Table 4.3. Screening of solvents

As shown in Table 4.4, the screening of different nickel sources showed no improvement when using a nickel source other than $NiBr_2$·diglyme. Similar results were obtained with nickel salts having chloride or bromide counterions (entries 1 to 4), whereas lower or no yield was obtained with $Ni(COD)_2$ or $Ni(acac)_2$, respectively (entries 5 and 6). The higher yields obtained with NiX_2 salts could be explained by the ability of halide anions to facilitate inner-sphere SET processes by acting as bridging ligands.[42] The results obtained with $Ni(COD)_2$ can

tentatively be attributed to the presence of 1,5-cyclooctadiene in solution that can compete with the alkyne for coordination to the nickel catalyst. The lack of reactivity when catalytic amounts of $Ni(acac)_2$ are used is rather surprising, as this Ni source has been successfully used in reductive cross-coupling reactions in combination with phenanthroline- and bipyridine-type ligands.[43,44] However, it is possible that the lower lability of acac compared to halide ligands hampers reactivity.

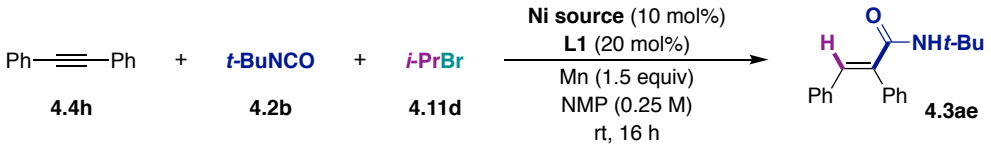

Entry	Ni source	Conversion of 4.4h (%)[a]	Yield of 4.3ae (%)[a]
1	$NiBr_2$·diglyme	100	91
2	$NiBr_2$·glyme	100	84
3	$NiBr_2$	87	81
4	$NiCl_2$·glyme	100	86
5	$Ni(COD)_2$	77	68
6	$Ni(acac)_2$	0	0

Reaction conditions: 4.4h (0.25 mmol), **4.2b** (0.38 mmol), *i*-PrBr (0.38 mmol), Ni-source (10 mol%), **L1** (20 mol%), Mn (0.38 mmol), NMP (1 mL) at rt, 16 h. [a] HPLC conversion and yield using naphthalene as internal standard. Mass balance accounts for *cis*- and *trans*-stilbene and trace hydroalkylation of **4.4h**.

Table 4.4. Screening of nickel sources

Considering that the previous screenings led to the identification of a better hydride source and solvent, a second ligand screening was performed in order to confirm whether **L1** continued to give the best results (Table 4.5). Indeed, lower yields of amide **4.3ae** were obtained when other bipyridine- and phenanthroline- type ligands were screened (entry 1 vs. 2 to 6). Given that phosphine ligands have been used in the formation of 2-pyridones,[26] and in metal-catalyzed alkyne trimerizations,[28] we questioned whether the hydroamidation would still be viable using these ligands. This was indeed the case, although incomplete conversion of **4.4h** and lower yields of **4.3ae** were observed (entries 7 and 8).

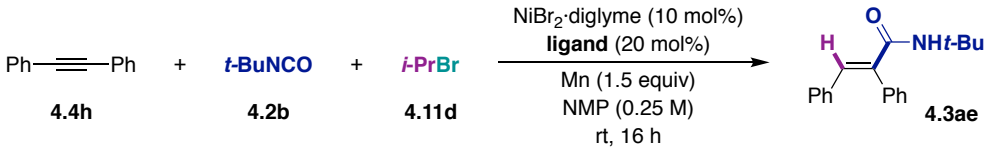

Entry	Ligand	Conversion of 4.4h (%)[a]	Yield of 4.3ae (%)[a]
1	bathocuproine (**L1**)	100	91[b]
2	2,2'-bipyridine (**L2**)	49	0
3	6,6'-dimethyl-2,2'-bipyridine (**L4**)	75	45
4	1,10-phenanthroline (**L5**)	40	0
5	2,9-dibutyl-4,7-diphenyl-1,10-phenanthroline (**L10**)	75	64
6	2,9-dibutyl-4,7-dimethyl-1,10-phenanthroline (**L11**)	74	66
7	PPh_3 (**L12**)	50	38[c]
8	PCy_3 (**L13**)	69	66[c]

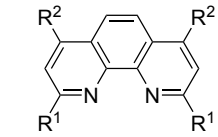

R^1 = *n*-Bu, R^2 = Ph, **L10**
R^1 = *n*-Bu, R^2 = Me, **L11**

Reaction conditions: 4.4h (0.25 mmol), **4.4b** (0.38 mmol), *i*-PrBr (0.38 mmol), $NiBr_2$·diglyme (10 mol%), ligand (20 mol%), Mn (0.38 mmol), NMP (1 mL) at rt, 16 h. [a] HPLC conversion and yield using naphthalene as internal standard. [b] Isolated yield.

Table 4.5. Screening of ligands under the new reaction conditions

Given that small amounts of the amidation of isopropyl bromide were obtained in the reaction crudes, we questioned whether *tert*-butyl bromide could serve as a better hydride source, as it possesses three more hydrogen atoms that statistically favor β-hydride elimination. Additionally, and in light with the knowledge acquired in Chapter 3, it is unlikely that *tert*-butyl bromide undergoes the amidation reaction. This hypothesis was however met with little success as lower yields of **4.3ae** were obtained when using this hydride source (Table 4.6, entry 2). It is likely that the steric hindrance of the *tert*-butyl group makes oxidative addition, via SET and recombination, a challenging process. In fact, only few methods for the metal-catalyzed coupling of tertiary alkyl halides have been reported.[44–48]

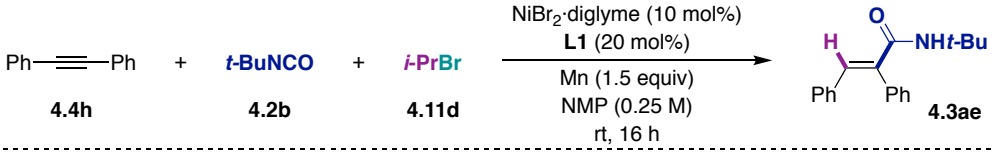

Entry	Deviation from Standard Conditions	Conversion of 4.4h (%)[a]	Yield of 4.3ae (%)[a]
1	none	100	91[b]
2	*t*-BuBr (**4.11e**)	100	69
3	Zn instead of Mn	100	54[c]
4	50 °C instead of rt	73[d]	15
5	1.0 equiv of *t*-BuNCO instead of 1.5 equiv	100	67
6	1.1 equiv of *i*-PrBr instead of 1.5 equiv	89	70
7	5 mol% $NiBr_2$·diglyme instead of 10 mol%	85	83
8	Leaving out $NiBr_2$·diglyme	0	0
9	Leaving out **L1**	0	0
10	Leaving out Mn	0	0
11	Leaving out **4.11d**	0	0

Reaction conditions: **4.4h** (0.25 mmol), **4.2b** (0.38 mmol), *i*-PrBr (0.38 mmol), $NiBr_2$·diglyme (10 mol%), **L1** (20 mol%), Mn (0.38 mmol), NMP (1 mL) at rt, 16 h. [a] HPLC conversion and yield using naphthalene as internal standard. [b] Isolated yield. [c] *E:Z* = 5:1. [d] Mass balance accounts for *cis*- and *trans*-stilbene and trace hydroalkylation of **4.4h**.

Table 4.6. Fine-tuning of the reaction conditions

Interestingly, *E/Z* mixtures of acrylamide **4.3ae** were observed when Zn was used as reducing agent (entry 3). One might argue that this could be explained by the formation of vinyl-zinc species originating from transmetalation of Zn^{2+} with the *in situ* generated vinyl-nickel intermediates.[49–51] However, this pathway is highly unlikely as alkenylzinc species are known to be configurationally stable.[52] In contrast, *E/Z* isomerizations of alkenylnickel species have been previously reported and are postulated to occur via Ni-carbene-like zwitterionic intermediates.[53–55] Although speculative, if one supposes that isocyanate insertion occurs from alkenylnickel(I) species, a slow reduction of the vinyl-nickel(II) to vinyl-nickel(I) species might favor the *E/Z* isomerization prior to isocyanate insertion. The use of a reductant with a lower reduction potential, such as Zn instead of Mn ($E°$= −0.76 and −1.185 V vs. SHE at 25 °C, respectively[38]), might indeed account for the observed results.

The reaction is also sensitive to temperature, for example entry 4 shows an increase in alkyne reduction when conducting the reaction at 50 °C. The use of lower amounts of *tert*-butyl isocyanate or isopropyl bromide had a deleterious effect on the reaction yield, probably due to the competitive amidation of **4.11d**, and the formation of small amounts of alkenes and urea as side-products (entries 5 and 6). Unfortunately, lower catalyst loadings afforded lower yields and incomplete conversions, even when running the reaction for longer periods of time (entry 7). Finally, no reactivity was observed when omitting the nickel(II) salt, the ligand, the manganese, or the

hydride source; showing that all reaction parameters were necessary to achieve the desired hydroamidation reaction (entries 8 to 11).

With the aim of stressing the importance of using a mild hydride source formed *in situ*, the reaction was carried out in the presence of hydride sources commonly used in hydrometalation reactions (Table 4.7). Only low yields of product were observed when diethoxymethyl silane was used in combination with a base (entry 1), whereas no product was obtained using hydrogen or ionic hydride sources such as $NaBH_4$ (entries 2 and 3). As expected, no hydroamidation was observed when *tert*-butanol was used (entry 4). This result contrasts the hydrocarboxylation of alkynes developed in our group,[29] but is predictable as alcohols can readily react with isocyanates to afford the corresponding carbamates.

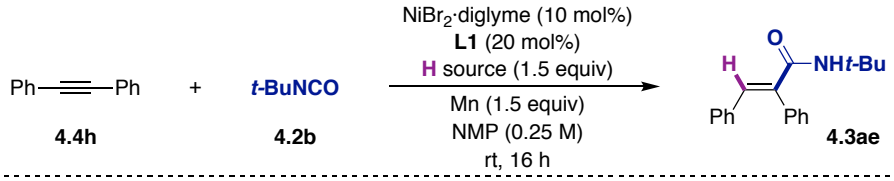

Entry	H source	Conversion of 4.4h (%)[a]	Yield of 4.3ae (%)[a]
1	$Me(EtO)_2SiH$ (0.75 mmol)[b]	64	17
2	H_2	86[b]	0
3	$NaBH_4$	89	0
4	*t*-BuOH	7	0

Reaction conditions: **4.4h** (0.25 mmol), **4.2b** (0.38 mmol), **H** source (0.38 mmol), $NiBr_2$·diglyme (10 mol%), **L1** (20 mol%), Mn (0.38 mmol), NMP (1 mL) at rt, 16 h. [a] HPLC conversion and yield using naphthalene as internal standard. [b] Na_2CO_3 (0.75 mmol), no Mn. [b] Mass balance accounts for *cis*- and *trans*-stilbene.

Table 4.7. Screening of hydride sources commonly used in metal-catalyzed hydrofunctionalizations

4.3.2. Preparative Substrate Scope

4.3.2.1. Preparative Scope and Limitations of Alkynes

The generality of the hydroamidation was studied by applying the optimized reaction conditions to an array of aryl- and alkyl-substituted alkynes, which were readily prepared using Sonogashira couplings. In all cases, the acrylamides were obtained as a single regioisomer with good levels of diastereoselectivity. The assigned regio- and diastereoselectivity was based on the NMR spectroscopic analysis of the products and corroborated by X-ray crystallography (**4.3ap**) (Scheme 4.10). Under the optimized conditions, symmetrical diaryl-alkynes could be employed regardless of the electronic properties of the substituents present in the aryl moiety (**4.3ae** to **4.3aj**). Aryl-alkyl-substituted alkynes could be as well accommodated, albeit with a slight erosion in diastereoselectivity (**4.3ak** to **4.3aq**). Substrates commonly used in Ni-catalyzed cross-coupling reactions afforded the desired acrylamides in good yields, as no competitive benzamide formation or other side-reactions were observed for aryl pivalates (**4.3af**), chlorides (**4.3ag**) and tosylates (**4.3ap**).[56,57] In contrast to the nickel-catalyzed amidation of alkyl bromides,[35] but in parallel to the amidation of aryl pivalates,[37] nitrile groups could be tolerated (**4.3aq**). Gratifyingly, internal dialkyl alkynes could be used as substrates delivering the corresponding products in moderate yields (**4.3ar** and **4.3as**), although a slight modification of the reaction conditions, using neocuproine as ligand and lower reaction temperatures, was necessary to obtain acrylamide **4.3ar**. The moderate diastereoselectivity observed for this product might be attributed to the lack of stabilizing aryl moieties or electron withdrawing groups in the starting alkyne. Additionally, the synthetic applicability of the hydroamidation was illustrated by the synthesis of **4.3ae** in 80% yield, starting from 5.0 mmol (891 mg) of diphenylacetylene.

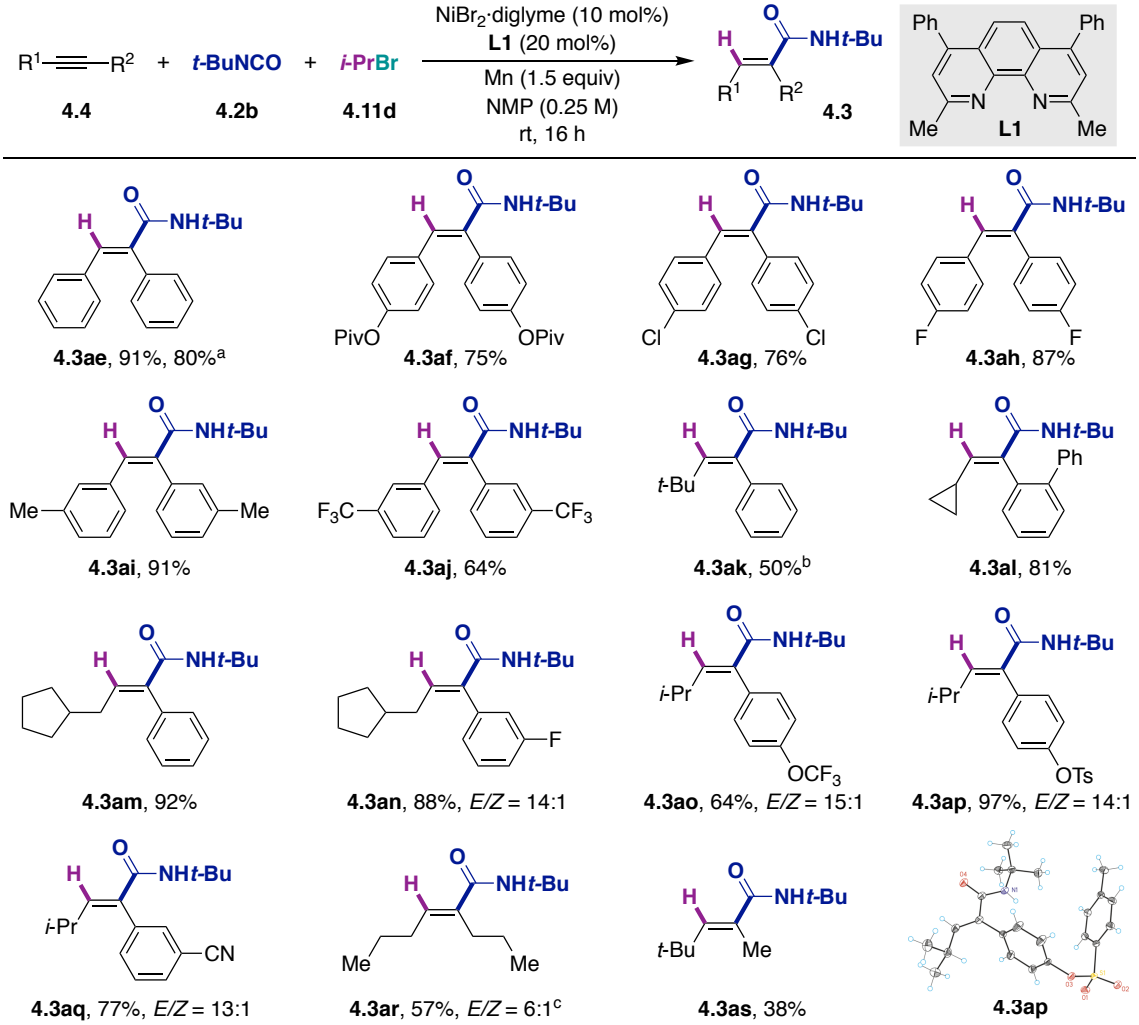

Reaction conditions: **4.4** (0.50 mmol), **4.2b** (0.75 mmol), **4.11d** (0.75 mmol), $NiBr_2$·diglyme (10 mol%), **L1** (20 mol%), Mn (0.75 mmol), NMP (2 mL) at rt, 16 h. [a] **4.4** (5.00 mmol). [b] 35 °C, 72 h. [c] using **L6** (20 mol%) as ligand at 10 °C. Yields of isolated product, average of at least two independent runs

Scheme 4.10. Scope of aryl- and alkyl-substituted alkynes with *tert*-butyl isocyanate

Prompted by the synthetical utility of silyl- and boryl-vinyl moieties as starting materials in a large variety of organic transformations, the applicability of the hydroamidation to silyl- and boryl-substituted acetylenes was studied. Scheme 4.11 shows that a broad array of silyl-substituted alkynes could be used to generate the corresponding acrylamides in good yields and with high selectivity. In all cases, the amide group was located adjacent to the aryl or vinyl groups, which stabilize the vinyl-nickel intermediate. For substrates such as **4.3bh**, lacking aryl or vinyl substituents, a regioselectivity switch was observed. This could be explained by the preferential formation of an intermediate containing the Ni-center adjacent to the silyl group. In this species, the silicon has a dual role of stabilizing the Ni—C σ-bond by hyperconjugation with the empty silicon *d*-orbitals, and of directing the hydride insertion to the more electrophilic β-carbon, stabilized by hyperconjugation of the Si—C σ-bond with the alkyne π-orbital.[58]

The application of the hydroamidation was met with less success for boryl-substituted acetylenes derived from commonly used Bpin derivatives (vide infra, unsuccessful substrates). However, the use of more robust and air-stable MIDA boronates allowed for the preparation of **4.3at**, albeit in low yields. These boronate esters are stable, present low reactivity towards oxidants and acidic conditions, and do not readily undergo transmetalation, even at high temperatures.[59] Deprotection of the MIDA-boronates to afford the boronic acids can be readily

performed under mild aqueous basic conditions, which allows for iterative cross-coupling[60] and even the slow release of the corresponding boronic acid.[61] In general, a wide functional group tolerance was observed when silyl- and boryl-substituted alkynes were used, with acetals (**4.3au**), esters (**4.3ay** and **4.3bc**), heterocycles (**4.3bf**), fluorides (**4.3bd**), and functional groups commonly used in metal-catalyzed cross-couplings (**4.3ay**, **4.3az**, **4.3ba** and **4.3bb**) being well tolerated. Furthermore, the reaction could be scaled-up to generate **4.3av** in good yields from 4.8 mmol (837 mg) of the starting alkyne.

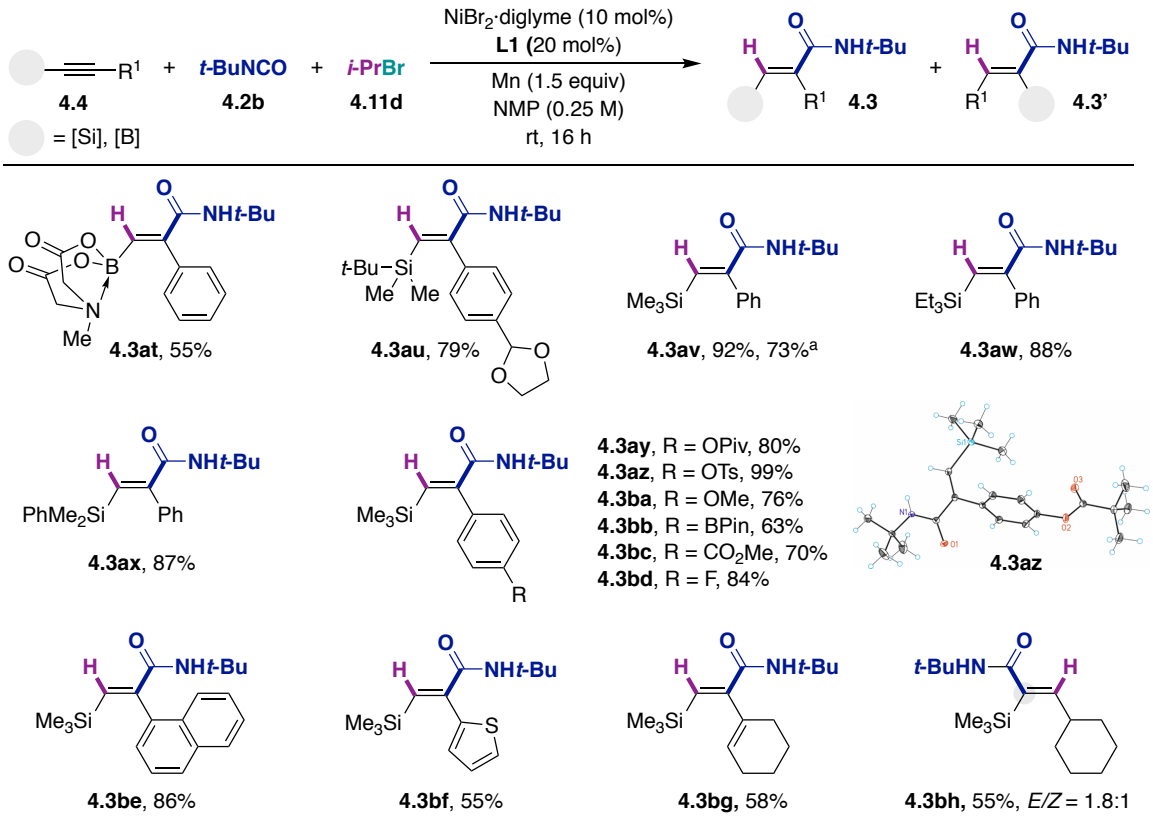

Reaction conditions: **4.4** (0.50 mmol), **4.2b** (0.75 mmol), **4.11d** (0.75 mmol), $NiBr_2$·diglyme (10 mol%), **L1** (20 mol%), Mn (0.75 mmol), NMP (2 mL) at rt, 16 h. [a] **4.4** (4.82 mmol). Yields of isolated product, average of at least two independent runs.

Scheme 4.11. Scope of silyl- and boryl-substituted alkynes with *tert*-butyl isocyanate

The limitations on the alkyne coupling partner were identified while studying the scope of the reaction (Scheme 4.12). When unsymmetrically-substituted 1,2-diaryl alkynes were employed mixtures of diastereomers and regioisomers were obtained (**4.4az** to **4.4bc**), even when using biased substrates such as **4.4bb**. The use of other aryl-alkyl-substituted alkynes resulted in low diastereoselectivity or low yields (**4.4bd** to **4.4bf**). Complex mixtures of side-products, presumably corresponding to the reduction of the ketone and ester moiety, were observed for substrates **4.4bg** to **4.4bi** and **4.4bl**. Likewise, complex mixtures of unidentified products were observed with boryl- and stannyl-substituted alkynes (**4.4o** to **4.4bm)**. No or little conversion was observed with alkynes substituted by heterocycles containing nitrogen atoms that might coordinate to the nickel center (**4.4bn** and **4.4bq)**, or with unsymmetrical alkynes possessing *ortho*-substituents (**4.4bo**). A re-optimization attempt of the reaction parameters invariably resulted in the trimerization and reduction of the starting alkyne when aromatic or aliphatic terminal alkynes were employed.

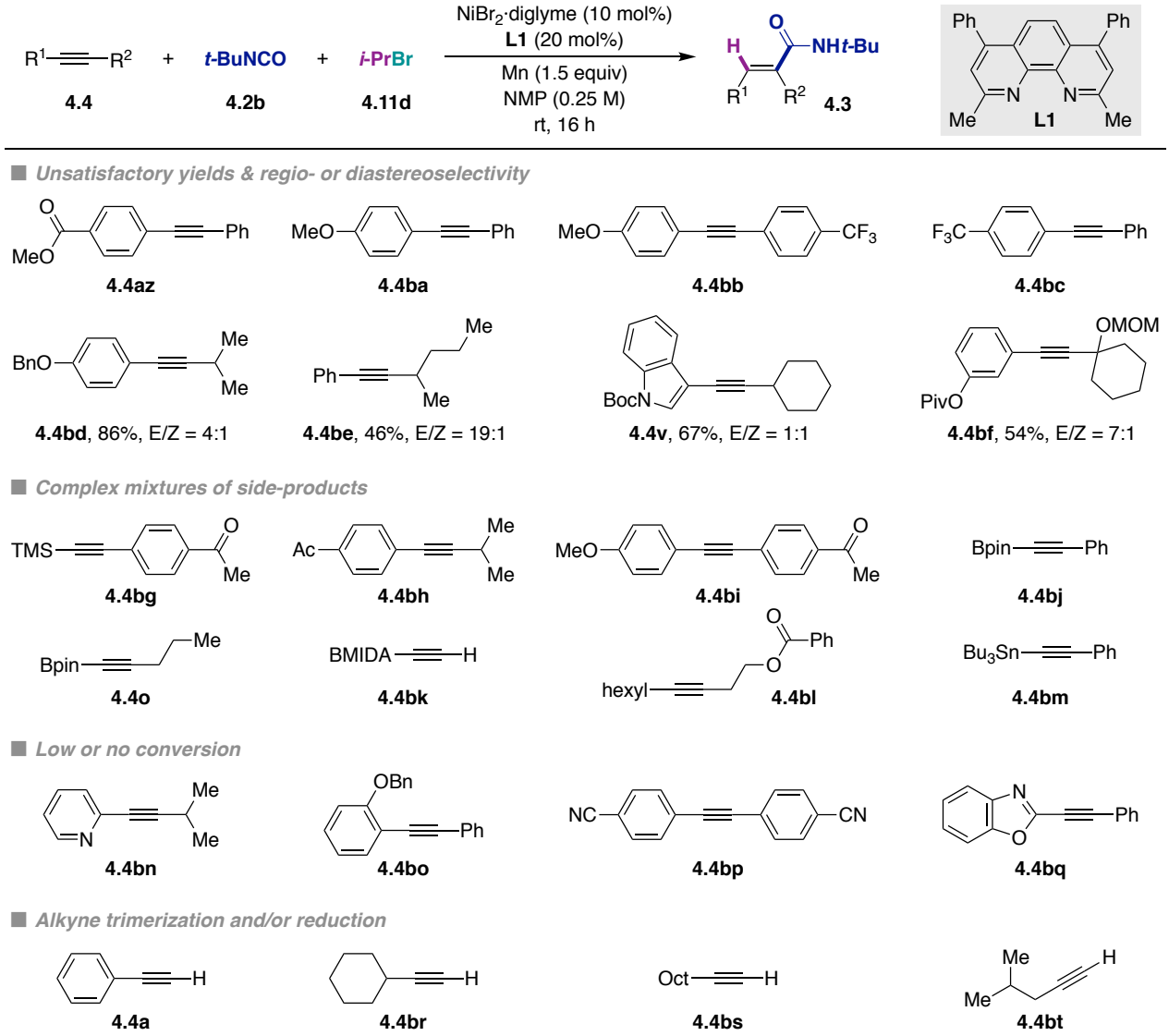

Reaction conditions: **4.4** (0.50 mmol), **4.2b** (0.75 mmol), **4.11d** (0.75 mmol), $NiBr_2$·diglyme (10 mol%), **L1** (20 mol%), Mn (0.75 mmol), NMP (2 mL) at rt, 16 h.

Scheme 4.12. Unsuccessful alkynes

4.3.2.2. Preparative Scope and Limitations of Isocyanates

The use of different alkyl and aryl isocyanates in combination with 1,2-diaryl and silyl-aryl-substituted alkynes is shown in Scheme 4.13. In parallel with Chapter 2, only bulky and electron rich isocyanates could be employed. Conversely in this transformation, an alkyl isocyanate containing a styrenyl motif was tolerated (**4.3bn**). Compared to the amidation of alkyl bromides, no re-optimization of the reaction conditions was necessary in order to accommodate the different successful isocyanates, and the reactions afforded even higher yields of the desired products. Moreover, the formation of isocyanate side-products, such as urea and isocyanurates, was rarely observed and the reaction crudes were cleaner than those obtained when using alkyl bromides as coupling partners (Chapters 2 and 3). The rationale behind this observation could be that the alkyne, having a stronger σ-donor π–acceptor character, competes with the isocyanate for coordination to the nickel-center, which could prevent undesired isocyanate decomposition. Another plausible explanation would be a faster isocyanate insertion that diminishes the probability of the isocyanate undergoing unproductive pathways. However, no kinetic experiments for either transformation were performed and with the present experimental results it is not possible to compare the reaction rates.

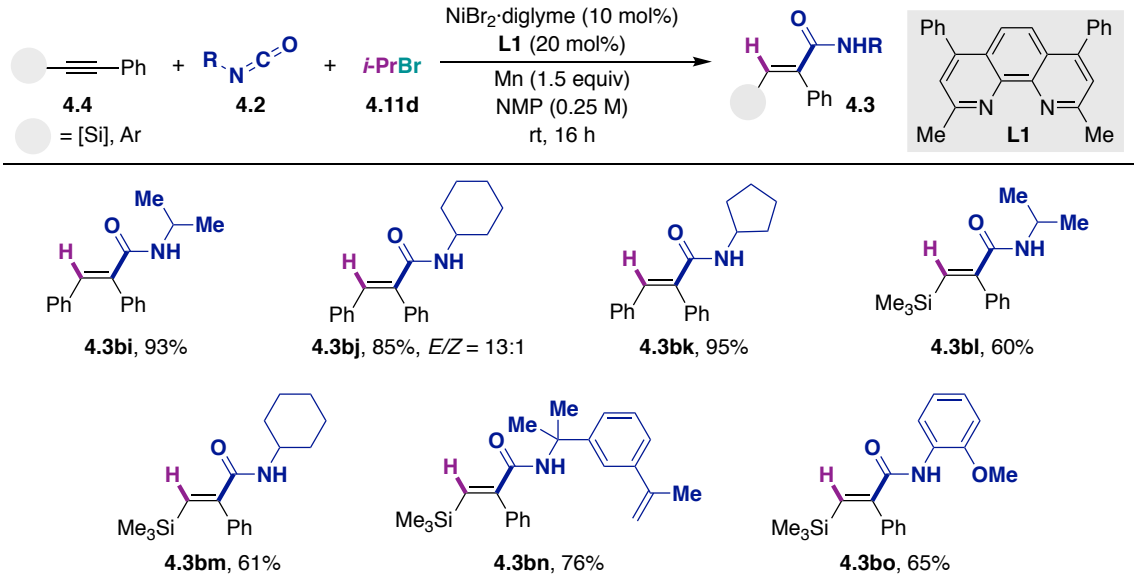

Reaction conditions: **4.4** (0.50 mmol), **4.2** (0.75 mmol), **4.11d** (0.75 mmol), $NiBr_2$·diglyme (10 mol%), **L1** (20 mol%), Mn (0.75 mmol), NMP (2 mL) at rt, 16 h. Yields of isolated product, average of at least two independent runs.

Scheme 4.13. Scope of isocyanates with silyl- and aryl-substituted alkynes

Unfortunately, several of the isocyanates that were evaluated did not lead to acrylamide formation or led to low yields of the desired product, despite substantial screening efforts (Scheme 4.14). In line with the results obtained in Chapter 2, most aryl isocyanates trimerized to isocyanurates, or oligomerized under the optimized reaction conditions (**4.2k** to **4.2p**). The use of alkyl isocyanates lacking steric hindrance also led to trimerization, oligomerization and urea formation (**4.4q** to **4.4s**). Undoubtedly, the narrow isocyanate scope observed is one of the major limitations of our hydroamidation methodology.

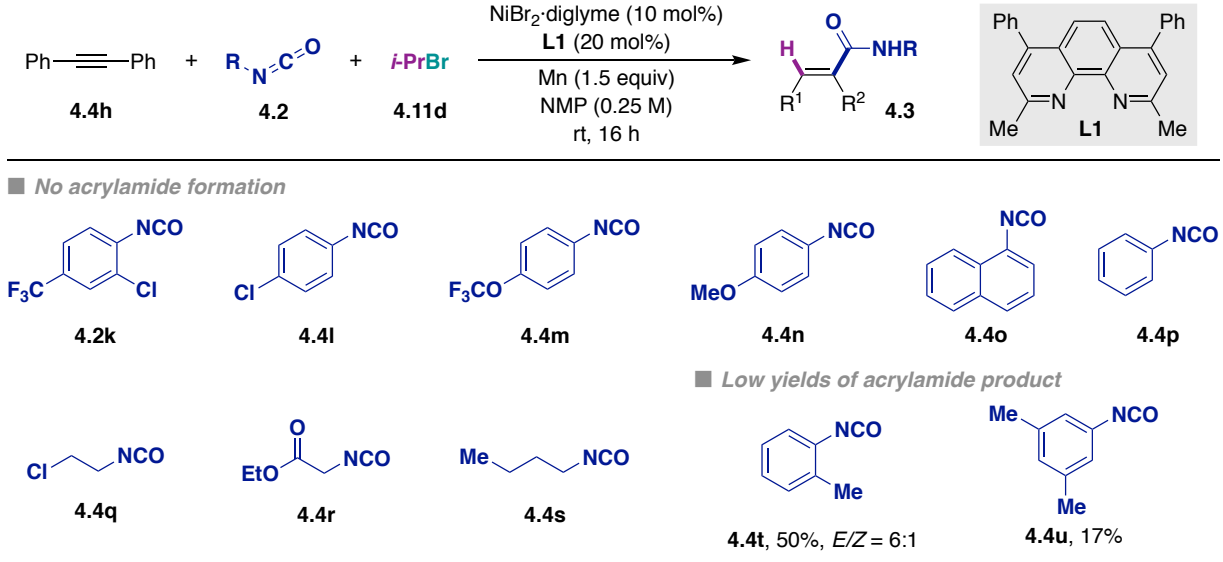

Reaction conditions: **4.4h** (0.50 mmol), **4.2** (0.75 mmol), **4.11d** (0.75 mmol), $NiBr_2$·diglyme (10 mol%), **L1** (20 mol%), Mn (0.75 mmol), NMP (2 mL) at rt, 16 h.

Scheme 4.14. Unsuccessful isocyanates for the hydroamidation of alkynes

4.3.3. Derivatization of the Prepared Acrylamides

4.3.3.1. Synthesis of Primary Amides and Terminal Acrylamides

The extension of the protocol to the synthesis of primary amides was achieved by using previously reported conditions for the deprotection of *tert*-butyl acrylamides in neat TFA (Scheme 4.15, left).[10,62] Moreover, protodesilylation triggered by fluoride anions afforded terminal acrylamide **4.13** in high yield. The synthesis of this 1,1-disubstituted acrylamide is complementary to the method developed by Jamison using α-olefins and isocyanates, as styrenes gave <10% yield of desired product with this methodology.[11]

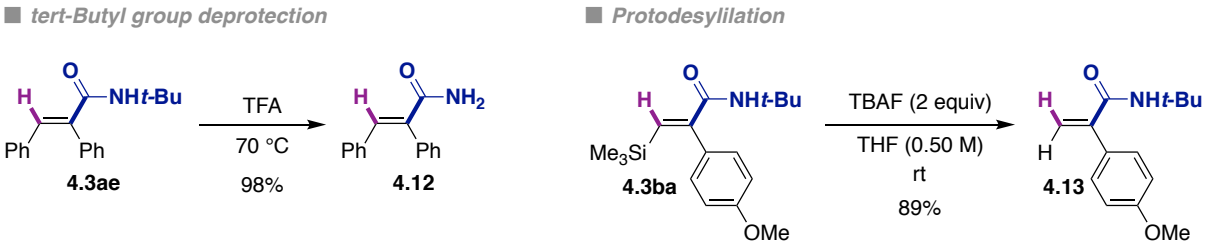

Scheme 4.15. Synthesis of Primary Amides and Terminal Acrylamides

4.3.3.2. Attempted Synthesis of Tertiary Amides via Sequential Electrophile Addition

Following the hypothesis postulated in Chapter 2, the one-pot synthesis of *N*-tertiary amides by the sequential addition of a third electrophile was evaluated under the hydroamidation reaction conditions and using model substrate **4.4h** (Scheme 4.16). Unfortunately, clean formation of the desired *N*-tertiary amides was not observed and instead complex mixtures of unidentified products, and recovered isomeric mixtures of secondary *N*-*tert*-butyl amide were obtained **(4.14a** to **4.14c**). Only traces of the desired *N*-methyl-*tert*-butyl amide were observed when methyl iodide was used. The addition of benzyl bromide only led to its homocoupling, and the use of benzoyl chloride degraded the amide to the nitrile and to other unidentified products.[63] Due to conjugation with the alkene's π-system, it is possible that the formed acrylamidates (**XII**) are less nucleophilic than the corresponding aliphatic amidates, generated from the amidation of alkyl bromides with isocyanates in Chapter 2.

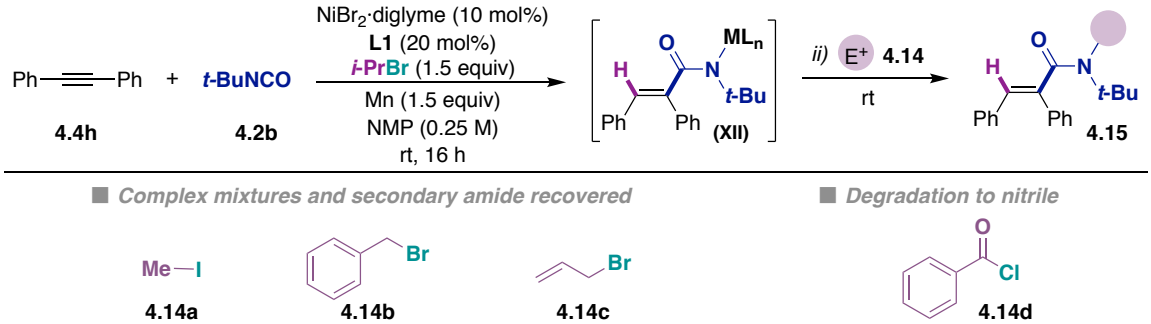

Reaction conditions: 4.4h (0.50 mmol), **4.2b** (0.75 mmol), **4.11d** (0.75 mmol), $NiBr_2$·diglyme (10 mol%), **L1** (20 mol%), Mn (0.75 mmol), NMP (2 mL) at rt, 16 h, then addition of **4.14** (5 equiv), rt.

Scheme 4.16. Unsuccessful synthesis of *N*-tertiary amides by the sequential addition of a third electrophile

4.3.3.3. Derivatization to Vinyl Halides and Cross-Coupling Example

To showcase the synthetical versatility of the silyl-substituted acrylamides prepared, vinyl chloride (**4.17**) and vinyl iodide (**4.18**) were synthesized via halodesilylation reactions (Scheme 4.17). Initial attempts to directly convert secondary amide (**4.3ba**) into the corresponding vinyl halides were unsuccessful, but the observed

undesired reactivity could be circumvented by the quantitative preparation of tertiary amide (**4.16**). As shown above, quenching of the reaction with MeI as performed in Chapter 2 failed, and a one-pot two step sequence was necessary to prepare the corresponding *N-tert*-butyl-methyl amide. Starting from **4.16**, the desired halogen-substituted acrylamides were obtained in high yields and with no erosion of the diastereoselectivity. To address the limitation of our protocol to the use of symmetrically aryl alkynes and extend the synthetic scope of the transformation, vinyl iodide (**4.18**) was subjected to Suzuki-Miyaura conditions to afford unsymmetrical acrylamide **4.19** in good yields.

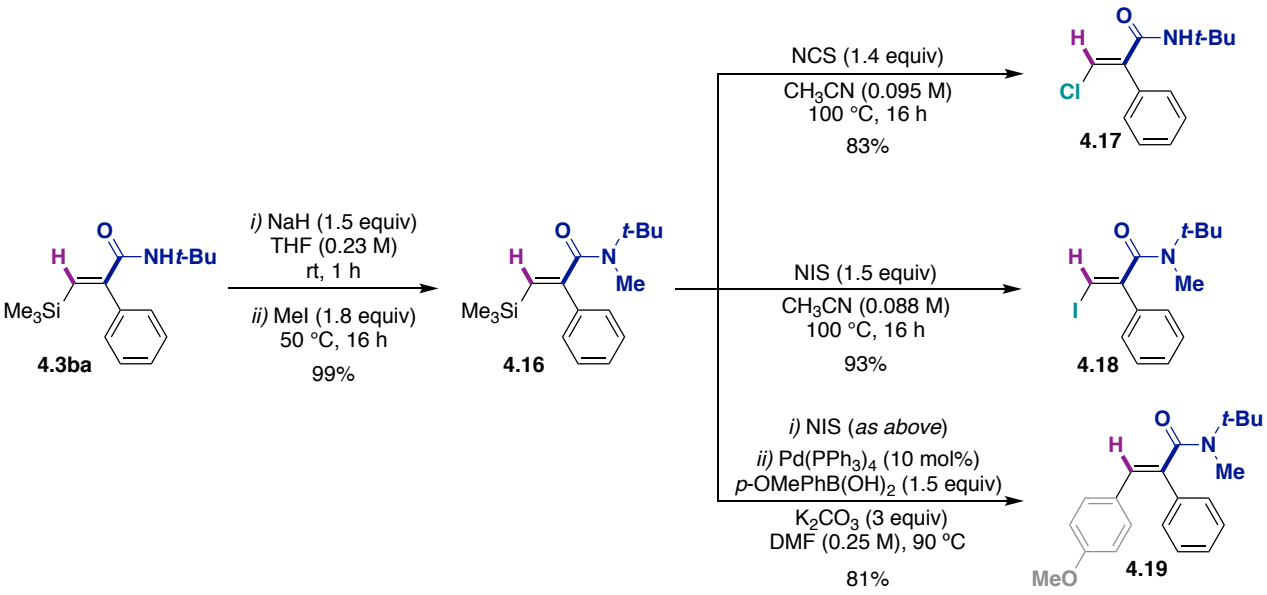

Scheme 4.17. Synthesis of halogen-substituted acrylamides and their use in Suzuki-Miyaura cross-couplings

4.3.4. Preliminary Mechanistic Studies

4.3.4.1. Deuteration Experiments

With the aim of gaining information about the possible hydride sources present in the reaction, deuteration experiments were carried out with d_7-, d_6-, and d_1-isopropyl bromide, as well as d_6-bathocuproine (Scheme 4.18). Full deuterium incorporation into the product was observed when d_7-isopropyl bromide was employed, whereas when using d_6- or d_1-isopropyl bromide 75% and 15% D-content were observed, respectively. These results indicate that β-hydride elimination is responsible for generating the transient Ni—H species, and also suggests that rapid re-insertion of the *in situ* generated Ni(II)-hydrides across the alkene occurs prior to alkyne binding. No deuterium incorporation was observed when the ligand containing deuterated *ortho*-substituents (d_6-**L1**) was employed, indicating that the ligand is not likely to participate as a hydride source.

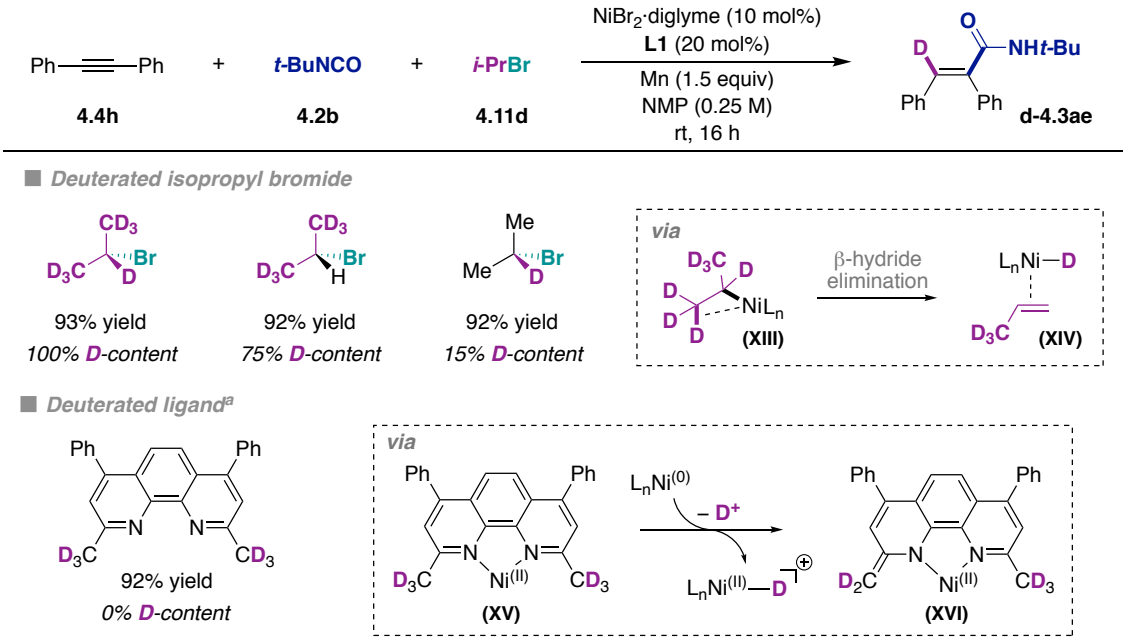

Reaction conditions: **4.4h** (0.50 mmol), **4.2b** (0.75 mmol), ***d*-4.11d** (0.75 mmol), $NiBr_2$·diglyme (10 mol%), **L1** (20 mol%), Mn (0.75 mmol), NMP (2 mL) at rt, 16 h. [a] Using ***d*₆-L1.** The percentage of deuteration was determined by ^{1}H-NMR.

Scheme 4.18. Deuteration experiment using d-isopropyl bromide and *d*₆-bathocuproine

4.3.4.2. Stoichiometric Experiments

In order to shine some light onto the reaction mechanism and help determining the identity of the putative nickel reaction intermediates, different stoichiometric studies were performed using Ni(**L1**)$_2$, which was easily prepared from Ni(COD)$_2$ and **L1** (Scheme 4.19).[64] In line with the results obtained in Chapter 2, stoichiometric experiments in the presence of isopropyl bromide afforded the desired product regardless of whether Mn was present in the reaction mixture or not (Scheme 4.20, left). Nevertheless, this result does not allow to clarify if isocyanate insertion takes place via vinyl-Ni(I) or vinyl-Ni(II) intermediates; which could have been hypothesized if no product formation had been observed or if a yield higher than 50% had been obtained, respectively. In agreement with the results obtained in the deuteration experiments, no product was obtained in the absence of isopropyl bromide, indicating that an oxidative cyclization mechanism via **XVII**, such as the one proposed by Hoberg and Jamison, does not intervene under our reaction conditions (Scheme 4.20, right).

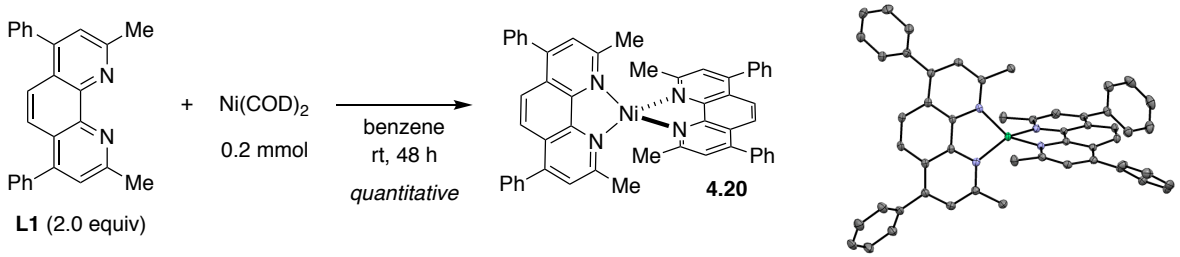

Scheme 4.19. Synthesis and ORTEP representation of Ni(bathocuproine)$_2$

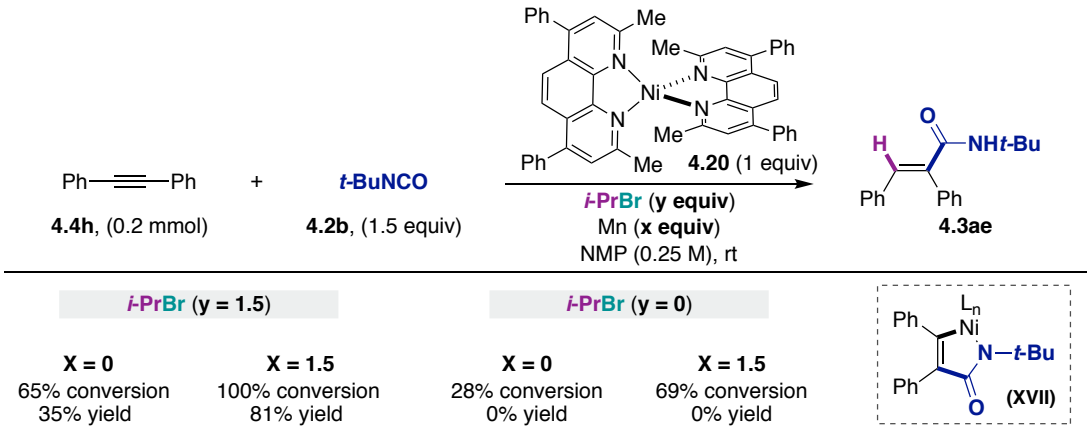

Scheme 4.20. Stoichiometric experiments with Ni(bathocuproine)$_2$ complex

4.3.5. Plausible Reaction Mechanisms

Taking together the information obtained from the stoichiometric and deuterium-labelling experiments, two plausible mechanistic pictures are proposed for the developed hydroamidation reaction. In both pathways, the nickel(II) salt is reduced to Ni(0) via SET from Mn, followed by oxidative addition of the secondary alkyl bromide to generate **XVIII**. Subsequently, β-hydride elimination leads to the formation of the critical Ni(II)-hydride species. Olefin displacement, alkyne coordination and hydrometallation, ultimately generate an alkenyl nickel(II) intermediate (**XX**) that will lead to the desired product via isocyanate insertion into the vinyl—Ni bond. Scheme 4.21, shows a first proposal where isocyanate insertion takes place directly from this vinyl-nickel(II) species, whereas Scheme 4.22 highlights the possibility of an isocyanate insertion occurring from vinyl-nickel(I) species (**XVIII**).

Unfortunately, the results obtained from the stoichiometric experiments cannot be used to rule out the intermediacy of Ni(II) or Ni(I) species preceding isocyanate insertion, as non-negligible amounts of acrylamide where obtained in the absence of reducing agent (vide supra). However, this result does point against the possibility of generating well-defined alkenyl manganese species. Moreover, there is no evidence for whether the nickel(I) intermediates are formed via comproportionation of Ni(II) with Ni(0),[65–67] or via SET from Mn.[68] Given that Ni(I) species are more nucleophilic, we tentatively hypothesize that isocyanate insertion occurs via these intermediates. A final reductive transmetallation of the nickel-amidate with Mn recovers the Ni(0) catalyst and affords a manganese-amidate(**XXII**), which is quenched with aqueous 5% HCl or a saturated solution of ammonium chloride to generate the final product.

As mentioned in the optimization of the reaction conditions, *N*-(*tert*-butyl)butyramide and traces of *N*-(*tert*-butyl)isobutyramide were detected by the GC-MS analysis of the crude reaction mixtures. This indicates that a small portion of the alkyl—Ni(II)—Br intermediate (**XVIII**) undergoes the amidation described in Chapter 3. In order to obtain high yields of the hydroamidation product, the use of a ligand that favors β-hydride elimination from the alkyl—Ni(II)—Br intermediate is crucial. The enhanced π-acidity of bathocuproine with respect to other substituted phenanthrolines could contribute to the observed results. Indeed, when comparing a series of molybdenum phenanthroline complexes a correlation between the substitution pattern of the ligand and the CO stretching frequency can be observed, which is indicative of the π-accepting character of the ligand (for example for bathocuproine υ_{CO} = 2016.5 and for bathophenanthroline υ_{CO} = 2015.5 cm^{-1}).[69] The use of a more π-acidic ligand removes electron density from the Ni, and thus enhances its electrophilicity. This results in a stronger agostic interaction with the C—H$_\beta$ bond – in this agostic interaction the σ-donation from the C—H$_\beta$ bond to the

metal is greater than the π-backdonation from the metal to the σ* C—H bond. Therefore, β-hydride elimination is promoted by weakening of the C—$H_β$ bond when a more π-acidic ligand such as **L1** is used.[70] Moreover, the steric hindrance imparted by the presence of two *ortho*-substituents on the ligand could favor the formation of cationic Ni species by extrusion of the bromide ligand, generating species that are more electrophilic and hence promote β-hydride elimination. Taking into account that the best results for the remote amidation of secondary alkyl bromides were obtained when using *ortho*-substituted bipyridine-type ligands (vide Chapter 3), whereas phenanthroline-type ligands gave optimal yields in the hydroamidation of alkynes, it is possible that not only π-acidity is involved in the promotion or prevention of β-hydride elimination. Other effects such as the ligand backbone and the rigidity of the complex are very likely to come into play in the systems developed by us.[71]

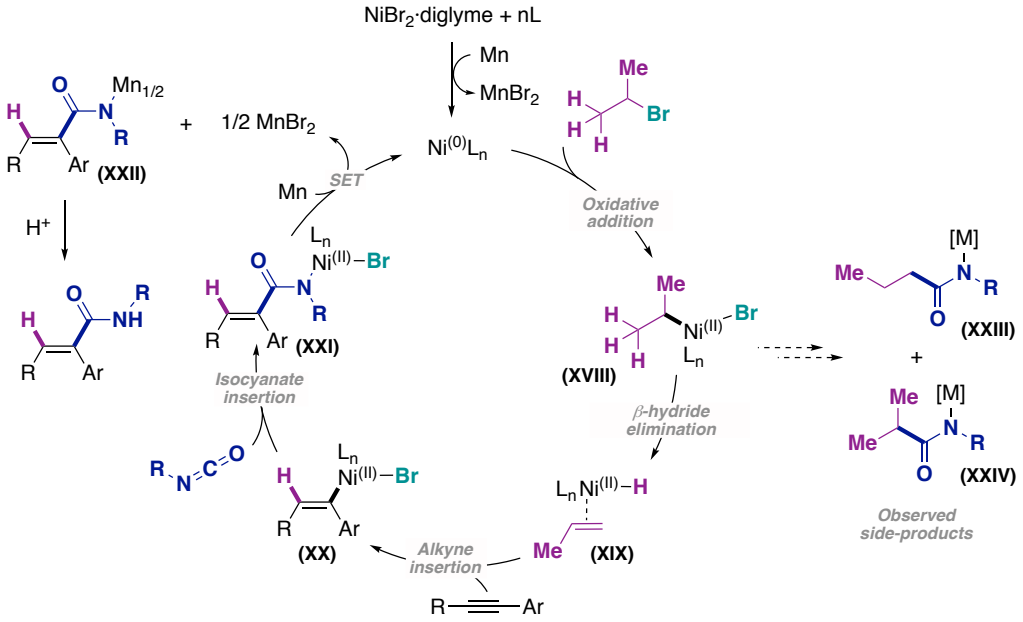

Scheme 4.21. Proposed reaction mechanism involving isocyanate insertion from alkenylnickel(II) species

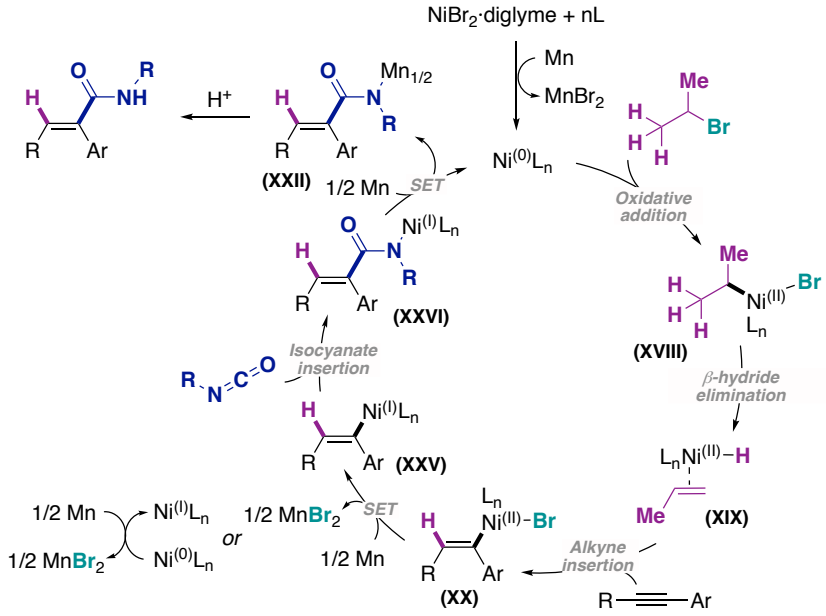

Scheme 4.22. Proposed reaction mechanism involving isocyanate insertion from alkenylnickel(I) species

As for the regio- and stereoselectivity of the hydroamidation, the formation of a single regioisomer of the acrylamide can be explained by the selective insertion of the nickel adjacent to the aryl moiety, where the Ni is stabilized through π-back donation from the *d* metal orbitals to the C—Ar σ* orbital. Additionally, the H-insertion is preferred at the non-benzylic position, where the newly formed C—H bond is stronger.[70] In the case of aliphatic internal alkynes, the regioselectivity is dictated only by steric factors. As for the observed diastereoselectivity, the insertion of Ni—H species to the triple bond is expected to occur with *syn*-selectivity.

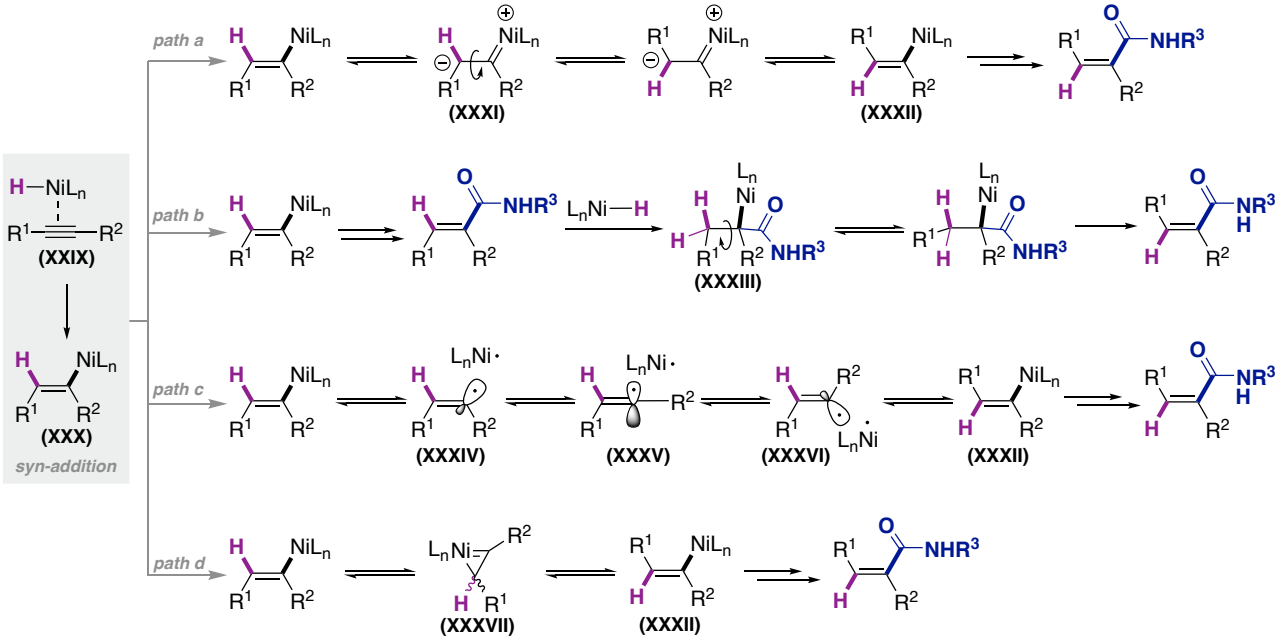

Scheme 4.23. Proposed pathways for the formation of diastereomeric *E/Z* mixtures

The *E/Z* mixtures observed for some of the products could be explained by the formation of zwitterionic Ni-carbene-like intermediates, from which rotation around the single bond can lead to the more stable *trans*-intermediate (Scheme 4.23, path a). These zwitterionic metal-carbene-like species have been previously proposed in Ni-catalyzed processes[53–55] and in numerous Pd-catalyzed reactions involving the formation of *syn*-alkenylmetal intermediates that interconvert to *anti*-alkenylmetal species.[72] This proposal is reminiscent to that of Ojima for Rh-catalyzed hydrosilylation.[73] Another possible scenario is the insertion of a second Ni—H species to the formed product, followed by isomerization and β-hydride elimination (path b). Alternatively, the homolytic cleavage of the newly formed Ni—C bond might afford a stabilized benzylic or a stabilized secondary alkyl radical, leading to an isomerization via an *sp* orbital and recombination to afford the *trans*-addition product (path c). Finally, a less likely possibility is the formation of a metallacyclopropene intermediate such as proposed by Crabtree in Ir-catalyzed hydrosilylations (path d);[74,75] however, this pathway is less probable given the smaller size of Ni.

4.4. Conclusions

In conclusion, the use of alkyl bromides as *in situ* hydride sources has allowed for the development of a highly regio- and diastereoselective Ni-catalyzed hydroamidation of alkynes with isocyanates. The mild conditions associated with reductive cross-couplings and the use of a catalytic hydride source allowed for a broad functional group tolerance for the coupling of aryl-, alkyl-, silyl- and boryl-substituted alkynes. The versatility of the obtained acrylamides was demonstrated by the deprotection of the *N*-tert-butyl group to afford *N*-primary amides, and by the deprotosilylation or halodesilylation of trimethylsilyl-substituted acrylamides. The initial limitation of our methodology to the synthesis of symmetrically substituted 1,2-diaryl acrylamides was surmounted via the formation of vinyl iodide species that were used under Pd-catalyzed Suzuki-Miyaura conditions to afford unsymmetrically substituted 1,2-diaryl acrylamides. The scope of our hydroamidation is complementary to that shown by Jamison using α-olefins and isocyanates,[10] as not only 1,1-disubstituted acrylamides but 1,2-disubstituted acrylamides could be synthesized. Moreover, our method allows for the synthesis of *N*-secondary amides which are not within reach using the current hydrocarbamoylations protocols using formamides.[22,23] The major drawback of the developed transformation is once again the limited scope of isocyanates that can be utilized. The design of an isocyanate surrogate for the *in situ* and gradual formation of the isocyanate coupling partner could circumvent the undesired pathways leading to isocyanate side-products, under the reaction conditions. Finally, the use of alkyl halides as *in situ* catalytic hydride sources has great potential and has already inspired other researchers, as described in the following section.

4.5. Alkyl Halides as Hydride Sources: Synthetic Methods Inspired by this Chapter's work

4.5.1. Pd-Catalyzed Halogenation of 1,6-enynes:

The year after the results that are the subject of this chapter were reported, the Lautens' group used *n*-butyl iodide or HX·Et_3N as HX surrogates for the catalytic formation of H—Pd(II)—X species, which were used as intermediates in the hydrohalogenation of 1,6-enynes *en route* to pyridinones (Scheme 4.24).[76] This method is the first example of a transfer hydrohalogenation[77,78] and constitutes an advantage over the hydrohalogenation of alkenes and alkynes with strong acids that are either added to the reaction, or generated *in situ*, and induce a loss of the chemoselectivity in the transformation due to the strongly-acidic conditions needed.[76]

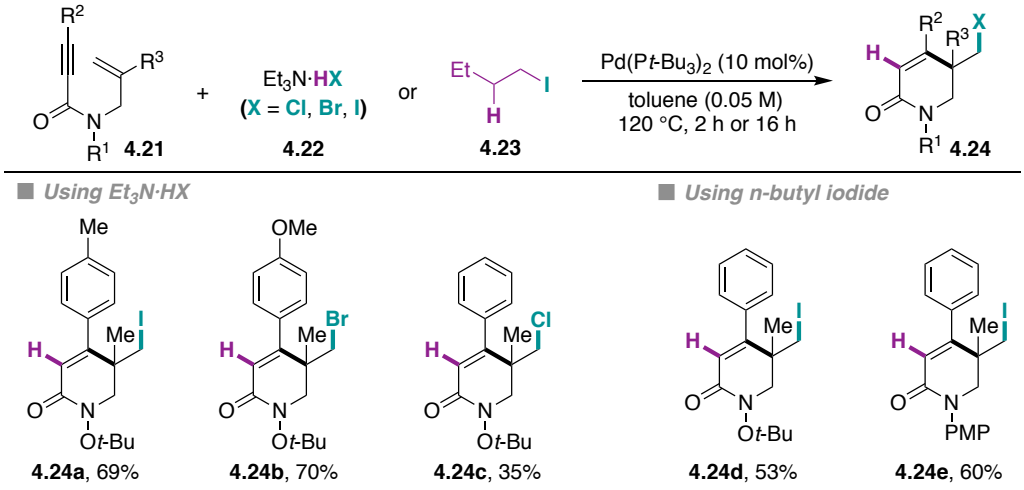

Scheme 4.24. Pd-catalyzed hydrohalogenation of 1,6-enynes with HX surrogates

4.5.2. Ni-Catalyzed Remote Arylation of Alkyl Bromides and Olefins:

That same year, the Zhu group reported the Ni-catalyzed chain-walking arylation of unactivated alkyl bromides or olefins with aryl bromides, enabled by the *in situ* generation of Ni—H species from light alkyl bromides (Scheme 4.25).[79] In this report, the addition of **4.11b** ensured that sufficient amounts of Ni—H species were available in the reaction, providing high yields of the desired remote cross-coupling products with high selectivity. The *n*-PrBr/Mn system replaced their previously developed method in which the chain-walking arylation of olefins was achieved using PMHS with CsF as hydride source and base needed to generate the catalytic Ni—H species.[80]

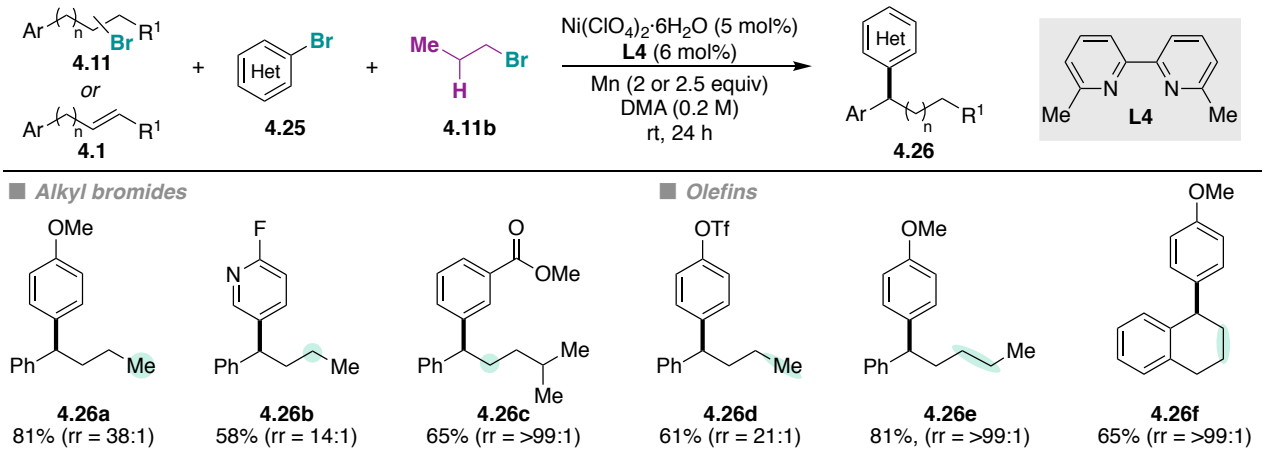

Scheme 4.25.Ni-catalyzed remote arylation of alkyl bromides and olefins

4.6. Bibliography

1. Ananikov, V. P. & Beletskaya, I. P. Alkyne and Alkene Insertion into Metal–Heteroatom and Metal–Hydrogen Bonds: The Key Stages of Hydrofunctionalization Process. in *Topics in Organometallic Chemistry* **43,** 1–20 (2013).
2. Negishi, E.-I. & Choueiry, D. Carbon with One Heteroatom Attached by a Single Bond: 2.19 Vinyl and Arylmetals. in *Comprehensive Organic Functional Group Transformations* (eds. Katritzky, A. R., Meth-Cohn, O. & Rees, C. W.) **2,** 951–995 (Elsevier, 1995).
3. Trost, B. M. & Ball, Z. T. Addition of Metalloid Hydrides to Alkynes: Hydrometallation with Boron, Silicon, and Tin. *Synthesis* **2005,** 853–887 (2005).
4. Trost, B. M. When Is a Proton Not a Proton? *Chem. Eur. J.* **4,** 2405–2412 (1998).
5. Herth, G., Schornick, G. & Buchholz, F. L. *Polyacrylamides and Poly(Acrylic Acids)*. *Ullmann's Encyclopedia of Industrial Chemistry* (Wiley-VCH Verlag GmbH & Co. KGaA, 2015).
6. Ekici, Ö. D. *et al.* Design, Synthesis, and Evaluation of Aza-Peptide Michael Acceptors as Selective and Potent Inhibitors of Caspases-2, -3, -6, -7, -8, -9, and -10. *J. Med. Chem.* **49,** 5728–5749 (2006).
7. Davies, I. R., Cheeseman, M., Niyadurupola, D. G. & Bull, S. D. An Efficient Synthesis of Semiplenamide C. *Tetrahedron Lett.* **46,** 5547–5549 (2005).
8. Hoberg, H., Sümmermann, K. & Milchereit, A. CC Bond Formation of Alkenes with Isocyanates on Ni^0 Complexes—a New Synthesis of Acrylamides. *Angew. Chem. Int. Ed.* **24,** 325–326 (1985).
9. Hoberg, H. & Hernandez, E. Nickel(0)-catalysed Synthesis of Unsaturated Carboxylic Acid Anilides from Ethene and Phenyl Isocyanate. *J. Chem. Soc. Chem. Commun.* **0,** 544–545 (1986).
10. Schleicher, K. D. & Jamison, T. F. Nickel-Catalyzed Synthesis of Acrylamides from α-Olefins and Isocyanates. *Org. Lett.* **9,** 875–878 (2007).
11. Schleicher, K. D. I. Nickel-Catalyzed Preparation of Acrylamides from Alpha Olefins and Isocyanates II. Synthetic Studies Toward Ripostatin A. (Massachusetts Institute of Technology, 2010).
12. Hoberg, H., Sümmermann, K. & Milchereit, A. C-C-Verknüpfung von Alkenen mit Isocyanaten am Nickel(0). *J. Organomet. Chem.* **288,** 237–248 (1985).
13. Hoberg, H. & Hernandez, E. Intermolekulare CC-Verknüpfung von Azanickelacyclopentanonen, α,ω-Disäureamide aus Alkenen und Phenylisocyanat. *J. Organomet. Chem.* **311,** 307–312 (1986).
14. Hoberg, H. & Guhl, D. Nickel(O)-Catalyzed Preparation of Isomeric Carboxamides – Ligand-Controlled β-H or β'-H Elimination. *Angew. Chem. Int. Ed.* **28,** 1035–1036 (1989).
15. Duong, H. A., Cross, M. J. & Louie, J. N-Heterocyclic Carbenes as Highly Efficient Catalysts for the Cyclotrimerization of Isocyanates. *Org. Lett.* **6,** 4679–4681 (2004).
16. El Ali, B., El-Ghanam, A., Fettouhi, M. & Tijani, J. Palladium(II)-Catalyzed Regioselective Carbonylative Coupling of Aniline Derivatives with Terminal Aryl Acetylenes to give Acrylamides under Syngas Conditions. *Tetrahedron Lett.* **41,** 5761–5764 (2000).
17. Li, Y., Alper, H. & Yu, Z. Palladium-Catalyzed Regiospecific Aminocarbonylation of Alkynes in the Ionic Liquid [bmim][Tf_2N]. *Org. Lett.* **8,** 5199–5201 (2006).
18. El Ali, B. & Tijani, J. Catalytic and regioselective synthesis of gem- or trans-α,β-unsaturated amides by carbonylation of alkyl alkynes with aniline derivatives by palladium(II) and phosphine. *Appl. Organomet. Chem.* **17,** 921–931 (2003).
19. Torii, S., Okumoto, H., Sadakane, M. & Xu, L. H. Organic Iodide Aided Carbonylation of Terminal Acetylenes with Palladium Catalyst. *Chem. Lett.* **20,** 1673–1676 (1991).
20. Brennführer, A., Neumann, H. & Beller, M. Palladium-Catalyzed Carbonylation Reactions of Alkenes and Alkynes. *ChemCatChem* **1,** 28–41 (2009).
21. Kobayashi, Y., Kamisaki, H., Yanada, K., Yanada, R. & Takemoto, Y. A convenient synthesis of (E)-α-alkylidene-γ-lactams and (E)-3-alkylideneoxindoles by rhodium-catalyzed intramolecular hydroamidation. *Tetrahedron Lett.* **46,** 7549–7552 (2005).
22. Nakao, Y., Idei, H., Kanyiva, K. S. & Hiyama, T. Hydrocarbamoylation of Unsaturated Bonds by Nickel/Lewis-Acid Catalysis. *J. Am. Chem. Soc.* **131,** 5070–5071 (2009).
23. Fujihara, T., Katafuchi, Y., Iwai, T., Terao, J. & Tsuji, Y. Palladium-Catalyzed Intermolecular Addition of Formamides to Alkynes. *J. Am. Chem. Soc.* **132,** 2094–2098 (2010).
24. Lindhardt, A. T., Mantel, M. L. H. & Skrydstrup, T. Palladium-Catalyzed Intermolecular Ene–Yne Coupling: Development of an Atom-Efficient Mizoroki–Heck-Type Reaction. *Angew. Chem. Int. Ed.* **47,** 2668–2672 (2008).
25. Duong, H. A., Cross, M. J. & Louie, J. Nickel-Catalyzed Cycloaddition of Alkynes and Isocyanates. *J. Am. Chem. Soc.* **126,** 11438–11439 (2004).
26. Duong, H. A. & Louie, J. Regioselectivity in Nickel(0)/phosphine Catalyzed Cycloadditions of Alkynes and Isocyanates. *J. Organomet. Chem.* **690,** 5098–5104 (2005).
27. Duong, H. A. & Louie, J. A nickel(0) catalyzed cycloaddition of alkynes and isocyanates that affords pyrimidine-diones. *Tetrahedron* **62,** 7552–7559 (2006).
28. Saito, S. & Yamamoto, Y. Recent Advances in the Transition-Metal-Catalyzed Regioselective Approaches to Polysubstituted Benzene Derivatives. *Chem. Rev.* **100,** 2901–2915 (2000).
29. Wang, X., Nakajima, M. & Martin, R. Ni-Catalyzed Regioselective Hydrocarboxylation of Alkynes with CO_2 by Using Simple Alcohols as Proton Sources. *J. Am. Chem. Soc.* **137,** 8924–8927 (2015).
30. Li, S., Yuan, W. & Ma, S. Highly Regio- and Stereoselective Three-Component Nickel-Catalyzed syn-Hydrocarboxylation of Alkynes with Diethyl Zinc and Carbon Dioxide. *Angew. Chem. Int. Ed.* **50,** 2578–2582 (2011).
31. Fujihara, T., Xu, T., Semba, K., Terao, J. & Tsuji, Y. Copper-Catalyzed Hydrocarboxylation of Alkynes Using Carbon

Dioxide and Hydrosilanes. *Angew. Chem. Int. Ed.* **50,** 523–527 (2011).
32. Burkhart, G. & Hoberg, H. Oxanickelacyclopentene Derivatives from Nickel(0), Carbon Dioxide, and Alkynes. *Angew. Chem. Int. Ed.* **21,** 76 (1982).
33. Cárdenas, D. J. Towards Efficient and Wide-Scope Metal-Catalyzed Alkyl-Alkyl Cross-Coupling Reactions. *Angew. Chem. Int. Ed.* **38,** 3018–3020 (1999).
34. Cárdenas, D. J. Advances in Functional-Group-Tolerant Metal-Catalyzed Alkyl-Alkyl Cross-Coupling Reactions. *Angew. Chem. Int. Ed.* **42,** 384–387 (2003).
35. Serrano, E. & Martin, R. Nickel-Catalyzed Reductive Amidation of Unactivated Alkyl Bromides. *Angew. Chem. Int. Ed.* **55,** 11207–11211 (2016).
36. Börjesson, M., Moragas, T., Gallego, D. & Martin, R. Metal-Catalyzed Carboxylation of Organic (Pseudo)halides with CO_2. *ACS Catalysis* **6,** 6739–6749 (2016).
37. Correa, A. & Martin, R. Ni-Catalyzed Direct Reductive Amidation via C-O Bond Cleavage. *J. Am. Chem. Soc.* **136,** 7253–7256 (2014).
38. *CRC Handbook of Chemistry and Physics*. (ed. Lide, D. R.) (CRC Press, 2003).
39. Jutand, A. The Use of Conductivity Measurements for the Characterization of Cationic Palladium(II) Complexes and for the Determination of Kinetic and Thermodynamic Data in Palladium-Catalyzed Reactions. *Eur. J. Inorg. Chem.* **2003,** 2017–2040 (2003).
40. Feth, M. P., Klein, A. & Bertagnolli, H. Investigation of the Ligand Exchange Behavior of Square-Planar Nickel(II) Complexes by X-ray Absorption Spectroscopy and X-ray Diffraction. *Eur. J. Inorg. Chem.* **2003,** 839–852 (2003).
41. Klein, A. *et al.* Halide ligands - More than just σ-donors? A structural and spectroscopic study of homologous organonickel complexes. *Inorg. Chem.* **47,** 11324–11333 (2008).
42. Taube, H. & Gould, E. S. Organic Molecules as Bridging Groups in Electron-Transfer Reactions. *Acc. Chem. Res.* **2,** 321–329 (1969).
43. Wu, F., Lu, W., Qian, Q., Ren, Q. & Gong, H. Ketone Formation via Mild Nickel-Catalyzed Reductive Coupling of Alkyl Halides with Aryl Acid Chlorides. *Org. Lett.* **14,** 3044–3047 (2012).
44. Zhao, C., Jia, X., Wang, X. & Gong, H. Ni-Catalyzed Reductive Coupling of Alkyl Acids with Unactivated Tertiary Alkyl and Glycosyl Halides. *J. Am. Chem. Soc.* **136,** 17645–17651 (2014).
45. Dudnik, A. S. & Fu, G. C. Nickel-Catalyzed Coupling Reactions of Alkyl Electrophiles, Including Unactivated Tertiary Halides, To Generate Carbon−Boron Bonds. *J. Am. Chem. Soc.* **134,** 10693–10697 (2012).
46. Zultanski, S. L. & Fu, G. C. Nickel-Catalyzed Carbon−Carbon Bond-Forming Reactions of Unactivated Tertiary Alkyl Halides: Suzuki Arylations. *J. Am. Chem. Soc.* **135,** 624–627 (2013).
47. Börjesson, M., Moragas, T. & Martin, R. Ni-Catalyzed Carboxylation of Unactivated Alkyl Chlorides with CO_2. *J. Am. Chem. Soc.* **138,** 7504–7507 (2016).
48. Wang, X., Wang, S., Xue, W. & Gong, H. Nickel-Catalyzed Reductive Coupling of Aryl Bromides with Tertiary Alkyl Halides. *J. Am. Chem. Soc.* **137,** 11562–11565 (2015).
49. Cheung, C. W., Zhurkin, F. E. & Hu, X. Z-Selective Olefin Synthesis via Iron-Catalyzed Reductive Coupling of Alkyl Halides with Terminal Arylalkynes. *J. Am. Chem. Soc.* **137,** 4932–4935 (2015).
50. Cheung, C. W. & Hu, X. Stereoselective Synthesis of Trisubstituted Alkenes through Sequential Iron-Catalyzed Reductive anti-Carbozincation of Terminal Alkynes and Base-Metal-Catalyzed Negishi Cross-Coupling. *Chem. Eur. J.* **21,** 18439–18444 (2015).
51. Zhurkin, F. E. & Hu, X. γ-Selective Allylation of (E)-Alkenylzinc Iodides Prepared by Reductive Coupling of Arylacetylenes with Alkyl Iodides. *J. Org. Chem.* **81,** 5795–5802 (2016).
52. Guijarro, A. Dynamic Behavior of Organozinc Compounds. in *The Chemistry of Organozinc Compounds* (eds. Rappoport, Z. & Marek, I.) 193–236 (John Wiley & Sons, Ltd, 2006).
53. Yamamoto, A. & Suginome, M. Nickel-Catalyzed trans-Alkynylboration of Alkynes via Activation of a Boron-Chlorine Bond. *J. Am. Chem. Soc.* **127,** 15706–15707 (2005).
54. Daini, M., Yamamoto, A. & Suginome, M. Nickel-Catalyzed Cyclizative trans-Carboboration of Alkynes through Activation of Boron-Chlorine Bonds by Using Organometallic Reagents as Donors of Organic Groups. *Asian J. Org. Chem.* **2,** 968–976 (2013).
55. Clarke, C., Incerti-Pradillos, C. A. & Lam, H. W. Enantioselective Nickel-Catalyzed anti-Carbometallative Cyclizations of Alkynyl Electrophiles Enabled by Reversible Alkenylnickel E/Z Isomerization. *J. Am. Chem. Soc.* **138,** 8068–8071 (2016).
56. Knappke, C. E. I. *et al.* Reductive Cross-Coupling Reactions between Two Electrophiles. *Chem. Eur. J.* **20,** 6828–6842 (2014).
57. Moragas, T., Correa, A. & Martin, R. Metal-Catalyzed Reductive Coupling Reactions of Organic Halides with Carbonyl-Type Compounds. *Chem. Eur. J.* **20,** 8242–8258 (2014).
58. Magnus, P. D., Sarkar, T. & Djuric, S. Organosilicon Compounds in Organic Synthesis. in *Comprehensive Organometallic Chemistry* (eds. Wilkinson, G., Gordon, F., Stone, A. & Abel, E. W.) **7,** 515–659 (Elsevier, 1982).
59. Gillis, E. P. & Burke, M. D. A Simple and Modular Strategy for Small Molecule Synthesis: Iterative Suzuki-Miyaura Coupling of B-Protected Haloboronic Acid Building Blocks. *J. Am. Chem. Soc.* **129,** 6716–6717 (2007).
60. Suk, J. L., Gray, K. C., Paek, J. S. & Burke, M. D. Simple, Efficient, and Modular Syntheses of Polyene Natural Products via Iterative Cross-Coupling. *J. Am. Chem. Soc.* **130,** 466–468 (2008).
61. Knapp, D. M., Gillis, E. P. & Burke, M. D. A General Solution for Unstable Boronic Acids: Slow-Release Cross-Coupling from Air-Stable MIDA Boronates. *J. Am. Chem. Soc.* **131,** 6961–6963 (2009).
62. Lacey, R. N. The Acid-Catalysed Heterolysis of Amides with Alkyl- Nitrogen Fission (AAL). *J. Chem. Soc.* **0,** 1633–1639 (1960).

63. Phillips, B. A., Fodor, G., Gal, J., Letourneau, F. & Ryan, J. J. Mechanism of the von Braun Amide Degradations with Carbonyl Bromide or Phosphorus Pentabromide. *Tetrahedron* **29,** 3309–3327 (1973).
64. Powers, D. C., Anderson, B. L. & Nocera, D. G. Two-Electron HCl to H_2 Photocycle Promoted by Ni(II) Polypyridyl Halide Complexes. *J. Am. Chem. Soc.* **135,** 18876–18883 (2013).
65. Jones, G. D. *et al.* Ligand Redox Effects in the Synthesis, Electronic Structure, and Reactivity of an Alkyl-Alkyl Cross-Coupling Catalyst. *J. Am. Chem. Soc.* **128,** 13175–13183 (2006).
66. Velian, A., Lin, S., Miller, A. J. M., Day, M. W. & Agapie, T. Synthesis and C-C coupling reactivity of a dinuclear Ni^{I}-Ni^{I} Complex Supported by a Terphenyl Diphosphine. *J. Am. Chem. Soc.* **132,** 6296–6297 (2010).
67. Cornella, J., Gómez-Bengoa, E. & Martin, R. Combined Experimental and Theoretical Study on the Reductive Cleavage of Inert C–O Bonds with Silanes: Ruling out a Classical Ni(0)/Ni(II) Catalytic Couple and Evidence for Ni(I) Intermediates. *J. Am. Chem. Soc.* **135,** 1997–2009 (2013).
68. Fujihara, T. *et al.* Nickel-Catalyzed Double Carboxylation of Alkynes Employing Carbon Dioxide. *Org. Lett.* **16,** 4960–4963 (2014).
69. Clauti, G., Zassinovich, G. & Mestroni, G. Carbonyl Complexes of Rh(I), Ir(I) and Mo(0) Containing Substituted Derivatives of 1,10-Phenanthroline and 2,2′-Bipyridine. *Inorg. Chim. Acta* **112,** 103–106 (1986).
70. Crabtree, R. H. *The Organometallic Chemistry of the Transition Metals*. (John Wiley & Sons, Inc., 2014).
71. Vitek, A. K., Leone, A. K., McNeil, A. J. & Zimmerman, P. M. Spin-Switching Transmetalation at Ni Diimine Catalysts. *ACS Catal.* **8,** 3655–3666 (2018).
72. *Metal-Catalyzed Cross-Coupling Reactions*. (eds. de Meijere, A. & Diederich, F.) (Wiley-VCH Verlag GmbH & Co. KGaA, 2004).
73. Ojima, I., Clos, N., Donovan, R. J. & Ingallina, P. Hydrosilylation of 1-Hexyne Catalyzed by Rhodium and Cobalt–Rhodium Mixed-Metal Complexes. Mechanism of Apparent Trans Addition. *Organometallics* **9,** 3127–3133 (1990).
74. Jun, C.-H. & Crabtree, R. H. Dehydrogenative silation, isomerization and the control of syn- vs. anti-addition in the hydrosilation of alkynes. *J. Organomet. Chem.* **447,** 177–187 (1993).
75. Crabtree, R. H. An η^2-vinyl pathway may explain net trans hydrosilylation via transition metal catalysis even in cyclic cases. *New J. Chem.* **27,** 771–772 (2003).
76. Petrone, D. A. *et al.* Palladium-Catalyzed Hydrohalogenation of 1,6-Enynes: Hydrogen Halide Salts and Alkyl Halides as Convenient HX Surrogates. *J. Am. Chem. Soc.* **139,** 3546–3557 (2017).
77. Bhawal, B. N. & Morandi, B. Shuttle Catalysis—New Strategies in Organic Synthesis. *Chem. Eur. J.* **23,** 12004–12013 (2017).
78. Bhawal, B. N. & Morandi, B. Catalytic Transfer Functionalization through Shuttle Catalysis. *ACS Catal.* **6,** 7528–7535 (2016).
79. Chen, F. *et al.* Remote Migratory Cross-Electrophile Coupling and Olefin Hydroarylation Reactions Enabled by in situ Generation of NiH. *J. Am. Chem. Soc.* **139,** 13929–13935 (2017).
80. He, Y., Cai, Y. & Zhu, S. Mild and Regioselective Benzylic C–H Functionalization: Ni-Catalyzed Reductive Arylation of Remote and Proximal Olefins. *J. Am. Chem. Soc.* **139,** 1061–1064 (2017).

4.7. Experimental Section

4.7.1. General Considerations

Reagents. All reactions were conducted in screw-cap test tubes under argon atmosphere. $NiBr_2$·glyme and manganese powder (99.9% trace metal basis) were purchased from Aldrich. All other nickel catalysts and ligands were purchased from Aldrich or Strem. Bathocuproine and isopropyl bromide were purchased from TCI. *tert*-butyl isocyanate (97% purity) and cyclohexyl isocyanate (98% purity) were purchased from Aldrich. Other isocyanates were purchased from TCI (NOTE: *the purity of the isocyanates was found crucial for the reaction*; higher yields and better reproducibility were achieved by purifying the isocyanates through a short plug of dried neutral alumina inside a nitrogen-filled glovebox. Old batches of isocyanates provide consistently lower yields and variable results). Anhydrous *N,N*-dimethylformamide (DMF, 99.8% purity), *N,N*-dimethylacetamide (DMA, 99.5% purity) and *N*-methylpyrrolidone (NMP, 99.5% purity) were purchased from Acros Organics and used as received (NOTE: *it is critical to have appropriately dried DMF and DMA to obtain reproducible results*, since old batches of these solvents provided variable results). All other reagents were purchased from commercial sources and used as received. The alkynes used as starting materials were prepared via Sonogashira reactions.

Analytical methods. ^{1}H NMR, ^{13}C NMR spectra and melting points (where applicable) are included for all compounds. ^{1}H and ^{13}C-NMR spectra were recorded on a Bruker 300 MHz, 400 MHz and 500 MHz at 20 °C. All ^{1}H-NMR spectra are reported in parts per million (ppm) downfield of TMS and are reported relative to the signal of residual $CHCl_3$ (7.26 ppm), unless indicated otherwise. All ^{13}C-NMR spectra are reported in ppm relative to residual $CHCl_3$ (77.2 ppm), unless otherwise indicated, and were measured with ^{1}H decoupling. Coupling constants, *J*, are reported in Hertz. HSQC, HMBC, DEPTQ and COSY experiments were used to assist the assignment of the signals. Melting points were measured using open glass capillaries in a Büchi B540 apparatus. IR spectra were measured on a Bruker Optics FT-IR GmbH Alpha spectrometer with a Platinum-ATR module. Gas chromatographic analyses were performed on a Hewlett-Packard 6890 gas chromatography instrument with an FID detector. High Pressure Liquid Chromatographic (HPLC) analyses were performed on Agilent Technologies Model 1260 Infinity HPLC chromatography instrument equipped with Agilent Eclipse Plus C18 (3.5 um, 4.6 x 100 mm) column and UV/VIS detector. Column chromatography was performed with EM Science silica gel 60 (230-400 mesh). Thin layer chromatography was carried out using Merck TLC Silica gel 60 F_{254}. $KMnO_4$ or vanillin stains were used as TLC stains for amides. The yields reported refer to isolated yields and represent an average of at least two independent runs.

4.7.2. Preparative Scope

General Procedure A: An oven-dried screw cap test tube containing a stirring bar was charged with diphenylacetylene (89.2 mg, 0.50 mmol), **L1** (36 mg, 0.1 mmol), Mn powder (41.2 mg, 0.75 mmol) and $NiBr_2$·diglyme (18 mg, 0.05 mmol). The tube was then sealed, evacuated and back-filled with argon three times. *i*-PrBr (71.2 μL, 0.75 mmol), *t*-BuNCO (85.6 μL, 0.75 mmol) and NMP (2 mL) were then added by syringe. Once added, the reaction mixture was stirred overnight at room temperature. The mixture was quenched with HCl (5% aq) or NH_4Cl (saturated solution) and extracted with ethyl acetate three times. The combined organic layers were washed with brine and dried over anhydrous $MgSO_4$ and evaporated. The residue was purified by column chromatography on a silica gel (hexane/ethyl acetate = 30/1 to 10/1).

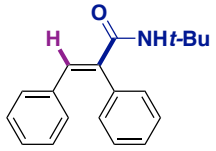

(*E*)-*N*-(*tert*-butyl)-2,3-diphenylacrylamide (4.3ae). Following the general procedure using 1,2-diphenylethyne to afford **4.3ae** as a colorless solid (127.1 mg, 91% yield). m. p. = 92 - 94 °C. ^{1}H NMR (500 MHz, $CDCl_3$) δ 7.80 (s, 1H), 7.49 – 7.36 (m, 3H), 7.27 – 7.21 (m, 2H), 7.18 – 7.08 (m, 3H), 7.00 – 6.93 (m, 2H), 5.34 (s, 1H), 1.31 (s, 9H) ppm. ^{13}C NMR (126 MHz, $CDCl_3$) δ 166.5, 136.7, 136.3, 135.8, 135.3, 130.4, 130.0, 129.6, 128.5, 128.4, 128.2, 51.6, 28.8 ppm. IR (neat, cm^{-1}): 3411, 2974, 1666, 1614, 1500, 1199, 781, 692. HRMS *calcd.* for ($C_{19}H_{21}NO$+H): 280.1696, *found:* 280.1689.

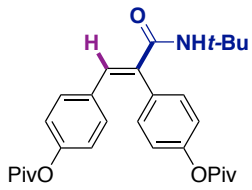

(*E*)-*N*-(*tert*-butyl)-2,3-bis(pivaloyloxyphenyl)acrylamide (4.3af). Following the general procedure using ethyne-1,2-diylbis(4,1-phenylene) bis(2,2-dimethylpropanoate)to afford **4.3af** as a colorless solid (180.8 mg, 75% yield). m. p. = 145 – 147 °C. ^{1}H NMR (400 MHz, $CDCl_3$) δ 7.79 (s, 1H), 7.27 (d, *J* = 8.7 Hz, 2H), 7.16 (d, *J* = 8.7 Hz, 2H), 7.04 – 6.98 (m, 2H), 6.88 (d, *J* = 8.7 Hz, 2H), 5.36 (s, 1H), 1.41 (s, 9H), 1.34 (s, 9H), 1.32 (s, 9H) ppm. ^{13}C NMR (101 MHz, $CDCl_3$) δ 177.0, 176.9, 166.2, 151.3, 151.1, 135.8, 134.8, 133.6, 132.6, 131.4, 130.0, 123.0, 121.4, 51.7, 39.3, 39.2, 28.8, 27.3, 27.19 (2C) ppm. IR (neat, cm^{-1}): 3432, 2973, 1747, 1674, 1501, 1270, 1196, 1164, 1106, 894. HRMS calcd. for ($C_{29}H_{37}NO_5$+H): 480.2744, found: 480.2745.

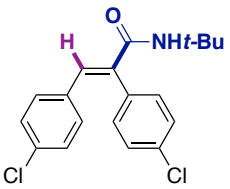

(*E*)-*N*-(*tert*-butyl)-2,3-bis(4-chlorophenyl)acrylamide (4.3ag). Following the general procedure using 1,2-bis(4-chlorophenyl)ethyne to afford **4.3ag** as a colorless solid (132.2 mg, 76% yield). m. p. = 124 - 125 °C. ^{1}H NMR (300 MHz, $CDCl_3$) δ 7.72 (s, 1H), 7.41 (d, *J* = 8.0 Hz, 2H), 7.21 7.08 (m, 4H), 6.88 (d, *J* = 8.5 Hz, 2H), 5.28 (s, 1H), 1.32 (s, 9H) ppm. ^{13}C NMR (126 MHz, $CDCl_3$) δ 165.7, 135.5, 135.2, 134.8, 134.6, 134.5, 133.4, 131.4, 131.3, 130.0, 128.6, 51.7, 28.7 ppm. IR (neat, cm^{-1}): 3420, 2965, 1668, 1618, 1503, 1271, 1095, 1010, 824, 743. HRMS *calcd.* for ($C_{19}H_{19}Cl_2NO$+Na): 370.0741, *found:* 370.0736.

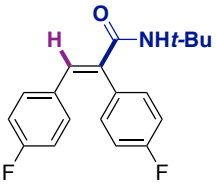

(*E*)-*N*-(*tert*-butyl)-2,3-bis(4-fluorophenyl)acrylamide (4.3ah). Following the general procedure using 1,2-bis(4-fluorophenyl)ethyne to afford **4.3ah** as a colorless solid (137.3 mg, 87% yield). m. p. = 109 - 111 °C. ^{1}H NMR (400 MHz, $CDCl_3$) δ 7.74 (s, 1H), 7.24 – 7.08 (m, 3H), 6.98 – 6.87 (m, 2H), 6.83 (dd, *J* = 8.9, 2.0 Hz, 2H), 5.27 (s, 1H), 1.31 (s, 9H) ppm. ^{13}C NMR (101 MHz, $CDCl_3$) δ 166.2, 164.0 (d, *J* = 19.6 Hz), 161.5 (d, *J* = 20.7 Hz), 135.6, 134.5, 132.3 (d, *J* = 3.7 Hz), 132.1 (d, *J* = 8.2 Hz), 131.9 (d, *J* = 8.1 Hz), 131.3 (d, *J* = 3.4 Hz), 117.0 (d, *J* = 21.5 Hz), 115.5 (d, *J* = 21.5 Hz), 51.7, 28.8 ppm. ^{19}F NMR (376 MHz, $CDCl_3$) δ -112.0, -112.5 ppm. IR (neat, cm^{-1}): 3424, 2966, 1670, 1496, 1222, 1157, 837. 808. HRMS *calcd.* for ($C_{19}H_{19}F_2NO$+Na): 338.1327, *found:* 338.1318.

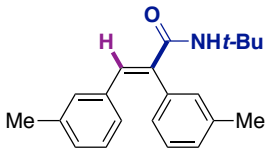

(*E*)-*N*-(*tert*-butyl)-2,3-di-*m*-tolylacrylamide (4.3ai). Following the general procedure using 1,2-di-*m*-tolylethyne to afford **4.3ai** as a colorless solid (139.8 mg, 91% yield). m. p. = 115 – 116 °C. ^{1}H NMR (500 MHz, $CDCl_3$) δ 7.77 (s, 1H), 7.33 (td, *J* = 7.4, 1.0 Hz, 1H), 7.24 – 7.20 (m, 1H), 7.10 – 6.94 (m, 4H), 6.84 (dq, *J* = 1.7, 0.8 Hz, 1H), 6.78 – 6.73 (m, 1H), 5.42 (s, 1H), 2.37 (s, 3H), 2.18 (s, 3H), 1.34 (s, 9H) ppm. ^{13}C NMR (126 MHz, $CDCl_3$) δ 166.5, 139.2, 137.5, 136.6, 136.0, 135.5, 135.2, 131.3, 130.2, 129.4, 129.1, 129.1, 128.0, 127.3, 126.8, 51.4, 28.7, 21.5, 21.3 ppm. IR (neat, cm^{-1}): 3270, 2958, 1633, 1613, 1537, 1450, 1314, 1222, 1091, 921. 783. HRMS *calcd.* for ($C_{21}H_{25}NO$+Na): 330.1834, *found:* 330.1840.

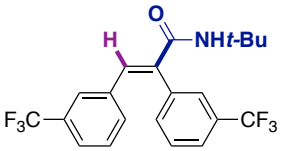

(*E*)-*N*-(*tert*-butyl)-2,3-bis(3-(trifluoromethyl)phenyl)acrylamide (4.3aj). Following the general procedure using 1,2-bis(3-(trifluoromethyl)phenyl)ethyne to afford **4.3aj** as a colorless solid (133.2 mg, 64% yield). m. p. = 64 - 65 °C. ^{1}H NMR (400 MHz, $CDCl_3$) δ 7.79 (s, 1H), 7.69 (d, *J* = 7.9 Hz, 1H), 7.58 (t, *J* = 7.8 Hz, 1H), 7.49 (s, 1H), 7.46 – 7.38 (m, 2H), 7.28 (dd, *J* = 9.7, 5.9 Hz, 1H), 7.14 (d, *J* = 7.8 Hz, 1H), 7.08 (s, 1H), 5.32 (s, 1H), 1.34 (s, 9H) ppm. ^{13}C NMR (101 MHz, $CDCl_3$) δ 165.2, 136.7, 136.6, 135.5, 135.4, 133.2 (2C), 132.1 (q, *J* = 32.7 Hz), 130.7 (q, *J* = 33.5 Hz), 130.2, 128.9, 126.7 (q, *J* = 3.7 Hz), 126.4 (q, *J* = 3.9 Hz), 125.5 (q, *J* = 3.8 Hz), 125.1 (q, *J* = 3.7 Hz), 123.6 (2C, q, *J* = 273 Hz), 51.9, 28.6 ppm. ^{19}F NMR (376 MHz, $CDCl_3$) δ -63.2, -63.5 ppm. IR (neat, cm^{-1}): 3275, 2971, 1638, 1548, 1322, 1118, 1072, 912, 698. HRMS *calcd.* for ($C_{21}H_{20}F_6NO$+H): 416.1444, *found:* 416.1438.

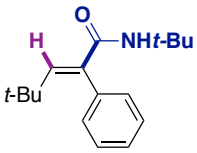

(*E*)-*N*-(*tert*-butyl)-4,4-dimethyl-2-phenylpent-2-enamide (4.3ak). Following the general procedure but at 35 °C for three days using (3,3-dimethylbut-1-yn-1-yl)benzene to afford **4.3ak** as a colorless solid (65.5 mg, 50% yield). m. p. = 99 - 100 °C. ^{1}H NMR (300 MHz, $CDCl_3$) δ 7.39 – 7.31 (m, 3H), 7.21 – 7.13 (m, 2H), 7.01 (s, 1H), 5.06 (s, 1H), 1.22 (s, 9H), 0.88 (s, 9H) ppm. ^{13}C NMR (75 MHz, $CDCl_3$) δ 166.8, 148.5, 136.9, 133.6, 130.3, 128.4, 127.9, 51.1, 33.7, 30.5, 28.6 ppm. IR (neat, cm^{-1}): 3293, 2960, 1621, 1533, 1452, 1358, 1306, 1219, 1157, 708. HRMS *calcd.* for ($C_{17}H_{26}NO$+H): 260.2009, *found:* 260.2005.

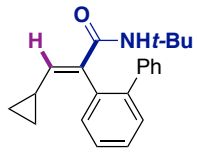

(*E*)-2-([1,1'-biphenyl]-2-yl)-*N*-(*tert*-butyl)-3-cyclopropylacrylamide (4.3ai). Following the general procedure using 2-(cyclopropylethynyl)-1,1'-biphenyl to afford **4.3ai** as a colorless solid (129.8 mg, 81% yield). m. p. = 104 - 106 °C. ^{1}H NMR (300 MHz, $CDCl_3$) δ 7.52 – 7.26 (m, 9H), 6.27 (d, *J* = 10.9 Hz, 1H), 4.98 (s, 1H), 1.38 – 1.19 (m, 1H), 1.04 (s, 9H), 0.90 – 0.77 (m, 1H), 0.77 – 0.59 (m, 1H), 0.59 – 0.40 (m, 1H) ppm. ^{13}C NMR (101 MHz, $CDCl_3$) δ 165.0, 146.0, 142.0, 140.8, 134.5, 134.1, 132.2, 130.5, 129.0, 128.7, 128.3, 127.9, 127.4, 50.9, 28.5, 12.5, 8.3, 8.2 ppm. IR (neat, cm^{-1}): 3424, 2965, 1666, 1621, 1505, 743, 703, 499. HRMS *calcd.* for ($C_{22}H_{25}NO$+H): 320.2009, *found:* 320.1999.

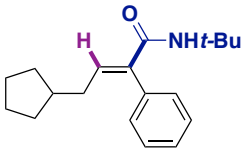

(*E*)-*N*-(*tert*-butyl)-4-cyclopentyl-2-phenylbut-2-enamide (4.3am). Following the general procedure using (3-cyclopentylprop-1-yn-1-yl)benzene to afford **4.3am** as a colorless solid (131.3 mg, 92% yield). m. p. = 61 – 62 °C. ^{1}H NMR (400 MHz, $CDCl_3$) δ 7.59 – 7.28 (m, 3H), 7.20 – 7.06 (m, 2H), 6.98 (t, J = 7.5 Hz, 1H), 5.14 (s, 1H), 1.99 – 1.90 (m, 2H), 1.91 – 1.80 (m, 1H), 1.76 – 1.66 (m, 2H), 1.55 – 1.41 (m, 4H), 1.26 (s, 9H), 1.11 – 0.96 (m, 2H) ppm. ^{13}C NMR (101 MHz, $CDCl_3$) δ 166.3, 139.8, 136.8, 136.5, 130.0, 128.9, 128.0, 51.3, 39.9, 35.4, 32.5, 29.0, 25.1 ppm. IR (neat, cm^{-1}): 3295, 2948, 2865, 1619, 1531, 1222, 700. HRMS *calcd.* for ($C_{19}H_{27}NO$+Na): 308.1985, *found:* 308.1980.

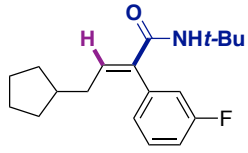

E/*Z* = 14:1

(*E*)-*N*-(*tert*-butyl)-4-cyclopentyl-2-(3-fluorophenyl)but-2-enamide (4.3an). Following the general procedure using 1-(3-cyclopentylprop-1-yn-1-yl)-3-fluoro-benzene to afford **4.3an** as a colorless solid (133.3 mg**, 4.3an:4.3an'** *E*/*Z* = 14:1 88% yield). m. p. = 74 - 76 °C. Spectroscopic data for the major isomer (**4.3an**): ^{1}H NMR (400 MHz, $CDCl_3$) δ 7.51 – 7.33 (m, 1H), 7.06 (td, *J* = 8.5, 2.7, 1H), 7.02 – 6.92 (m, 2H), 6.88 (dd, *J* = 9.4, 2.6, 1H), 5.10 (s, 1H), 1.99 – 1.94 (m, 1H) 1.93 – 1.79 (m, 2H), 1.79 – 1.66 (m, 2H), 1.59 – 1.44 (m, 4H), 1.29 (s, 9H), 1.11 – 0.95 (m, 2H) ppm. ^{13}C NMR (101 MHz, $CDCl_3$) δ 165.7, 162.9 (d, *J* = 247.6 Hz), 140.6, 138.8 (d, *J* = 7.5 Hz), 135.8, 130.6 (d, *J* = 8.5 Hz), 125.7 (d, *J* = 3.1 Hz), 117.0 (d, *J* = 21.2 Hz), 115.1 (d, *J* = 21.0 Hz), 51.5, 39.8, 35.4, 32.6, 28.9, 25.1 ppm. ^{19}F NMR (376 MHz, $CDCl_3$) δ -111.70 ppm. IR (neat, cm^{-1}): 3281, 2957, 2865, 1624, 1539, 1223, 740, 678. HRMS *calcd.* for ($C_{19}H_{26}FNO$+H): 304.2071, *found:* 304.2063.

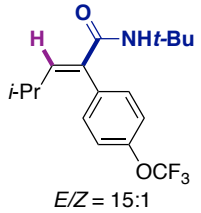

E/*Z* = 15:1

(*E*)-*N*-(*tert*-butyl)-4-methyl-2-(4-(trifluoromethoxy)phenyl)pent-2-enamide (4.3ao). Following the general procedure using 1-(3-methylbut-1-yn-1-yl)-4-(trifluoromethoxy)benzene to afford **4.3ao** as a colorless solid (105.4 mg, **4.3ao:4.3ao'** *E*/*Z* = 15:1, 64% yield). m. p. = 66 – 69 °C. Spectroscopic data for the major isomer (**4.3ao**): ^{1}H NMR (400 MHz, $CDCl_3$) δ 7.35 – 7.14 (m, 4H), 6.73 (d, *J* = 10.6 Hz, 1H), 5.07 (s, 1H), 2.22 – 2.13 (m, 1H), 1.29 (s, 9H), 0.96 (d, J = 6.6 Hz, 6H) ppm. ^{13}C NMR (101 MHz, $CDCl_3$) δ 166.0, 149.0 (q, *J* = 1.7 Hz), 147.2, 135.1, 133.5, 131.3, 121.7, 120.6 (q, *J* = 257.4 Hz), 51.5, 28.8, 28.6, 22.4 ppm. ^{19}F NMR (376 MHz, $CDCl_3$) δ -57.90 ppm. IR (neat, cm^{-1}): 3296, 2960, 1612, 1534, 1250, 1159. HRMS *calcd.* for ($C_{17}H_{22}F_3NO$+Na): 352.1495, *found:* 352.1491.

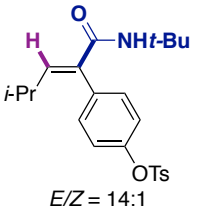

E/*Z* = 14:1

(*E*)-4-(1-(*tert*-butylamino)-4-methyl-1-oxopent-2-en-2-yl)phenyl 4-methylbenzene sulfonate (4.3ap). Following the general procedure using 4-(3-methylbut-1-yn-1-yl)phenyl 4-methylbenzenesulfonate to afford **4.3ap** as a colorless solid (202.8 mg, **4.3ap:4.3ap'** *E*/*Z* = 14:1, 97% yield). m. p. = 123 – 125 °C. Spectroscopic data for the major isomer (**4.3ap**): ^{1}H NMR (400 MHz, $CDCl_3$) δ 7.65 (d, *J* = 8.3 Hz, 2H), 7.25 (d, *J* = 7.9 Hz, 2H), 7.08 – 7.02 (m, 2H), 7.02 – 6.94 (m, 2H), 6.63 (d, *J* = 10.5 Hz, 1H), 4.95 (s, 1H), 2.38 (s, 3H), 2.17 – 1.86 (m, 1H), 1.21 (s, 9H), 0.87 (d, *J* = 6.6 Hz, 6H) ppm. ^{13}C NMR (101 MHz, $CDCl_3$) δ 165.8, 149.2, 146.9, 145.6, 135.3, 133.4, 132.2, 130.9, 129.8, 128.5, 122.7, 51.3, 28.6, 28.4, 22.3, 21.7 ppm. IR (neat, cm^{-1}): 3423, 2965, 1668, 1497, 1361, 1153, 858, 549. HRMS *calcd.* for ($C_{23}H_{30}NO_4S$+Na): 416.1890, *found:* 416.1891.

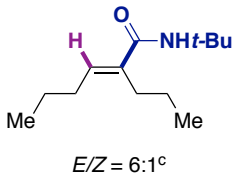

E/*Z* = 6:1[c]

(*E*)-N-(tert-butyl)-2-propylhex-2-enamide (4.3ar). Following the general procedure using oct-4-yne, neocuproine (21 mg, 20 mol%) as ligand, Mn (54 mg, 2.0 equiv.) at 10°C, to afford **4.3ar** as an off-white solid (60.2 mg, **4.3ar**:**4.3ar'** *E*/*Z* = 6:1, 57% yield). m. p. = 39.2 – 40.7 °C. Spectroscopic data for the major isomer (**4.3ar**): ^{1}H NMR (400 MHz, $CDCl_3$) δ 5.33 (tt, *J* = 7.5, 1.2 Hz, 1H), 5.25 (bs, 1H), 2.18 – 2.04 (m, 4H), 1.47 – 1.39 (m, 4H), 1.38 (s, 9H), 0.93 – 0.88 ppm (m, 6H). ^{13}C NMR (126 MHz, $CDCl_3$) δ 167.0, 139.3, 129.5, 51.5, 37.2, 31.4, 29.1, 23.1, 21.6, 14.0, 13.8 ppm. IR (neat, cm^{-1}): 3276, 2958, 2929, 2871, 1624, 1535, 1452, 1360, 1224. HRMS *calcd.* for ($C_{13}H_{25}NO$+H): 212.2009, found: 212.2007.

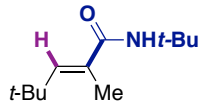

(*E*)-*N*-(*tert*-butyl)-2,4,4-trimethylpent-2-enamide (4.3as). Following the general procedure using 4,4-dimethylpent-2-yne to afford **4.3as** as an off-white solid (37.8 mg, 38% yield). m. p. = 88.5 – 89.6 °C. ^{1}H NMR (300 MHz, $CDCl_3$) δ 6.19 (q, *J* = 1.3 Hz, 1H), 5.50 (bs, 1H), 1.92 (d, *J* = 1.4 Hz, 3H), 1.38 (s, 9H), 1.15 ppm (s, 9H). ^{13}C NMR (126 MHz, $CDCl_3$) δ 170.6, 143.9, 131.7, 51.2, 32.7, 30.5, 28.9, 13.9 ppm. IR (neat, cm^{-1}): 3304, 2972, 2957, 2929, 1652, 1617, 1522, 1359, 1304, 1220. HRMS *calcd.* for ($C_{12}H_{23}NO$+H): 198.1852, found: 198.1853.

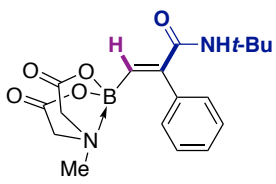

(*E*)-N-(*tert*-butyl)-3-(6-methyl-4,8-dioxo-1,3,6,2-dioxazaborocan-2-yl)-2 phenylac-rylamide (4.3at). Following the general procedure using 6-methyl-2-(phenylethynyl)-1,3,6,2-dioxazaborocane-4,8-dioneto afford **4.3at** as a pale yellow solid (99.0 mg, 55% yield). m. p. = 249.6 – 254.9 °C (decomposition). ^{1}H NMR (400 MHz, CD_3CN) δ 7.38- 7.32 (m, 3H), 7.26 – 7.22 (m, 2H), 6.54 (s, 1H), 5.70 (s, 1H), 3.80 (d, *J* = 16.9 Hz, 2H), 3.56 (d, *J* = 16.8 Hz, 2H), 2.85 (s, 3H), 1.25 (s, 9H) ppm. ^{13}C NMR (126 MHz, CD_3CN) δ 168.6, 167.9, 151.9, 138.9, 130.0, 129.1, 128.6, 118.3, 62.6, 51.7, 47.6, 28.7 ppm. IR (neat, cm^{-1}): 3420, 2960, 1757, 1657, 1512, 1268, 1039, 855. HRMS *calcd.* for ($C_{18}H_{23}BN_2O_5$+Na) 381.1596, *found*: 381.1590.

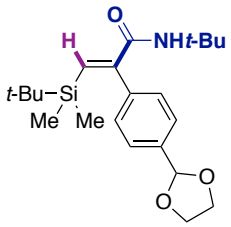

(*E*)-2-(4-(1,3-dioxolan-2-yl)phenyl)-*N*-(*tert*-butyl)-3-(*tert*-butyldimethylsilyl)-acrylamide (4.3au). Following the general procedure using ((4-(1,3-dioxolan-2-yl)phenyl)ethynyl)(tert-butyl)dimethylsilane to afford **4.3au** as a clear oil (153.9 mg, 79% yield). ^{1}H NMR (300 MHz, $CDCl_3$) δ 7.46 (d, *J* = 8.0 Hz, 1H), 7.22 (s, 1H), 7.19 (d, *J* = 7.9 Hz, 2H), 5.78 (s, 1H), 5.20 (s, 1H), 4.15 – 3.98 (m, 4H), 1.22 (s, 9H), 0.83 (s, 9H), -0.41 (s, 6H) ppm. ^{13}C NMR (101 MHz, $CDCl_3$) δ 165.1, 150.9, 139.8, 137.9, 137.4, 129.6, 126.7, 103.4, 65.4, 51.4, 28.7, 26.6, 16.8, -5.4 ppm. IR (neat, cm^{-1}): 3423, 2954, 2928, 2883, 2856, 1669, 1504, 1453, 1265, 1212, 1081, 825. HRMS *calcd.* for ($C_{22}H_{35}NOSi$+H): 390.2459, *found:* 390.2454.

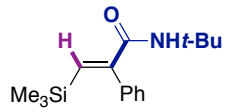

(*E*)-*N*-(*tert*-butyl)-2-phenyl-3-(triethylsilyl)acrylamide (4.3av). Following the general procedure using trimethyl(phenylethynyl)silane to afford **4.3av** as a colorless solid (139.7 mg, 88% yield). m. p. = 50 – 52 °C. ^{1}H NMR (400 MHz, $CDCl_3$) δ 7.35 – 7.33 (m, 3H), 7.22 – 7.15 (m, 2H), 7.13 (s, 1H), 5.27 (s, 1H), 1.25 (s, 9H), 0.79 (t, *J* = 7.9 Hz, 9H), 0.28 (q, *J* = 7.9 Hz, 6H) ppm. ^{13}C NMR (101 MHz, $CDCl_3$) δ 165.4, 151.3, 139.0, 137.2, 129.4, 128.5, 128.3, 51.4, 28.7, 7.5, 3.9 ppm. IR (neat, cm^{-1}) 3279, 2952, 2875, 1636, 1533, 1285, 1224, 839, 699. HRMS *calcd.* for ($C_{19}H_{31}NOSi$+H): 318.2248, *found:* 318.2244.

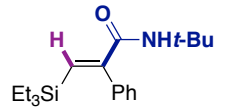

(*E*)-*N*-(*tert*-butyl)-2-phenyl-3-(trimethylsilyl)acrylamide (4.3aw). Following the general procedure using triethyl(phenylethynyl)silane to afford **4.3aw** as a colorless solid (127.0 mg, 92% yield). m. p. = 104 – 106 °C. ^{1}H NMR (300 MHz, $CDCl_3$) δ 7.50 – 7.29 (m, 3H), 7.24 – 7.09 (m, 3H), 5.30 (s, 1H), 1.25 (s, 9H), -0.19 (s, 9H) ppm. ^{13}C NMR (101 MHz, $CDCl_3$) δ 165.6, 150.7, 139.8, 138.8, 129.6, 128.6, 128.3, 51.4, 28.7, -0.6 ppm. IR (neat, cm^{-1}): 3293, 2973, 1636, 1537, 836, 697. HRMS *calcd.* for ($C_{16}H_{25}NOSi$+Na): 298.1598, *found:* 298.1597.

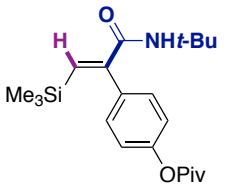

(*E*)-4-(3-(*tert*-butylamino)-3-oxo-1-(trimethylsilyl)prop-1-en-2-yl)phenyl pivalate (4.3ay). Following the general procedure using 4-((trimethylsilyl)ethynyl)phenyl pivalate to afford **4.3ay** as a colorless solid (150.0 mg, 80% yield). m. p. = 121 – 122 °C. ^{1}H NMR (400 MHz, $CDCl_3$) δ 7.18 (d, *J* = 8.4 Hz, 2H), 7.12 (s, 1H), 7.05 (d, *J* = 8.5 Hz, 2H), 5.28 (s, 1H), 1.33 (s, 9H), 1.24 (s, 9H), -0.18 (s, 9H) ppm. ^{13}C NMR (101 MHz, $CDCl_3$) δ 177.0, 165.4, 151.2, 149.8, 140.4, 136.0, 130.5, 121.8, 51.5, 39.2, 28.6, 27.2, -0.6 ppm. IR (neat, cm^{-1}) 3367, 2965, 1749, 1632, 1526, 1197, 1115, 860, 833. HRMS *calcd.* for ($C_{21}H_{33}NOSi$+H): 376.2302, *found:* 376.2314.

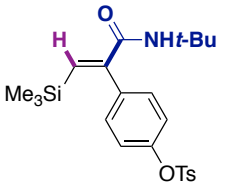

(*E*)-4-(3-(*tert*-butylamino)-3-oxo-1-(trimethylsilyl)prop-1-en-2-yl)phenyl 4-meth-ylbenzenesulfonate (4.3az). Following the general procedure using 4-((trimethylsilyl)ethynyl)phenyl 4-methylbenzenesulfonate to afford **4.3az** as a colorless solid (222.0 mg, 99% yield). m. p. = 143 – 145 °C. ^{1}H NMR (400 MHz, $CDCl_3$) δ 7.66 (d, *J* = 8.4 Hz, 2H), 7.26 (d, *J* = 8.0 Hz, 2H), 7.11 (d, *J* = 8.5 Hz, 2H), 7.06 (s, 1H), 6.99 (d, *J* = 8.5 Hz, 2H), 5.15 (s, 1H), 2.41 (s, 3H), 1.24 (s, 9H), -0.21 (s, 9H) ppm. ^{13}C NMR (101 MHz, $CDCl_3$) δ 165.2, 149.6, 149.5, 145.7, 140.5, 137.8, 132.0, 130.8, 129.9, 128.7, 122.6, 51.6, 28.6, 21.8, -0.6 ppm. IR (neat, cm^{-1}) 3347, 2975, 1524, 1373, 1149, 866, 552. HRMS *calcd.* for ($C_{23}H_{31}NO_4SSi$+H): 446.1816, *found:* 446.1814

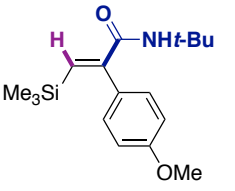

(*E*)-*N*-(*tert*-butyl)-2-(4-methoxylphenyl)-3-(trimethylsilyl)acrylamide (4.3ba). Follo-wing the general procedure using ((4-methoxyphenyl)ethynyl)trimethylsilane to afford **4.3ba** as a colorless solid (116.8 mg, 76% yield). m. p. = 97 – 99 °C. ^{1}H NMR (300 MHz, $CDCl_3$) δ 7.17 – 7.05 (m, 3H), 6.95 – 6.84 (m, 2H), 5.37 (s, 1H), 3.83 (s, 3H), 1.27 (s, 9H),

-0.16 (s, 9H) ppm. ^{13}C NMR (75 MHz, $CDCl_3$) δ 166.0, 159.6, 150.3, 139.7, 130.8, 113.9, 55.4, 51.4, 28.7, -0.5 ppm. HRMS *calcd.* for ($C_{17}H_{28}NO_2Si$+H): 306.1884, *found:* 316.1882.

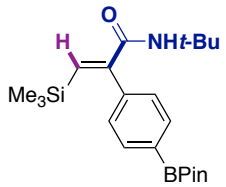

(*E*)-*N*-(*tert*-butyl)-2-(4-(4,4,5,5-tetramethyl-1,3,2-dioxaborolan-2-yl)phenyl)-3-(trimethylsilyl)acrylamide (4.3bb). Following the general procedure using trimethyl((4-(4,4,5,5-tetramethyl-1,3,2-dioxaborolan-2-yl)phenyl)ethynyl)silane to afford **4.3bb** as a colorless solid (126.2 mg, 63% yield). m. p. = 157 – 158 °C. ^{1}H NMR (400 MHz, $CDCl_3$) δ 7.82 (d, *J* = 8.0 Hz, 2H), 7.23 (d, *J* = 8.0 Hz, 2H), 7.19 (s, 1H), 5.29 (s, 1H), 1.39 (s, 12H), 1.28 (s, 9H), -0.15 (s, 9H) ppm. ^{13}C NMR (101 MHz, $CDCl_3$) δ 165.3, 150.6, 141.7, 140.0, 134.9, 128.9, 84.2, 51.5, 28.7, 25.1, -0.5 ppm. IR (neat, cm^{-1}): 3424, 2973, 1667, 1594, 1506, 1396, 1359, 1215, 1143, 1088, 837, 659. HRMS *calcd.* for ($C_{22}H_{36}BNO_3Si$): 401.2558, *found:* 401.2667.

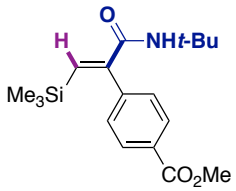

(*E*)-methyl-4-(3-(*tert*-butylamino)-3-oxo-1-(trimethylsilyl)prop-1-en-2-yl)benzoa-te (4.3bc). Following the general procedure using methyl 4-((trimethylsilyl)ethynyl)benzoate to afford **4.3bc** as a colorless solid (116.8 mg, 70% yield). m. p. = 97 – 99 °C. ^{1}H NMR (400 MHz, $CDCl_3$) δ 8.04 (d, *J* = 8.3 Hz, 2H), 7.29 (d, *J* = 8.3 Hz, 2H), 7.14 (s, 1H), 5.17 (s, 1H), 3.92 (s, 3H), 1.25 (s, 9H), -0.18 (s, 9H) ppm. ^{13}C NMR (101 MHz, $CDCl_3$) δ 166.7, 165.0, 149.9, 143.8, 140.6, 130.1, 129.8, 129.7, 52.4, 51.7, 28.7, -0.6 ppm. IR (neat, cm^{-1}) 3114, 2968, 1725, 1636, 1525, 1273, 831, 710. HRMS *calcd.* for ($C_{18}H_{27}NO_3Si$+Na): 356.1652, *found:* 356.1641.

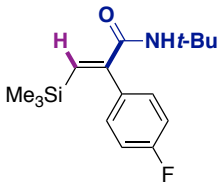

(*E*)-*N*-(*tert*-butyl)-2-(4-fluorophenyl)-3-(trimethylsilyl)acrylamide (4.3bd). Following the general procedure using ((4-fluorophenyl)ethynyl)trimethylsilane to afford **4.3bd** as a colorless solid (123.2 mg, 84% yield). m. p. = 98 – 99 °C. 1H NMR (300 MHz, $CDCl_3$) δ 7.43 – 7.33 (m, 2H), 7.27 (s, 1H), 7.18 – 7.13 (m, 2H), 5.32 (s, 1H), 1.34 (s, 9H), -0.10 (s, 9H) ppm. ^{13}C NMR (75 MHz, $CDCl_3$) δ 165.5, 164.3, 161.0, 149.7, 140.3, 134.7, 134.6, 131.3, 131.2, 115.7, 115.4, 51.5, 28.6, -0.6 ppm. ^{19}F NMR (376 MHz, $CDCl_3$) δ -113.3 (tt, *J* = 8.6, 5.4 Hz) ppm. IR (neat, cm^{-1}): 3296, 2968, 1634, 1605, 1539, 1505, 1290, 1218, 1157, 838. HRMS *calcd.* for ($C_{16}H_{24}FNOSi$+Na): 316.1509, *found:* 316.1503.

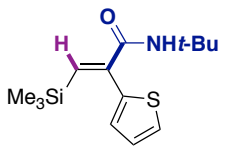

(*Z*)-*N*-(*tert*-butyl)-2-(thiophen-2-yl)-3-(trimethylsilyl)acrylamide (4.3bf). Following the general procedure using trimethyl(thiophen-2-ylethynyl)silane to afford **4.3bf** as a brown solid (77.1 mg, 55% yield). m. p. = 101 – 102 °C. ^{1}H NMR (400 MHz, $CDCl_3$) δ 7.38 (dd, *J* = 5.1, 1.2 Hz, 1H), 7.28 (s, 1H), 7.05 (dd, *J* = 5.1, 3.5 Hz, 1H), 6.95 (dd, *J* = 3.5, 1.2 Hz, 1H), 5.70 (s, 1H), 1.32 (s, 9H), -0.06 (s, 9H) ppm. ^{13}C NMR (101 MHz, $CDCl_3$) δ 165.1, 144.0, 143.1, 139.1, 128.6, 127.1, 127.0, 51.5, 28.6, -0.8 ppm. IR (neat, cm^{-1}): 3315, 2961, 1638, 1534, 1454, 1287, 1220, 830, 695. HRMS *calcd.* for ($C_{19}H_{19}F_2NO$+Na): 338.1327, *found:* 338.1318.

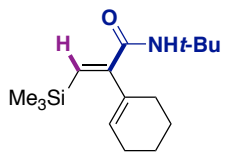

(*E*)-*N*-(*tert*-butyl)-2-(cyclohex-1-en-1-yl)-3-(trimethylsilyl)acrylamide (4.3bg). Following the general procedure using (cyclohex-1-en-1-ylethynyl)trimethylsilane to afford **4.3bg** (81.3 mg, 58% yield) as a pale yellow solid. m. p. = 111.9 – 114.7 °C. ^{1}H NMR (500 MHz, $CDCl_3$) δ 6.64 (s, 1H), 5.85 (s, 1H), 5.69 – 5.67 (m, 1H), 2.15 – 2.11 (m, 2H), 2.07 – 2.00 (m, 2H), 1.72 – 1.60 (m, 4H), 1.35 (s, 9H), 0.09 (s, 9H) ppm. ^{13}C NMR (126 MHz, $CDCl_3$) δ 165.9, 154.1, 137.4, 135.7 129.0, 51.1, 29.2, 28.7, 25.3, 22.9, 21.9, 0.0 ppm. IR (neat, cm^{-1}): 3295, 2926, 2858, 1634, 1586, 1531, 1243, 834. HRMS *calcd.* for ($C_{16}H_{29}NOSi$+Na) 302.1911, *found*: 302.1917.

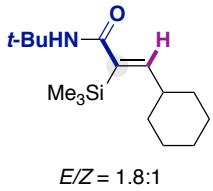

E/*Z* = 1.8:1

(*Z*)-*N*-(*tert*-butyl)-3-cyclohexyl-2-(trimethylsilyl)acrylamide (4.3bh'). Following the general procedure using (cyclohexylethynyl)trimethylsilane to afford **4.3bh** (76.5 mg, **4.3bh':4.3bh''** *E*/*Z* = 1.8:1, 54% yield) as a pale yellow solid. m. p. = 93.2 – 95.6 °C. Spectroscopic data for the major isomer (**4.3bh'**): ^{1}H NMR (500 MHz, $CDCl_3$) δ 6.10 (d, J = 10.2 Hz, 1H), 5.23 (s, 1H), 2.22 – 2.11 (m, 1H), 1.77 – 1.56 (m, 5H), 1.34 (s, 9H), 1.30 – 1.01 (m, 5H), 0.18 (s, 9H) ppm. ^{13}C NMR (126 MHz, $CDCl_3$) δ 173.8, 151.3, 140.0, 51.2, 40.9, 32.8, 29.0, 25.9, 25.7, 0.4 ppm. IR (neat, cm^{-1}): 3320, 2923, 2850, 1626, 1520, 1448, 1246, 839. HRMS *calcd.* for ($C_{16}H_{31}NOSi$+Na) 304.2067, *found*: 304.2064.

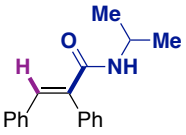

(*E*)-*N*-*iso*propyl-2,3-diphenylacrylamide (4.3bi). Following the general procedure using 1,2-diphenylethyne to afford **4.3bi** as a colorless solid (123.4 mg, 93% yield). m. p. = 82 - 84 °C. ^{1}H NMR (400 MHz, $CDCl_3$) δ 7.83 (s, 1H), 7.55 – 7.32 (m, 3H), 7.25 – 7.19 (m, 2H), 7.19 – 7.03 (m, 3H), 7.03 – 6.82 (m, 2H), 5.28 (d, *J* = 7.8 Hz, 1H), 4.16 (m, 6.5 Hz, 1H), 1.07 (d, *J* = 6.6 Hz, 6H) ppm. ^{13}C NMR (101 MHz, $CDCl_3$) δ 166.3, 136.9, 136.3, 135.2, 134.8, 130.3, 129.9, 129.6, 128.5, 128.5, 128.2, 42.0, 22.7 ppm. IR (neat, cm^{-1}): 3304, 2970, 1649, 1510, 690. HRMS *calcd.* for ($C_{18}H_{19}NO$+H): 266.1539, *found:* 266.1535.

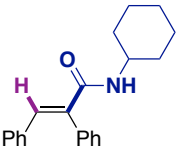

E/*Z* = 13:1

(*E*)-*N*-cyclohexyl-2,3-diphenylacrylamide (4.3bj). Following the general procedure using 1,2-diphenylethyne to afford **4.3bj** as a colorless solid (129.8 mg, **34.3bj:4.3bj'** (*E*:*Z*) = 13:1, 85% yield). m. p. = 104 - 106 °C. Spectroscopic data for the major isomer (**4.3bj**): ^{1}H NMR (400 MHz, $CDCl_3$) δ 7.82 (s, 1H), 7.60 – 7.32 (m, 3H), 7.25 – 7.20 (m, 2H), 7.17 – 7.02 (m, 3H), 7.02 – 6.71 (m, 2H), 5.35 (d, *J* = 8.2 Hz, 1H), 3.92 – 3.83 (m 1H), 1.84 (dt, *J* = 12.6, 4.3 Hz, 2H), 1.59 – 1.51 (m, 3H), 1.47 – 1.27 (m, 2H), 1.18 – 0.87 (m, 3H) ppm. ^{13}C NMR (101 MHz, $CDCl_3$) δ 166.1, 136.8, 136.4, 135.2, 134.8, 130.3, 129.9, 129.6, 128.5, 128.4, 128.2, 48.6, 32.8, 25.6, 24.7 ppm. IR (neat, cm^{-1}): 3423, 2929, 2854, 1664, 1618, 1496, 1203, 709, 692. HRMS *calcd.* for ($C_{21}H_{23}NO$+H): 306.1852, *found:* 306.1838.

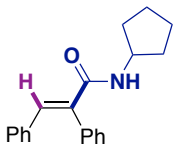

(*E*)-*N*-cyclopentyl-2,3-diphenylacrylamide (4.3bk). Following the general procedure using 1,2-diphenylethyne to afford **4.3bk** as a colorless solid (138.4 mg, 95% yield). m. p. = 84 - 86 °C. ^{1}H NMR (400 MHz, $CDCl_3$) δ 7.83 (s, 1H), 7.59 – 7.31 (m, 3H), 7.25 – 7.20 (m, 2H), 7.15 – 7.06 (m, 3H), 7.00 – 6.92 (m, 2H), 5.40 (d, *J* = 7.7 Hz, 1H), 4.32 – 4.23 (m, 1H), 2.15 – 1.79 (m, 2H), 1.58 – 1.50 (m, 4H), 1.37 – 1.08 (m, 2H) ppm. ^{13}C NMR (101 MHz, $CDCl_3$) δ 166.7, 136.8, 136.4, 135.2, 134.7, 130.3, 129.9, 129.6, 128.5, 128.5, 128.2, 51.8, 33.1, 23.7 ppm. IR (neat, cm^{-1}): 3422, 2961, 1667, 1618, 1495, 1205, 692. HRMS *calcd.* for ($C_{20}H_{21}NO$+H): 292.1696, *found:* 292.1688.

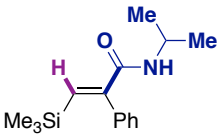

(*E*)-*N*-isopropyl-2-phenyl-3-(trimethylsilyl)acrylamide (4.3bl). Following the general procedure using trimethyl(phenylethynyl)silane to afford **4.3bl** as a colorless solid (78.4 mg, 60% yield). m. p. = 105 – 107 °C. ^{1}H NMR (500 MHz, $CDCl_3$) δ 7.58 – 7.34 (m, 3H), 7.26 – 7.05 (m, 3H), 5.26 (s, 1H), 4.14 – 4.07 (m, 6.6 Hz, 1H), 1.07 (d, *J* = 6.6 Hz, 6H), -0.15 (s, 9H) ppm. ^{13}C NMR (126 MHz, $CDCl_3$) δ 165.4, 149.7, 140.7, 138.6, 129.7, 128.6, 128.4, 42.1, 22.7, -0.6 ppm. IR (neat, cm^{-1}) 3274, 2974, 1626, 1581, 1543, 1244, 835, 694. HRMS *calcd.* for ($C_{15}H_{23}NOSi$+H): 262.1622, *found:* 262.1616.

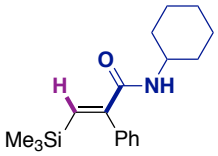

(*E*)-*N*-cyclohexyl-2-phenyl-3-(trimethylsilyl)acrylamide (4.3bm). Following the general procedure using trimethyl(phenylethynyl)silane to afford **4.3bm** as a colorless solid (91.6 mg, 61% yield). m. p. = 108 – 109 °C. ^{1}H NMR (500 MHz, $CDCl_3$) δ 7.42 – 7.33 (m, 3H), 7.23 – 7.16 (m, 3H), 5.30 (s, 1H), 3.79 (tdt, *J* = 10.3, 8.0, 3.9 Hz, 1H), 1.89 – 1.67 (m, 2H), 1.61 – 1.47 (m, 3H), 1.39 – 1.27 (m, 2H), 1.16 – 0.88 (m, 3H), -0.18 (s, 9H) ppm. ^{13}C NMR (126 MHz, $CDCl_3$) δ 165.3, 149.8, 140.6, 138.6, 129.6, 128.6, 128.4, 48.7, 32.8, 25.6, 24.7, -0.6 ppm. IR (neat, cm^{-1}) 3268, 2933, 2854, 1627, 1533, 1242, 861, 836, 696. HRMS *calcd.* for ($C_{18}H_{27}NOSi$+H): 302.1935, *found:* 302.1942.

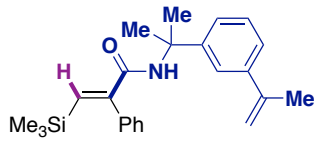

(*E*)-2-phenyl-*N*-(2-(3-(prop-1-en-2-yl)phenyl)propan-2-yl)-3-(trimethylsilyl)acry-lamide (4.3bn). Following the general procedure using trimethyl(phenylethynyl)silane to afford **4.3bn** as a colorless solid (128 mg, 68% yield). m. p. = 86 – 87 °C. ^{1}H NMR (500 MHz, $CDCl_3$) δ 7.48 – 7.33 (m, 4H), 7.33 – 7.23 (m, 4H), 7.23 – 7.13 (m, 2H), 5.82 (s, 1H), 5.31 (dd, *J* = 1.6, 0.8 Hz, 1H), 5.08 (t, *J* = 1.5 Hz, 1H), 2.13 (dd, *J* = 1.5, 0.8 Hz, 3H), 1.65 (s, 6H), -0.15 (s, 9H) ppm. ^{13}C NMR (126 MHz, $CDCl_3$) δ 165.0, 150.0, 146.6, 143.3, 141.2, 140.3, 138.5, 129.3, 128.5, 128.2, 128.1, 123.8, 123.5, 121.5, 112.3, 56.1, 28.7, 21.8, -0.9 ppm. IR (neat, cm^{-1}) 3279, 2954, 1639, 1525, 1244, 860, 832, 696. HRMS *calcd.* for ($C_{24}H_{31}NOSi$+Na): 400.2067, *found:* 400.2076.

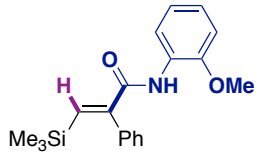

(*E*)-*N*-(2-methoxyphenyl)-2-phenyl-3-(trimethylsilyl)acrylamide (4.3bo). Following the general procedure using trimethyl(phenylethynyl)silane to afford **4.3bo** as a clear oil (106.3 mg, 65% yield). ^{1}H NMR (400 MHz, $CDCl_3$) δ 8.46 (dd, *J* = 7.7, 2.0 Hz, 1H), 8.00 (s, 1H), 7.49 – 7.38 (m, 3H), 7.36 (s, 1H), 7.34 – 7.28 (m, 2H), 7.01 – 6.91 (m, 2H), 6.75 (dd, *J* = 7.8, 1.7 Hz, 1H), 3.58 (s, 3H), -0.11 (s, 9H) ppm. ^{13}C NMR (101 MHz, $CDCl_3$) δ 163.8, 150.2, 148.3, 141.7, 138.2, 129.9, 128.6, 128.5, 128.0, 123.9, 121.3, 119.5, 110.1, 55.8, -0.6 ppm. IR (neat, cm^{-1}) 3391, 2954, 1673, 1520, 1459, 1247, 833, 745, 703. HRMS *calcd.* for ($C_{19}H_{24}NO_2Si$+H): 326.1571, *found:* 326.1569.

4.7.3. *tert*-Butyl Group Deprotection

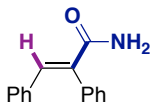

(*E*)-2,3-diphenylacrylamide (4.12). A round bottom flask charged with **4.3ae** (560 mg, 2 mmol) and TFA (18 mL) was stirred at 70 °C for 16 hours. The reaction mixture was cooled to room temperature and the excess of TFA was removed under reduced pressure. The crude solid was filtered over a short pad of silica gel (EtOAc) affording the product **4.12** as a colorless solid (436 mg, 98%). m. p. = 134 – 135 °C. ^{1}H NMR (300 MHz, $CDCl_3$) δ 7.94 (bs, 1H), 7.44 (bs, 3H), 7.31 – 7.24 (m, 2H), 7.16 (dt, *J* = 14.5, 7.1 Hz, 3H), 7.02 (d, *J* = 7.5 Hz, 2H), 5.59 (bs, 1H) ppm. ^{13}C NMR (126 MHz, $CDCl_3$) δ 169.2, 138.3, 136.6, 134.8, 133.8, 130.6, 129.8, 129.8, 128.9, 128.7, 128.3 ppm. IR (neat, cm^{-1}): 3463, 3141, 1671, 1581, 1490, 1445, 1358, 798706, 684. HRMS *calcd.* for ($C_{15}H_{13}NO$+Na) 246.0889, *found*: 246.0896.

4.7.4. Protodesilylation

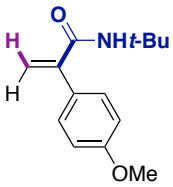

***N*-(*tert*-butyl)-2-(4-methoxyphenyl)acrylamide (4.13). 4.3ba** (91.6 mg, 0.3 mmol) was charged in an oven-dried reaction vial equipped with a stir bar. Then, the vial was sealed with a septum and a solution of 1M TBAF in THF (600 µL, 0.6 mmol) was added under a nitrogen atmosphere. After stirring the reaction mixture at room temperature for 2.5 hours, the reaction mixture was directly absorbed on silica. Purification via column chromatography over silica gel (hexane/EtOAc 6:1) afforded **4.13** as a colorless solid (62 mg, 89%). m. p. = 60 – 69 °C. ^{1}H NMR (400 MHz, $CDCl_3$) δ 7.34 – 7.27 (m, 2H), 6.93 – 6.86 (m, 2H), 5.92 (d, *J* = 1.3 Hz, 1H), 5.56 (s, 1H), 5.48 (d, *J* = 1.3 Hz, 1H), 3.82 (s, 3H), 1.37 (s, 9H) ppm. ^{13}C NMR (101 MHz, $CDCl_3$) δ 167.2, 159.7, 145.5, 129.6, 129.2,

119.4, 114.0, 77.3, 77.0, 76.7, 55.3, 51.5, 28.7 ppm. IR (neat, cm^{-1}): 3246, 2966, 2930, 1641, 1606, 1509, 1249, 1176, 1030, 830. HRMS *calcd.* for ($C_{14}H_{19}NNaO_2$) 256,1308, *found*: 256,1304.

4.7.5. Synthetic Applications

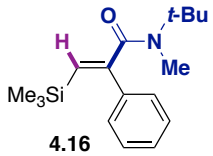

4.16

(*E*)-*N*-(*tert*-butyl)-*N*-methyl-2-phenyl-3-(trimethylsilyl)acrylamide (4.16). An oven-dried round bottom flask was charged NaH (60% dispersion in mineral oil, 340 mg, 8.50 mmol), evacuated and back-filled with nitrogen. Then, a solution of **4.3ba** (1.55 g, 5.63 mmol) in anhydrous THF (25 mL) was added via a syringe and the suspension was stirred vigorously at room temperature for 1 hour. Methyl iodide (0.62 mL, 10 mmol) was added in one portion and the reaction mixture was stirred at 50 °C for 16 hours. The reaction was quenched by the addition of silica gel and the solvent was removed under reduced pressure. Purification of the crude product by column chromatography over silica gel provided **4.16** as a brown solid (1.63 g, quantitative). m. p. = 45 – 47 °C. ^{1}H NMR (300 MHz, $CDCl_3$) δ 7.46 – 7.22 (m, 5H), 5.90 (s, 1H), 2.88 (s, 3H), 1.44 (s, 9H), -0.03 (s, 9H) ppm. ^{13}C NMR (126 MHz, $CDCl_3$) δ 173.6, 156.0, 138.7, 131.1, 128.4, 128.1, 128.0, 56.4, 34.1, 28.0, -0.1 ppm. IR (neat, cm^{-1}): 2959, 1625, 1475, 1363, 1247, 1120, 960, 830, 763, 703. HRMS *calcd.* for ($C_{17}H_{27}NOSi$+H) 290.1935, *found*: 290.1930.

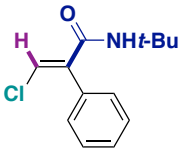

(*E*)-*N*-(*tert*-butyl)-3-chloro-*N*-methyl-2-phenylacrylamide (4.17). A 10-mL reaction tube was charged with **4.16** (110.2 mg, 0.38 mmol) and NCS (117.0 mg, 0.52 mmol). Anhydrous acetonitrile (4 mL) was added and the reaction mixture was heated at 100 °C for 16 hours. The solvent was removed under reduced pressure and the crude product was purified by column chromatography over silica gel (hexane/EtOAc 10:1) providing **4.17** as a clear oil (81 mg, 84%). ^{1}H NMR (400 MHz, $CDCl_3$) δ 7.61 – 7.53 (m, 2H), 7.46 – 7.34 (m, 3H), 6.54 (s, 1H), 2.80 (s, 3H), 1.45 (s, 9H) ppm. ^{13}C NMR (101 MHz, $CDCl_3$) δ 169.3, 141.4, 133.2, 128.6, 128.6, 128.5, 119.7, 57.0, 34.0, 27.8 ppm. IR (neat, cm^{-1}): 3060, 2962, 2924, 1637, 1471, 1365, 1212, 1116, 977, 875, 774, 695, 654. HRMS *calcd.* for ($C_{14}H_{18}ClNO$+Na) 274.0969, *found*: 274.0965.

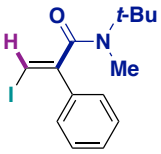

(*E*)-*N*-(*tert*-butyl)-3-iodo-*N*-methyl-2-phenylacrylamide (4.18). A round bottom flask equipped with a condenser was charged with **4.16** (869 mg, 3.0 mmol) and NIS (1.0 g, 4.5 mmol). Anhydrous acetonitrile (34 mL) was added and the reaction mixture was heated at 100 °C for 16 hours. The solvent was removed under reduced pressure and the crude product was purified by column chromatography over silica gel (hexane/EtOAc 20:1 -> 10:1) providing **4.18** as a yellowish oil (958 mg, 93%). ^{1}H NMR (400 MHz, $CDCl_3$) δ 7.60 – 7.50 (m, 2H), 7.46 – 7.33 (m, 3H), 6.83 (s, 1H), 2.85 (s, 3H), 1.43 (s, 9H) ppm. ^{13}C NMR (101 MHz, $CDCl_3$) δ 169.2, 150.5, 136.7, 128.7, 128.4, 128.2, 82.4, 57.0, 33.9, 27.8 ppm. IR (neat, cm-1): 2960, 2922, 1634, 1471, 1363, 1209, 1109, 963, 807, 767, 697. HRMS *calcd.* for ($C_{14}H_{19}INO^+$) 344.0506 *found*: 344.0502.

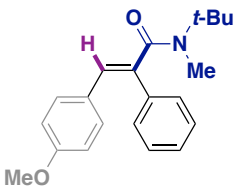

(*E*)-*N*-(*tert*-butyl)-3-(4-methoxyphenyl)-*N*-methyl-2-phenylacrylamide (4.19). A reaction tube was charged with **4.16** (49.4 mg, 0.15 mmol), 4-methoxyphenylboronic acid (34.2 mg, 0.225 mmol), K_2CO_3 (62.2 mg, 0.45 mmol) and $Pd(PPh_3)_4$ (17.3 mg, 0.015 mmol). The tube was sealed, evacuated and back-filled with argon. Then, degassed DMF (0.6 mL) and degassed water (60 μL) were added and the reaction mixture was stirred at 90 °C for 5 hours. Afterwards, the reaction mixture was directly purified via column chromatography over silica gel (hexane/EtOAc 10:1) affording **4.19** as a brown gum (42 mg, 87%). ^{1}H NMR (500 MHz, $CDCl_3$) δ 7.44 – 7.26 (m, 5H), 7.09 – 7.03 (m, 2H), 6.74 – 6.70 (m, 3H), 3.78 (s, 3H), 2.90 (s, 3H), 1.48 (s, 9H) ppm. ^{13}C NMR (126 MHz, $CDCl_3$) δ 173.4, 159.2, 138.6, 136.5, 130.9, 129.8, 129.2, 128.7, 128.3, 127.7, 113.6, 56.5,

55.3, 34.2, 27.9 ppm. IR (neat, cm^{-1}): 2958, 2836, 1631, 1605, 1509, 1470, 1362, 1297, 1248, 1176, 1105, 1031, 981, 909, 827, 731, 699. HRMS *calcd*. for ($C_{21}H_{25}NO_2$+Na) 346.1777, *found*: 346.1773

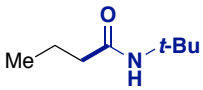

***N*-(*tert*-butyl)butyramide.** ^{1}H-NMR (300 MHz, $CDCl_3$) δ 5.26 (s, 1H, *NH*), 2.05 (t, *J* = 7.4 Hz, 2H, *CH₂*), 1.68 – 1.56 (m, 2H, *CH₂*), 1.34 (s, 9H, *t-Bu*), 0.92 (t, *J* = 7.4 Hz, 3H, *CH₃*) ppm. ^{13}C-NMR (126 MHz, $CDCl_3$) δ 172.5, 51.2, 39.8, 29.0, 19.3, 13.8 ppm. IR (neat, cm^{-1}): 3303, 3076, 2963, 2931, 2874, 1643, 1548, 1453, 1361, 1225.

4.7.6. Preliminary Mechanistic Studies

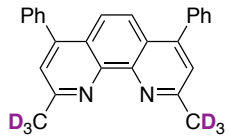

Bathocuproine-*d*$_6$ (*d*$_6$-L1). A 12 mL reaction tube was charged with bathocuproine (180 mg, 0.5 mmol) and anhydrous $CoCl_2$ (6.5 mg, 0.05 mmol). After anhydrous THF (2 mL) and D_2O (2 mL) was added, the tube was flushed with argon, sealed and stirred vigorously at 125 °C for 24 hours. Afterward, the solvents were removed under reduced pressure. The residual solid was purified via column chromatography over silica gel (CH_2Cl_2:MeOH 20:1) affording a beige solid (144 mg, 79%). m. p. = 291 – 293 °C. ^{1}H NMR (400 MHz, $CDCl_3$) δ 7.71 (s, 2H), 7.51 – 7.38 (m, 12H) ppm. ^{13}C NMR (101 MHz, $CDCl_3$) δ 158.4, 148.3, 145.8, 138.0, 129.4, 128.3, 128.1, 124.5, 123.7, 122.7, 31.9 – 20.5 (m) ppm. IR (neat, cm-1): 3055, 3024, 1619, 1567, 1478, 1443, 1368, 1027, 766, 703. HRMS *calcd*. for ($C_{26}H_{14}D_6N_2$+H) 367.2064, *found*: 367.2076.

4.7.6.1. Isotope Labelling Studies:

- With ***d*$_7$-4.11d:** Following the general procedure to afford ***d*-4.3ae** (92% yield, 75% D-content) as a colorless solid. D-content was determined by ^{1}H NMR analysis.
- With ***d*$_6$-4.11d**: Following the general procedure using to afford ***d*-4.3ae** (92% yield, 15% D-content) as a colorless solid. D-content was detected by ^{1}H NMR analysis
- With ***d*$_1$-4.11d**: Following the general procedure using to afford ***d*-4.3ae** (92% yield, 100% D-content) as a colorless solid. D-content was detected by ^{1}H NMR analysis.
- With ***d*$_6$-L1:** Following the general procedure to afford **4.3ae** (92% yield, 0% D-content) as a colorless solid. D-content was detected by ^{1}H NMR analysis.

4.7.6.2. Stoichiometric Experiments

A Schlenk tube containing a stirring bar was charged inside a glovebox with Ni(**L1**)$_2$[64] (156 mg, 0.2 mmol), diphenylacetylene (35.6 mg, 0.2 mmol) and manganese (16.5 mg, 0.3 mmol). Once outside the glovebox, *i*-PrBr (28.2 µL, 0.3 mmol), *t*-BuNCO (34.3 µL, 0.3 mmol) and NMP (0.8 mL) were added by syringe under an argon atmosphere, the tube was then sealed and the mixture stirred overnight at room temperature. The mixture was quenched with HCl (5%) and extracted with CH_2Cl_2. The crude reaction mixture was analyzed by GC-FID using naphthalene as internal standard (corrected yields are given).

- Following the above procedure, when no Mn was added, **4.3ae** was obtained in 35% yield.
- Following the above procedure, when no Mn and no *i*-PrBr were added, no desired product **4.3ae** was obtained.
- Following the above procedure, **4.3ae** was obtained in 81% yield.
- Following the above procedure, when Mn was used, but no *i*-PrBr was added, no desired product **4.3ae** was obtained.

4.7.7. X-ray Crystallographic Analysis

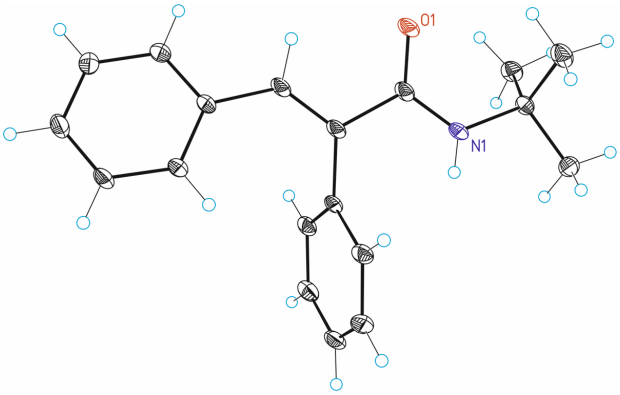

Table 1. Crystal data and structure refinement for **4.3ae.**

Identification code	**4.3ae**
Empirical formula	$C_{19}H_{21}NO$
Formula weight	279.37
Temperature	100(2) K
Wavelength	0.71073 Å
Crystal system	Monoclinic
Space group	Cc
Unit cell dimensions	a = 5.827(3)Å ⟨= 90°.
	b = 18.141(6)Å ® = 98.777(9)°.
	c = 14.817(6)Å © = 90°.
Volume	1547.9(11) $Å^3$
Z	4
Density (calculated)	1.199 Mg/m^3
Absorption coefficient	0.073 mm^{-1}
F(000)	600
Crystal size	0.25 x 0.20 x 0.10 mm^3
Theta range for data collection	2.245 to 32.118°.
Index ranges	-8<=h<=8,-26<=k<=26,-22<=l<=22
Reflections collected	10678
Independent reflections	4997[R(int) = 0.0647]
Completeness to theta =32.118°	99.7%
Absorption correction	Empirical
Max. and min. transmission	0.993 and 0.764
Refinement method	Full-matrix least-squares on F^2
Data / restraints / parameters	4997/ 2/ 193
Goodness-of-fit on F^2	1.027
Final R indices [I>2sigma(I)]	R1 = 0.0565, wR2 = 0.1429
R indices (all data)	R1 = 0.0596, wR2 = 0.1442
Flack parameter	x =-1.0(10)
Largest diff. peak and hole	0.632 and -0.300 $e.Å^{-3}$

Table 2. Bond lengths [Å] and angles [°] for **4.3ae**

Bond lengths----			
C1-C2	1.347(3)	C9-C10	1.405(3)
C1-C9	1.491(3)	C10-C11	1.398(3)
C1-C15	1.521(3)	C11-C12	1.388(4)
C2-C3	1.468(3)	C12-C13	1.395(4)
C3-C8	1.403(3)	C13-C14	1.394(3)
C3-C4	1.407(3)	C15-O1	1.236(3)
C4-C5	1.396(3)	C15-N1	1.352(3)
C5-C6	1.390(3)	C16-N1	1.483(3)
C6-C7	1.396(3)	C16-C17	1.528(3)
C7-C8	1.391(3)	C16-C18	1.535(3)
C9-C14	1.399(3)	C16-C19	1.535(3)
Angles----------			
C2-C1-C9	125.59(18)	C11-C10-C9	120.2(2)
C2-C1-C15	114.67(17)	C12-C11-C10	120.5(2)
C9-C1-C15	119.52(17)	C11-C12-C13	119.8(2)
C1-C2-C3	130.69(19)	C14-C13-C12	119.7(2)
C8-C3-C4	118.45(19)	C13-C14-C9	121.2(2)
C8-C3-C2	116.83(18)	O1-C15-N1	123.08(19)
C4-C3-C2	124.67(19)	O1-C15-C1	121.06(19)
C5-C4-C3	120.2(2)	N1-C15-C1	115.86(17)
C6-C5-C4	120.43(19)	N1-C16-C17	106.34(17)
C5-C6-C7	120.0(2)	N1-C16-C18	111.35(18)
C8-C7-C6	119.6(2)	C17-C16-C18	109.18(19)
C7-C8-C3	121.16(19)	N1-C16-C19	108.85(18)
C14-C9-C10	118.52(19)	C17-C16-C19	109.91(19)
C14-C9-C1	120.07(19)	C18-C16-C19	111.11(18)
C10-C9-C1	121.34(19)	C15-N1-C16	124.73(17)

Table 3. Torsion angles [°] for **4.3ae**

C9-C1-C2-C3	5.9(4)	C2-C3-C8-C7	179.6(2)
C15-C1-C2-C3	-179.6(2)	C2-C1-C9-C14	68.1(3)
C1-C2-C3-C8	-154.6(2)	C15-C1-C9-C14	-106.0(2)
C1-C2-C3-C4	28.1(4)	C2-C1-C9-C10	-115.0(2)
C8-C3-C4-C5	1.1(3)	C15-C1-C9-C10	70.8(3)
C2-C3-C4-C5	178.3(2)	C14-C9-C10-C11	0.1(3)
C3-C4-C5-C6	1.4(4)	C1-C9-C10-C11	-176.87(19)
C4-C5-C6-C7	-2.1(4)	C9-C10-C11-C12	1.4(3)
C5-C6-C7-C8	0.3(4)	C10-C11-C12-C13	-1.8(3)
C6-C7-C8-C3	2.2(4)	C11-C12-C13-C14	0.8(3)
C4-C3-C8-C7	-2.9(3)	C12-C13-C14-C9	0.7(3)

C10-C9-C14-C13	-1.1(3)	O1-C15-N1-C16	-9.2(4)
C1-C9-C14-C13	175.84(19)	C1-C15-N1-C16	170.03(19)
C2-C1-C15-O1	2.6(3)	C17-C16-N1-C15	176.8(2)
C9-C1-C15-O1	177.4(2)	C18-C16-N1-C15	57.9(3)
C2-C1-C15-N1	-176.62(19)	C19-C16-N1-C15	-64.9(3)
C9-C1-C15-N1	-1.8(3)		

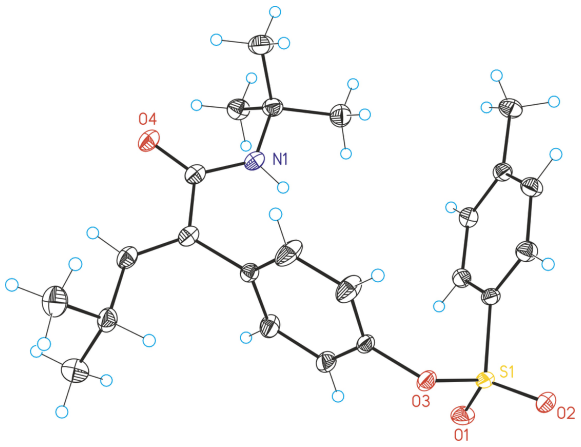

Table 1. Crystal data and structure refinement for **4.3ap**

Identification code	**4.3ap**
Empirical formula	$C_{29}H_{29}NO_4S$
Formula weight	415.53
Temperature	100(2) K
Wavelength	0.71073 Å
Crystal system	Monoclinic
Space group	P2(1)/n
Unit cell dimensions	a = 9.6344(10)Å ⟨= 90°.
	b = 9.5419(12)Å ® = 101.317(4)°.
	c = 24.422(3)Å © = 90°.
Volume	2201.4(4) $Å^3$
Z	4
Density (calculated)	1.254 Mg/m^3
Absorption coefficient	0.175 mm^{-1}
F(000)	888
Crystal size	0.10 x 0.20 x 0.30 mm^3
Theta range for data collection	3.264 to 28.298°.
Index ranges	-12<=h<=8,-12<=k<=12,-32<=l<=24
Reflections collected	17729
Independent reflections	4807[R(int) = 0.0260]
Completeness to theta =28.298°	89.0%
Absorption correction	Multi-scan

Max. and min. transmission	0.966 and 0.743
Refinement method	Full-matrix least-squares on F^2
Data / restraints / parameters	4807/ 0/ 272
Goodness-of-fit on F^2	1.048
Final R indices [I>2sigma(I)]	R1 = 0.0327, wR2 = 0.0857
R indices (all data)	R1 = 0.0356, wR2 = 0.0871
Largest diff. peak and hole	0.364 and -0.402 e.Å^{-3}

Table 2. Bond lengths [Å] and angles [°] for **4.3ap**

Bond lengths----

C1-C6	1.3862(17)	C12-C13	1.3940(16)
C1-C2	1.3918(16)	C14-C15	1.3371(18)
C1-S1	1.7517(12)	C14-C19	1.5100(17)
C2-C3	1.3870(17)	C15-C16	1.4968(18)
C3-C4	1.3956(18)	C16-C18	1.5301(18)
C4-C5	1.3930(16)	C16-C17	1.5320(18)
C4-C7	1.5046(16)	C19-O4	1.2330(14)
C5-C6	1.3880(17)	C19-N1	1.3486(17)
C8-C13	1.3752(17)	C20-N1	1.4798(17)
C8-C9	1.3769(16)	C20-C23	1.5267(17)
C8-O3	1.4154(13)	C20-C21	1.5270(18)
C9-C10	1.3877(17)	C20-C22	1.5339(16)
C10-C11	1.3875(17)	O1-S1	1.4252(9)
C11-C12	1.3906(15)	O2-S1	1.4269(9)
C11-C14	1.4976(15)	O3-S1	1.6033(9)

Angles----------

C6-C1-C2	121.56(11)	C11-C12-C13	121.41(11)
C6-C1-S1	119.42(9)	C8-C13-C12	118.43(10)
C2-C1-S1	119.02(9)	C15-C14-C11	122.04(11)
C3-C2-C1	118.79(11)	C15-C14-C19	118.26(10)
C2-C3-C4	120.84(11)	C11-C14-C19	119.67(11)
C5-C4-C3	118.98(11)	C14-C15-C16	126.57(11)
C5-C4-C7	120.38(11)	C15-C16-C18	111.09(11)
C3-C4-C7	120.63(11)	C15-C16-C17	109.39(11)
C6-C5-C4	121.06(11)	C18-C16-C17	110.05(11)
C1-C6-C5	118.72(10)	O4-C19-N1	123.25(12)
C13-C8-C9	121.98(11)	O4-C19-C14	121.61(11)
C13-C8-O3	122.00(10)	N1-C19-C14	115.13(10)
C9-C8-O3	115.98(10)	N1-C20-C23	110.35(10)
C8-C9-C10	118.53(11)	N1-C20-C21	105.68(10)
C11-C10-C9	121.64(11)	C23-C20-C21	109.66(11)
C10-C11-C12	118.00(10)	N1-C20-C22	109.88(11)
C10-C11-C14	121.02(10)	C23-C20-C22	110.80(10)
C12-C11-C14	120.97(10)	C21-C20-C22	110.36(11)

C19-N1-C20	126.75(10)	O2-S1-O3	103.19(5)
C8-O3-S1	118.79(8)	O1-S1-C1	109.42(6)
O1-S1-O2	119.73(5)	O2-S1-C1	110.26(5)
O1-S1-O3	109.07(5)	O3-S1-C1	103.85(5)

Table 3. Torsion angles [°] for **4.3ap**

C6-C1-C2-C3	-1.41(18)	C11-C14-C15-C16	2.06(19)
S1-C1-C2-C3	178.60(9)	C19-C14-C15-C16	-176.30(11)
C1-C2-C3-C4	-0.66(18)	C14-C15-C16-C18	-113.78(14)
C2-C3-C4-C5	1.86(18)	C14-C15-C16-C17	124.54(13)
C2-C3-C4-C7	-177.41(11)	C15-C14-C19-O4	7.22(17)
C3-C4-C5-C6	-1.04(18)	C11-C14-C19-O4	-171.18(11)
C7-C4-C5-C6	178.24(11)	C15-C14-C19-N1	-173.40(11)
C2-C1-C6-C5	2.21(17)	C11-C14-C19-N1	8.20(15)
S1-C1-C6-C5	-177.80(9)	O4-C19-N1-C20	0.32(19)
C4-C5-C6-C1	-0.96(17)	C14-C19-N1-C20	-179.05(10)
C13-C8-C9-C10	-0.3(2)	C23-C20-N1-C19	-60.19(15)
O3-C8-C9-C10	-178.05(13)	C21-C20-N1-C19	-178.67(11)
C8-C9-C10-C11	0.2(2)	C22-C20-N1-C19	62.27(15)
C9-C10-C11-C12	-0.2(2)	C13-C8-O3-S1	64.74(14)
C9-C10-C11-C14	178.94(13)	C9-C8-O3-S1	-117.55(11)
C10-C11-C12-C13	0.4(2)	C8-O3-S1-O1	-69.22(9)
C14-C11-C12-C13	-178.81(12)	C8-O3-S1-O2	162.46(8)
C9-C8-C13-C12	0.5(2)	C8-O3-S1-C1	47.37(9)
O3-C8-C13-C12	178.03(11)	C6-C1-S1-O1	14.35(11)
C11-C12-C13-C8	-0.5(2)	C2-C1-S1-O1	-165.66(9)
C10-C11-C14-C15	-99.37(16)	C6-C1-S1-O2	148.03(9)
C12-C11-C14-C15	79.78(16)	C2-C1-S1-O2	-31.98(11)
C10-C11-C14-C19	78.96(16)	C6-C1-S1-O3	-102.00(10)
C12-C11-C14-C19	-101.89(14)	C2-C1-S1-O3	77.99(10)

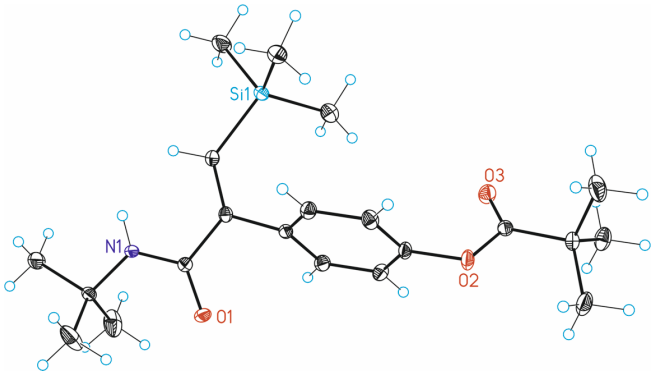

Table 1. Crystal data and structure refinement for **4.3az**

Identification code	**4.3az**
Empirical formula	$C_{21}H_{31}NO_3Si$
Formula weight	375.57
Temperature	100(2) K
Wavelength	0.71073 Å
Crystal system	Monoclinic
Space group	P2(1)/c
Unit cell dimensions	a = 10.0373(8)Å a= 90°.
	b = 20.8698(17)Å b = 91.723(2)°.
	c = 10.3716(8)Å g = 90°.
Volume	2171.6(3) $Å^3$
Z	4
Density (calculated)	1.149 Mg/m^3
Absorption coefficient	0.127 mm^{-1}
F(000)	816
Crystal size	0.50 x 0.40 x 0.20 mm^3
Theta range for data collection	2.194 to 27.471°.
Index ranges	-12<=h<=13,-27<=k<=27,-13<=l<=13
Reflections collected	40741
Independent reflections	4966[R(int) = 0.0260]
Completeness to theta =27.471°	99.8%
Absorption correction	Multi-scan
Max. and min. transmission	0.975 and 0.75
Refinement method	Full-matrix least-squares on F^2
Data / restraints / parameters	4966/ 0/ 244
Goodness-of-fit on F^2	1.064
Final R indices [I>2sigma(I)]	R1 = 0.0310, wR2 = 0.0844
R indices (all data)	R1 = 0.0341, wR2 = 0.0862
Largest diff. peak and hole	0.368 and -0.211 $e.Å^{-3}$

Table 2. Bond lengths [Å] and angles [°] for **4.3az**

Bond lengths----

C1-C2	1.3436(13)	C10-C11	1.3860(14)
C1-Si1	1.8835(10)	C11-C12	1.3813(15)
C2-C8	1.4951(13)	C11-O2	1.4123(11)
C2-C3	1.5191(13)	C12-C13	1.3953(13)
C3-O1	1.2368(12)	C14-O3	1.1991(12)
C3-N1	1.3452(12)	C14-O2	1.3659(12)
C4-C7	1.5225(14)	C14-C15	1.5273(13)
C5-C7	1.5250(15)	C15-C16	1.5249(14)
C6-C7	1.5261(14)	C15-C17	1.5299(14)
C7-N1	1.4827(12)	C15-C18	1.5380(15)
C8-C13	1.3961(13)	C19-Si1	1.8735(11)
C8-C9	1.3987(14)	C20-Si1	1.8708(11)
C9-C10	1.3902(14)	C21-Si1	1.8691(11)

Angles----------

C2-C1-Si1	129.13(7)	C14-C15-C17	108.38(8)
C1-C2-C8	120.35(8)	C16-C15-C18	110.30(9)
C1-C2-C3	123.94(8)	C14-C15-C18	106.16(8)
C8-C2-C3	115.64(8)	C17-C15-C18	109.33(9)
O1-C3-N1	122.59(9)	C3-N1-C7	124.50(8)
O1-C3-C2	119.60(8)	C14-O2-C11	116.21(7)
N1-C3-C2	117.81(8)	C21-Si1-C20	108.91(5)
N1-C7-C4	110.56(8)	C21-Si1-C19	109.14(6)
N1-C7-C5	110.24(8)	C20-Si1-C19	109.78(5)
C4-C7-C5	110.93(10)	C21-Si1-C1	104.26(5)
N1-C7-C6	106.90(8)	C20-Si1-C1	113.28(5)
C4-C7-C6	109.23(9)	C19-Si1-C1	111.26(5)
C5-C7-C6	108.89(9)		
C13-C8-C9	118.68(9)		
C13-C8-C2	119.59(8)		
C9-C8-C2	121.55(9)		
C10-C9-C8	120.74(9)		
C11-C10-C9	119.01(9)		
C12-C11-C10	121.75(9)		
C12-C11-O2	118.13(9)		
C10-C11-O2	120.08(9)		
C11-C12-C13	118.65(9)		
C12-C13-C8	121.04(9)		
O3-C14-O2	122.65(9)		
O3-C14-C15	125.01(9)		
O2-C14-C15	112.28(8)		
C16-C15-C14	112.65(8)		
C16-C15-C17	109.91(9)		

Table 3. Torsion angles [°] for **4.3az**

Si1-C1-C2-C8	11.72(14)
Si1-C1-C2-C3	-165.04(7)
C1-C2-C3-O1	173.66(9)
C8-C2-C3-O1	-3.24(12)
C1-C2-C3-N1	-5.34(14)
C8-C2-C3-N1	177.77(8)
C1-C2-C8-C13	60.06(13)
C3-C2-C8-C13	-122.93(9)
C1-C2-C8-C9	-115.03(11)
C3-C2-C8-C9	61.98(12)
C13-C8-C9-C10	-3.53(14)
C2-C8-C9-C10	171.60(9)
C8-C9-C10-C11	1.00(15)
C9-C10-C11-C12	2.00(15)
C9-C10-C11-O2	179.55(9)
C10-C11-C12-C13	-2.35(15)
O2-C11-C12-C13	-179.95(8)
C11-C12-C13-C8	-0.30(15)
C9-C8-C13-C12	3.18(14)
C2-C8-C13-C12	-172.05(9)
O3-C14-C15-C16	-159.09(10)
O2-C14-C15-C16	23.61(12)
O3-C14-C15-C17	-37.26(13)
O2-C14-C15-C17	145.45(9)
O3-C14-C15-C18	80.09(12)
O2-C14-C15-C18	-97.20(10)
O1-C3-N1-C7	-0.71(15)
C2-C3-N1-C7	178.25(8)
C4-C7-N1-C3	60.07(13)
C5-C7-N1-C3	-62.94(13)
C6-C7-N1-C3	178.85(9)
O3-C14-O2-C11	2.85(14)
C15-C14-O2-C11	-179.78(8)
C12-C11-O2-C14	-110.75(10)
C10-C11-O2-C14	71.61(12)
C2-C1-Si1-C21	155.35(10)
C2-C1-Si1-C20	-86.40(10)
C2-C1-Si1-C19	37.85(11)

4.8. ^{1}H-NMR and ^{13}C-NMR Spectra

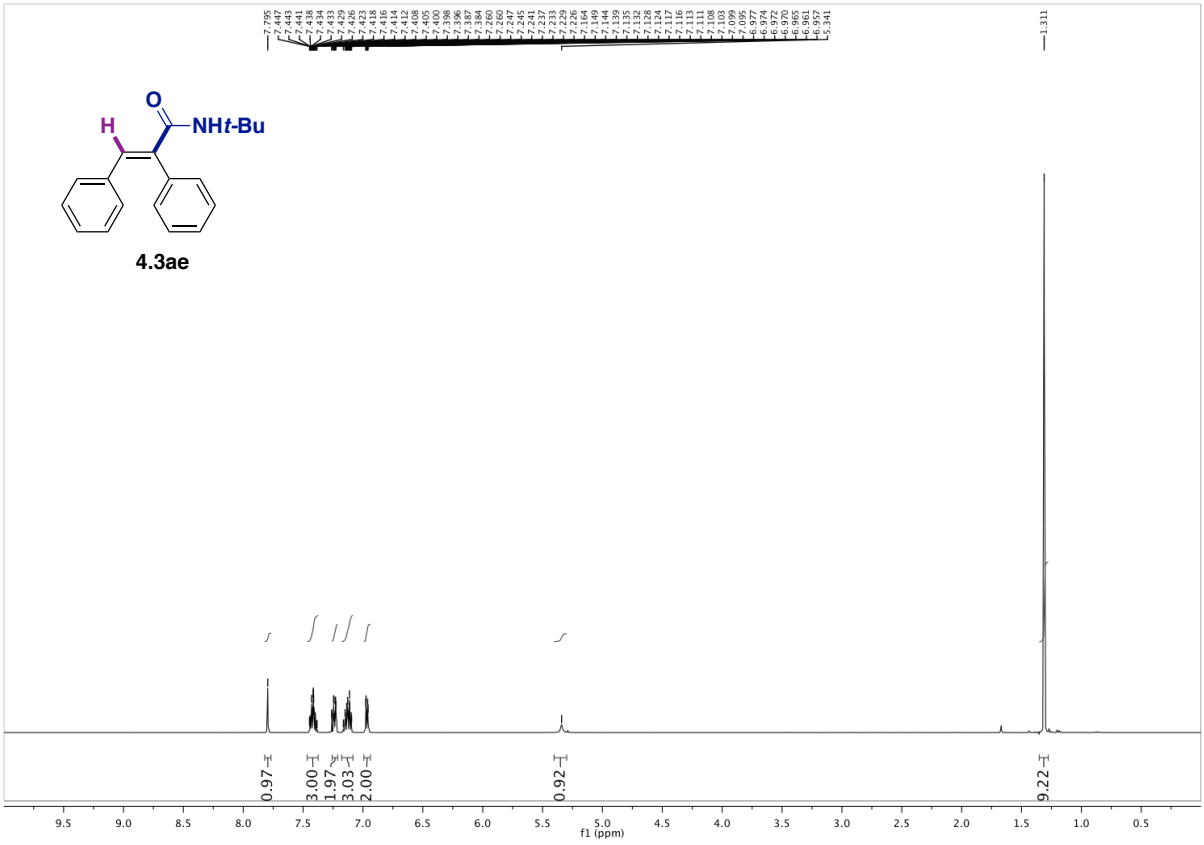

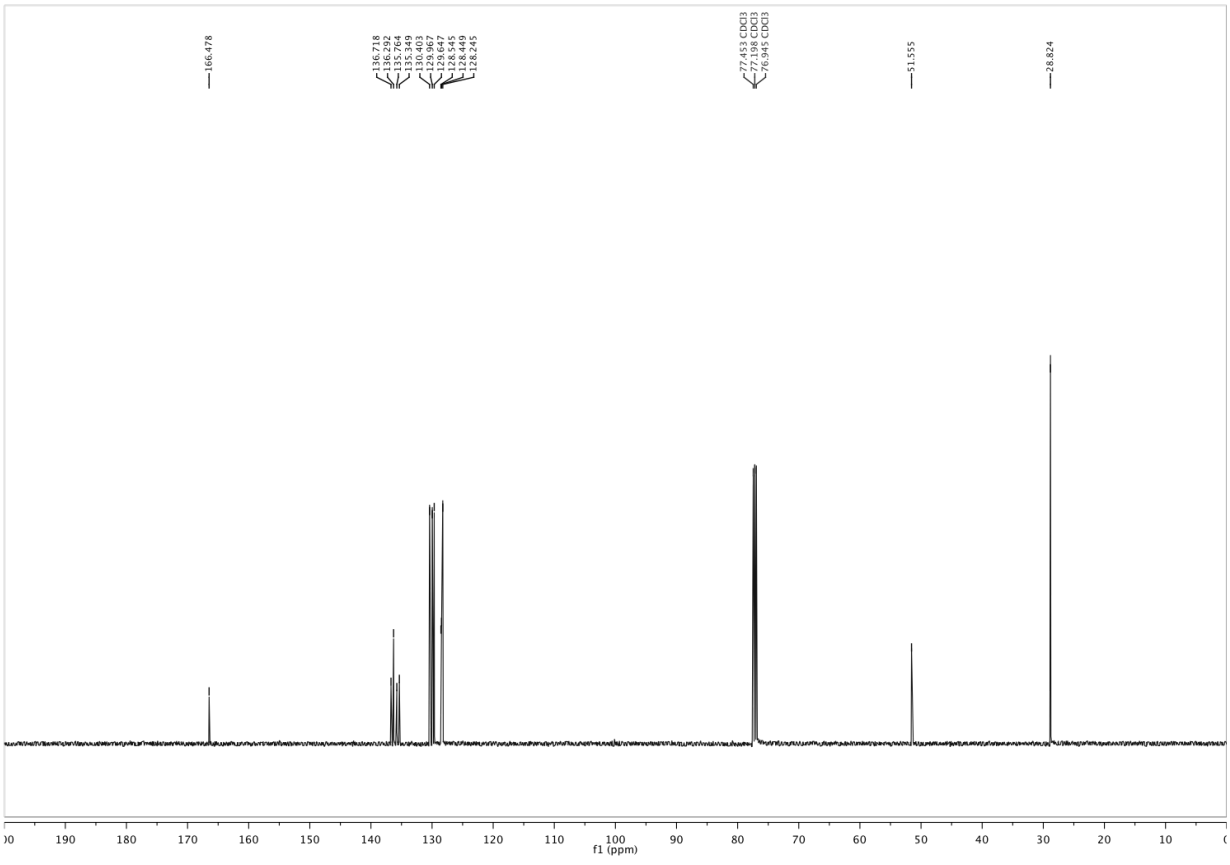

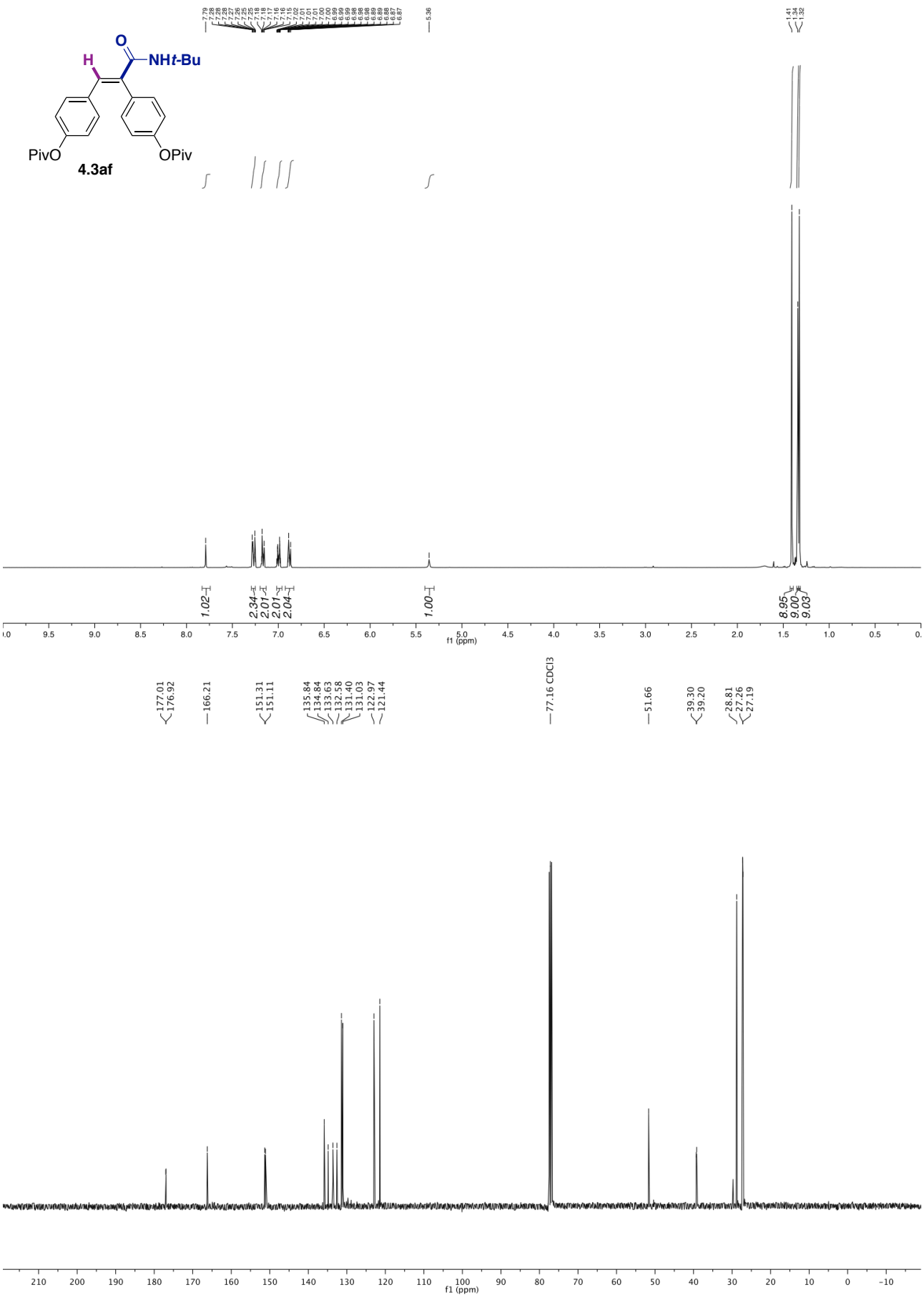
O
H
NHt-Bu
PivO
OPiv
4.3af
f1 (ppm)

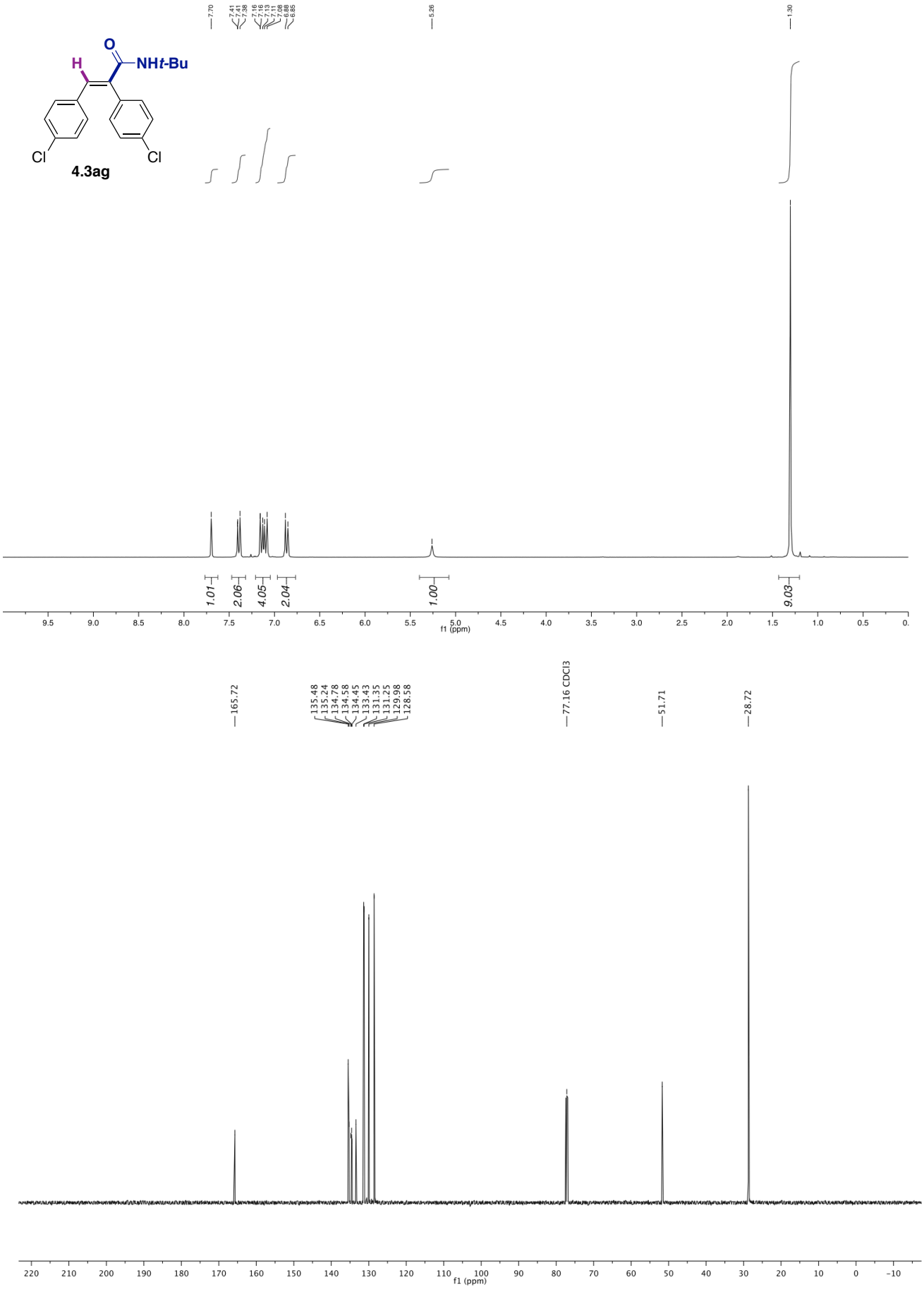
O
H
NHt-Bu
Cl
Cl
4.3ag
7.70
7.41
7.41
7.38
7.16
7.15
7.13
7.11
7.11
6.88
6.85
5.26
1.30
1.01
2.06
4.05
2.04
1.00
9.03
f1 (ppm)
165.72
135.48
135.24
134.78
134.58
134.45
133.43
131.35
131.25
129.98
128.58
77.16 CDCl3
51.71
28.72
f1 (ppm)

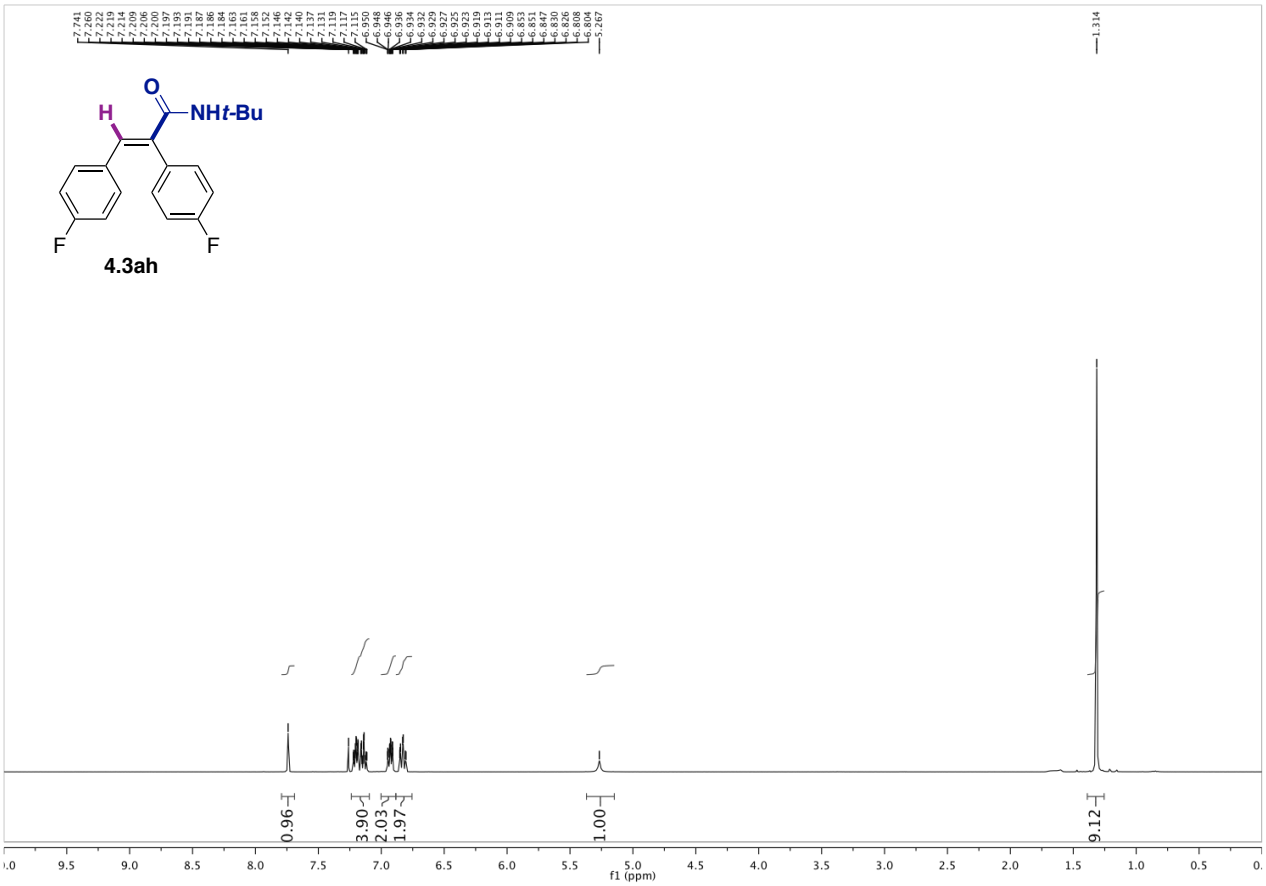
O
H
NHt-Bu
F
F
4.3ah
0.96
3.90
2.03
1.97
1.00
9.12
f1 (ppm)

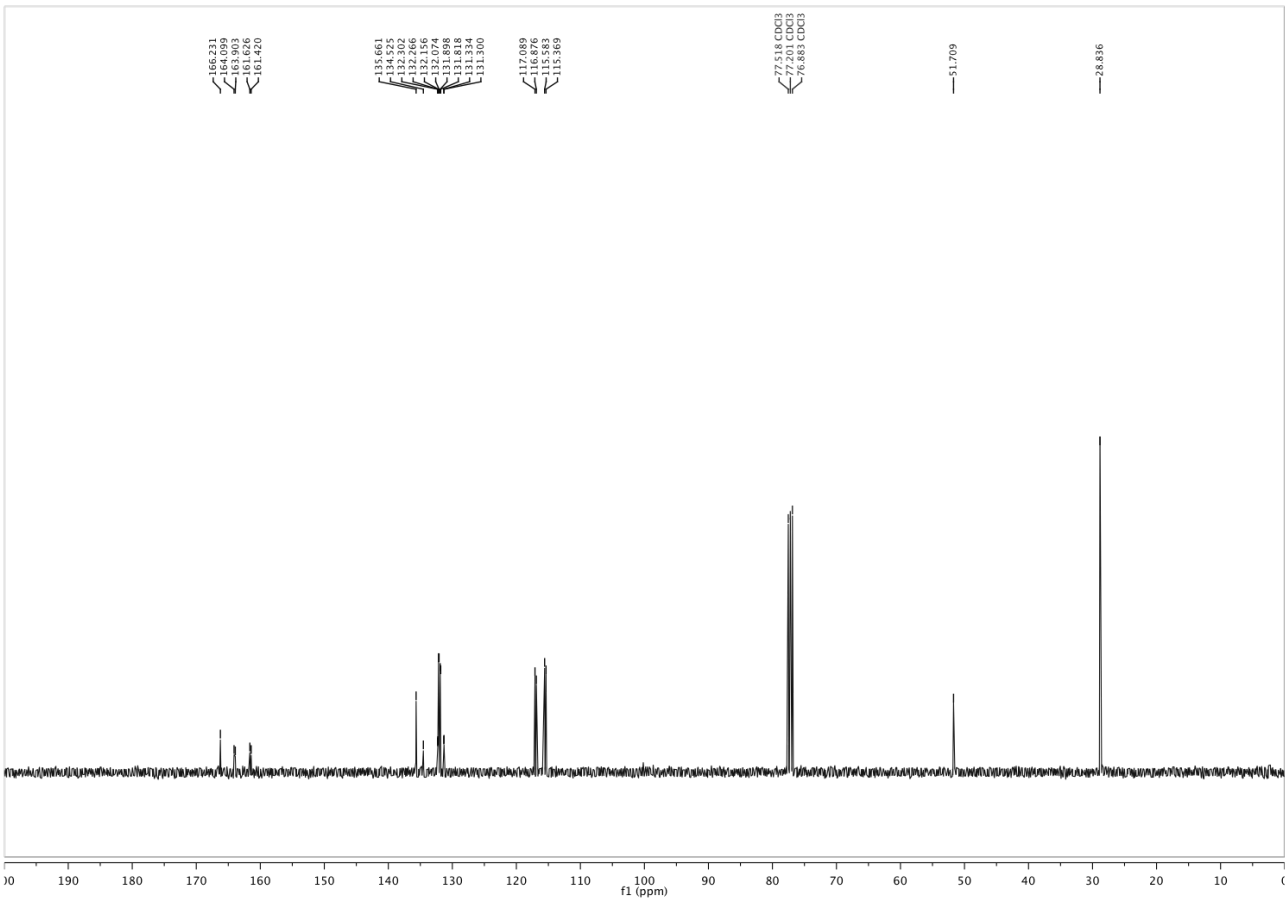
166.231
164.099
163.093
161.626
161.420
135.661
134.325
132.302
132.266
132.156
132.074
131.988
131.818
131.334
131.300
117.089
116.876
115.533
115.369
77.518 CDCl3
77.201 CDCl3
76.883 CDCl3
51.709
28.836
f1 (ppm)

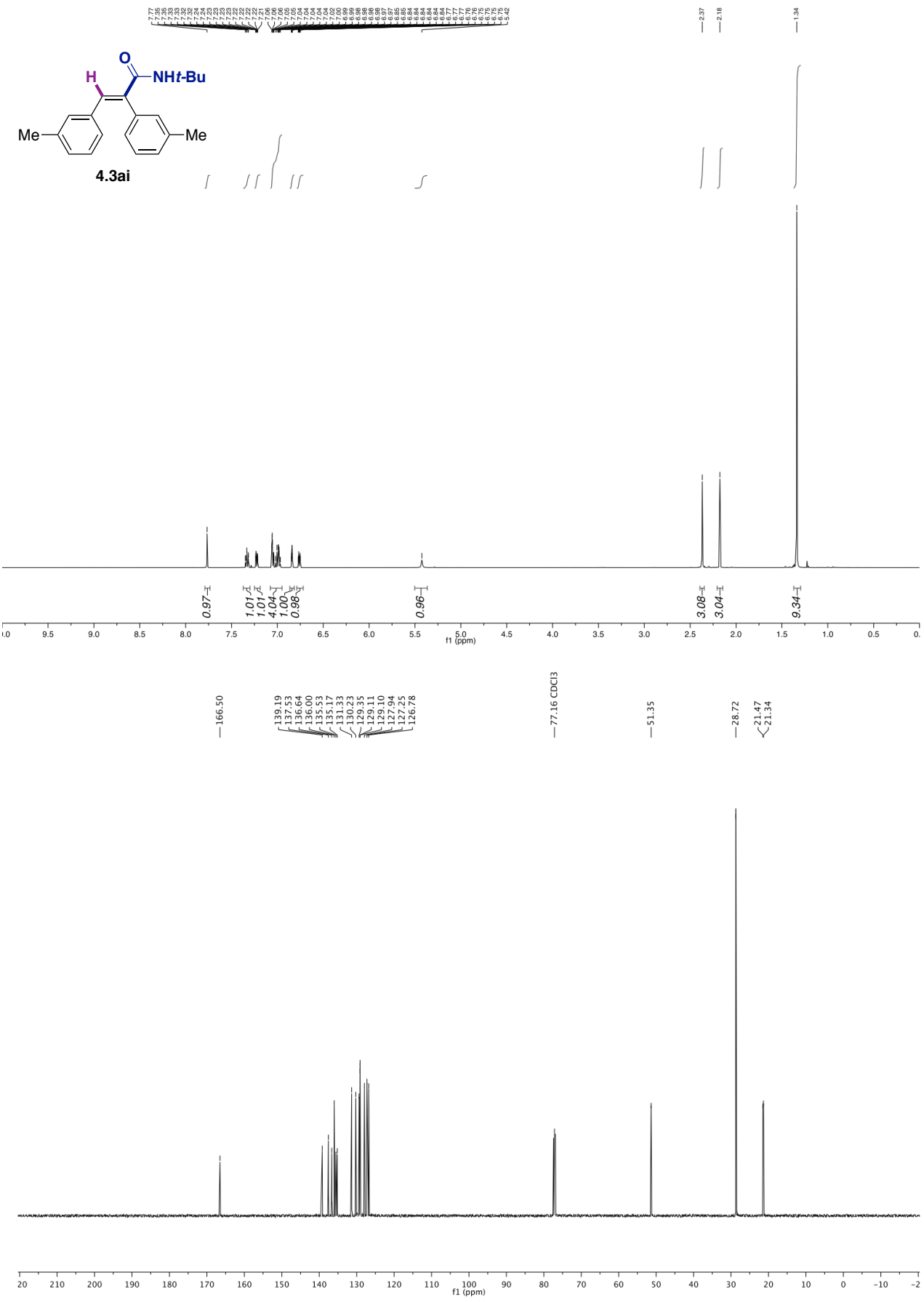
NHt-Bu
Me
Me
4.3ai
f1 (ppm)
CDCl3

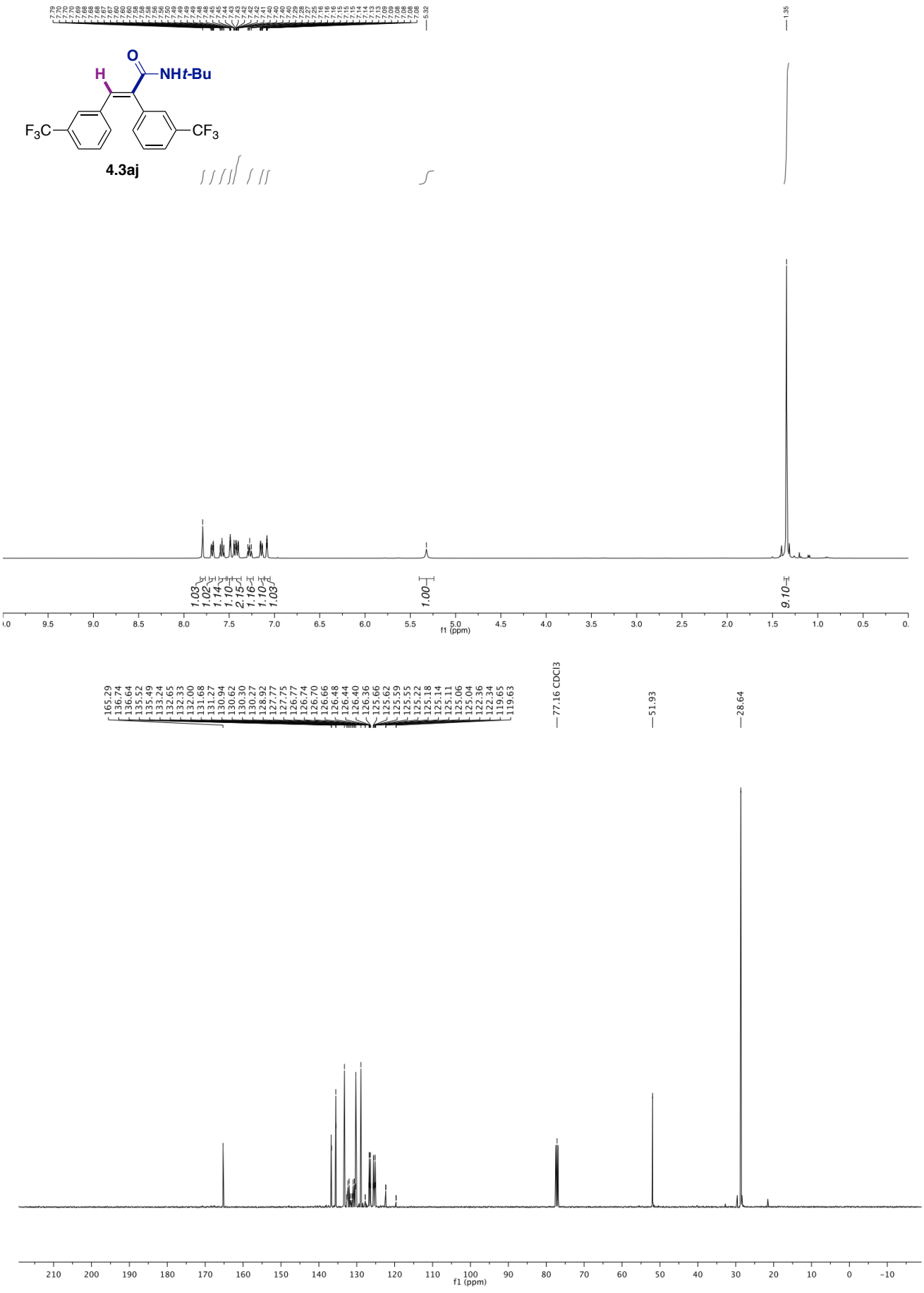
O
H
NHt-Bu
F3C
CF3
4.3aj
f1 (ppm)
77.16 CDCl3
51.93
28.64

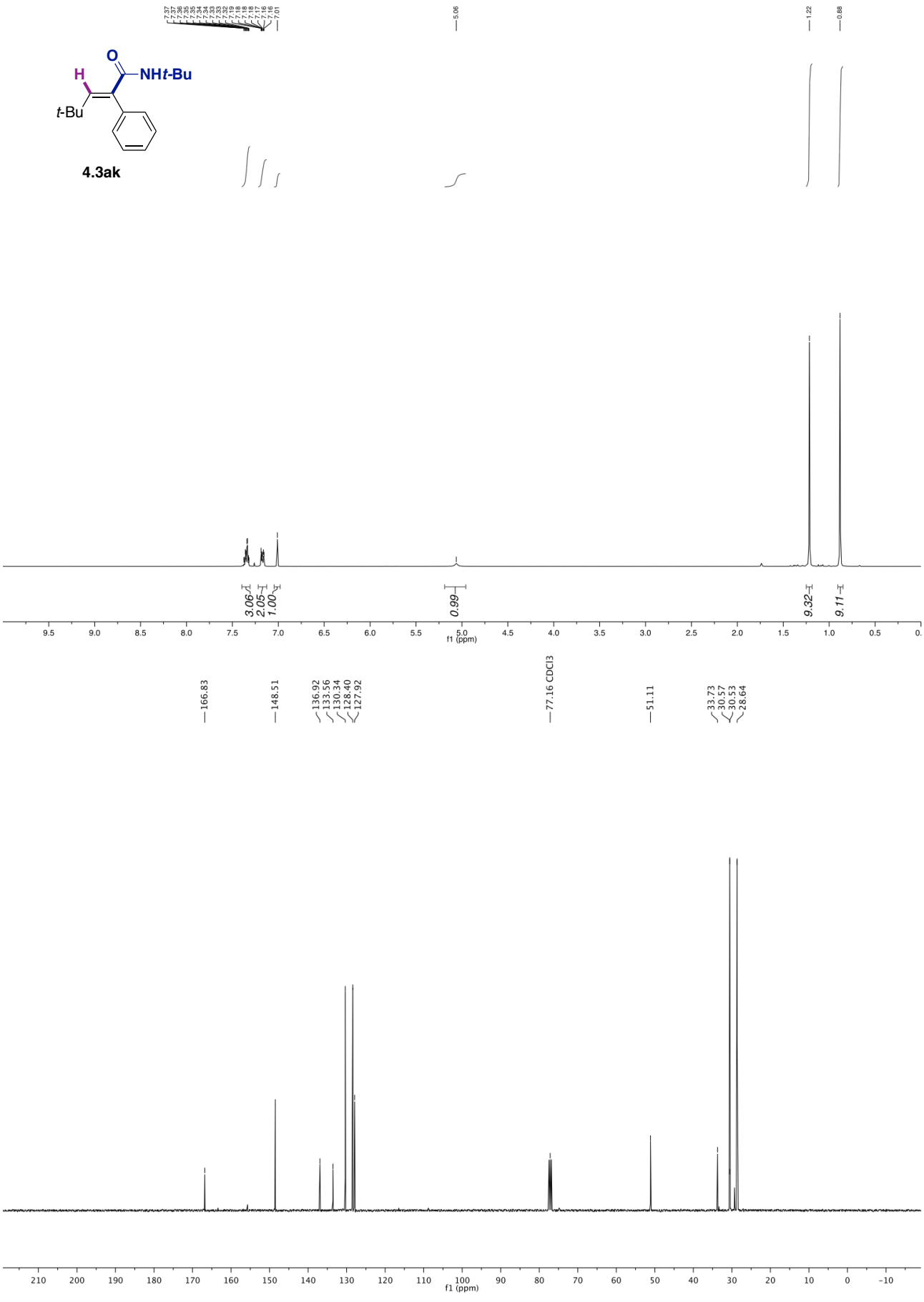
H
O
NHt-Bu
t-Bu
4.3ak
7.37
7.37
7.36
7.35
7.35
7.34
7.34
7.33
7.32
7.19
7.18
7.18
7.17
7.17
7.16
7.01
5.06
1.22
0.88
3.06
2.05
1.00
0.99
9.32
9.11
f1 (ppm)
166.83
148.51
136.92
133.56
130.34
128.40
127.92
77.16 CDCl3
51.11
33.73
30.57
30.53
28.64
f1 (ppm)

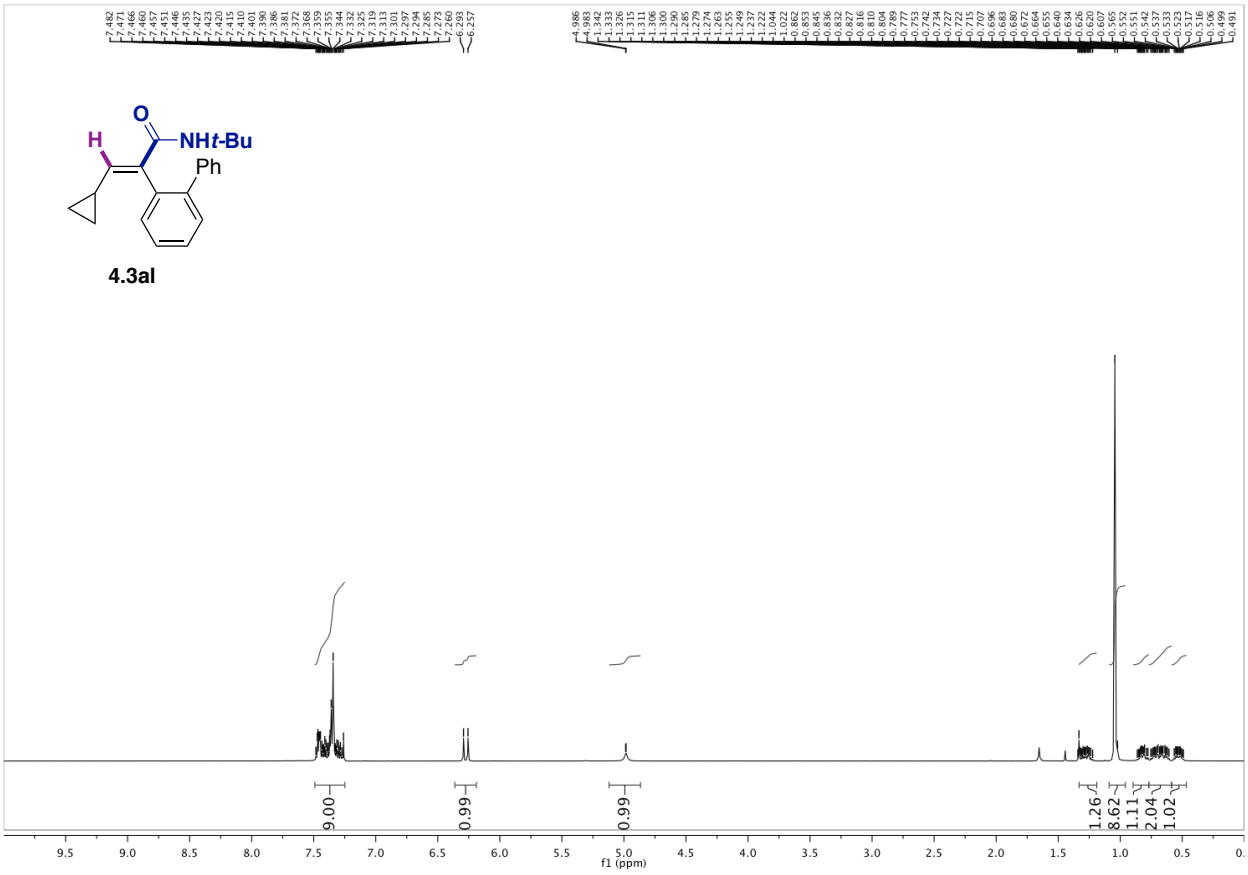
O
H
NHt-Bu
Ph
4.3al
9.00
0.99
0.99
1.26
8.62
1.11
2.04
1.02
f1 (ppm)

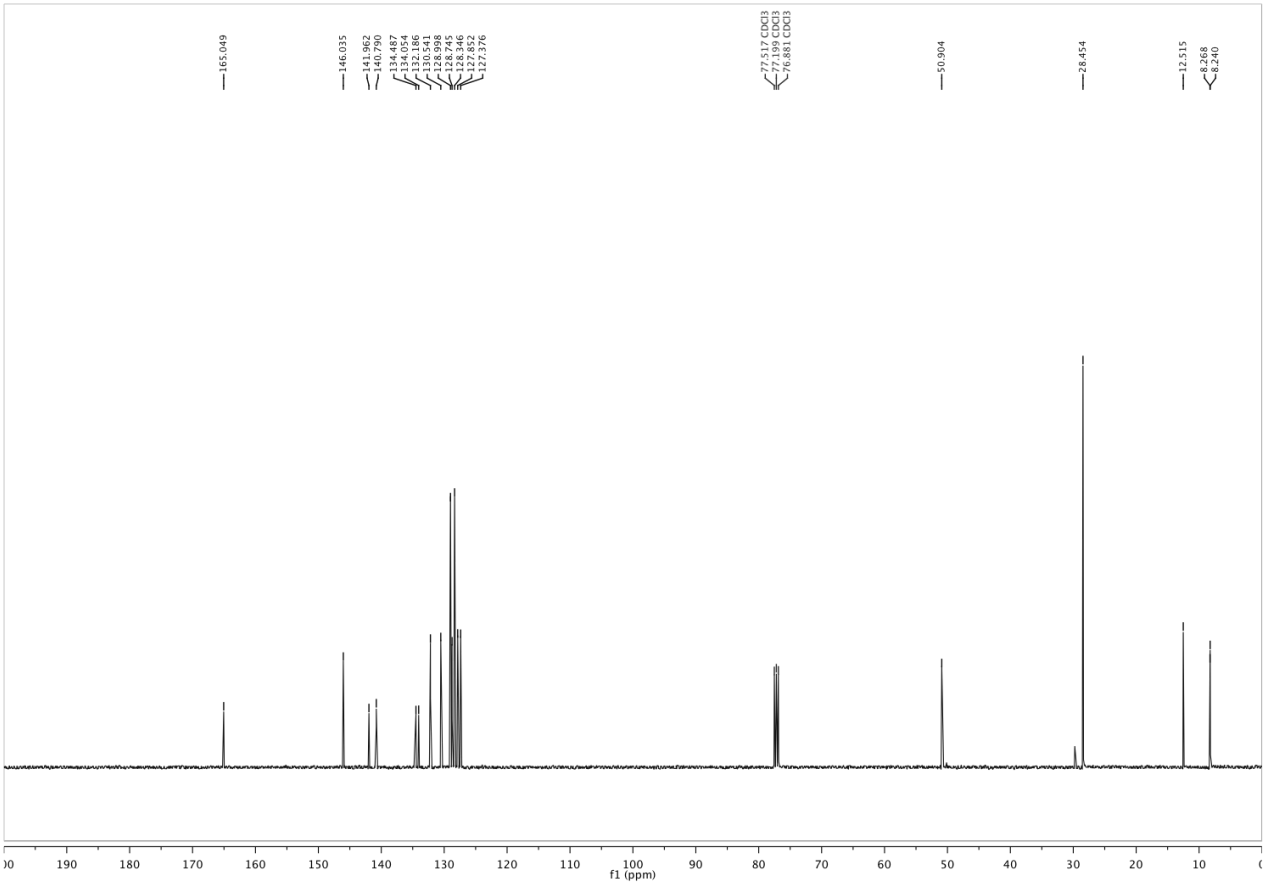
165.049
146.035
141.962
140.790
134.487
134.054
132.186
130.541
128.998
128.745
128.346
127.852
127.376
77.517 CDCl3
77.199 CDCl3
76.881 CDCl3
50.904
28.454
12.515
8.268
8.240
f1 (ppm)

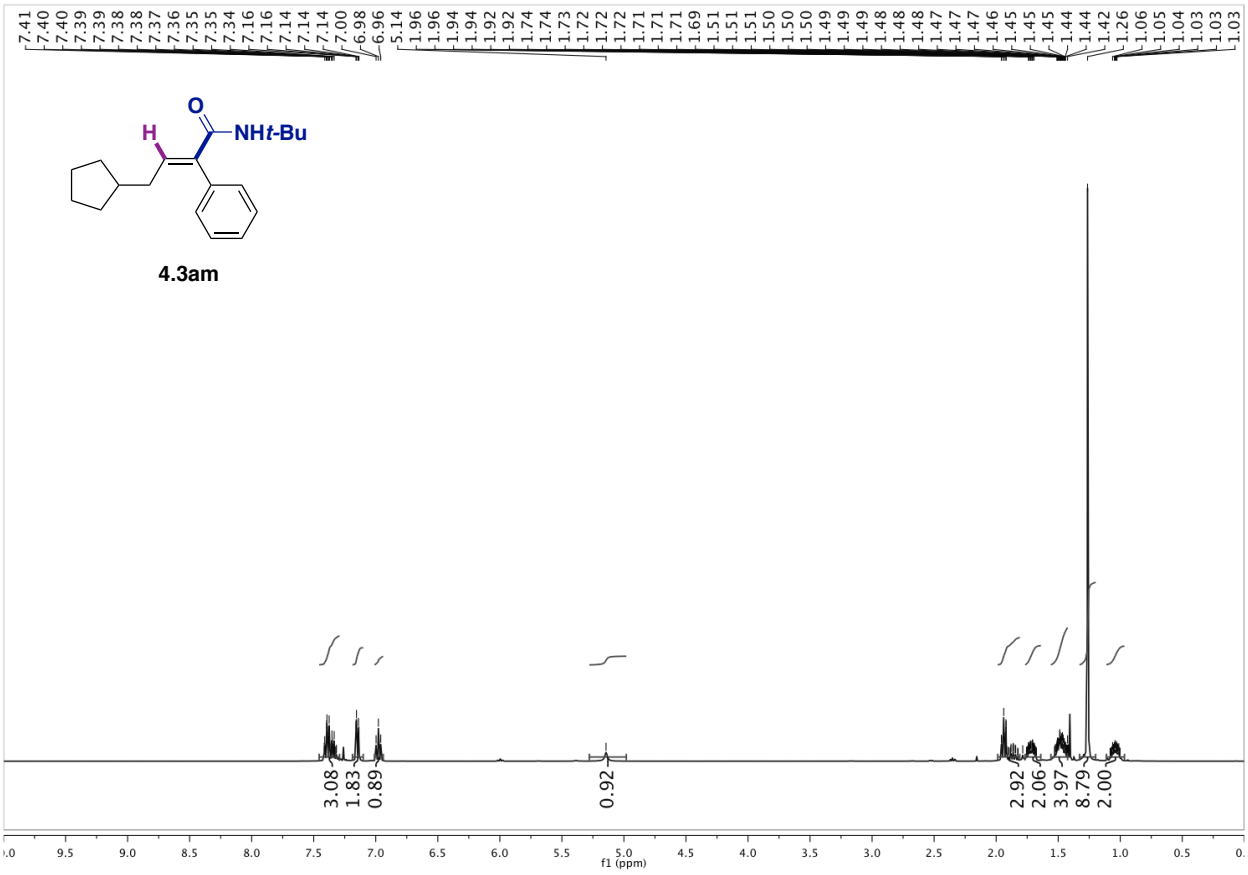
7.41 7.40 7.40 7.39 7.39 7.38 7.38 7.37 7.36 7.35 7.35 7.34 7.16 7.16 7.14 7.14 7.14 7.00 6.98 6.96
5.14 1.96 1.96 1.94 1.94 1.92 1.92 1.74 1.74 1.73 1.72 1.72 1.72 1.71 1.71 1.71 1.69 1.51 1.51 1.51 1.50 1.50 1.50 1.49 1.49 1.49 1.48 1.48 1.48 1.47 1.47 1.47 1.46 1.45 1.45 1.45 1.44 1.44 1.42 1.26 1.06 1.05 1.04 1.03 1.03 1.03
O
H
NHt-Bu
4.3am
3.08
1.83
0.89
0.92
2.92
2.06
3.97
8.79
2.00
f1 (ppm)

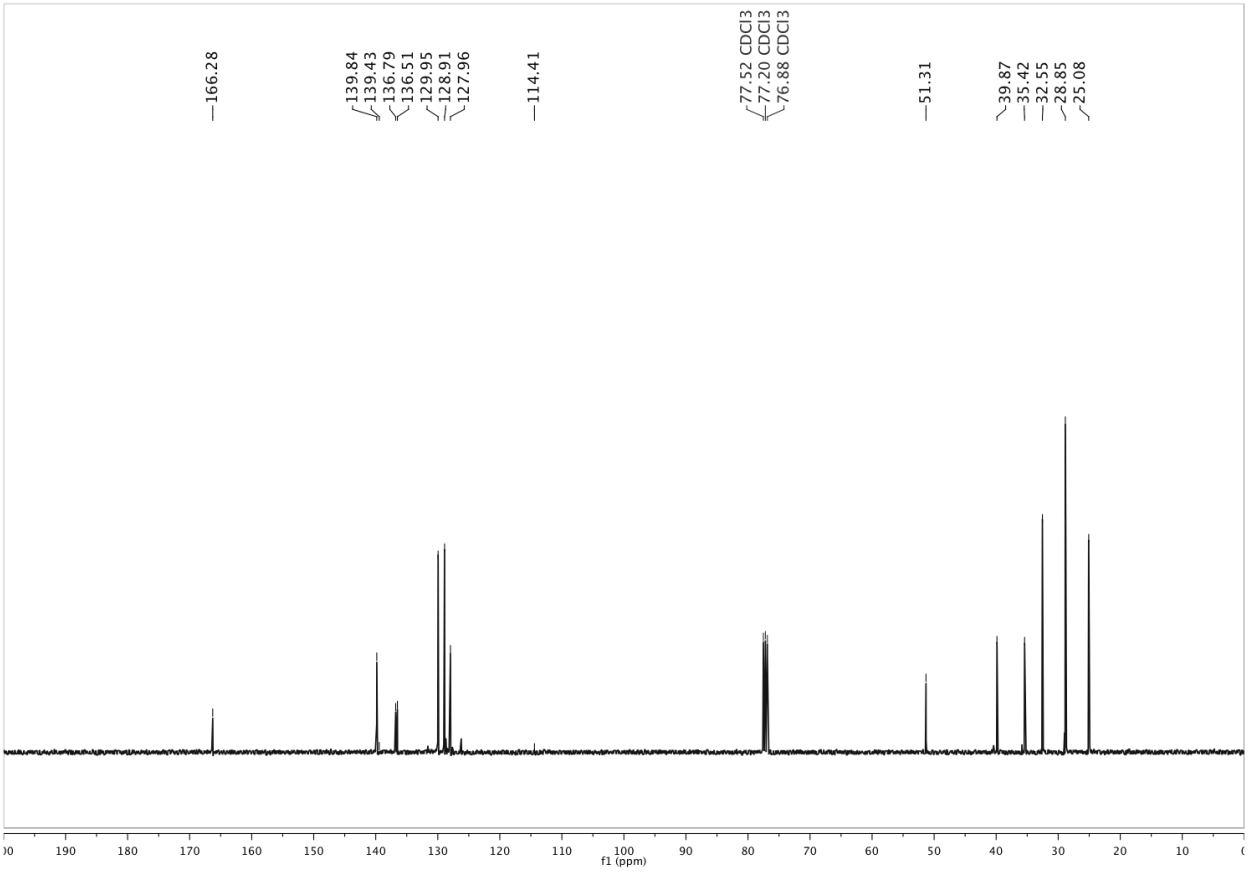
166.28
139.84
139.43
136.79
136.51
129.95
128.91
127.96
114.41
77.52 CDCl3
77.20 CDCl3
76.88 CDCl3
51.31
39.87
35.42
32.55
28.85
25.08
f1 (ppm)

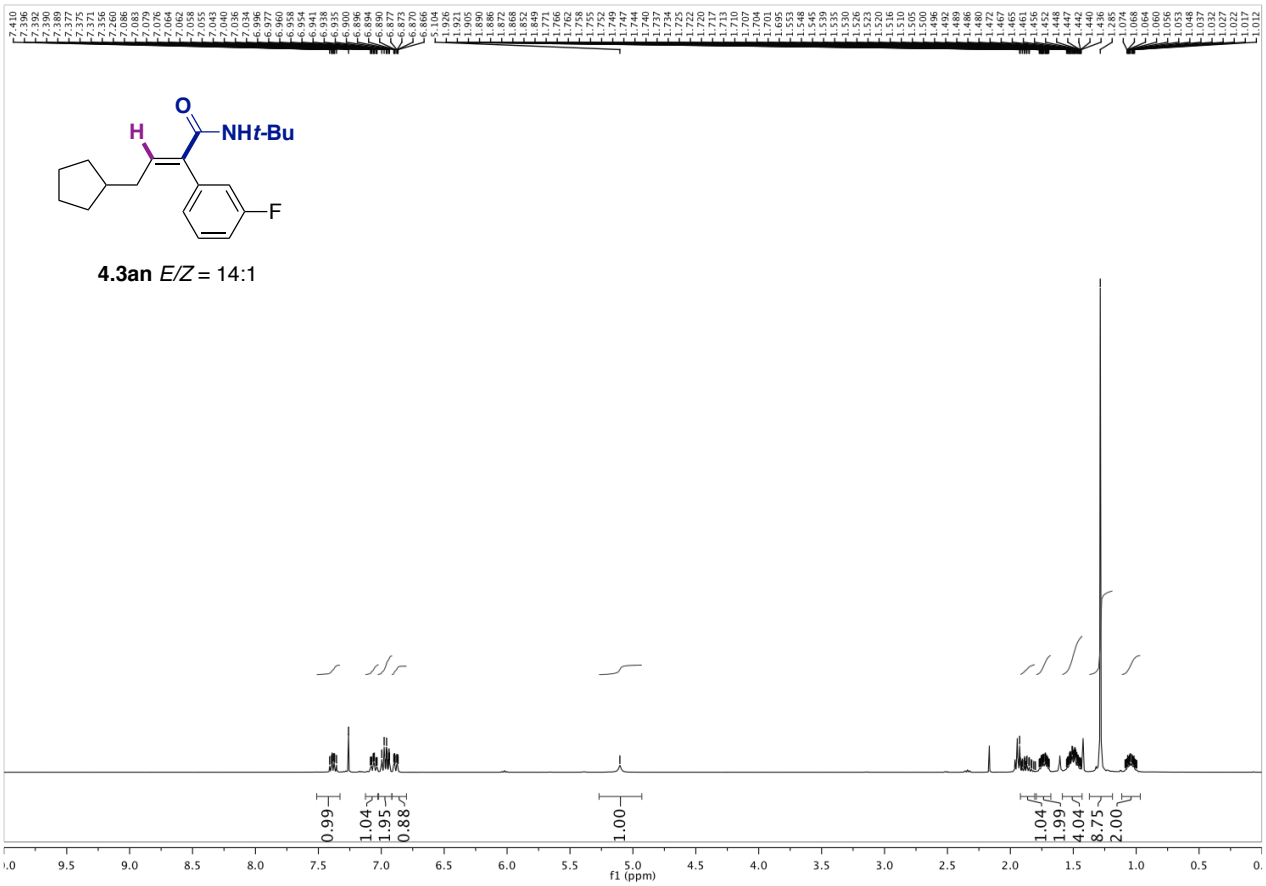
O
H
NHt-Bu
F
0.99
1.04
1.95
0.88
1.00
1.04
1.99
4.04
8.75
2.00
f1 (ppm)

4.3an *E*/*Z* = 14:1

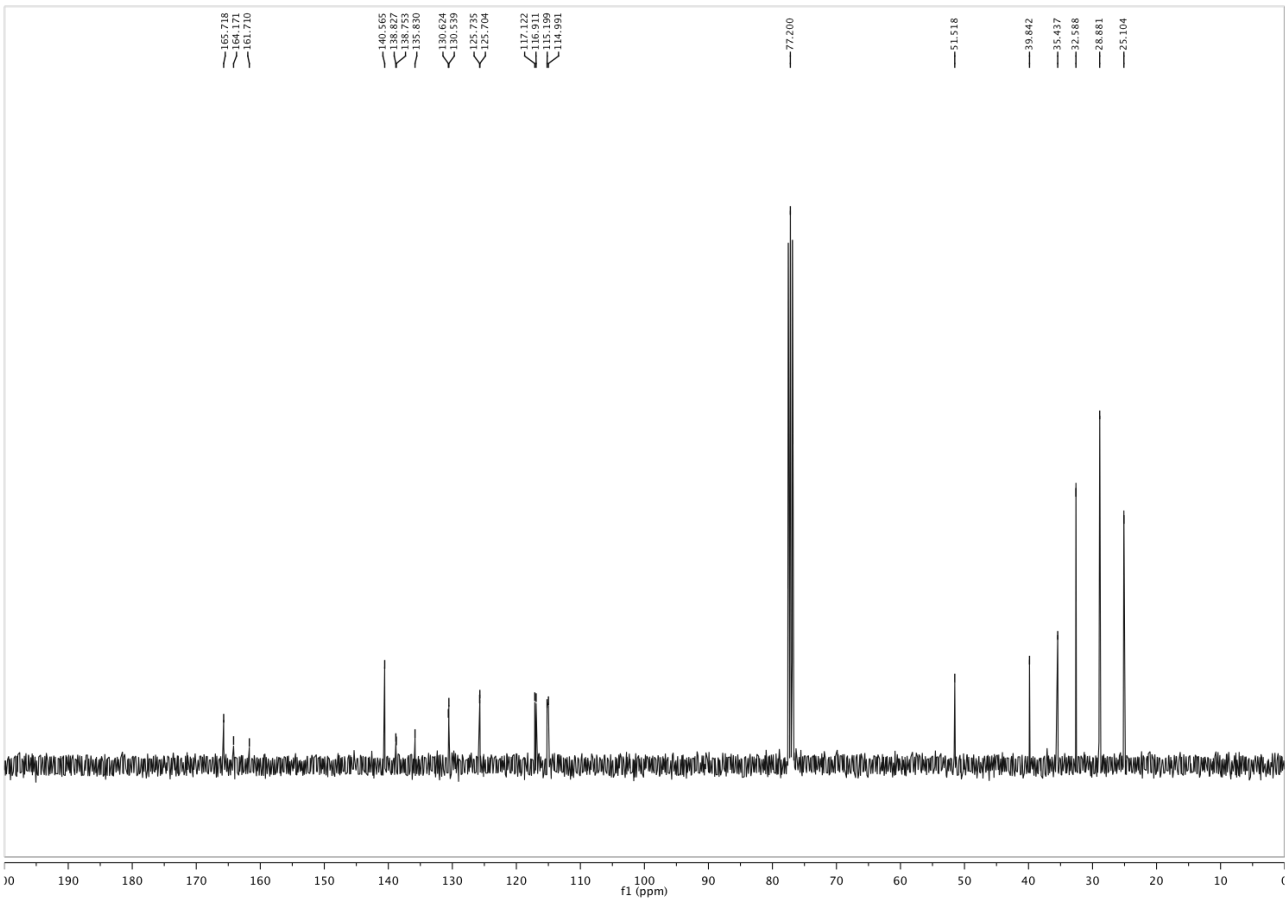
165.718
164.771
161.710
140.565
138.827
138.755
135.830
130.624
130.539
125.735
125.704
117.122
116.911
115.399
114.991
77.200
51.518
39.842
35.437
32.588
28.881
25.104
f1 (ppm)

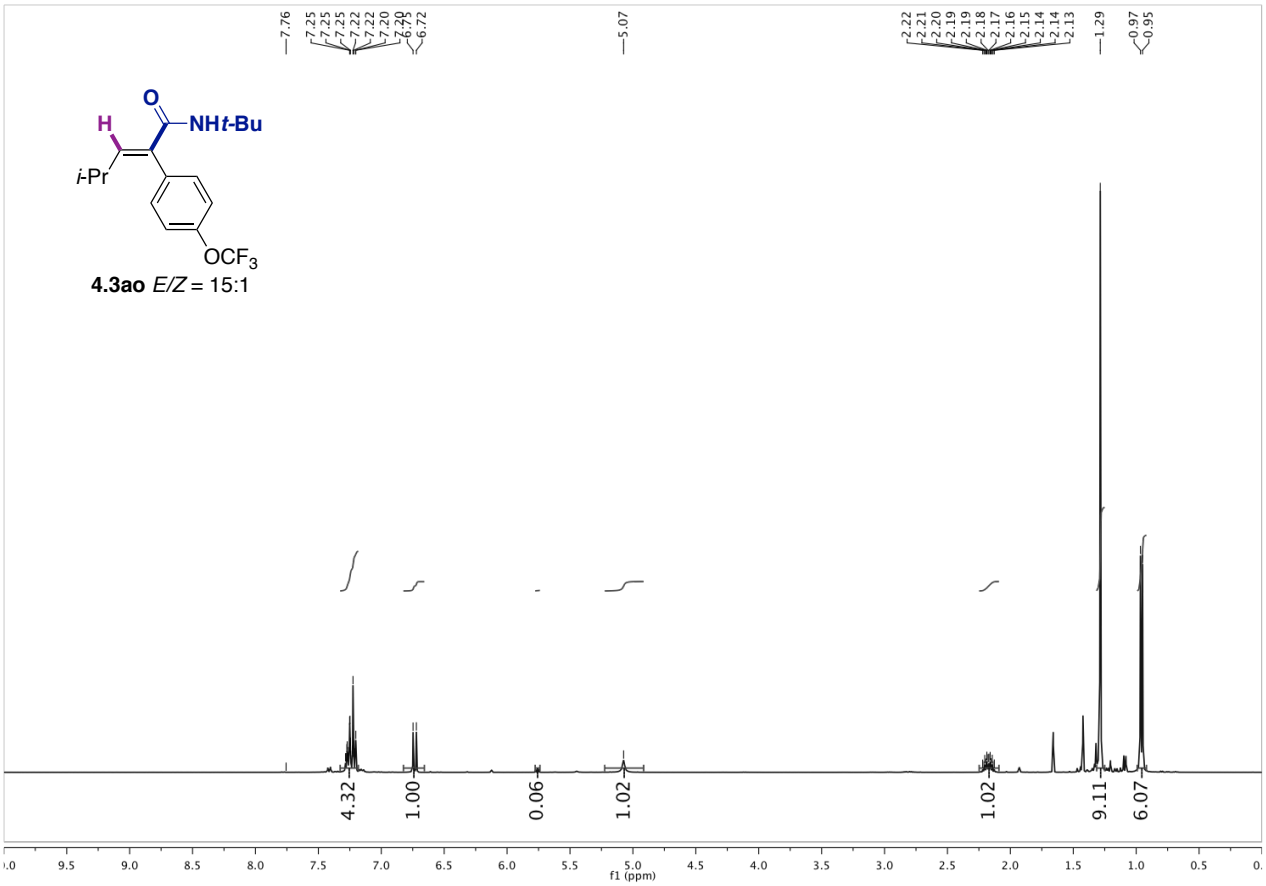
7.76
7.25
7.25
7.25
7.22
7.22
7.20
7.20
6.75
6.72
5.07
2.22
2.21
2.20
2.19
2.19
2.18
2.17
2.16
2.15
2.14
2.14
2.13
1.29
0.97
0.95
O
H
NHt-Bu
i-Pr
OCF3
4.32
1.00
0.06
1.02
1.02
9.11
6.07
f1 (ppm)

4.3ao *E/Z* = 15:1

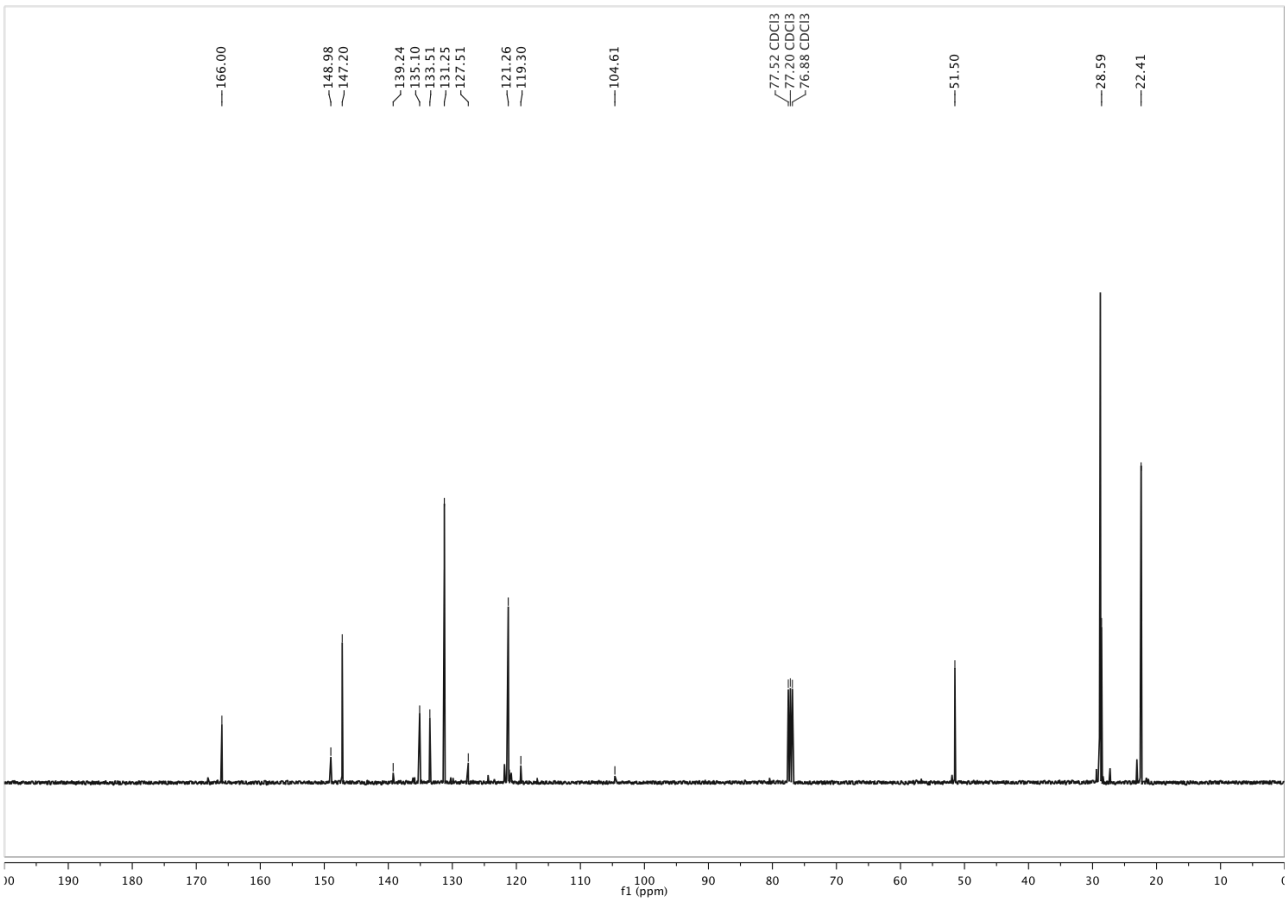
166.00
148.98
147.20
139.24
135.10
133.51
131.25
127.51
121.26
119.30
104.61
77.52 CDCl3
77.20 CDCl3
76.88 CDCl3
51.50
28.59
22.41
f1 (ppm)

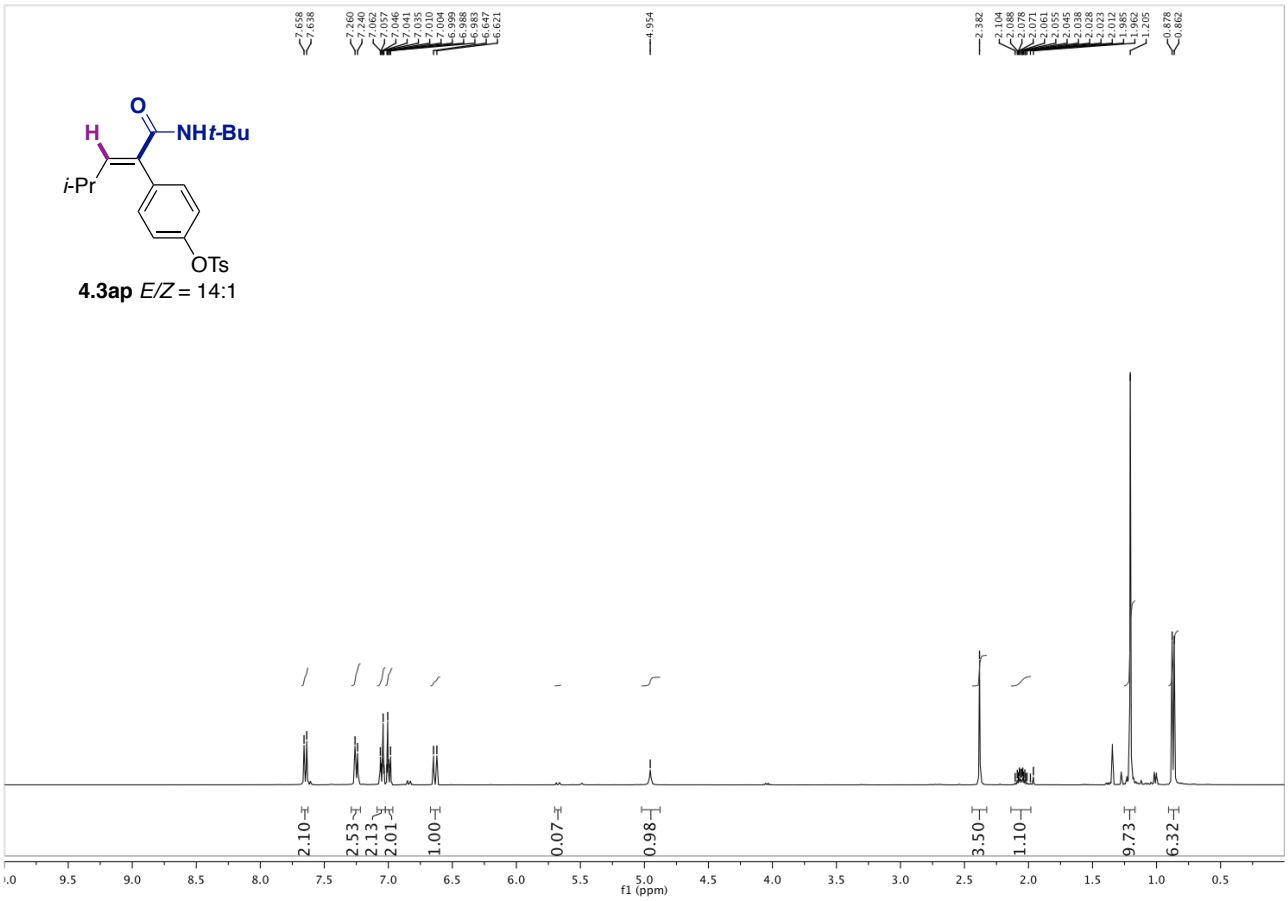
7.658
7.638
7.260
7.240
7.062
7.057
7.046
7.041
7.035
7.010
7.004
6.999
6.988
6.983
6.647
6.621
4.954
2.382
2.104
2.088
2.078
2.071
2.061
2.055
2.045
2.038
2.028
2.023
2.012
1.985
1.962
1.265
0.878
0.862
O
NH*t*-Bu
H
i-Pr
OTs
2.10
2.53
2.13
2.01
1.00
0.07
0.98
3.50
1.10
9.73
6.32
f1 (ppm)

4.3ap *E*/*Z* = 14:1

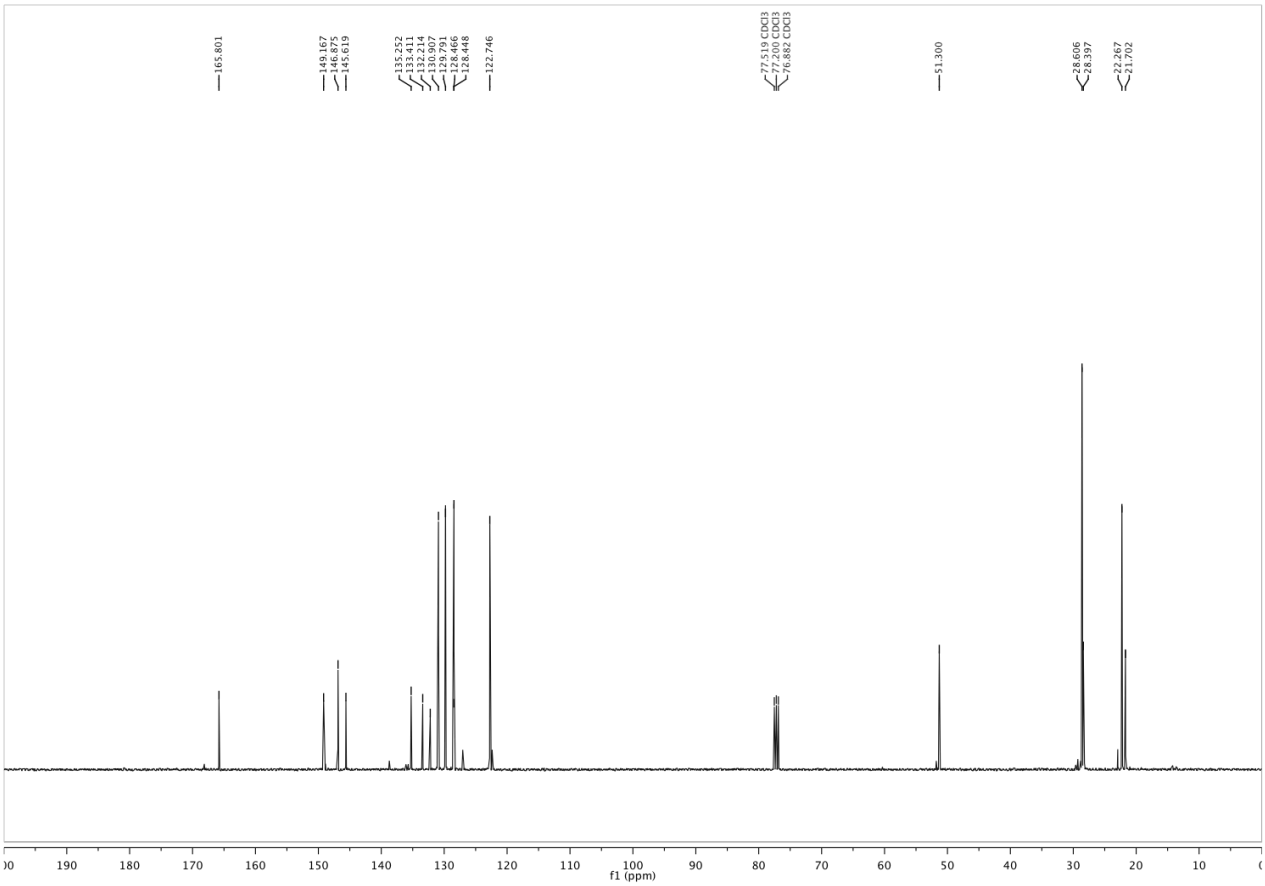
165.801
149.167
146.835
145.619
135.252
133.411
132.214
130.607
129.791
128.466
128.448
122.746
77.519 CDCl3
77.200 CDCl3
76.882 CDCl3
51.300
28.606
28.397
22.267
21.702
f1 (ppm)

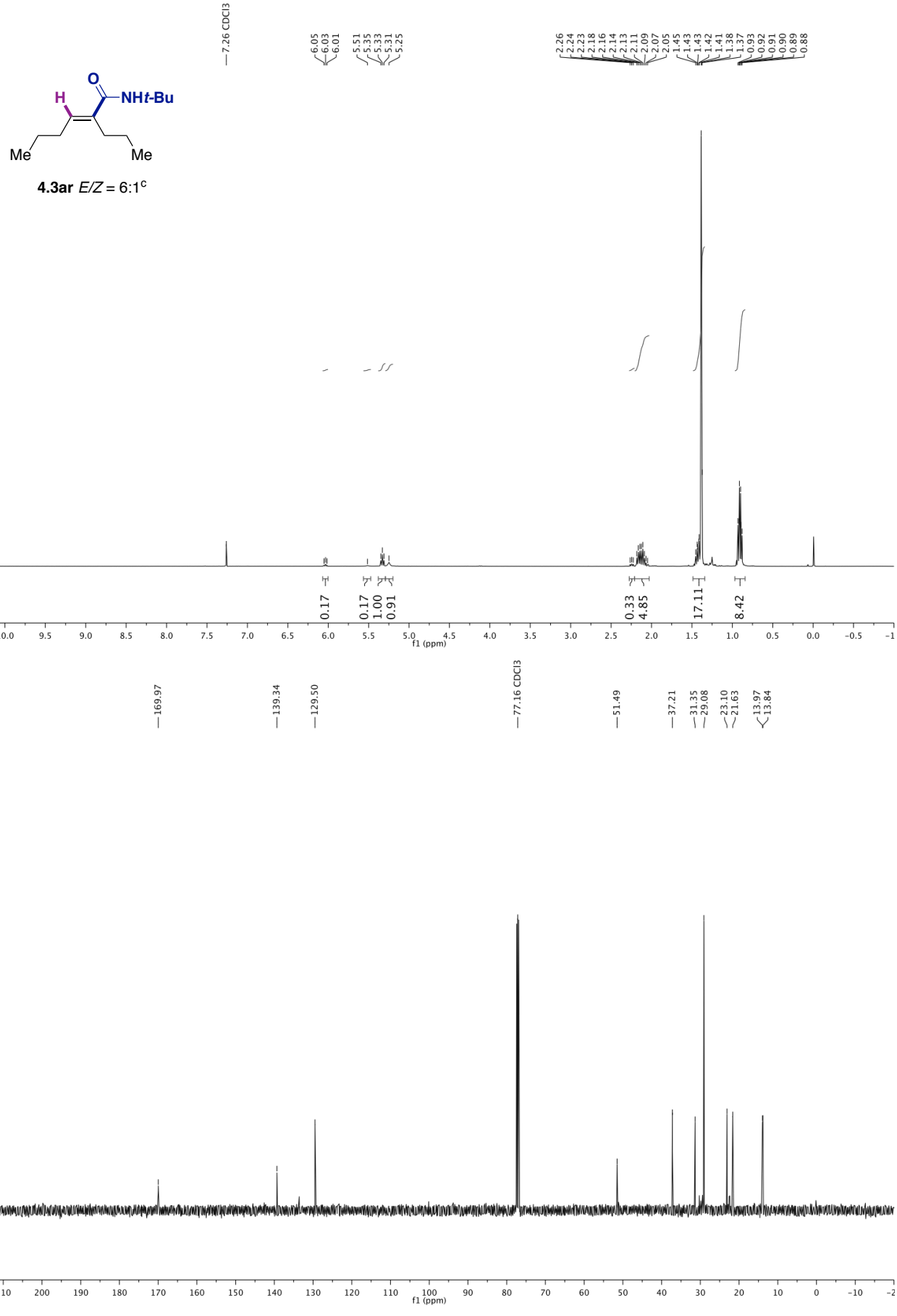
7.26 CDCl3
6.05
6.03
6.01
5.51
5.35
5.33
5.31
5.25
2.26
2.24
2.23
2.18
2.16
2.14
2.13
2.11
2.09
2.07
2.05
1.45
1.43
1.43
1.42
1.41
1.38
1.37
0.93
0.92
0.91
0.90
0.89
0.88
O
H
NHt-Bu
Me
Me
0.17
0.17
1.00
0.91
0.33
4.85
17.11
8.42
f1 (ppm)
169.97
139.34
129.50
77.16 CDCl3
51.49
37.21
31.35
29.08
23.10
21.63
13.97
13.84
f1 (ppm)

4.3ar *E/Z* = 6:1[c]

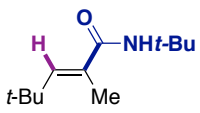
O
H
NH*t*-Bu
t-Bu
Me

4.3as

7.26 CDCl3
6.20
6.19
6.19
6.18
5.50
1.92
1.92
1.38
1.15
1.00
0.92
3.01
9.29
9.04
f1 (ppm)

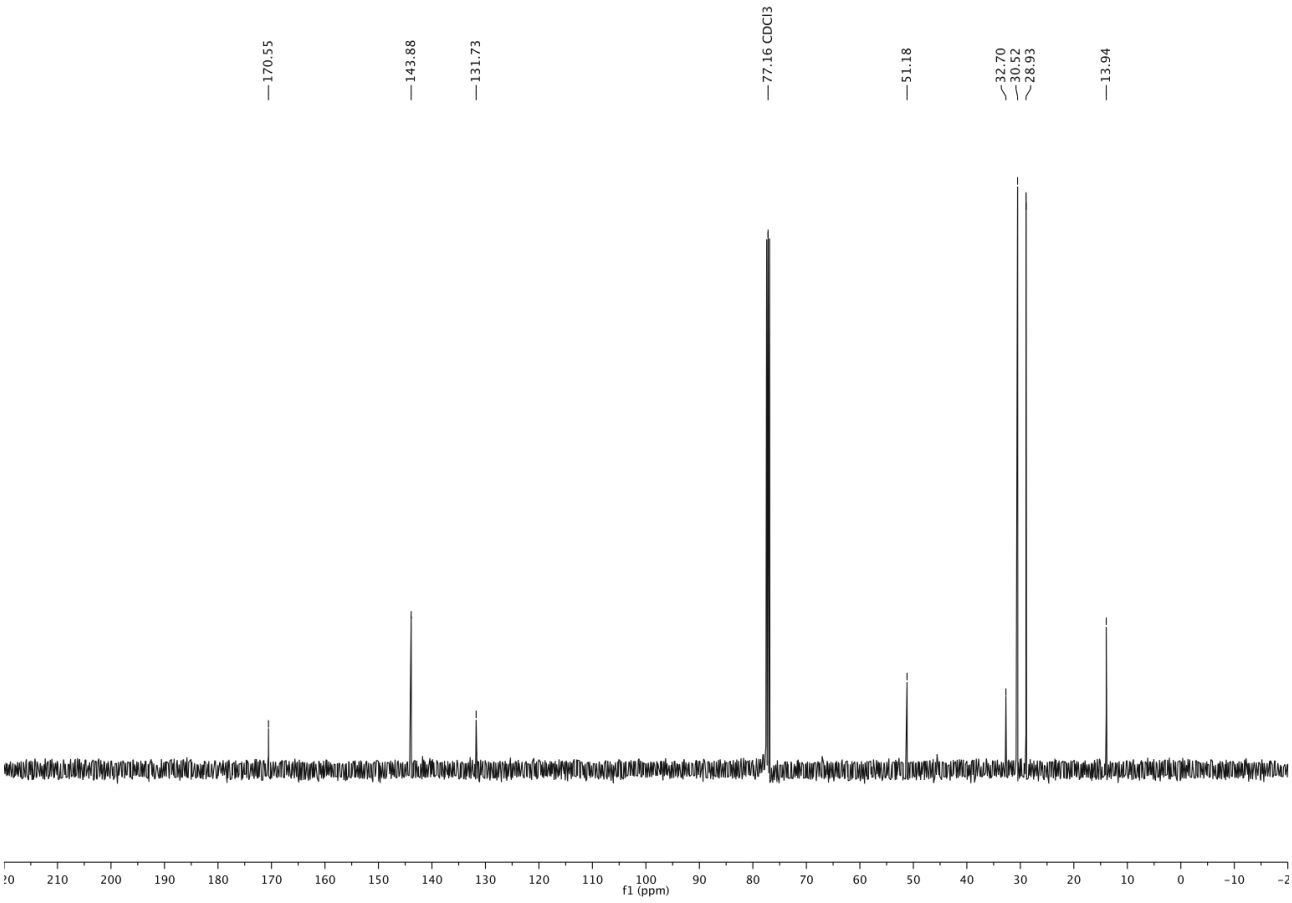
170.55
143.88
131.73
77.16 CDCl3
51.18
32.70
30.52
28.93
13.94
f1 (ppm)

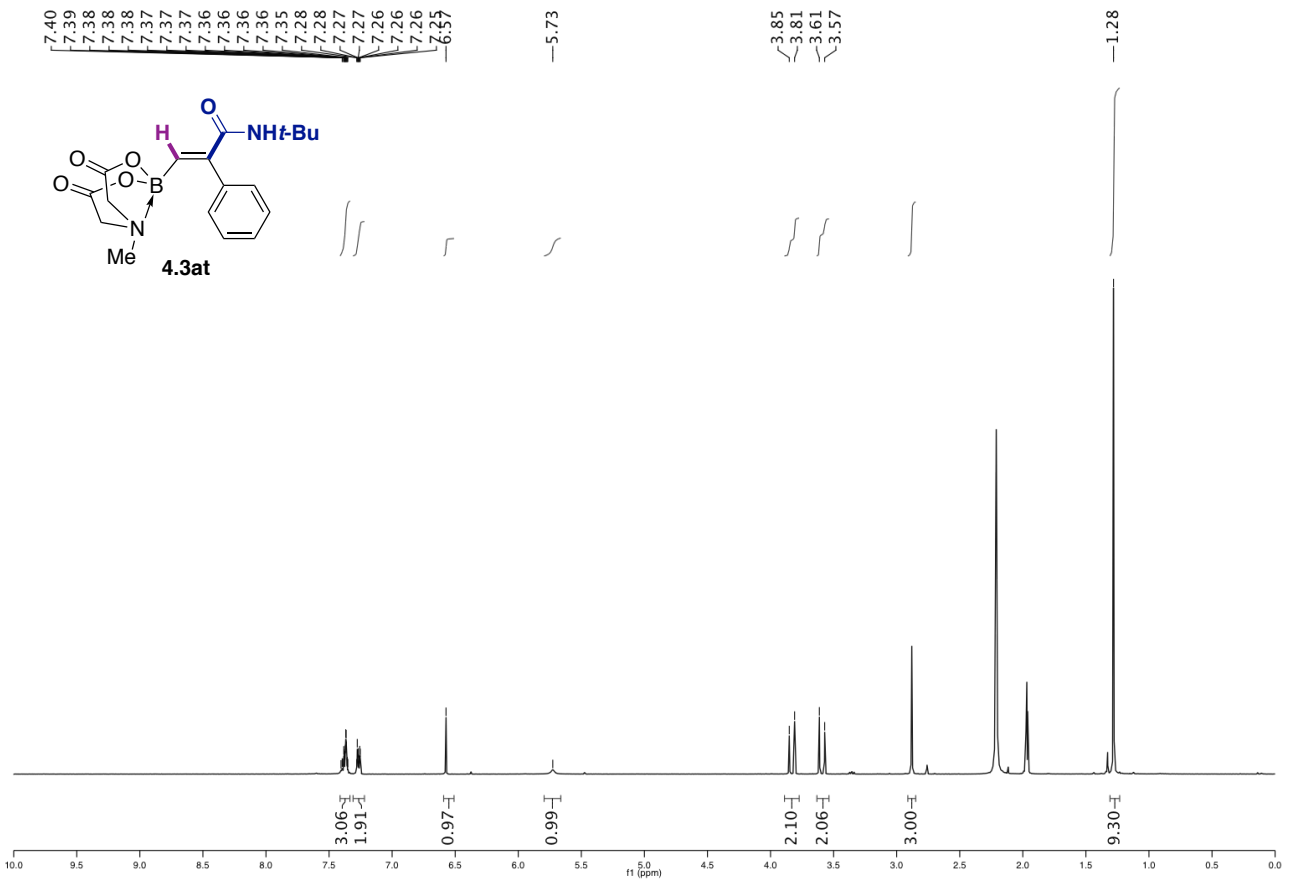
7.40
7.39
7.38
7.38
7.38
7.37
7.37
7.37
7.36
7.36
7.36
7.35
7.28
7.28
7.27
7.27
7.26
7.26
7.26
7.25
6.57
5.73
3.85
3.81
3.61
3.57
1.28
O
NHt-Bu
H
O
O
O
O
B
N
Me
4.3at
3.06
1.91
0.97
0.99
2.10
2.06
3.00
9.30
f1 (ppm)

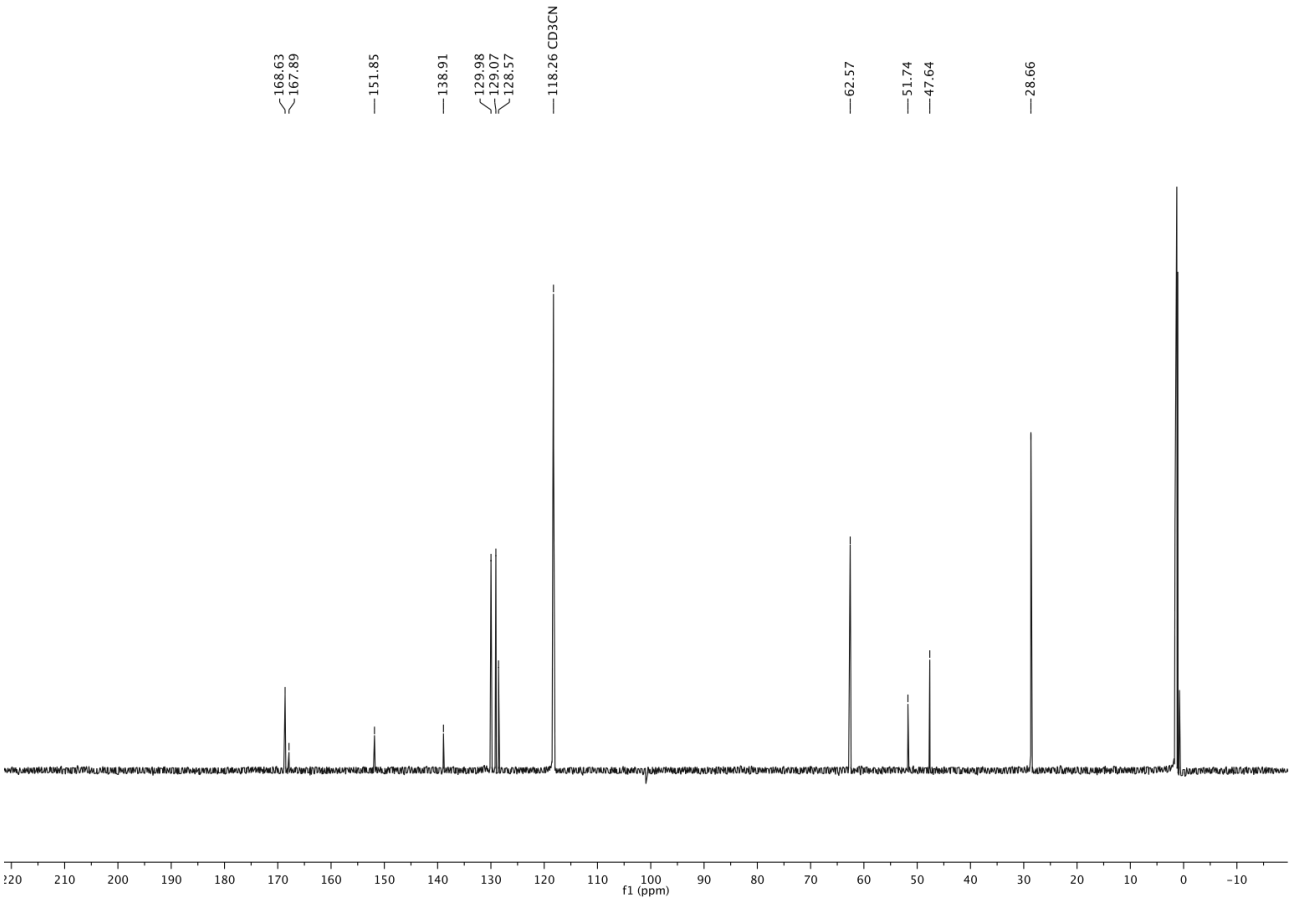
168.63
167.89
151.85
138.91
129.98
129.07
128.57
118.26 CD3CN
62.57
51.74
47.64
28.66
f1 (ppm)

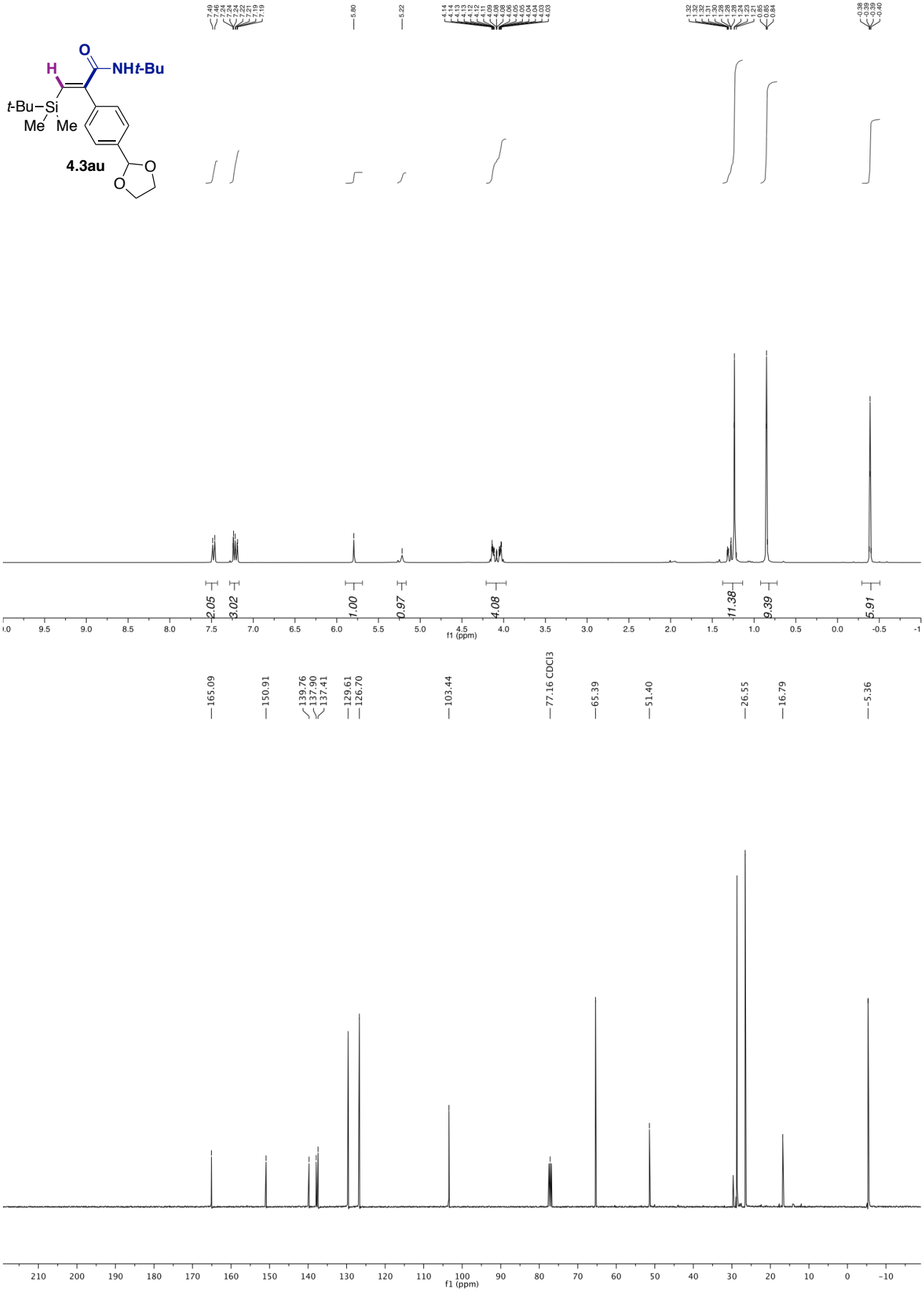
O
H
NHt-Bu
t-Bu–Si
Me Me
4.3au
O
O
f1 (ppm)
f1 (ppm)

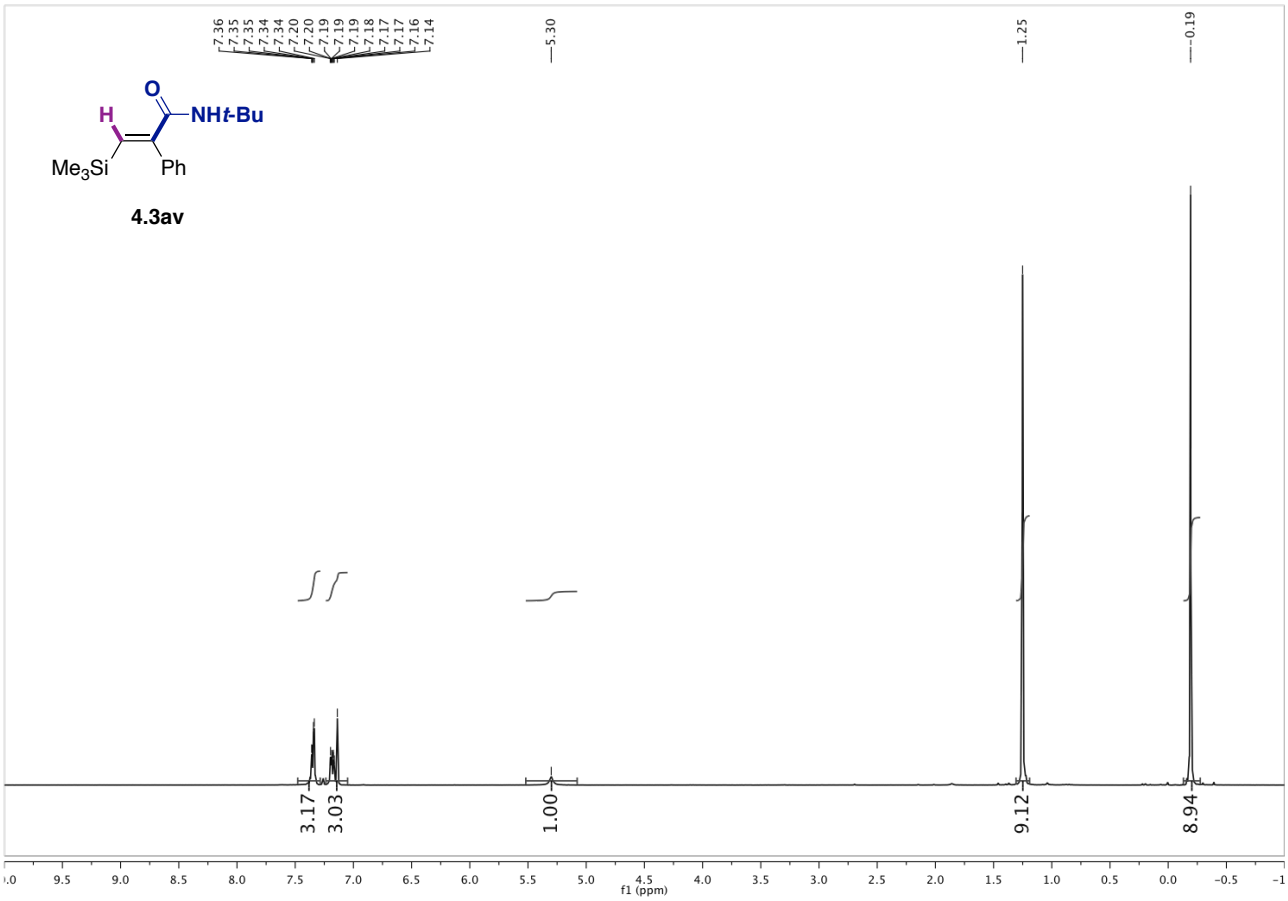
7.36
7.35
7.35
7.34
7.34
7.20
7.19
7.19
7.18
7.17
7.17
7.16
7.14
5.30
1.25
0.19
O
H
NHt-Bu
Me3Si
Ph
4.3av
3.17
3.03
1.00
9.12
8.94
f1 (ppm)

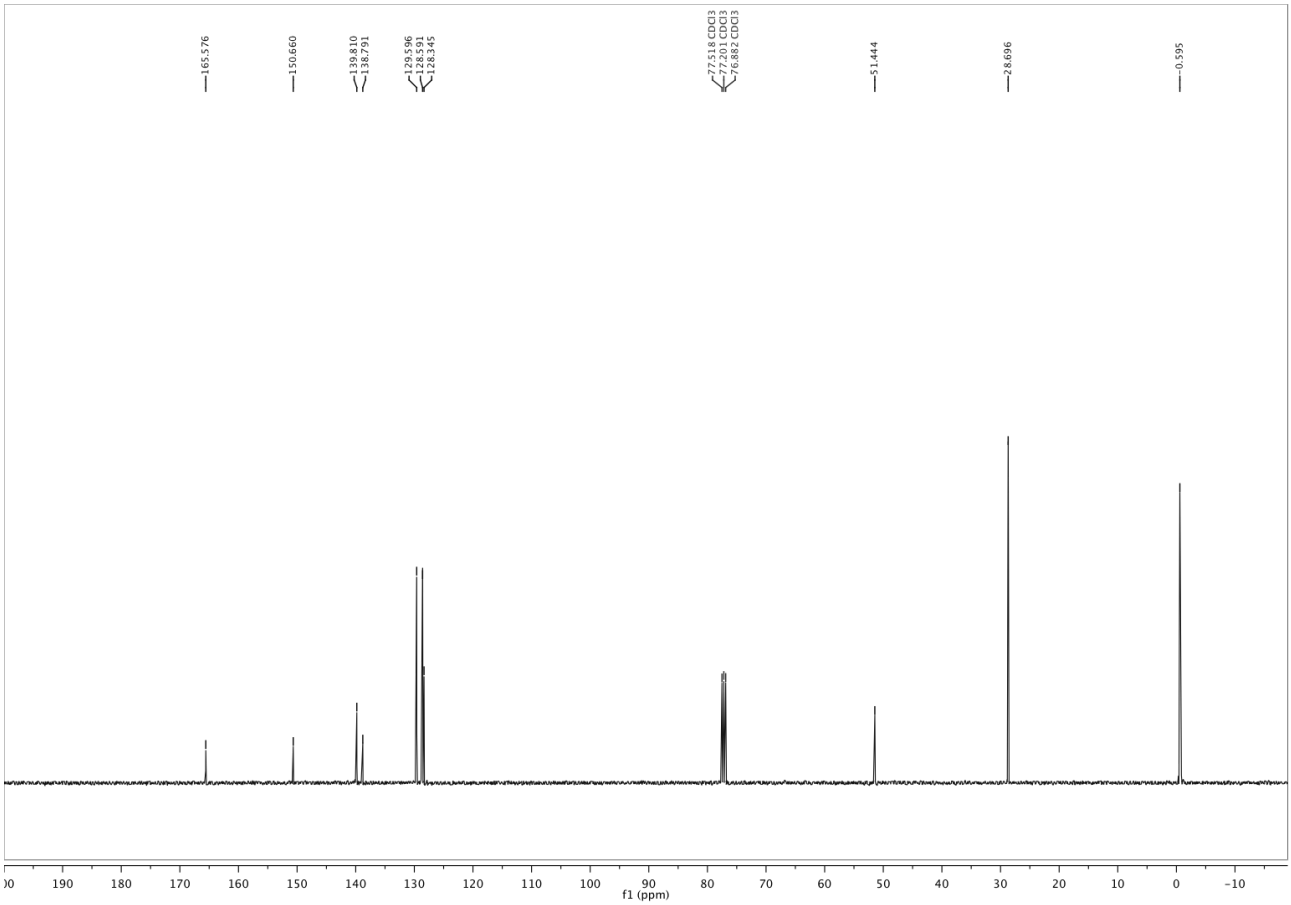
165.576
150.660
139.810
138.791
129.596
128.591
128.345
77.518 CDCl3
77.201 CDCl3
76.882 CDCl3
51.444
28.696
0.595
f1 (ppm)

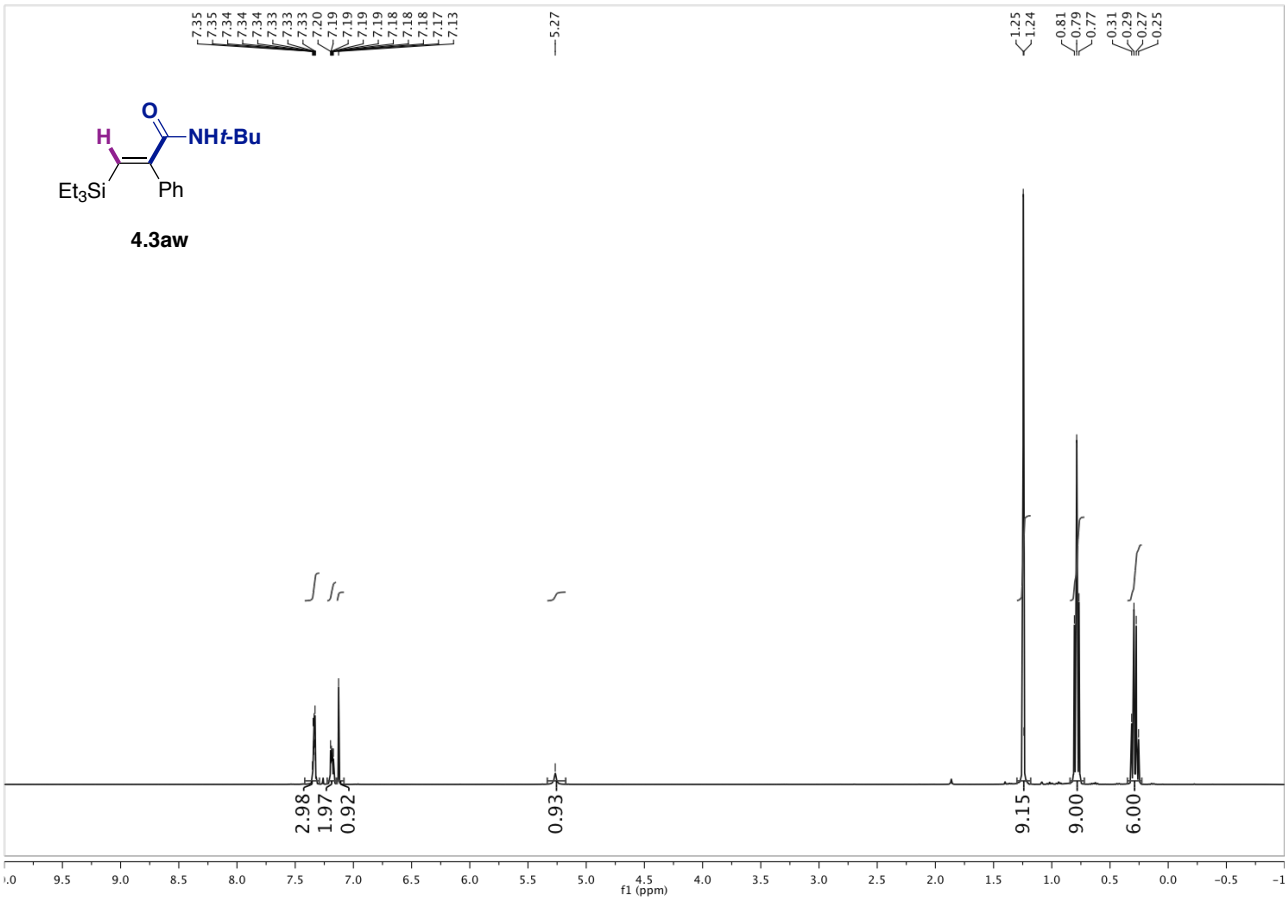
7.35
7.35
7.34
7.34
7.34
7.33
7.33
7.33
7.20
7.19
7.19
7.19
7.19
7.18
7.18
7.18
7.17
7.13
5.27
1.25
1.24
0.81
0.79
0.77
0.31
0.29
0.27
0.25
O
H
NHt-Bu
Et3Si
Ph
4.3aw
2.98
1.97
0.92
0.93
9.15
9.00
6.00
f1 (ppm)

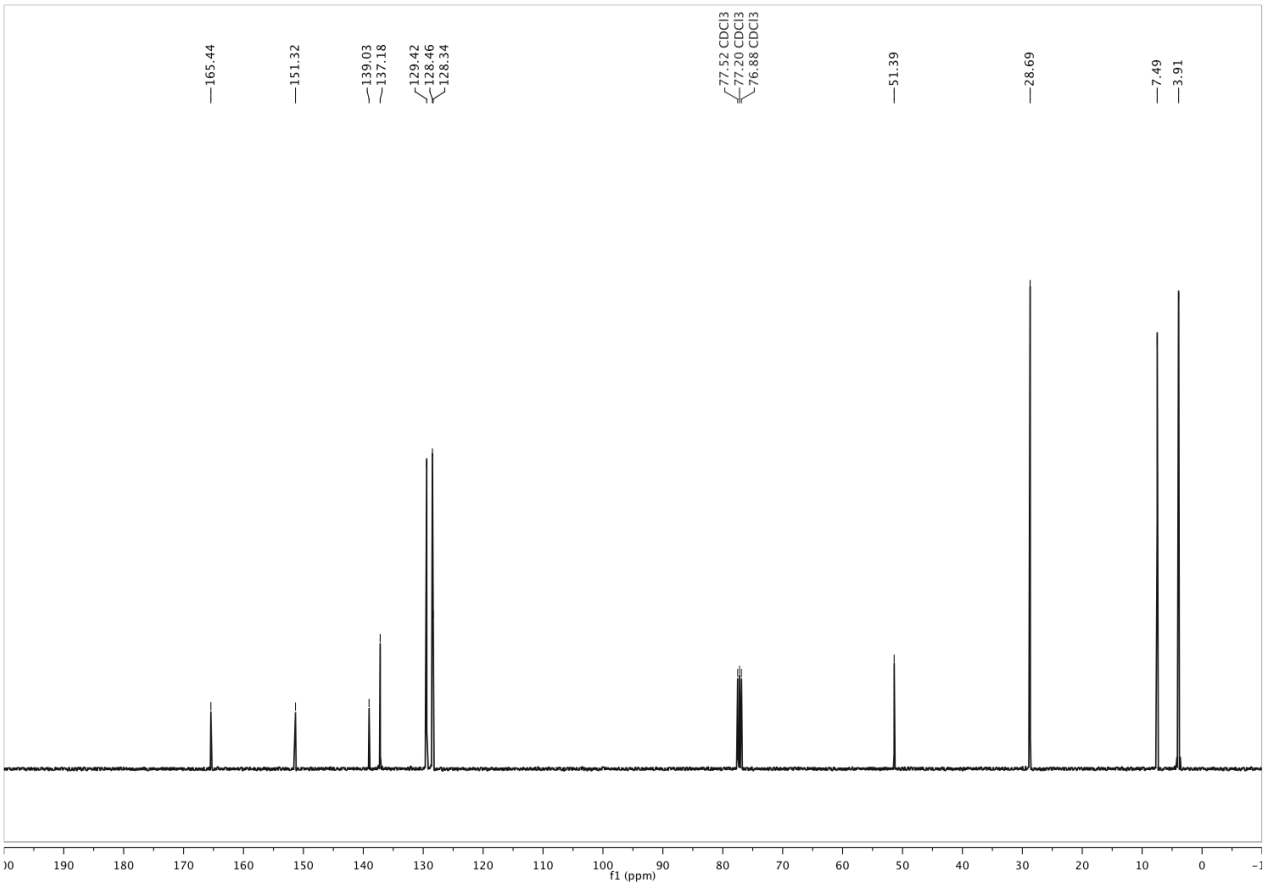
165.44
151.32
139.03
137.18
129.42
128.46
128.34
77.52 CDCl3
77.20 CDCl3
76.88 CDCl3
51.39
28.69
7.49
3.91
f1 (ppm)

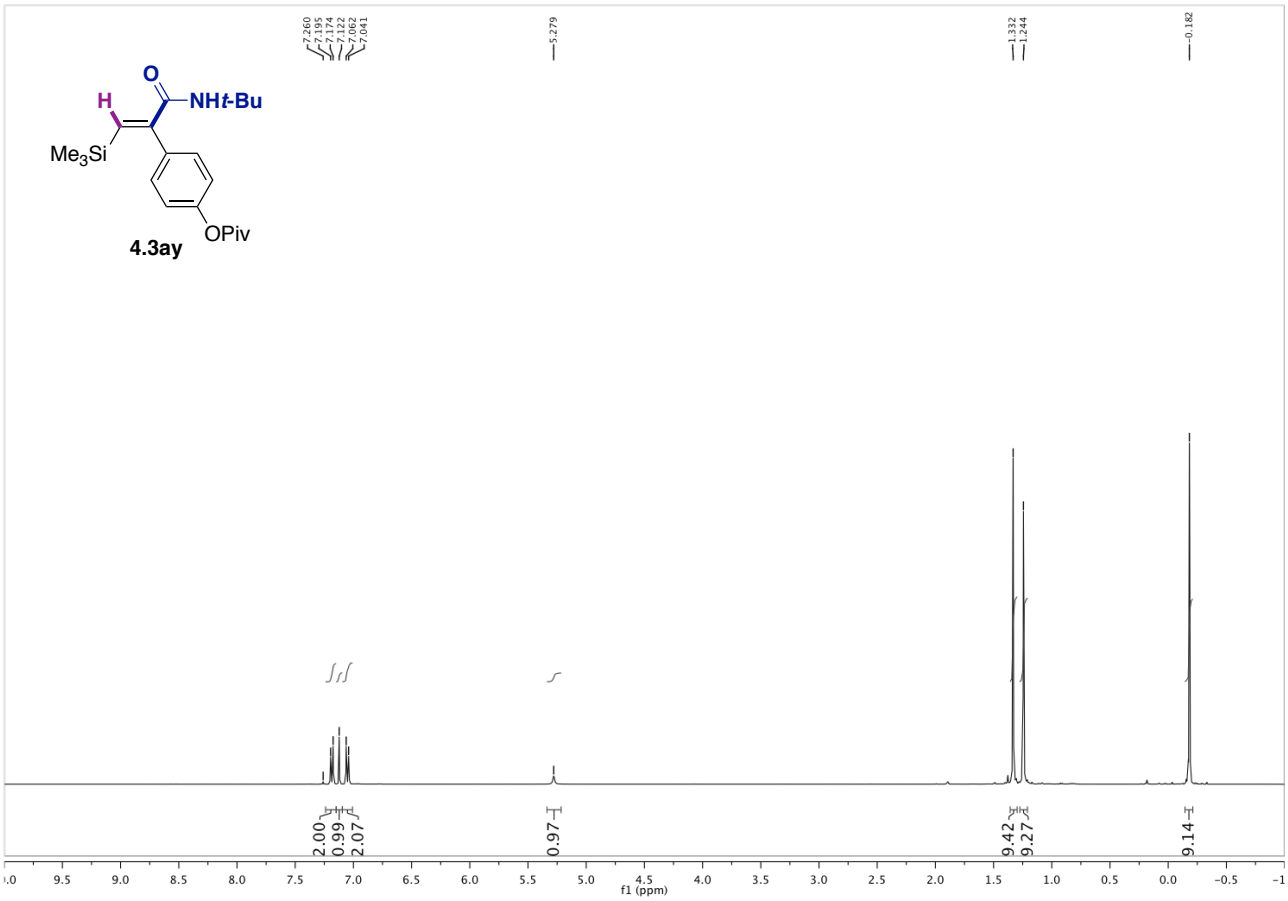
7.260
7.195
7.174
7.122
7.062
7.041
5.279
1.332
1.244
0.182
O
H
NHt-Bu
Me3Si
OPiv
4.3ay
2.00
0.99
2.07
0.97
9.42
9.27
9.14
f1 (ppm)

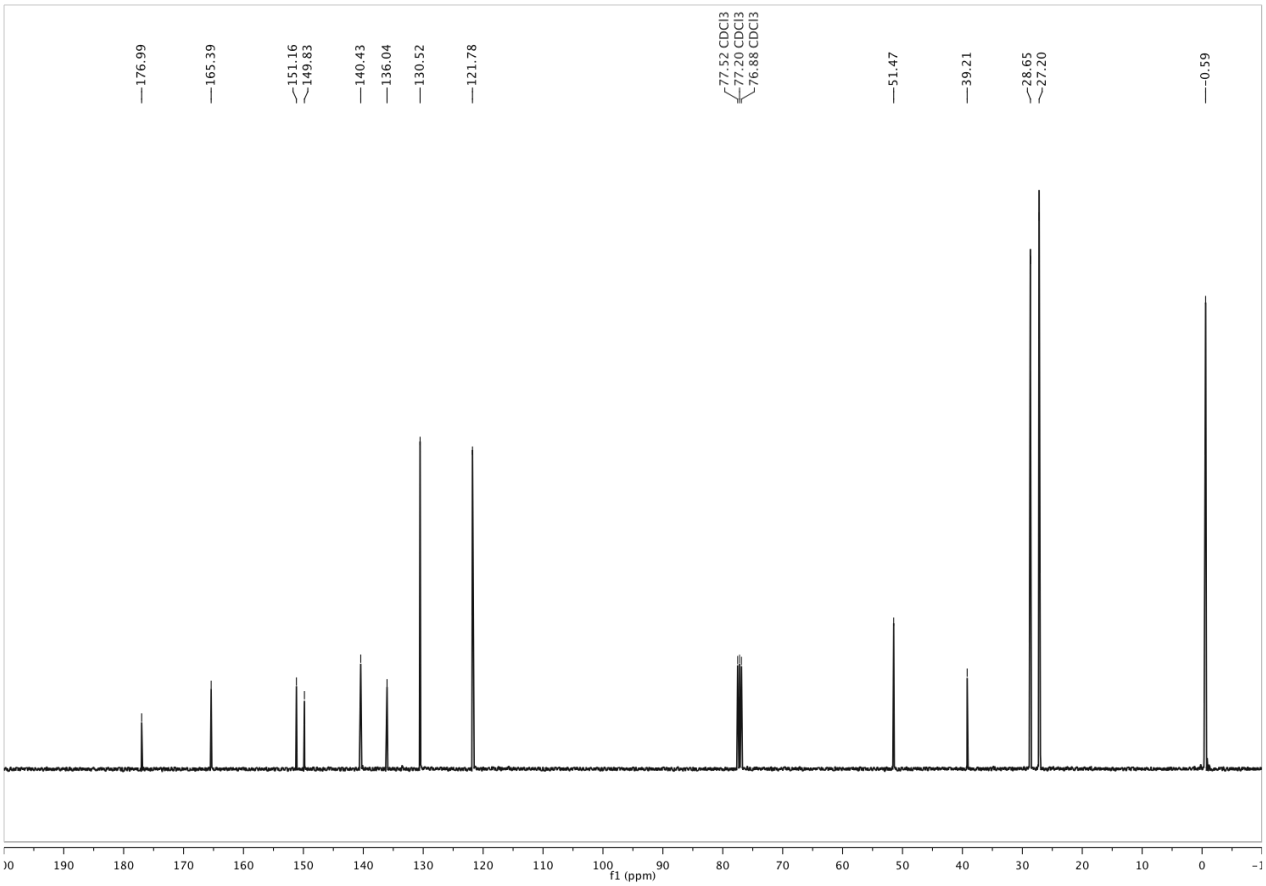
176.99
165.39
151.16
149.83
140.43
136.04
130.52
121.78
77.52 CDCl3
77.20 CDCl3
76.88 CDCl3
51.47
39.21
28.65
27.20
0.59
f1 (ppm)

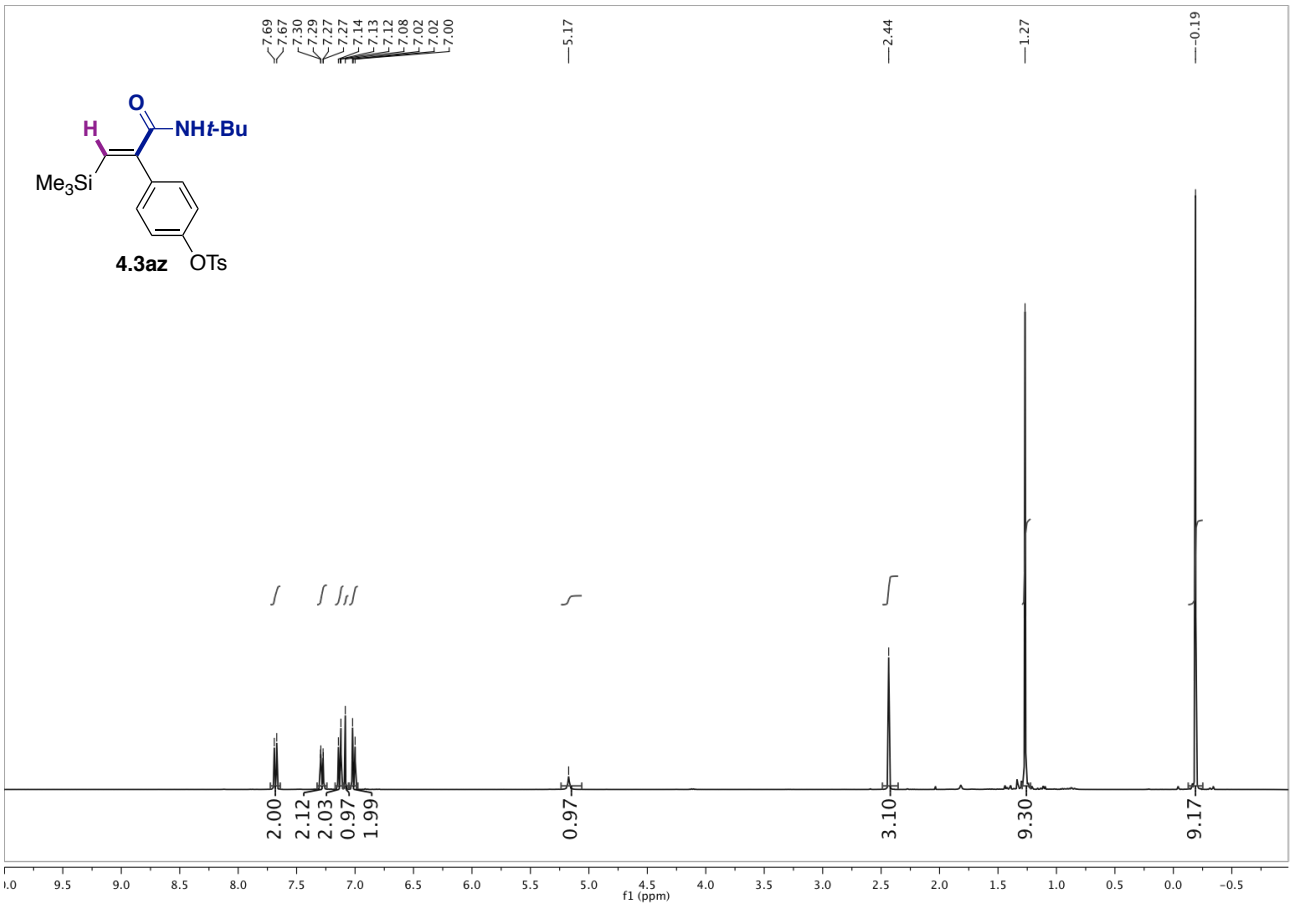
7.69
7.67
7.30
7.29
7.27
7.27
7.14
7.13
7.12
7.08
7.02
7.02
7.00
5.17
2.44
1.27
0.19
O
NHt-Bu
H
Me3Si
4.3az
OTs
2.00
2.12
2.03
0.97
1.99
0.97
3.10
9.30
9.17
f1 (ppm)

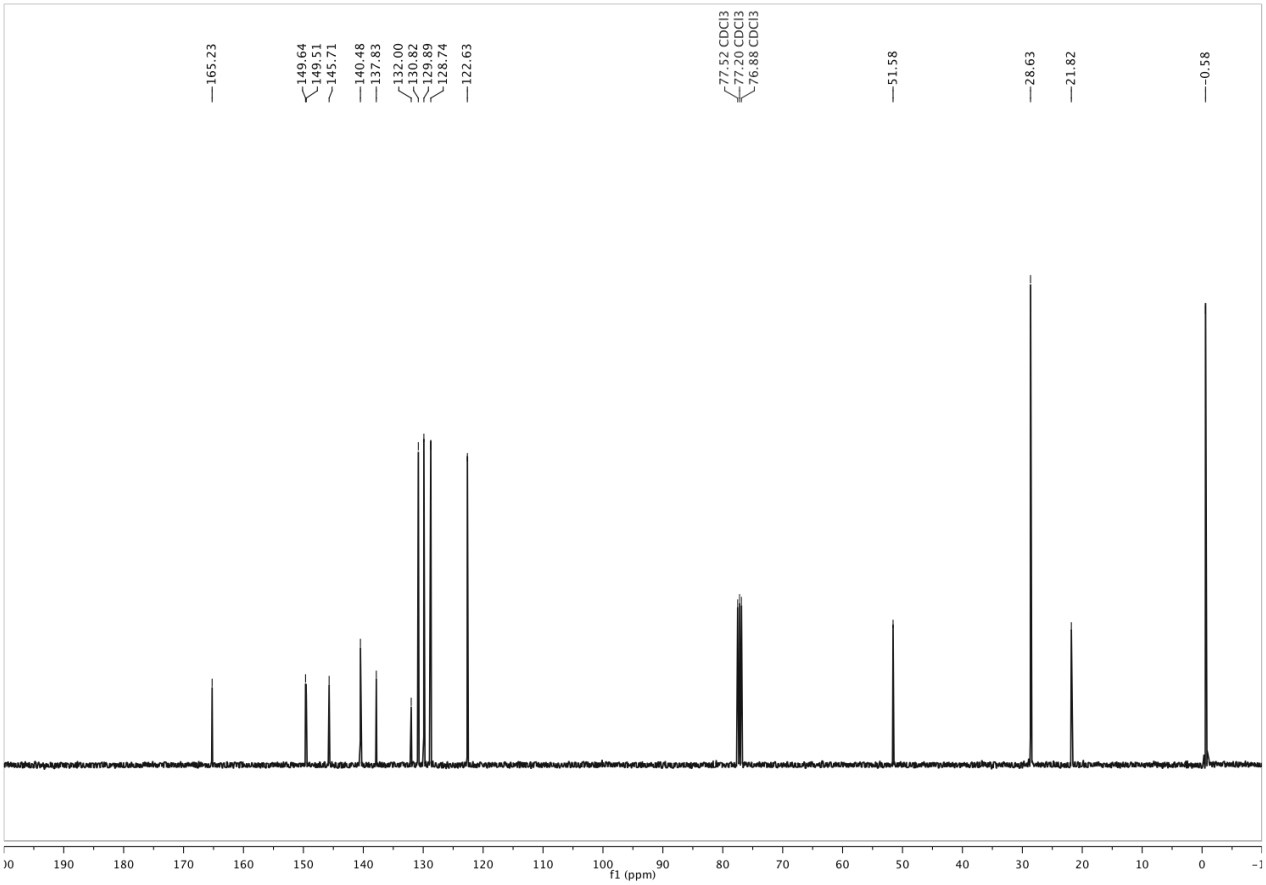
165.23
149.64
149.51
145.71
140.48
137.83
132.00
130.82
129.89
128.74
122.63
77.52 CDCl3
77.20 CDCl3
76.88 CDCl3
51.58
28.63
21.82
0.58
f1 (ppm)

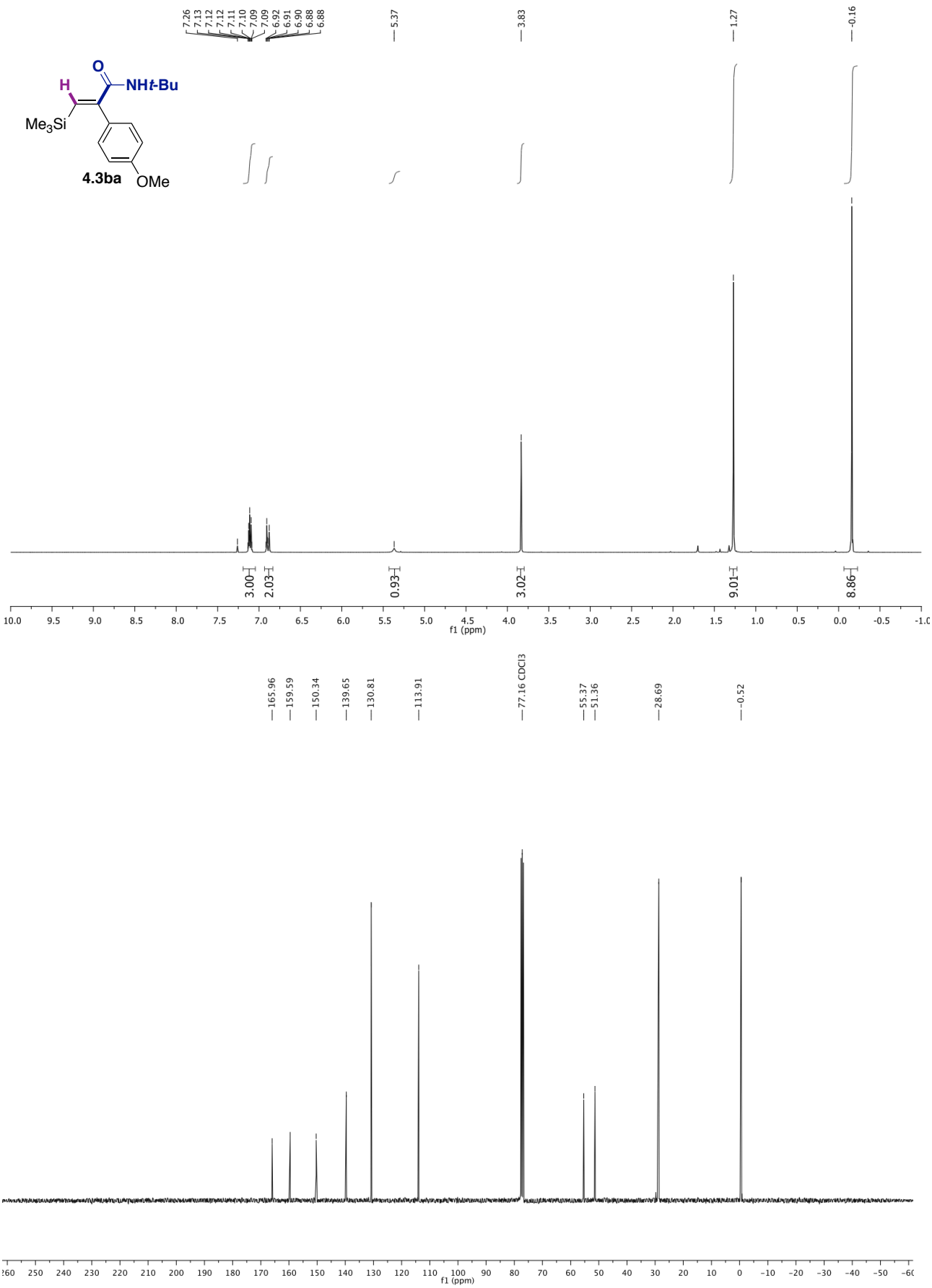
7.26
7.13
7.12
7.12
7.11
7.10
7.09
7.09
6.92
6.91
6.90
6.88
6.88
5.37
3.83
1.27
-0.16
O
H
NHt-Bu
Me3Si
4.3ba
OMe
3.00
2.03
0.93
3.02
9.01
8.86
f1 (ppm)
165.96
159.59
150.34
139.65
130.81
113.91
77.16 CDCl3
55.37
51.36
28.69
-0.52
f1 (ppm)

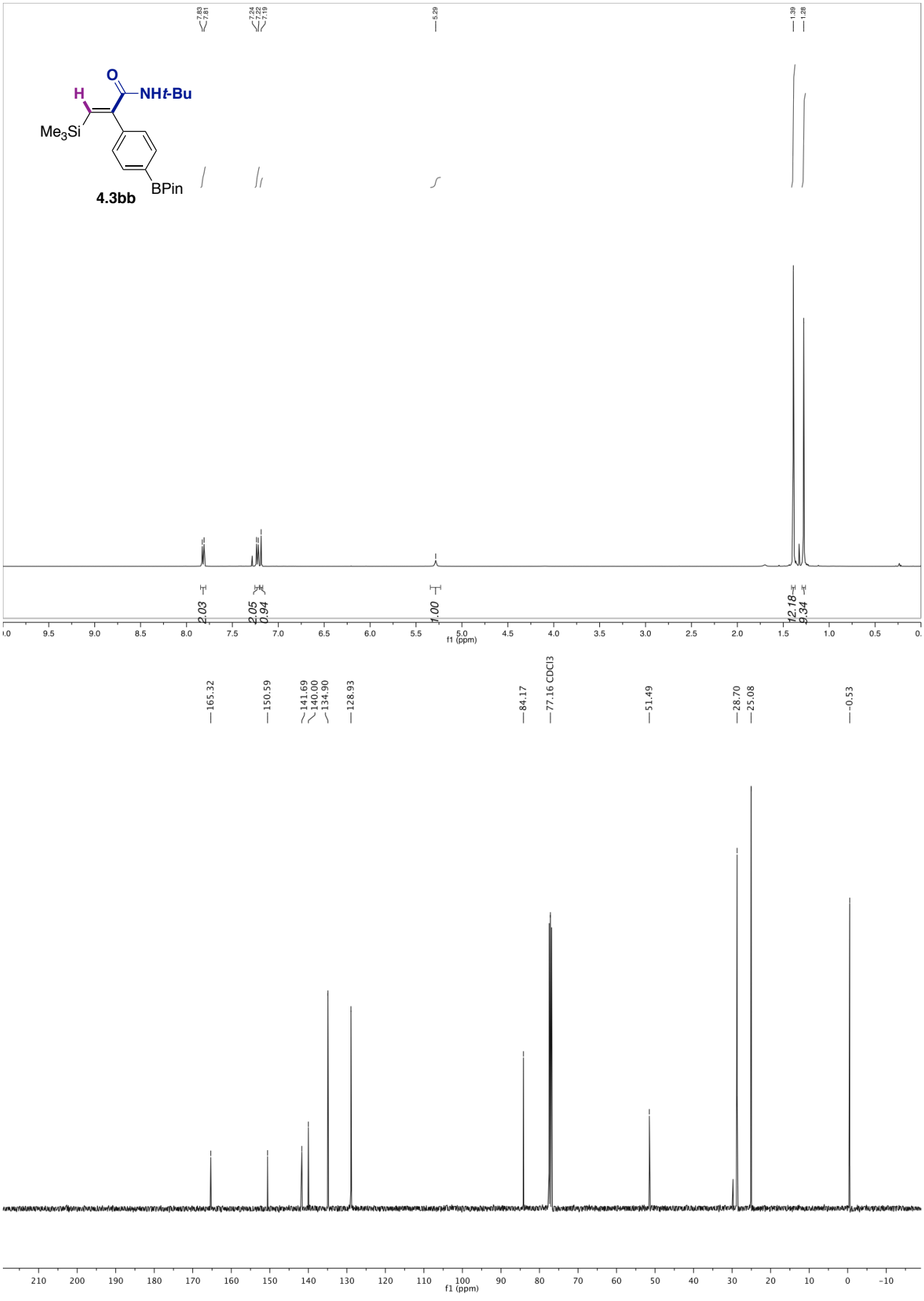
7.83
7.81
7.24
7.22
7.19
5.29
1.39
1.28
O
H
NHt-Bu
Me3Si
BPin
4.3bb
2.03
2.05
0.94
1.00
12.18
9.34
f1 (ppm)
165.32
150.59
141.69
140.00
134.90
128.93
84.17
77.16 CDCl3
51.49
28.70
25.08
-0.53
f1 (ppm)

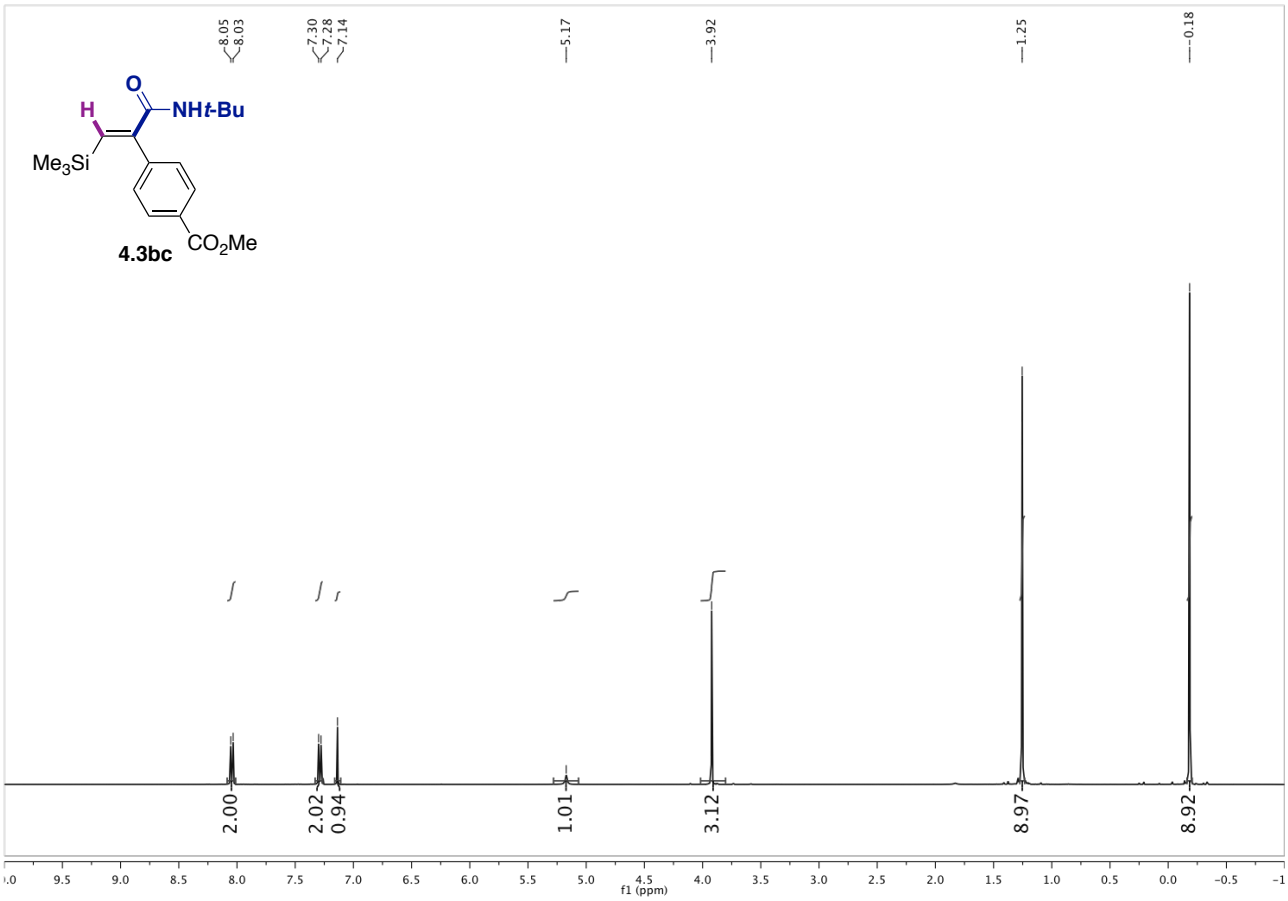
8.05
8.03
7.30
7.28
7.14
5.17
3.92
1.25
0.18
O
H
NHt-Bu
Me3Si
CO2Me
4.3bc
2.00
2.02
0.94
1.01
3.12
8.97
8.92
f1 (ppm)

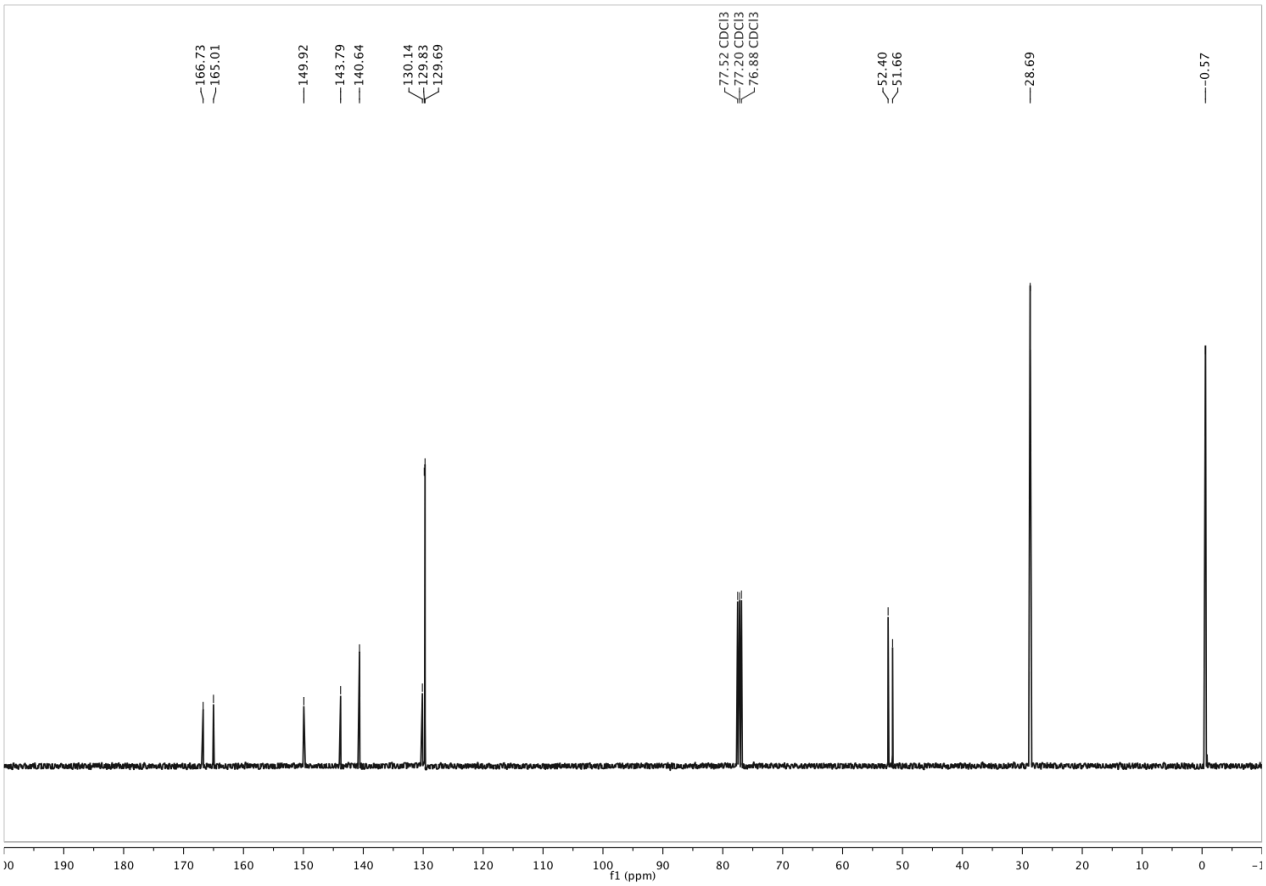
166.73
165.01
149.92
143.79
140.64
130.14
129.83
129.69
77.52 CDCl3
77.20 CDCl3
76.88 CDCl3
52.40
51.66
28.69
0.57
f1 (ppm)

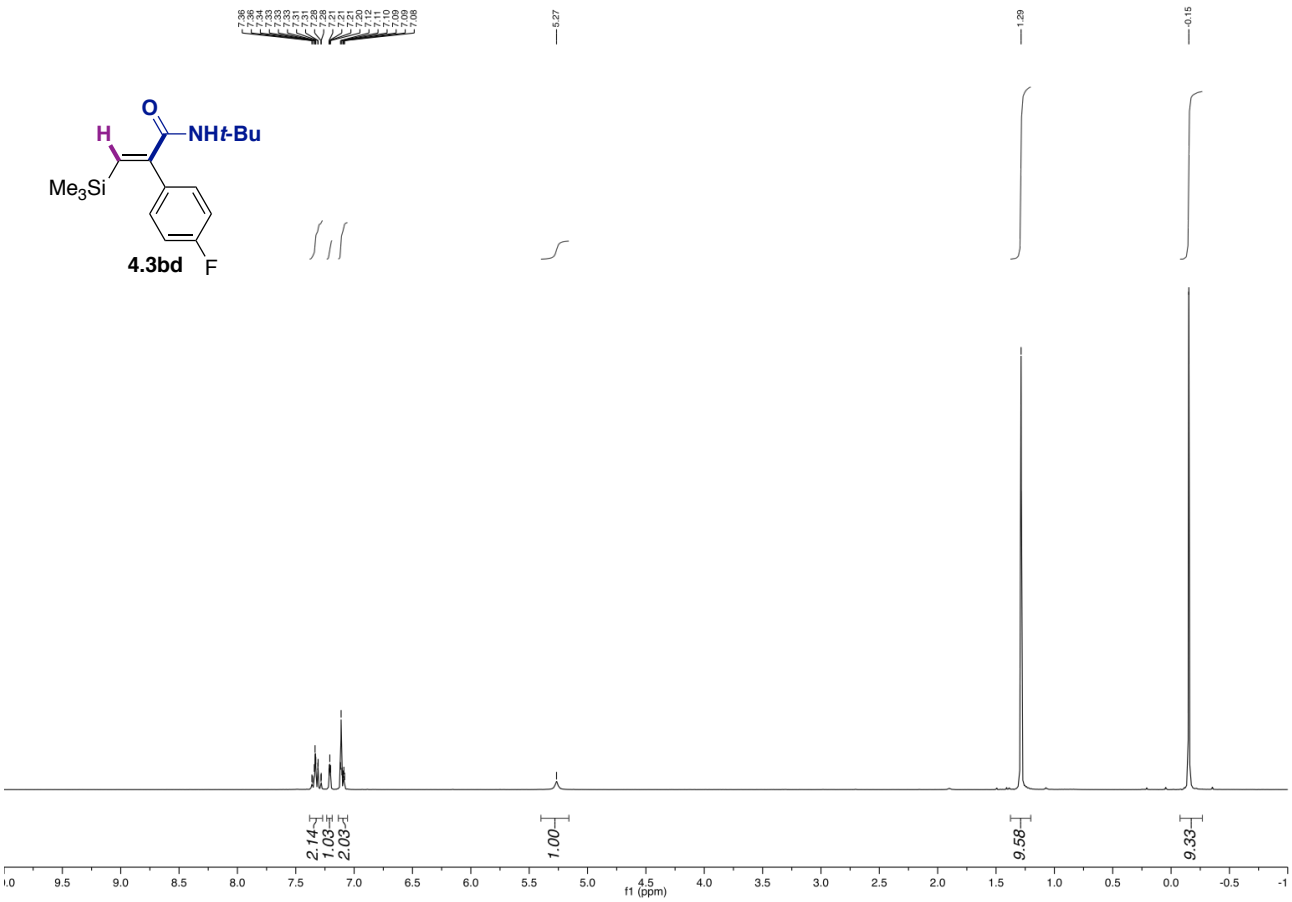
O
NHt-Bu
H
Me3Si
4.3bd
F
5.27
1.29
0.15
2.14
1.03
2.03
1.00
9.58
9.33
f1 (ppm)

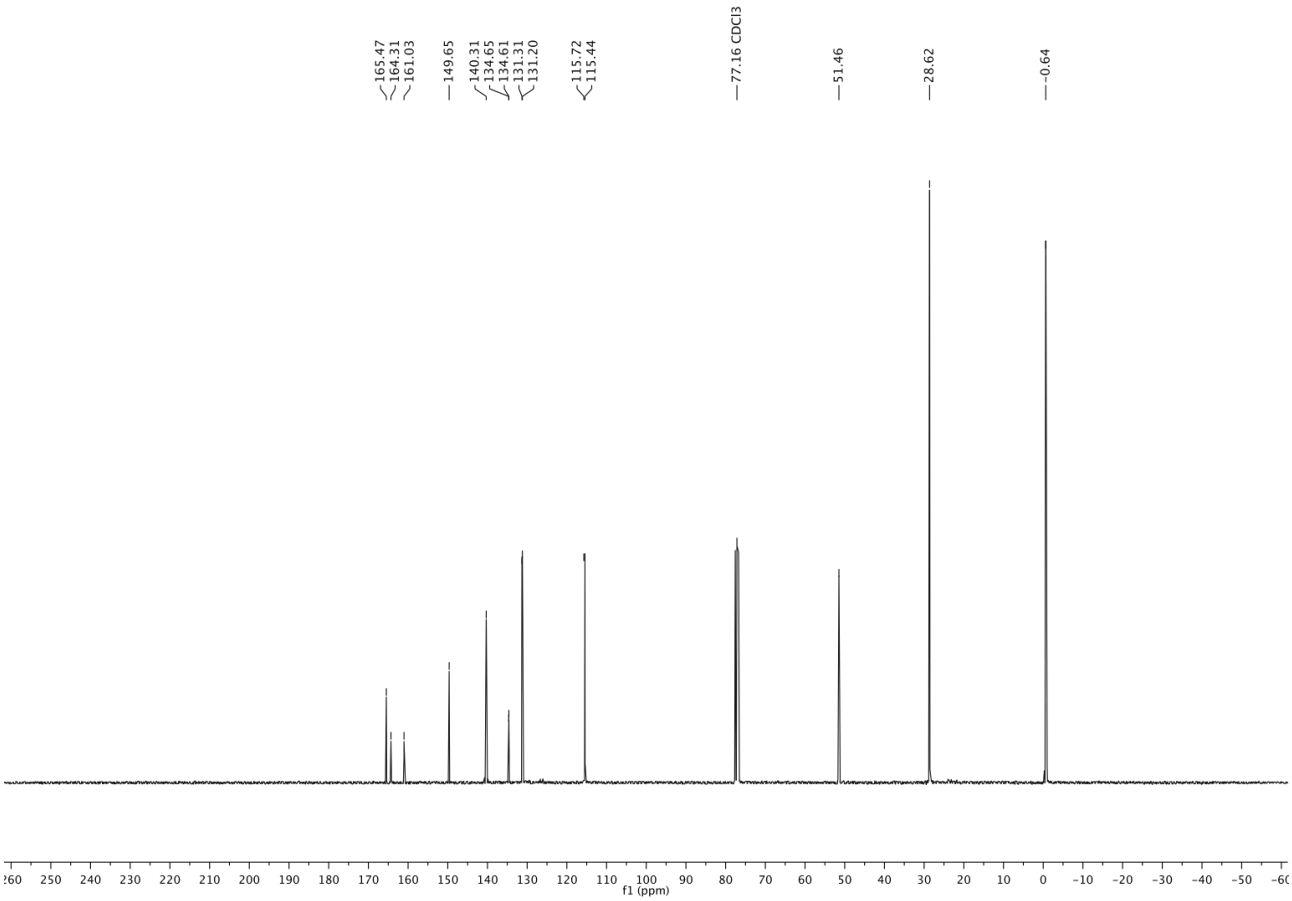
165.47
164.31
161.03
149.65
140.31
134.65
134.61
131.31
131.20
115.72
115.44
77.16 CDCl3
51.46
28.62
0.64
f1 (ppm)

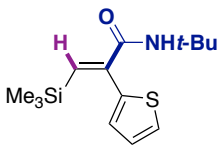
O
NH*t*-Bu
H
Me3Si
S

4.3bf

7.39
7.39
7.38
7.37
7.36
7.06
7.05
7.05
7.04
6.96
6.95
6.95
6.94
5.70
1.32
0.06
0.98
1.08
1.01
1.00
0.97
9.54
9.27
f1 (ppm)

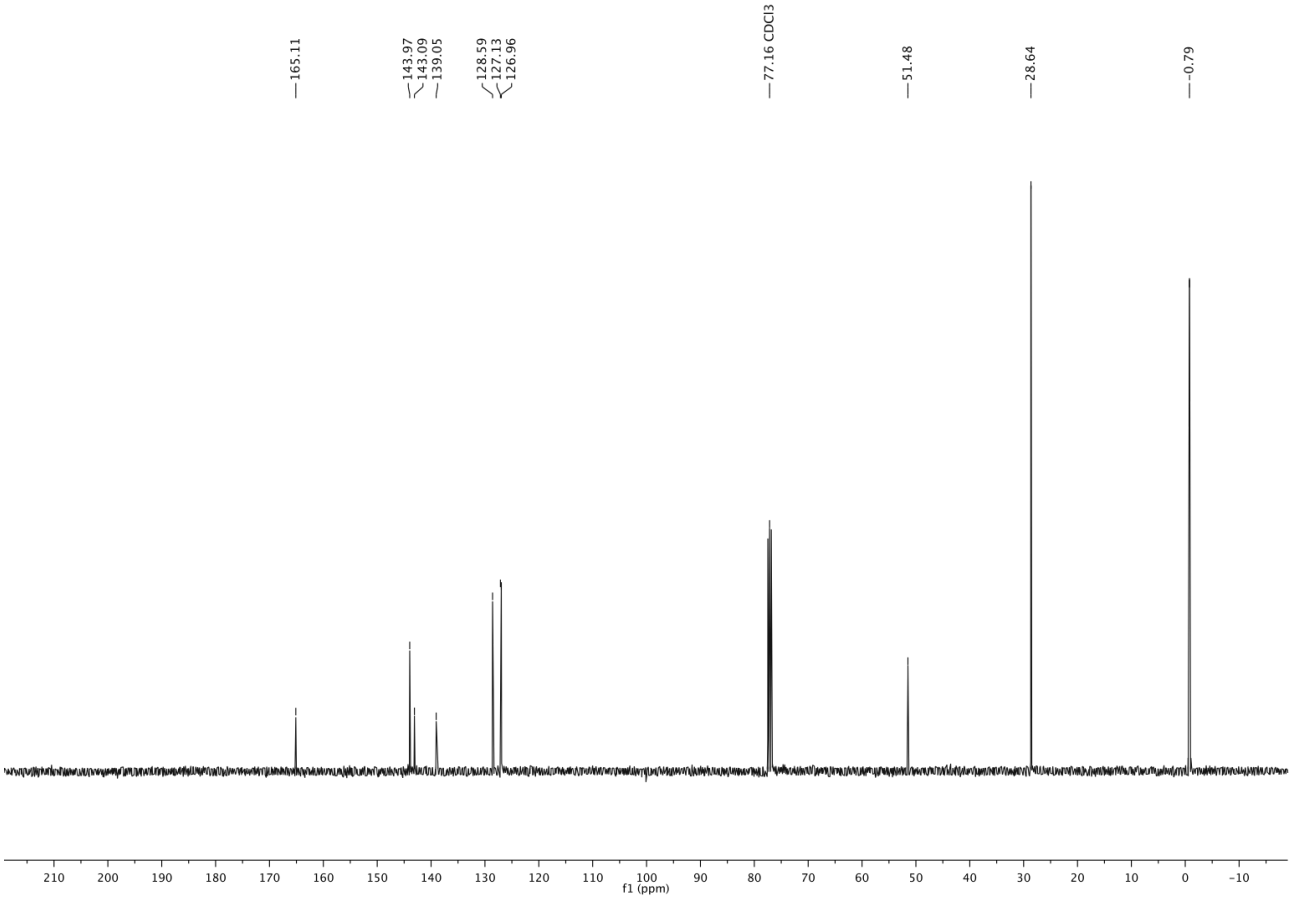
165.11
143.97
143.09
139.05
128.59
127.13
126.96
77.16 CDCl3
51.48
28.64
-0.79
f1 (ppm)

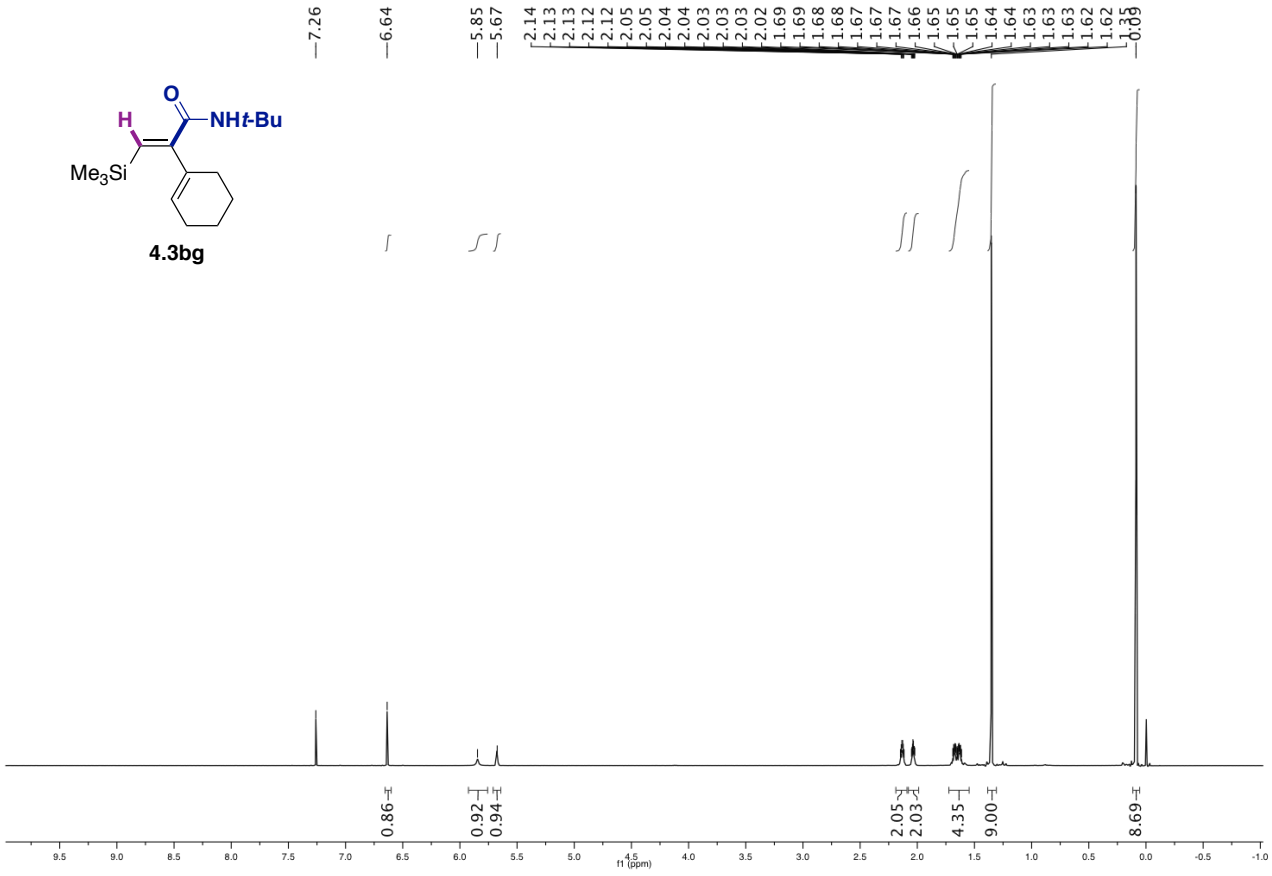
7.26
6.64
5.85
5.67
2.14
2.13
2.13
2.12
2.12
2.05
2.05
2.04
2.04
2.03
2.03
2.03
2.02
1.69
1.69
1.68
1.68
1.67
1.67
1.67
1.66
1.65
1.65
1.65
1.64
1.64
1.63
1.63
1.62
1.62
1.35
0.09
O
NHt-Bu
H
Me3Si
4.3bg
0.86
0.92
0.94
2.05
2.03
4.35
9.00
8.69
f1 (ppm)

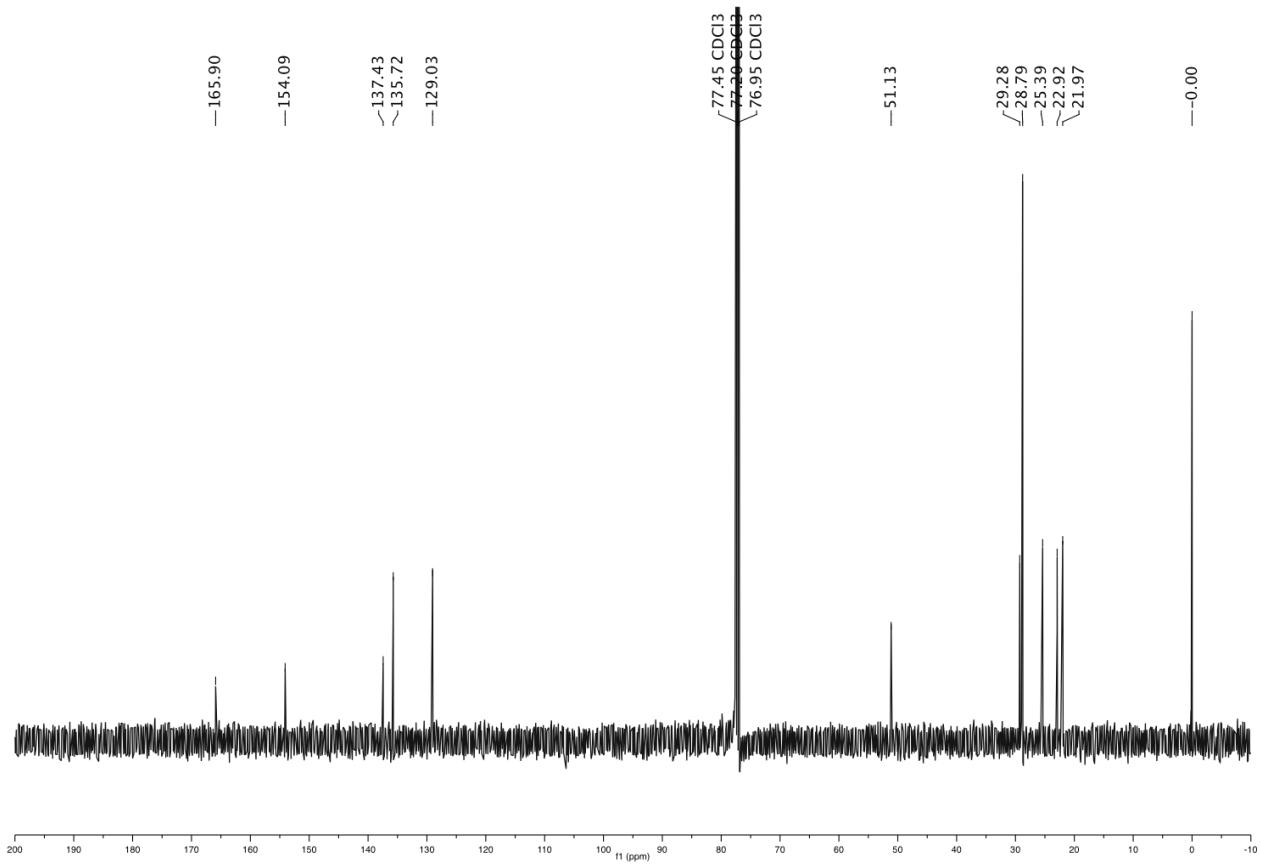
165.90
154.09
137.43
135.72
129.03
77.45 CDCl3
77.20 CDCl3
76.95 CDCl3
51.13
29.28
28.79
25.39
22.92
21.97
0.00
f1 (ppm)

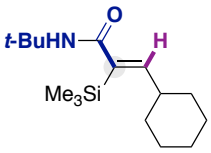
t-BuHN
O
H
Me3Si

4.3bh,, *E/Z* = 1.8:1

7.26
6.11
6.09
5.57
5.55
5.23
5.03
2.35
2.32
2.30
2.20
2.18
2.15
2.13
1.92
1.72
1.70
1.67
1.64
1.62
1.60
1.59
1.36
1.34
1.27
1.25
1.22
1.19
1.17
1.11
1.09
1.05
0.18
0.10
1.00
0.56
0.98
0.53
0.62
1.07
8.97
15.87
9.77
9.29
5.29
f1 (ppm)

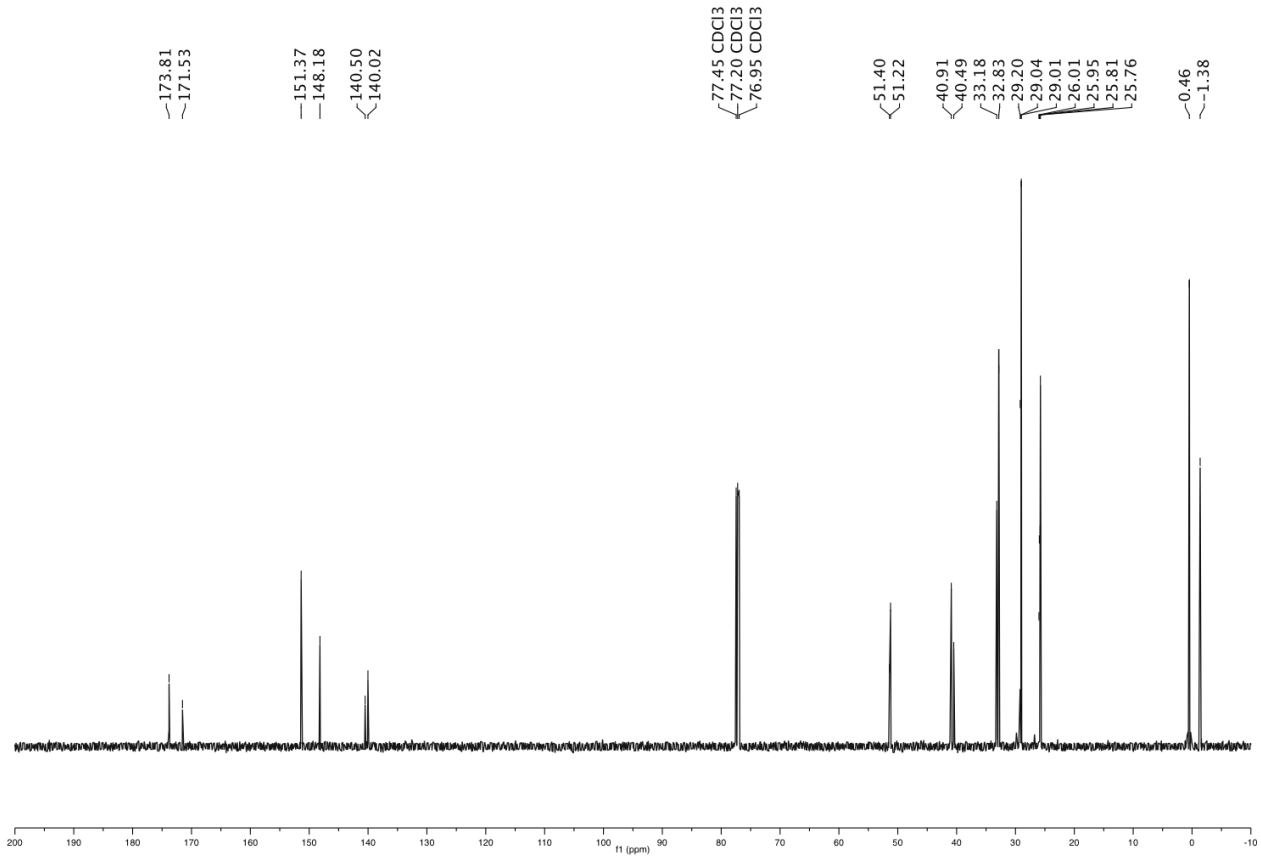
173.81
171.53
151.37
148.18
140.50
140.02
77.45 CDCl3
77.20 CDCl3
76.95 CDCl3
51.40
51.22
40.91
40.49
33.18
32.83
29.20
29.04
29.01
26.01
25.95
25.81
25.76
0.46
-1.38
f1 (ppm)

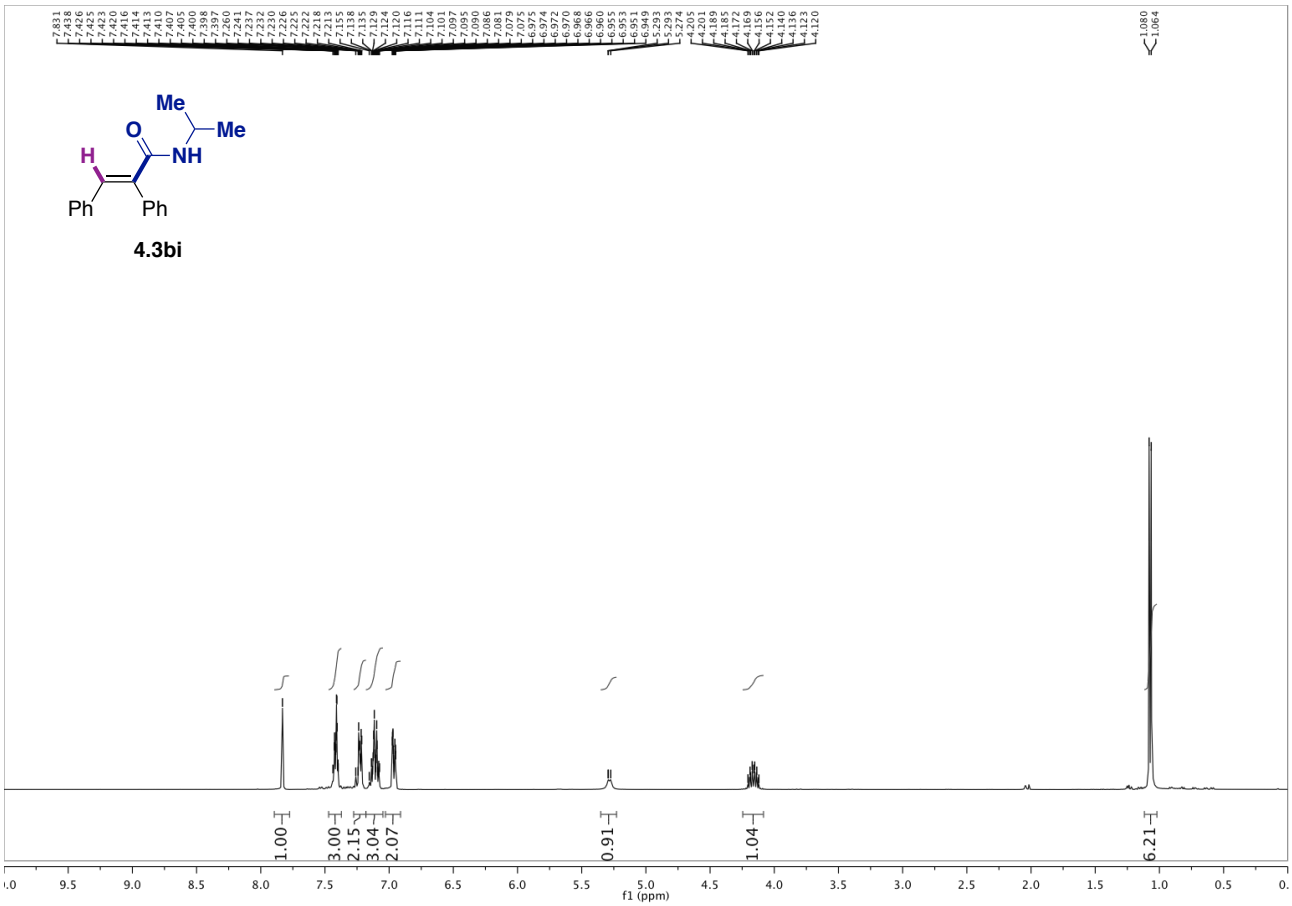
Me
O
Me
NH
H
Ph
Ph
4.3bi
1.00
3.00
2.15
3.04
2.07
0.91
1.04
6.21
f1 (ppm)

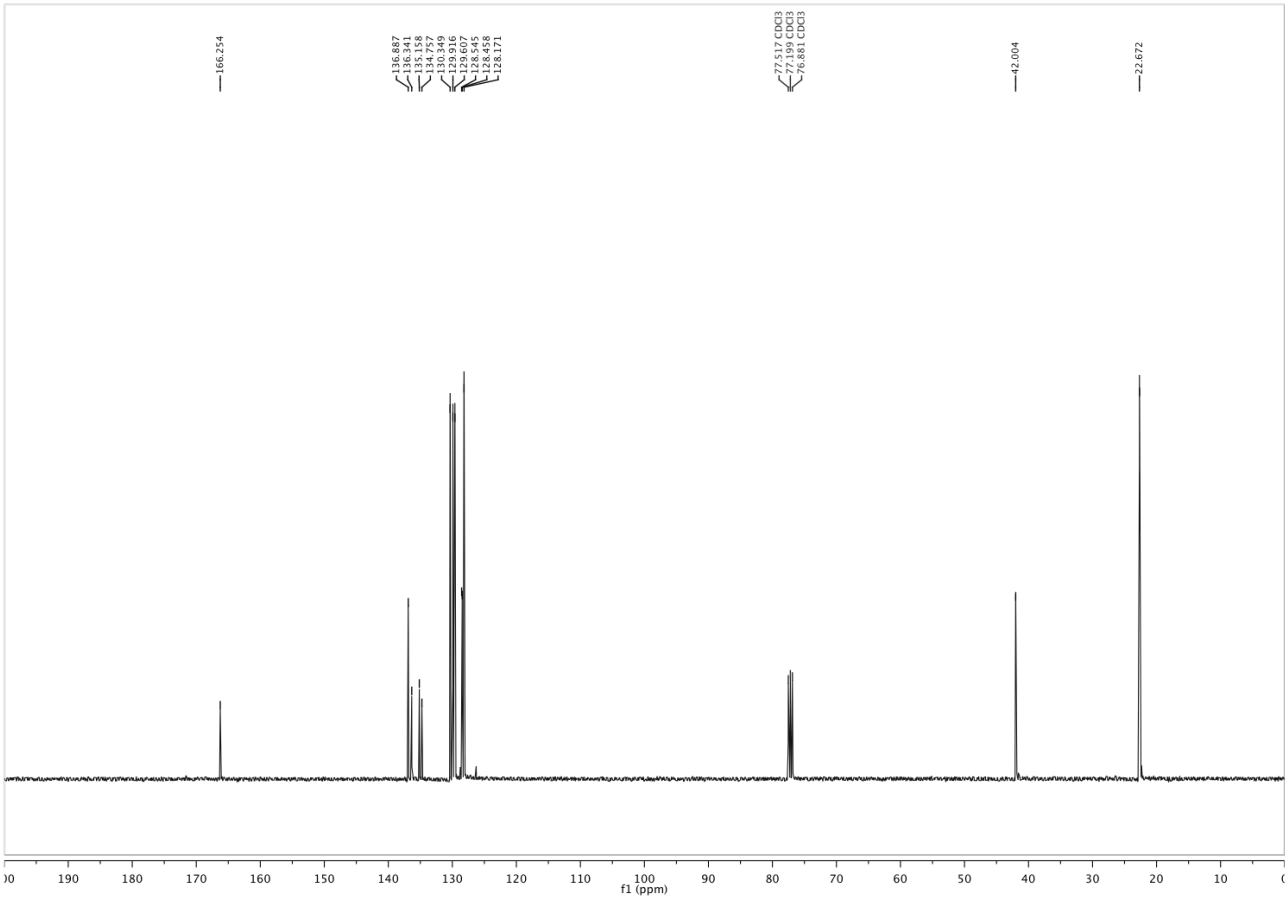
166.254
136.887
136.341
135.158
134.757
130.349
129.916
129.607
128.645
128.458
128.171
77.517 CDCl3
77.199 CDCl3
76.881 CDCl3
42.004
22.672
f1 (ppm)

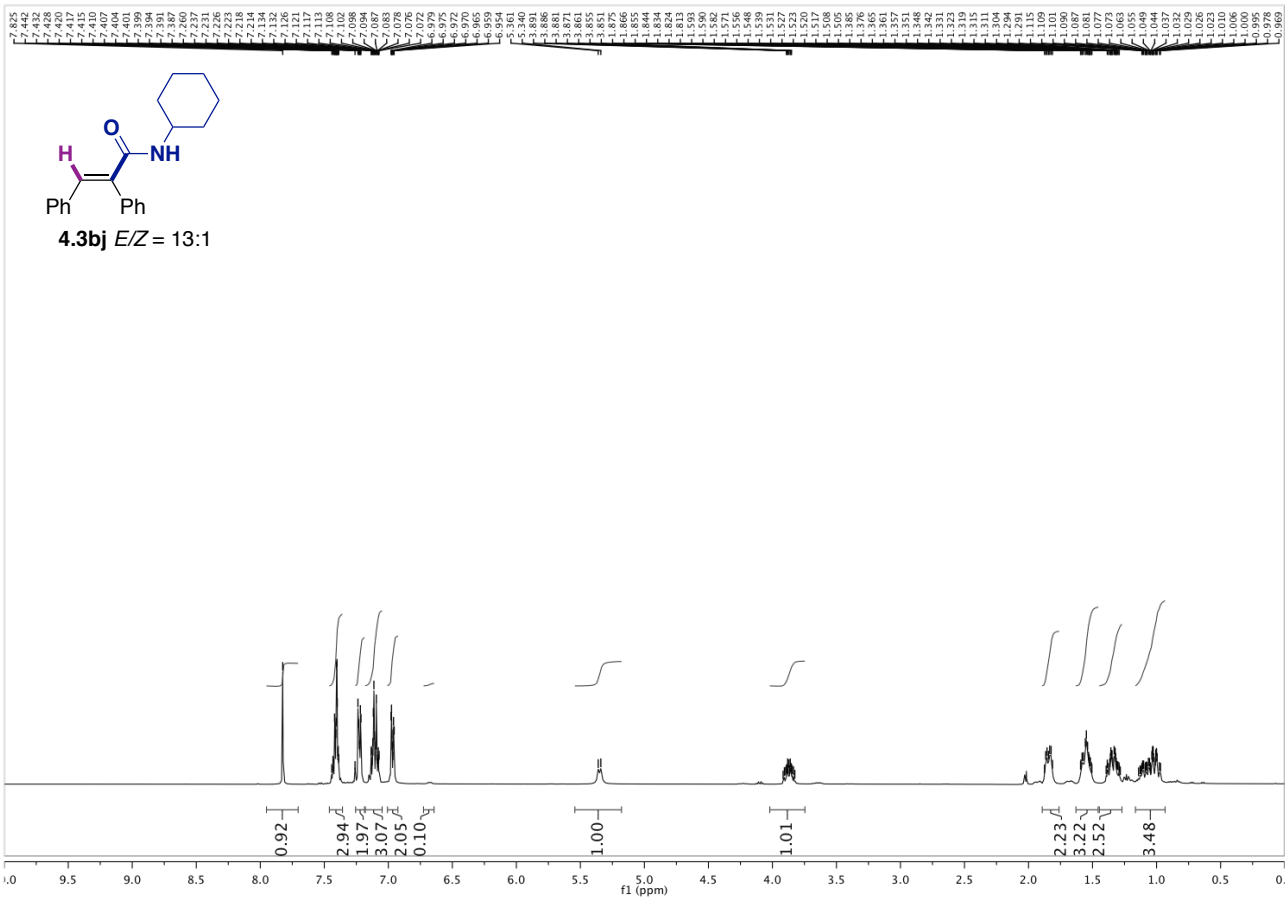
O
NH
H
Ph
Ph
0.92
2.94
1.97
3.07
2.05
0.10
1.00
1.01
2.23
3.22
2.52
3.48
f1 (ppm)

4.3bj *E/Z* = 13:1

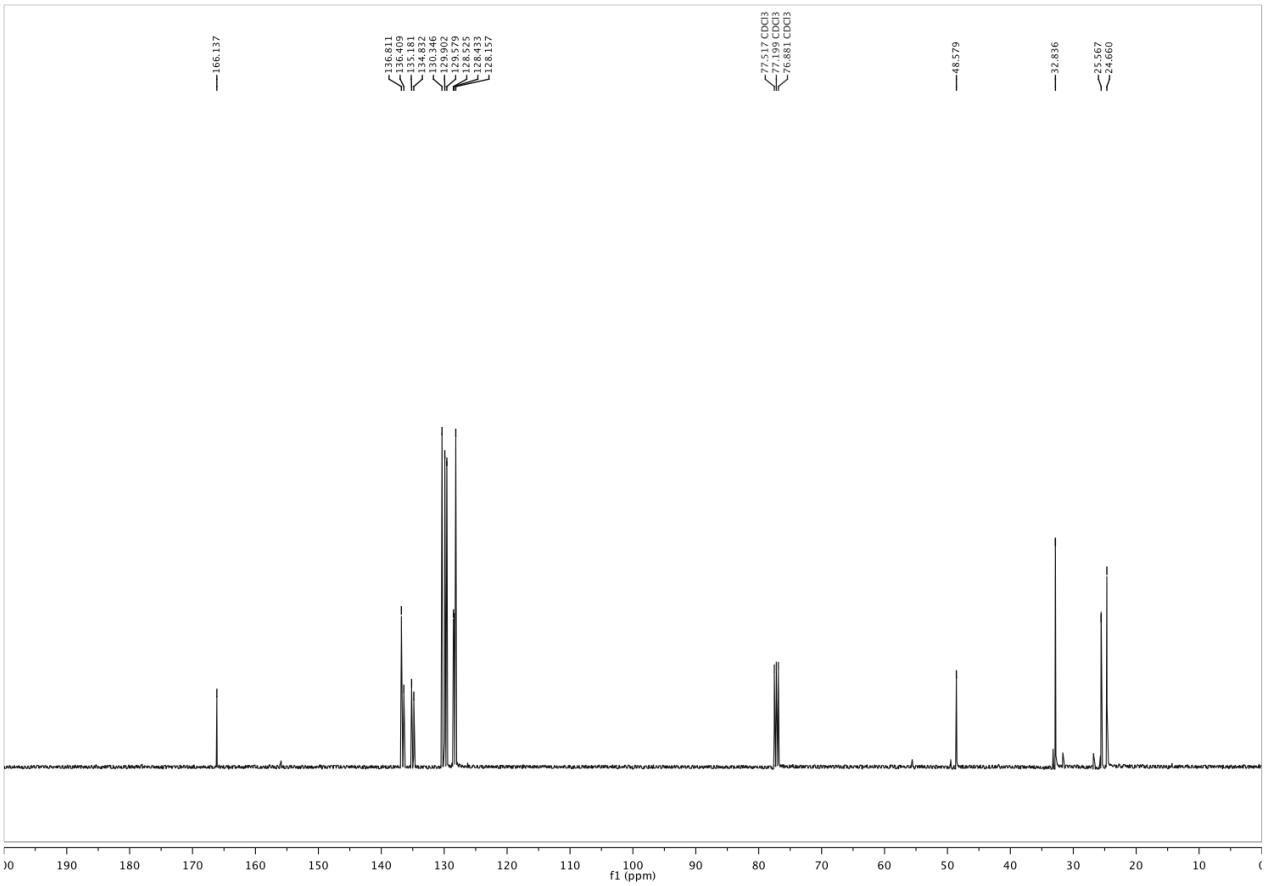
166.137
136.811
136.409
135.181
134.832
130.446
129.902
129.579
128.525
128.433
128.157
77.517 CDCl3
77.199 CDCl3
76.881 CDCl3
48.579
32.836
25.567
24.660
f1 (ppm)

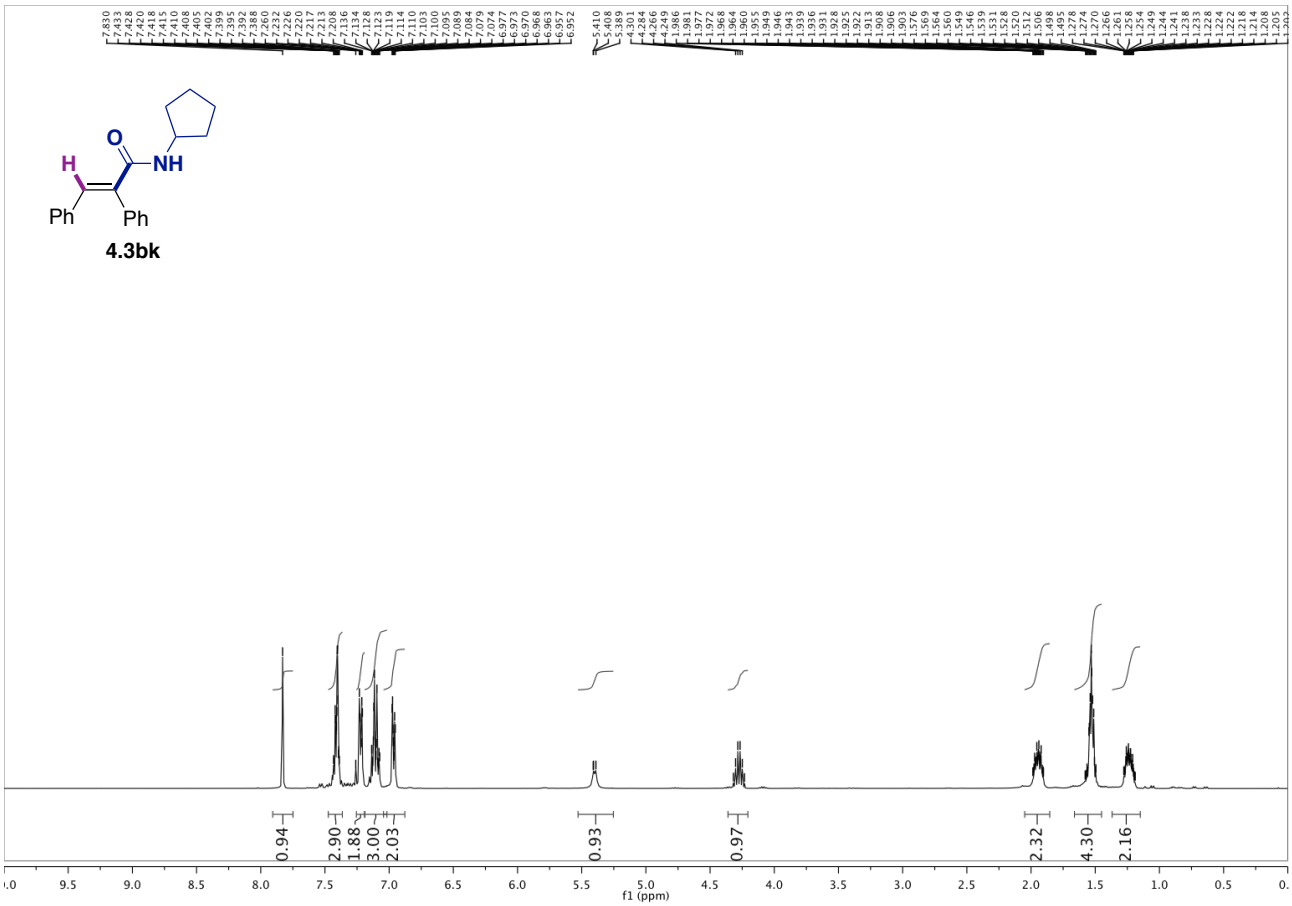
O
NH
H
Ph
Ph
4.3bk
0.94
2.90
1.88
3.00
2.03
0.93
0.97
2.32
4.30
2.16
f1 (ppm)

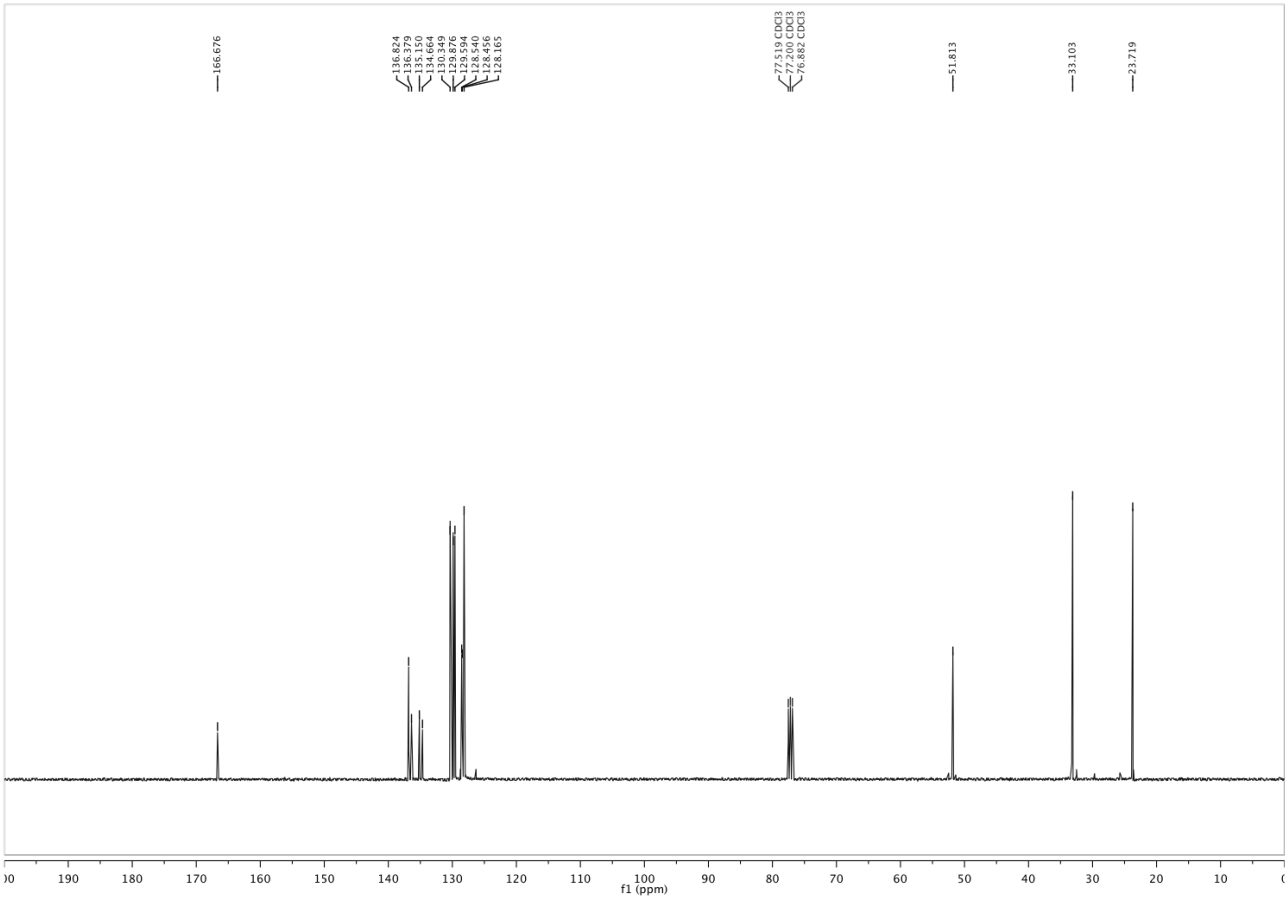
166.676
136.824
136.379
135.550
134.664
130.349
129.876
129.594
128.640
128.456
128.165
77.519 CDCl3
77.200 CDCl3
76.882 CDCl3
51.813
33.103
23.719
f1 (ppm)

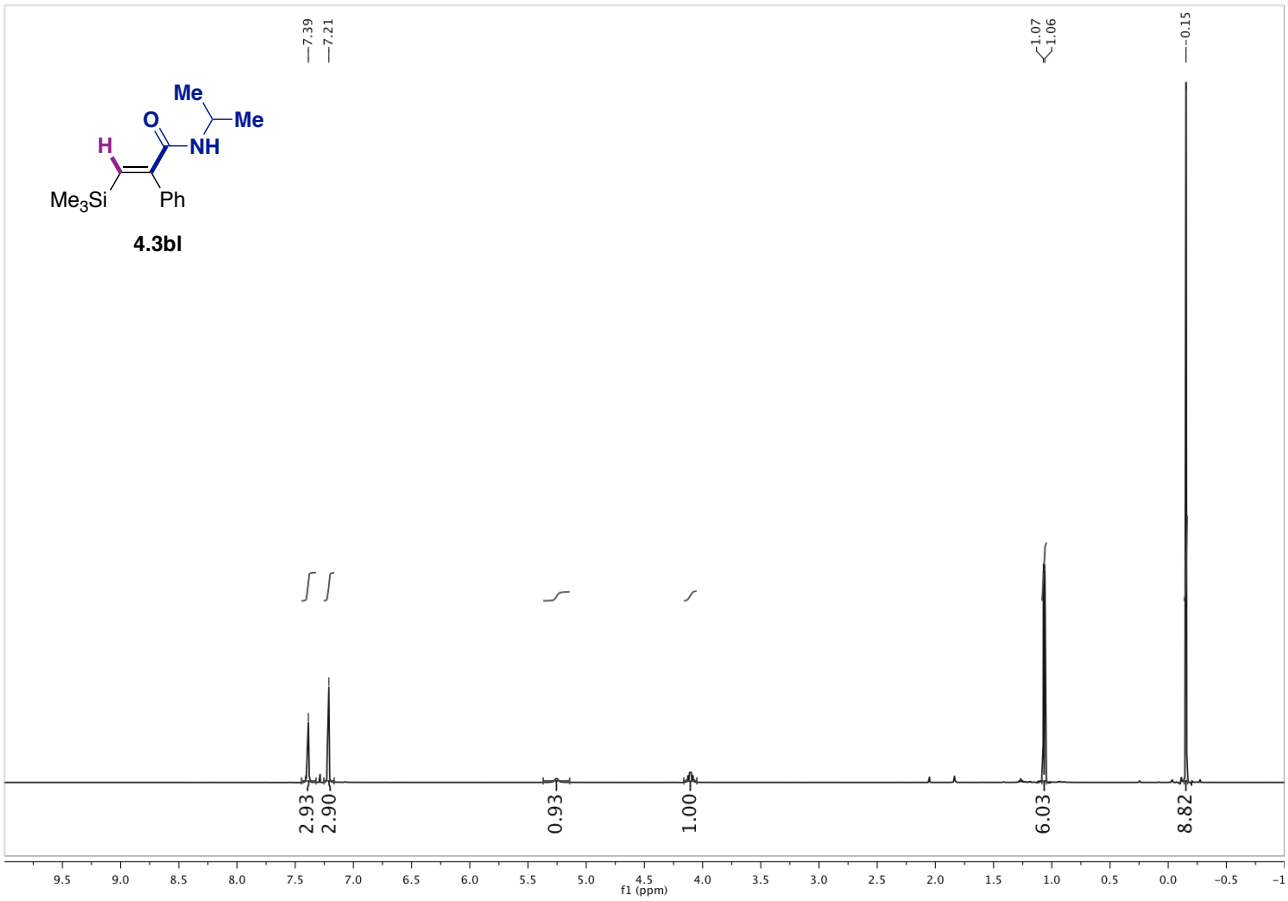
Me
Me
O
NH
H
Me3Si
Ph
7.39
7.21
1.07
1.06
0.15
2.93
2.90
0.93
1.00
6.03
8.82
f1 (ppm)

4.3bl

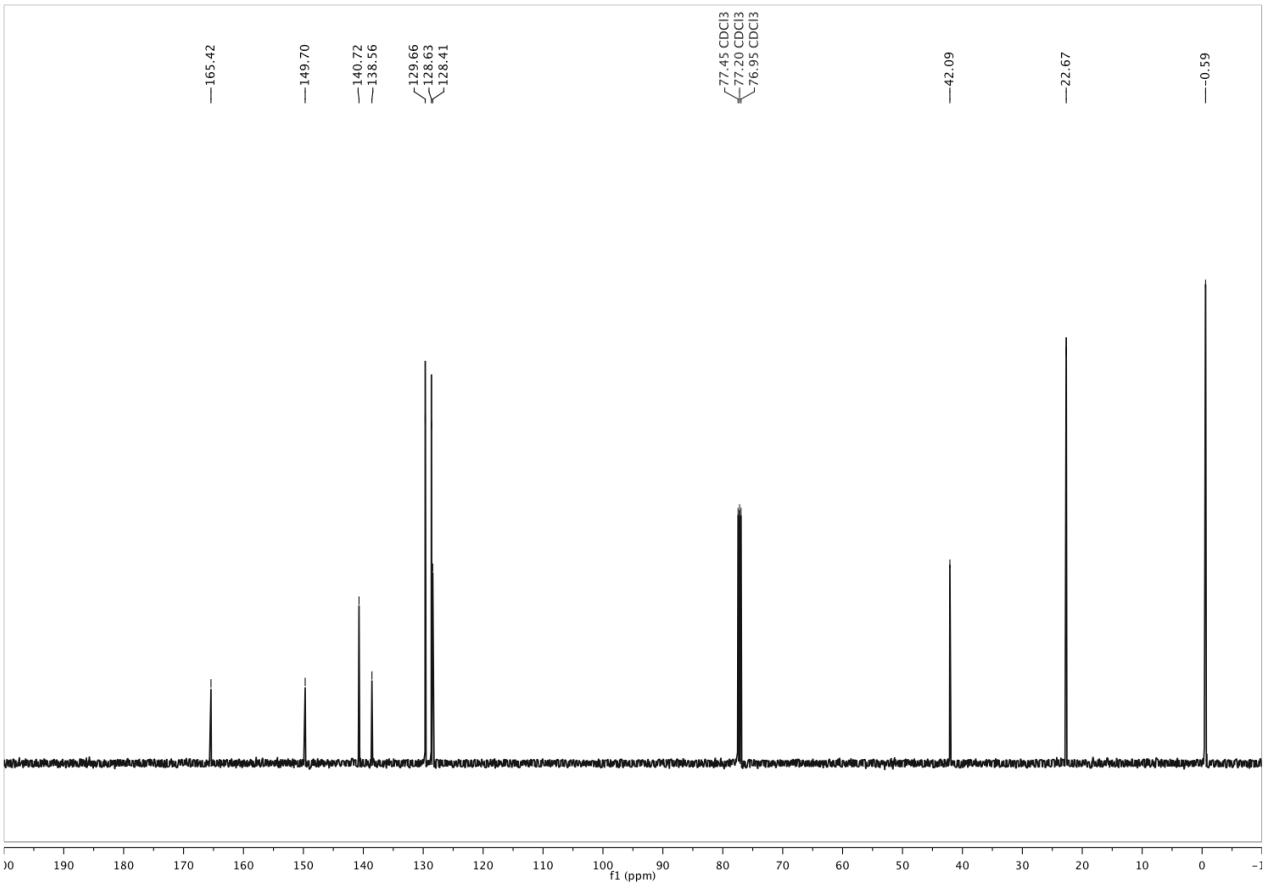
165.42
149.70
140.72
138.56
129.66
128.63
128.41
77.45 CDCl3
77.20 CDCl3
76.95 CDCl3
42.09
22.67
0.59
f1 (ppm)

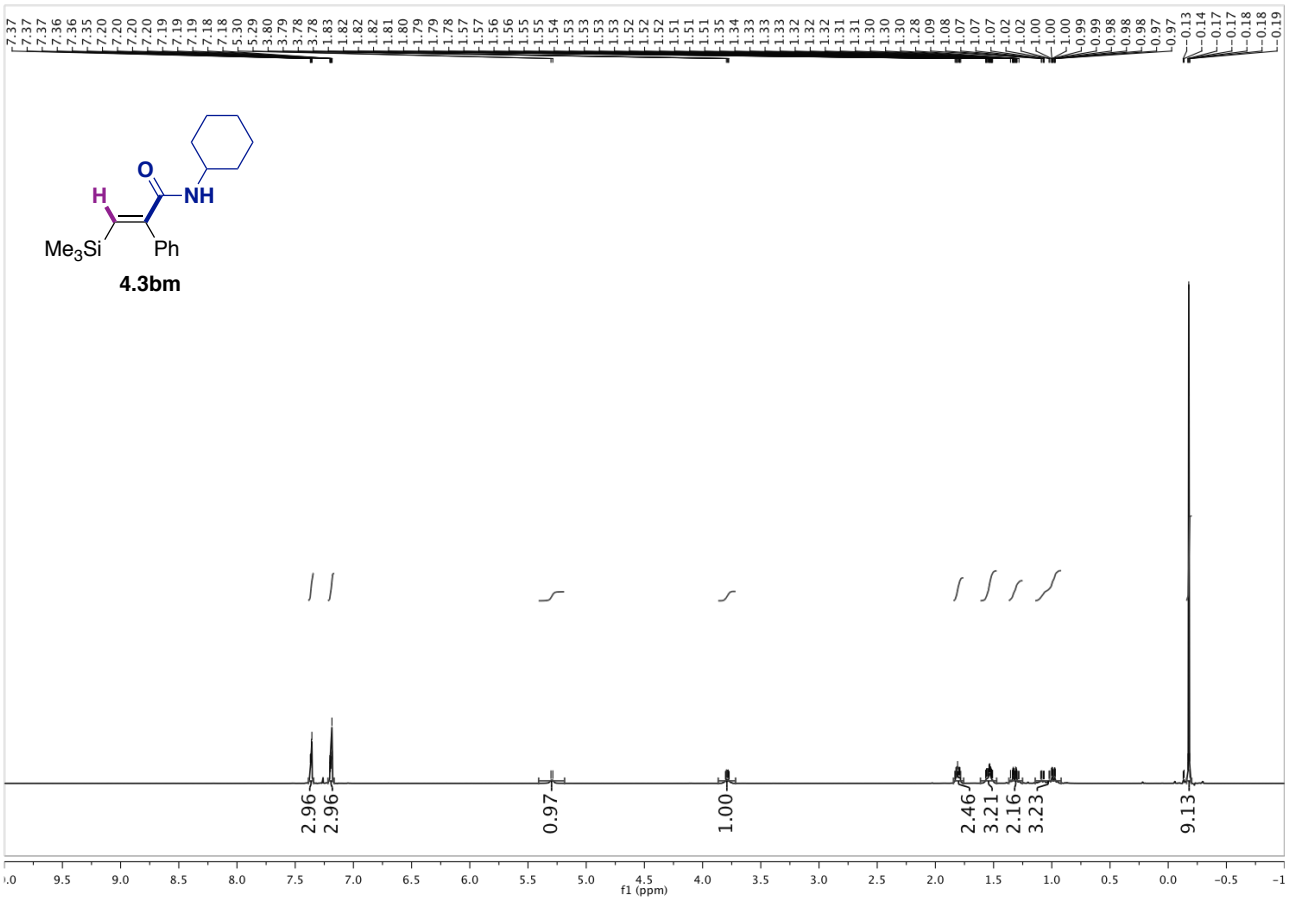
O
NH
H
Me3Si
Ph
4.3bm
2.96
2.96
0.97
1.00
2.46
3.21
2.16
3.23
9.13
f1 (ppm)

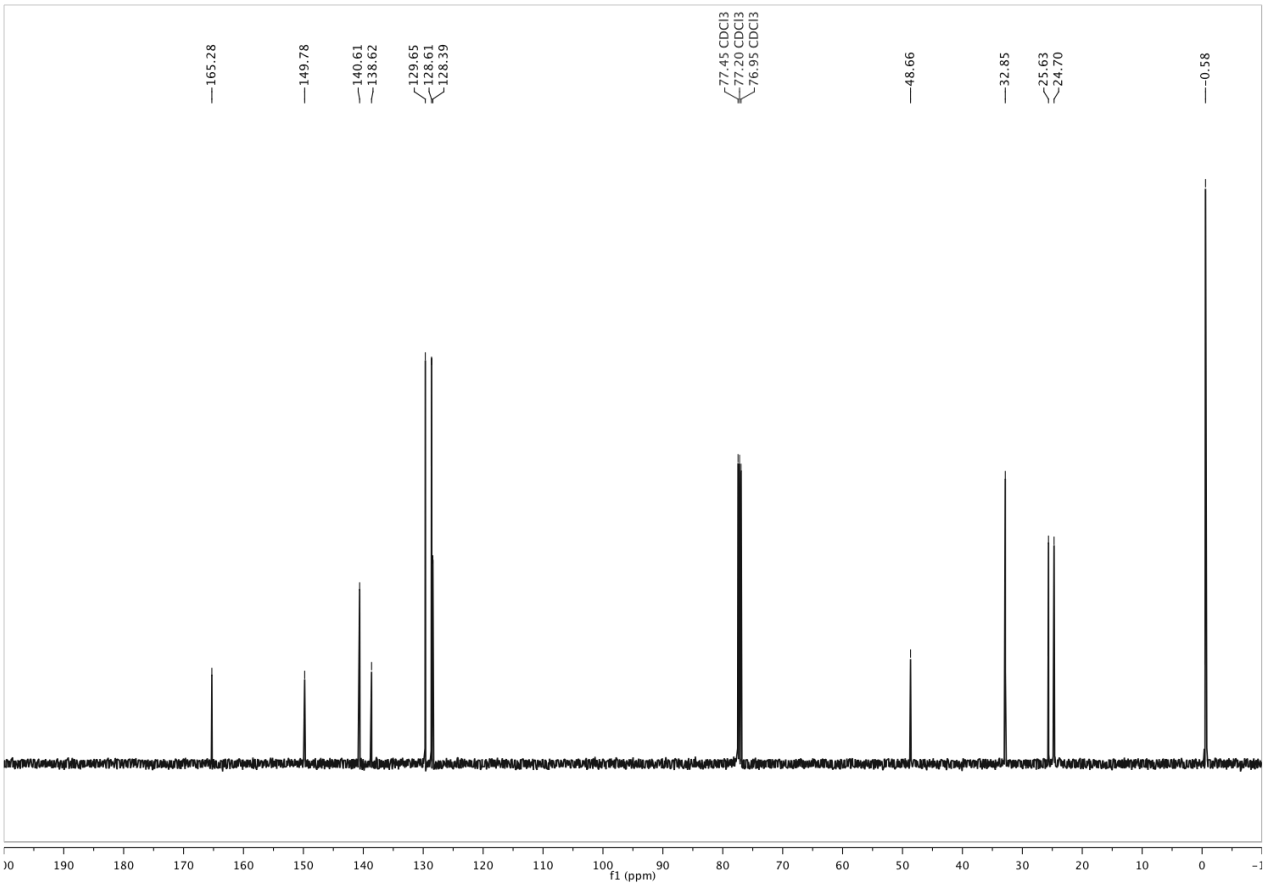
165.28
149.78
140.61
138.62
129.65
128.61
128.39
77.45 CDCl3
77.20 CDCl3
76.95 CDCl3
48.66
32.85
25.63
24.70
-0.58
f1 (ppm)

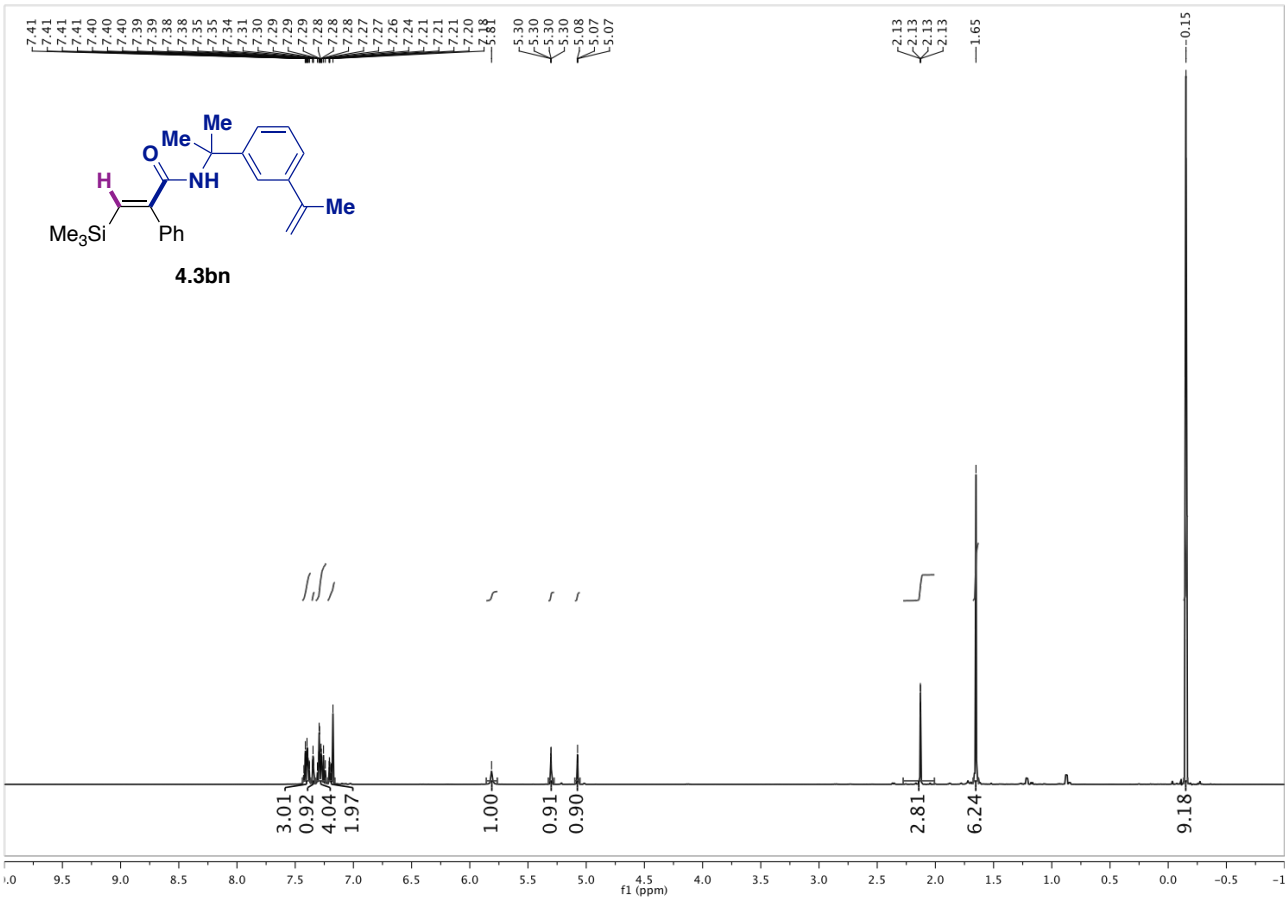
Me
Me
O
NH
H
Me
Me3Si
Ph
4.3bn
f1 (ppm)

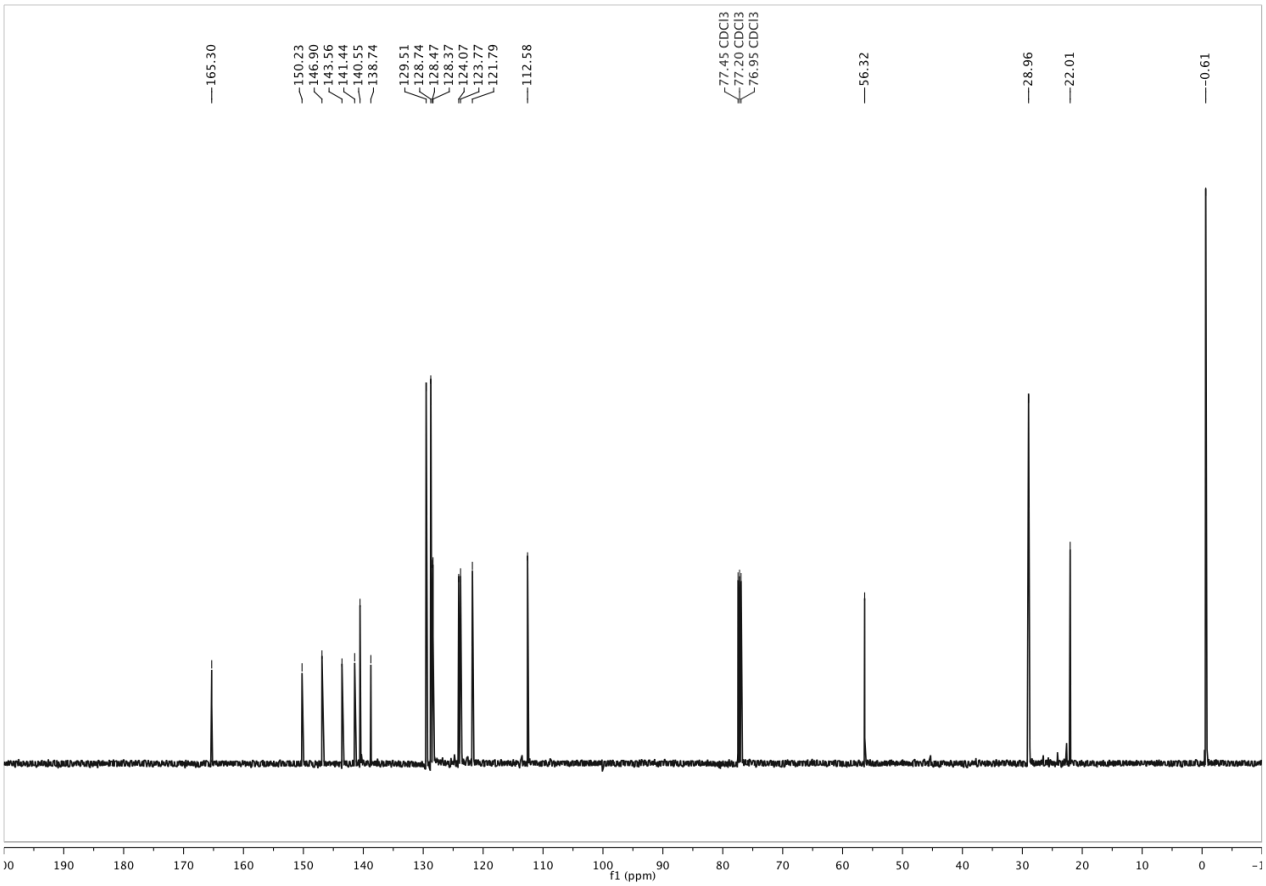
f1 (ppm)

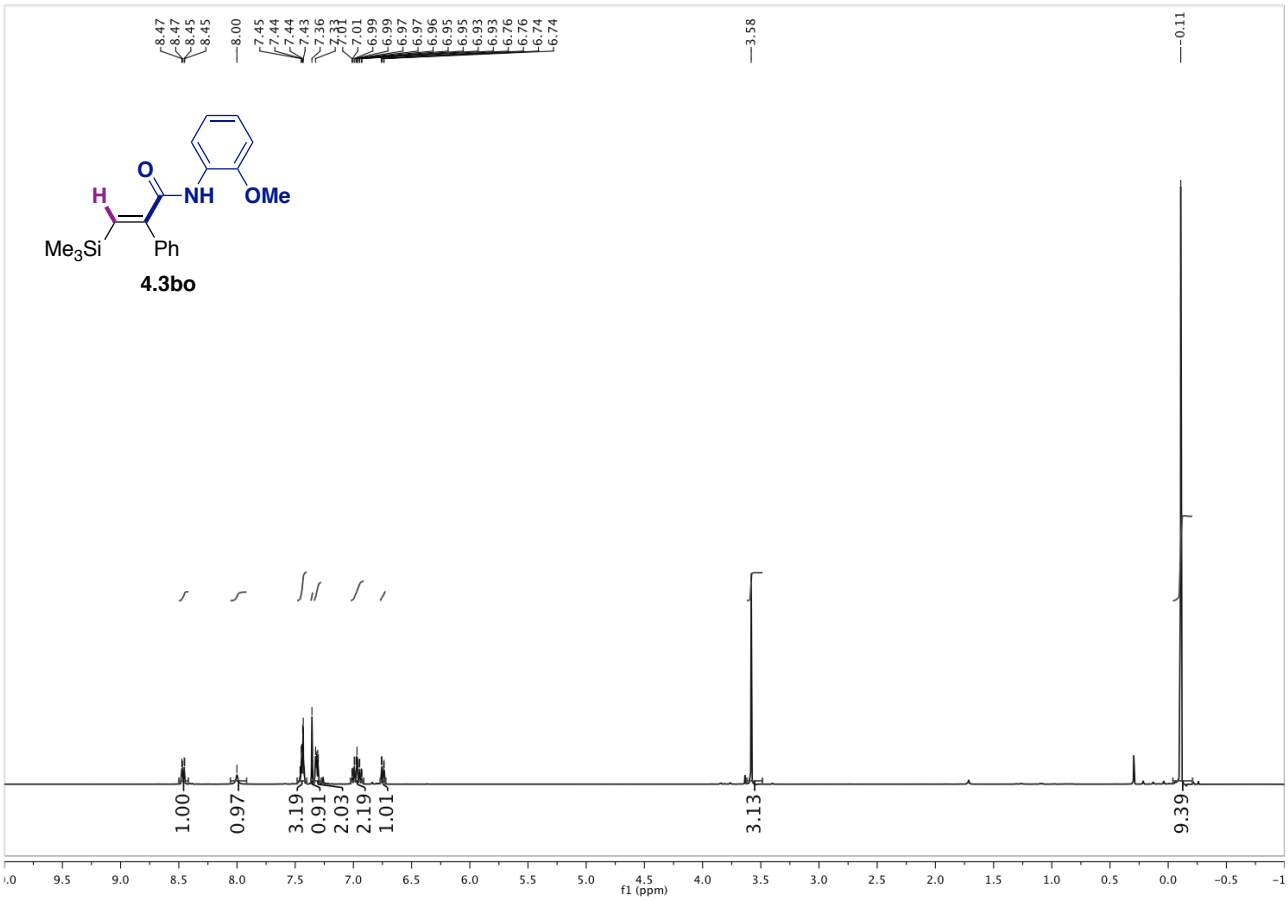
8.47
8.47
8.45
8.45
8.00
7.45
7.44
7.44
7.43
7.36
7.33
7.01
6.99
6.99
6.97
6.97
6.96
6.95
6.95
6.93
6.76
6.76
6.74
6.74
3.58
0.11
O
H
NH
OMe
Me3Si
Ph
4.3bo
1.00
0.97
3.19
0.91
2.03
2.19
1.01
3.13
9.39
f1 (ppm)

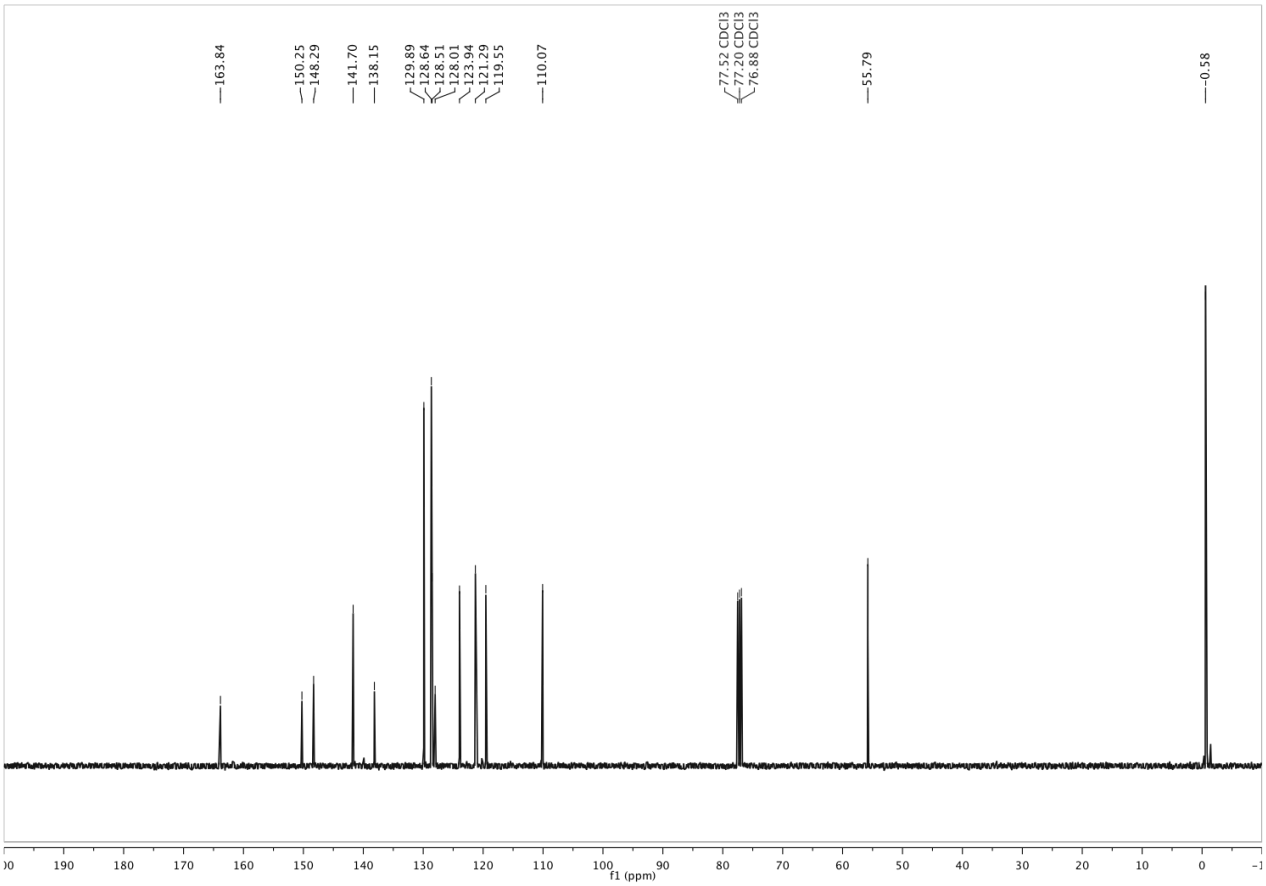
163.84
150.25
148.29
141.70
138.15
129.89
128.64
128.51
128.01
123.94
121.29
119.55
110.07
77.52 CDCl3
77.20 CDCl3
76.88 CDCl3
55.79
-0.58
f1 (ppm)

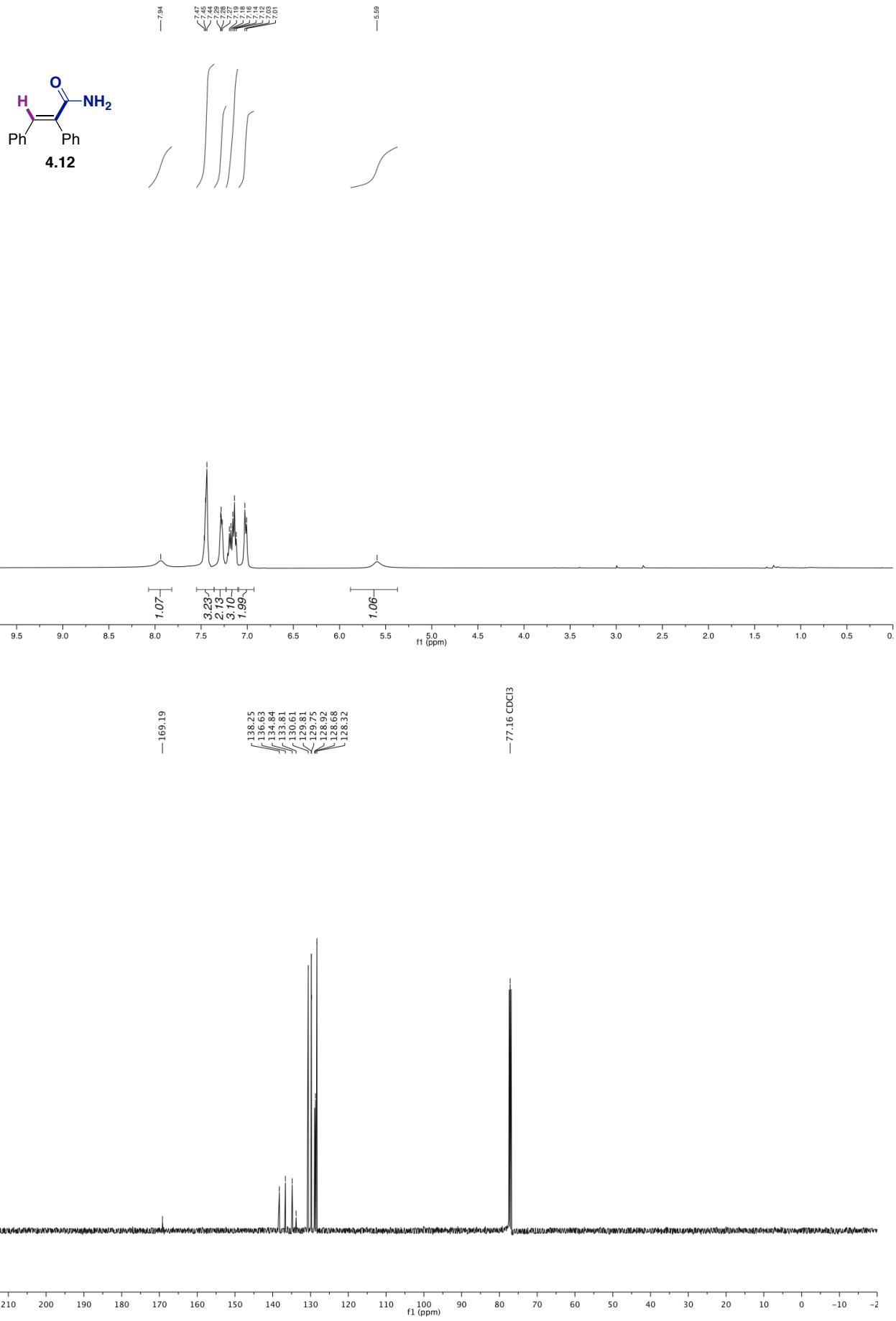
7.94
7.47
7.45
7.44
7.29
7.28
7.27
7.19
7.18
7.16
7.14
7.12
7.03
7.01
5.59
O
H
NH2
Ph
Ph
4.12
1.07
3.23
2.13
3.10
1.99
1.06
f1 (ppm)
169.19
138.25
136.63
134.84
133.81
130.61
129.81
129.75
128.92
128.68
128.32
77.16 CDCl3
f1 (ppm)

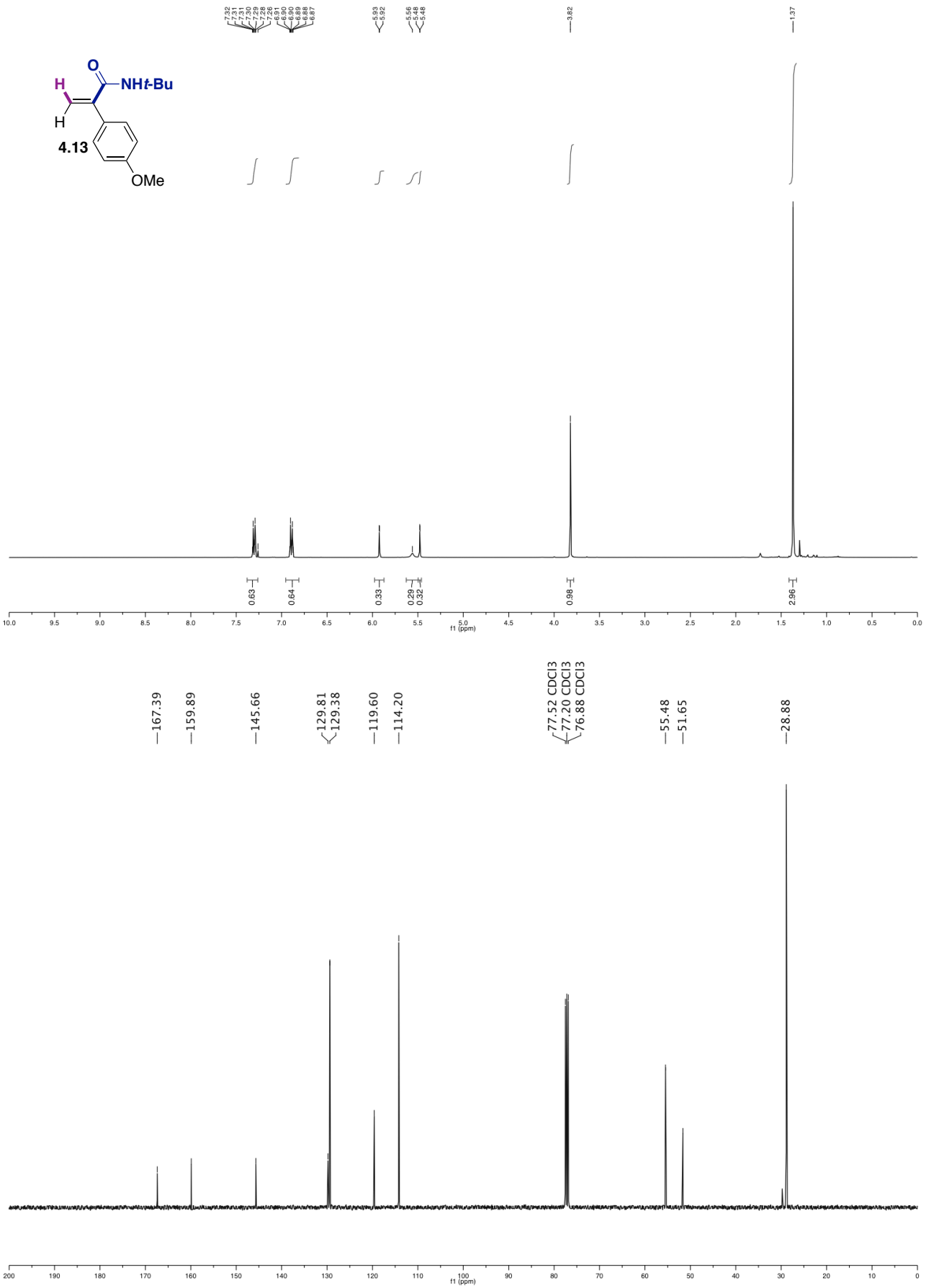
7.32
7.31
7.31
7.30
7.28
7.28
7.26
6.91
6.90
6.90
6.89
6.88
6.87
5.93
5.92
5.56
5.48
5.48
3.82
1.37
O
NHt-Bu
H
H
4.13
OMe
0.63
0.64
0.33
0.29
0.32
0.98
2.96
f1 (ppm)
167.39
159.89
145.66
129.81
129.38
119.60
114.20
77.52 CDCl3
77.20 CDCl3
76.88 CDCl3
55.48
51.65
28.88
f1 (ppm)

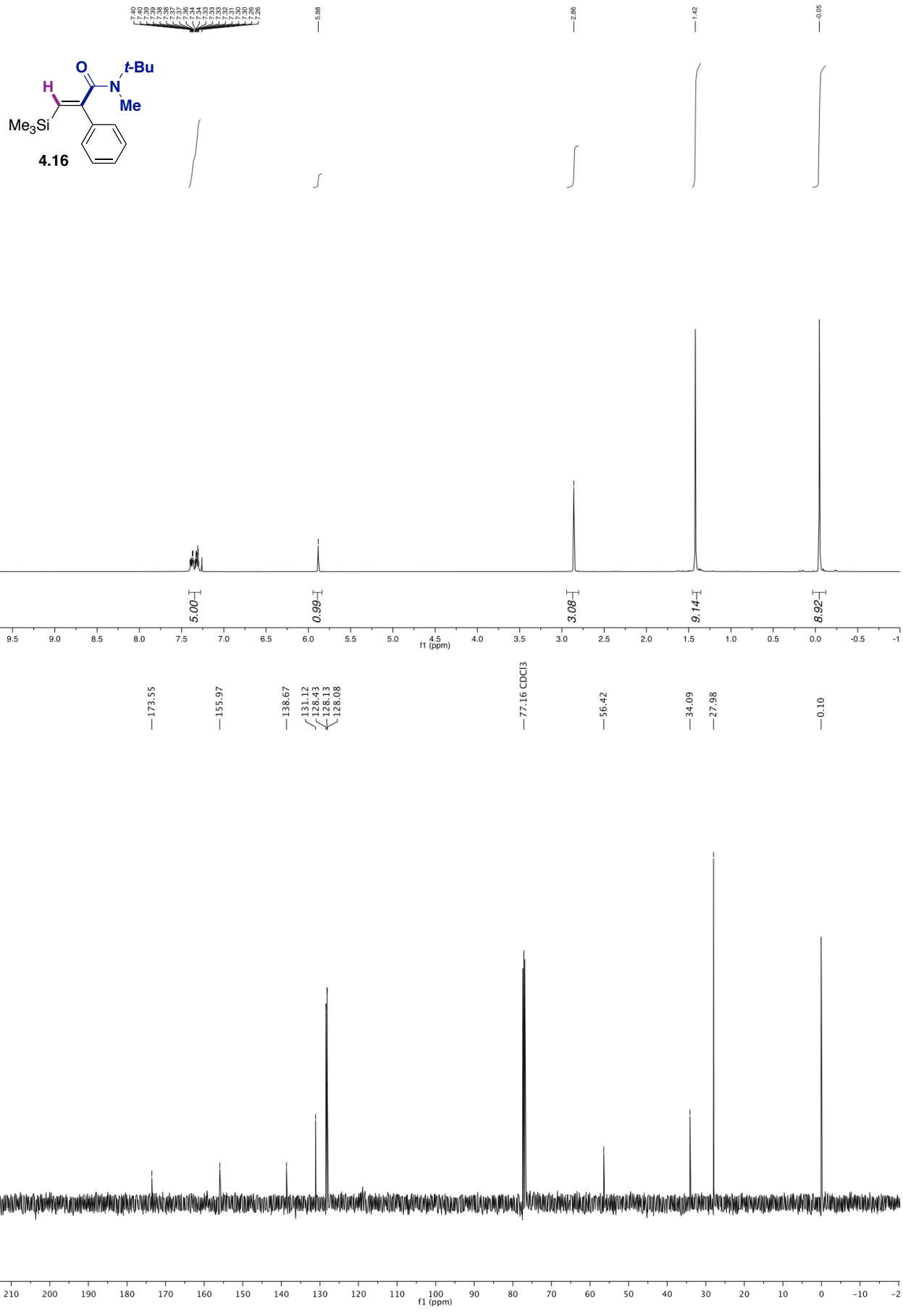
O
t-Bu
H
N
Me
Me3Si
4.16
5.00
0.99
3.08
9.14
8.92
f1 (ppm)
173.55
155.97
138.67
131.12
128.43
128.13
128.08
77.16 CDCl3
56.42
34.09
27.98
0.10
f1 (ppm)

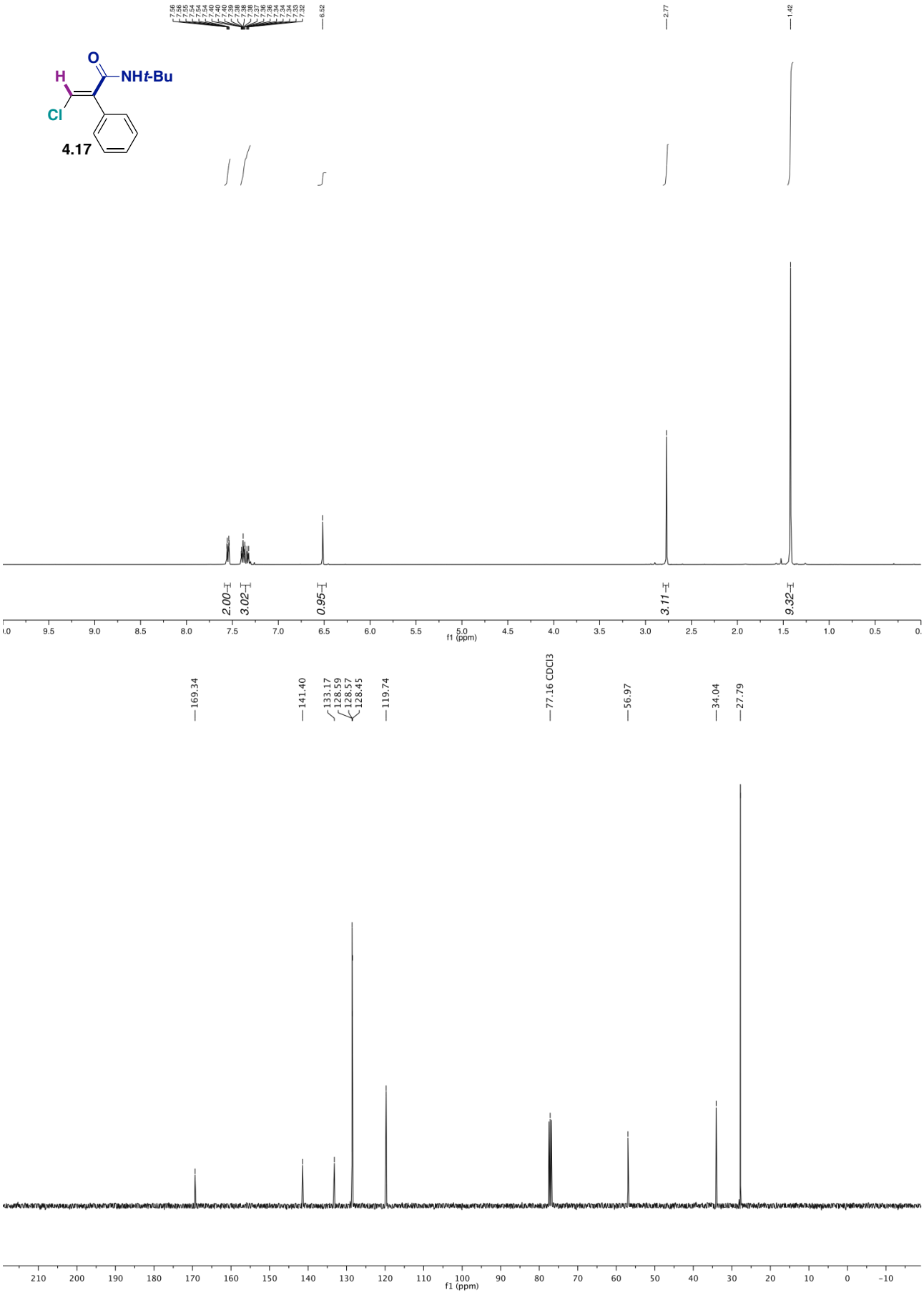
O
H
NHt-Bu
Cl
4.17
7.56
7.56
7.55
7.55
7.54
7.54
7.40
7.40
7.39
7.39
7.38
7.38
7.38
7.37
7.36
7.36
7.34
7.34
7.33
7.33
6.52
2.77
1.42
2.00
3.02
0.95
3.11
9.32
f1 (ppm)
169.34
141.40
133.17
128.59
128.57
128.45
119.74
77.16 CDCl3
56.97
34.04
27.79
f1 (ppm)

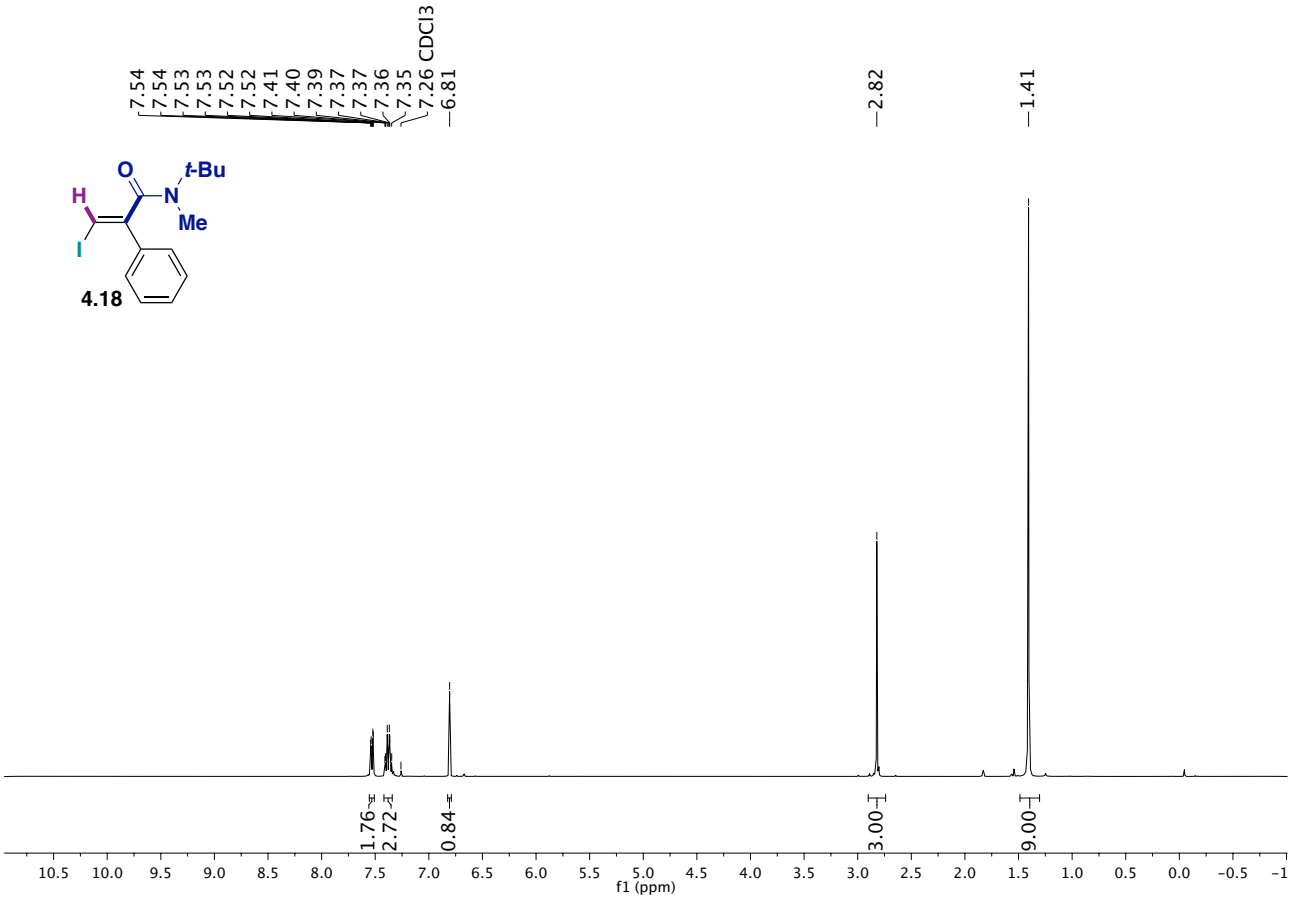
7.54
7.54
7.53
7.53
7.52
7.52
7.41
7.40
7.39
7.37
7.37
7.36
7.35
7.26 CDCl3
6.81
2.82
1.41
O
t-Bu
N
H
Me
I
4.18
1.76
2.72
0.84
3.00
9.00
f1 (ppm)

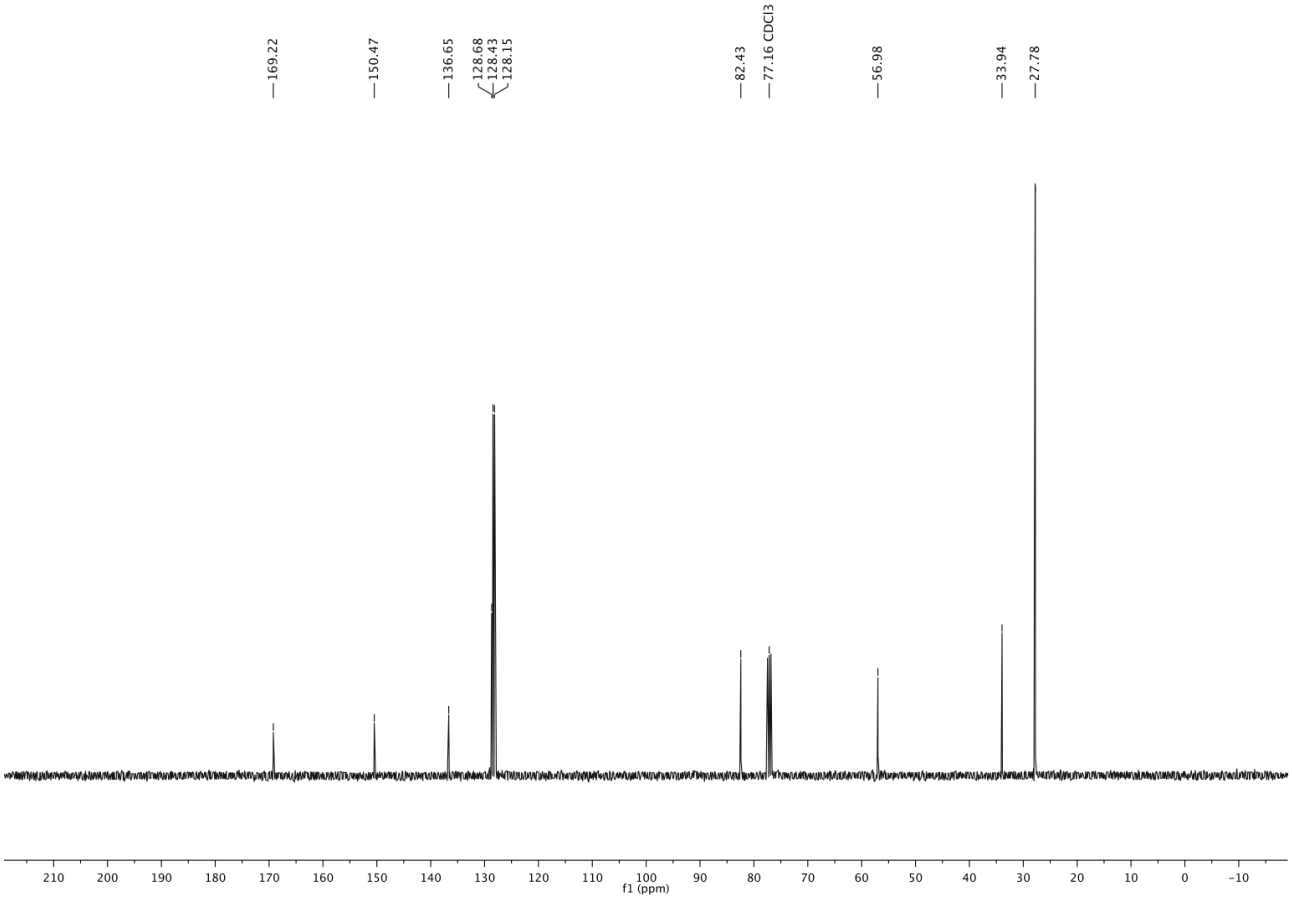
169.22
150.47
136.65
128.68
128.43
128.15
82.43
77.16 CDCl3
56.98
33.94
27.78
f1 (ppm)

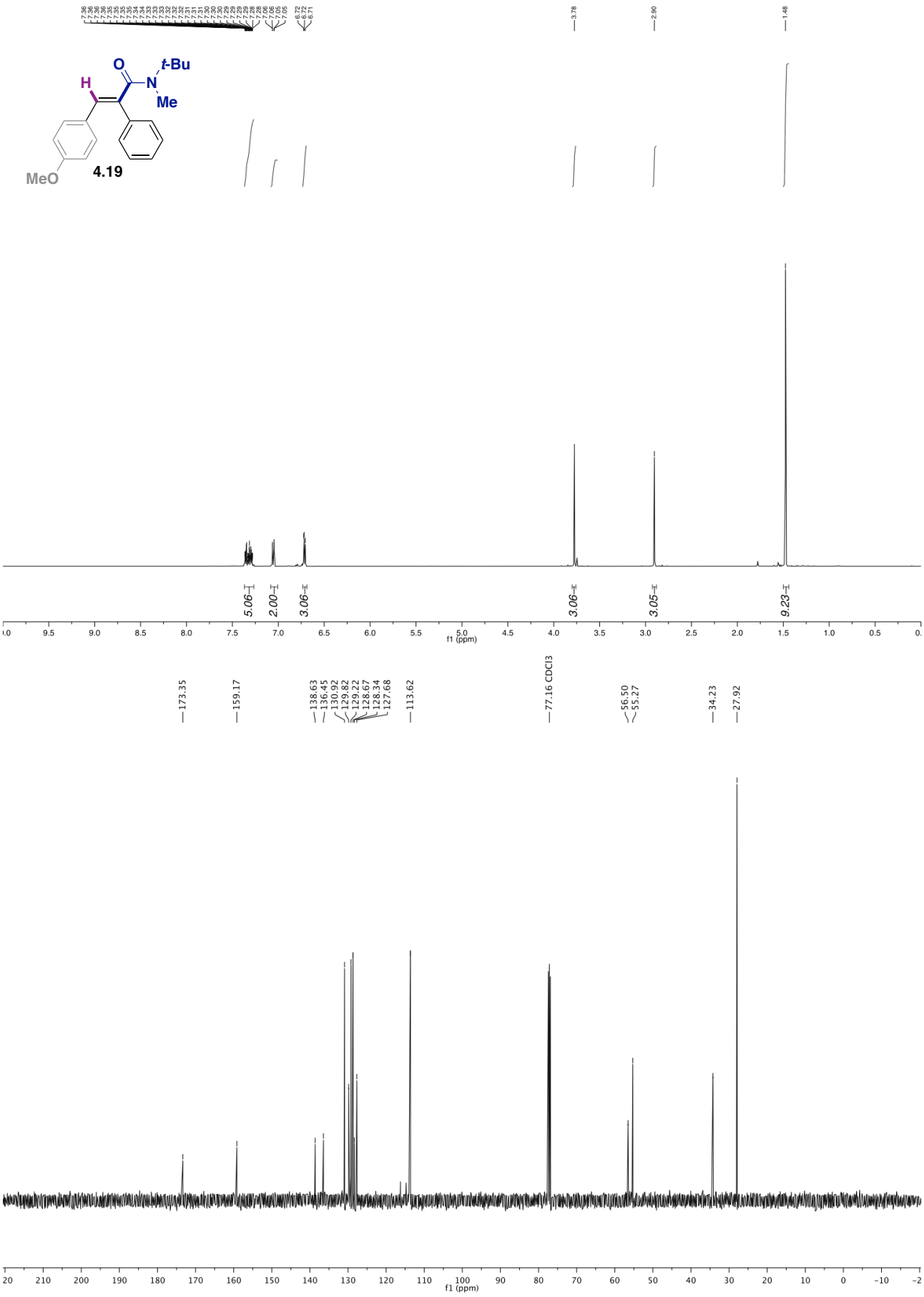
O
t-Bu
H
N
Me
MeO
4.19
3.78
2.90
1.48
5.06
2.00
3.06
3.06
3.05
9.23
f1 (ppm)
173.35
159.17
138.63
136.45
130.92
129.82
129.22
128.67
128.34
127.68
113.62
77.16 CDCl3
56.50
55.27
34.23
27.92
f1 (ppm)

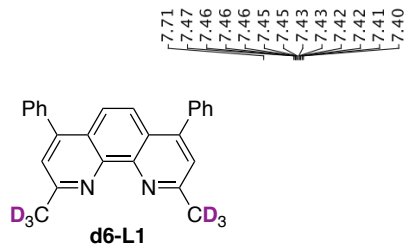
7.71
7.47
7.46
7.46
7.46
7.45
7.45
7.43
7.43
7.42
7.42
7.41
7.40
Ph
Ph
N
N
D3C
CD3

d6-L1

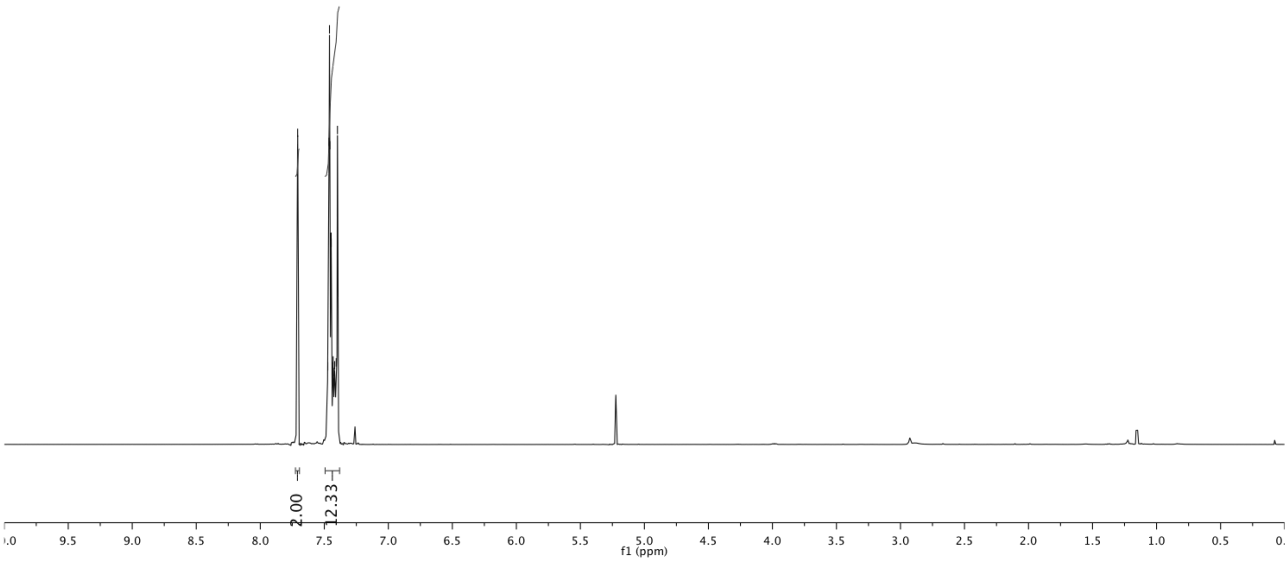
2.00
12.33
f1 (ppm)

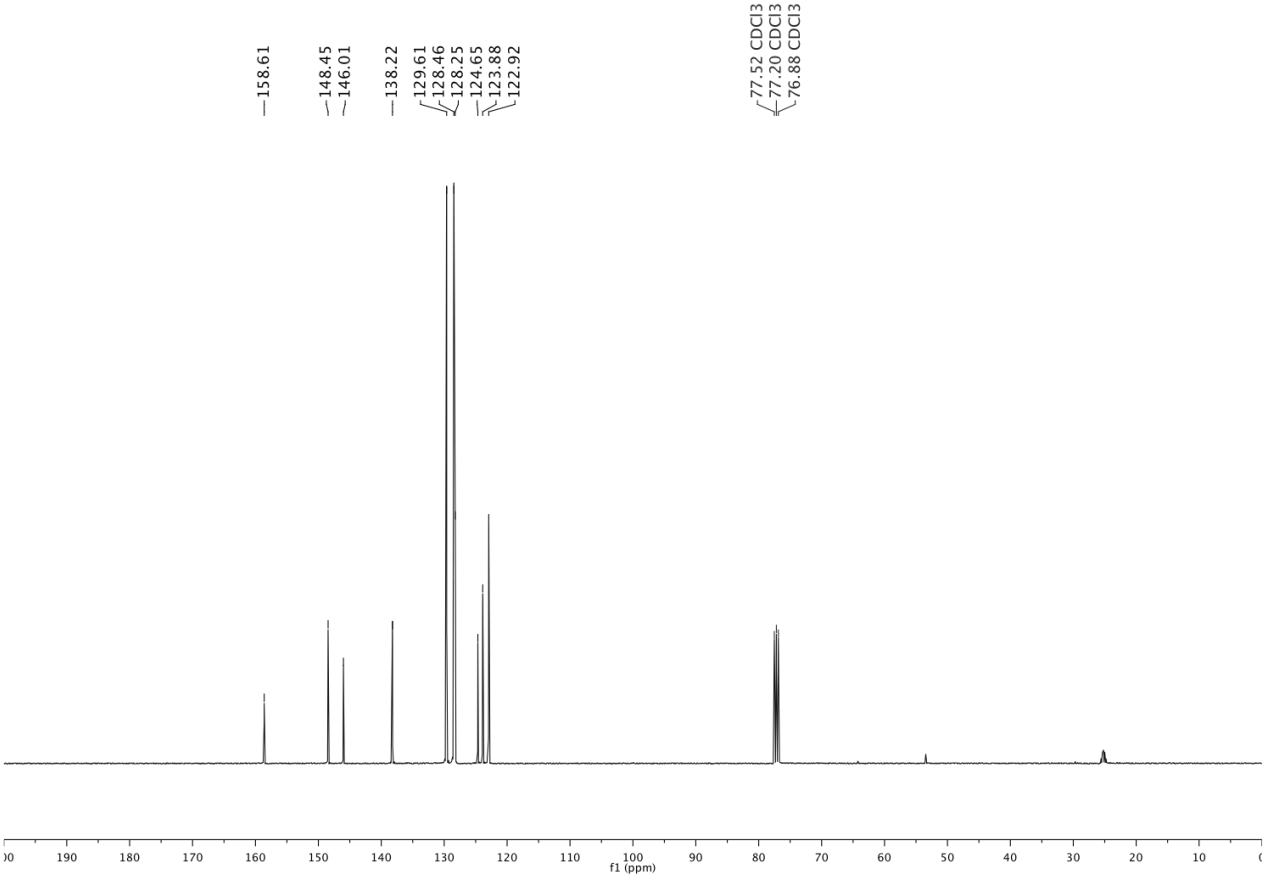
158.61
148.45
146.01
138.22
129.61
128.46
128.25
124.65
123.88
122.92
77.52 CDCl3
77.20 CDCl3
76.88 CDCl3
f1 (ppm)

UNIVERSITAT ROVIRA I VIRGILI
AMIDE FORMATION VIA NI-CATALYZED REDUCTIVE COUPLING REACTIONS WITH ISOCYANATES
Eloísa Sofía Serrano Robledo

Chapter 5.

General Conclusions

The synthetic methods developed during this Doctoral Thesis give access to a variety of aliphatic amides and acrylamides via Ni-catalyzed reductive couplings using isocyanates as the amide synthon. These reactions are carried out under mild conditions using catalytic systems based on Ni(II) salts as pre-catalysts and bipyridine- or phenanthroline-type ligands, with Mn as the reducing agent in coordinating solvents such as DMF or NMP. Starting from primary, secondary and tertiary unactivated alkyl bromides in combination with aryl and alkyl isocyanates, a broad scope of *N*-secondary aliphatic amides was prepared. When primary alkyl bromides were used, the sequential addition of a third electrophile allowed for the preparation of *N*-tertiary amides. The use of *tert*-butyl isocyanate as coupling partner has a synthetic advantage, as deprotection of *N*-*tert*-butyl-amides under Lewis acids gave access to *N*-primary amides or *N*-methyl amides that would formally arise from the use of toxic methyl isocyanate. Initial limitations associated with the use of acyclic secondary alkyl bromides could be overcome by avoiding β-hydride elimination through the use of low reaction temperatures and a finely-tuned bipyridine ligand. Following recent developments by our research group on the remote carboxylation of halogenated hydrocarbon chains, efforts towards the development of a chain-walking sp^3 C—H amidation of secondary alkyl halides were presented. Finally, the ability to form Ni—H species *in situ* from light alkyl bromides was exploited in the hydroamidation of alkynes with isocyanates to afford a wide variety of acrylamides.

Although in-depth mechanistic studies are necessary, evidence for a SET-recombination oxidative addition of the unactivated alkyl bromides was obtained when an enantiopure starting material afforded a racemic mixture of amides under the reaction conditions. For both the amidation of unactivated primary alkyl bromides and the hydroamidation of alkynes, stoichiometric studies with Ni(0) complexes, performed in the presence and absence of a reducing agent, pointed towards the intermediacy of Ni(I) species. However, due to non-negligible amounts of product generated in the absence of Mn, the intermediacy of Ni(II) species cannot entirely be ruled out. A strong indication for the *in situ* formation of Ni—H species was obtained when d_7-isopropyl bromide was used in the hydroamidation of alkynes, leading to fully deuterated acrylamides.

One of the major limitations of the amidations that derive from this Doctoral Thesis is the narrow scope of isocyanates. Specifically, only bulky and electron rich isocyanates can be used as others oligomerize under our catalytic conditions and afford only traces of the desired product. One possibility towards overcoming this limitation could be the use of isocyanate surrogates, such as carbamates, which could potentially slowly form the desired isocyanates *in situ*. Moreover, the need for superstoichiometric quantities of metal powders as reductants, which need to be quenched at the end of the reaction and generate metal waste, can be considered as a drawback for the wide application of reductive cross-electrophile reactions. The use of organic reductants such as TDAE could be an alternative; however, their high price makes their use less attractive.

Finally, the Ni-catalyzed reductive couplings with isocyanates developed during this Doctoral Thesis complement the previous methods for the metal-catalyzed synthesis of amides via C—C bond formation. Our work grants access to a broad scope of aliphatic amides and acrylamides, including hindered combinations that are often difficult to prepare via traditional coupling of activated carboxylic acid derivatives and amines. The use of isocyanates for the formation of aliphatic amides has inspired the development of a metallaphotoredox transformation using these synthons with alkyl silicates employing dual Ni/Ir-catalysis. This method circumvents the use of metallic reductants, and offers a broader scope of iso(thio)cyanates. Moreover, the discovery of the *in situ* formation of Ni—H species from light alkyl bromides has already inspired other members of the organic chemistry community for the development of Pd- and Ni-catalyzed transformations.